TERTIARY LYMPHOID STRUCTURES: FROM BASIC BIOLOGY TO TRANSLATIONAL IMPACT IN CANCER

EDITED BY: Vivek Verma, Catherine Sautes-Fridman and Anna Dimberg
PUBLISHED IN: Frontiers in Immunology

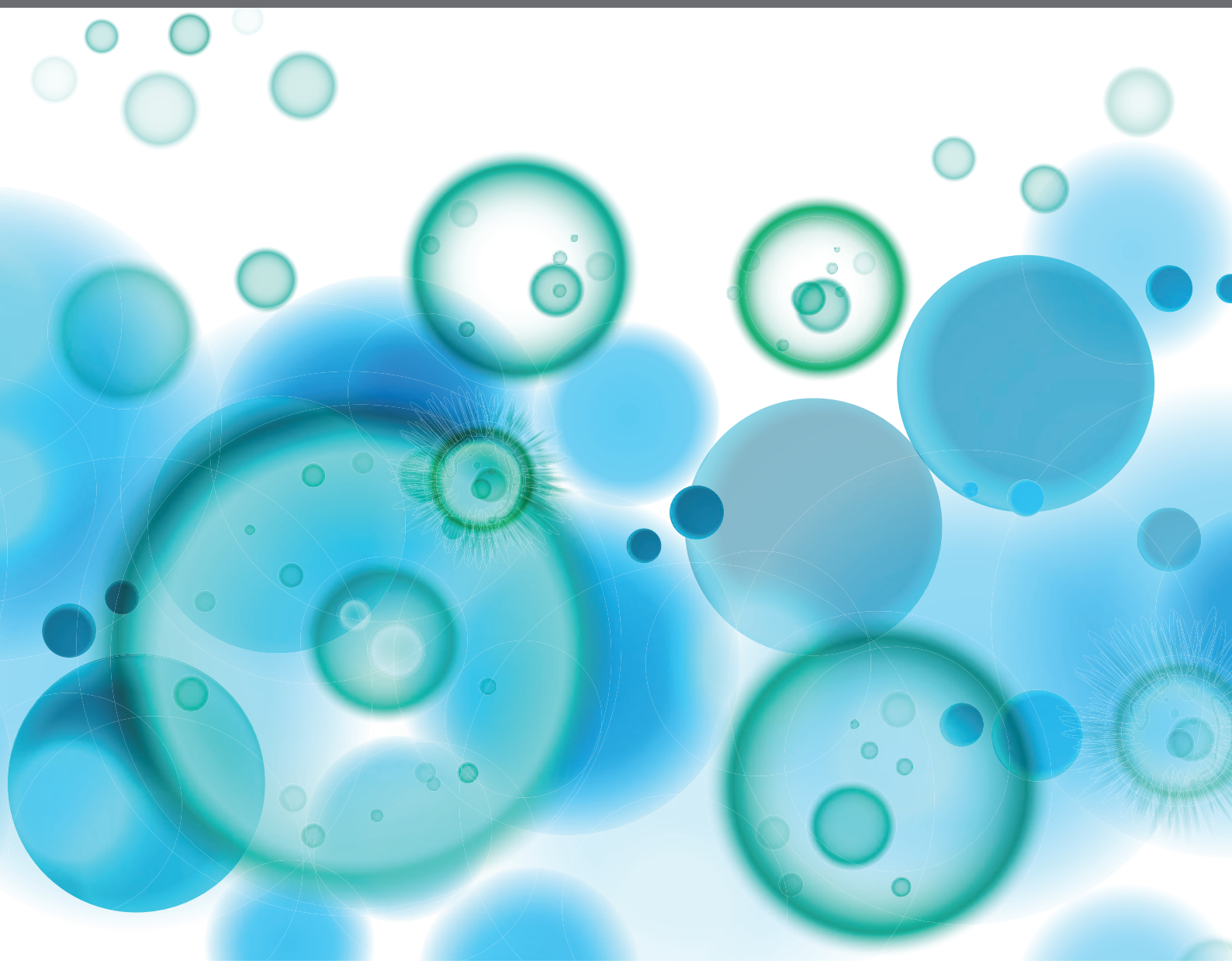

frontiers Research Topics

frontiers

Frontiers eBook Copyright Statement

The copyright in the text of individual articles in this eBook is the property of their respective authors or their respective institutions or funders. The copyright in graphics and images within each article may be subject to copyright of other parties. In both cases this is subject to a license granted to Frontiers.

The compilation of articles constituting this eBook is the property of Frontiers.

Each article within this eBook, and the eBook itself, are published under the most recent version of the Creative Commons CC-BY licence. The version current at the date of publication of this eBook is CC-BY 4.0. If the CC-BY licence is updated, the licence granted by Frontiers is automatically updated to the new version.

When exercising any right under the CC-BY licence, Frontiers must be attributed as the original publisher of the article or eBook, as applicable.

Authors have the responsibility of ensuring that any graphics or other materials which are the property of others may be included in the CC-BY licence, but this should be checked before relying on the CC-BY licence to reproduce those materials. Any copyright notices relating to those materials must be complied with.

Copyright and source acknowledgement notices may not be removed and must be displayed in any copy, derivative work or partial copy which includes the elements in question.

All copyright, and all rights therein, are protected by national and international copyright laws. The above represents a summary only. For further information please read Frontiers' Conditions for Website Use and Copyright Statement, and the applicable CC-BY licence.

ISSN 1664-8714
ISBN 978-2-88974-862-4
DOI 10.3389/978-2-88974-862-4

About Frontiers

Frontiers is more than just an open-access publisher of scholarly articles: it is a pioneering approach to the world of academia, radically improving the way scholarly research is managed. The grand vision of Frontiers is a world where all people have an equal opportunity to seek, share and generate knowledge. Frontiers provides immediate and permanent online open access to all its publications, but this alone is not enough to realize our grand goals.

Frontiers Journal Series

The Frontiers Journal Series is a multi-tier and interdisciplinary set of open-access, online journals, promising a paradigm shift from the current review, selection and dissemination processes in academic publishing. All Frontiers journals are driven by researchers for researchers; therefore, they constitute a service to the scholarly community. At the same time, the Frontiers Journal Series operates on a revolutionary invention, the tiered publishing system, initially addressing specific communities of scholars, and gradually climbing up to broader public understanding, thus serving the interests of the lay society, too.

Dedication to Quality

Each Frontiers article is a landmark of the highest quality, thanks to genuinely collaborative interactions between authors and review editors, who include some of the world's best academicians. Research must be certified by peers before entering a stream of knowledge that may eventually reach the public - and shape society; therefore, Frontiers only applies the most rigorous and unbiased reviews.
Frontiers revolutionizes research publishing by freely delivering the most outstanding research, evaluated with no bias from both the academic and social point of view. By applying the most advanced information technologies, Frontiers is catapulting scholarly publishing into a new generation.

What are Frontiers Research Topics?

Frontiers Research Topics are very popular trademarks of the Frontiers Journals Series: they are collections of at least ten articles, all centered on a particular subject. With their unique mix of varied contributions from Original Research to Review Articles, Frontiers Research Topics unify the most influential researchers, the latest key findings and historical advances in a hot research area! Find out more on how to host your own Frontiers Research Topic or contribute to one as an author by contacting the Frontiers Editorial Office: frontiersin.org/about/contact

TERTIARY LYMPHOID STRUCTURES: FROM BASIC BIOLOGY TO TRANSLATIONAL IMPACT IN CANCER

Topic Editors:
Vivek Verma, University of Minnesota Twin Cities, United States
Catherine Sautes-Fridman, INSERM U1138 Centre de Recherche des Cordeliers (CRC), France
Anna Dimberg, Uppsala University, Sweden

Citation: Verma, V., Sautes-Fridman, C., Dimberg, A., eds. (2022). Tertiary Lymphoid Structures: From Basic Biology to Translational Impact in Cancer. Lausanne: Frontiers Media SA. doi: 10.3389/978-2-88974-862-4

Table of Contents

frontiers in Immunology

EDITORIAL
published: 16 March 2022
doi: 10.3389/fimmu.2022.870862

Editorial: Tertiary Lymphoid Structures: From Basic Biology to Translational Impact in Cancer

Catherine Sautès-Fridman[1,2]*, *Anna Dimberg*[3] *and Vivek Verma*[4]

[1] Centre de Recherche des Cordeliers, INSERM, Université de Paris, Sorbonne Université, Equipe inflammation, complément et cancer, Paris, France, [2] Equipe labellisée Ligue contre le Cancer, INSERM, Université de Paris, Sorbonne Université, Equipe Inflammation, Complément et Cancer, Paris, France, [3] Department of Immunology, Genetics and Pathology, Rudbeck Laboratory, Science for Life Laboratory, Uppsala University, Uppsala, Sweden, [4] The Hormel Institute, University of Minnesota, Austin, MN, United States

Keywords: biomarker, development, tumor microenvironment, *in situ* immune response activation, *in situ* generation method

Editorial on the Research Topic

Tertiary Lymphoid Structures: From Basic Biology to Translational Impact in Cancer

OPEN ACCESS

Edited and reviewed by:
Katy Rezvani,
University of Texas MD Anderson Cancer Center, United States

***Correspondence:**
Catherine Sautès-Fridman
catherine.fridman@crc.jussieu.fr

Specialty section:
This article was submitted to Cancer Immunity and Immunotherapy, a section of the journal Frontiers in Immunology

Received: *07 February 2022*
Accepted: *10 February 2022*
Published: *16 March 2022*

Citation:
Sautès-Fridman C, Dimberg A and Verma V (2022) Editorial: Tertiary Lymphoid Structures: From Basic Biology to Translational Impact in Cancer. Front. Immunol. 13:870862. doi: 10.3389/fimmu.2022.870862

Tertiary lymphoid structures (TLSs) are organized lymphoid aggregates developing in inflamed tissues upon infection, auto-immune reactions, and in tumors. As potential biomarkers of response to antibodies against immune checkpoints, TLSs have recently become prominent, highlighting the need to increase basic knowledge of these structures. This Research Topic presents 14 articles covering TLS heterogeneity and relationships with tumor mutational burden (TMB) as well as strategies for their induction in mouse models and in artificial scaffolds.

THE EARLY EVENTS TRIGGERING TLS FORMATION

The question regarding the early events that lead to TLS formation has been addressed in mouse models. Johansson-Percival and Ganss highlight that development of lymphoid tissue involves a crosstalk between Podoplanin$^+$ICAM$^+$/αSMA$^+$ stromal cells expressing LTβR and TNFR [LT organizer cells (LTo)] and immune cells including macrophages, dendritic cells (DCs), and T and B cells [LT inducer cells (LTi)]. This interaction sustains the production of CCL19/21/CXCL13 by stromal cells through production of TNFα, LTα and β, LIGHT, IL1β, and CCL21. They discuss the LTi role of each of the immune cell types to support mature TLS formation. They hypothesize that CCL19-secreting cancer-associated fibroblasts, TNFα-secreting macrophages, and LTβ-secreting DCs could be the originators of TLSs in human cancers. Filderman et al. cite the role of interferon (IFN) and IL1 family members (ILF9/IL36γ), in association with activation of T cell-mediated anti-tumor functions for TLS induction.

TLSs are surrounded by high endothelial venules (HEV). Filderman et al. provide a comprehensive review on the chemokines and cytokines involved in HEV formation and TLS induction from studies in mouse models. TNFR- over LTβR-mediated signaling is dominant for HEV and TLS neogenesis (Filderman et al.), both pathways being necessary for acquisition of a fully

mature HEV phenotype (Vella et al.). HEVs can be modulated by immune cells, DCs favor their formation and Tregs suppress it. Vella et al. provide evidence suggesting that altered HEVs could allow formation of a pre-metastatic niche permissive for tumor cells, and allow tumor cell intravasation into the bloodstream.

TLSs: A SET OF STRUCTURES WITH DISTINCT CELLULAR COMPOSITION AND FUNCTIONS

By analogy with secondary lymphoid organs (SLOs), three classes of TLSs are being considered (1): primary follicle-like TLSs with $CD21^+$ follicular dendritic cells (FDCs) (2), mature TLSs with CD23+CD21+ FDC within germinal centers (GC) and lymphoid aggregates of T and B cells, and (3) so-called, although not demonstrated, "early-TLSs" or "immature TLSs".

One of the current key issues is to deeply characterize these distinct TLSs and understand their relationships with the immune infiltrate and the surrounding tissue. Two papers address these questions in urothelial cancers (UCs). UCs develop below inflamed areas of the bladder and can become invasive in the muscle. By analyzing 40 tumor samples of muscle invasive bladder cancer patients (MIBC), Pagliarulo et al. show that immature TLSs have an increased proportion of T cells and reduced proportion of total B cells when compared to mature TLSs. Presence of mature TLSs correlates with higher lymphocytic infiltration in many cancer types. Analyzing the TME, Pagliarulo et al. find that the majority of TLS-high tumors show B and T cell co-infiltration harboring naïve (PD1-TCF7+) and progenitor-like (PD1+TCF7+) CD8 T cells and activated B cells (PD1+), whereas only a minority of TLS-low tumors present this type of infiltration. These differences are independent of TLS maturation stages. Pagliarulo et al. therefore suggest a role of B cells and CD8 T cell interactions sustaining the presence of PD1+ TCF1+ T cells in the TME. Trüb and Zippelius also discuss the mechanisms underlying the potential crosstalk between B cells and CD8 T cells, either direct as suggested by Pagliarulo et al. or through DCs or CD4 T cells, leading to optimal cancer immunosurveillance. Which molecules are involved in a potential direct B cell-CD8 T cell crosstalk need to be further explored.

Van Dijk et al. compare TLSs in cystectomy specimens and in superficial transurethral resection (TUR) biopsies of 31 UC patients. TLSs located in TUR biopsies display higher numbers of CD4 T cells, a higher fraction of early TLS, and lower germinal center (GC+) TLS than submucosal ones. TUR specimens contain superficial tissue that is highly exposed to inflammation stimuli, urinary toxins, and microbial pathogens. The Van Dijk et al. report is reminiscent of studies showing that the early hepatic lesions that precede transformation to hepatocellular carcinoma (HCC) also display immature TLS and show elevated expression of immune inhibitory molecules that may favor immune evasion (1). Further experiments are needed to investigate the prognostic impact of these distinct entities and the antigens recognized. In the same line, Werner et al. investigate TLS composition and location by seven-color multiplex staining of whole tissue sections in 48 patients with primary cutaneous melanoma and 39 distant/late metastases. Whereas only early TLSs were found in one third of primary tumors, half of the metastases contained secondary follicle-like TLSs most of which were located in the extratumoral compartment within 1 mm distance to the invasive tumor. Most of these TLSs lack BCl6+ lymphatic cells and canonic GC polarity. This paper shows that the "mature TLS" stage defined using CD21+CD23+FDC may, depending on the tumor site, include heterogeneous phenotypes with variable BCl6 expression levels in B cells, likely reflecting the strength of B cell signaling and of T cell help, and thus the fate of B cell differentiation into antibody secreting cells. Other types of TLS heterogeneity could influence the impact of mature TLS on prognosis. Johansson-Percival and Ganss mention that TLSs with high densities of M2 macrophages and T helper cells expressing GATA3, a master regulator of Th2 differentiation, were found to contribute to immune suppression and correlate with relapse in colorectal cancer (2). Domblides et al. and Kang et al. also discuss the negative impact of Tregs on functions of mature TLSs.

In conclusion, 1) "early TLSs" or "immature TLSs" exhibit distinct cellular composition and functions compared to "mature TLSs", 2) "mature TLSs" are heterogenous and need to be defined by additional markers other than CD21+CD23+ FDC. The role of TLSs in maintaining immune niches for TCF1+PD1+ stem cells needs to be further investigated (3).

TLS FORMATION EXHIBITS NO STRICT DEPENDENCE ON TUMOR MUTATIONAL BURDEN (TMB)

By analyzing diagnostic hematoxylin and eosin (H&E) images and genetic features of MIBC tumors in TCGA data, Pagliarulo et al. show that TLS density is a significant favorable prognostic factor without direct correlation with TMB. Both favorable prognosticators synergize. They propose a joint TLS-TMB score independent of tumor stage and vascular invasion. Domblides et al. also address this question and present a comprehensive analysis of the literature comparing genomic instability, oncogenic drivers, as well as viruses and TLS presence in human tumors. Presence of TLS in transcriptomic data could be assessed using the 12-chemokine (12-CK) score (4). Li et al. performed a pan-cancer comparison between the expression levels of the 12-CK score in tumors and normal samples with the TMB in tumors from TCGA. They found that 12-CK scores generally corresponded with the median tumor mutational burden (TMB) ($r=0.46$, $p=0.01$). However, mutationally silent testicular seminoma as well as several tumors with low mutational burden such as soft tissue sarcoma (5) and melanoma (6) exhibit TLSs confirming that other antigenic stimuli than TMB may be involved in TLS formation. High 12-CK scores were seen amongst cancers with high TMB, presumably with high neoantigenic stimuli to trigger a strong immunogenic response, high immune infiltrate, and presence of mature TLS, and were associated with favorable

outcome for the patients. Li et al. also provide arguments supporting the use of the 12-CK score to predict response to immune checkpoint blockade. Whether the score can be refined further to take into account the TLS heterogeneity described above is an open question.

THERAPEUTIC INDUCTION OF TLS

The presence of intratumoral TLSs in many cancer forms are predictive of a positive response to cancer immunotherapies (Trüb and Zippelius), sparking an interest in inducing TLSs as a means to improve immunotherapy responses. Van de Walle et al. hypothesize that this may be of special benefit in CNS tumors, where TLSs could provide a local site for T cell priming. That would circumvent the need for transport of tumor antigens and trafficking of antigen-presenting cells from the CNS into cervical lymph nodes. Several papers cite the importance of vascular normalization for TLS induction in tumors (Johansson-Percival and Ganss; Vella et al.; Filderman et al.). STING (STimulator of INterferon Genes) agonists originally developed as anti-angiogenic agents induce immature TLSs in mice. Their use in therapy would require activation of CXCL13 production to induce TLS maturation, that could be provided upon stimulation of stromal cells (Filderman et al.). Cytokine fusion compounds which deliver TNF or IFNβ to tumor vessels, do not induce mature TLSs as monotherapies, but could be used in combination with antibodies targeting immune checkpoint molecules as immunotherapeutic tools (Johansson-Percival and Ganss). Kang et al. propose to combine the induction of HEVs and inhibition of local immunosuppression using anti-checkpoint antibodies to induce TLSs, arguing for a better knowledge of the mechanisms of regulation of HEV formation.

Domblides et al. comprehensively review the syngeneic, humanized, carcinogen-induced, and genetically engineered tumor models to induce TLSs as well as artificial approaches using organoids or spheroids. Aoyama et al. focus on approaches to artificially induce TLS formation using the LTβR-chemokine axis embedded in a variety of three-dimensional materials that are permissible to cellular infiltration and that may allow for cell-scaffold interactions. They compare the use of collagen-based matrices, hydrogels or cryogels, silica-based scaffolds, and liposome based-micro and nanoparticles with delayed release of soluble factors. Some of these materials can induce an inflammatory response due to local activation of neutrophils and macrophages, which may interfere with formation of TLSs with anti-tumor function. Aoyama et al. anticipate the challenges to translate such approaches to the clinic given the multimodal processes involved in their development.

Altogether, this Research Topic emphasizes the importance of intrinsic and cancer-dependent TLS heterogeneity, unveiling the need for their detailed and robust characterization. It also highlights the need for nomenclature adjustment in order to allow an integration of reports, and facilitate the development of new concepts and strategies for their induction.

AUTHOR CONTRIBUTIONS

All authors listed have made a substantial, direct, and intellectual contribution to the work and approved it for publication.

REFERENCES

1. Meylan M, Petitprez F, Lacroix L, Di Tommaso L, Roncalli M, Bougoüin A, et al. Early Hepatic Lesions Display Immature Tertiary Lymphoid Structures and Show Elevated Expression of Immune Inhibitory and Immunosuppressive Molecules. *Clin Cancer Res* (2020) 26)16:4381–89. doi: 10.1158/1078-0432.CCR-19-2929
2. Yamaguchi K, Ito M, Ohmura H, Hanamura F, Nakano M, Tsuchihashi K, et al. Helper T Cell-Dominant Tertiary Lymphoid Structures Are Associated With Disease Relapse of Advanced Colorectal Cancer. *Oncoimmunology* (2020) 9 (1):1724763. doi: 10.1080/2162402X.2020.1724763
3. Jansen CS, Prokhnevska N, Master VA, Sanda MG, Carlisle JW, Bilen MA, et al. An Intra-Tumoral Niche Maintains and Differentiates Stem-Like CD8 T Cells. *Nature* (2019) 576(7787):465–70. doi: 10.1038/s41586-019-1836-5
4. Coppola D, Nebozhyn M, Khalil F, Dai H, Yeatman T, Loboda A, et al. Unique Ectopic Lymph Node-Like Structures Present in Human Primary Colorectal Carcinoma Are Identified by Immune Gene Array Profiling. *Am J Pathol* (2011) 179(1):37–45. doi: 10.1016/j.ajpath.2011.03.007
5. Petitprez F, de Reynies A, Keung EZ, Chen TW, Sun CM, Calderaro J, et al. B Cells Are Associated With Survival and Immunotherapy Response in Sarcoma. *Nature* (2020) 577(7791):556–60. doi: 10.1038/s41586-019-1906-8
6. Cabrita R, Lauss M, Sanna A, Donia M, Skaarup Larsen M, Mitra S, et al. Tertiary Lymphoid Structures Improve Immunotherapy and Survival in Melanoma. *Nature* (2020) 577(7791):561–5. doi: 10.1038/s41586-019-1914-8

Conflict of Interest: The authors declare that the research was conducted in the absence of any commercial or financial relationships that could be construed as a potential conflict of interest.

Publisher's Note: All claims expressed in this article are solely those of the authors and do not necessarily represent those of their affiliated organizations, or those of the publisher, the editors and the reviewers. Any product that may be evaluated in this article, or claim that may be made by its manufacturer, is not guaranteed or endorsed by the publisher.

Copyright © 2022 Sautès-Fridman, Dimberg and Verma. This is an open-access article distributed under the terms of the Creative Commons Attribution License (CC BY). The use, distribution or reproduction in other forums is permitted, provided the original author(s) and the copyright owner(s) are credited and that the original publication in this journal is cited, in accordance with accepted academic practice. No use, distribution or reproduction is permitted which does not comply with these terms.

frontiers in Immunology

MINI REVIEW
published: 12 May 2021
doi: 10.3389/fimmu.2021.674565

Tertiary Lymphoid Structures as a Predictive Biomarker of Response to Cancer Immunotherapies

Marta Trüb [1*] *and Alfred Zippelius* [1,2]

[1] Laboratory of Cancer Immunology, Department of Biomedicine, University of Basel, University Hospital Basel, Basel, Switzerland, [2] Medical Oncology, University Hospital Basel, Basel, Switzerland

Tertiary lymphoid structures (TLS) are ectopic lymphoid formations which are formed under long-lasting inflammatory conditions, including tumours. TLS are composed predominantly of B cells, T cells and dendritic cells, and display various levels of organisation, from locally concentrated aggregates of immune cells, through clearly defined B cell follicles to mature follicles containing germinal centres. Their presence has been strongly associated with improved survival and clinical outcome upon cancer immunotherapies for patients with solid tumours, indicating potential for TLS to be used as a prognostic and predictive factor. Although signals involved in TLS generation and main cellular components of TLS have been extensively characterised, the exact mechanism by which TLS contribute to the anti-tumour response remain unclear. Here, we summarise the most recent development in our understanding of their role in cancer and in particular in the response to cancer immunotherapy. Deciphering the relationship between B cells and T cells found in TLS is a highly exciting field of investigation, with the potential to lead to novel, B-cell focused immunotherapies.

Keywords: TLS, tertiary lymphoid structures, tumour, cancer immunotherapy, novel therapies, B cells

OPEN ACCESS

Edited by:
Catherine Sautes-Fridman, INSERM U1138 Centre de Recherche des Cordeliers (CRC), France

Reviewed by:
Graham Robert Leggatt, The University of Queensland, Australia
Eric Vivier, INSERM U1104 Centre d'immunologie de Marseille-Luminy (CIML), France

***Correspondence:**
Marta Trüb
marta.trueb@unibas.ch

Specialty section:
This article was submitted to Cancer Immunity and Immunotherapy, a section of the journal Frontiers in Immunology

Received: *01 March 2021*
Accepted: *08 April 2021*
Published: *12 May 2021*

Citation:
Trüb M and Zippelius A (2021) Tertiary Lymphoid Structures as a Predictive Biomarker of Response to Cancer Immunotherapies. Front. Immunol. 12:674565. doi: 10.3389/fimmu.2021.674565

B CELLS IN THE CANCER IMMUNOTHERAPY SPOTLIGHT

Immunotherapy is a recent breakthrough in oncology treatment which focuses on harnessing the power of the immune system to fight cancer. Immune checkpoint blockade (ICB) therapy mainly targets PD-(L)-1 and CTLA-4 receptors and provides durable responses in cancer patients. T cells have been at the forefront of research surrounding ICB but other immune cells are also increasingly being found to take part in the response (1, 2). Recent studies from human patients (and also mouse models) have put the spotlight on B cells as additional important players in immunotherapy. For example, the presence of B cells and TLS is associated with favourable response to immune checkpoint blockade in patients with soft tissue sarcomas (3), metastatic melanoma (4, 5) and renal cell carcinoma (5). While the field has been so far primarily focused on T cells, these findings call for further investigation into the active role of TLS and B cells in ICB treatment. This review aims to summarise our understanding of the role of B cells and TLS in immunotherapy response and mechanisms in the cellular network of the tumour microenvironment with a focus on the potential cross-talk between B cells and cytotoxic T cells.

TLS COMPOSITION

Orchestrated immune response to cancer is elicited systemically in secondary lymphoid organs (SLO, such as lymph nodes and spleen) and locally, in ectopic lymphoid formations called tertiary lymphoid structures (TLS) found at the tumour site. TLS are composed predominantly of aggregates of B cells and T cells displaying various stages of organisation. Immature TLS present clearly visible foci of immune cells with segregated B and T cell zones, but lack follicular dendritic cells (FDCs) and germinal centres (GCs), with the latter being sites of active B cell proliferation and affinity maturation (6). In the intermediate maturation stage, B and T cell areas are enriched by FDCs but not GCs. Finally, mature TLS contain both FDCs and GCs (7). In general, mature TLS resemble well structure of SLO (8). Of note, TLS are also known to be formed and play role in other chronic inflammatory conditions, such as viral infections (9–11), autoimmune disorders (11–13) and after tissue transplantation (14, 15). Alongside B cells, other immune cells found in the TLS include dendritic cells [DCs (16–18)], CD4+ T follicular helper cells [Tfh (19)], CD4+ regulatory T cells [Tregs (20)], CD8+ cytotoxic T cells (21–23) and macrophages (16), as well as innate lymphoid cells (24). Importantly, TLS are also accompanied by lymphatic and blood vessels (including high endothelial venules), which aid in immune cell trafficking into the tumour (25). Therefore, TLS create the niche which provides opportunity for immune cell interaction in the inflammatory tumour environment.

THE PROGNOSTIC VALUE OF TLS IN CANCER

The prognostic potential of TLS structures was described for many tumours, including non-small cell lung cancer [NSCLC (26)], colorectal cancer (18, 27), breast (19, 28), pancreatic and gastric cancers (29, 30), melanoma (17) as well as ovarian (31) and oral cancer (32). The presence of TLS carries therefore a positive prognostic value in most solid tumours (33, 34). It is important to keep in mind that different studies used varying methods for TLS quantification, such as the presence of CD208+ DCs found exclusively in TLS (in lung cancer), presence of FDC markers CD21 and CD23 or co-localisation of CD3+ T cells and CD20+ B cells. TLS can be nowadays investigated by state-of the art digital and computational pathology utilizing methods incorporating deep-learning and artificial intelligence (35). Additionally, it is vital to consider other patient-related factors while assessing TLS presence, since co-morbidities (such as chronic inflammation) or treatments (e.g. with corticosteroids) impact TLS formation and maturation (7). Importantly, TLS presence was shown to be independent of tumour mutational burden (which influences immune response to tumours) in several tumour entities (4, 22).

B cells found in tumours display wide variety of phenotypes, ranging from naïve B cells, through actively proliferating GC B cells to memory B cells and terminally differentiated plasma cells. It is important to distinguish between investigations assessing the prognostic role of TLS or individual B cell subsets. For example, presence of memory B cells was associated with poorer survival prognosis in pan-cancer analysis of many solid tumours [including lung squamous cell carcinoma, colon and gastric cancers (36)], although these tumour entities show improved prognosis upon TLS assessment (7, 27). Additionally, in pancreatic cancer, high density of B cells was associated with improved survival prognosis but only if the cells were forming TLS (30). Therefore, it is important to characterise B cell organisation while assessing their prognostic potential. Of note, considering the presence of B cells and TLS often strengthens the prognostic potential of CD8 T cells (4, 37, 38). In ovarian cancer patients, CD8 intratumoral T cells only carried prognostic value in the presence of CD20+ B cells and plasma cells, with the latter population associated with the most robust responses (22).

In conclusion, presence of B cells and TLS is a strong prognostic factor for cancer patient survival on its own and in combination with CD8 T cells, which may suggest an active cooperation of these cell subsets in eliciting successful anti-tumour immune response.

B CELLS IN TUMOURS: HETEROGENEITY OF PHENOTYPES LEADS TO PLEIOTROPIC FUNCTION

The heterogeneity of B cell phenotypes has functional consequences, as B cell subsets display pleiotropic character. B cell functions fall into two broad categories, namely humoral and non-humoral responses. The humoral responses are consequences of GC reaction and extrafollicular plasma cell activity within TLS and have been extensively reviewed elsewhere (39). Meta-analysis showed positive association of plasma cell signature in most of solid tumours [except for the brain and large cell carcinoma (39)]. Antigen specificity of intratumoral B cells is an emerging topic of interest. Alongside B cells specific for tumour antigens [such as e.g. aberrantly glycosylated mucin 1 (40)], recent studies in patients with head and neck cancer infected with human papilloma virus (HPV) provided evidence of HPV-specific antibody production at the tumour site (41, 42). Whether B cells specific for tumour-derived antigen, self-peptides or viral proteins display different phenotypical and functional state remains to be established.

The non-humoral activities of B cells encompass functions which require direct cell to cell contact, such as antigen presentation (*via* MHC class II and class I molecules) and engagement of co-stimulatory molecules (such as CD40, CD80, CD86, ICOS-L, CD27 and 4-1BBL) or co-inhibitory receptors (including PD-L1 and PD-L2) to CD4 and CD8 T cells. Additionally, B cells secrete a wide range of cytokines, which have potential to influence multiple cell types, including T cells, NK cells and myeloid cells. This includes, again, cytokines with anti-tumoral effects [such as IL-6, IL-12, IL-13, TNF-α and IFN-γ (43)] as well as pro-tumoral character [such as IL-10, IL-35 and TGF-β (44)]. Regulatory B cell subsets (Bregs) which play a tumour-promoting role have also been identified in tumours (45, 46).

Summing up, intratumoral B cells are a multifaceted subset and even though they can display both pro- and anti-tumoral roles (43), there is overwhelming evidence of improved prognosis for cancer patients when B cells form TLS (34). A major challenge is to link B cell phenotypes to effector functions, so that precise therapies aiming at depleting or promoting certain populations can be developed. Additionally, B cell plasticity between different subsets and intra-subset heterogeneity are not fully understood. Whether function of individual cells changes over time depending on tumour stage, microenvironment, TLS formation or applied therapies (including immunotherapy) remains to be explored.

TLS ARE A PREDICTIVE FACTOR IN THE RESPONSE TO IMMUNOTHERAPY

Study of TLS in response to immunotherapy in sarcoma, melanoma and renal cell carcinoma patients showed strong associations between presence of TLS at the baseline and positive outcome of the ICB treatment (3–5). Whether TLS density increases in ICB-responding patients during the treatment is currently not clear. CD20 density (assessed by histology) was higher at the baseline for ICB responding patients and, crucially, was further increased after ICB therapy, while non-responding patients had low CD20 density before and after treatment (5). However, evaluation of TLS by histology did not show statistically significant increase in TLS density in ICB responders (compared to non-responders) although increased ratio of TLS to tumour was found for the former group (5). Studies with prospective validation with larger and more homogenous patient cohort will help to establish whether ICB therapy actively induces TLS formation, and if confirmed it will provide further strong evidence of active and beneficial role of TLS in immunotherapy.

Further evidence for positive role of TLS in immunotherapy comes from the analysis of sarcoma patients treated with anti-PD-1 blockade (3). Petitprez et al. divided sarcoma tumours into 5 different classes (based on the tumour microenvironment signature derived from RNA sequencing) and showed that tumours with high level of infiltration by immune cells (including B and T cell populations) carried strong prognostic value for improved patients' survival prior to the ICB treatment. Interestingly, when response to anti-PD-1 immunotherapy was analysed, tumours with high immune cell infiltration lost their predictive value, unless they contained TLS. This study argues that what matters in response to immunotherapy is not only the presence of immune cells, but also their organisation into TLS.

HUMORAL B CELL RESPONSES IN IMMUNOTHERAPY

It is currently not clear whether B cells play an active role in anti-tumour responses e.g. *via* antibody-mediated mechanisms. Increased BCR diversity and expansion of memory B cells within the tumour was associated with the response to ICB in melanoma patients (5). However, no differences in the populations of GC-like B cells and plasma cells were found between responders and non-responders to ICB (5). Another study showed, however, expansion of CD69+ B cells with transcriptional signature resembling GC B cells in ICB-responding melanoma patients (4). More evidence is therefore needed to understand the extent to which the humoral functions of B cells contribute to immunotherapy response.

CROSS TALK BETWEEN B CELLS AND CD8 T CELLS: AN EXCITING AND UNEXPLORED AVENUE

One of the important unanswered questions surrounding response to ICB is whether there is a direct cross-talk between main subsets forming TLS (B cells) and effector cells directly involved in eliminating tumour response (e.g. CD8 T cells or natural killer cells).

There are several arguments speaking for a strong possibility of CD8 and B cell communication. The colocalization of B cells and CD8 T cells within the TLS is well established by numerous studies assessing TLS presence in several tumour entities [(37, 38, 43), reviewed in (34)]. Secondly, there is some evidence that CD8 T cells can actively recruit B cells to the tumours. Cabrita et al. (4) divided metastatic melanoma tumours in three groups (based on their T and B cell content), namely tumours with no T cells or B cells, containing T cells only or with both T and B cells present. The fact that no tumour group with B cells only was identified may suggest that T cells appear early at the tumour site and subsequently facilitate B cell recruitment. This is corroborated by several studies which identity CD8 T cells as a source of CXCL13 (47–49), a potent B cell chemoattractant. It is therefore reasonable to speculate that T cells possibly take active part in B cell recruitment and TLS formation, although that hypothesis remains to be vigorously tested.

The potential advantages for CD8 T cells resulting from B cell recruitment are not fully understood. B cells exhibit a variety of functions, which can affect CD8 T cells directly or indirectly (**Figure 1**). Direct effects include antigen presentation, delivery of co-stimulatory or co-inhibitory receptors and cytokine secretion (38, 50), which can ultimately guide CD8 T cell activation, differentiation and effector function (as discussed above). An alternative explanation for TLS facilitating T cell-mediated ICB response is that it provides favourable niche for T cells to acquire their functional role, without direct role for B cell-mediated activation. As mentioned, other immune cell populations capable of antigen presentation are found within the TLS, such as mature CD208+ DCs (39, 51, 52). This mature DC subset was found to locate almost exclusively to TLS in lung cancer and is often used as a TLS marker (51). However, this phenomenon is limited to lung cancer and does not explain the supportive role of TLS in other tumour entities. Whether different antigen presenting cell populations support particular subsets of T cells, act at different stages of immune response to tumours or play interchangeable

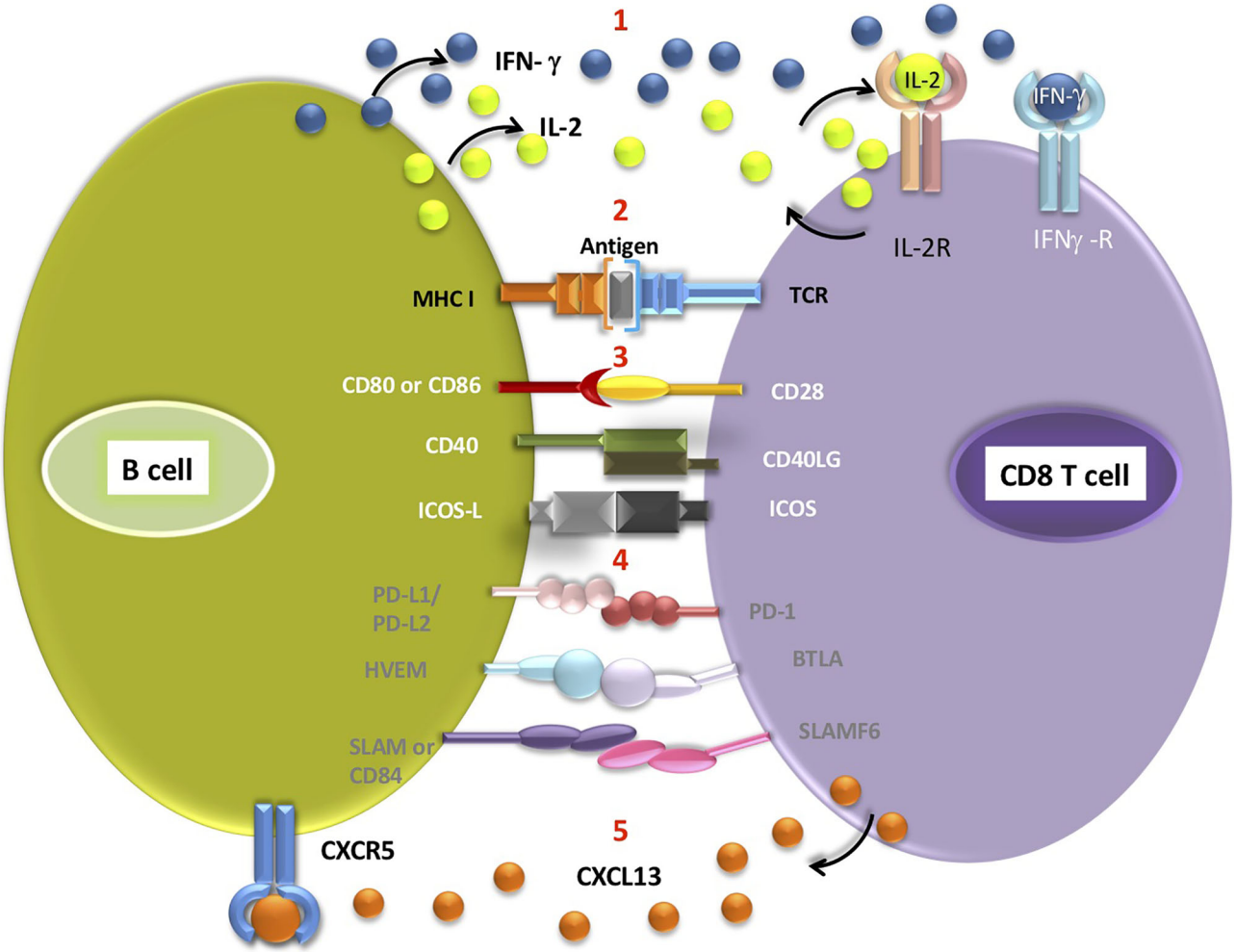

FIGURE 1 | Interactions potentially occurring between the B cell and CD8 T cells located in the TLS (1). B cells secrete cytokines such as IFN-γ and IL-2, which can then bind to appropriate receptors on CD8 T cells (2). Antigen presentation on MHC class I molecule expressed by B cell triggers signalling from TCR receptor on T cell. Engagement of receptors on B cells and corresponding T cell receptors delivers co-stimulatory (3, white font) or co-inhibitory (4, grey font) signals to T cells (5). CD8 T cells secrete CXCL13, a B-cell chemoattractant which binds to CXCR5 receptors on B cells. Antigen cross-presentation by intratumoral B cells requires further experimental validation.

roles, remains to be seen. Additionally, B cells may support CD8 T cells indirectly *via* CD40-CD40L interactions with CD4+ T follicular helper cells, which would then provide enhanced help to effector T cells (53).

Furthermore, TLS creates microenvironment with a unique cytokine milieu (34). Apart from abundance of transcripts encoding cytokines involved in TLS generation (such as CXCL13, CCL19 and CCL21 (34, 50) many cytokines and chemokines involved in improving anti-tumour function and trafficking of T cells and DCs [eg. CXCR1, CCL20, IL-12, IFN-γ (38, 39)] and affecting other immune cells [e.g. macrophage chemoattractants CCL3, CCL4, CCL5 and neutrophil chemoattractant IL-8 (50)] are also found within the TLS.

Careful analysis of CD3 T cells (with both CD4 and CD8 populations included) revealed that T cells isolated from tumours with TLS have different transcription signature from T cells isolated from tumours without TLS, and this also differs to T cells isolated from TLS themselves (4). T cells isolated from B cell-rich tumours expressed more mRNA for *Tcf7* and *Tcf1* (involved in maintenance of stem-like T cell population), *Il7r* and *Sell* (encoding CD62L) as well as lower levels of transcripts for granzyme-encoding genes and *Ptpn22* (54), a negative regulator of TCR signalling (4). Additionally, analysis of CD8 T cells positioned within the TLS revealed elevated expression of activation markers compared to CD8 T cells placed outside TLS (5). This strongly supports the fact that there are significant differences in the gene and protein expression profile of T cells based on their location with respect to TLS. Interestingly, tumour-reactive, exhausted CD8+ T cell subset was found to locate predominantly in the TLS in lung cancer patients (47). Whether all CD8 T cells found within TLS are specific for tumour antigens and actively primed within the TLS remains

an important and open question. Phenotypical, transcriptional and functional comparison of CD8 T cells positioned inside and outside TLS would reveal valuable insights about potential influence of TLS on cytotoxic effector T cells.

CONCLUSIONS AND FUTURE DIRECTIONS IN TLS INVESTIGATION

Investigations of intratumoral T cells have paved the way in immunotherapy and their exploitation brought great clinical benefit to cancer patients. Currently the field is dynamically broadened to include other immune cells types and alternative immunotherapy approaches, including DC vaccinations (55), adoptive T cell and NK cell transfers (56) and agents targeting myeloid cell populations (57). Whether immunotherapeutic strategies can be tailored to target B cells remains to be determined, and the exact design of such therapies will depend on which B cell subset and function can be harnessed for the optimal clinical benefit. For example, it would be interesting to establish whether adoptive B cell transfer can lead to TLS induction (and recapitulate its complex spatial arrangement) to evoke durable immune response in cancer patients.

Future research will surely make most of the cutting-edge technologies, already employed for T cell-focused investigations, to characterise B cells and TLS. Although RNA sequencing [including single cell sequencing (58)] is an extremally useful tool for unbiased characterisation of intratumoral B cells, it does not contain information on spatial positioning of the cell within the tumour. On the other hand, multiplex imaging technologies are getting advanced at great speed to enable visualisation of up to 50-60 markers from a single tissue slide (59, 60). This is a very useful approach for thorough analysis of TME, and especially immune compartment, with the limitations of its biased approach (as analysis is restricted to antibodies available for imaging). Spatial sequencing, with provides information on transcriptome composition together with tissue coordinate of each cell, is a perfect tool for TLS-based investigation. However, in this case transcriptome analysis is derived from a cluster of cells rather than a single cell [although resolution of this technology is increasing rapidly (61)], which can lead to difficulties in deciphering gene expression profiles from adjacent T and B cells. Therefore, combination of unbiased and targeted experimental approach (62, 63) is an exciting direction for deciphering role of TLS in cancer immunotherapy.

Our appreciation of TLS and their active role in immunotherapy is continuously growing, but the phenomenon is still far from being completely understood. It would be of great importance to the scientific community to address the question of ICB treatment on phenotype and function of B cell populations. Studies addressing functional connections to CD8 T cells in ICB would optimally guide the treatment strategies targeting selected aspects of TLS and B cell biology. Identification of mechanistic insights will provide an exciting and immediate avenue for translation of B cell-based immunotherapies into clinics, complementary to existing T cell-centric strategies.

AUTHOR CONTRIBUTIONS

MT and AZ wrote the manuscript. All authors contributed to the article and approved the submitted version.

FUNDING

MT is supported by University of Basel Research Grant and Cancer League Basel. AZ is supported by grants from the Swiss National Science Foundation (320030_188576/1; CRSII5_170929).

ACKNOWLEDGMENTS

We thank Dr. Marina Natoli for her advice on the manuscript.

REFERENCES

1. Tsou P, Katayama H, Ostrin EJ, Hanash SM. The Emerging Role of B Cells in Tumor Immunity. *Cancer Res* (2016) 76(19):5597–601. doi: 10.1158/0008-5472.CAN-16-0431
2. Fridman WH, Zitvogel L, Sautès-Fridman C, Kroemer G. The Immune Contexture in Cancer Prognosis and Treatment. *Nat Rev Clin Oncol* (2017) 14(12):717–34. doi: 10.1038/nrclinonc.2017.101
3. Petitprez F, de Reyniès A, Keung EZ, Chen TW-W, Sun C-M, Calderaro J, et al. B Cells are Associated With Survival and Immunotherapy Response in Sarcoma. *Nature* (2020) 577(7791):556–60. doi: 10.1038/s41586-019-1906-8
4. Cabrita R, Lauss M, Sanna A, Donia M, Larsen MS, Mitra S, et al. Tertiary Lymphoid Structures Improve Immunotherapy and Survival in Melanoma. *Nature* (2020) 577(7791):561–5. doi: 10.1038/s41586-019-1914-8
5. Helmink BA, Reddy SM, Gao J, Zhang S, Basar R, Thakur R, et al. B Cells and Tertiary Lymphoid Structures Promote Immunotherapy Response. *Nature* (2020) 577(7791):549–55. doi: 10.1038/s41586-019-1922-8
6. De Silva NS, Klein U. Dynamics of B Cells in Germinal Centres. *Nat Rev Immunol* (2015) 15(3):137–48. doi: 10.1038/nri3804
7. Siliņa K, Soltermann A, Attar FM, Casanova R, Uckeley ZM, Thut H, et al. Germinal Centers Determine the Prognostic Relevance of Tertiary Lymphoid Structures and Are Impaired by Corticosteroids in Lung Squamous Cell Carcinoma. *Cancer Res* (2018) 78(5):1308–20. doi: 10.1158/0008-5472.CAN-17-1987
8. Germain C, Gnjatic S, Dieu-Nosjean MC. Tertiary Lymphoid Structure-Associated B Cells are Key Players in Anti-Tumor Immunity. *Front Immunol* (2015) 6:67. doi: 10.3389/fimmu.2015.00067
9. Moyron-Quiroz JE, Rangel-Moreno J, Kusser K, Hartson L, Sprague F, Goodrich S, et al. Role of Inducible Bronchus Associated Lymphoid Tissue (iBALT) in Respiratory Immunity. *Nat Med* (2004) 10(9):927–34. doi: 10.1038/nm1091
10. Foo SY, Phipps S. Regulation of Inducible BALT Formation and Contribution to Immunity and Pathology. *Mucosal Immunol* (2010) 3(6):537–44. doi: 10.1038/mi.2010.52
11. Neyt K, Perros F, GeurtsvanKessel CH, Hammad H, Lambrecht BN. Tertiary Lymphoid Organs in Infection and Autoimmunity. *Trends Immunol* (2012) 33(6):297–305. doi: 10.1016/j.it.2012.04.006
12. Pitzalis C, Jones GW, Bombardieri M, Jones SA. Ectopic Lymphoid-Like Structures in Infection, Cancer and Autoimmunity. *Nat Rev Immunol* (2014) 14(7):447–62. doi: 10.1038/nri3700
13. Pipi E, Nayar S, Gardner DH, Colafrancesco S, Smith C, Barone F. Tertiary Lymphoid Structures: Autoimmunity Goes Local. *Front Immunol* (2018) 9:1952. doi: 10.3389/fimmu.2018.01952

14. Koenig A, Thaunat O. Lymphoid Neogenesis and Tertiary Lymphoid Organs in Transplanted Organs. *Front Immunol* (2016) 7:646. doi: 10.3389/fimmu.2016.00646
15. Corsiero E, Delvecchio FR, Bombardieri M, Pitzalis C. B Cells in the Formation of Tertiary Lymphoid Organs in Autoimmunity, Transplantation and Tumorigenesis. *Curr Opin Immunol* (2019) 57:46–52. doi: 10.1016/j.coi.2019.01.004
16. Dieu-Nosjean MC, Antoine M, Danel C, Heudes D, Wislez M, Poulot V, et al. Long-Term Survival for Patients With non-Small-Cell Lung Cancer With Intratumoral Lymphoid Structures. *J Clin Oncol* (2008) 26(27):4410–7. doi: 10.1200/JCO.2007.15.0284
17. Ladányi A, Kiss J, Somlai B, Gilde K, Fejős Z, Mohos A, et al. Density of DC-LAMP(+) Mature Dendritic Cells in Combination With Activated T Lymphocytes Infiltrating Primary Cutaneous Melanoma is a Strong Independent Prognostic Factor. *Cancer Immunol Immunother* (2007) 56 (9):1459–69. doi: 10.1007/s00262-007-0286-3
18. McMullen TP, Lai R, Dabbagh L, Wallace TM, de Gara CJ. Survival in Rectal Cancer is Predicted by T Cell Infiltration of Tumour-Associated Lymphoid Nodules. *Clin Exp Immunol* (2010) 161(1):81–8. doi: 10.1111/j.1365-2249.2010.04147.x
19. Gu-Trantien C, Loi S, Garaud S, Equeter C, Libin M, de Wind A, et al. $CD4^+$ Follicular Helper T Cell Infiltration Predicts Breast Cancer Survival. *J Clin Invest* (2013) 123(7):2873–92. doi: 10.1172/JCI67428
20. Gobert M, Treilleux I, Bendriss-Vermare N, Bachelot T, Goddard-Leon S, Arfi V, et al. Regulatory T Cells Recruited Through CCL22/CCR4 are Selectively Activated in Lymphoid Infiltrates Surrounding Primary Breast Tumors and Lead to an Adverse Clinical Outcome. *Cancer Res* (2009) 69(5):2000–9. doi: 10.1158/0008-5472.CAN-08-2360
21. Goc J, Germain C, Vo-Bourgais TK, Lupo A, Klein C, Knockaert S, et al. Dendritic Cells in Tumor-Associated Tertiary Lymphoid Structures Signal a Th1 Cytotoxic Immune Contexture and License the Positive Prognostic Value of Infiltrating CD8+ T Cells. *Cancer Res* (2014) 74(3):705–15. doi: 10.1158/0008-5472.CAN-13-1342
22. Kroeger DR, Milne K, Nelson BH. Tumor-Infiltrating Plasma Cells Are Associated With Tertiary Lymphoid Structures, Cytolytic T-Cell Responses, and Superior Prognosis in Ovarian Cancer. *Clin Cancer Res* (2016) 22 (12):3005–15. doi: 10.1158/1078-0432.CCR-15-2762
23. Hennequin A, Derangère V, Boidot R, Apetoh L, Vincent J, Orry D, et al. Tumor Infiltration by Tbet+ Effector T Cells and CD20+ B Cells is Associated With Survival in Gastric Cancer Patients. *Oncoimmunology* (2015) 5(2): e1054598. doi: 10.1080/2162402X.2015.1054598
24. Ikeda A, Ogino T, Kayama H, Okuzaki D, Nishimura J, Fujino S, et al. Human NKp44+ Group 3 Innate Lymphoid Cells Associate With Tumor-Associated Tertiary Lymphoid Structures in Colorectal Cancer. *Cancer Immunol Res* (2020) 8(6):724–31. doi: 10.1158/2326-6066.CIR-19-0775
25. Ruddle NH. High Endothelial Venules and Lymphatic Vessels in Tertiary Lymphoid Organs: Characteristics, Functions, and Regulation. *Front Immunol* (2016) 7:491. doi: 10.3389/fimmu.2016.00491
26. Germain C, Gnjatic S, Tamzalit F, Knockaert S, Remark R, Goc J, et al. Presence of B Cells in Tertiary Lymphoid Structures is Associated With a Protective Immunity in Patients With Lung Cancer. *Am J Respir Crit Care Med* (2014) 189(7):832–44. doi: 10.1164/rccm.201309-1611OC
27. Di Caro G, Bergomas F, Grizzi F, Doni A, Bianchi P, Malesci A, et al. Occurrence of Tertiary Lymphoid Tissue is Associated With T-cell Infiltration and Predicts Better Prognosis in Early-Stage Colorectal Cancers. *Clin Cancer Res* (2014) 20(8):2147–58. doi: 10.1158/1078-0432.CCR-13-2590
28. Martinet L, Garrido I, Filleron T, Le Guellec S, Bellard E, Fournie J-J, et al. Human Solid Tumors Contain High Endothelial Venules: Association With T- and B-lymphocyte Infiltration and Favorable Prognosis in Breast Cancer. *Cancer Res* (2011) 71(17):5678–87. doi: 10.1158/0008-5472.CAN-11-0431
29. Hiraoka N, Ino Y, Yamazaki-Itoh R, Kanai Y, Kosuge T, Shimada K. Intratumoral Tertiary Lymphoid Organ is a Favourable Prognosticator in Patients With Pancreatic Cancer. *Br J Cancer* (2015) 112(11):1782–90. doi: 10.1038/bjc.2015.145
30. Castino GF, Cortese N, Capretti G, Serio S, Di Caro G, Mineri R, et al. Spatial Distribution of B Cells Predicts Prognosis in Human Pancreatic Adenocarcinoma. *Oncoimmunology* (2015) 5(4):e1085147. doi: 10.1080/2162402X.2015.1085147
31. Milne K, Köbel M, Kalloger SE, Barnes RO, Gao D, Gilks CB, et al. Systematic Analysis of Immune Infiltrates in High-Grade Serous Ovarian Cancer Reveals CD20, FoxP3 and TIA-1 as Positive Prognostic Factors. *PloS One* (2009) 4(7): e6412. doi: 10.1371/journal.pone.0006412
32. Wirsing AM, Ervik IK, Seppola M, Uhlin-Hansen L, Steigen SE, Hadler-Olsen E. Presence of High-Endothelial Venules Correlates With a Favorable Immune Microenvironment in Oral Squamous Cell Carcinoma. *Mod Pathol* (2018) 31(6):910–22. doi: 10.1038/s41379-018-0019-5
33. Sautès-Fridman C, Lawand M, Giraldo NA, Kaplon H, Germain C, Fridman WH, et al. Tertiary Lymphoid Structures in Cancers: Prognostic Value, Regulation, and Manipulation for Therapeutic Intervention. *Front Immunol* (2016) 7:407. doi: 10.3389/fimmu.2016.00407
34. Sautès-Fridman C, Petitprez F, Calderaro J, Fridman WH. Tertiary Lymphoid Structures in the Era of Cancer Immunotherapy. *Nat Rev Cancer* (2019) 19 (6):307–25. doi: 10.1038/s41568-019-0144-6
35. Cui M, Zhang DY. Artificial Intelligence and Computational Pathology. *Lab Invest* (2021) 101(4):412–22. doi: 10.1038/s41374-020-00514-0
36. Gentles AJ, Newman AM, Liu CL, Bratman SV, Feng W, Kim D, et al. The Prognostic Landscape of Genes and Infiltrating Immune Cells Across Human Cancers. *Nat Med* (2015) 21(8):938–45. doi: 10.1038/nm.3909
37. Ladányi A, Kiss J, Mohos A, Somlai B, Liszkay G, Gilde K, et al. Prognostic Impact of B-cell Density in Cutaneous Melanoma. *Cancer Immunol Immunother* (2011) 60(12):1729–38. doi: 10.1007/s00262-011-1071-x
38. Shi JY, Gao Q, Wang ZC, Zhou J, Wang X-Y, Min Z-H, et al. Margin-Infiltrating CD20(+) B Cells Display an Atypical Memory Phenotype and Correlate With Favorable Prognosis in Hepatocellular Carcinoma. *Clin Cancer Res* (2013) 19(21):5994–6005. doi: 10.1158/1078-0432.CCR-12-3497
39. Sharonov GV, Serebrovskaya EO, Yuzhakova DV, Britanova OV, Chudakov DM. B Cells, Plasma Cells and Antibody Repertoires in the Tumour Microenvironment. *Nat Rev Immunol* (2020) 20(5):294–307. doi: 10.1038/s41577-019-0257-x
40. Brockhausen I, Yang JM, Burchell J, Whitehouse C, Taylor-Papadimitriou J. Mechanisms Underlying Aberrant Glycosylation of MUC1 Mucin in Breast Cancer Cells. *Eur J Biochem* (1995) 233(2):607–17. doi: 10.1111/j.1432-1033.1995.607_2.x
41. Wieland A, Patel MR, Cardenas MA, Eberhardt CS, Hudson WH, Obeng RC, et al. Defining HPV-Specific B Cell Responses in Patients With Head and Neck Cancer. *Nature* (2020). doi: 10.1038/s41586-020-2931-3
42. Cillo AR, Kürten CHL, Tabib T, Qi Z, Onkar S, Wang T, et al. Immune Landscape of Viral- and Carcinogen-Driven Head and Neck Cancer. *Immunity* (2020) 52(1):183–99.e9. doi: 10.1016/j.immuni.2019.11.014
43. Guo FF, Cui JW. The Role of Tumor-Infiltrating B Cells in Tumor Immunity. *J Oncol* (2019) 2019:2592419. doi: 10.1155/2019/2592419
44. Shang J, Zha H, Sun Y. Phenotypes, Functions, and Clinical Relevance of Regulatory B Cells in Cancer. *Front Immunol* (2020) 11:582657. doi: 10.3389/fimmu.2020.582657
45. Murakami Y, Saito H, Shimizu S, Kono Y, Shishido Y, Miyatani K, et al. Increased Regulatory B Cells are Involved in Immune Evasion in Patients With Gastric Cancer. *Sci Rep* (2019) 9(1):13083. doi: 10.1038/s41598-019-49581-4
46. Horii M, Matsushita T. Regulatory B Cells and T Cell Regulation in Cancer. *J Mol Biol* (2021) 433(1):166685. doi: 10.1016/j.jmb.2020.10.019
47. Thommen DS, Koelzer VH, Herzig P, Roller A, Trefny M, Dimeloe S, et al. A Transcriptionally and Functionally Distinct PD-1+ CD8+ T Cell Pool With Predictive Potential in Non-Small-Cell Lung Cancer Treated With PD-1 Blockade. *Nat Med* (2018) 24(7):994–1004. doi: 10.1038/s41591-018-0057-z
48. Workel HH, Lubbers JM, Arnold R, Prins TM, van der Vlies P, de Lange K, et al. A Transcriptionally Distinct CXCL13+CD103+CD8+ T-cell Population Is Associated with B-cell Recruitment and Neoantigen Load in Human Cancer. *Cancer Immunol Res* (2019) 7(5):784–96. doi: 10.1158/2326-6066.CIR-18-0517
49. Li H, van der Leun AM, Yofe I, Cell YL. Dysfunctional CD8 T Cells Form a Proliferative, Dynamically Regulated Compartment within Human Melanoma. *Cell* (2019) 176(4):775–89.e18. doi: 10.1016/j.cell.2020.04.017
50. Griss J, Bauer W, Wagner C, Simon M, Chen M, Grabmeier-Pfistershammer K, et al. B Cells Sustain Inflammation and Predict Response to Immune Checkpoint Blockade in Human Melanoma. *Nat Commun* (2019) 10(1):4186. doi: 10.1038/s41467-019-12160-2
51. Dieu-Nosjean MC, Goc J, Giraldo NA, Sautès-Fridman C, Fridman WH. Tertiary Lymphoid Structures in Cancer and Beyond. *Trends Immunol* (2014) 35(11):571–80. doi: 10.1016/j.it.2014.09.006

52. Hughes CE, Benson RA, Bedaj M, Maffia P. Antigen-Presenting Cells and Antigen Presentation in Tertiary Lymphoid Organs. *Front Immunol* (2016) 7:481. doi: 10.3389/fimmu.2016.00481
53. Sautès-Fridman C, Verneau J, Sun CM, Moreira M, Chen TW-W, Meylan M, et al. Tertiary Lymphoid Structures and B Cells: Clinical Impact and Therapeutic Modulation in Cancer. *Semin Immunol* (2020) 48:101406. doi: 10.1016/j.smim.2020.101406
54. Brownlie RJ, Zamoyska R, Salmond RJ. Regulation of Autoimmune and Anti-Tumour T-cell Responses by PTPN22. *Immunology* (2018) 154(3):377–82. doi: 10.1111/imm.12919
55. Perez CR, De Palma M. Engineering Dendritic Cell Vaccines to Improve Cancer Immunotherapy. *Nat Commun* (2019) 10(1):5408. doi: 10.1038/s41467-019-13368-y
56. Myers JA, Miller JS. Exploring the NK Cell Platform for Cancer Immunotherapy. *Nat Rev Clin Oncol* (2021) 18(2):85–100. doi: 10.1038/s41571-020-0426-7
57. Engblom C, Pfirschke C, Pittet MJ. The Role of Myeloid Cells in Cancer Therapies. *Nat Rev Cancer* (2016) 16(7):447–62. doi: 10.1038/nrc.2016.54
58. Hwang B, Lee JH, Bang D. Single-Cell RNA Sequencing Technologies and Bioinformatics Pipelines. *Exp Mol Med* (2018) 50(8):1–14. doi: 10.1038/s12276-018-0071-8
59. Goltsev Y, Samusik N, Kennedy-Darling J, Bhate S, Hale M, Vasquez G, et al. Deep Profiling of Mouse Splenic Architecture With CODEX Multiplexed Imaging. *Cell* (2018) 174(4):968–81.e15. doi: 10.1016/j.cell.2018.07.010
60. Giesen C, Wang HA, Schapiro D, Zivanovic N, Jacobs A, Hattendorf B, et al. Highly Multiplexed Imaging of Tumor Tissues With Subcellular Resolution by Mass Cytometry. *Nat Methods* (2014) 11(4):417–22. doi: 10.1038/nmeth.2869
61. Eng CL, Lawson M, Zhu Q, Dries R, Koulena N, Takei Y, et al. Transcriptome-Scale Super-Resolved Imaging in Tissues by RNA Seqfish. *Nature* (2019) 568 (7751):235–9. doi: 10.1038/s41586-019-1049-y
62. Moncada R, Barkley D, Wagner F, Chiodin M, Devlin JC, Baron M, et al. Integrating Microarray-Based Spatial Transcriptomics and Single-Cell RNA-seq Reveals Tissue Architecture in Pancreatic Ductal Adenocarcinomas. *Nat Biotechnol* (2020) 38(3):333–42. doi: 10.1038/s41587-019-0392-8
63. Andersson A, Bergenstråhle J, Asp M, Bergenstråhle L, Jurek A, Navarro JF, et al. Single-Cell and Spatial Transcriptomics Enables Probabilistic Inference of Cell Type Topography. *Commun Biol* (2020) 3(1):565. doi: 10.1038/s42003-020-01247-y

Conflict of Interest: The authors declare that the research was conducted in the absence of any commercial or financial relationships that could be construed as a potential conflict of interest.

Copyright © 2021 Trüb and Zippelius. This is an open-access article distributed under the terms of the Creative Commons Attribution License (CC BY). The use, distribution or reproduction in other forums is permitted, provided the original author(s) and the copyright owner(s) are credited and that the original publication in this journal is cited, in accordance with accepted academic practice. No use, distribution or reproduction is permitted which does not comply with these terms.

frontiers in Immunology

MINI REVIEW
published: 13 May 2021
doi: 10.3389/fimmu.2021.690105

STINGing the Tumor Microenvironment to Promote Therapeutic Tertiary Lymphoid Structure Development

Jessica N. Filderman[1†], Mark Appleman[2†], Manoj Chelvanambi[1], Jennifer L. Taylor[2] and Walter J. Storkus[1,2,3,4]*

[1] Department of Immunology, University of Pittsburgh School of Medicine, Pittsburgh, PA, United States, [2] Department of Dermatology, University of Pittsburgh School of Medicine, Pittsburgh, PA, United States, [3] Department of Pathology, University of Pittsburgh School of Medicine, Pittsburgh, PA, United States, [4] Department of Bioengineering, University of Pittsburgh School of Medicine, Pittsburgh, PA, United States

OPEN ACCESS

Edited by:
Catherine Sautes-Fridman, U1138 Centre de Recherche des Cordeliers (INSERM), France

Reviewed by:
Itziar Otano, Research Institute Hospital 12 de Octubre, Spain
Eduardo Huarte, PTC Therapeutics, United States
Awen Gallimore, Cardiff University, United Kingdom

***Correspondence:**
Walter J. Storkus
storkuswj@upmc.edu

[†]These authors have contributed equally to this work and share first authorship

Specialty section:
This article was submitted to Cancer Immunity and Immunotherapy, a section of the journal Frontiers in Immunology

Received: 02 April 2021
Accepted: 30 April 2021
Published: 13 May 2021

Citation:
Filderman JN, Appleman M, Chelvanambi M, Taylor JL and Storkus WJ (2021) STINGing the Tumor Microenvironment to Promote Therapeutic Tertiary Lymphoid Structure Development. Front. Immunol. 12:690105. doi: 10.3389/fimmu.2021.690105

Tertiary lymphoid structures (TLS), also known as ectopic lymphoid structures (ELS) or tertiary lymphoid organs (TLO), represent a unique subset of lymphoid tissues noted for their architectural similarity to lymph nodes, but which conditionally form in peripheral tissues in a milieu of sustained inflammation. TLS serve as regional sites for induction and expansion of the host B and T cell repertoires *via* an operational paradigm involving mature dendritic cells (DC) and specialized endothelial cells (i.e. high endothelial venules; HEV) in a process directed by TLS-associated cytokines and chemokines. Recent clinical correlations have been reported for the presence of TLS within tumor biopsies with overall patient survival and responsiveness to interventional immunotherapy. Hence, therapeutic strategies to conditionally reinforce TLS formation within the tumor microenvironment (TME) *via* the targeting of DC, vascular endothelial cells (VEC) and local cytokine/chemokine profiles are actively being developed and tested in translational tumor models and early phase clinical trials. In this regard, a subset of agents that promote tumor vascular normalization (VN) have been observed to coordinately support the development of a pro-inflammatory TME, maturation of DC and VEC, local production of TLS-inducing cytokines and chemokines, and therapeutic TLS formation. This mini-review will focus on STING agonists, which were originally developed as anti-angiogenic agents, but which have recently been shown to be effective in promoting VN and TLS formation within the therapeutic TME. Future application of these drugs in combination immunotherapy approaches for greater therapeutic efficacy is further discussed.

Keywords: dendritic cells, immunotherapy, STING agonists, tertiary lymphoid structures, T cells, tumor, vaccine, vascular normalization

CHRONIC INFLAMMATION AND TLS ORGANOGENESIS: GENERAL OVERVIEW AND CANCER INDICATIONS

TLS are non-encapsulated aggregates of lymphoid cells that form at sites of sustained inflammation, including tissues impacted by autoimmune disease, chronic infection, and cancer (1, 2). Recent findings suggest that the presence of TLS within tumor lesions positively correlates with favorable prognosis in most forms of solid cancer (1–4). TLS are associated with specialized vascular structures (i.e. HEV) that differentiate from $CD31^+$ VEC or endothelial progenitor cells under pro-inflammatory, pro-angiogenic conditions (5–7). HEV express the cell surface marker peripheral node addressin (PNAd, a binding partner for CD62L expressed on lymphocytes) and produce chemokines (CCL19, CCL21, CXCL13), which facilitate the recruitment of naïve/central memory $CD62L^+CCR7^+$ T cells, naïve $CD62L^+CXCR5^+$ B cells, $CXCR5^+$ T follicular helper (Tfh) cells and mature $CCR7^+$ DC into the TME (1). In this context, it is believed that TLS serve as local sites for the *de novo (*cross) priming, expansion, and differentiation of tumor-specific T and B cells, leading to more efficient/effective anti-tumor responses within sites of active disease (2, 8–13). TLS also appear to define an operational site in which the T cell and B cell repertoires may expand their specificity against a broadened range of tumor antigenic targets, *via* the paradigms of epitope spreading or determinant spreading (14). Notably, TLS exhibit heterogeneity in their cellular composition and in the organization of their integrated cell subsets, which is believed to be reflective of their maturational status (2, 15). Classical (mature) TLS are characterized by the presence of i.) $PNAd^+$ HEV surrounded by ii.) aggregates of T cells and mature DCs and iii.) distinct B cell zones containing naïve B cells around germinal center (GC)-like structures (1–3, 16, 17). Non-classical (immature) TLS contain some but not all of these three characteristics (i.e. typically lacking B cells/GC) (16). Strikingly, the presence of either classical TLS or non-classical TLS in TME portends superior prognoses in cancer patients (1–3, 10, 16–27).

TLS HOMEOSTATIC CYTOKINES/ CHEMOKINES ARE MODULATED BY AGENTS THAT PROMOTE VASCULAR NORMALIZATION (VN) IN TUMORS

An important component of TLS formation in peripheral tissues is sustained local production of homeostatic chemokines that recruit immune cells into affected tissue sites and serve as cues for establishing organized interactions between infiltrating lymphocytes and antigen presenting cells (APC). This topic has been well-described in other publications (28, 29) and elsewhere in the current volume and is therefore only briefly discussed below.

One key homeostatic chemokine associated with TLS development is CXCL13 (also known as B lymphocyte chemoattractant [BLC] or B cell-attracting chemokine 1 [BCA-1]), the ligand for CXCR5 (28). The production of CXCL13 by tumor-associated fibroblasts, Tfh cells, follicular dendritic cells (FDC) and HEV is positively-correlated with the formation of GC that contain $CXCR5^+$ B cells (29, 30). While not yet investigated in the tumor setting, forced expression of CXCL13 in normal pancreatic β cells leads to the formation of TLS containing HEV, B cells and T cells *via* a process dependent on the initial infiltration of B cells into tissue and the activation of the lymphotoxin (LT)αβ-LTβR signaling cascade (31). Two additional major TLS-associated homeostatic chemokines produced by mature DC and HEV are CCL19 and CCL21, both of which serve as ligands for CCR7 (28). In normal mouse pancreatic tissue, ectopic overexpression of CCL19 or CCL21 induces the formation of TLS containing $CD4^+$ T cells, $CD11c^+$ DCs, and $B220^+$ B cells surrounding HEV *via* a process dependent on CCL19/21-induced expression of $LT\alpha_1\beta_2$ complexes on $CD4^+$ T cells (32). Although TLS were not formally evaluated in their endpoint analyses, several studies have shown that treatment of murine tumors by injection with recombinant CCL19, viruses encoding CCL19 or CCL21, or DC engineered to express CCL21 results in robust tumor infiltration by T cells and DC in association with slowed tumor growth and extended overall survival (33–36).

In addition to these chemokines, tumor necrosis factor (TNF), interferon (IFN) and interleukin (IL)-1 superfamily cytokines also play major roles in TLS neogenesis. Lymphotoxins (LTα/TNFSF1 and LTβ/TNFSF3) and LIGHT/ TNFSF14 produced by immune cells play canonical roles in the formation of TLS (29, 37). Lymphotoxins form bioactive heterotrimers ($LT\alpha_3$, $LT\alpha_1\beta_2$, $LT\alpha_2\beta_1$) that bind to LTβR/ TNFRSF3, with $LT\alpha_3$ also binding and mediating signals through the TNFR1/TNFRSF1A, TNFR2/TNFSF1B and herpesvirus entry mediator (HVEM)/TNFRSF14 receptors (38). LIGHT also binds to HVEM/TNFRSF14 (39). TNF receptors represent important signaling receptors for endothelial cell function and proliferation and they facilitate TLS neogenesis. TNFR1/2 expression on endothelial cells has been shown to be necessary for HEV formation and T cell infiltration into murine melanoma (40). Mice lacking TNFR1/2 on the endothelium or LTα on $CD8^+$ T cells have significantly decreased PNAd expression, demonstrating that $LT\alpha_3$ engagement of TNFR1 induces PNAd expression on the tumor vascular endothelium (40). In kidney and pancreatic tissues, the forced overexpression of LTα promotes lymphoid aggregate formation (containing T cells, B cells, and APCs) and tumor vascular reprograming, as indicated by increased expression of VCAM-1, ICAM-1, MAdCAM, and PNAd on VEC/HEV (41). Additionally, combined overexpression of LTα and LTβ further enhances infiltration of naïve lymphocytes and expression of homeostatic chemokines when compared to LTα overexpression alone, suggesting the synergistic action of these cytokines in TLS formation (42). In line with such findings, B16.F10 melanoma-bearing mice treated with a tumor-targeted GD2 scFv-LTα fusion protein demonstrate increased densities of intratumoral HEV and develop a diverse T cell repertoire in association with

TLS neogenesis (43). Remarkably, recent reports in murine transplantable and carcinogen-induced tumor models support the operational dominance of TNFR- over LTβR-mediated signaling for HEV/TLS neogenesis in the TME (40, 44), findings which contrast with the canonical importance of LTβR-mediated signaling for HEV/TLS formation in normal tissues and in ontogenic secondary lymphoid organogenesis (1, 29, 30, 40, 44). Beyond lymphotoxins, LIGHT activation of VEC has also been shown to play a role in TLS formation in cancer models. C57BL/6 mice bearing intracranial NSCG glioblastomas treated with a fusion protein encoding LIGHT and a vascular targeting peptide (LIGHT-VTP) displayed VN and induction of classical TLS within the TME (45). In murine fibrosarcoma models, forced expression of LIGHT prompted naïve T cell infiltration and local production of homeostatic chemokines, leading to tumor rejection in the therapy setting (8, 46).

Type I IFNs have also been reported to drive TLS formation in normal tissues (47, 48). In murine models, a subset of PDGFRα$^+$ lung fibroblasts produce CXCL13 in response to infection with influenza virus or intranasal administration of IFNβ (48). IFN-I receptor (IFNAR) activation in these cells results in increased recruitment of CXCR5$^+$ B cells and ectopic germinal center formation in the lungs, which in turn promotes the development of a broadly neutralizing repertoire of antiviral antibodies conferring cross-strain protection (48). In a hydrocarbon (TMPD)-induced model of autoimmune SLE, mice with intact IFN-I signaling had worse clinical scores and increased lupus-specific autoantibody production compared to IFNAR-deficient mice (49). It was shown that IFN-I produced by activated DCs in this model was associated with the formation of classical TLS containing B cells, CD4$^+$ T cells, and DC along with coordinate expression of TLS homeostatic chemokines (CCL19, CCL21, CXCL13) and their receptors (CCR7, CXCR5) (50). Sustained IFN-I/IFNAR signaling in tissues has similarly been shown to promote TLS formation in additional studies *via* local production of pro-inflammatory CXCR3 ligand chemokines (CXCL10/11) and lymphotoxins (51, 52).

Furthermore, gene therapy delivering IL-1 family member IL-F9/IL-36γ induces HEV and TLS formation in mouse colon carcinomas in association with the development of superior T cell-mediated anti-tumor immunity and tumor growth suppression (11). Notably, the activation of IL-36R on immune and stromal cell populations has been shown to upregulate local production of pro-inflammatory, pro-TLS factors including CXCL10, LTα and IFNs (53). In humans, IL-36γ is expressed by the tumor vasculature in colorectal cancers and has been correlated with an increased density of CD20$^+$ B cells localized in TLS in these tumors (54).

STING SIGNALING ENFORCES A PRO-INFLAMMATORY, PRO-TLS TME

STING (STimulator of INterferon Genes) is a cytosolic DNA sensing protein that is activated upon binding to cGAMP, a catalyzed dsDNA product of cytosolic GMP/AMP synthase (cGAS) (55). Activation of STING leads to secondary activation of transcription factor IRF3 by facilitating IRF3 interaction with Tank Binding Kinase 1 (TBK1), phosphorylation of IRF3 (pIRF3), pIRF3 dimerization and translocation into the nucleus where it transactivates IFNβ and other pro-inflammatory genes (55).

As a consequence of defects in the expression/functionality of DNA repair proteins, tumors are commonly characterized by genetic instability (56, 57) and contain high concentrations of cytoplasmic DNA leading to intrinsic cGAS/STING activation and secretion of proinflammatory mediators (58–60). Progressively growing tumors have been reported to develop defects in the STING signaling pathway to avoid STING-induced apoptosis and immune surveillance (60–62). Nevertheless, dying tumor cells still release dsDNA (and/or 2'3' cGAMP, its cGAS catalyzed product) into the TME, which may result in the activation of STING$^+$ cells in the tumor stroma, including DC and VEC (63–65). This intrinsic inflammatory process may be therapeutically enhanced by local or systemic delivery of synthetic STING agonists (66, 67).

Activation of STING in tumor-associated VEC leads to VN (67, 68) characterized by increased vascular perfusion and upregulated expression of E-selectin/CD62E, VCAM-1 and ICAM-1 which facilitates circulating immune cell adhesion to the endothelium and consequent recruitment of tumor-infiltrating lymphocytes into the TME (63, 67, 68). This operating paradigm may underlie observations of cancers with reduced DNA repair proficiency and high comparative mutational burden presenting with brisk proinflammatory immune cell infiltrates (i.e. "hot tumors") that are more prone to develop TLS (69, 70) and to be more responsive to interventional immunotherapy (71, 72). Notably, provision of low doses of STING agonists cGAMP and ADU-S100 (aka ML-RR-S2-CDA, MIW815) coordinately promote VN and CD8$^+$ T cell-dependent control of tumor growth in murine models of breast carcinoma, lung carcinoma and melanoma (67, 68, 73). Yang et al. (68) further confirmed the importance of STING agonist-induced Type-I IFN produced by tumor VEC with the therapeutic benefits associated with this treatment approach. Most recently (**Figure 1**), Chelvanambi et al. has demonstrated that VN induced by intratumoral administration of low doses of the STING agonist ADU-S100 results in sustained inflammation within the TME of B16 melanomas and local production of homeostatic cytokines/chemokines (LTα, LTβ, LIGHT, CCL19 and CCL21, but remarkably not CXCL13) and pro-inflammatory/pro-TLS mediators (CXCL10, IL-36β, IFNβ) (67). These therapy-associated changes were associated with coordinate neogenesis of non-classical TLS and the development of a unique tumor-infiltrating T cell receptor (TCR) repertoire in the TLS$^+$ TME that was not detectable in the peripheral immune cell compartment (67). Parallel studies using STING-KO mice confirmed the strict requirement for STING expression in host but not tumor cells for therapeutic response to intratumoral administration of ADU-S100, including TLS formation and slowed tumor growth (67).

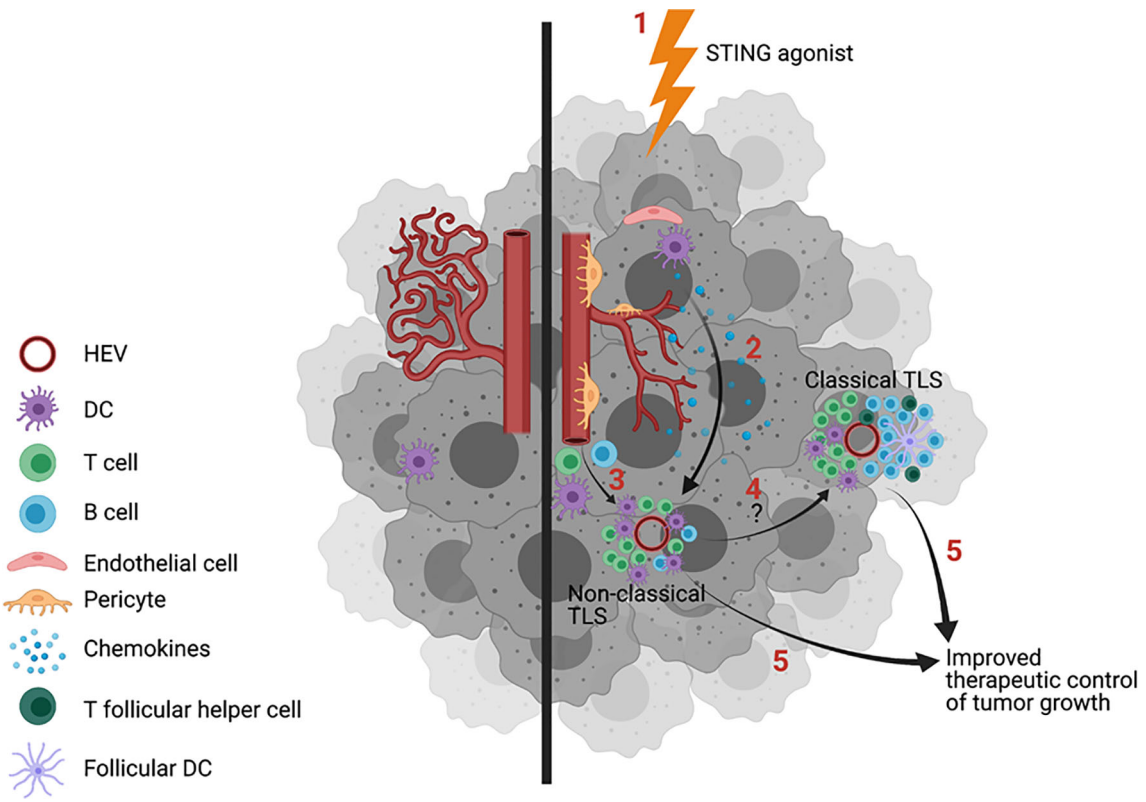

FIGURE 1 | Treatment of tumors with STING agonists induces vascular normalization (VN), increased inflammatory immune cell infiltration and TLS formation. Untreated tumors exhibit dysfunctional blood vessels that limit immune cell entry into the tumor microenvironment (TME) in support of tumor progression (left). Provision of STING agonists (1, right) into the TME leads to the activation of STING$^+$ stromal cells (2), including dendritic cells (DC) and vascular endothelial cells (VEC), leading to enhanced endothelial cell expression of adhesion molecules, improved vascular integrity/perfusion, and pro-inflammatory immune cell infiltration. A subset of therapeutically-conditioned VEC may differentiate into PNAd$^+$ high endothelial venules (HEV). STING activated DC and HEV produce TLS-promoting cytokines/chemokines CCL19, CCL21, lymphotoxins, CXCL10 and IFNβ, which serve to recruit T cells and DC into the TME in support of non-classic, immature TLS formation proximal to HEV (3). CXCL13, required for optimal B cell recruitment into the TME and for germinal center (GC) formation within TLS, is only poorly produced in the STING agonist-conditioned tumors, precluding formation of classical, mature TLS. Combination protocols will likely be required for conversion of immature TLS into B cell/GC-rich classical, mature TLS (4) and/or to improve the therapeutic benefits associated with treatment-induced TLS formation (5). Image created with BioRender.com.

COMBINATION STING AGONIST THERAPIES MAY BE REQUIRED TO PROMOTE THE NEOGENESIS OF CLASSICAL, MATURE TLS IN THE TME

The finding that STING agonists promote the formation of non-classical/immature TLS is consistent with the inability of these agents to augment production of CXCL13 within the treated TME, a prerequisite for CXCR5$^+$ B cell/Tfh cell recruitment and the formation of GC within classical/mature TLS (67). While the exact mechanism underlying this deficiency in CXCL13 production remains unclear, it could relate to the known regulatory action of STING signaling in B cells. For instance, the activation of STING in B cells *via* genetic engineering to express a constitutively activated form of STING or by treatment of B cells with STING agonists results in endoplasmic reticulum (ER)-associated degradation of membrane-bound immunoglobulin, muted BCR signaling *via* enhanced SHP1 phosphatase activity and increased rates of B cell apoptosis (74–76).

Since STING agonist-associated treatment benefits occur in association with non-classical/immature TLS formation, with seemingly minimal input from B cells, these findings also reenergize discussions related to the operational importance of B cells in therapeutic anti-tumor immune responses. Despite several recent reports citing the association of B cells and GC within tumor-associated TLS and positive clinical prognosis and response to interventional immunotherapy (19, 77–80), the literature is balanced by observations for an immunosuppressive influence for intratumoral B cells in promoting tumor progression, poor patient prognosis and immune-related adverse events (irAEs) in response to immunotherapy (80–82). Translational modeling in murine tumor models has similarly provided equivocal findings. Hence, B cell deficiency (muMT) or B cell depletion (using anti-CD20 mAbs) has resulted in either decreased (83–86) or

increased (87) tumor growth. In the former cases, B cells are hypothesized to serve as intrinsic immunoregulatory cells or facilitators of Treg recruitment/development/function (82–85), while in the latter situation, B cells are believed to serve as supportive antigen-presenting cells and/or producers of pro-TLS cytokines (i.e. LIGHT) and therapeutic anti-tumor antibodies (19, 78, 88–93).

In recent years, more attention has been devoted to discerning the impact of B cells in TLS that form in patients' tumors with a generally beneficial role for B cells emerging. In both melanoma and renal cell carcinoma, B cell gene signatures are enriched in the tumors of patients who respond to immune checkpoint blockade with positive correlations observed at baseline and on-treatment (79). When tumor samples were histologically analyzed, TLS containing B cells were more commonly identified in tumor biopsies obtained from clinical responders vs. non-responders, and these mature TLS appeared more secondary-follicle-like and contained $CD21^+$ follicular DC and $CD23^+$ germinal center B cells (79). Furthermore, the presence of B cells in classical, mature TLS was associated with T cells exhibiting more activated, functional phenotypes and expanded repertoires (79, 94–96).

If these more recent observations can be generalized, they suggest that optimal benefits from interventional immunotherapies may require treatment-associated development of classic, mature TLS containing B cells. As such, STING agonist-based regimens should be combined (synchronously or potentially after STING agonists) with co-treatments that coordinately induce the entry of therapeutic B cells, as well as FDC and Tfh cells, into the TME to improve TLS-associated anti-tumor immune responses. Candidate co-therapies include a range of toll-receptor agonists (97–104), agonist anti-TNFR1 antibodies (105) and DNA methylase inhibitors (106) which have each been reported to augment production of CXCL13 by stromal cell populations. This augmentation would be expected to improve tumor infiltrating B cell content and GC formation within the TLS^+ TME, conceivably improving immune-mediated control of tumor growth. Indeed, several recent reports support therapeutic synergy using treatment regimens combining STING agonists and TLR1/2 agonist Pam3Csk (97), TLR4 agonist monophosphoryl lipid A (102), TLR7/8 agonist MEDI9197 (103) or TLR9 agonist CpG (104). Although the impact of these interventional protocols on TLS formation within the TME and the evolving anti-tumor immune response remains unknown, these aspects are expected to be actively pursued in future studies.

COMBINING STING AGONISTS WITH AGENTS CAPABLE OF ANTAGONIZING COMPENSATORY REGULATORY PATHWAYS FOR IMPROVED THERAPEUTIC EFFICACY

Given the ability of STING agonists to promote robust pro-inflammatory responses in tumor-associated stromal cells, it is perhaps not surprising that these agents are competent to initiate the development of non-classical, immature TLS within the TME (67). And even though treatment of tumor-bearing mice with STING agonists leads to reduced levels of tumor-associated myeloid-derived suppressor cells (MDSC) and Treg cells (107, 108), these regimens promote compensatory activation of immune regulatory pathways by augmenting expression of arginase-2 (ARG2), cyclooxygenase-2 (COX2/PTGS2), indoleamine 2,3 dioxygenase (IDO), programmed death-1 (PD-1), programmed death ligand-1 (PD-L1) and prostaglandin E synthase (PTGES) within the TME (67, 109–111). Hence, combined treatment protocols that include STING agonists and antagonists of these regulatory pathways would be anticipated to enhance/sustain inflammation within the TME in support of TLS formation/maintenance and improved host control of tumor growth. While the formation of TLS has yet to be investigated as a therapeutic endpoint in translational models of such combination treatment protocols, therapeutic synergy has been observed for regimens combining STING agonists with inhibitors of COX2 (Celecoxib) or IDO (BMS-986205), or antagonist anti-PD1 and/or anti-PD-L1 antibodies (107, 109, 112).

DISCUSSION AND FUTURE PERSPECTIVES

TLS are increasingly viewed as important operational components supporting the development and maintenance of protective immune responses that impact patient prognosis and response to interventional immunotherapy. The ability to predictably and reproducibly promote or augment TLS formation in a patient's tumor(s) *via* the administration of therapeutic agents may dramatically improve objective response rates over those currently observed for standard of care treatments, including immune checkpoint blockade antibodies. Although previous animal modeling of gene therapy and targeted antibody approaches to deliver individual TLS homeostatic cytokines/chemokines have proven successful in controlling tumor growth and promoting TLS formation in mice (113–115), these strategies have yet to be effectively translated into the clinic, and they rely on the biologic dominance of a single agent to initiate the complex biologic process of TLS formation. In this regard, STING agonism provides the opportunity to coordinately activate a range of tumor-associated stromal cell populations, including vascular endothelial cells and immune cells, leading to VN, enhanced immune cell infiltration, and the establishment of a pro-inflammatory TME in which TLS-associated homeostatic chemokines and cytokines are produced and TLS formation is facilitated. While provision of STING agonist ADU-S100 into B16 melanomas resulted in the development of a T cell repertoire unique to the therapeutic TLS^+ TME and to some abscopal benefit in regulating the growth of distal, untreated tumor lesions, the current approach has several limitations.

First, the approach involves direct injection of a second-generation STING agonist (which can only be administered locally) into an accessible lesion, with the intent to treat disseminated disease. In this regard, while local injection of STING agonists [i.e. ADU-S100/MIW815 (NCT02675439), MK-1454 (NCT03010176)] as monotherapies has provided some evidence for pro-inflammatory changes in the TME or patient sera, therapeutic benefits have been minimal (i.e. < 5% objective response rate) in early phase clinical trials treating advanced-stage cancer patients (as described in greater detail in a series of recent outstanding reviews) (55, 116, 117). This deficiency may be circumvented by the provision of next-generation, systemic STING agonists for more effective treatment of patients with multifocal, disseminated disease in visceral tissue sites. Several of these agents (i.e. E7766 [NCT04109092], GSK-3745417 [NCT03843359], MSA-2, SB-11285 [NCT04096638], TAK-676 [NCT04420884]) (55, 118, 119) are planned for, or are currently being evaluated in, phase I clinical trials. Given the pro-apoptotic impact of high-doses of STING agonists on VEC (i.e. vasoablative) and immune cell populations (67, 73–76, 120, 121), but the ability of low-dose regimens to promote VN and enhanced pro-inflammatory immune function in pre-clinical models, it might be anticipated that low-dose protocols will provide optimal immunotherapeutic benefits in these trials. While it is not clear that the formation of TLS represents an exploratory endpoint in these ongoing trial designs, one might expect that low-dose regimens of these next-generation STING agonists will prove effective in inducing *de novo* development of TLS or expansion of existing TLS within the tumor of treated patients. It is also possible given enhanced autoimmune manifestations in older (cancer) patients (122), many of which have known associations with the formation of TLS in affected tissues (123), that treatment with systemic STING agonists may exacerbate the incidence and severity of irAEs.

Second, the TLS promoted by ADU-S100 in the TME appear rich in $CD8^+$ T cells, DC and HEV, but they are poor in CXCL13 production and infiltrating B cell/GC content (67) [i.e. representative of non-classical, immature TLS (2, 16)]. If B cells are indeed crucial to superior therapeutic benefits associated with TLS formation in tumors, additional co-therapies that i.) reinforce local CXCL13 production, ii.) B cell, Tfh and FDC infiltration and iii.) GC formation, may need to be combined with STING agonists to achieve maximal interventional benefit.

Third, the natural checks and balances in evolving immune responses must be considered in conditionally optimizing STING agonist-based immunotherapies. The robust pro-inflammatory responses evoked by these agents result in an upregulation in immune regulatory pathways within the TME, including but not limited to prostaglandin E production and immune suppression mediated by arginase, IDO and co-inhibitory receptors (67, 68). These regulatory pathways may be antagonized (individually or collectively) in combination STING agonist protocols using available, in-clinic targeted inhibitors. Such approaches would be expected to augment and prolong inflammation within the TME in support of TLS formation and the mobilization of broadly-reactive anti-tumor immune responses in the therapy setting. However, as suggested above, such deregulated reinforcement of TLS formation in tumors and normal tissues carries increased risk for the evolution of severe (autoimmune) irAEs.

Finally, previous findings suggest that in certain cases, STING activation and the presence of HEV/TLS may be associated with tumor progression. Hence, in murine lung carcinoma models (109, 111), provision of STING agonists (i.e. CDA) initially slowed primary tumor growth but ultimately resulted in disease progression and metastasis due to treatment-associated enhancement in immune regulatory/tolerogenic pathways (COX2, IDO, PD-1), which could be mitigated using targeted inhibitors in combination protocols (109, 111). Furthermore, tumors with pronounced chromosomal instability and intrinsic STING signaling competency have been reported to exhibit STING-dependent metastatic potential (124), which might be envisioned to be further exacerbated by treatment with STING agonists. Additional reports caution that TLS enriched in Treg cells or immature (thin-walled) HEV may be associated with poor immune infiltration of tumors, poor patient prognosis and increased tumor metastasis (125). Therefore, baseline tumor STING signaling competency and the quality and cell composition of STING-agonized TLS should be carefully monitored for correlative impact on cancer patient outcome.

AUTHOR CONTRIBUTIONS

All authors contributed to the article and approved the submitted version.

FUNDING

This work was supported by NIH grants R01 CA204419 and P01 CA234212 (both to WS) and NIH T32 CA082084 (to JF).

REFERENCES

1. Engelhard VH, Rodriguez AB, Mauldin IS, Woods AN, Peske JD, Slingluff CL. Immune Cell Infiltration and Tertiary Lymphoid Structures as Determinants of Antitumor Immunity. *J Immunol* (2018) 200:432–42. doi: 10.4049/jimmunol.1701269
2. Weinstein AM, Storkus WJ. Therapeutic Lymphoid Organogenesis in the Tumor Microenvironment. *Adv Cancer Res* (2015) 128:197–233. doi: 10.1016/bs.acr.2015.04.003
3. Sautès-Fridman C, Lawand M, Giraldo NA, Kaplon H, Germain C, Fridman WH, et al. Tertiary Lymphoid Structures in Cancers: Prognostic Value, Regulation, and Manipulation for Therapeutic Intervention. *Front Immunol* (2016) 7:407. doi: 10.3389/fimmu.2016.00407
4. Dieu-Nosjean M-C, Giraldo NA, Kaplon H, Germain C, Fridman WH, Sautès-Fridman C. Tertiary Lymphoid Structures, Drivers of the Anti-Tumor Responses in Human Cancers. *Immunol Rev* (2016) 271:260–75. doi: 10.1111/imr.12405

5. Weinstein AM, Storkus WJ. Biosynthesis and Functional Significance of Peripheral Node Addressin in Cancer-Associated TLO. *Front Immunol* (2016) 7:301. doi: 10.3389/fimmu.2016.00301
6. Jones E, Gallimore A, Ager A. Defining High Endothelial Venules and Tertiary Lymphoid Structures in Cancer. *Methods Mol Biol* (2018) 1845:99–118. doi: 10.1007/978-1-4939-8709-2_7
7. Ager A, May MJ. Understanding High Endothelial Venules: Lessons for Cancer Immunology. *Oncoimmunology* (2015) 4:e1008791. doi: 10.1080/2162402X.2015.1008791
8. Yu P, Lee Y, Liu W, Chin RK, Wang J, Wang Y, et al. Priming of Naive T Cells Inside Tumors Leads to Eradication of Established Tumors. *Nat Immunol* (2004) 5:141–9. doi: 10.1038/ni1029
9. Thompson ED, Enriquez HL, Fu YX, Engelhard VH. Tumor Masses Support Naive T Cell Infiltration, Activation, and Differentiation Into Effectors. *J Exp Med* (2010) 207:1791–804. doi: 10.1084/jem.20092454
10. Teillaud J-L, Dieu-Nosjean M-C. Tertiary Lymphoid Structures: An Anti-Tumor School for Adaptive Immune Cells and an Antibody Factory to Fight Cancer? *Front Immunol* (2017) 8:830. doi: 10.3389/fimmu.2017.00830
11. Weinstein AM, Chen L, Brzana EA, Patil PR, Taylor JL, Fabian KL, et al. Tbet and IL-36γ Cooperate in Therapeutic DC-mediated Promotion of Ectopic Lymphoid Organogenesis in the Tumor Microenvironment. *OncoImmunology* (2017) 6:e1322238. doi: 10.1080/2162402X.2017.1322238
12. Goc J, Germain C, Vo-Bourgais TKD, Lupo A, Klein C, Knockaert S, et al. Dendritic Cells in Tumor-Associated Tertiary Lymphoid Structures Signal a Th1 Cytotoxic Immune Contexture and License the Positive Prognostic Value of Infiltrating $CD8^+$ T Cells. *Cancer Res* (2014) 74:705–15. doi: 10.1158/0008-5472.CAN-13-1342
13. Halle S, Dujardin HC, Bakocevic N, Fleige H, Danzer H, Willenzon S, et al. Induced Bronchus-Associated Lymphoid Tissue Serves as a General Priming Site for T Cells and is Maintained by Dendritic Cells. *J Exp Med* (2009) 206:2593–601. doi: 10.1084/jem.20091472
14. Kuerten S, Schickel A, Kerkloh C, Recks MS, Addicks K, Ruddle NH, et al. Tertiary Lymphoid Organ Development Coincides With Determinant Spreading of the Myelin-Specific T Cell Response. *Acta Neuropathol* (2012) 124:861–73. doi: 10.1007/s00401-012-1023-3
15. Posch F, Silina K, Leibl S, Mündlein A, Moch H, Siebenhüner A, et al. Maturation of Tertiary Lymphoid Structures and Recurrence of Stage II and III Colorectal Cancer. *Oncoimmunology* (2017) 7:e1378844. doi: 10.1080/2162402X.2017.1378844
16. Hiraoka N, Ino Y, Yamazaki-Itoh R. Tertiary Lymphoid Organs in Cancer Tissues. *Front Immunol* (2016) 7:244. doi: 10.3389/fimmu.2016.00244
17. Stowman AM, Hickman AW, Mauldin IS, Mahmutovic A, Gru AA, Slingluff CL Jr. Lymphoid Aggregates in Desmoplastic Melanoma Have Features of Tertiary Lymphoid Structures. *Melanoma Res* (2018) 28:237–45. doi: 10.1097/CMR.0000000000000439
18. Wirsing AM, Rikardsen OG, Steigen SE, Uhlin-Hansen L, Hadler-Olsen E. Characterisation and Prognostic Value of Tertiary Lymphoid Structures in Oral Squamous Cell Carcinoma. *BMC Clin Pathol* (2014) 14:38. doi: 10.1186/1472-6890-14-38
19. Germain C, Gnjatic S, Tamzalit F, Knockaert S, Remark R, Goc J, et al. Presence of B Cells in Tertiary Lymphoid Structures is Associated With a Protective Immunity in Patients With Lung Cancer. *Am J Respir Crit Care Med* (2014) 189:832–44. doi: 10.1164/rccm.201309-1611OC
20. Kroeger DR, Milne K, Nelson BH. Tumor Infiltrating Plasma Cells are Associated With Tertiary Lymphoid Structures, Cytolytic T-cell Responses, and Superior Prognosis in Ovarian Cancer. *Clin Cancer Res* (2016) 22:3005–15. doi: 10.1158/1078-0432.CCR-15-2762
21. Dieu-Nosjean MC, Antoine M, Danel C, Heudes D, Wislez M, Poulot V, et al. Long-Term Survival for Patients With Non- Small-Cell Lung Cancer With Intratumoral Lymphoid Structures. *J Clin Oncol* (2008) 26:4410–7. doi: 10.1200/JCO.2007.15.0284
22. Siliņa K, Soltermann A, Attar FM, Casanova R, Uckeley ZM, Thut H, et al. Germinal Centers Determine the Prognostic Relevance of Tertiary Lymphoid Structures and are Impaired by Corticosteroids in Lung Squamous Cell Carcinoma. *Cancer Res* (2018) 78:1308–20. doi: 10.1158/0008-5472.CAN-17-1987
23. Castino GF, Cortese N, Capretti G, Serio S, Di Caro G, Mineri R, et al. Spatial Distribution of B Cells Predicts Prognosis in Human Pancreatic Adenocarcinoma. *Oncoimmunology* (2016) 5:e1085147. doi: 10.1080/2162402X.2015.1085147
24. Di Caro G, Bergomas F, Grizzi F, Doni A, Bianchi P, Malesci A, et al. Occurrence of Tertiary Lymphoid Tissue is Associated With T Cell Infiltration and Predicts Better Prognosis in Early- Stage Colorectal Cancers. *Clin Cancer Res* (2014) 20:2147–58. doi: 10.1158/1078-0432.CCR-13-2590
25. Lee HJ, Kim JY, Park IA, Song IH, Yu JH, Ahn JH, et al. Prognostic Significance of Tumor Infiltrating Lymphocytes and the Tertiary Lymphoid Structures in HER2-positive Breast Cancer Treated With Adjuvant Trastuzumab. *Am J Clin Pathol* (2015) 144:278–88. doi: 10.1309/AJCPIXUYDVZ0RZ3G
26. Savas P, Salgado R, Sotiriou C, Denkert C, Darcy PK, Smyth MJ, et al. Clinical Relevance of Host Immunity in Breast Cancer: From TILs to the Clinic. *Nat Rev Clin Oncol* (2016) 13:228–41. doi: 10.1038/nrclinonc.2015.215
27. Martinet L, Filleron T, Le Guellec S, Rochaix P, Garrido I, Girardet JP. High Endothelial Venule Blood Vessels for Tumor-Infiltrating Lymphocytes are Associated With Lymphotoxin β-Producing Dendritic Cells in Human Breast Cancer. *J Immunol* (2013) 191:2001–8. doi: 10.4049/jimmunol.1300872
28. Nerviani A, Pitzalis C. Role of Chemokines in Ectopic Lymphoid Structures Formation in Autoimmunity and Cancer. *J Leukoc Biol* (2018) 104:333–41. doi: 10.1002/JLB.3MR0218-062R
29. Ruddle NH. Lymphoid Neo-Organogenesis: Lymphotoxin's Role in Inflammation and Development. *Immunol Res* (1999) 19:119–25. doi: 10.1007/BF02786481
30. Furtado GC, Marinkovic T, Martin AP, Garin A, Hoch B, Hubner W, et al. Lymphotoxin Beta Receptor Signaling is Required for Inflammatory Lymphangiogenesis in the Thyroid. *Proc Natl Acad Sci USA* (2007) 104:5026–31. doi: 10.1073/pnas.0606697104
31. Luther SA, Lopez T, Bai W, Hanahan D, Cyster JG. BLC Expression in Pancreatic Islets Causes B Cell Recruitment and Lymphotoxin-Dependent Lymphoid Neogenesis. *Immunity* (2000) 12:471–81. doi: 10.1016/s1074-7613(00)80199-5
32. Luther SA, Bidgol A, Hargreaves DC, Schmidt A, Xu Y, Paniyadi J, et al. Differing Activities of Homeostatic Chemokines CCL19, CCL21, and CXCL12 in Lymphocyte and Dendritic Cell Recruitment and Lymphoid Neogenesis. *J Immunol* (2002) 169:424–33. doi: 10.4049/jimmunol.169.1.424
33. Sharma S, Stolina M, Luo J, Strieter RM, Burdick M, Li X, et al. Secondary Lymphoid Tissue Chemokine Mediates T Cell-Dependent Antitumor Responses In Vivo. *J Immunol* (2000) 164:4558–63. doi: 10.4049/jimmunol.164.9.4558
34. Li J, O'Malley M, Sampath P, Kalinski P, Bartlett DL, Thorne SH. Expression of CCL19 From Oncolytic Vaccinia Enhances Immunotherapeutic Potential While Maintaining Oncolytic Activity. *Neoplasia* (2012) 14:1115–21. doi: 10.1593/neo.121272
35. Chen P, Luo S, Wen YJ, Li YH, Li J, Wang YS, et al. Low-Dose Paclitaxel Improves the Therapeutic Efficacy of Recombinant Adenovirus Encoding CCL21 Chemokine Against Murine Cancer. *Cancer Sci* (2014) 105:1393–401. doi: 10.1111/cas.12537
36. Lee JM, Lee MH, Garon E, Goldman JW, Salehi-Rad R, Baratelli FE, et al. Phase I Trial of Intratumoral Injection of CCL21 Gene-Modified Dendritic Cells in Lung Cancer Elicits Tumor-Specific Immune Responses and $CD8^+$ T-Cell Infiltration. *Clin Cancer Res* (2017) 23:4556–68. doi: 10.1158/1078-0432
37. Tang H, Zhu M, Qiao J, Fu YX. Lymphotoxin Signalling in Tertiary Lymphoid Structures and Immunotherapy. *Cell Mol Immunol* (2017) 14:809–18. doi: 10.1038/cmi.2017.13
38. Upadhyay V, Fu YX. Lymphotoxin Signalling in Immune Homeostasis and the Control of Microorganisms. *Nat Rev Immunol* (2013) 13:270–9. doi: 10.1038/nri3406
39. Ware CF. Targeting Lymphocyte Activation Through the Lymphotoxin and LIGHT Pathways. *Immunol Rev* (2008) 223:86–201. doi: 10.1111/j.1600-065X.2008.00629.x
40. Peske JD, Thompson ED, Gemta L, Baylis RA, Fu Y-X, Engelhard VH. Effector Lymphocyte-Induced Lymph Node-Like Vasculature Enables Naive

T-Cell Entry Into Tumours and Enhanced Anti-Tumour Immunity. *Nat Commun* (2015) 6:7114. doi: 10.1038/ncomms8114
41. Kratz A, Campos-Neto A, Hanson MS, Ruddle NH. Chronic Inflammation Caused by Lymphotoxin is Lymphoid Neogenesis. *J Exp Med* (1996) 183:1461–72. doi: 10.1084/jem.183.4.1461
42. Drayton DL, Ying X, Lee J, Lesslauer W, Ruddle NH. Ectopic LT Alpha Beta Directs Lymphoid Organ Neogenesis With Concomitant Expression of Peripheral Node Addressin and a HEV-restricted Sulfotransferase. *J Exp Med* (2003) 197:1153–63. doi: 10.1084/jem.20021761
43. Schrama D, thor Straten P, Fischer WH, McLellan AD, Brocker EB, Reisfeld RA, et al. Targeting of Lymphotoxin-Alpha to the Tumor Elicits an Efficient Immune Response Associated With Induction of Peripheral Lymphoid-Like Tissue. *Immunity* (2001) 14:111–21. doi: 10.1016/s1074-7613(01)00094-2
44. Colbeck EJ, Jones E, Hindley JP, Smart K, Schulz R, Browne M, et al. Treg Depletion Licenses T Cell-Driven HEV Neogenesis and Promotes Tumor Destruction. *Cancer Immunol Res* (2017) 5:1005–15. doi: 10.1158/2326-6066.CIR-17-0131
45. He B, Jabouille A, Steri V, Johansson-Percival A, Michael IP, Kotamraju VR, et al. Vascular Targeting of LIGHT Normalizes Blood Vessels in Primary Brain Cancer and Induces Intratumoural High Endothelial Venules. *J Pathol* (2018) 245:209–21. doi: 10.1002/path.5080
46. Fan Z, Yu P, Wang Y, Wang Y, Fu ML, Liu W, et al. NK-Cell Activation by LIGHT Triggers Tumor-Specific $CD8^+$ T-Cell Immunity to Reject Established Tumors. *Blood* (2006) 107:1342–51. doi: 10.1182/blood-2005-08-3485
47. Mourik BC, Lubberts E, de Steenwinkel JEM, Ottenhoff THM, Leenen PJM. Interactions Between Type 1 Interferons and the Th17 Response in Tuberculosis: Lessons Learned From Autoimmune Diseases. *Front Immunol* (2017) 8:294. doi: 10.3389/fimmu.2017.00294
48. Denton AE, Innocentin S, Carr EJ, Bradford BM, Lafouresse F, Mabbott NA, et al. Type I Interferon Induces CXCL13 to Support Ectopic Germinal Center Formation. *J Exp Med* (2019) 216:621–37. doi: 10.1084/jem.20181216
49. Nacionales DC, Kelly-Scumpia KM, Lee PY, Weinstein JS, Lyons R, Sobel E, et al. Deficiency of the Type I Interferon Receptor Protects Mice From Experimental Lupus. *Arthritis Rheumatol* (2007) 56:3770–83. doi: 10.1002/art.23023
50. Nacionales DC, Kelly KM, Lee PY, Zhuang H, Li Y, Weinstein JS, et al. Type I Interferon Production by Tertiary Lymphoid Tissue Developing in Response to 2,6,10,14-Tetramethyl-Pentadecane (Pristane). *Am J Pathol* (2006) 168:1227–40. doi: 10.2353/ajpath.2006.050125
51. Ogasawara K, Hida S, Weng Y, Saiura A, Sato K, Takayanagi H, et al. Requirement of the IFN-alpha/beta-induced CXCR3 Chemokine Signalling for $CD8^+$ T Cell Activation. *Genes Cells* (2002) 7:309–20. doi: 10.1046/j.1365-2443.2002.00515.x
52. Banks TA, Rickert S, Benedict CA, Ma L, Ko M, Meier J, et al. A lymphotoxin-IFN-beta Axis Essential for Lymphocyte Survival Revealed During Cytomegalovirus Infection. *J Immunol* (2005) 174:7217–25. doi: 10.4049/jimmunol.174.11.7217
53. Chelvanambi M, Weinstein AM, Storkus WJ. Il-36 Signaling in the Tumor Microenvironment. *Adv Exp Med Biol* (2020) 1240:95–110. doi: 10.1007/978-3-030-38315-2_8
54. Weinstein AM, Giraldo NA, Petitprez F, Julie C, Lacroix L, Peschaud F, et al. Association of IL-36γ With Tertiary Lymphoid Structures and Inflammatory Immune Infiltrates in Human Colorectal Cancer. *Cancer Immunol Immunother* (2019) 68:109–20. doi: 10.1007/s00262-018-2259-0
55. Flood BA, Higgs EF, Li S, Luke JJ, Gajewski TF. STING Pathway Agonism as a Cancer Therapeutic. *Immunol Rev* (2019) 290:24–38. doi: 10.1111/imr.12765
56. Kiwerska K, Szyfter K. DNA Repair in Cancer Initiation, Progression, and Therapy-a Double-Edged Sword. *J Appl Genet* (2019) 60:329–34. doi: 10.1007/s13353-019-00516-9
57. Hoeijmakers JH. Genome Maintenance Mechanisms for Preventing Cancer. *Nature* (2001) 411:366–74. doi: 10.1038/35077232
58. Bhattacharya S, Srinivasan K, Abdisalaam S, Su F, Raj P, Dozmorov I, et al. RAD51 Interconnects Between DNA Replication, DNA Repair and Immunity. *Nucleic Acids Res* (2017) 45:4590–605. doi: 10.1093/nar/gkx126
59. Guan J, Lu C, Jin Q, Lu H, Chen X, Tian L, et al. Deficiency-Triggered DNA Hyperexcision by Exonuclease 1 Activates the cGAS-STING Pathway. *Cancer Cell* (2021) 39:109–21. doi: 10.1016/j.ccell.2020.11.004
60. Talens F, Van Vugt MATM. Inflammatory Signaling in Genomically Instable Cancers. *Cell Cycle* (2019) 18:1830–48. doi: 10.1080/15384101.2019.1638192
61. He L, Xiao X, Yang X, Zhang Z, Wu L, Liu Z. STING Signaling in Tumorigenesis and Cancer Therapy: A Friend or Foe? *Cancer Lett* (2017) 402:203–12. doi: 10.1016/j.canlet.2017.05.026
62. Reisländer T, Groelly FJ, Tarsounas M. DNA Damage and Cancer Immunotherapy: A STING in the Tale. *Mol Cell* (2020) 80:21–8. doi: 10.1016/j.molcel.2020.07.026
63. Campisi M, Sundararaman SK, Shelton SE, Knelson EH, Mahadevan NR, Yoshida R, et al. Tumor-Derived cGAMP Regulates Activation of the Vasculature. *Front Immunol* (2020) 11:2090. doi: 10.3389/fimmu.2020.02090
64. Schadt L, Sparano C, Schweiger NA, Silina K, Cecconi V, Lucchiari G, et al. Cancer-Cell-Intrinsic Cgas Expression Mediates Tumor Immunogenicity. *Cell Rep* (2019) 29:1236–48. doi: 10.1016/j.celrep.2019.09.065
65. Andzinski L, Spanier J, Kasnitz N, Kröger A, Jin L, Brinkmann MM, et al. Growing Tumors Induce a Local STING Dependent Type I IFN Response in Dendritic Cells. *Int J Cancer* (2016) 139:1350–7. doi: 10.1002/ijc.30159
66. Corrales L, Glickman LH, McWhirter SM, Kanne DB, Sivick KE, Katibah GE, et al. Direct Activation of STING in the Tumor Microenvironment Leads to Potent and Systemic Tumor Regression and Immunity. *Cell Rep* (2015) 11:1018–30. doi: 10.1016/j.celrep.2015.04.031
67. Chelvanambi M, Fecek RJ, Taylor JL, Storkus WJ. STING Agonist-Based Treatment Promotes Vascular Normalization and Tertiary Lymphoid Structure Formation in the Therapeutic Melanoma Microenvironment. *J Immunother Cancer* (2021) 9:e001906. doi: 10.1136/jitc-2020-001906
68. Yang H, Lee WS, Kong SJ, Kim CG, Kim JH, Chang SK, et al. STING Activation Reprograms Tumor Vasculatures and Synergizes With VEGFR2 Blockade. *J Clin Invest* (2019) 129:4350–64. doi: 10.1172/JCI125413
69. Lin Z, Huang L, Li S, Gu J, Cui X, Zhou Y. Pan-Cancer Analysis of Genomic Properties and Clinical Outcome Associated With Tumor Tertiary Lymphoid Structure. *Sci Rep* (2020) 10:21530. doi: 10.1038/s41598-020-78560-3
70. Salem D, Chelvanambi M, Storkus WJ, Fecek RJ. Cutaneous Melanoma: Mutational Status and Potential Links to Tertiary Lymphoid Structure Formation. *Front Immunol* (2021) 12:629519. doi: 10.3389/fimmu.2021.629519
71. Samstein RM, Lee CH, Shoushtari AN, Hellmann MD, Shen R, Janjigian YY, et al. Tumor Mutational Load Predicts Survival After Immunotherapy Across Multiple Cancer Types. *Nat Genet* (2019) 51:202–6. doi: 10.1038/s41588-018-0312-8
72. Goodman AM, Kato S, Bazhenova L, Patel SP, Frampton GM, Miller V, et al. Tumor Mutational Burden as an Independent Predictor of Response to Immunotherapy in Diverse Cancers. *Mol Cancer Ther* (2017) 16:2598–608. doi: 10.1158/1535-7163.MCT-17-0386
73. Farshchi Adli AD, Jahanban-Esfahlan R, Seidi K, Samandari-Rad S, Zarghami N. An Overview on Vadimezan (Dmxaa): The Vascular Disrupting Agent. *Chem Biol Drug Des* (2018) 91:996–1006. doi: 10.1111/cbdd.13166
74. Tang CHA, Lee AC, Chang S, Xu Q, Shao A, Lo Y, et al. STING Regulates BCR Signaling in Normal and Malignant B Cells. *Cell Mol Immunol* (2021) 18:1016–31. doi: 10.1038/s41423-020-00552-0.Online ahead of print
75. Tang CHA, Zundell JA, Ranatunga S, Lin C, Nefedova Y, Del Valle JR, et al. Agonist-Mediated Activation of STING Induces Apoptosis in Malignant B Cells. *Cancer Res* (2016) 76:2137–52. doi: 10.1158/0008-5472.CAN-15-1885
76. Jing Y, Dai X, Yang L, Kang D, Jiang P, Li N, et al. STING Couples With PI3K to Regulate Actin Reorganization During BCR Activation. *Sci Adv* (2020) 6:eaax9455. doi: 10.1126/sciadv.aax9455
77. Sakimura C, Tanaka H, Okuno T, Hiramatsu S, Muguruma K, Hirakawa K, et al. B Cells in Tertiary Lymphoid Structures are Associated With Favorable Prognosis in Gastric Cancer. *J Surg Res* (2017) 215:74–82. doi: 10.1016/j.jss.2017.03.033

78. Cabrita R, Lauss M, Sanna A, Donia M, Skaarup Larsen M, Mitra S, et al. Tertiary Lymphoid Structures Improve Immunotherapy and Survival in Melanoma. *Nature* (2020) 577:561–5. doi: 10.1038/s41586-019-1914-8
79. Helmink BA, Reddy SM, Gao J, Zhang S, Basar R, Thakur R, et al. B Cells and Tertiary Lymphoid Structures Promote Immunotherapy Response. *Nature* (2020) 577:549–55. doi: 10.1038/s41586-019-1922-8
80. Willsmore ZN, Harris RJ, Crescioli S, Hussein K, Kakkassery H, Thapa D, et al. B Cells in Patients With Melanoma: Implications for Treatment With Checkpoint Inhibitor Antibodies. *Front Immunol* (2021) 11:622442. doi: 10.3389/fimmu.2020.622442
81. Corsiero E, Delvecchio FR, Bombardieri M, Pitzalis C. B Cells in the Formation of Tertiary Lymphoid Organs in Autoimmunity, Transplantation and Tumorigenesis. *Curr Opin Immunol* (2019) 57:46–52. doi: 10.1016/j.coi.2019.01.004
82. Zhang Y, Gallastegui N, Rosenblatt JD. Regulatory B Cells in Anti-Tumor Immunity. *Int Immunol* (2015) 27:521–30. doi: 10.1093/intimm/dxv034
83. Zhang Y, Eliav Y, Shin SU, Schreiber TH, Podack ER, Tadmor T, et al. B Lymphocyte Inhibition of Anti-Tumor Response Depends on Expansion of Treg But is Independent of B-cell Il-10 Secretion. *Cancer Immunol Immunother* (2013) 62:87–99. doi: 10.1007/s00262-012-1313-6
84. Shah S, Divekar AA, Hilchey SP, Cho HM, Newman CL, Shin SU, et al. Increased Rejection of Primary Tumors in Mice Lacking B Cells: Inhibition of Anti-Tumor CTL and TH1 Cytokine Responses by B Cells. *Int J Cancer* (2005) 117:574–86. doi: 10.1002/ijc.21177
85. Zhang Y, Morgan R, Chen C, Cai Y, Clark E, Noor Khan W, et al. Mammary-Tumor-Educated B Cells Acquire LAP/TGF-β and PD-L1 Expression and Suppress Anti-Tumor Immune Responses. *Int Immunol* (2016) 28:423–33. doi: 10.1093/intimm/dxw007
86. Xiao X, Lao XM, Chen MM, Liu RX, Wei Y, Ouyang FZ, et al. PD-1^{hi} Identifies a Novel Regulatory B Cell Population in Human Hepatoma That Promotes Disease Progression. *Cancer Discovery* (2016) 6:546–59. doi: 10.1158/2159-8290.CD-15-1408
87. DiLillo DJ, Yanaba K, Tedder TF. B Cells are Required for Optimal CD4$^+$ and CD8$^+$ T Cell Tumor Immunity: Therapeutic B Cell Depletion Enhances B16 Melanoma Growth in Mice. *J Immunol* (2010) 184:4006–16. doi: 10.4049/jimmunol.0903009
88. Fridman WH, Petitprez F, Meylan M, Chen TWW, Sun CM, Roumenina LT, et al. B Cells and Cancer: to B or Not to B? *J Exp Med* (2021) 218:e20200851. doi: 10.1084/jem.20200851
89. Nelson BH. CD20$^+$ B Cells: The Other Tumor-Infiltrating Lymphocytes. *J Immunol* (2010) 185:4977–82. doi: 10.4049/jimmunol.1001323
90. Kang YM, Kim SY, Kang JH, Han SW, Nam EJ, Kyung HS, et al. LIGHT Up-Regulated on B Lymphocytes and Monocytes in Rheumatoid Arthritis Mediates Cellular Adhesion and Metalloproteinase Production by Synoviocytes. *Arthritis Rheumatol* (2007) 56:1106–17. doi: 10.1002/art.22493
91. Schlößer HA, Thelen M, Lechner A, Wennhold K, Garcia-Marquez MA, Rothschild SI, et al. B Cells in Esophago-Gastric Adenocarcinoma are Highly Differentiated, Organize in Tertiary Lymphoid Structures and Produce Tumor Specific Antibodies. *Oncoimmunology* (2019) 8:e1512458. doi: 10.1080/2162402X.2018.1512458
92. Coronella JA, Spier C, Welch M, Trevor KT, Stopeck AT, Villar H, et al. Antigen-Driven Oligoclonal Expansion of Tumor- Infiltrating B Cells in Infiltrating Ductal Carcinoma of the Breast. *J Immunol* (2002) 169:1829–36. doi: 10.4049/jimmunol.169.4.1829
93. Nzula S, Going JJ, Stott DI. Antigen- Driven Clonal Proliferation, Somatic Hypermutation, and Selection of B Lymphocytes Infiltrating Human Ductal Breast Carcinomas. *Cancer Res* (2003) 63:3275–80.
94. Zhu W, Germain C, Liu Z, Sebastian Y, Devi P, Knockaert S, et al. A High Density of Tertiary Lymphoid Structure B Cells in Lung Tumors is Associated With Increased CD4$^+$ T Cell Receptor Repertoire Clonality. *Oncoimmunology* (2015) 4:e1051922. doi: 10.1080/2162402X.2015.1051922
95. Gnjatic S, Atanackovic D, Jäger E, Matsuo M, Selvakumar A, Altorki NK, et al. Survey of Naturally Occurring CD4$^+$ T Cell Responses Against NY-ESO-1 in Cancer Patients: Correlation With Antibody Responses. *Proc Natl Acad Sci USA* (2003) 100:8862–7. doi: 10.1073/pnas.1133324100
96. Montfort A, Pearce O, Maniati E, Vincent BG, Bixby L, Böhmet S, et al. A Strong B Cell Response is Part of the Immune Landscape in Human High-Grade Serous Ovarian Metastases. *Clin Cancer Res* (2017) 23:250–62. doi: 10.1158/1078-0432.CCR-16-0081
97. Hu HG, Wu J, Zhang BD, Li WH, Li YM. Pam 3 CSK 4-Cdg SF Augments Antitumor Immunotherapy by Synergistically Activating TLR1/2 and STING. *Bioconjug Chem* (2020) 31:2499–503. doi: 10.1021/acs.bioconjchem.0c00522
98. Vanpouille-Box C, Hoffmann JA, Galluzzi L. Pharmacological Modulation of Nucleic Acid Sensors - Therapeutic Potential and Persisting Obstacles. *Nat Rev Drug Discovery* (2019) 18:845–67. doi: 10.1038/s41573-019-0043-2
99. Moreth K, Brodbeck R, Babelova A, Gretz N, Spieker T, Zeng-Brouwers J, et al. The Proteoglycan Biglycan Regulates Expression of the B Cell Chemoattractant CXCL13 and Aggravates Murine Lupus Nephritis. *J Clin Invest* (2010) 120:4251–72. doi: 10.1172/JCI42213
100. Bellamri N, Viel R, Morzadec C, Lecureur V, Joannes A, de Latour B, et al. TNF-Alpha and IL-10 Control CXCL13 Expression in Human Macrophages. *J Immunol* (2020) 204:2492–502. doi: 10.4049/jimmunol.1900790
101. Robinet M, Villeret B, Maillard S, Cron MA, Berrih-Aknin S, Le Panse R. Use of Toll-Like Receptor Agonists to Induce Ectopic Lymphoid Structures in Myasthenia Gravis Mouse Models. *Front Immunol* (2017) 8:1029. doi: 10.3389/fimmu.2017.01029
102. Lorkowski ME, Atukorale PU, Bielecki PA, Tong KH, Covarrubias G, Zhang Y, et al. Immunostimulatory Nanoparticle Incorporating Two Immune Agonists for the Treatment of Pancreatic Tumors. *J Control Release* (2021) 330:1095–105. doi: 10.1016/j.jconrel.2020.11.014
103. Mullins SR, Vasilakos JP, Deschler K, Grigsby I, Gillis P, John J, et al. Intratumoral Immunotherapy With TLR7/8 Agonist MEDI9197 Modulates the Tumor Microenvironment Leading to Enhanced Activity When Combined With Other Immunotherapies. *J Immunother Cancer* (2019) 7:244. doi: 10.1186/s40425-019-0724-8.(B16)
104. Temizoz B, Kuroda E, Ohata K, Jounai N, Ozasa K, Kobiyama K, et al. TLR9 and STING Agonists Synergistically Induce Innate and Adaptive type-II Ifn. *Eur J Immunol* (2015) 45:1159–69. doi: 10.1002/eji.201445132
105. Mandik-Nayak L, Huang G, Sheehan KC, Erikson J, Chaplin DD. Signaling Through TNF Receptor p55 in TNF-Alpha-Deficient Mice Alters the CXCL13/CCL19/CCL21 Ratio in the Spleen and Induces Maturation and Migration of Anergic B Cells Into the B Cell Follicle. *J Immunol* (2001) 167:1920–8. doi: 10.4049/jimmunol.167.4.1920
106. Ma D, Fan SB, Hua N, Li GH, Chang Q , Liu X. Hypermethylation of Single CpG Dinucleotides At the Promoter of CXCL13 Gene Promote Cell Migration in Cervical Cancer. *Curr Cancer Drug Targets* (2020) 20:355–63. doi: 10.2174/1568009620666200102123635
107. Ager CR, Reilley MJ, Nicholas C, Bartkowiak T, Jaiswal AR, Curran MA. Intratumoral STING Activation With T-cell Checkpoint Modulation Generates Systemic Antitumor Immunity. *Cancer Immunol Res* (2017) 5:676–84. doi: 10.1158/2326-6066.CIR-17-0049
108. Zhang CX, Ye SB, Ni JJ, Cai TT, Liu YN, Huang DJ, et al. STING Signaling Remodels the Tumor Microenvironment by Antagonizing Myeloid-Derived Suppressor Cell Expansion. *Cell Death Differ* (2019) 26:2314–28. doi: 10.1038/s41418-019-0302-0
109. Lemos H, Ou R, McCardle C, Lin Y, Calver J, Minett J, et al. Overcoming Resistance to STING Agonist Therapy to Incite Durable Protective Antitumor Immunity. *J Immunother Cancer* (2020) 8:e001182. doi: 10.1136/jitc-2020-001182
110. Chin EN, Yu C, Vartabedian VF, Jia Y, Kumar M, Gamo AM, et al. Antitumor Activity of a Systemic STING-activating non-Nucleotide cGAMP Mimetic. *Science* (2020) 369:993–9. doi: 10.1126/science.abb4255
111. Lemos H, Mohamed E, Huang L, Ou R, Pacholczyk G, Arbab AS, et al. Sting Promotes the Growth of Tumors Characterized by Low Antigenicity via IDO Activation. *Cancer Res* (2016) 76:2076–81. doi: 10.1158/0008-5472.CAN-15-1456
112. Cheng N, Watkins-Schulz R, Junkins RD, David CN, Johnson BM, Montgomery SA, et al. A Nanoparticle-Incorporated STING Activator Enhances Antitumor Immunity in PD-L1-insensitive Models of Triple-Negative Breast Cancer. *JCI Insight* (2018) 3:e120638. doi: 10.1172/jci.insight.120638
113. Sharma S, Kadam P, Dubinett S. CCL21 Programs Immune Activity in Tumor Microenvironment. *Adv Exp Med Biol* (2020) 1231:67–78. doi: 10.1007/978-3-030-36667-4_7

114. Hisada M, Yoshimoto T, Kamiya S, Magami Y, Miyaji H, Yoneto T, et al. Synergistic Antitumor Effect by Coexpression of Chemokine CCL21/SLC and Costimulatory Molecule LIGHT. *Cancer Gene Ther* (2004) 11:280–8. doi: 10.1038/sj.cgt.7700676
115. Skeate JG, Otsmaa ME, Prins R, Fernandez DJ, Da Silva DM, Kast WM. TNFSF14: LIGHTing the Way for Effective Cancer Immunotherapy. *Front Immunol* (2020) 11:922. doi: 10.3389/fimmu.2020.00922
116. Le Naour J, Zitvogel L, Galluzzi L, Vacchelli E, Kroemer G. Trial Watch: STING Agonists in Cancer Therapy. *Oncoimmunology* (2020) 9:1777624. doi: 10.1080/2162402X.2020.1777624
117. Gogoi H, Mansouri S, Jin L. The Age of Cyclic Dinucleotide Vaccine Adjuvants. *Vaccines* (2020) 8:453. doi: 10.3390/vaccines8030453
118. Pan BS, Perera SA, Piesvaux JA, Presland JP, Schroeder GK, Cumming JN, et al. An Orally Available non-Nucleotide STING Agonist With Antitumor Activity. *Science* (2020) 369:eaba6098. doi: 10.1126/science.aba6098
119. Aval LM, Pease JE, Sharma R, Pinato DJ. Challenges and Opportunities in the Clinical Development of STING Agonists for Cancer Immunotherapy. *J Clin Med* (2020) 9:3323. doi: 10.3390/jcm9103323
120. Baguley BC. Antivascular Therapy of Cancer: DMXAA. *Lancet Oncol* (2003) 4:141–8. doi: 10.1016/s1470-2045(03)01018-0
121. Wu J, Chen YJ, Dobbs N, Sakai T, Liou J, Miner JJ, et al. STING-Mediated Disruption of Calcium Homeostasis Chronically Activates ER Stress and Primes T Cell Death. *J Exp Med* (2019) 216:867–83. doi: 10.1084/jem.20182192
122. Furman D, Campisi J, Verdin E, Carrera-Bastos P, Targ S. Franceschi, CChronic Inflammation in the Etiology of Disease Across the Life Span. *Nat Med* (2019) 25:1822–32. doi: 10.1038/s41591-019-0675-0
123. Pipi E, Nayar S, Gardner DH, Colafrancesco S, Smith C, Barone F. Tertiary Lymphoid Structures: Autoimmunity Goes Local. *Front Immunol* (2018) 9:1952. doi: 10.3389/fimmu.2018.01952
124. Bakhoum SF, Ngo B, Laughney AM, Cavallo JA, Murphy CJ, Ly P, et al. Chromosomal Instability Drives Metastasis Through a Cytosolic DNA Response. *Nature* (2018) 553:467–72. doi: 10.1038/nature25432
125. Milutinovic S, Abe J, Godkin A, Stein JV, Gallimore A. The Dual Role of High Endothelial Venules in Cancer Progression Versus Immunity. *Trends Cancer* (2021) 7:214–25. doi: 10.1016/j.trecan.2020.10.001

Conflict of Interest: The authors declare that the research was conducted in the absence of any commercial or financial relationships that could be construed as a potential conflict of interest.

Copyright © 2021 Filderman, Appleman, Chelvanambi, Taylor and Storkus. This is an open-access article distributed under the terms of the Creative Commons Attribution License (CC BY). The use, distribution or reproduction in other forums is permitted, provided the original author(s) and the copyright owner(s) are credited and that the original publication in this journal is cited, in accordance with accepted academic practice. No use, distribution or reproduction is permitted which does not comply with these terms.

frontiers in Immunology

REVIEW
published: 14 May 2021
doi: 10.3389/fimmu.2021.675538

Inducible Tertiary Lymphoid Structures: Promise and Challenges for Translating a New Class of Immunotherapy

Shota Aoyama[1†], *Ryosuke Nakagawa*[1†], *James J. Mulé*[2,3] *and Adam W. Mailloux*[4*]

[1] Department of Surgery, Institute of Gastroenterology, Tokyo Women's Medical University, Tokyo, Japan, [2] Immunology Program, Moffitt Cancer Center, Tampa, FL, United States, [3] Cutaneous Oncology Program, Moffitt Cancer Center, Tampa, FL, United States, [4] Department of Microbiology and Immunology, University of Iowa, Iowa City, IA, United States

Tertiary lymphoid structures (TLS) are ectopically formed aggregates of organized lymphocytes and antigen-presenting cells that occur in solid tissues as part of a chronic inflammation response. Sharing structural and functional characteristics with conventional secondary lymphoid organs (SLO) including discrete T cell zones, B cell zones, marginal zones with antigen presenting cells, reticular stromal networks, and high endothelial venues (HEV), TLS are prominent centers of antigen presentation and adaptive immune activation within the periphery. TLS share many signaling axes and leukocyte recruitment schemes with SLO regarding their formation and function. In cancer, their presence confers positive prognostic value across a wide spectrum of indications, spurring interest in their artificial induction as either a new form of immunotherapy, or as a means to augment other cell or immunotherapies. Here, we review approaches for inducible (iTLS) that utilize chemokines, inflammatory factors, or cellular analogues vital to TLS formation and that often mirror conventional SLO organogenesis. This review also addresses biomaterials that have been or might be suitable for iTLS, and discusses remaining challenges facing iTLS manufacturing approaches for clinical translation.

Keywords: immunotherapy, tertiary lymphoid structure (TLS), cancer, bioengineering, biomaterials

OPEN ACCESS

Edited by:
Vivek Verma,
Georgetown University, United States

Reviewed by:
Iain Comerford,
University of Adelaide, Australia
Saba Nayar,
University of Birmingham, United Kingdom

****Correspondence:***
Adam W. Mailloux
adam-mailloux@uiowa.edu

†These authors have contributed equally to this work and share first authorship

Specialty section:
This article was submitted to Cancer Immunity and Immunotherapy, a section of the journal Frontiers in Immunology

Received: *03 March 2021*
Accepted: *27 April 2021*
Published: *14 May 2021*

Citation:
Aoyama S, Nakagawa R, Mulé JJ and Mailloux AW (2021) Inducible Tertiary Lymphoid Structures: Promise and Challenges for Translating a New Class of Immunotherapy. Front. Immunol. 12:675538. doi: 10.3389/fimmu.2021.675538

INTRODUCTION

The presence of infiltrating immune cell populations is a prominent histological feature of most solid tumors that with some exceptions (1, 2), often confers positive prognostic significance across a wide spectrum of indications (3). This benefit is often contingent on the number and phenotypic makeup of the immune infiltrate, and on the ratios of beneficial effector cells to immune suppressive populations (3, 4). This may entail elevated numbers of activated $CD8^+$ cytotoxic T cells (T_C), type-I polarized $CD4^+$ helper T (T_H1) cells, and B cells, signifying an adaptive anti-tumor immune response (3, 5, 6). In a similar fashion, infiltrating antigen-presenting cells such as macrophage and dendritic cells (DC) confer positive prognostic value in many tumor types (7, 8), and in particular those antigen presenting cells with type I polarization attributes are especially equipped to support anti-tumor immunity (9, 10). It is an important understated fact that elements associated with

antigen presentation and immune polarization are found inside solid tumors and confer prognostic benefit alongside effector lymphocyte populations. This infers that active antigen presentation, and the structural organization needed to support it, must occur at the tumor site; thus, an anti-tumor immune response is not limited to remote activation of effector lymphocytes in draining secondary lymphoid organs (SLO), but also occurs locally within and proximal to the tumor mass (4).

It is now understood that many tumors are associated with the presence of tertiary lymph node structures (TLS) (11). TLS consist of structural features analogous to conventional SLO, including discrete B cell zones, T cell zones, marginal zones with activated macrophage and DC, reticular fibroblast cell (RFC) networks (or RFC-like stromal networks), and vasculature permissive to immune cell extravasation (11–13). In mature TLS, this high level of organization can consist of networks of supportive infrastructure are compartmentalized just as they are in SLO, with activated mature DC supporting T_H1 activation in T cell zones (14, 15), and follicular DC localizing to B cell zones in support of humoral immunity (16, 17). TLS form *de novo* in the microenvironment of solid tissues in response to protracted inflammatory stimuli, and may dissipate upon the resolution of inflammation (18). TLS can additionally foster tumor antigen presentation and T cell activation, including germinal centers (19, 20), B cell class switching (21), activated antigen presenting cells (22), and T cell clonal expansion (23, 24). In human cancers, TLS are associated with better disease outcomes across a broad spectrum of indications including ovarian (25, 26), metastatic melanoma (27, 28), breast (29, 30), colorectal (11, 31), and non-small cell lung cancers (7, 14), and can augment the efficacy of immunotherapies such as imune chackpoint inhibitors (28). In murine models, TLS can reduce orthotopic growth of colon carcinoma (32), melanoma (33), and fibrosarcoma (34). These associations and clear demonstrations of beneficial anti-tumor immunity by TLS embody a majority of scenarios that are overwhelmingly positive in nature and that provide a strong basis for pursuing the artificial induction of TLS as a therapeutic modality. However, there are reports in which TLS are associated with negative prognostication or disease progression. This is best exemplified in hepatocellular carcinoma (HCC) (35), and suggests that while TLS represent an integral part of the anti-tumor immune response, their function is likely influenced by a number of contextual signals, including those afforded by local stroma, secreted inflammatory factors, other resident immune populations, local vasculature, and epithelium (36). This may also indicate that different types of TLS exist that are susceptible to immune polarization or can even serve an immune suppressive role depending on and subsequent to microenvironmental context (37). This review will focus on approaches that can be taken to artificially induce TLS as a novel immunotherapy or as a means of augmenting immunotherapies. The prognostic value of TLS has been well reviewed (38, 39).

The clear benefit of TLS has prompted investigation into their potential therapeutic use, both as a standalone treatment or as an adjuvant to adoptive transfer-based cell therapies (40, 41). As such, artificial or inducible TLS (iTLS) hold great promise as a novel immunotherapy, but significant challenges must first be overcome that preclude their advent. These challenges range from knowledge gaps in basic TLS biology to complexities associated with clinical grade biomaterials and autologous cell processing. This review provides an overview of what strategies have been and might be employed to artificially induce TLS, how iTLS may be employed as a novel therapeutic, and what technical difficulties must be addressed prior to manufacturing iTLS at a clinical level.

LESSONS FROM SLO ORGANOGENESIS: STRATEGIES FOR THERAPEUTIC TLS INDUCTION

TLS formation is a complex process incorporating many processes that overlap conceptually with conventional SLO organogenesis (42), although multiple contextual and spacial constraints add complexity to TLS formation. In addition, not all TLS develop to the same level of structural and functional maturity. The level of TLS organization, what ectopic factors contribute to their function and development and how these factors play into prognostication have been well reviewed (36). In this review, we focus on approaches to artificially induce TLS formation, which have thus far been guided by our understanding of shared pathways between SLO organogenesis and natural TLS formation. Any successfully implemented iTLS will likely be subject to the same functional and organizational variations as seen in natural TLS caused by diverse microenvironmental cues present in different organs and indications. Thus, any clincial translation of iTLS must expect disease-specific challenges and variations regarding efficacy.

SLO initiate during embryogenesis following expression of lymphotoxin alpha-1, beta-2 ($LT\alpha1\beta2$) on specialized lymphoid tissue inducer cells (LTi) (43) that binds to lymphotoxin beta receptor (LTBR) expressed on lymphoid tissue organizer cells (LTo), an early mesenchymal-derived fibroblast (42). Engagement of LTBR induces the expression of numerous NF-κB target genes (44, 45) that orchestrate the recruitment of different immune cells. NF-κB signals *via* two separate pathways, canonical and non-canonical. Canonical signaling leads to the translocation of p50/RelA dimers to the nucleus, where they induce CCL4, CXCL2, and CCL2 among other gene targets, while non-canonical NF-κB signaling leads to the translocation of p52/RelB dimers to the nucleus inducing CXCL13, CCL19, and CCL21 (44). This results in the recruitment of early $CD11c^+$ myeloid populations followed by mass immigration of B and T cells which segregate into discrete T cell zones and B cell follicles (46, 47). This influx of lymphocyte subsets coincides with the LTBR-dependent development of high endothelial venules (HEV), and is followed by the LTBR-dependent appearance of antigen-presenting cells such as follicular DC (FDC) (48–50). As the SLO develops, LTo cells differentiate into RFC through continued LTBR signaling (51). Importantly, SLO formation

requires both NF-κB signaling pathways to properly develop, although the non-canonical pathway appears more indispensable (45). In adults, there is no clear evidence that LTi or LTo cells persist, and so for TLS formation it is less clear which cell types fill these roles. However, overexpression of LTα1β2 markedly increase TLS (2), whereas LTBR blockade prevents TLS in murine models (52); this suggests that any cell expressing LTα1β2 has the potential to function as a LTi analogue, and any $LTBR^+$ stromal cell capable of chemokine production has the potential to function as a LTo analogue. Importantly, most mesenchymal-derived stroma throughout the body expresses LTBR (53), including RFC (54). Additionally, LTα1β2 is expressed on activated T cells, B cells, and dendritic cells (55), giving this signaling axis wide-reaching potential for TLS induction if the correct environmental inflammatory cues are met. Importantly, engagement of LTBR on many types of mesenchymal-derived stroma induces analogous expression of both canonical and non-canonical NF-κB target genes as compared to LTo, including the lymphoid tissue homeostatic cytokines CXCL13, CCL19 and CCL21 necessary for SLO development (1). In addition to LTα1β2, another LTBR ligand, homologous to lymphotoxin, exhibits inducible expression and competes with HSV glycoprotein D for binding to herpesvirus entry mediator, a receptor expressed on T lymphocytes (LIGHT) effectively elicits chemokine gene targets on $LTBR^+$ stroma through NF-κB (56). LIGHT signaling can also lead to TLS formation, and while also binding to other receptors such as Herpesvirus entry mediator (HVEM), LIGHT acts analogous to LTα1β2 in its capacity to induce TLS formation (34, 57).

The role of chemokines in both SLO organogenesis and in TLS formation cannot be understated. For SLO, the narrow set of homeostatic chemokines required for organogenesis reflects the chemokine receptor patterns expressed by naïve and resting memory T cells, and coincides with the chemokine receptors expressed by DC and macrophage (58). Activated lymphocytes follow different trafficking patterns throughout the periphery owing to the downregulation of SLO-homing chemokine receptors and the up-regulation of alternative chemokine receptor sets that allow for emigration from SLO and infiltration into inflamed peripheral sites (59). It is thus unsurprising that gene signatures associated with TLS formation in tumors encompass not only SLO-associated homeostatic chemokines, but many other chemokines capable of recruiting lymphocytes in various stages of activation and effector function and that are associated with peripheral lymphocyte trafficking (13). A TLS gene signature which incorporates 12 chemokines (12CK-GES) that was associated with better patient survival independent of tumor staging, was first identified in patients with colorectal carcinoma (11) and was soon after used to predict the presence of TLS in wide range of tumor types including melanoma, lung, breast, and colorectal (13, 29). Importantly, nine of the chemokines identified in the 12CK-GES have reported up-regulation by LTBR signaling in mesenchymal-derived stroma through canonical or non-canonical NF-κB signaling, whereas the remaining three are hallmark products of tumor-associated macrophages (TAM), or type-II polarized macrophages (60–64) which themselves are recruited by multiple members of the 12CK-GES (**Table 1**). Insights from the 12CK-GES, and the parallels to SLO organogenesis can easily lead one to speculate that TLS form *via* a sequential or semi-sequential recruitment of immune subsets in response to chronic LTBR stimulation, and that any chemokines in the 12CK-GES not directly produced by $LTBR^+$ stroma might be indirectly accounted for by subsequently recruited immune populations. In addition to TLS-associated chemokines, LTBR signaling also regulates the expression of a number of homeostatic cytokines and growth factors important to SLO organogenesis and to TLS formation, including IL-7, IL-15, and B cell activating factor (BAFF) (44, 72). However, to prove that any components of TLS organization form through sequential recruitment steps requires an experimental model of TLS formation in which temporal data can be acquired. When considering TLS induction as an anti-cancer therapeutic, such models may be necessary to deduce which components of TLS formation are required for anti-tumor activity, and which component might be expendable for anti-tumor effect.

Strategies for iTLS can either utilize methods to initiate sustained LTBR signaling, thereby taking advantage of the same

TABLE 1 | 12CK-GES and associated NF-κB signaling pathways.

Chemokine signature	LTBR target	NF-κB pathway	Reference	Recruitment potential	Cognate Receptor(s)
CCL2	Yes	Canonical	(44)	T, M, MDSC, TAM	CCR2, CCR3,
CCL4	Yes	Canonical	(44)	M, MDSC, TAM	CCR5
CXCL10	Yes	Canonical	(65)	T, NK, TAM	CXCR3
CXCL11	Yes	Canonical	(66)	T, NK, TAM	CXCR3,
CCL5	Yes	Non-canonical	(67, 68)	T, M	CCR1, CCR3, CCR5
CCL19	Yes	Non-canonical	(44)	T, DC	CCR7
CCL21	Yes	Non-canonical	(44)	T, DC	CCR7
CXCL13	Yes	Non-canonical	(44)	B	CXCR5
CCL3	Yes	Canonical	(69)	M, T, NK, DC	CCR1, CCR5
CCL8	No	Canonical	(69)	M, NK, T, B, DC	CCR2
CCL18	No	No	(70)	DC	CCR8
CXCL9	No	No	(71)	T, NK	CXCR3

Beneficial Cell Types: T, T cell; B, B cell; M, monocyte/macrophage; NK, Natural Killer Cell; DC, Dendritic Cells.
Suppressive Cell Types: MDSC, Myeloid-derived Suppressor Cell; TAM, Tumor-associated Macrophage.

cascade of events that leads to naturally occurring TLS, by introducing cellular components engineered with constitutively active LTBR or with transgenic expression of LTBR gene targets, by some combination of the above approaches, or by complete TLS manufacture ex vivo prior to adoptive transfer/retransfer (**Figure 1**). iTLS methods that involve the introduction of isolated or cultivated cellular components have an additional appeal beyond the iTLS itself. The central role that antigen presenting cells play in TLS formation and function (73) and the effector cell-recruiting potential TLS create in the tumor microenvironment (57) make iTLS an ideal platform for the delivery of DC-based anti-tumor vaccines or as an adjuvant for chimeric antigen receptor-transduced T cell (CAR-T) or tumor-infiltrating lymphocyte (TIL) adoptive transfer therapies. Given the breadth of possible approaches, novel iTLS-based therapies can be designed with goals ranging from early interventional to multi-modal combination therapies that bridge cellular therapies, immunotherapies, and/or chemotherapeutic and radiation therapies.

Early demonstrations that the LTBR-chemokine axis can be utilized for iTLS occurred in transgenic model systems in which mice overexpressing chemokines or LTα developed lymph node-like structures in certain tissues (74). In mice expressing LTα under the rat insulin promoter, a promotor with transgene expression limited to pancreatic beta cells and proximal tubule of the kidney, TLS formation was observed in both the pancreas and kidney, especially in proximity to vasculature where the formation of HEV was evident (74). Under the same promoter, transgenic CCL21 induced HEV-containing TLS in the pancreas as well (75, 76), but using a promoter with skin-specific CCL21 expression did not result in TLS; these data suggest that additional cues or microenvironmental constraints are needed for TLS beyond CCL21 expression alone (75). Other examples include LTBR ligand targeting strategies, such as delivery of recombinant LIGHT tagged to vascular-targeting peptide. This chimeric compound induced TLS in pancreatic neuroendocrine tumors and in glioblastoma in areas surrounding dense vasculature that contain discrete B cell zones, T cell zones, macrophage, HEV, and DC (32, 77). Delivery of LTBR ligands to induce TLS is also possible *via* adoptive cell transfer of transgenic cells. DC transduced with the type-I polarizing transcription factor T-bet induced the expression of LIGHT and LTα, and subsequently CCL21, when injected into murine colon adenocarcinoma, slowing tumor growth (73, 78). Lastly, delivery of $LTBR^{+}$ stroma demonstrates functional TLS formation when injected subcutaneously juxtaposed to established MC-38 murine colon carcinoma tumors, slowing tumor growth and actively priming T cell response (79). Despite the precedent that TLS can be induced by taking advantage of the LTBR-chemokine axis, the greatest benefit from iTLS will likely result from injectable or implantable preparations that do not require additional microenvironmental cues from the recipient host. This way, they may be applied to a wider range of tissues and organs as part of a microenvironment reprogramming

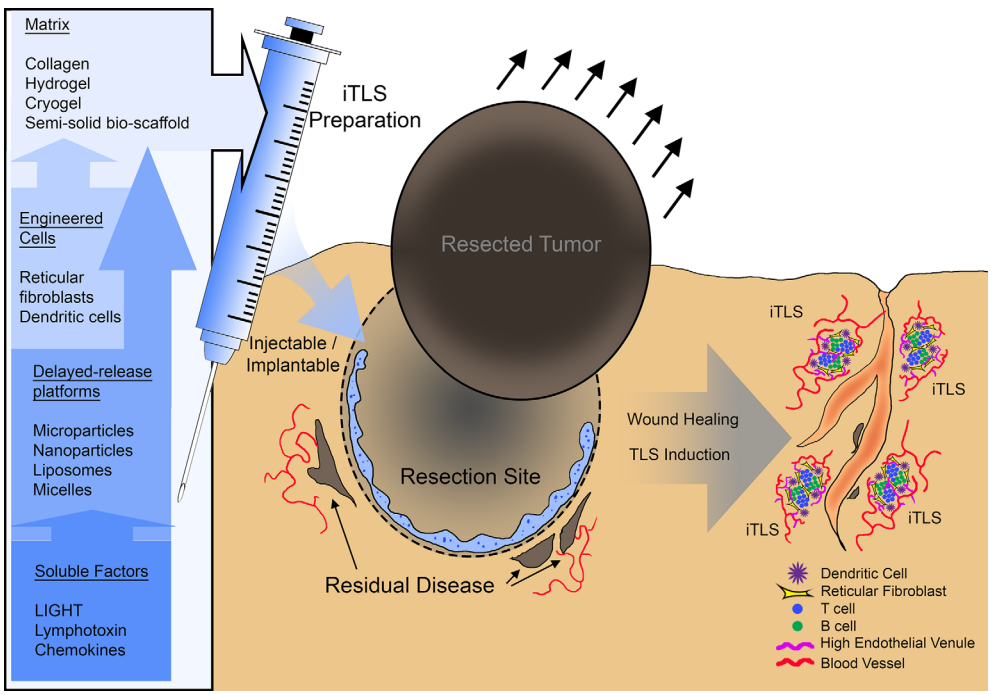

FIGURE 1 | A summary schematic of potential therapeutic use of inducible tertiary lymphoid structures (iTLS). iTLS preparations may include cellular components such as dendritic cells, or reticular fibroblasts modified to engage the LTBR pathway, or co-delivered with soluble LTBR-ligands *via* a delayed-release platform such as liposomes, nanoparticles, or micelles. Injectable or implantable iTLS preparations could be administered at the site of tumor resection to induce TLS and subsequently control residual disease or counteract reoccurrence.

strategy. Discussed below are biocompatible matrixes and micro/nanoparticles that may be suitable as scaffolding material for iTLS or for the sustained release of biologics aimed at TLS induction respectively.

BIOMATERIALS WITH PROPOSED SUITABILITY FOR ITLS

A variety of three-dimensional materials that are permissible to cellular infiltration and that may allow for cell-scaffold interactions have been used for tissue engineering, regenerative medicine, and ex vivo scientific investigation (80). Some bio-scaffolds derived from animal or cell-based products such as Matrigel® (Corning Life Sciences) have a decades-long precedent. These products isolate entire acid-soluble constituents of tumor cell line-derived extracellular matrix, and thus represent a more physiologically complete microenvironment than synthetic scaffolds. However, such products are not immunologically inert, and contain growth factors and biologically active components that have well described angiogenic, adipogenic, and inflammatory properties (81). This is even true of "growth factor reduced" product versions (albeit improved) (81, 82). As such, use of such cell or animal-derived matrixes often invites scientific scrutiny (83), and thus more advanced synthetic alternatives are typically sought for bioengineering endeavors which contain less lot-to-lot variation, display a more immunologically inert background, and lack any confounding variables caused by biologically active carryover components (81).

Collagen Matrixes

Collagens constitute the major framework of the extracellular matrix (ECM) with distinct primary, secondary, tertiary, and quaternary structures that create a range of ECM scaffold superstructures in different tissues and organs from rope-like fibrils to web-like networks, anchoring structures, and can even complex with transmembrane collagens (84). In vertebrates, at least 29 types of collagen are coded by at least 45 separate genes (85). Given the complexity of collagen, tissues from animals or human-sourced raw materials are often used to make collagen-based scaffolding materials (86). Recombinant sources of collagen monomers or peptides are commercially available (87) but small yields and the lack of the tertiary and quaternary structural complexity that would be afforded by multi-collagen type complexes limit their use as a scaffold for bioengineering (86). Most collagen products are manufactured in one of two ways: from decellularization of existing ECM, resulting in an intact ECM superstructure (88), or through the breakdown, solubilization, extraction, and reformulation of collagen, often with the addition of crosslinking agents such as glycosaminoglycans (89, 90), elastins (91, 92), or chitosans (93, 94). The precise methodologies used to manufacture commercial collagen matrix products should be carefully considered prior to implementation in iTLS approaches since most collagen-based matrixes are derived from animal or human tissues (86). While more purified than bulk ECM products like Matrigel®, biologically active impurities may still carry over from raw materials (95). A major strength of collagen-based matrixes is their versatility in available formats, including sheets, sponges, disks, granulated tablets, or even nano-scale spheres (96).

One of the first successful demonstrations of iTLS using implantable artificial matrix was performed by Suematsu and Wantanabe using a collagen sponge biomatrix impregnated with a thymus-derived stromal cell line modified to constitutively express LTα. Following implantation, functionality of iTLS was demonstrated by vaccination with 4-hydroxy3-nitrophenylacetyl-ovalbumin (NP-OVA). Three weeks after subcutaneous implantation, discrete B cell and T cell zones formed in the stromal cell-impregnated collagen sponge with interacting DC, as well as HEV-like structures. Recipient mice that were vaccinated with NP-OVA produced anti-NP-OVA IgG-producing B cells within iTLS. This effect was bolstered if NP-OVA-pulsed DC were included in preparations. Furthermore, these NP-OVA-primed iTLS could be resected after their formation, and transplanted to syngeneic recipient mice wherein they could mount effective secondary response to NP-OVA (97). These iTLS were later shown to be able to produce a potent secondary immune response when transplanted into severe combined immunodeficiency (SCID) recipient mice, repopulating SLO and bone marrow with anti-NP-OVA IgG-producing B cells (98). An alternative approach using chemokine and VCAM-1-loaded collagen matrix instead of stromal cells soon followed, recapitulating the successes of stromal-cell line-loaded collagen sponges. These chemokine-induced TLS incorporated B cell zones, T cell zones, and supporting DC and were able to prime a similar anti-NP-OVA response. HEV were not interrogated in these iTLS (99).

Hydrogels

Hydrogel refers to a large class of biomaterials that are made of three-dimensional crosslinked polymers with a large capacity for water uptake and retention that are prepared in aqueous solution (100). Depending on the types of polymers and crosslinking reagents used, a wide variety of hydrogels can be prepared that have different properties regarding biologic interactivity or inertness, physical rigidity or elasticity, temperature sensitivity, pH sensitivity, shape memory properties, or capacity to carry and deliver soluble drugs or cellular payloads (101–103). Hydrogels can be classified according to physical structure, charge, size or chemical properties (102). Of relevance to iTLS efforts, most hydrogel preparations can be injectable or transplantable depending on the timing and chemistries of the crosslinking steps, and can be formulated in large injection/implantation volumes or in micro or even nanoscale particle preparations (104). Because of their large capacity to hold aqueous solution, many hydrogel preparation methodologies are widely compatible with cell culture conditions so long as the chemistries required for crosslinking do not stray from physiologic pH, temperature, salinity, and other cell culture ranges (105–107). For this reason, crosslinking chemistries that utilize mild temperature or pH changes such as warming from 4°C to 37°C or changing from a slightly acidic solution to slightly basic are ideal for injectable preparations, as such hydrogels would crosslink *after* injection into living recipients (105, 107).

When used as an *in vitro* model for iTLS, hydrogel preparations with BAFF-producing stromal cells and IL-4 support the compartmentalization, expansion, and class-switching of primary B cells (108, 109). When used as a model of cell therapy delivery, hydrogels have been successfully deployed to carry CAR-T cells in conjunction with delivering stimulator of IFN genes (STING) agonist cyclic di-GMP. This preparation was then placed in resection sites of murine pancreatic tumors, or alongside pancreatic tumors mimicking non-resectable masses. These implants produced a significant anti-tumor effect compared to intravenously delivered CAR-T, activated host DC, and induced significant infiltration of immune cells at the implantation sites (110).

Cryogels, a subset of hydrogels prepared at sub 0°C, may be of particular interest to iTLS efforts. Their preparation creates a larger pore size than typical hydrogels, which are typically measured in the nanometer range. Such a small pore size requires hydrogel breakdown or active turnover by infiltrating populations to emigrate or infiltrate transferred materials, significantly limiting cellular involvement (111, 112). Cryogels are formed when polymer and cross linkers are displaced by ice crystal formation, causing concentration spikes in localized spaces in between ice crystals. When the cryogels are subsequently thawed, the space occupied by the ice crystals leaves a porous network measured on a micron scale or larger (113, 114). Thus, cryogels provide a more cell-invasive alternative to conventional cryogels, although, their freeze/thaw preparation method requires any would-be cellular components to be loaded after formation and precludes any formation post injection, somewhat limiting their use to implantation. Cryogels have been be used to deliver chemotherapies and cancer vaccines (115), and when incorporated with DC activating components and tumor antigen vaccination strategies, induces the recruitment of DC and lymphocytes (113, 116, 117), although the organization of these infiltrates was not investigated.

Other Solid or Semi-Solid Bio-Scaffolds

A wide array of scaffolding material distinct from hydrogels or tissue-derived collagen matrixes have been derived for use in tissue repair, wound-healing, or other bioengineering endeavors (118). Among these are matrixes made from mesoporous silica rods, which have been used to boost the immunogenicity of tumor antigen peptide-based vaccine approaches in mice bearing B16F10 melanoma or CT26 colon carcinoma tumors. In these models, tumor associated antigen pools were loaded into mesoporous silica rod matrixes and injected subcutaneously. While the organization of infiltrates was not analyzed histologically, vaccination using this matrix approach greatly enhanced lymphocyte infiltration, and activation, as well as mediated anti-tumor effects on lung nodule growth (119). While not evidence of iTLS, this study does provide precedence for silica as a biomaterial supportive of lymphocyte recruitment, DC activation, and antigen priming. Another bio-matrix that may be permissive to iTLS are polyamide fiber preparations. In what represents one of the earliest attempt to manufacture iTLS entirely in situ, non-woven sheets of polyamide fibers were loaded with antigen-primed primed DC (in this case, cytomegalovirus lysate) and sealed inside a closed and chambered bioreactor system in which lymphocytes isolated from peripheral blood mononuclear cells (PBMC) were continuously circulated. After two weeks, this bioreactor approach resulted in TLS-like structures with discrete B cell and T cell clusters around DC inside the polyamide fiber sheets. Cytokine production suggests that these lymphocytes were activated by the primed DC (120).

Micro and Nanoparticles in iTLS

While bio-scaffolds can, in some instances, impart delayed release of soluble factors, another class of biomaterials has been refined over time with delayed-release of soluble factors as one of several defining characteristics. Microparticles or nanoparticles represent entire fields of materials science in their own right (121). Here, microparticles and nanoparticles are proposed as cooperative biomaterial elements that can be used as an incorporated element within bio-scaffolding to mediate controlled release of chemokines, LTBR ligands, or other TLS-inducing factors. Of these, liposomes represent the most studied and characterized class of micro or nanoscale biomaterials that can serve as carriers for a wide range of compounds. Liposomes form when lipid components assemble into spherical bilayers leaving an aqueous compartment that carry a water-soluble payload (122). The physical properties of liposomes can be easily controlled by altering the types of lipids used for incorporation (123–126), and their size can be controlled by deploying different production methods such as sonication, which delivers liposomes in the 20-40 nm range (127), microfluidic mixing in the 20-80 nm range (128, 129), high pressure homogenization in the 20-140 nm range (130), flow focusing in the 50-150 nm range (131), and extrusion in the 70-415 nm range (132). Many liposomes are already incorporated as part of FDA-approved drugs (133, 134) giving precedent to their clinical translatability and patient safety, and there are now multitudes of methodologies that can deliver on a wide range of specifications, cost, uniformity, and bulk manufacturing requirements (135).

Unmodified liposomes were first described 55 years ago (136), and while successful, have limitations due to their unprotected outer lipid surface, making them subject to fusion with other liposomes as natural result of surface tension reduction (137, 138). Unmodified liposomes are also susceptible to opsonization of serum protein following injection which can lead to phagocytic uptake, or clearance in the liver (139, 140). Any such alteration manipulates drug release kinetics or limits payload delivery to intended targets. A second generation of liposomes was created by modifying liposomal surfaces with integrated polymers, providing structural stabilization and interfering with serum protein binding (139, 141), the most successful of which has been polyethylene glycol (PEG) (142, 143). Additional modification strategies have been employed to liposomes within the last 20 years that not only aim to stabilize liposomal formulations, but to also impart drug target selectivity or more precisely control drug release. Examples of such modifications include liposomes with surface-attached bioactive ligands, such as aptamers, peptides, or most

commonly immunoglobulin or immunoglobulin fragments (144). By incorporating moieties with known affinities for antigens expressed on target tissues (or tumors), liposomes can then specifically interact with intended targets. Such incorporations can be accomplished by including recombinant protein products in the initial lipid formulations that either naturally contain hydrophobic regions or that are themselves modified to contain hydrophobic regions, or by covalent binding to hydrophilic regions of incorporated lipids (145). Of particular relevance to iTLS, liposomes can offer extended release kinetics of their payloads, or even be designed for content release in response to an external trigger, such as temperature (146), magnetic fields (147), or light (148, 149). In addition, liposomes are compatible with other bio-scaffolding materials such as hydrogels, cryogels, or polymeric matrixes (150), and have a demonstrated ability for delayed release of chemokines such as CXCL13 (151).

Other nanoscale particles capable of delivering or releasing inflammatory mediators include micelles which are created by self-assembling amphiphilic polymers (152, 153). Micelles have proven capacity to deliver cytokines (154), antigens (155), and interfering RNAs (156, 157), and thus represent a plausible alternative to liposomes to deliver factors for iTLS. In addition, nanoparticles made from aliphatic polyesters (PLGA) are also an attractive option to incorporate delayed-release of soluble factors, and are already FDA-approved in many clinical contexts (158–160). PLGA nanoparticles are biodegradable, and like micelles, are capable of tumor antigen delivery (161, 162) and immunotherapeutic biologics (163, 164). In what is perhaps the most robust example of iTLS generated in animal models, Kobayashi and Watanabe combined microscale gelatin-based hydrogels loaded with LTα1β2, CCL19, CCL21, CXCL12, CXCL13, and soluble RANKL inside a macroscale implantable collagen sponge. This preparation was then implanted onto the kidney capsule of recipient mice, and after three weeks produced mature iTLS with discrete T cell zones, B cell zones, RFC networks, FDC in what appears to be a marginal zone, HEV, and lymphatic vasculature. These iTLS were also able to prime primary and secondary IgG responses to NP-OVA (165). Another example of combined biomaterial approaches utilized lipid-coated silica microspheres harboring IL-15/IL-15Ra fusion proteins and anti-CD3, anti-CD18, and anti-CD137 antibodies to act as artificial antigen-presenting cells inserted into alginate hydrogels loaded with NKG2D-CAR-expressing murine T cells. This construct, when implanted next to partially resected established subcutaneous 4T1 breast cancer tumor-bearing mice, elicited significant anti-tumor reactivity and slowed tumor growth (166). While not necessarily iTLS, this study further establishes precedent that combination biomaterials can deliver and expand effector lymphocytes.

Challenges Awaiting iTLS for Clinical Translation

Avoiding Foreign Body Response for Incorporated Biomaterials

One general drawback to the use of biomaterials is the induction of a foreign body response (FBR), an acute inflammatory reaction against the material itself (167). FBR can result in a wide range of unintended consequences including but not limited to vascularization, fibrotic encapsulation, and infiltration of innate immune cells (168, 169). Neutrophils and macrophages are among the earliest effector cells responding to the FBR and can destroy implanted biomaterials through the release of cytotoxic granules, reactive oxygen species, proteolytic enzymes, and phagocytosis (170–173). Of particular importance to iTLS, recruited and activated macrophages and neutrophils produce high levels of chemokines associated with FBR such as CXCL8, CCL2, CCL4 (174, 175). While CCL2 and CCL4 are part of the 12CK-GES associated with TLS presence in human tumors, CXCL8 is not (11), and none of these chemokines encompass the SLO homeostatic chemokines CXCL13, CCL19 and CCL21 previously used for iTLS, as discussed above. In addition, physical macrophage adherence to many biomaterials polarizes them to a M2 phenotype, which may be detrimental to iTLS formation for anti-tumor immunity (176). To avoid a FBR, it is advantageous to select biomaterials with low antigenicity that have little or no carryover of soluble factors from animal sources (167). In addition, biomaterial topography has also been identified as a contributing factor to FBR, and thus biomaterial size, shape, and texture can be modified to minimize FBR (177, 178). However, any such measure would need to be weighed against the need to recruit cellular infiltrate as part of the iTLS.

Generating cGMP Materials for iTLS Manufacture

As ever more complex components and methodologies are used to innovate iTLS as a potential therapy, so too do the challenges associated with translating such approaches to the clinic. To fully qualify for the Food and Drug Administration's (FDA) approval, components used to make any would-be iTLS therapy need to graduate to clinical-grade materials by the time pivotal trials are conducted, meaning the components themselves must be manufactured under cGMP conditions (179). Not only does this add difficulty to the process, but in almost every scenario, results in elevated manufacturing cost (180, 181). Cell therapies utilizing one cell type with one gene modification can easily exceed $400,000 per dose due in no small part to the elevated cost of manufacturing cell therapies at a cGMP level (182). Given the potentially multimodal processes involved in iTLS development, this new class of immunotherapy may incur clinical-grade manufacturing costs reflective of cell therapies, biomaterials, and biologics combined. In addition to cost, there are also regulatory challenges. Biomaterial products which contain no cellular or bioactive components, such as an inert scaffolding material, might be considered from a regulatory perspective as a "medical device" depending on their mode of action, but should such material be combined with cellular components or biologics, it will most certainly be considered a drug (183). Careful consideration will then need to be taken when defining what components are drug product versus drug substance. Conventionally, the drug substance is whatever components entail the "active ingredient(s)," whereas the drug product is the entirety of the components and compositions used in the manufacturing process. These definitions are critical to the regulatory success of new investigational drugs, but may be less

clear for iTLS, which may combine novel biomaterials with varying amounts of bioactivity (184), with active biologics and cell therapies which may contain genetic modifications. Similar to the advent of cell therapies over the past few decades, the clinical translation of bioengineered constructs such as iTLS may be codependent on the FDA's creation of a new guidelines that are developed in concert with the scientific field (185).

CONCLUDING REMARKS

The progress toward utilizing TLS as a therapeutic intervention has made great strides over the last few decades and has come to incorporate many new and technologies, particularly in the biomaterials space. iTLS have to potential to become an entire new class of immunotherapy combining elements of biologic compounds, cellular therapeutics, and biofabrication techniques. However, significant challenges and unanswered questions remain. These include identifying the optimal bio-scaffold/nanomaterial combinations for sustained release of TLS-inducing soluble factors and identifying the minimal combination of chemokines, LTBR ligands, and other soluble factors required for robust iTLS formation. Another prominent point of consideration is to further evaluate if stromal and/or DC components are needed for iTLS approaches. Their involvement has been critical to early iTLS successes, but recent advances demonstrate iTLS can be achieved using cell-free constructs (165). This would have obvious benefits when translating to clinical-grade manufacturing processes, and allow for less costly clinical translation.

AUTHOR CONTRIBUTIONS

SA and RN performed literature searches, outlined sections, and reviewed and edited the manuscript, JJM reviewed and edited the manuscript, and provided funding, AWM wrote the manuscript, created the figure and table, reviewed and edited the manuscript, and provided funding. All authors contributed to the article and approved the submitted version.

FUNDING

This work was funded by the NCI-NIH (1R01 CA148995, 1R01 CA184845, P30 CA076292, P50 CA168536, and 5R21CA214285), Cindy and Jon Gruden Fund, Chris Sullivan Fund, V Foundation, and the Dr. Miriam and Sheldon G. Adelson Medical Research Foundation.

REFERENCES

1. Fernandes MT, Dejardin E, dos Santos NR. Context-Dependent Roles for Lymphotoxin-Beta Receptor Signaling in Cancer Development. *Biochim Biophys Acta* (2016) 1865(2):204–19. doi: 10.1016/j.bbcan.2016.02.005
2. Wolf MJ, Seleznik GM, Zeller N, Heikenwalder M. The Unexpected Role of Lymphotoxin Beta Receptor Signaling in Carcinogenesis: From Lymphoid Tissue Formation to Liver and Prostate Cancer Development. *Oncogene* (2010) 29(36):5006–18. doi: 10.1038/onc.2010.260
3. Senovilla L, Vacchelli E, Galon J, Adjemian S, Eggermont A, Fridman WH, et al. Trial Watch: Prognostic and Predictive Value of the Immune Infiltrate in Cancer. *Oncoimmunology* (2012) 1(8):1323–43. doi: 10.4161/onci.22009
4. Goc J, Fridman WH, Sautes-Fridman C, Dieu-Nosjean MC. Characteristics of Tertiary Lymphoid Structures in Primary Cancers. *Oncoimmunology* (2013) 2(12):e26836. doi: 10.4161/onci.26836
5. Fridman WH, Pages F, Sautes-Fridman C, Galon J. The Immune Contexture in Human Tumours: Impact on Clinical Outcome. *Nat Rev Cancer* (2012) 12(4):298–306. doi: 10.1038/nrc3245
6. Nielsen JS, Sahota RA, Milne K, Kost SE, Nesslinger NJ, Watson PH, et al. CD20+ Tumor-Infiltrating Lymphocytes Have an Atypical CD27- Memory Phenotype and Together With CD8+ T Cells Promote Favorable Prognosis in Ovarian Cancer. *Clin Cancer Res* (2012) 18(12):3281–92. doi: 10.1158/1078-0432.CCR-12-0234
7. Dieu-Nosjean MC, Antoine M, Danel C, Heudes D, Wislez M, Poulot V, et al. Long-Term Survival for Patients With Non-Small-Cell Lung Cancer With Intratumoral Lymphoid Structures. *J Clin Oncol* (2008) 26(27):4410–7. doi: 10.1200/JCO.2007.15.0284
8. Remark R, Alifano M, Cremer I, Lupo A, Dieu-Nosjean MC, Riquet M, et al. Characteristics and Clinical Impacts of the Immune Environments in Colorectal and Renal Cell Carcinoma Lung Metastases: Influence of Tumor Origin. *Clin Cancer Res* (2013) 19(15):4079–91. doi: 10.1158/1078-0432.CCR-12-3847
9. Najafi M, Hashemi Goradel N, Farhood B, Salehi E, Nashtaei MS, Khanlarkhani N, et al. Macrophage Polarity in Cancer: A Review. *J Cell Biochem* (2019) 120(3):2756–65. doi: 10.1002/jcb.27646
10. Jayasingam SD, Citartan M, Thang TH, Mat Zin AA, Ang KC, Ch'ng ES. Evaluating the Polarization of Tumor-Associated Macrophages Into M1 and M2 Phenotypes in Human Cancer Tissue: Technicalities and Challenges in Routine Clinical Practice. *Front Oncol* (2019) 9:1512. doi: 10.3389/fonc.2019.01512
11. Coppola D, Nebozhyn M, Khalil F, Dai H, Yeatman T, Loboda A, et al. Unique Ectopic Lymph Node-Like Structures Present in Human Primary Colorectal Carcinoma are Identified by Immune Gene Array Profiling. *Am J Pathol* (2011) 179(1):37–45. doi: 10.1016/j.ajpath.2011.03.007
12. Dieu-Nosjean MC, Goc J, Giraldo NA, Sautes-Fridman C, Fridman WH. Tertiary Lymphoid Structures in Cancer and Beyond. *Trends Immunol* (2014) 35(11):571–80. doi: 10.1016/j.it.2014.09.006
13. Messina JL, Fenstermacher DA, Eschrich S, Qu X, Berglund AE, Lloyd MC, et al. 12-Chemokine Gene Signature Identifies Lymph Node-Like Structures in Melanoma: Potential for Patient Selection for Immunotherapy? *Sci Rep* (2012) 2:765. doi: 10.1038/srep00765
14. Goc J, Germain C, Vo-Bourgais TK, Lupo A, Klein C, Knockaert S, et al. Dendritic Cells in Tumor-Associated Tertiary Lymphoid Structures Signal a Th1 Cytotoxic Immune Contexture and License the Positive Prognostic Value of Infiltrating CD8+ T Cells. *Cancer Res* (2014) 74(3):705–15. doi: 10.1158/0008-5472.CAN-13-1342
15. Movassagh M, Spatz A, Davoust J, Lebecque S, Romero P, Pittet M, et al. Selective Accumulation of Mature DC-Lamp+ Dendritic Cells in Tumor Sites is Associated With Efficient T-Cell-Mediated Antitumor Response and Control of Metastatic Dissemination in Melanoma. *Cancer Res* (2004) 64(6):2192–8. doi: 10.1158/0008-5472.CAN-03-2969
16. Bergomas F, Grizzi F, Doni A, Pesce S, Laghi L, Allavena P, et al. Tertiary Intratumor Lymphoid Tissue in Colo-Rectal Cancer. *Cancers (Basel)* (2011) 4(1):1–10. doi: 10.3390/cancers4010001
17. Drayton DL, Ying X, Lee J, Lesslauer W, Ruddle NH. Ectopic LT Alpha Beta Directs Lymphoid Organ Neogenesis With Concomitant Expression of Peripheral Node Addressin and a HEV-Restricted Sulfotransferase. *J Exp Med* (2003) 197(9):1153–63. doi: 10.1084/jem.20021761
18. Moyron-Quiroz JE, Rangel-Moreno J, Kusser K, Hartson L, Sprague F, Goodrich S, et al. Role of Inducible Bronchus Associated Lymphoid Tissue

(Ibalt) in Respiratory Immunity. *Nat Med* (2004) 10(9):927–34. doi: 10.1038/nm1091
19. de Chaisemartin L, Goc J, Damotte D, Validire P, Magdeleinat P, Alifano M, et al. Characterization of Chemokines and Adhesion Molecules Associated With T Cell Presence in Tertiary Lymphoid Structures in Human Lung Cancer. *Cancer Res* (2011) 71(20):6391–9. doi: 10.1158/0008-5472.CAN-11-0952
20. Silina K, Soltermann A, Attar FM, Casanova R, Uckeley ZM, Thut H, et al. Germinal Centers Determine the Prognostic Relevance of Tertiary Lymphoid Structures and are Impaired by Corticosteroids in Lung Squamous Cell Carcinoma. *Cancer Res* (2018) 78(5):1308–20. doi: 10.1158/0008-5472.CAN-17-1987
21. Schroder AE, Greiner A, Seyfert C, Berek C. Differentiation of B Cells in the Nonlymphoid Tissue of the Synovial Membrane of Patients With Rheumatoid Arthritis. *Proc Natl Acad Sci USA* (1996) 93(1):221–5. doi: 10.1073/pnas.93.1.221
22. Hughes CE, Benson RA, Bedaj M, Maffia P. Antigen-Presenting Cells and Antigen Presentation in Tertiary Lymphoid Organs. *Front Immunol* (2016) 7:481. doi: 10.3389/fimmu.2016.00481
23. Joshi NS, Akama-Garren EH, Lu Y, Lee DY, Chang GP, Li A, et al. Regulatory T Cells in Tumor-Associated Tertiary Lymphoid Structures Suppress Anti-Tumor T Cell Responses. *Immunity* (2015) 43(3):579–90. doi: 10.1016/j.immuni.2015.08.006
24. Zhu W, Germain C, Liu Z, Sebastian Y, Devi P, Knockaert S, et al. A High Density of Tertiary Lymphoid Structure B Cells in Lung Tumors is Associated With Increased CD4(+) T Cell Receptor Repertoire Clonality. *Oncoimmunology* (2015) 4(12):e1051922. doi: 10.1080/2162402X.2015.1051922
25. Kroeger DR, Milne K, Nelson BH. Tumor-Infiltrating Plasma Cells are Associated With Tertiary Lymphoid Structures, Cytolytic T-Cell Responses, and Superior Prognosis in Ovarian Cancer. *Clin Cancer Res* (2016) 22 (12):3005–15. doi: 10.1158/1078-0432.CCR-15-2762
26. Truxova I, Kasikova L, Hensler M, Skapa P, Laco J, Pecen L, et al. Mature Dendritic Cells Correlate With Favorable Immune Infiltrate and Improved Prognosis in Ovarian Carcinoma Patients. *J Immunother Cancer* (2018) 6 (1):139. doi: 10.1186/s40425-018-0446-3
27. Mattlage AE, Ashenden AL, Lentz AA, Rippee MA, Billinger SA. Submaximal and Peak Cardiorespiratory Response After Moderate-High Intensity Exercise Training in Subacute Stroke. *Cardiopulm Phys Ther J* (2013) 24(3):14–20. doi: 10.1097/01823246-201324030-00003
28. Cabrita R, Lauss M, Sanna A, Donia M, Skaarup Larsen M, Mitra S, et al. Tertiary Lymphoid Structures Improve Immunotherapy and Survival in Melanoma. *Nature* (2020) 577(7791):561–5. doi: 10.1038/s41586-019-1914-8
29. Prabhakaran S, Rizk VT, Ma Z, Cheng CH, Berglund AE, Coppola D, et al. Evaluation of Invasive Breast Cancer Samples Using a 12-Chemokine Gene Expression Score: Correlation With Clinical Outcomes. *Breast Cancer Res* (2017) 19(1):71. doi: 10.1186/s13058-017-0864-z
30. Liu X, Tsang JYS, Hlaing T, Hu J, Ni YB, Chan SK, et al. Distinct Tertiary Lymphoid Structure Associations and Their Prognostic Relevance in HER2 Positive and Negative Breast Cancers. *Oncologist* (2017) 22(11):1316–24. doi: 10.1634/theoncologist.2017-0029
31. Posch F, Silina K, Leibl S, Mundlein A, Moch H, Siebenhuner A, et al. Maturation of Tertiary Lymphoid Structures and Recurrence of Stage II and III Colorectal Cancer. *Oncoimmunology* (2018) 7(2):e1378844. doi: 10.1080/2162402X.2017.1378844
32. Tang H, Wang Y, Chlewicki LK, Zhang Y, Guo J, Liang W, et al. Facilitating T Cell Infiltration in Tumor Microenvironment Overcomes Resistance to PD-L1 Blockade. *Cancer Cell* (2016) 29(3):285–96. doi: 10.1016/j.ccell.2016.02.004
33. Schrama D, thor Straten P, Fischer WH, McLellan AD, Brocker EB, Reisfeld RA, et al. Targeting of Lymphotoxin-Alpha to the Tumor Elicits an Efficient Immune Response Associated With Induction of Peripheral Lymphoid-Like Tissue. *Immunity* (2001) 14(2):111–21. doi: 10.1016/S1074-7613(01)00094-2
34. Yu P, Lee Y, Liu W, Chin RK, Wang J, Wang Y, et al. Priming of Naive T Cells Inside Tumors Leads to Eradication of Established Tumors. *Nat Immunol* (2004) 5(2):141–9. doi: 10.1038/ni1029
35. Finkin S, Yuan D, Stein I, Taniguchi K, Weber A, Unger K, et al. Ectopic Lymphoid Structures Function as Microniches for Tumor Progenitor Cells in Hepatocellular Carcinoma. *Nat Immunol* (2015) 16(12):1235–44. doi: 10.1038/ni.3290
36. Rodriguez AB, Engelhard VH. Insights Into Tumor-Associated Tertiary Lymphoid Structures: Novel Targets for Antitumor Immunity and Cancer Immunotherapy. *Cancer Immunol Res* (2020) 8(11):1338–45. doi: 10.1158/2326-6066.CIR-20-0432
37. Sautes-Fridman C, Verneau J, Sun CM, Moreira M, Chen TW, Meylan M, et al. Tertiary Lymphoid Structures and B Cells: Clinical Impact and Therapeutic Modulation in Cancer. *Semin Immunol* (2020) 48:101406. doi: 10.1016/j.smim.2020.101406
38. Munoz-Erazo L, Rhodes JL, Marion VC, Kemp RA. Tertiary Lymphoid Structures in Cancer - Considerations for Patient Prognosis. *Cell Mol Immunol* (2020) 17(6):570–5. doi: 10.1038/s41423-020-0457-0
39. Jacquelot N, Tellier J, Nutt SI, Belz Gt. Tertiary Lymphoid Structures and B Lymphocytes in Cancer Prognosis and Response to Immunotherapies. *Oncoimmunology* (2021) 10(1):1900508. doi: 10.1080/2162402X.2021.1900508
40. Zhu G, Falahat R, Wang K, Mailloux A, Artzi N, Mule JJ. Tumor-Associated Tertiary Lymphoid Structures: Gene-Expression Profiling and Their Bioengineering. *Front Immunol* (2017) 8:767. doi: 10.3389/fimmu.2017.00767
41. Sautes-Fridman C, Petitprez F, Calderaro J, Fridman WH. Tertiary Lymphoid Structures in the Era of Cancer Immunotherapy. *Nat Rev Cancer* (2019) 19(6):307–25. doi: 10.1038/s41568-019-0144-6
42. Pitzalis C, Jones GW, Bombardieri M, Jones SA. Ectopic Lymphoid-Like Structures in Infection, Cancer and Autoimmunity. *Nat Rev Immunol* (2014) 14(7):447–62. doi: 10.1038/nri3700
43. Yoshida H, Naito A, Inoue J, Satoh M, Santee-Cooper SM, Ware CF, et al. Different Cytokines Induce Surface Lymphotoxin-Alphabeta on IL-7 Receptor-Alpha Cells That Differentially Engender Lymph Nodes and Peyer's Patches. *Immunity* (2002) 17(6):823–33. doi: 10.1016/S1074-7613(02)00479-X
44. Dejardin E, Droin NM, Delhase M, Haas E, Cao Y, Makris C, et al. The Lymphotoxin-Beta Receptor Induces Different Patterns of Gene Expression Via Two NF-Kappab Pathways. *Immunity* (2002) 17(4):525–35. doi: 10.1016/S1074-7613(02)00423-5
45. Yilmaz ZB, Weih DS, Sivakumar V, Weih F. Relb is Required for Peyer's Patch Development: Differential Regulation of P52-Relb by Lymphotoxin and TNF. *EMBO J* (2003) 22(1):121–30. doi: 10.1093/emboj/cdg004
46. Mebius RE, Streeter PR, Michie S, Butcher EC, Weissman IL. A Developmental Switch in Lymphocyte Homing Receptor and Endothelial Vascular Addressin Expression Regulates Lymphocyte Homing and Permits CD4+ CD3- Cells to Colonize Lymph Nodes. *Proc Natl Acad Sci USA* (1996) 93(20):11019–24. doi: 10.1073/pnas.93.20.11019
47. Cupedo T, Crellin NK, Papazian N, Rombouts EJ, Weijer K, Grogan JL, et al. Human Fetal Lymphoid Tissue-Inducer Cells are Interleukin 17-Producing Precursors to RORC+ CD127+ Natural Killer-Like Cells. *Nat Immunol* (2009) 10(1):66–74. doi: 10.1038/ni.1668
48. Browning JL, Allaire N, Ngam-Ek A, Notidis E, Hunt J, Perrin S, et al. Lymphotoxin-Beta Receptor Signaling is Required for the Homeostatic Control of HEV Differentiation and Function. *Immunity* (2005) 23 (5):539–50. doi: 10.1016/j.immuni.2005.10.002
49. Krautler NJ, Kana V, Kranich J, Tian Y, Perera D, Lemm D, et al. Follicular Dendritic Cells Emerge From Ubiquitous Perivascular Precursors. *Cell* (2012) 150(1):194–206. doi: 10.1016/j.cell.2012.05.032
50. Jeucken KCM, Koning JJ, Mebius RE, Tas SW. The Role of Endothelial Cells and TNF-Receptor Superfamily Members in Lymphoid Organogenesis and Function During Health and Inflammation. *Front Immunol* (2019) 10:2700. doi: 10.3389/fimmu.2019.02700
51. Cheng HW, Onder L, Novkovic M, Soneson C, Lutge M, Pikor N, et al. Origin and Differentiation Trajectories of Fibroblastic Reticular Cells in the Splenic White Pulp. *Nat Commun* (2019) 10(1):1739. doi: 10.1038/s41467-019-09728-3
52. Grabner R, Lotzer K, Dopping S, Hildner M, Radke D, Beer M, et al. Lymphotoxin Beta Receptor Signaling Promotes Tertiary Lymphoid Organogenesis in the Aorta Adventitia of Aged Apoe-/- Mice. *J Exp Med* (2009) 206(1):233–48. doi: 10.1084/jem.20080752
53. Degli-Esposti MA, Davis-Smith T, Din WS, Smolak PJ, Goodwin RG, Smith CA. Activation of the Lymphotoxin Beta Receptor by Cross-Linking Induces

Chemokine Production and Growth Arrest in A375 Melanoma Cells. *J Immunol* (1997) 158(4):1756–62.
54. Chai Q, Onder L, Scandella E, Gil-Cruz C, Perez-Shibayama C, Cupovic J, et al. Maturation of Lymph Node Fibroblastic Reticular Cells From Myofibroblastic Precursors is Critical for Antiviral Immunity. *Immunity* (2013) 38(5):1013–24. doi: 10.1016/j.immuni.2013.03.012
55. Browning JL, Sizing ID, Lawton P, Bourdon PR, Rennert PD, Majeau GR, et al. Characterization of Lymphotoxin-Alpha Beta Complexes on the Surface of Mouse Lymphocytes. *J Immunol* (1997) 159(7):3288–98.
56. Ware CF. Targeting Lymphocyte Activation Through the Lymphotoxin and LIGHT Pathways. *Immunol Rev* (2008) 223:186–201. doi: 10.1111/j.1600-065X.2008.00629.x
57. Lee Y, Chin RK, Christiansen P, Sun Y, Tumanov AV, Wang J, et al. Recruitment and Activation of Naive T Cells in the Islets by Lymphotoxin Beta Receptor-Dependent Tertiary Lymphoid Structure. *Immunity* (2006) 25(3):499–509. doi: 10.1016/j.immuni.2006.06.016
58. Randall TD, Carragher DM, Rangel-Moreno J. Development of Secondary Lymphoid Organs. *Annu Rev Immunol* (2008) 26:627–50. doi: 10.1146/annurev.immunol.26.021607.090257
59. Hampton HR, Chtanova T. Lymphatic Migration of Immune Cells. *Front Immunol* (2019) 10:1168. doi: 10.3389/fimmu.2019.01168
60. Zhang X, Chen L, Dang WQ, Cao MF, Xiao JF, Lv SQ, et al. CCL8 Secreted by Tumor-Associated Macrophages Promotes Invasion and Stemness of Glioblastoma Cells Via ERK1/2 Signaling. *Lab Invest* (2020) 100(4):619–29. doi: 10.1038/s41374-019-0345-3
61. Pascual-Garcia M, Bonfill-Teixidor E, Planas-Rigol E, Rubio-Perez C, Iurlaro R, Arias A, et al. LIF Regulates CXCL9 in Tumor-Associated Macrophages and Prevents CD8(+) T Cell Tumor-Infiltration Impairing Anti-PD1 Therapy. *Nat Commun* (2019) 10(1):2416. doi: 10.1038/s41467-019-10369-9
62. Qu Y, Wen J, Thomas G, Yang W, Prior W, He W, et al. Baseline Frequency of Inflammatory Cxcl9-Expressing Tumor-Associated Macrophages Predicts Response to Avelumab Treatment. *Cell Rep* (2020) 32(1):107873. doi: 10.1016/j.celrep.2020.107873
63. Kodelja V, Muller C, Politz O, Hakij N, Orfanos CE, Goerdt S. Alternative Macrophage Activation-Associated CC-Chemokine-1, a Novel Structural Homologue of Macrophage Inflammatory Protein-1 Alpha With a Th2-Associated Expression Pattern. *J Immunol* (1998) 160(3):1411–8.
64. Chen J, Yao Y, Gong C, Yu F, Su S, Chen J, et al. Ccl18 From Tumor-Associated Macrophages Promotes Breast Cancer Metastasis Via Pitpnm3. *Cancer Cell* (2011) 19(4):541–55. doi: 10.1016/j.ccr.2011.02.006
65. Bista P, Zeng W, Ryan S, Bailly V, Browning JL, Lukashev ME. TRAF3 Controls Activation of the Canonical and Alternative Nfkappab by the Lymphotoxin Beta Receptor. *J Biol Chem* (2010) 285(17):12971–8. doi: 10.1074/jbc.M109.076091
66. Lau TS, Chung TK, Cheung TH, Chan LK, Cheung LW, Yim SF, et al. Cancer Cell-Derived Lymphotoxin Mediates Reciprocal Tumour-Stromal Interactions in Human Ovarian Cancer by Inducing CXCL11 in Fibroblasts. *J Pathol* (2014) 232(1):43–56. doi: 10.1002/path.4258
67. Yeh DY, Wu CC, Chin YP, Lu CJ, Wang YH, Chen MC. Mechanisms of Human Lymphotoxin Beta Receptor Activation on Upregulation of CCL5/RANTES Production. *Int Immunopharmacol* (2015) 28(1):220–9. doi: 10.1016/j.intimp.2015.06.010
68. Grandoch M, Feldmann K, Gothert JR, Dick LS, Homann S, Klatt C, et al. Deficiency in Lymphotoxin Beta Receptor Protects From Atherosclerosis in Apoe-Deficient Mice. *Circ Res* (2015) 116(8):e57–68. doi: 10.1161/CIRCRESAHA.116.305723
69. Bonizzi G, Karin M. The Two NF-Kappab Activation Pathways and Their Role in Innate and Adaptive Immunity. *Trends Immunol* (2004) 25(6):280–8. doi: 10.1016/j.it.2004.03.008
70. Vulcano M, Struyf S, Scapini P, Cassatella M, Bernasconi S, Bonecchi R, et al. Unique Regulation of CCL18 Production by Maturing Dendritic Cells. *J Immunol* (2003) 170(7):3843–9. doi: 10.4049/jimmunol.170.7.3843
71. Proost P, Verpoest S, Van de Borne K, Schutyser E, Struyf S, Put W, et al. Synergistic Induction of CXCL9 and CXCL11 by Toll-Like Receptor Ligands and Interferon-Gamma in Fibroblasts Correlates With Elevated Levels of CXCR3 Ligands in Septic Arthritis Synovial Fluids. *J Leukoc Biol* (2004) 75(5):777–84. doi: 10.1189/jlb.1003524
72. Vondenhoff MF, Greuter M, Goverse G, Elewaut D, Dewint P, Ware CF, et al. Ltbetar Signaling Induces Cytokine Expression and Up-Regulates Lymphangiogenic Factors in Lymph Node Anlagen. *J Immunol* (2009) 182(9):5439–45. doi: 10.4049/jimmunol.0801165
73. Weinstein AM, Chen L, Brzana EA, Patil PR, Taylor JL, Fabian KL, et al. Tbet and IL-36gamma Cooperate in Therapeutic DC-Mediated Promotion of Ectopic Lymphoid Organogenesis in the Tumor Microenvironment. *Oncoimmunology* (2017) 6(6):e1322238. doi: 10.1080/2162402X.2017.1322238
74. Kratz A, Campos-Neto A, Hanson MS, Ruddle NH. Chronic Inflammation Caused by Lymphotoxin is Lymphoid Neogenesis. *J Exp Med* (1996) 183(4):1461–72. doi: 10.1084/jem.183.4.1461
75. Chen SC, Vassileva G, Kinsley D, Holzmann S, Manfra D, Wiekowski MT, et al. Ectopic Expression of the Murine Chemokines CCL21a and CCL21b Induces the Formation of Lymph Node-Like Structures in Pancreas, But Not Skin, of Transgenic Mice. *J Immunol* (2002) 168(3):1001–8. doi: 10.4049/jimmunol.168.3.1001
76. Fan L, Reilly CR, Luo Y, Dorf ME, Lo D. Cutting Edge: Ectopic Expression of the Chemokine TCA4/SLC is Sufficient to Trigger Lymphoid Neogenesis. *J Immunol* (2000) 164(8):3955–9. doi: 10.4049/jimmunol.164.8.3955
77. Johansson-Percival A, He B, Li ZJ, Kjellen A, Russell K, Li J, et al. De Novo Induction of Intratumoral Lymphoid Structures and Vessel Normalization Enhances Immunotherapy in Resistant Tumors. *Nat Immunol* (2017) 18(11):1207–17. doi: 10.1038/ni.3836
78. Chen L, Fabian KL, Taylor JL, Storkus WJ. Therapeutic Use of Dendritic Cells to Promote the Extranodal Priming of Anti-Tumor Immunity. *Front Immunol* (2013) 4:388. doi: 10.3389/fimmu.2013.00388
79. Zhu G, Nemoto S, Mailloux AW, Perez-Villarroel P, Nakagawa R, Falahat R, et al. Induction of Tertiary Lymphoid Structures With Antitumor Function by a Lymph Node-Derived Stromal Cell Line. *Front Immunol* (2018) 9:1609. doi: 10.3389/fimmu.2018.01609
80. Weiden J, Tel J, Figdor CG. Synthetic Immune Niches for Cancer Immunotherapy. *Nat Rev Immunol* (2018) 18(3):212–9. doi: 10.1038/nri.2017.89
81. Aisenbrey EA, Murphy WL. Synthetic Alternatives to Matrigel. *Nat Rev Mater* (2020) 5(7):539–51. doi: 10.1038/s41578-020-0199-8
82. Vukicevic S, Kleinman HK, Luyten FP, Roberts AB, Roche NS, Reddi AH. Identification of Multiple Active Growth Factors in Basement Membrane Matrigel Suggests Caution in Interpretation of Cellular Activity Related to Extracellular Matrix Components. *Exp Cell Res* (1992) 202(1):1–8. doi: 10.1016/0014-4827(92)90397-Q
83. Polykandriotis E, Arkudas A, Horch RE, Kneser U. To Matrigel or Not to Matrigel. *Am J Pathol* (2008) 172(5):1441; author reply –2. doi: 10.2353/ajpath.2008.071215
84. Liu X, Zheng C, Luo X, Wang X, Jiang H. Recent Advances of Collagen-Based Biomaterials: Multi-Hierarchical Structure, Modification and Biomedical Applications. *Mater Sci Eng C Mater Biol Appl* (2019) 99:1509–22. doi: 10.1016/j.msec.2019.02.070
85. Shoulders MD, Raines RT. Collagen Structure and Stability. *Annu Rev Biochem* (2009) 78:929–58. doi: 10.1146/annurev.biochem.77.032207.120833
86. Meyer M. Processing of Collagen Based Biomaterials and the Resulting Materials Properties. *BioMed Eng Online* (2019) 18(1):24. doi: 10.1186/s12938-019-0647-0
87. Werkmeister JA, Ramshaw JA. Recombinant Protein Scaffolds for Tissue Engineering. *BioMed Mater* (2012) 7(1):012002. doi: 10.1088/1748-6041/7/1/012002
88. Gilbert TW, Sellaro TL, Badylak SF. Decellularization of Tissues and Organs. *Biomaterials* (2006) 27(19):3675–83. doi: 10.1016/j.biomaterials.2006.02.014
89. Chen P, Marsilio E, Goldstein RH, Yannas IV, Spector M. Formation of Lung Alveolar-Like Structures in Collagen-Glycosaminoglycan Scaffolds in Vitro. *Tissue Eng* (2005) 11(9-10):1436–48. doi: 10.1089/ten.2005.11.1436
90. Boyce ST, Christianson DJ, Hansbrough JF. Structure of a Collagen-GAG Dermal Skin Substitute Optimized for Cultured Human Epidermal Keratinocytes. *J BioMed Mater Res* (1988) 22(10):939–57. doi: 10.1002/jbm.820221008
91. Gerhold D, Caskey CT. It's the Genes! *EST Access to Hum Genome content. Bioessays* (1996) 18(12):973–81. doi: 10.1002/bies.950181207
92. Aprahamian M, Lambert A, Balboni G, Lefebvre F, Schmitthaeusler R, Damge C, et al. A New Reconstituted Connective Tissue Matrix:

Preparation, Biochemical, Structural and Mechanical Studies. *J BioMed Mater Res* (1987) 21(8):965–77. doi: 10.1002/jbm.820210803
93. Wu X, Black L, Santacana-Laffitte G, Patrick CW Jr. Preparation and Assessment of Glutaraldehyde-Crosslinked Collagen-Chitosan Hydrogels for Adipose Tissue Engineering. *J BioMed Mater Res A* (2007) 81(1):59–65. doi: 10.1002/jbm.a.31003
94. Shahabeddin L, Berthod F, Damour O, Collombel C. Characterization of Skin Reconstructed on a Chitosan-Cross-Linked Collagen-Glycosaminoglycan Matrix. *Skin Pharmacol* (1990) 3(2):107–14. doi: 10.1159/000210857
95. Irawan V, Sung TC, Higuchi A, Ikoma T. Collagen Scaffolds in Cartilage Tissue Engineering and Relevant Approaches for Future Development. *Tissue Eng Regener Med* (2018) 15(6):673–97. doi: 10.1007/s13770-018-0135-9
96. Khan R, Khan MH. Use of Collagen as a Biomaterial: An Update. *J Indian Soc Periodontol* (2013) 17(4):539–42. doi: 10.4103/0972-124X.118333
97. Suematsu S, Watanabe T. Generation of a Synthetic Lymphoid Tissue-Like Organoid in Mice. *Nat Biotechnol* (2004) 22(12):1539–45. doi: 10.1038/nbt1039
98. Okamoto N, Chihara R, Shimizu C, Nishimoto S, Watanabe T. Artificial Lymph Nodes Induce Potent Secondary Immune Responses in Naive and Immunodeficient Mice. *J Clin Invest* (2007) 117(4):997–1007. doi: 10.1172/JCI30379
99. Kobayashi Y, Kato K, Watanabe T. Synthesis of Functional Artificial Lymphoid Tissues. *Discovery Med* (2011) 12(65):351–62.
100. Bashir S, Hina M, Iqbal J, Rajpar AH, Mujtaba MA, Alghamdi NA, et al. Fundamental Concepts of Hydrogels: Synthesis, Properties, and Their Applications. *Polymers (Basel)* (2020) 12(11). doi: 10.3390/polym12112702
101. Lowenberg C, Balk M, Wischke C, Behl M, Lendlein A. Shape-Memory Hydrogels: Evolution of Structural Principles to Enable Shape Switching of Hydrophilic Polymer Networks. *Acc Chem Res* (2017) 50(4):723–32. doi: 10.1021/acs.accounts.6b00584
102. Mahinroosta M, Jomeh Farsangi Z, Allahverdi A, Shakoori Z. Hydrogels as Intelligent Materials: A Brief Review of Synthesis, Properties and Applications. *Materials Today Chem* (2018) 8:42–55. doi: 10.1016/j.mtchem.2018.02.004
103. Wang Q. *Smart Materials for Tissue Engineering: Applications: Royal Society of Chemistry*. Royal Society of Chemistry (2017). doi: 10.1039/9781788010542
104. Kabanov AV, Vinogradov SV. Nanogels as Pharmaceutical Carriers: Finite Networks of Infinite Capabilities. *Angewandte Chemie* (2009) 48: (30):5418–29. doi: 10.1002/anie.200900441
105. Dusek K, Duskova-Smrckova M. Volume Phase Transition in Gels: Its Discovery and Development. *Gels* (2020) 6(3):1–12. doi: 10.3390/gels6030022
106. Grinberg VY, Dubovik AS, Kuznetsov DV, Grinberg NV, Grosberg AY, Tanaka T. Studies of the Thermal Volume Transition of Poly(N-Isopropylacrylamide) Hydrogels by High-Sensitivity Differential Scanning Microcalorimetry. 2. Thermodynamic Functions. *Macromolecules* (2000) 33 (23):8685–92. doi: 10.1021/ma000527w
107. Schild HG. Poly(N-Isopropylacrylamide): Experiment, Theory and Application. *Prog Polymer Sci* (1992) 17(2):163–249. doi: 10.1016/0079-6700(92)90023-R
108. Purwada A, Singh A. Immuno-Engineered Organoids for Regulating the Kinetics of B-Cell Development and Antibody Production. *Nat Protoc* (2017) 12(1):168–82. doi: 10.1038/nprot.2016.157
109. Purwada A, Jaiswal MK, Ahn H, Nojima T, Kitamura D, Gaharwar AK, et al. Ex Vivo Engineered Immune Organoids for Controlled Germinal Center Reactions. *Biomaterials* (2015) 63:24–34. doi: 10.1016/j.biomaterials.2015.06.002
110. Smith TT, Moffett HF, Stephan SB, Opel CF, Dumigan AG, Jiang X, et al. Biopolymers Codelivering Engineered T Cells and STING Agonists Can Eliminate Heterogeneous Tumors. *J Clin Invest* (2017) 127(6):2176–91. doi: 10.1172/JCI87624
111. Pedde RD, Mirani B, Navaei A, Styan T, Wong S, Mehrali M, et al. Emerging Biofabrication Strategies for Engineering Complex Tissue Constructs. *Adv Mater* (2017) 29(19):1–27. doi: 10.1002/adma.201606061
112. Wegst UG, Bai H, Saiz E, Tomsia AP, Ritchie RO. Bioinspired Structural Materials. *Nat Mater* (2015) 14(1):23–36. doi: 10.1038/nmat4089
113. Bencherif SA, Warren Sands R, Ali OA, Li WA, Lewin SA, Braschler TM, et al. Injectable Cryogel-Based Whole-Cell Cancer Vaccines. *Nat Commun* (2015) 6:7556. doi: 10.1038/ncomms8556
114. Bencherif SA, Sands RW, Bhatta D, Arany P, Verbeke CS, Edwards DA, et al. Injectable Preformed Scaffolds With Shape-Memory Properties. *Proc Natl Acad Sci USA* (2012) 109(48):19590–5. doi: 10.1073/pnas.1211516109
115. Bauleth-Ramos T, Shih T-Y, Shahbazi M-A, Najibi AJ, Mao AS, Liu D, et al. Acetalated Dextran Nanoparticles Loaded Into an Injectable Alginate Cryogel for Combined Chemotherapy and Cancer Vaccination. *Adv Funct Mater* (2019) 29(35):1903686. doi: 10.1002/adfm.201903686
116. Singh A, Suri S, Roy K. In-Situ Crosslinking Hydrogels for Combinatorial Delivery of Chemokines and Sirna-DNA Carrying Microparticles to Dendritic Cells. *Biomaterials* (2009) 30(28):5187–200. doi: 10.1016/j.biomaterials.2009.06.001
117. Singh A, Qin H, Fernandez I, Wei J, Lin J, Kwak LW, et al. An Injectable Synthetic Immune-Priming Center Mediates Efficient T-Cell Class Switching and T-Helper 1 Response Against B Cell Lymphoma. *J Control Release* (2011) 155(2):184–92. doi: 10.1016/j.jconrel.2011.06.008
118. Najibi AJ, Mooney DJ. Cell and Tissue Engineering in Lymph Nodes for Cancer Immunotherapy. *Adv Drug Delivery Rev* (2020) 161-162:42–62. doi: 10.1016/j.addr.2020.07.023
119. Li AW, Sobral MC, Badrinath S, Choi Y, Graveline A, Stafford AG, et al. A Facile Approach to Enhance Antigen Response for Personalized Cancer Vaccination. *Nat Mater* (2018) 17(6):528–34. doi: 10.1038/s41563-018-0028-2
120. Giese C, Demmler CD, Ammer R, Hartmann S, Lubitz A, Miller L, et al. A Human Lymph Node in Vitro–Challenges and Progress. *Artif Organs* (2006) 30(10):803–8. doi: 10.1111/j.1525-1594.2006.00303.x
121. Lakshmanan VK, Jindal S, Packirisamy G, Ojha S, Lian S, Kaushik A, et al. Nanomedicine-Based Cancer Immunotherapy: Recent Trends and Future Perspectives. *Cancer Gene Ther* (2021). doi: 10.1038/s41417-021-00299-4
122. Kim EM, Jeong HJ. Liposomes: Biomedical Applications. *Chonnam Med J* (2021) 57(1):27–35. doi: 10.4068/cmj.2021.57.1.27
123. Plotnick AN. Lipid-Based Formulations of Amphotericin B. *J Am Vet Med Assoc* (2000) 216(6):838–41. doi: 10.2460/javma.2000.216.838
124. Patel HM. Serum Opsonins and Liposomes: Their Interaction and Opsonophagocytosis. *Crit Rev Ther Drug Carrier Syst* (1992) 9(1):39–90.
125. Scherphof GL, Dijkstra J, Spanjer HH, Derksen JT, Roerdink FH. Uptake and Intracellular Processing of Targeted and Nontargeted Liposomes by Rat Kupffer Cells in Vivo and in Vitro. *Ann N Y Acad Sci* (1985) 446:368–84. doi: 10.1111/j.1749-6632.1985.tb18414.x
126. Alving CR, Steck EA, Chapman WLJr., Waits VB, Hendricks LD, Swartz GMJr., et al. Therapy of Leishmaniasis: Superior Efficacies of Liposome-Encapsulated Drugs. *Proc Natl Acad Sci USA* (1978) 75(6):2959–63. doi: 10.1073/pnas.75.6.2959
127. Mayer LD, Hope MJ, Cullis PR. Vesicles of Variable Sizes Produced by a Rapid Extrusion Procedure. *Biochim Biophys Acta* (1986) 858(1):161–8. doi: 10.1016/0005-2736(86)90302-0
128. Jahn A, Stavis SM, Hong JS, Vreeland WN, DeVoe DL, Gaitan M. Microfluidic Mixing and the Formation of Nanoscale Lipid Vesicles. *ACS Nano* (2010) 4(4):2077–87. doi: 10.1021/nn901676x
129. Zhigaltsev IV, Belliveau N, Hafez I, Leung AK, Huft J, Hansen C, et al. Bottom-Up Design and Synthesis of Limit Size Lipid Nanoparticle Systems With Aqueous and Triglyceride Cores Using Millisecond Microfluidic Mixing. *Langmuir* (2012) 28(7):3633–40. doi: 10.1021/la204833h
130. Gregoriadis G. *Liposome Technology. 2nd ed.* Boca Raton, Fla: CRC Press (1993).
131. Jahn A, Vreeland WN, DeVoe DL, Locascio LE, Gaitan M. Microfluidic Directed Formation of Liposomes of Controlled Size. *Langmuir* (2007) 23 (11):6289–93. doi: 10.1021/la070051a
132. Hinna A, Steiniger F, Hupfeld S, Stein P, Kuntsche J, Brandl M. Filter-Extruded Liposomes Revisited: A Study Into Size Distributions and Morphologies in Relation to Lipid-Composition and Process Parameters. *J Liposome Res* (2016) 26(1):11–20. doi: 10.3109/08982104.2015.1022556
133. Panahi Y, Farshbaf M, Mohammadhosseini M, Mirahadi M, Khalilov R, Saghfi S, et al. Recent Advances on Liposomal Nanoparticles: Synthesis, Characterization and Biomedical Applications. *Artif Cells Nanomed Biotechnol* (2017) 45(4):788–99. doi: 10.1080/21691401.2017.1282496

134. Bulbake U, Doppalapudi S, Kommineni N, Khan W. Liposomal Formulations in Clinical Use: An Updated Review. *Pharmaceutics* (2017) 9(2):1–33. doi: 10.3390/pharmaceutics9020012
135. Has C, Sunthar P. A Comprehensive Review on Recent Preparation Techniques of Liposomes. *J Liposome Res* (2020) 30(4):336–65. doi: 10.1080/08982104.2019.1668010
136. Bangham AD, Horne RW. Negative Staining of Phospholipids and Their Structural Modification by Surface-Active Agents as Observed in the Electron Microscope. *J Mol Biol* (1964) 8:660–8. doi: 10.1016/S0022-2836(64)80115-7
137. Haluska CK, Riske KA, Marchi-Artzner V, Lehn JM, Lipowsky R, Dimova R. Time Scales of Membrane Fusion Revealed by Direct Imaging of Vesicle Fusion With High Temporal Resolution. *Proc Natl Acad Sci USA* (2006) 103 (43):15841–6. doi: 10.1073/pnas.0602766103
138. Marrink SJ, Mark AE. The Mechanism of Vesicle Fusion as Revealed by Molecular Dynamics Simulations. *J Am Chem Soc* (2003) 125(37):11144–5. doi: 10.1021/ja036138+
139. Gabizon A, Papahadjopoulos D. Liposome Formulations With Prolonged Circulation Time in Blood and Enhanced Uptake by Tumors. *Proc Natl Acad Sci USA* (1988) 85(18):6949–53. doi: 10.1073/pnas.85.18.6949
140. Senior J, Gregoriadis G. Is Half-Life of Circulating Liposomes Determined by Changes in Their Permeability? *FEBS Lett* (1982) 145(1):109–14. doi: 10.1016/0014-5793(82)81216-7
141. Immordino ML, Dosio F, Cattel L. Stealth Liposomes: Review of the Basic Science, Rationale, and Clinical Applications, Existing and Potential. *Int J Nanomedicine* (2006) 1(3):297–315.
142. Drummond DC, Meyer O, Hong K, Kirpotin DB, Papahadjopoulos D. Optimizing Liposomes for Delivery of Chemotherapeutic Agents to Solid Tumors. *Pharmacol Rev* (1999) 51(4):691–743.
143. Allen TM, Hansen C, Martin F, Redemann C, Yau-Young A. Liposomes Containing Synthetic Lipid Derivatives of Poly(Ethylene Glycol) Show Prolonged Circulation Half-Lives in Vivo. *Biochim Biophys Acta* (1991) 1066(1):29–36. doi: 10.1016/0005-2736(91)90246-5
144. Khan AA, Allemailem KS, Almatroodi SA, Almatroudi A, Rahmani AH. Recent Strategies Towards the Surface Modification of Liposomes: An Innovative Approach for Different Clinical Applications. *3 Biotech* (2020) 10(4):163. doi: 10.1007/s13205-020-2144-3
145. Willis M, Forssen E. Ligand-Targeted Liposomes. *Adv Drug Delivery Rev* (1998) 29(3):249–71. doi: 10.1016/S0169-409X(97)00083-5
146. Ponce AM, Vujaskovic Z, Yuan F, Needham D, Dewhirst MW. Hyperthermia Mediated Liposomal Drug Delivery. *Int J Hyperthermia* (2006) 22(3):205–13. doi: 10.1080/02656730600582956
147. Kaur R, Morris R, Bencsik M, Vangala A, Rades T, Perrie Y. Development of a Novel Magnetic Resonance Imaging Contrast Agent for Pressure Measurements Using Lipid-Coated Microbubbles. *J BioMed Nanotechnol* (2009) 5(6):707–15. doi: 10.1166/jbn.2009.1087
148. Shum P, Kim JM, Thompson DH. Phototriggering of Liposomal Drug Delivery Systems. *Adv Drug Delivery Rev* (2001) 53(3):273–84. doi: 10.1016/S0169-409X(01)00232-0
149. Yavlovich A, Singh A, Blumenthal R, Puri A. A Novel Class of Photo-Triggerable Liposomes Containing DPPC:DC(8,9)PC as Vehicles for Delivery of Doxorubcin to Cells. *Biochim Biophys Acta* (2011) 1808 (1):117–26. doi: 10.1016/j.bbamem.2010.07.030
150. Yu JR, Janssen M, Liang BJ, Huang HC, Fisher JP. A Liposome/Gelatin Methacrylate Nanocomposite Hydrogel System for Delivery of Stromal Cell-Derived Factor-1alpha and Stimulation of Cell Migration. *Acta Biomater* (2020) 108:67–76. doi: 10.1016/j.actbio.2020.03.015
151. Rubio AJ, Zhong X, Porter TM. In Vitro Characterization of Chemokine-Loaded Liposomes. *Cogent Biol* (2019) 5(1):1–17. doi: 10.1080/23312025.2019.1662931
152. Liu T, Liu Z, Chen J, Jin R, Bai Y, Zhou Y, et al. Redox-Responsive Supramolecular Micelles for Targeted Imaging and Drug Delivery to Tumor. *J BioMed Nanotechnol* (2018) 14(6):1107–16. doi: 10.1166/jbn.2018.2573
153. Letchford K, Burt H. A Review of the Formation and Classification of Amphiphilic Block Copolymer Nanoparticulate Structures: Micelles, Nanospheres, Nanocapsules and Polymersomes. *Eur J Pharm Biopharm* (2007) 65(3):259–69. doi: 10.1016/j.ejpb.2006.11.009
154. Ishii S, Kaneko J, Nagasaki Y. Development of a Long-Acting, Protein-Loaded, Redox-Active, Injectable Gel Formed by a Polyion Complex for Local Protein Therapeutics. *Biomaterials* (2016) 84:210–8. doi: 10.1016/j.biomaterials.2016.01.029
155. Li H, Li Y, Wang X, Hou Y, Hong X, Gong T, et al. Rational Design of Polymeric Hybrid Micelles to Overcome Lymphatic and Intracellular Delivery Barriers in Cancer Immunotherapy. *Theranostics* (2017) 7 (18):4383–98. doi: 10.7150/thno.20745
156. Liu L, Yi H, Wang C, He H, Li P, Pan H, et al. Integrated Nanovaccine With Microrna-148a Inhibition Reprograms Tumor-Associated Dendritic Cells by Modulating Mir-148a/DNMT1/SOCS1 Axis. *J Immunol* (2016) 197 (4):1231–41. doi: 10.4049/jimmunol.1600182
157. Li C, Zhang X, Chen Q, Zhang J, Li W, Hu H, et al. Synthetic Polymeric Mixed Micelles Targeting Lymph Nodes Trigger Enhanced Cellular and Humoral Immune Responses. *ACS Appl Mater Interfaces* (2018) 10(3):2874–89. doi: 10.1021/acsami.7b14004
158. Danhier F, Ansorena E, Silva JM, Coco R, Le Breton A, Preat V. PLGA-Based Nanoparticles: An Overview of Biomedical Applications. *J Control Release* (2012) 161(2):505–22. doi: 10.1016/j.jconrel.2012.01.043
159. Shive MS, Anderson JM. Biodegradation and Biocompatibility of PLA and PLGA Microspheres. *Adv Drug Delivery Rev* (1997) 28(1):5–24. doi: 10.1016/S0169-409X(97)00048-3
160. Hamdy S, Haddadi A, Hung RW, Lavasanifar A. Targeting Dendritic Cells With Nano-Particulate Plga Cancer Vaccine Formulations. *Adv Drug Delivery Rev* (2011) 63(10-11):943–55. doi: 10.1016/j.addr.2011.05.021
161. Guo Y, Wang D, Song Q, Wu T, Zhuang X, Bao Y, et al. Erythrocyte Membrane-Enveloped Polymeric Nanoparticles as Nanovaccine for Induction of Antitumor Immunity Against Melanoma. *ACS Nano* (2015) 9 (7):6918–33. doi: 10.1021/acsnano.5b01042
162. Fang RH, Hu CM, Luk BT, Gao W, Copp JA, Tai Y, et al. Cancer Cell Membrane-Coated Nanoparticles for Anticancer Vaccination and Drug Delivery. *Nano Lett* (2014) 14(4):2181–8. doi: 10.1021/nl500618u
163. Mi Y, Smith CC, Yang F, Qi Y, Roche KC, Serody JS, et al. A Dual Immunotherapy Nanoparticle Improves T-Cell Activation and Cancer Immunotherapy. *Adv Mater* (2018) 30(25):e1706098. doi: 10.1002/adma.201706098
164. Rosalia RA, Cruz LJ, van Duikeren S, Tromp AT, Silva AL, Jiskoot W, et al. CD40-Targeted Dendritic Cell Delivery of PLGA-Nanoparticle Vaccines Induce Potent Anti-Tumor Responses. *Biomaterials* (2015) 40:88–97. doi: 10.1016/j.biomaterials.2014.10.053
165. Kobayashi Y, Watanabe T. Gel-Trapped Lymphorganogenic Chemokines Trigger Artificial Tertiary Lymphoid Organs and Mount Adaptive Immune Responses in Vivo. *Front Immunol* (2016) 7:316. doi: 10.3389/fimmu.2016.00316
166. Stephan SB, Taber AM, Jileaeva I, Pegues EP, Sentman CL, Stephan MT. Biopolymer Implants Enhance the Efficacy of Adoptive T-Cell Therapy. *Nat Biotechnol* (2015) 33(1):97–101. doi: 10.1038/nbt.3104
167. Mariani E, Lisignoli G, Borzi RM, Pulsatelli L. Biomaterials: Foreign Bodies or Tuners for the Immune Response? *Int J Mol Sci* (2019) 20(3):1–42. doi: 10.3390/ijms20030636
168. Chung L, Maestas DRJr., Housseau F, Elisseeff JH. Key Players in the Immune Response to Biomaterial Scaffolds for Regenerative Medicine. *Adv Drug Delivery Rev* (2017) 114:184–92. doi: 10.1016/j.addr.2017.07.006
169. Christo SN, Diener KR, Bachhuka A, Vasilev K, Hayball JD. Innate Immunity and Biomaterials At the Nexus: Friends or Foes. *BioMed Res Int* (2015) 2015:342304. doi: 10.1155/2015/342304
170. Labow RS, Meek E, Santerre JP. Neutrophil-Mediated Biodegradation of Medical Implant Materials. *J Cell Physiol* (2001) 186(1):95–103. doi: 10.1002/1097-4652(200101)186:1<95::AID-JCP1008>3.0.CO;2-0
171. Nimeri G, Ohman L, Elwing H, Wettero J, Bengtsson T. The Influence of Plasma Proteins and Platelets on Oxygen Radical Production and F-Actin Distribution in Neutrophils Adhering to Polymer Surfaces. *Biomaterials* (2002) 23(8):1785–95. doi: 10.1016/S0142-9612(01)00305-2
172. Nimeri G, Majeed M, Elwing H, Ohman L, Wettero J, Bengtsson T. Oxygen Radical Production in Neutrophils Interacting With Platelets and Surface-Immobilized Plasma Proteins: Role of Tyrosine Phosphorylation. *J BioMed Mater Res A* (2003) 67(2):439–47. doi: 10.1002/jbm.a.10081
173. Wettero J, Bengtsson T, Tengvall P. Complement Activation on Immunoglobulin G-Coated Hydrophobic Surfaces Enhances the Release of Oxygen Radicals From Neutrophils Through an Actin-Dependent

Mechanism. *J BioMed Mater Res* (2000) 51(4):742–51. doi: 10.1002/1097-4636(20000915)51:4<742::AID-JBM24>3.0.CO;2-D
174. Jones JA, Chang DT, Meyerson H, Colton E, Kwon IK, Matsuda T, et al. Proteomic Analysis and Quantification of Cytokines and Chemokines From Biomaterial Surface-Adherent Macrophages and Foreign Body Giant Cells. *J BioMed Mater Res A* (2007) 83(3):585–96. doi: 10.1002/jbm.a.31221
175. Yamashiro S, Kamohara H, Wang JM, Yang D, Gong WH, Yoshimura T. Phenotypic and Functional Change of Cytokine-Activated Neutrophils: Inflammatory Neutrophils are Heterogeneous and Enhance Adaptive Immune Responses. *J Leukoc Biol* (2001) 69(5):698–704.
176. Garg K, Pullen NA, Oskeritzian CA, Ryan JJ, Bowlin GL. Macrophage Functional Polarization (M1/M2) in Response to Varying Fiber and Pore Dimensions of Electrospun Scaffolds. *Biomaterials* (2013) 34(18):4439–51. doi: 10.1016/j.biomaterials.2013.02.065
177. Chen S, Jones JA, Xu Y, Low HY, Anderson JM, Leong KW. Characterization of Topographical Effects on Macrophage Behavior in a Foreign Body Response Model. *Biomaterials* (2010) 31(13):3479–91. doi: 10.1016/j.biomaterials.2010.01.074
178. Fink J, Fuhrmann R, Scharnweber T, Franke RP. Stimulation of Monocytes and Macrophages: Possible Influence of Surface Roughness. *Clin Hemorheol Microcirc* (2008) 39(1-4):205–12. doi: 10.3233/CH-2008-1090
179. Nutrition CfFSaA, Medicine CfV, Affairs OoR, Research CfDEa, Health CfDaR and Research CfBEa. *Part 11, Electronic Records; Electronic Signatures - Scope and Application*. U.S. Food and drug Administration (2003).
180. Tinkle S, McNeil SE, Muhlebach S, Bawa R, Borchard G, Barenholz YC, et al. Nanomedicines: Addressing the Scientific and Regulatory Gap. *Ann N Y Acad Sci* (2014) 1313:35–56. doi: 10.1111/nyas.12403
181. Teli MK, Mutalik S, Rajanikant GK. Nanotechnology and Nanomedicine: Going Small Means Aiming Big. *Curr Pharm Des* (2010) 16(16):1882–92. doi: 10.2174/138161210791208992
182. Hernandez I, Prasad V, Gellad WF. Total Costs of Chimeric Antigen Receptor T-Cell Immunotherapy. *JAMA Oncol* (2018) 4(7):994–6. doi: 10.1001/jamaoncol.2018.0977
183. Administration FaD. *Definition of Primary Mode of Action of a Combination Product*. Federal Register (2004). pp. 25527–33.
184. Boehler RM, Graham JG, Shea LD. Tissue Engineering Tools for Modulation of the Immune Response. *Biotechniques* (2011) 51(4):239–40, 42, 44 passim. doi: 10.2144/000113754
185. Mendicino M, Fan Y, Griffin D, Gunter KC, Nichols K. Current State of U.S. Food and Drug Administration Regulation for Cellular and Gene Therapy Products: Potential Cures on the Horizon. *Cytotherapy* (2019) 21(7):699–724. doi: 10.1016/j.jcyt.2019.04.002

Conflict of Interest: The authors declare that the research was conducted in the absence of any commercial or financial relationships that could be construed as a potential conflict of interest.

Copyright © 2021 Aoyama, Nakagawa, Mulé and Mailloux. This is an open-access article distributed under the terms of the Creative Commons Attribution License (CC BY). The use, distribution or reproduction in other forums is permitted, provided the original author(s) and the copyright owner(s) are credited and that the original publication in this journal is cited, in accordance with accepted academic practice. No use, distribution or reproduction is permitted which does not comply with these terms.

frontiers in Immunology

REVIEW
published: 27 May 2021
doi: 10.3389/fimmu.2021.674375

Therapeutic Induction of Tertiary Lymphoid Structures in Cancer Through Stromal Remodeling

Anna Johansson-Percival[1,2]* *and Ruth Ganss*[1,2]

[1] Cancer Microenvironment Laboratory, Harry Perkins Institute of Medical Research, QEII Medical Centre, Nedlands, WA, Australia, [2] Centre for Medical Research, The University of Western Australia, Crawley, WA, Australia

Improving the effectiveness of anti-cancer immunotherapy remains a major clinical challenge. Cytotoxic T cell infiltration is crucial for immune-mediated tumor rejection, however, the suppressive tumor microenvironment impedes their recruitment, activation, maturation and function. Nevertheless, solid tumors can harbor specialized lymph node vasculature and immune cell clusters that are organized into tertiary lymphoid structures (TLS). These TLS support naïve T cell infiltration and intratumoral priming. In many human cancers, their presence is a positive prognostic factor, and importantly, predictive for responsiveness to immune checkpoint blockade. Thus, therapeutic induction of TLS is an attractive concept to boost anti-cancer immunotherapy. However, our understanding of how cancer-associated TLS could be initiated is rudimentary. Exciting new reagents which induce TLS in preclinical cancer models provide mechanistic insights into the exquisite stromal orchestration of TLS formation, a process often associated with a more functional or "normalized" tumor vasculature and fueled by LIGHT/LTα/LTβ, TNFα and CC/CXC chemokine signaling. These emerging insights provide innovative opportunities to induce and shape TLS in the tumor microenvironment to improve immunotherapies.

Keywords: light, LTβR, tumor, TLS, ICB, vascular normalization

OPEN ACCESS

Edited by:
Anna Dimberg,
Uppsala University, Sweden

Reviewed by:
Tibor Bakacs,
Alfred Renyi Institute of Mathematics, Hungary
Tiziana Schioppa,
University of Brescia, Italy

***Correspondence:**
Anna Johansson-Percival
anna.a.johansson@perkins.org.au

Specialty section:
This article was submitted to Cancer Immunity and Immunotherapy, a section of the journal Frontiers in Immunology

Received: *01 March 2021*
Accepted: *04 May 2021*
Published: *27 May 2021*

Citation:
Johansson-Percival A and Ganss R (2021) Therapeutic Induction of Tertiary Lymphoid Structures in Cancer Through Stromal Remodeling. Front. Immunol. 12:674375. doi: 10.3389/fimmu.2021.674375

INTRODUCTION

Unprecedented success of immune checkpoint blockade (ICB) in melanoma patients has sparked considerable interest in immunotherapies (1). Treatment with immune modulatory antibodies has also highlighted the critical importance of an immune "hot" tumor environment for therapeutic responsiveness (2). Considerable efforts are now being directed into increasing responsiveness to ICB in all cancer patients.

The tumor microenvironment including stromal innate immune cells, fibroblasts and the vasculature has become a major target for new therapies aiming to increase intratumoral T cell numbers and their activation status prior to ICB (3, 4). Spontaneous and/or therapeutic increase of T cell numbers into tumors can result in the formation of TLS (3, 5). These TLS have the ability to effectively prime naïve T cells entering through high endothelia venules (HEV) (6). Notably, the presence of TLS predicts and improves efficacy of immunotherapy in mice and humans (7).

In this review, we delineate common features of peripheral lymph nodes (LNs), inflammation- and cancer-associated TLS, and discuss the relationship between the presence of TLS, lymphocyte

priming and response to immunotherapy. We further elaborate on potential drivers for intratumoral TLS formation and how TLS could be exploited therapeutically, in particular for non-responsive, immune "cold" cancers.

THE BEGINNING: DEVELOPMENT OF LYMPHOID TISSUE

The immune system is comprised of organs and cell types that protect the host from foreign pathogens and disease. The highly specialized adaptive immune system consists of T and B lymphocytes that form in the bone marrow and later reside in secondary lymphoid organs (SLOs). SLOs are strategically placed to facilitate immune surveillance and priming of naïve T cells and also include LNs (8). The structural framework of LNs are fibroblastic reticular cells (FRCs) which mediate cross-talk between various immune cell populations throughout the LN. In addition, follicular dendritic cells (FDCs) that reside within B cell zones maximize interactions between antigens, antigen presenting cells and naïve lymphocytes (9). Embedded in the paracortical region of LNs are HEVs, highly specialized post capillary venules that serve as entry portals for naïve and central memory lymphocytes from the blood; this migration process is mediated by interactions of L-selectin expressed on lymphocytes and peripheral node addressins (PNAds) on HEVs (10). TLS are lymphoid aggregates similar to SLOs which develop in non-lymphoid tissue, for instance at sites of chronic inflammation (11). TLS vary in composition and maturity but share with SLOs separated B and T cell zones, stromal cells, and HEVs.

One proposed mechanism for the initiation of LN development is upregulation of chemokine (C-X-C motif) ligand 13 (Cxcl13) by lymphotoxin beta receptor (LTβR) expressing mesenchymal precursors known as lymphoid tissue organizer (LTo) cells (12). Cxcl13 subsequently attracts hematopoietic precursors or lymphoid tissue inducer (LTi) cells resulting in the first cluster of LTi cells and the initiation of LN development (12). Mature LTi express lymphotoxin alpha 1 beta 2 ($LT\alpha_1ß_2$) which binds LTβR in activated LTo, resulting in further LTo maturation and expression of intercellular adhesion molecule 1 (ICAM1), vascular cell adhesion molecule 1 (VCAM1), chemokine (C-C motif) ligand 19 (Ccl19) and 21 (Ccl21), and Cxcl13 which recruit more LTi and promote interactions between LTi and LTo (8, 9). Mouse LTo may give rise to stromal lineages such as FRCs, FDCs, lymphatic endothelium and vascular endothelium within adult LNs (13).

Emerging evidence also highlights a crucial role of vascular endothelium in the development of LNs. In adult LNs, endothelial cells (ECs) and lymphatic endothelial cells (LECs) express LTβR; EC-specific deletion of LTβR by crossing vascular endothelial cadherin (VE-Cad)-Cre and $LT\beta R^{fl/fl}$ mice results in compromised LN development with a reduced HEV network demonstrating the importance of EC-specific LTβR for HEV development and lymphocyte trafficking (14). Moreover, EC and to a lesser extent LEC-specific deletion of NFκB-inducing kinase (NIK), one of the major pathways downstream of LTβR signaling, results in an almost complete loss of peripheral LNs (15). In the remaining LN anlagen of these mice, $CD4^+$ LTi cells are drastically reduced coinciding with very low VCAM1, ICAM1, Cxcl13 and Ccl19 expression levels suggesting that failure of LTi to engage with ECs during LN development prevents LTo activation. Furthermore, forced retention of LTi following treatment of pregnant mice with the drug FTY720 which sequesters lymphocytes in LNs, results in formation of mature ectopic LNs in the inguinal fat pad of the progeny (15). These findings imply that the numbers of LTi retained by EC/LECs may be an additional determinant of LN development, alongside interactions between LTi and mesenchymal LTo (16).

TLS FORM UNDER INFLAMMATORY CONDITIONS IN MICE

Although the initial events of LN development are not fully resolved, LTβR signaling is crucial for subsequent LN maturation, and also plays a major role in TLS formation during chronic inflammation in mice (**Figure 1**). For instance, in apolipoprotein E $(ApoE)^{-/-}$ mice, LTβR expressing aortic smooth muscle cells (SMC) over time become activated and produce TLS inducing cytokines such as Cxcl13, Ccl21 and LTβ (17). This leads to the formation of mature aortic TLS containing B cell follicles and germinal centers (GCs), T cells and HEVs. Importantly, TLS assembly can be prevented by blocking LTβR signaling *in vivo* (17).

LTβR binds two ligands, the developmentally important LN-inducing cytokine $LT\alpha_1ß_2$ and tumor necrosis factor superfamily (TNFSF) 14 or LIGHT. Increased LIGHT expression coincides with TLS formation in the pancreas of aged non-obese diabetic (NOD) mice; *in vivo* inhibition of LTβR prevents TLS formation and diabetes (18). TLS in mouse pancreatic islets can also be induced by overexpressing C-X-C chemokine receptor type 5 (Cxcr5), the receptor for Cxcl13 (19), Cxcl12, Ccl19 or Ccl21 (20) under the control of the rat insulin gene promotor. Interestingly, LTβR or LTα1β2 blockade prevents TLS formation in chemokine overexpressing mice (19, 20), implying that LTα1β2 and/or LIGHT are *bona fide* TLS inducers under inflammatory conditions. However, mechanisms leading to inflammation-associated TLS formation are complex and can involve a network of multiple immune and stromal cell types, and - besides $LT\alpha_1\beta_2$ – other cytokines such as tumor necrosis factor alpha (TNFα), IL6, IL13, IL17, IL22 and IL23 (21–25).

In mouse inflammatory lesions, stromal cells can function as LTo by upregulation of the FRC markers podoplanin, Ccl19, Ccl21 and Cxcl13 which in turn stimulate lymphocyte recruitment to sites of inflammation (26, 27). For instance, in patients with primary Sjögren's syndrome (pSS) and a mouse model of salivary gland inflammation, IL13 production by activated fibroblast activation protein $(FAP)^+$ $podoplanin^+$ fibroblasts, termed "immunofibroblasts", is the earliest detectable event during TLS neogenesis which precedes lymphocyte recruitment into tissue and subsequent IL22/$LT\alpha_1\beta_2$ secretion (24). As demonstrated in mice deficient for

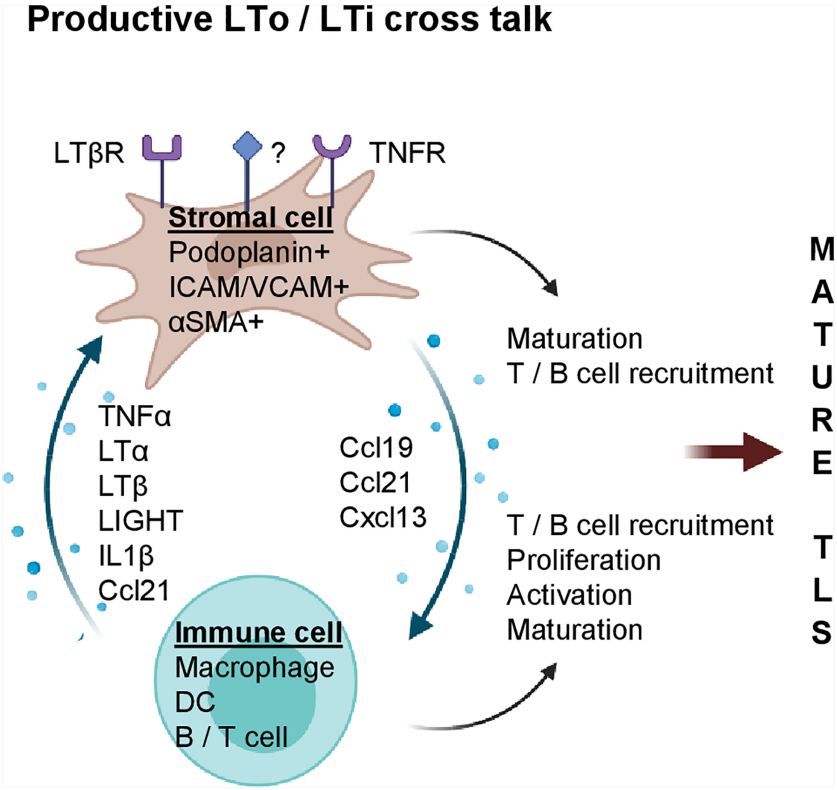

FIGURE 1 | Stromal and immune cell cross talk mediate TLS formation during chronic inflammation. Potential cytokines/chemokines involved in immune (LTi) and stromal cell (LTo) cross-talk. Stromal cells express cytokine receptors such as LTβR and TNFR (and potentially others, marked with "?"); upon activation, LN inducing chemokines such as Ccl19, Ccl21 and Cxcl13 are secreted by stromal cells which increase immune cell density and foster their own maturation. Activated stroma and immune cells coordinate formation of LN aggregates which can mature into clusters containing T cells, B cells, FDCs and MECA79$^+$ HEVs (mature TLS). Created with BioRender.com.

IL13 or its receptor IL4R, "immunofibroblast" activation is dependent on IL13/IL4R signaling and precedes their expansion which is subsequently regulated by lymphocyte-derived IL22 (28). Furthermore, genetic deletion of FAP$^+$ fibroblasts abolishes TLS formation highlighting the LTo role of fibroblasts during TLS formation (24).

During ear inflammation in mice, induction of podoplanin$^+$ stromal cells is dependent on myeloid cells, since depletion of CD11$^+$ Gr1$^+$ cells using monoclonal antibodies significantly reduces podoplanin$^+$ cells (26). This suggests that circulating monocytes can acquire a postnatal role as LTi. Indeed, myeloid cells have been implicated in the development of TLS in various experimental systems. For instance, global overexpression of TNFα in mice by expressing a stabilized TNFα mRNA (TNF$^{\Delta ARE}$) leads to the development of TLS in the intestine in a process which is dependent on F4/80$^+$ myeloid cells (21). Mechanistically, F4/80$^+$CD11b$^+$ myeloid cells in the LN anlagen are the major source of TNFα and inducers of stromal maturation and expression of LTo chemokines such as Cxcl13, Ccl19 and Ccl21. The potency of these myeloid cells was further demonstrated by surgical transplantation of LN anlagen from TNF/RORc(γt)$^{-/-}$ mice under the kidney capsule of RORC(γt)$^{-/-}$ mice that lack classical LTi; this leads to LN development in the majority of mice thus demonstrating that TNFα producing myeloid cells have the capacity to induce LN formation (21). In atherosclerosis, M1-polarized macrophages act as LTi cells and produce high levels of LN-inducing cytokines such as TNFα and LTα (29). *In vitro* stimulation of vascular SMCs (vSMC) with M1 macrophage conditioned media induces an LTo profile and triggers the formation of TLS *in vivo* following vSMC injection (29). VSMC activation is dependent on TNFR signaling as blockade of TNFR1/2 *in vivo* abolishes the LTo phenotype and prevents TLS formation. Similarly, adipose tissue-associated TLS formation is dependent on myeloid derived TNFα and stromal expression of TNFR, but independent of LTβR signaling (27).

The effects of DCs on lymph angiogenesis and TLS induction have also been studied in multiple models (30–35). For instance, in a mouse model of atopic dermatitis, CD11c$^+$ DCs accumulate around newly formed HEVs; inhibition of LTβR signaling or depletion of CD11c$^+$ cells inhibits HEV formation (33). Similarly, following influenza virus infection in mice, lung CD11c$^+$ DCs express TLS-inducing cytokines such as LTβ, Cxcl13, Ccl19 and Ccl21 which correlates with formation of

mature TLS; *in vivo* depletion of $CD11c^+$ cells or inhibition of LTβR signaling perturbs TLS formation (34). Moreover, in plaques arising in $ApoE^{-/-}$ mice, LTβ producing $CD11c^+$ $CD68^+$ $Ly6C^{lo}$ monocytes reside in close proximity to vSMCs and induce Cxcl13 and Ccl21 secretion, indicating a potential role of DCs as LTi (17). Overall, multiple models of chronic inflammation show that stromal cells can gain LTo function whilst inflammatory myeloid cells play a crucial role as LTi. Moreover, in the process of TLS formation, TNFα and LTβ serve important non-redundant roles.

SPONTANEOUS TLS FORMATION IN HUMAN CANCER

Tumors are described as "wounds that never heal" (36), and indeed rely on continuous stromal remodeling, inflammation and angiogenesis to support the rapidly growing cancer. The abnormal angiogenic tumor vasculature often lacks adhesion molecules such as ICAM/VCAM which prevents efficient lymphocyte-EC binding (37, 38). However, despite this "anergic" tumor vasculature, the tumor microenvironment (TME) can support naïve T cell infiltration, and spontaneous intratumoral TLS formation has been observed in a subset of patients across cancer types (7).

Although the precise mechanism of spontaneous TLS formation in human cancers is unknown, the presence of intratumoral TLS structures is often associated with a favorable clinical outcome and extended disease-free survival (7, 39–47). In hepatocellular carcinoma (HCC) for instance, the presence of intratumoral TLS reduces the risk for early relapse following tumor resection (43). In addition, mature TLS harboring GCs rather than poorly defined lymphocyte aggregates have the lowest recurrence risk (43). In human breast cancer, the presence of HEVs correlates with overall T and B cell infiltration, and improved prognosis (44, 45). Moreover, flow cytometry and gene expression analysis of $CD4^+$ T cell subsets revealed that highly infiltrated breast cancers also harbor TLS, and express markers such as Cxcl13, ICOS, IFNγ and TBX21/T-bet, commonly associated with follicular T helper (T_{fh}) and Th1 profiles (39, 40). In multiple human cancers such as lung, breast, pancreatic, gastric cancers and melanoma, TLS^{high} tumors harbor more activated, cytotoxic or naïve $CD8^+$ T cells together with $CD4^+$ T cells which are skewed to a Th1 and/or Th17 phenotype when compared to TLS^{low} tumors (41, 42, 44–47).

The presence of intratumoral TLS can be determined by analyzing chemokine gene-expression signatures which were first described in colorectal cancer (48) and subsequently validated for other types of cancer such as HCC, breast cancer and melanoma (43, 49, 50). The ability to assess TLS status prior to therapy is of clinical significance and may offer an opportunity to improve immunotherapy (49).

However, the predictive value of TLS for patient outcome is complex, and other parameters besides presence or absence of lymphocyte aggregates seem to be important. In colorectal cancer, for instance, TLS structures with high densities of M2 macrophages and T helper cells expressing GATA3, a master regulator of Th2 differentiation, contribute to immune suppression and thus correlate with relapse rather than improved prognosis (51). In HCC, TLS in the tumor margin are associated with an increased risk of recurrence (52). Moreover, TLS which arise in HCC patients, or mice with persistent and high NFκB activation in hepatocytes, promote tumor progression rather than anti-tumor immunity (52). Similarly, early human hepatic lesions can harbor immature TLS characterized by the expression of immune suppressive cytokines and T cell exhaustion markers such as IL10RA, TGFβ1, TIM-3 and PD-L2 (53). In other cancer types, for instance breast, colorectal and pancreatic cancers, TLS are often found in peri-tumoral locations, and are associated with more advanced disease (41, 54, 55). Overall, these studies indicate that intratumoral location and TLS maturity are crucial parameters for productive anti-tumor immunity and improved patient outcome (7, 56).

TLS AS INTRATUMORAL PRIMING SITES FOR ADAPTIVE IMMUNITY

It is commonly accepted that naïve lymphocytes do not enter peripheral tissues or tumors, but circulate through lymphoid organs to encounter cognate antigen for activation. However, there is emerging evidence that HEV^+ TLS may activate effector T cells intratumorally thus bypassing the need for tumor-antigen presentation in draining LNs (57). For instance, LIGHT accelerates development of diabetes in NOD mice even after surgical removal of pancreatic draining LNs implying that naïve T cells are primed within TLS in pancreatic islets (18). In B16 melanoma-bearing mice, adoptively transferred naïve anti-tumor T cells differentiate into effector cells, reduce tumor growth and improve survival even when lymphocyte egress from LNs is blocked by FTY720 (6, 58). This suggests that HEV^+ mouse melanomas can facilitate naïve T cell infiltration, and support subsequent priming and differentiation (6).

Naïve T cell activation in TLS relies on the presence of antigen presenting cells such as B cells and DCs. Indeed, in lung (42, 59), breast (60) and renal cancers (61), a high density of TLS-associated mature DCs correlates with the degree of Th1 effector T cell infiltration and improved prognosis. Interestingly, DCs are also involved in HEV function. In peripheral LNs, for instance, DCs maintain HEV maturity and thus naïve T cell infiltration through LTβR signaling (30). In human breast cancer, DCs produce high levels of LTβ and the density of mature $DC\text{-}LAMP^+$ DCs strongly correlates with the frequency of HEVs (60). Collectively, this indicates that DCs maintain HEV maturity and facilitate T cell egress and priming in both LNs and TLS.

B cells are an integral part of mature TLS and potent antigen presenting cells. In some cancers, B cells have been shown to foster tumor development by secreting factors which contribute to a pro-tumorigenic immune environment (62). However, mature B cells in TLS produce antibodies within GCs which correlates with a higher degree of T cell infiltration and disease free survival (63–65). Improved prognosis in human breast

cancer is associated with $CD4^+$ T_{fh} cells which produce an abundance of Cxcl13 and support B cell differentiation, TLS formation and GC maturation (39, 66). In pancreatic adenocarcinoma (PDAC), the presence of B cells within mature TLS correlates with improved prognosis in patients, or increased immune response to vaccination in mice (67). Furthermore, initial evidence in human melanoma suggested a potential link between antibody producing B cells and ICB responsiveness (68, 69). This has now been confirmed in a series of studies which performed in-depth molecular analyses in ICB responder and non-responder tumor tissues (70–72). For instance in human sarcoma, ICB responders are characterized by B cell-rich intratumoral TLS and an immune gene signature related to T cell infiltration and activation, immune checkpoints and expression of Cxcl13 (70). In human melanoma, B cell-enriched TLS confer improved survival and responsiveness to ICB, and also contain naïve and/or memory T cells and an immune signature indicative of enhanced B-T cell interactions and antigen presentation (71, 72). In contrast, T cells in TLS negative melanomas expressed elevated TIM3 and PD-1 levels which may indicate a dysfunctional state (72). Furthermore, RNA-seq analysis of B cell receptors (BCRs) in melanomas showed greater BCR diversity and B cell maturity in ICB responders versus non-responders supporting an active role for B cells in anti-tumor immunity (71). In summary, these studies demonstrate a major role of TLS-associated B cells in antigen presentation, T cell polarization and activation thus placing B cells at the center of TLS function (62, 70–75).

The efficacy of anti-cancer effector T cells is intimately linked to the presence or absence of $CD4^+CD25^+FoxP3^+$ regulatory T cells (T regs), and interestingly, T reg depletion induces TLS. For instance, in a mouse model of chemically induced fibrosarcoma genetic T reg deletion triggers intratumoral HEV formation, T cell recruitment and tumor control (76, 77). Similarly, T-reg depletion in a model of autochthonous lung adenocarcinoma induces TLS, increases T cell proliferation and DC activation with ensuing tumor control (78).

Overall, current evidence strongly supports a role of intratumoral TLS as priming sites for anti-tumor immunity and prognostic indicators for ICB efficacy. Spontaneous formation of mature and functional TLS in cancer is highly orchestrated and context-dependent; insights into this process will provide exciting opportunities for innovative drug development.

FROM CONCEPT TO TREATMENT: THERAPEUTIC INDUCTION OF TLS

Experimental TLS induction in animal models provides an important opportunity to study the complex interplay between immune cell populations which foster adaptive anti-cancer immunity. Therapeutic TLS induction in cancer patients holds the promise to advance immunotherapy. Numerous attempts have been made to induce TLS in mouse models, so far with mixed outcomes. For instance, both Ccl21 and LTβR play important roles during peripheral LN development. Early work in a mouse melanoma model indeed found that a recombinant antibody targeting LTα to melanoma cells induced intratumoral HEVs, B and T cell zones, and improved survival (79). In contrast, Ccl21 overexpressing melanoma cells promoted infiltration of suppressive immune cells and cytokines which collectively stimulate tumor growth (80). Thus, to harness TLS therapeutically better mechanistic insights into intratumoral TLS formation are urgently needed.

More recent attempts to induce TLS in mouse tumors have employed sophisticated technologies such as artificial scaffolds, gene engineering, and vaccination strategies. Given the crucial role of LTo cells in the recruitment of LTi during LN development (8, 12), a role of stromal cells as TLS inducers has been widely explored (48, 81–83). For instance, LTα overexpression in a stromal cell line derived from thymus induces lymphoid-like organoids in mice when co-implanted with DCs in a collagenous scaffold (81). Moreover, a collagen sponge with a cocktail of LN-inducing cytokines when implanted under the kidney capsule also initiates formation of artificial LN-like TLS (artTLS) with distinct B/T cell zones, FDC/FRCs and HEVs. Intriguingly, implantation of these sponges into immunodeficient mice generates antibody producing cells following immunization (82), further supporting a role of TLS in adaptive immunity. Similarly, a LN-derived stromal cell line which expresses high levels of the FRC marker podoplanin and chemokines such as Ccl19, Ccl21, Cxcl10 and Cxcl13 - reminiscent of the chemokine gene signature first identified in human colorectal cancer (48) - when implanted subcutaneously in mice also generates TLS (83). Within these TLS, resident T cells were successfully activated into effector T cells by tumor-lysate-pulsed DCs which suppressed the growth of adjacent MC38 colon cancer cells (83).

In gene engineering studies, DCs were generated to produce high levels of T-bet/Tbx21, a transcription factor that drives the development and functionality of immune cells, particularly by producing the key Th1 cytokine IFNγ. T-bet overexpressing DCs also produce high levels of pro-inflammatory cytokines such as TNFα, IL12p40 and IL-36γ, and induce TLS in a mouse colon cancer model; even in the absence of peripheral LNs intratumoral DC-Tbet therapy prolongs survival (84). In contrast, tumor growth control is abolished in IL36R-deficient mice indicating a crucial role of T-bet/IL-36γ in therapeutic TLS induction (84). This is supported by findings in human colon cancer where IL-36γ is highly expressed in M1 macrophages and cells of the vasculature, including vSMCs and HEVs, and correlates with spontaneous TLS formation (85).

In human papilloma virus (HPV) 16-positive cervical cancer, intramuscular vaccination targeting HPV16 E6/E7 antigens induces intratumoral TLS which contain antigen-experienced effector memory T cells (86). Moreover, TLS-rich tumor stroma harbors a typical Th1 gene signature with increased levels of Cxcr3, TBX21, IFNγ and IFNβ.

In human PDAC, T cell infiltration and activation is positively linked to survival in some patients (87, 88), and TLS can be induced following an allogeneic granulocyte-macrophage

colony stimulating factor secreting vaccine (GVAX) when given in combination with T reg-depleting cyclophosphamide (89). TLS display a distinct Th17 gene signature, a high T effector to T reg ratio, and serve as a prognostic tool to segregate long term from short term survivors (89). Although this clinical trial provides rare evidence for therapeutic TLS induction in humans, PDAC can harbor spontaneous intratumoral TLS which are linked to better prognosis (41). Interestingly, spontaneous TLS in PDAC are associated with a more mature vascular network that expresses the vascular adhesion molecule VE-Cadherin and is covered by αSMA^+ pericytes, a mural cell type which wraps around and supports the endothelium (41), suggesting a possible link between TLS formation and stabilized tumor vessels.

A POTENTIAL LINK BETWEEN VASCULAR NORMALIZATION AND TLS INDUCTION

T cell infiltration into solid cancers is controlled by the vasculature which co-evolves with an immune-suppressive microenvironment and plays an active part in limiting T cell influx (37, 90–93). In contrast, activating tumor blood vessels to express adhesion molecules such as ICAM and VCAM enables productive endothelial-T cell interactions and fosters effector T cell transmigration (3, 92, 94–97). Moreover, tumor vessel normalization which improves vascular morphology and function lowers hypoxia and indirectly changes the tumor microenvironment to support Th1-driven anti-tumor immunity (98–100). Therefore, compounds which normalize tumor blood vessels and attract T cells may have the capacity to induce intratumoral TLS. Indeed, a fusion compound of the cytokine LIGHT conjugated to a homing peptide (vascular targeting peptide or VTP) which delivers LIGHT specifically to angiogenic tumor vessels is such a reagent (95). LTβR and Herpes virus entry mediator (HVEM) are major LIGHT receptors, expressed in stroma and immune cells, respectively, and thus link LIGHT to LN neogenesis and immune regulation (101–106). Treatment of neuroendocrine pancreatic cancer (PNET) in mice with low dose LIGHT-VTP normalizes blood vessels and induces intratumoral TLS with distinct B and T cell zones and high expression of the T cell attractant Ccl21 in vascular cells as well as macrophages (**Figures 2A, B**) (3, 95). Importantly, the capacity to induce TLS correlates with the degree of vessel normalization and is abolished with high dose LIGHT-VTP which induces vessel death, demonstrating a causal link between vessel normalization and TLS formation (3). Other treatment regimens which are known to normalize tumor vessels in PNET such as low dose anti-vascular endothelial growth factors (VEGF) or anti-angiopoietin-2/anti-VEGF therapies facilitate lymphocyte infiltration but do not induce TLS as monotherapies (107, 108). Similarly, cytokine fusion compounds which deliver for instance TNFα or IFNγ to tumor vessels in PNET induce vessel normalization and/or vessel wall inflammation without TLS formation demonstrating the unique opportunities of targeting LIGHT into the tumor microenvironment (97, 109). Furthermore, intratumoral treatment of melanoma-bearing mice with low dose stimulator

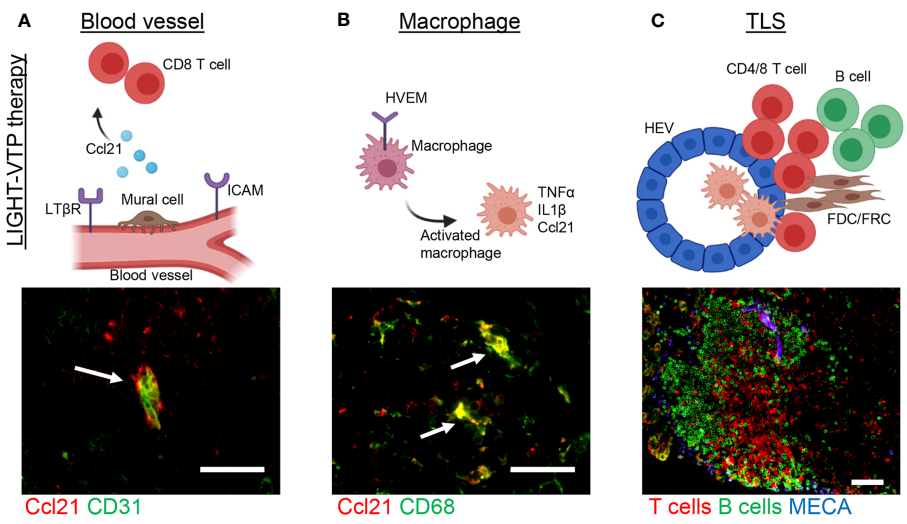

FIGURE 2 | Induction of cancer-associated TLS during LIGHT-VTP therapy. **(A, B)** Treatment of transgenic PNET-bearing mice with bi-weekly i.v. injections of 20 ng LIGHT-VTP specifically targets abnormal angiogenic blood vessels and induces chemokines important for TLS formation (e.g. Ccl21) in **(A)** vascular cells (co-staining of $CD31^+$ endothelium in green and Ccl21 in red, overlay in yellow marked by arrow) which attract $CD8^+$ T cells, and **(B)** tumor-resident $CD68^+$ macrophages which are recruited to the vascular niche (co-staining of CD68 in green and Ccl21 in red, overlay in yellow marked by arrows) and re-programmed to secrete other cytokines such as TNFα and IL1β which in turn attract T/B cells to form TLS (3). **(C)** Adoptive transfer of LIGHT-stimulated macrophages into PNET-bearing mice leads to $CD68^+$ macrophage accumulation in the TME and subsequent formation of mature TLS 8 days after transfer. TLS with organized T cell (red) and B cell (green) zones as well as $MECA79^+$ HEVs (blue) are depicted. Scale bars 50μm. Images are unpublished microscopic photographs similar to work published in (3). Created with BioRender.com.

of interferon genes (STING) agonist (ADU S-100) normalizes angiogenic blood vessels and upregulates TLS-inducing factors such as Ccl19, Ccl21, LTαβ and LIGHT (110). This induces unstructured HEV-containing lymphocyte aggregates resembling TLS which contain T cells and $CD11c^+$ DCs. STING activation enables recruitment of pre-primed peripheral T cells and expansion of unique T cell clonotypes in the TME thus further supporting the benefits of reagents with dual capacity to induce vessel normalization and intratumoral priming. Nevertheless, the anti-tumor effects of LIGHT-VTP or STING monotherapies are modest, and the clinical relevance of these reagents lies in increasing the potency of current immunotherapies (3, 110).

TLS AND IMMUNOTHERAPY

Immunotherapies which boost the host's intrinsic immunity such as anti-cancer vaccines and ICBs have dramatically changed clinical oncology. However, based on the increasing number of drug combination trials, ICB therapies will be predictably more effective in combination with other therapies such as TLS induction (7, 111).

The presence of spontaneously arising B cell-rich TLS within cancers has recently been shown to predict the response to ICB in patients with melanoma, soft-tissue sarcoma and renal cell carcinoma (see above) (70–72). In addition, a retrospective analysis of human lung cancer samples identified $PD\text{-}1^{hi}$ expressing $CD8^+$ T cells within TLS to predict response to PD-1 blockade (112). These proliferating $PD\text{-}1^{hi}$ T cells were highly tumor-reactive, secreted Cxcl13, and are thus potential drivers of TLS formation (112). Similarly, non-small cell lung carcinoma biopsies from PD-1 blockade responders are enriched in TLS and mature B cells (113). Furthermore, patients with desmoplastic melanoma, a subtype of melanoma with dense fibroblastic stroma and high frequency of TLS, respond particularly well to PD-1 blockade compared to other advanced forms of melanoma (114). Although the correlation of TLS frequency and patient responsiveness in retrospective studies might be biased, collectively these studies support the notion that TLS induction prior to ICB is beneficial and will improve response rates to immunotherapy.

Strong evidence for beneficial TME-immune stimulating combination therapies also comes from animal studies. For instance, experimental induction of TLS with LIGHT-VTP therapy renders PNET and Lewis lung carcinoma (LLC) sensitive to ICB targeting cytotoxic T-lymphocyte-associated protein 4 (CTLA-4) and PD-1. The combined treatment induces intratumoral activation of cytotoxic T cells with ensuing survival benefits which can be further improved when combined with anti-cancer vaccination. Notably, neither vaccination, ICB or a combination thereof match the survival outcome achieved with LIGHT-VTP combination treatment (3). In mouse breast cancer, PNET, and glioblastoma (GBM), VEGF inhibition renders tumors susceptible to anti-PD-L1 therapy. The combination treatment of anti-VEGF and anti-PD-L1 activates intratumoral DCs and T cells and reaches maximal efficacy when combined with agonistic LTRβ antibodies; this triple treatment induces HEV^+ immune clusters even in highly therapy-resistant GBM (115). In the same GBM tumor model, LIGHT-VTP treatment in combination with anti-VEGF and anti-PD-L1 is even more effective than agonistic LTβR antibodies, and generates an abundance of intratumoral HEV^+ TLS and granzyme B^+ (GrzB) $CD8^+$ effector T cells (116). This highlights the importance of LTβR signaling for TLS combination immune therapies but also the potential involvement of other pathways since LIGHT activates cells within the tumor microenvironment through multiple receptors including LTβR and HVEM.

Overall, there is already strong evidence that intratumoral TLS are an important prognostic tool for immunotherapies (70–72). However, beyond risk stratification, inducing TLS in combination with ICB generates a synergism which is likely to promote lymphocyte infiltration, intratumoral activation and immune rejection, in particular in immune-deserted or "cold" tumors. Given the significant toxicities of ICB as observed in recent combination trials of Nivolumab and Ipilimumab (117, 118), the presence of TLS may be helpful to select patients who will benefit most from ICB. In addition, TLS/ICB combination therapies could contribute to more effective anti-tumor responses with lower ICB doses. In this context, a preliminary study of low dose Nivolumab and Ipilimumab combined with IL-2 and hyperthermia treatment shows similar overall response rates when compared to high dose ICB with significantly lower overall toxicity (119). This indicates an exciting possibility to lower ICB doses when used in combination with other immune stimulating reagents.

SEARCHING FOR THE INSTIGATOR(S) IN CANCER-ASSOCIATED TLS

Much like LN neogenesis, formation of cancer-associated TLS presumably involves a network of stromal and immune cells linked by multiple cytokines/chemokines. However, mechanistic insights into this process are rudimentary. Since these interactions are precisely orchestrated in a 3D environment *in vitro* studies are challenging. Nevertheless, some cell types and cytokines/chemokines by virtue of their crucial role in experimental systems and presence in human TLS^+ cancer tissue deserve further consideration (**Figure 3**).

Non-Hematopoietic Stromal Cells: Blood Vessels and Fibroblasts

Tumor vasculature and TLS formation are intimately linked (3, 4, 110). For instance, LIGHT-VTP in mouse PNET increases the expression of Ccl21 in the vascular bed and in $CD68^+$ tumor-resident macrophages associated with TLS (**Figures 2A, B**) (3). Moreover, a 3D scaffold environment and slow interstitial flow are essential for Ccl21 expression by LN-derived FRCs both *in vitro* and *in vivo*; without lymph flow Ccl21 expression is not detectable suggesting that fluid flow dynamics may regulate

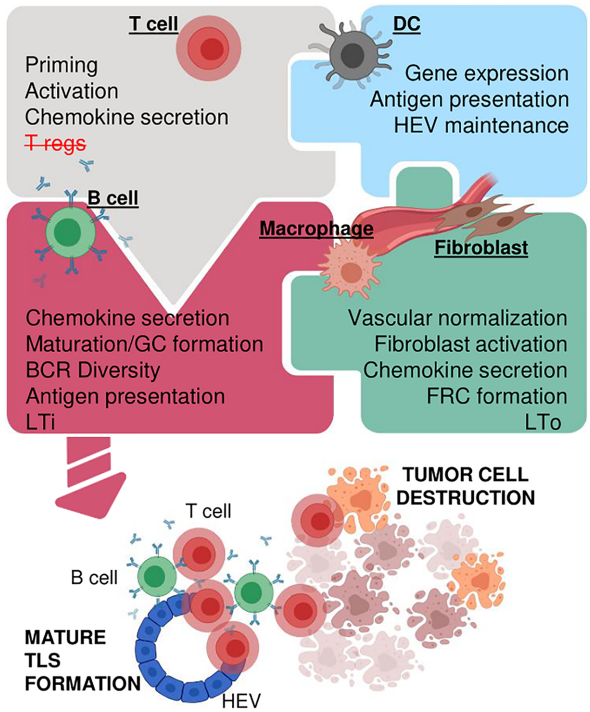

FIGURE 3 | Concepts for creating functional TLS in cancer. Multiple immune and stromal cell types orchestrate TLS formation potentially involving activated T cells and/or depletion of T regs (upper left), DCs which express TLS supporting cytokines/chemokines, maintain HEVs and promote antigen presentation (upper right), mature B cells which produce antibodies, enhance antigen presentation, act as LTi cells (lower left), and stromal cells such as fibroblasts, macrophages and vascular cells which can act as LTo, secrete chemotactic cytokines/chemokines and/or provide structural support (lower right). Some or all cell types may be necessary in an intricate network of simultaneous or consecutive interactions to generate mature TLS which in turn enhance immunotherapy and tumor destruction. Created with BioRender.com.

Ccl21 expression (120). It is therefore interesting to speculate that modulation of blood flow dynamics and transport of cytokines/chemokines during tumor blood vessel normalization may regulate Ccl21 expression levels in the vascular bed, and thus TLS formation *in vivo*.

Cancer associated fibroblasts (CAFs) form a large part of the tumor microenvironment, reduce fluid flow by increasing tumor stiffness, and support tumor-promoting inflammation (121). Thus, modulation of CAFs can enhance anti-cancer immunotherapy (121, 122) and potentially support TLS formation. More recently, a crucial role for CAFs as LTo and effector $CD8^+$ T cells/B cells as LTi was delineated in an intraperitoneal melanoma model of spontaneous TLS formation (4). Therein, effector T cells recruit FAP^- $podoplanin^+$ fibroblasts to HEVs where they differentiate into Cxcl13 secreting FRCs *via* TNFR signaling, similar to previous models of chronic inflammation (26, 27). This in turn promotes recruitment and proliferation of $LT\alpha_1\beta_2$ secreting B cells which further stimulate TLS formation in a positive feedback loop (4).

In human and mouse lung cancer, Ccl19 producing fibroblastic stromal cells (FSC) correlate with increased $CD8^+$ T cell infiltration and tumor growth control. Although TLS formation was not examined in this study, Ccl19-expressing FSCs reside in peri-vascular niches within LLC tumors and T cell recruitment is impaired upon Ccl19 gene deletion suggesting an early role of FSCs in forming immune-stimulating stromal niches (123). Collectively these studies support the notion that vascular cells and fibroblasts are important mediators of TLS neogenesis in cancer (4, 38, 94).

Hematopoietic Stromal Cells: Macrophages

Monocytes/macrophages are a major component of tumor stroma (124). In a hypoxic tumor environment, macrophages are immunosuppressive and support tumor growth. However, their phenotype is highly dynamic and macrophage "re-education" can support immunotherapy (125). In the context of TLS neogenesis, M1 macrophages can produce chemokines similar to those detected in TLS^+ human cancers, including Ccl21 and TNFα (3, 126). Furthermore, *ex vivo* LIGHT-stimulated macrophages in contrast to control macrophages when adoptively transferred into tumor-bearing mice are necessary and sufficient to induce intratumoral TLS in a T cell-dependent manner (**Figure 2C**) (3). In addition to Ccl21, these LIGHT-stimulated macrophages also express high levels of TNFα (**Figure 2B**) which is a key driver of inflammation-induced TLS formation in mice (21, 27). It is therefore possible that LIGHT-stimulated macrophages drive TLS formation *via* the TNFα/TNFR signaling pathway which has so far not been investigated. Whilst the importance of macrophages during TLS formation in cancer is understudied, robust data in inflammatory disease support their importance in TLS neogenesis (21, 27, 29), warranting further investigations in cancer.

Hematopoietic Stromal Cells: DCs

LTα/LTβ producing $CD11c^+$ DCs play a critical role in regulating lymphocyte trafficking and maintaining HEV phenotype and function in adult mouse LNs (30, 32), and are involved in TLS formation during chronic inflammation (30–35). In human tumors, DCs are a major source of LTβ and their density correlates with HEV formation and favorable clinical outcome in breast cancer (60). Similarly, in primary human lung and ovarian cancers the number of mature DCs correlates with the degree of $CD8^+$ T cell infiltration, anti-tumor cytotoxicity and survival (42, 127). Furthermore, immune-stimulating and vascular normalization therapies in mice increase intratumoral $CD11c^+$ DCs coinciding with the formation of lymphocyte aggregates and HEVs (110, 115). Treatment of B16 melanoma with low-dose STING agonist, for instance polarizes DCs to produce TLS-inducing cytokines such as LTα, IL36β and TNFα (110), implicating mature DCs in TLS neogenesis. Overall, mechanistic tumor data are still sparse; plasticity of myeloid cells as well as shared marker expression in myeloid cell and DC populations complicate interpretation of the data. Further analysis of stromal innate immune cells such as monocytes/

macrophage and DCs as initiators of cancer-associated TLS is therefore warranted.

CONCLUSIONS

Although immunotherapy has shown unprecedented success in some cancer patients and tumor types, the challenge ahead lies in improving the outcome for non-responsive patients. TLS as prognostic markers for improved patient outcomes have long been recognized (7). However, only recently have mature TLS been shown to predict ICB success in patients (70–72). It is imperative to now develop strategies to increase TLS frequency and/or maturation in cancers where they naturally occur. This may be achieved by providing further innate immune stimulation as demonstrated for instance with STING agonist treatment (110). Induction of *de novo* TLS formation holds great therapeutic potential to overcome intrinsic immune inhibitory mechanisms within the TME and render non-responsive, immune "cold" tumors susceptible for ICB. However, the orchestration of mature immune-supportive TLS formation in cancer is complex and involves multiple cellular compartments and cytokines/chemokines; this process may also be tumor type-dependent. Emerging mechanistic insight from mouse tumors demonstrate potential LTi roles for anti-tumor effectors such as T and surprisingly B cells which requires re-definition of the role of B cells in TLS and cancer (4). Therapeutic vessel normalization which enables lymphocyte infiltration into tumors may also promote access of these LTi into the TME for more effective TLS priming (3, 110). Furthermore, intratumoral stromal cell types such a monocytes/macrophages and fibroblasts are strong candidates for LTo cells which when reprogrammed in permissive tumor "niches" can drive TLS formation (3, 4). In this context, TNFR in addition to LTβR signaling may prove crucial for tumor-associated TLS formation as opposed to primarily LTβR driven processes as seen during peripheral LN development. Overall, improving existing TLS function or priming *de novo* TLS formation in cancer to maximize ICB efficacy holds the potential to induce more durable anti-tumor immune responses in a higher percentage of cancer patients and warrants urgent investigation.

AUTHOR CONTRIBUTIONS

AJ-P designed the figures. AJ-P and RG planned, constructed and wrote the paper. All authors contributed to the article and approved the submitted version.

FUNDING

This work was supported by the National Health and Medical Research Council of Australia (APP1157240, APP2001120), Cancer Council Western Australia, Cancer Research Institute Clinic and Laboratory Integration Program (CLIP), Worldwide Cancer Research and a Woodside Energy Fellowship (to RG). The funder was not involved in the study design, collection, analysis, interpretation of data, the writing of this article or the decision to submit it for publication.

REFERENCES

1. Hodi FS, O'Day SJ, McDermott DF, Weber RW, Sosman JA, Haanen JB, et al. Improved Survival With Ipilimumab in Patients With Metastatic Melanoma. *N Engl J Med* (2010) 363(8):711–23. doi: 10.1056/NEJMoa1003466
2. Gajewski TF, Corrales L, Williams J, Horton B, Sivan A, Spranger S. Cancer Immunotherapy Targets Based on Understanding the T Cell-Inflamed Versus non-T Cell-Inflamed Tumor Microenvironment. *Adv Exp Med Biol* (2017) 1036:19–31. doi: 10.1007/978-3-319-67577-0_2
3. Johansson-Percival A, He B, Li ZJ, Kjellen A, Russell K, Li J, et al. De Novo Induction of Intratumoral Lymphoid Structures and Vessel Normalization Enhances Immunotherapy in Resistant Tumors. *Nat Immunol* (2017) 18 (11):1207–17. doi: 10.1038/ni.3836
4. Rodriguez A, Peske JD, Woods AN, Leick KM, Mauldin IS, Young SJ, et al. Immune Mechanisms Orchestrate Tertiary Lymphoid Structures in Tumors Via Cancer-Associated Fibroblasts. *Immunity* (2020). doi: 10.2139/ssrn.3575119
5. Tang H, Wang Y, Chlewicki LK, Zhang Y, Guo J, Liang W, et al. Facilitating T Cell Infiltration in Tumor Microenvironment Overcomes Resistance to PD-L1 Blockade. *Cancer Cell* (2016) 30(3):500. doi: 10.1016/j.ccell.2016.08.011
6. Thompson ED, Enriquez HL, Fu YX, Engelhard VH. Tumor Masses Support Naive T Cell Infiltration, Activation, and Differentiation Into Effectors. *J Exp Med* (2010) 207(8):1791–804. doi: 10.1084/jem.20092454
7. Sautes-Fridman C, Petitprez F, Calderaro J, Fridman WH. Tertiary Lymphoid Structures in the Era of Cancer Immunotherapy. *Nat Rev Cancer* (2019) 19(6):307–25. doi: 10.1038/s41568-019-0144-6
8. van de Pavert SA, Mebius RE. New Insights Into the Development of Lymphoid Tissues. *Nat Rev Immunol* (2010) 10(9):664–74. doi: 10.1038/nri2832
9. Fletcher AL, Acton SE, Knoblich K. Lymph Node Fibroblastic Reticular Cells in Health and Disease. *Nat Rev Immunol* (2015) 15(6):350–61. doi: 10.1038/nri3846
10. Gallatin WM, Weissman IL, Butcher EC. A Cell-Surface Molecule Involved in Organ-Specific Homing of Lymphocytes. *Nature* (1983) 304(5921):30–4. doi: 10.1038/304030a0
11. Sautes-Fridman C, Lawand M, Giraldo NA, Kaplon H, Germain C, Fridman WH, et al. Tertiary Lymphoid Structures in Cancers: Prognostic Value, Regulation, and Manipulation for Therapeutic Intervention. *Front Immunol* (2016) 7:407. doi: 10.3389/fimmu.2016.00407
12. van de Pavert SA, Olivier BJ, Goverse G, Vondenhoff MF, Greuter M, Beke P, et al. Chemokine CXCL13 is Essential for Lymph Node Initiation and is Induced by Retinoic Acid and Neuronal Stimulation. *Nat Immunol* (2009) 10(11):1193–9. doi: 10.1038/ni.1789
13. Cupedo T, Jansen W, Kraal G, Mebius RE. Induction of Secondary and Tertiary Lymphoid Structures in the Skin. *Immunity* (2004) 21(5):655–67. doi: 10.1016/j.immuni.2004.09.006
14. Onder L, Danuser R, Scandella E, Firner S, Chai Q, Hehlgans T, et al. Endothelial Cell-Specific Lymphotoxin-Beta Receptor Signaling is Critical for Lymph Node and High Endothelial Venule Formation. *J Exp Med* (2013) 210(3):465–73. doi: 10.1084/jem.20121462
15. Onder L, Morbe U, Pikor N, Novkovic M, Cheng HW, Hehlgans T, et al. Lymphatic Endothelial Cells Control Initiation of Lymph Node Organogenesis. *Immunity* (2017) 47(1):80–92 e4. doi: 10.1016/j.immuni.2017.05.008
16. Onder L, Ludewig B. A Fresh View on Lymph Node Organogenesis. *Trends Immunol* (2018) 39(10):775–87. doi: 10.1016/j.it.2018.08.003
17. Grabner R, Lotzer K, Dopping S, Hildner M, Radke D, Beer M, et al. Lymphotoxin Beta Receptor Signaling Promotes Tertiary Lymphoid

Organogenesis in the Aorta Adventitia of Aged ApoE-/- Mice. *J Exp Med* (2009) 206(1):233–48. doi: 10.1084/jem.20080752
18. Lee Y, Chin RK, Christiansen P, Sun Y, Tumanov AV, Wang J, et al. Recruitment and Activation of Naive T Cells in the Islets by Lymphotoxin Beta Receptor-Dependent Tertiary Lymphoid Structure. *Immunity* (2006) 25(3):499–509. doi: 10.1016/j.immuni.2006.06.016
19. Luther SA, Lopez T, Bai W, Hanahan D, Cyster JG. BLC Expression in Pancreatic Islets Causes B Cell Recruitment and Lymphotoxin-Dependent Lymphoid Neogenesis. *Immunity* (2000) 12(5):471–81. doi: 10.1016/S1074-7613(00)80199-5
20. Luther SA, Bidgol A, Hargreaves DC, Schmidt A, Xu Y, Paniyadi J, et al. Differing Activities of Homeostatic Chemokines CCL19, CCL21, and CXCL12 in Lymphocyte and Dendritic Cell Recruitment and Lymphoid Neogenesis. *J Immunol* (2002) 169(1):424–33. doi: 10.4049/jimmunol.169.1.424
21. Furtado GC, Pacer ME, Bongers G, Benezech C, He Z, Chen L, et al. Tnfalpha-Dependent Development of Lymphoid Tissue in the Absence of RORgammat(+) Lymphoid Tissue Inducer Cells. *Mucosal Immunol* (2014) 7 (3):602–14. doi: 10.1038/mi.2013.79
22. Goya S, Matsuoka H, Mori M, Morishita H, Kida H, Kobashi Y, et al. Sustained Interleukin-6 Signalling Leads to the Development of Lymphoid Organ-Like Structures in the Lung. *J Pathol* (2003) 200(1):82–7. doi: 10.1002/path.1321
23. Rangel-Moreno J, Carragher DM, de la Luz Garcia-Hernandez M, Hwang JY, Kusser K, Hartson L, et al. The Development of Inducible Bronchus-Associated Lymphoid Tissue Depends on IL-17. *Nat Immunol* (2011) 12 (7):639–46. doi: 10.1038/ni.2053
24. Nayar S, Campos J, Smith CG, Iannizzotto V, Gardner DH, Mourcin F, et al. Immunofibroblasts are Pivotal Drivers of Tertiary Lymphoid Structure Formation and Local Pathology. *Proc Natl Acad Sci USA* (2019) 116 (27):13490–7. doi: 10.1073/pnas.1905301116
25. Canete JD, Celis R, Yeremenko N, Sanmarti R, van Duivenvoorde L, Ramirez J, et al. Ectopic Lymphoid Neogenesis is Strongly Associated With Activation of the IL-23 Pathway in Rheumatoid Synovitis. *Arthritis Res Ther* (2015) 17:173. doi: 10.1186/s13075-015-0688-0
26. Peduto L, Dulauroy S, Lochner M, Spath GF, Morales MA, Cumano A, et al. Inflammation Recapitulates the Ontogeny of Lymphoid Stromal Cells. *J Immunol* (2009) 182(9):5789–99. doi: 10.4049/jimmunol.0803974
27. Benezech C, Luu NT, Walker JA, Kruglov AA, Loo Y, Nakamura K, et al. Inflammation-Induced Formation of Fat-Associated Lymphoid Clusters. *Nat Immunol* (2015) 16(8):819–28. doi: 10.1038/ni.3215
28. Barone F, Nayar S, Campos J, Cloake T, Withers DR, Toellner KM, et al. Il-22 Regulates Lymphoid Chemokine Production and Assembly of Tertiary Lymphoid Organs. *Proc Natl Acad Sci USA* (2015) 112(35):11024–9. doi: 10.1073/pnas.1503315112
29. Guedj K, Khallou-Laschet J, Clement M, Morvan M, Gaston AT, Fornasa G, et al. M1 Macrophages Act as LTbetaR-independent Lymphoid Tissue Inducer Cells During Atherosclerosis-Related Lymphoid Neogenesis. *Cardiovasc Res* (2014) 101(3):434–43. doi: 10.1093/cvr/cvt263
30. Moussion C, Girard JP. Dendritic Cells Control Lymphocyte Entry to Lymph Nodes Through High Endothelial Venules. *Nature* (2011) 479 (7374):542–6. doi: 10.1038/nature10540
31. Marinkovic T, Garin A, Yokota Y, Fu YX, Ruddle NH, Furtado GC, et al. Interaction of Mature CD3+CD4+ T Cells With Dendritic Cells Triggers the Development of Tertiary Lymphoid Structures in the Thyroid. *J Clin Invest* (2006) 116(10):2622–32. doi: 10.1172/JCI28993.
32. Girard JP, Moussion C, Forster R. Hevs, Lymphatics and Homeostatic Immune Cell Trafficking in Lymph Nodes. *Nat Rev Immunol* (2012) 12 (11):762–73. doi: 10.1038/nri3298
33. Kanameishi S, Ono S, Honda T, Kabashima K. Lymphotoxin β Receptor Signaling and CD11c-positive Dendritic Cells Form High Endothelial Venule-Like Vessels in the Skin in Murine Atopic Dermatitis Model. *J Immunol* (2020) 204(1 Supplement):229.2–.2.
34. GeurtsvanKessel CH, Willart MA, Bergen IM, van Rijt LS, Muskens F, Elewaut D, et al. Dendritic Cells are Crucial for Maintenance of Tertiary Lymphoid Structures in the Lung of Influenza Virus-Infected Mice. *J Exp Med* (2009) 206(11):2339–49. doi: 10.1084/jem.20090410
35. Halle S, Dujardin HC, Bakocevic N, Fleige H, Danzer H, Willenzon S, et al. Induced Bronchus-Associated Lymphoid Tissue Serves as a General Priming Site for T Cells and is Maintained by Dendritic Cells. *J Exp Med* (2009) 206 (12):2593–601. doi: 10.1084/jem.20091472
36. Dvorak HF. Tumors: Wounds That do Not Heal. Similarities Between Tumor Stroma Generation and Wound Healing. *N Engl J Med* (1986) 315 (26):1650–9. doi: 10.1056/NEJM198612253152606
37. Dirkx AE, Oude Egbrink MG, Kuijpers MJ, van der Niet ST, Heijnen VV, Bouma-ter Steege JC, et al. Tumor Angiogenesis Modulates Leukocyte-Vessel Wall Interactions In Vivo by Reducing Endothelial Adhesion Molecule Expression. *Cancer Res* (2003) 63(9):2322–9.
38. Johansson A, Hamzah J, Ganss R. More Than a Scaffold: Stromal Modulation of Tumor Immunity. *Biochim Biophys Acta* (2016) 1865(1):3–13. doi: 10.1016/j.bbcan.2015.06.001
39. Gu-Trantien C, Loi S, Garaud S, Equeter C, Libin M, de Wind A, et al. CD4 (+) Follicular Helper T Cell Infiltration Predicts Breast Cancer Survival. *J Clin Invest* (2013) 123(7):2873–92. doi: 10.1172/JCI67428
40. Gu-Trantien C, Willard-Gallo K. Tumor-Infiltrating Follicular Helper T Cells: The New Kids on the Block. *Oncoimmunology* (2013) 2(10):e26066. doi: 10.4161/onci.26066
41. Hiraoka N, Ino Y, Yamazaki-Itoh R, Kanai Y, Kosuge T, Shimada K. Intratumoral Tertiary Lymphoid Organ is a Favourable Prognosticator in Patients With Pancreatic Cancer. *Br J Cancer* (2015) 112(11):1782–90. doi: 10.1038/bjc.2015.145
42. Goc J, Germain C, Vo-Bourgais TK, Lupo A, Klein C, Knockaert S, et al. Dendritic Cells in Tumor-Associated Tertiary Lymphoid Structures Signal a Th1 Cytotoxic Immune Contexture and License the Positive Prognostic Value of Infiltrating CD8+ T Cells. *Cancer Res* (2014) 74(3):705–15. doi: 10.1158/0008-5472.CAN-13-1342
43. Calderaro J, Petitprez F, Becht E, Laurent A, Hirsch TZ, Rousseau B, et al. Intra-Tumoral Tertiary Lymphoid Structures are Associated With a Low Risk of Early Recurrence of Hepatocellular Carcinoma. *J Hepatol* (2019) 70 (1):58–65. doi: 10.1016/j.jhep.2018.09.003
44. Martinet L, Garrido I, Filleron T, Le Guellec S, Bellard E, Fournie JJ, et al. Human Solid Tumors Contain High Endothelial Venules: Association With T- and B-lymphocyte Infiltration and Favorable Prognosis in Breast Cancer. *Cancer Res* (2011) 71(17):5678–87. doi: 10.1158/0008-5472.CAN-11-0431
45. Martinet L, Garrido I, Girard JP. Tumor High Endothelial Venules (Hevs) Predict Lymphocyte Infiltration and Favorable Prognosis in Breast Cancer. *Oncoimmunology* (2012) 1(5):789–90. doi: 10.4161/onci.19787
46. Martinet L, Le Guellec S, Filleron T, Lamant L, Meyer N, Rochaix P, et al. High Endothelial Venules (Hevs) in Human Melanoma Lesions: Major Gateways for Tumor-Infiltrating Lymphocytes. *Oncoimmunology* (2012) 1 (6):829–39. doi: 10.4161/onci.20492
47. Hennequin A, Derangere V, Boidot R, Apetoh L, Vincent J, Orry D, et al. Tumor Infiltration by Tbet+ Effector T Cells and CD20+ B Cells is Associated With Survival in Gastric Cancer Patients. *Oncoimmunology* (2016) 5(2):e1054598. doi: 10.1080/2162402X.2015.1054598
48. Coppola D, Nebozhyn M, Khalil F, Dai H, Yeatman T, Loboda A, et al. Unique Ectopic Lymph Node-Like Structures Present in Human Primary Colorectal Carcinoma are Identified by Immune Gene Array Profiling. *Am J Pathol* (2011) 179(1):37–45. doi: 10.1016/j.ajpath.2011.03.007
49. Messina JL, Fenstermacher DA, Eschrich S, Qu X, Berglund AE, Lloyd MC, et al. 12-Chemokine Gene Signature Identifies Lymph Node-Like Structures in Melanoma: Potential for Patient Selection for Immunotherapy? *Sci Rep* (2012) 2:765. doi: 10.1038/srep00765
50. Prabhakaran S, Rizk VT, Ma Z, Cheng CH, Berglund AE, Coppola D, et al. Evaluation of Invasive Breast Cancer Samples Using a 12-Chemokine Gene Expression Score: Correlation With Clinical Outcomes. *Breast Cancer Res* (2017) 19(1):71. doi: 10.1186/s13058-017-0864-z
51. Yamaguchi K, Ito M, Ohmura H, Hanamura F, Nakano M, Tsuchihashi K, et al. Helper T Cell-Dominant Tertiary Lymphoid Structures are Associated With Disease Relapse of Advanced Colorectal Cancer. *Oncoimmunology* (2020) 9(1):1724763. doi: 10.1080/2162402X.2020.1724763
52. Finkin S, Yuan D, Stein I, Taniguchi K, Weber A, Unger K, et al. Ectopic Lymphoid Structures Function as Microniches for Tumor Progenitor Cells in Hepatocellular Carcinoma. *Nat Immunol* (2015) 16(12):1235–44. doi: 10.1038/ni.3290

53. Meylan M, Petitprez F, Lacroix L, Di Tommaso L, Roncalli M, Bougouin A, et al. Early Hepatic Lesions Display Immature Tertiary Lymphoid Structures and Show Elevated Expression of Immune Inhibitory and Immunosuppressive Molecules. *Clin Cancer Res* (2020) 26(16):4381–9. doi: 10.1158/1078-0432.CCR-19-2929
54. Figenschau SL, Fismen S, Fenton KA, Fenton C, Mortensen ES. Tertiary Lymphoid Structures are Associated With Higher Tumor Grade in Primary Operable Breast Cancer Patients. *BMC Cancer* (2015) 15:101. doi: 10.1186/s12885-015-1116-1
55. Bento DC, Jones E, Junaid S, Tull J, Williams GT, Godkin A, et al. High Endothelial Venules are Rare in Colorectal Cancers But Accumulate in Extra-Tumoral Areas With Disease Progression. *Oncoimmunology* (2015) 4 (3):e974374. doi: 10.4161/2162402X.2014.974374
56. Engelhard VH, Rodriguez AB, Mauldin IS, Woods AN, Peske JD, Slingluff CLJr. Immune Cell Infiltration and Tertiary Lymphoid Structures as Determinants of Antitumor Immunity. *J Immunol* (2018) 200(2):432–42. doi: 10.4049/jimmunol.1701269
57. Dieu-Nosjean MC, Giraldo NA, Kaplon H, Germain C, Fridman WH, Sautes-Fridman C. Tertiary Lymphoid Structures, Drivers of the Anti-Tumor Responses in Human Cancers. *Immunol Rev* (2016) 271(1):260–75. doi: 10.1111/imr.12405
58. Peske JD, Woods AB, Engelhard VH. Control of CD8 T-Cell Infiltration Into Tumors by Vasculature and Microenvironment. *Adv Cancer Res* (2015) 128:263–307. doi: 10.1016/bs.acr.2015.05.001
59. Dieu-Nosjean MC, Antoine M, Danel C, Heudes D, Wislez M, Poulot V, et al. Long-Term Survival for Patients With non-Small-Cell Lung Cancer With Intratumoral Lymphoid Structures. *J Clin Oncol* (2008) 26(27):4410–7. doi: 10.1200/JCO.2007.15.0284
60. Martinet L, Filleron T, Le Guellec S, Rochaix P, Garrido I, Girard JP. High Endothelial Venule Blood Vessels for Tumor-Infiltrating Lymphocytes are Associated With Lymphotoxin Beta-Producing Dendritic Cells in Human Breast Cancer. *J Immunol* (2013) 191(4):2001–8. doi: 10.4049/jimmunol.1300872
61. Giraldo NA, Becht E, Pages F, Skliris G, Verkarre V, Vano Y, et al. Orchestration and Prognostic Significance of Immune Checkpoints in the Microenvironment of Primary and Metastatic Renal Cell Cancer. *Clin Cancer Res* (2015) 21(13):3031–40. doi: 10.1158/1078-0432.CCR-14-2926
62. Gunderson AJ, Coussens LM. B Cells and Their Mediators as Targets for Therapy in Solid Tumors. *Exp Cell Res* (2013) 319(11):1644–9. doi: 10.1016/j.yexcr.2013.03.005
63. Kroeger DR, Milne K, Nelson BH. Tumor-Infiltrating Plasma Cells Are Associated With Tertiary Lymphoid Structures, Cytolytic T-Cell Responses, and Superior Prognosis in Ovarian Cancer. *Clin Cancer Res* (2016) 22 (12):3005–15. doi: 10.1158/1078-0432.CCR-15-2762
64. Garaud S, Buisseret L, Solinas C, Gu-Trantien C, de Wind A, Van den Eynden G, et al. Tumor Infiltrating B-cells Signal Functional Humoral Immune Responses in Breast Cancer. *JCI Insight* (2019) 4(18):e129641. doi: 10.1172/jci.insight.129641
65. Germain C, Gnjatic S, Tamzalit F, Knockaert S, Remark R, Goc J, et al. Presence of B Cells in Tertiary Lymphoid Structures is Associated With a Protective Immunity in Patients With Lung Cancer. *Am J Respir Crit Care Med* (2014) 189(7):832–44. doi: 10.1164/rccm.201309-1611OC
66. Gu-Trantien C, Migliori E, Buisseret L, de Wind A, Brohee S, Garaud S, et al. CXCL13-Producing TFH Cells Link Immune Suppression and Adaptive Memory in Human Breast Cancer. *JCI Insight* (2017) 2(11):e91487. doi: 10.1172/jci.insight.91487
67. Castino GF, Cortese N, Capretti G, Serio S, Di Caro G, Mineri R, et al. Spatial Distribution of B Cells Predicts Prognosis in Human Pancreatic Adenocarcinoma. *Oncoimmunology* (2016) 5(4):e1085147. doi: 10.1080/2162402X.2015.1085147
68. Griss J, Bauer W, Wagner C, Simon M, Chen M, Grabmeier-Pfistershammer K, et al. B Cells Sustain Inflammation and Predict Response to Immune Checkpoint Blockade in Human Melanoma. *Nat Commun* (2019) 10 (1):4186. doi: 10.1038/s41467-019-12160-2
69. Selitsky SR, Mose LE, Smith CC, Chai S, Hoadley KA, Dittmer DP, et al. Prognostic Value of B Cells in Cutaneous Melanoma. *Genome Med* (2019) 11(1):36. doi: 10.1186/s13073-019-0647-5
70. Petitprez F, de Reynies A, Keung EZ, Chen TW, Sun CM, Calderaro J, et al. B Cells are Associated With Survival and Immunotherapy Response in Sarcoma. *Nature* (2020) 577(7791):556–60. doi: 10.1038/s41586-019-1906-8
71. Helmink BA, Reddy SM, Gao J, Zhang S, Basar R, Thakur R, et al. B Cells and Tertiary Lymphoid Structures Promote Immunotherapy Response. *Nature* (2020) 577(7791):549–55. doi: 10.1038/s41586-019-1922-8
72. Cabrita R, Lauss M, Sanna A, Donia M, Skaarup Larsen M, Mitra S, et al. Tertiary Lymphoid Structures Improve Immunotherapy and Survival in Melanoma. *Nature* (2020) 577(7791):561–5. doi: 10.1038/s41586-019-1914-8
73. Carmi Y, Spitzer MH, Linde IL, Burt BM, Prestwood TR, Perlman N, et al. Allogeneic IgG Combined With Dendritic Cell Stimuli Induce Antitumour T-cell Immunity. *Nature* (2015) 521(7550):99–104. doi: 10.1038/nature14424
74. Bruno TC, Ruffin A, Cillo A, Liu D, Kunning S, Ferris RL, et al. Tumor Infiltrating B Cells Co-Localize With CD4 T Effector Cells Within Organized Tertiary Lymphoid Structures to Present Antigen and Educate the Anti-Tumor Immune Response in Human Primary Tumors. *J Immunol* (2019) 202(1 Supplement):138.15–.15.
75. Teillaud JL, Dieu-Nosjean MC. Tertiary Lymphoid Structures: An Anti-Tumor School for Adaptive Immune Cells and an Antibody Factory to Fight Cancer? *Front Immunol* (2017) 8:830. doi: 10.3389/fimmu.2017.00830
76. Hindley JP, Jones E, Smart K, Bridgeman H, Lauder SN, Ondondo B, et al. T-Cell Trafficking Facilitated by High Endothelial Venules is Required for Tumor Control After Regulatory T-cell Depletion. *Cancer Res* (2012) 72 (21):5473–82. doi: 10.1158/0008-5472.CAN-12-1912
77. Colbeck EJ, Jones E, Hindley JP, Smart K, Schulz R, Browne M, et al. Treg Depletion Licenses T Cell-Driven HEV Neogenesis and Promotes Tumor Destruction. *Cancer Immunol Res* (2017) 5(11):1005–15. doi: 10.1158/2326-6066.CIR-17-0131
78. Joshi NS, Akama-Garren EH, Lu Y, Lee DY, Chang GP, Li A, et al. Regulatory T Cells in Tumor-Associated Tertiary Lymphoid Structures Suppress Anti-Tumor T Cell Responses. *Immunity* (2015) 43(3):579–90. doi: 10.1016/j.immuni.2015.08.006
79. Schrama D, thor Straten P, Fischer WH, McLellan AD, Brocker EB, Reisfeld RA, et al. Targeting of Lymphotoxin-Alpha to the Tumor Elicits an Efficient Immune Response Associated With Induction of Peripheral Lymphoid-Like Tissue. *Immunity* (2001) 14(2):111–21. doi: 10.1016/S1074-7613(01)00094-2
80. Shields JD, Kourtis IC, Tomei AA, Roberts JM, Swartz MA. Induction of Lymphoidlike Stroma and Immune Escape by Tumors That Express the Chemokine CCL21. *Science* (2010) 328(5979):749–52. doi: 10.1126/science.1185837
81. Suematsu S, Watanabe T. Generation of a Synthetic Lymphoid Tissue-Like Organoid in Mice. *Nat Biotechnol* (2004) 22(12):1539–45. doi: 10.1038/nbt1039
82. Kobayashi Y, Watanabe T. Gel-Trapped Lymphorganogenic Chemokines Trigger Artificial Tertiary Lymphoid Organs and Mount Adaptive Immune Responses In Vivo. *Front Immunol* (2016) 7:316. doi: 10.3389/fimmu.2016.00316
83. Zhu G, Nemoto S, Mailloux AW, Perez-Villarroel P, Nakagawa R, Falahat R, et al. Induction of Tertiary Lymphoid Structures With Antitumor Function by a Lymph Node-Derived Stromal Cell Line. *Front Immunol* (2018) 9:1609. doi: 10.3389/fimmu.2018.01609
84. Weinstein AM, Chen L, Brzana EA, Patil PR, Taylor JL, Fabian KL, et al. Tbet and IL-36gamma Cooperate in Therapeutic DC-mediated Promotion of Ectopic Lymphoid Organogenesis in the Tumor Microenvironment. *Oncoimmunology* (2017) 6(6):e1322238. doi: 10.1080/2162402X.2017.1322238
85. Weinstein AM, Giraldo NA, Petitprez F, Julie C, Lacroix L, Peschaud F, et al. Association of IL-36gamma With Tertiary Lymphoid Structures and Inflammatory Immune Infiltrates in Human Colorectal Cancer. *Cancer Immunol Immunother* (2019) 68(1):109–20. doi: 10.1007/s00262-018-2259-0
86. Maldonado L, Teague JE, Morrow MP, Jotova I, Wu TC, Wang C, et al. Intramuscular Therapeutic Vaccination Targeting HPV16 Induces T Cell Responses That Localize in Mucosal Lesions. *Sci Transl Med* (2014) 6 (221):221ra13. doi: 10.1126/scitranslmed.3007323

87. Tewari N, Zaitoun AM, Arora A, Madhusudan S, Ilyas M, Lobo DN. The Presence of Tumour-Associated Lymphocytes Confers a Good Prognosis in Pancreatic Ductal Adenocarcinoma: An Immunohistochemical Study of Tissue Microarrays. *BMC Cancer* (2013) 13:436. doi: 10.1186/1471-2407-13-436
88. Balachandran VP, Luksza M, Zhao JN, Makarov V, Moral JA, Remark R, et al. Identification of Unique Neoantigen Qualities in Long-Term Survivors of Pancreatic Cancer. *Nature* (2017) 551(7681):512–6. doi: 10.1038/nature24462
89. Lutz ER, Wu AA, Bigelow E, Sharma R, Mo G, Soares K, et al. Immunotherapy Converts Nonimmunogenic Pancreatic Tumors Into Immunogenic Foci of Immune Regulation. *Cancer Immunol Res* (2014) 2 (7):616–31. doi: 10.1158/2326-6066.CIR-14-0027
90. Vestweber D. How Leukocytes Cross the Vascular Endothelium. *Nat Rev Immunol* (2015) 15(11):692–704. doi: 10.1038/nri3908
91. Motz GT, Santoro SP, Wang LP, Garrabrant T, Lastra RR, Hagemann IS, et al. Tumor Endothelium FasL Establishes a Selective Immune Barrier Promoting Tolerance in Tumors. *Nat Med* (2014) 20(6):607–15. doi: 10.1038/nm.3541
92. Hamzah J, Jugold M, Kiessling F, Rigby P, Manzur M, Marti HH, et al. Vascular Normalization in Rgs5-deficient Tumours Promotes Immune Destruction. *Nature* (2008) 453(7193):410–4. doi: 10.1038/nature06868
93. Griffioen AW, Damen CA, Blijham GH, Groenewegen G. Tumor Angiogenesis is Accompanied by a Decreased Inflammatory Response of Tumor-Associated Endothelium. *Blood* (1996) 88(2):667–73. doi: 10.1182/blood.V88.2.667.bloodjournal882667
94. Johansson-Percival A, He B, Ganss R. Immunomodulation of Tumor Vessels: It Takes Two to Tango. *Trends Immunol* (2018) 39(10):801–14. doi: 10.1016/j.it.2018.08.001
95. Johansson-Percival A, Li ZJ, Lakhiani DD, He B, Wang X, Hamzah J, et al. Intratumoral LIGHT Restores Pericyte Contractile Properties and Vessel Integrity. *Cell Rep* (2015) 13(12):2687–98. doi: 10.1016/j.celrep.2015.12.004
96. Ganss R, Hanahan D. Tumor Microenvironment can Restrict the Effectiveness of Activated Antitumor Lymphocytes. *Cancer Res* (1998) 58 (20):4673–81.
97. Johansson A, Hamzah J, Payne CJ, Ganss R. Tumor-Targeted TNFalpha Stabilizes Tumor Vessels and Enhances Active Immunotherapy. *Proc Natl Acad Sci U S A* (2012) 109(20):7841–6. doi: 10.1073/pnas.1118296109
98. Ganss R, Ryschich E, Klar E, Arnold B, Hammerling GJ. Combination of T-cell Therapy and Trigger of Inflammation Induces Remodeling of the Vasculature and Tumor Eradication. *Cancer Res* (2002) 62(5):1462–70.
99. Tian L, Goldstein A, Wang H, Ching Lo H, Sun Kim I, Welte T, et al. Mutual Regulation of Tumour Vessel Normalization and Immunostimulatory Reprogramming. *Nature* (2017) 544(7649):250–4. doi: 10.1038/nature21724
100. Zheng X, Fang Z, Liu X, Deng S, Zhou P, Wang X, et al. Increased Vessel Perfusion Predicts the Efficacy of Immune Checkpoint Blockade. *J Clin Invest* (2018) 128(5):2104–15. doi: 10.1172/JCI96582
101. Crowe PD, VanArsdale TL, Walter BN, Ware CF, Hession C, Ehrenfels B, et al. A Lymphotoxin-Beta-Specific Receptor. *Science* (1994) 264(5159):707–10. doi: 10.1126/science.8171323
102. Montgomery RI, Warner MS, Lum BJ, Spear PG. Herpes Simplex Virus-1 Entry Into Cells Mediated by a Novel Member of the TNF/NGF Receptor Family. *Cell* (1996) 87(3):427–36. doi: 10.1016/S0092-8674(00)81363-X
103. Lu TT, Browning JL. Role of the Lymphotoxin/LIGHT System in the Development and Maintenance of Reticular Networks and Vasculature in Lymphoid Tissues. *Front Immunol* (2014) 5:47. doi: 10.3389/fimmu.2014.00047
104. Browning JL, Allaire N, Ngam-Ek A, Notidis E, Hunt J, Perrin S, et al. Lymphotoxin-Beta Receptor Signaling is Required for the Homeostatic Control of HEV Differentiation and Function. *Immunity* (2005) 23 (5):539–50. doi: 10.1016/j.immuni.2005.10.002
105. Chang YH, Hsieh SL, Chao Y, Chou YC, Lin WW. Proinflammatory Effects of LIGHT Through HVEM and LTbetaR Interactions in Cultured Human Umbilical Vein Endothelial Cells. *J BioMed Sci* (2005) 12(2):363–75. doi: 10.1007/s11373-005-1360-5
106. Morel Y, Schiano de Colella JM, Harrop J, Deen KC, Holmes SD, Wattam TA, et al. Reciprocal Expression of the TNF Family Receptor Herpes Virus Entry Mediator and its Ligand LIGHT on Activated T Cells: LIGHT Down-Regulates its Own Receptor. *J Immunol* (2000) 165(8):4397–404. doi: 10.4049/jimmunol.165.8.4397
107. Schmittnaegel M, Rigamonti N, Kadioglu E, Cassara A, Wyser Rmili C, Kiialainen A, et al. Dual Angiopoietin-2 and VEGFA Inhibition Elicits Antitumor Immunity That is Enhanced by PD-1 Checkpoint Blockade. *Sci Transl Med* (2017) 9(385):eaak9670. doi: 10.1126/scitranslmed.aak9670
108. Huang Y, Yuan J, Righi E, Kamoun WS, Ancukiewicz M, Nezivar J, et al. Vascular Normalizing Doses of Antiangiogenic Treatment Reprogram the Immunosuppressive Tumor Microenvironment and Enhance Immunotherapy. *Proc Natl Acad Sci U.S.A.* (2012) 109(43):17561–6. doi: 10.1073/pnas.1215397109
109. Johansson A, Hamzah J, Ganss R. Intratumoral TNFalpha Improves Immunotherapy. *Oncoimmunology* (2012) 1(8):1395–7. doi: 10.4161/onci.20981
110. Chelvanambi M, Fecek RJ, Taylor JL, Storkus WJ. STING Agonist-Based Treatment Promotes Vascular Normalization and Tertiary Lymphoid Structure Formation in the Therapeutic Melanoma Microenvironment. *J Immunother Cancer* (2021) 9(2):e001906. doi: 10.1136/jitc-2020-001906
111. Upadhaya S, Neftelino ST, Hodge JP, Oliva C, Campbell JR, Yu JX. Combinations Take Centre Stage in PD1/PDL1 Inhibitor Clinical Trials. *Nat Rev Drug Discovery* (2020) 20:168–9. doi: 10.1038/d41573-020-00204-y
112. Thommen DS, Koelzer VH, Herzig P, Roller A, Trefny M, Dimeloe S, et al. A Transcriptionally and Functionally Distinct PD-1(+) Cd8(+) T Cell Pool With Predictive Potential in non-Small-Cell Lung Cancer Treated With PD-1 Blockade. *Nat Med* (2018) 24(7):994–1004. doi: 10.1038/s41591-018-0057-z
113. Cottrell TR, Thompson ED, Forde PM, Stein JE, Duffield AS, Anagnostou V, et al. Pathologic Features of Response to Neoadjuvant anti-PD-1 in Resected non-Small-Cell Lung Carcinoma: A Proposal for Quantitative Immune-Related Pathologic Response Criteria (Irprc). *Ann Oncol* (2018) 29(8):1853–60. doi: 10.1093/annonc/mdy218
114. Eroglu Z, Zaretsky JM, Hu-Lieskovan S, Kim DW, Algazi A, Johnson DB, et al. High Response Rate to PD-1 Blockade in Desmoplastic Melanomas. *Nature* (2018) 553(7688):347–50. doi: 10.1038/nature25187
115. Allen E, Jabouille A, Rivera LB, Lodewijckx I, Missiaen R, Steri V, et al. Combined Antiangiogenic and anti-PD-L1 Therapy Stimulates Tumor Immunity Through HEV Formation. *Sci Transl Med* (2017) 9(385): eaak9679. doi: 10.1126/scitranslmed.aak9679
116. He B, Jabouille A, Steri V, Johansson-Percival A, Michael IP, Kotamraju VR, et al. Vascular Targeting of LIGHT Normalizes Blood Vessels in Primary Brain Cancer and Induces Intratumoural High Endothelial Venules. *J Pathol* (2018) 245(2):209–21. doi: 10.1002/path.5080
117. Xing P, Zhang F, Wang G, Xu Y, Li C, Wang S, et al. Incidence Rates of Immune-Related Adverse Events and Their Correlation With Response in Advanced Solid Tumours Treated With NIVO or NIVO+IPI: A Systematic Review and Meta-Analysis. *J Immunother Cancer* (2019) 7(1):341. doi: 10.1186/s40425-019-0779-6
118. Callahan MK, Kluger H, Postow MA, Segal NH, Lesokhin A, Atkins MB, et al. Nivolumab Plus Ipilimumab in Patients With Advanced Melanoma: Updated Survival, Response, and Safety Data in a Phase I Dose-Escalation Study. *J Clin Oncol* (2018) 36(4):391–8. doi: 10.1200/JCO.2017.72.2850
119. Kleef R, Nagy R, Baierl A, Bacher V, Bojar H, McKee DL, et al. Low-Dose Ipilimumab Plus Nivolumab Combined With IL-2 and Hyperthermia in Cancer Patients With Advanced Disease: Exploratory Findings of a Case Series of 131 Stage IV Cancers - a Retrospective Study of a Single Institution. *Cancer Immunol Immunother* (2021) 70(5):1393–403. doi: 10.1007/s00262-020-02751-0
120. Tomei AA, Siegert S, Britschgi MR, Luther SA, Swartz MA. Fluid Flow Regulates Stromal Cell Organization and CCL21 Expression in a Tissue-Engineered Lymph Node Microenvironment. *J Immunol* (2009) 183 (7):4273–83. doi: 10.4049/jimmunol.0900835
121. Liu T, Han C, Wang S, Fang P, Ma Z, Xu L, et al. Cancer-Associated Fibroblasts: An Emerging Target of Anti-Cancer Immunotherapy. *J Hematol Oncol* (2019) 12(1):86. doi: 10.1186/s13045-019-0770-1

122. Monteran L, Erez N. The Dark Side of Fibroblasts: Cancer-Associated Fibroblasts as Mediators of Immunosuppression in the Tumor Microenvironment. *Front Immunol* (2019) 10:1835. doi: 10.3389/fimmu.2019.01835
123. Cheng HW, Onder L, Cupovic J, Boesch M, Novkovic M, Pikor N, et al. CCL19-Producing Fibroblastic Stromal Cells Restrain Lung Carcinoma Growth by Promoting Local Antitumor T-cell Responses. *J Allergy Clin Immunol* (2018) 142(4):1257–71 e4. doi: 10.1016/j.jaci.2017.12.998
124. Mantovani A, Marchesi F, Malesci A, Laghi L, Allavena P. Tumour-Associated Macrophages as Treatment Targets in Oncology. *Nat Rev Clin Oncol* (2017) 14(7):399–416. doi: 10.1038/nrclinonc.2016.217
125. DeNardo DG, Ruffell B. Macrophages as Regulators of Tumour Immunity and Immunotherapy. *Nat Rev Immunol* (2019) 19(6):369–82. doi: 10.1038/s41577-019-0127-6
126. Allavena P, Sica A, Garlanda C, Mantovani A. The Yin-Yang of Tumor-Associated Macrophages in Neoplastic Progression and Immune Surveillance. *Immunol Rev* (2008) 222:155–61. doi: 10.1111/j.1600-065X.2008.00607.x
127. Truxova I, Kasikova L, Hensler M, Skapa P, Laco J, Pecen L, et al. Mature Dendritic Cells Correlate With Favorable Immune Infiltrate and Improved Prognosis in Ovarian Carcinoma Patients. *J Immunother Cancer* (2018) 6:139. doi: 10.1186/s40425-018-0446-3

Conflict of Interest: The authors declare that the research was conducted in the absence of any commercial or financial relationships that could be construed as a potential conflict of interest.

Copyright © 2021 Johansson-Percival and Ganss. This is an open-access article distributed under the terms of the Creative Commons Attribution License (CC BY). The use, distribution or reproduction in other forums is permitted, provided the original author(s) and the copyright owner(s) are credited and that the original publication in this journal is cited, in accordance with accepted academic practice. No use, distribution or reproduction is permitted which does not comply with these terms.

frontiers in Immunology

ORIGINAL RESEARCH
published: 24 June 2021
doi: 10.3389/fimmu.2021.675146

A Standardized Analysis of Tertiary Lymphoid Structures in Human Melanoma: Disease Progression- and Tumor Site-Associated Changes With Germinal Center Alteration

*Franziska Werner[1], Christine Wagner[1], Martin Simon[1], Katharina Glatz[2], Kirsten D. Mertz[3], Heinz Läubli[4], Johannes Griss[5] and Stephan N. Wagner[1]**

[1] Laboratory of Molecular Dermato-Oncology and Tumor Immunology, Department of Dermatology, Medical University of Vienna, Vienna, Austria, [2] Institute of Medical Genetics and Pathology, University Hospital Basel, University Basel, Basel, Switzerland, [3] Institute of Pathology, Cantonal Hospital Baselland, Liestal, Switzerland, [4] Laboratory for Cancer Immunotherapy, Department of Biomedicine and Medical Oncology, Department of Internal Medicine, University Hospital Basel, Basel, Switzerland, [5] Department of Dermatology, Medical University of Vienna, Vienna, Austria

OPEN ACCESS

Edited by:
Vivek Verma,
Georgetown University, United States

Reviewed by:
Pushpamali De Silva,
Massachusetts General Hospital and Harvard Medical School, United States
Adam William Mailloux,
The University of Iowa, United States

***Correspondence:**
Stephan N Wagner
stephan.wagner@meduniwien.ac.at

Specialty section:
This article was submitted to Cancer Immunity and Immunotherapy, a section of the journal Frontiers in Immunology

Received: 02 March 2021
Accepted: 10 June 2021
Published: 24 June 2021

Citation:
Werner F, Wagner C, Simon M, Glatz K, Mertz KD, Läubli H, Griss J and Wagner SN (2021) A Standardized Analysis of Tertiary Lymphoid Structures in Human Melanoma: Disease Progression- and Tumor Site-Associated Changes With Germinal Center Alteration. Front. Immunol. 12:675146. doi: 10.3389/fimmu.2021.675146

There is increasing evidence that tertiary lymphoid structures (TLS) control not only local adaptive B cell responses at melanoma tumor sites but also the cellular composition and function of other immune cells. In human melanoma, however, a comprehensive analysis of TLS phenotypes, density and spatial distribution at different disease stages is lacking. Here we used 7-color multiplex immunostaining of whole tissue sections from 103 human melanoma samples to characterize TLS phenotypes along the expression of established TLS-defining molecular and cellular components. TLS density and spatial distribution were determined by referring TLS counts to the tissue area within defined intra- and extratumoral perimeters around the invasive tumor front. We show that only a subgroup of primary human melanomas contains TLS. These TLS rarely formed germinal centers and mostly located intratumorally within 1 mm distance to the invasive tumor front. In contrast, melanoma metastases had a significantly increased density of secondary follicular TLS. They appeared preferentially in stromal areas within an extratumoral 1 mm distance to the invasive tumor front and their density varied over time and site of metastasis. Interestingly, secondary follicular TLS in melanoma often lacked $BCL6^+$ lymphatic cells and canonical germinal center polarity with the formation of dark and light zone areas. Our work provides an integrated qualitative, quantitative and spatial analysis of TLS in human melanoma and shows disease progression- and site-associated changes in TLS phenotypes, density and spatial distribution. The frequent absence of canonical germinal center polarity in melanoma TLS highlights the induction of TLS maturation as a potential additive to future immunotherapy studies. Given the variable evaluation strategies used in previous

TLS studies of human tumors, an important asset of this study is the standardized quantitative evaluation approach that provides a high degree of reproducibility.

Keywords: Tertiary Lymphoid Structures (TLS), TLS maturation, tumor microenvironment, multiplex immunohistochemistry (mIHC), germinal center polarity, spatial distribution, automated imaging and analysis, human melanoma

INTRODUCTION

Immune checkpoint blockade (ICB) aims to overcome inhibition of anti-tumor T cell effector functions in an inflamed but immunosuppressed tumor microenvironment (TME, *i.e.* tumor cells with surrounding extracellular matrix and stromal/immune host cells). That way, ICB has transformed the therapy of many cancer types, particularly of melanoma, where ICB has led to progression-free survival rates of 36% at 5 years in metastatic patients (1). Yet, the other 64% of patients experience disease progression and alternative therapeutic options are naught.

The outcome of ICB therapy in cancer patients has been linked to immune cell infiltration into the TME and the quality and magnitude of the induced activation of immune cells including T cells, NK cells and, more recently tumor-associated B cells. In human melanoma, up to 33% of the immune cells found in the TME can be B cells. Though B cells in human cancer have been shown to express immunoinhibitory cytokines, growth factors and cell surface molecules that impede anti-tumor immune and drug responses (2, 3), several reports suggest a role in supporting tumor immunity and limiting disease progression. They demonstrate a positive prognostic association of $CD20^+$ B cell numbers in primary human melanoma (4, 5) and, together with increased $CD138^+$ plasma cell numbers, in metastatic human melanoma (6). In line with these data, B cells have recently been shown to sustain inflammation and $CD8^+$ and $CD4^+$ T cell numbers in the TME of human melanoma, and to directly augment T cell activation by ICB (7). Furthermore, B cell markers were reported to be increased in tumor samples from responders to neoadjuvant ICB compared with non-responders in patients with high-risk resectable melanoma (8), and pretreatment B cell counts, particularly of plasmablast-like B cells, have been found to predict response and survival in metastatic melanoma patients receiving ICB (7).

Further independent comparative analyses of human melanoma and soft tissue sarcoma described higher numbers of mature tertiary lymphoid structures (TLS) in tumor samples from patients who responded to ICB treatment compared to non-responding patients (9–11). As ectopic lymphoid structures at tumor sites, TLS share many structural and functional features with canonical lymphoid structures from secondary lymphoid organs which are important drivers of adaptive B cell and T cell responses. Consistently, higher numbers of mature TLS are associated with clonal B cell expansion, increased B cell receptor diversity and increased frequency of class-switched memory, plasmablast/plasma cell-like and activated $CD69^+$ B cells in human melanoma (9, 10). Again, the number of intratumoral B cells before treatment, either together with increased or independent of $CD8^+$ T cell numbers, was shown to be predictive for improved patient survival (9). Together with the reported clonal amplification, somatic hypermutation and isotype switching of B cells in microdissected lymphoid follicles from human melanoma skin metastases (12) and our observation on the loss even of $CD20^-$ B cells from the human melanoma TME upon depletion of TLS by anti-CD20 therapy (7), these data strongly support the concept of TLS as the main generator of local adaptive B cell responses in melanoma. In addition, there is increasing evidence that TLS can also play a significant role in the induction of local adaptive T cell responses in human melanoma. Mature TLS also contain T cell zones where mature dendritic cells and most likely mature B cells present antigenic peptides to $CD4^+$ and $CD8^+$ T cells (13–16). Consistent with this, the density of mature dendritic cells is associated with strong infiltration by activated T cells and favorable survival in primary human melanoma (17) and $CD3^+$ T cells from inside TLS of human melanoma metastases show a higher expression of T cell activation markers compared with T cells from outside (10). Moreover, in TLS-enriched melanoma metastases, increased immune signatures for antigen presentation and processing, T cell receptor signaling and differentiation of T helper 1 and 2 cells were found (10), whereas in TLS-depleted melanomas, T cell signatures indicated a more dysfunctional state (9).

Similar to canonical lymphoid structures in secondary lymphoid organs, phenotypic changes of TLS have been described in human cancer and are associated with a variable composition of diverse cell types with distinct differentiation. Here, the cellular composition of TLS appears to vary between patients and cancer types, stages and sites (18–22). While there are some reports on the presence of distinct TLS-associated cell types in primary human melanoma (17, 23) and a smaller cohort of human melanoma skin metastases (12), a systematic comparative analysis of TLS phenotypes, their cellular composition and spatial distribution in human melanoma samples from different disease stages and sites is still lacking. Given the high variability of evaluation approaches used by previous studies for TLS definition and quantification, we applied 7-color multiplex immunohistochemistry to characterize TLS phenotypes along the coordinated expression of established TLS-defining molecular and cellular components together with a standardized evaluation strategy specifically adapted for high reproducibility. We found progression-, tumor site-, but not prognosis-associated changes in TLS phenotypes, density and spatial distribution. In contrast to secondary lymphoid organs, secondary follicular melanoma TLS showed a remarkable paucity of canonical germinal center formation.

MATERIALS AND METHODS

Patient Cohorts

Primary Human Melanomas and Matched Early/Regional Metastases

Whole tissue sections were obtained from routine formalin-fixed paraffin-embedded (FFPE) blocks of cutaneous primary melanomas from Caucasian patients who underwent surgery between the years 2002 and 2014 at the Cantonal Hospital Baselland, Liestal (5). All tumor samples were obtained with informed patients' consent and the pathology files retrieved as approved by the local Ethics Committee (EKNZ vote BASEC 2016-01499). Histological diagnoses were made by board-certified pathologists from the Cantonal Hospital under the guidance of KM. This cohort included 48 patients with primary cutaneous melanoma. 27 patients presented without metastasis within a follow-up interval of up to 140 months (mean: 42 months, **Table 1**); 21 patients were diagnosed with regional metastasis at the time of first diagnosis (**Table 2**).

From 10 of the latter patients additional 16 metastatic samples could also be included in our analysis. These early metastatic samples almost exclusively consisted of locoregional skin (n=4) and clinically detectable (macroscopic) nodal metastases (n=11, **Table 3**) where tumor deposits had completely or almost completely replaced lymph node tissue. None of these patients had received local or systemic antitumor treatment before surgery.

Late/Distant Metastases

In addition, we analyzed whole sections from 39 distant human melanoma metastases, mainly derived from cutaneous (n=15) and lymph node (n=13) sites (**Table 3**). These samples were collected between the years 2015 and 2019 at the University Hospital Basel. Tumor samples were obtained with informed patients' consent and the pathology files retrieved as approved by the local Ethics Committee (EKNZ vote BASEC 2019-00927). Histological diagnoses were made by board-certified pathologists from the Institute of Pathology, University Hospital Basel, under the guidance of KG. In lymph node metastases, tumor deposits had completely or almost completely replaced lymph node tissue. Desmoplastic subtypes of melanoma were not included in this study as they show a distinct clinical behavior (24).

TABLE 1 | Clinical and histopathological summary of melanoma patients without metastasis.

Number of patients		**27**
Follow-up (months)	Mean	42
	Median	28
	Range	8-140
Age (years)	Mean	67
	Median	70
	Range	31-93
Breslow depth (thickness in mm)	Mean	2,73
	Median	1,99
	Range	0,36-10
Location	Extremities	8
	Head/Neck	2
	Trunk	17
Ulceration	Present	10
	Absent	17
Histotype*	SSM	20
	NM	6
	NOS	1
Sex	Female	11
	Male	16

SSM, superficial spreading melanoma; NM, nodular Melanoma; NOS, not otherwise specified.

TABLE 2 | Clinical and histopathological summary of melanoma patients with metastasis at the time of first diagnosis.

Number of patients		**21**
Age (years)	Mean	66
	Median	67
	Range	31-91
Breslow depth (thickness in mm)*	Mean	6,30
	Median	5,73
	Range	1-15
Location*	Extremities	7
	Head/Neck	3
	Trunk	10
Ulceration*	Present	15
	Absent	5
Histotype**	SSM	6
	NM	15
Sex	Female	6
	Male	15

Three samples without information about Breslow depth, one about location, one about ulceration.
***SSM, superficial spreading melanoma; NM, nodular melanoma.*

TABLE 3 | Numbers of biopsy sites of melanoma patients with early and late metastases.

Biopsy site	**Number of patients**	
	early metastases	**late metastases**
Sum	16	39
Skin	4	15
Lymph node	11	13
Lung	1	4
Brain	0	3
Nerve	0	1
Kidney	0	1
Bone	0	1
Bladder	0	1

Seven Color Multiplex Immunohistochemical Staining

Tumor tissue analysis and read-out were approved by the Ethics Committee of the Medical University of Vienna (ethics vote 1999/2019). First, each of the following antibodies was established on four-micrometer sections from FFPE tissue of human tonsil: CD20 (mouse monoclonal IgG2a, clone L26, 1:2000, Agilent, M0755), CD4 (mouse monoclonal IgG1, clone 4B12, 1:500, Agilent, M7310), CXCL13 (rabbit polyclonal IgG, 1:1000, Proteintech, 10927-1-AP), CD21 (rabbit polyclonal IgG, 1:3600, Proteintech, 24374-1-AP), CD23 (rabbit monoclonal IgG, clone SP23, 1:900, Novus Biologicals, NB120-16702) and

BCL6 (mouse monoclonal IgG1, clone 1E6B1, 1:24000, Proteintech, 66340-1-Ig). Each antibody was assigned to one of the fluorophores Opal 520, Opal 540, Opal 570, Opal 620, Opal 650 and Opal 690 (Akoya Biosciences) diluted in 1X Plus Amplification Diluent (Akoya).

For multiplex stainings, these antibodies were successively applied to deparaffinized sections from FFPE tumor samples in six iterative rounds of immunostaining. Each round started with heated antigen retrieval with either citrate buffer (pH 6.0) or Tris-EDTA (pH 9.0) for 30 min, fixation with 7.5% neutralized formaldehyde (SAV Liquid Production) and a 15 min blocking step using 20% normal goat serum (Agilent, X0907). Thereafter, primary antibodies were applied followed by incubation with respective biotinylated anti-mouse/-rabbit secondary antibodies (Agilent, K5003), Streptavidin-HRP (Agilent, K5003) and Opal fluorophore dye (Akoya). After six rounds of immunostainings, nuclei were counterstained with DAPI (PerkinElmer, FP1490). A detailed protocol of the immunohistochemistry staining procedure was previously described by us (7).

Tyramid signal amplification-based visualization of the primary antibodies was established on control tonsil tissue, the gold standard for lymphocyte antigen detection in pathology, and the signal balanced by diluting the primary antibodies to obtain staining levels and cell frequencies comparable to conventional immunofluorescence staining. Negative controls included the use of isotype instead of primary antibodies and stainings without primary antibodies. Single antibody stainings were run in parallel to control for false positive (incomplete stripping of antibody-tyramide complexes) and false negative results (antigen masking by multiple antibodies, "umbrella-effect") as well as for spillover effects (detection of fluorophores in adjacent channels), again as described by us before (7).

Additional immunofluorescent double stainings were performed with antibodies against BCL6 (mouse monoclonal IgG1, clone 1E6B1, 1:24000, Proteintech, 66340-1-Ig)-Opal 650 and Ki67 (mouse monoclonal IgG1, clone MIB-1, 1:1600, Agilent, M7240)-Opal 570.

Automated Acquisition and Quantification of TLS

Multiplexed slides of the whole tissue sections were scanned on the Vectra 3 Automated Quantitative Pathology Imaging System (version 3.0.5., Akoya) and potential TLS were acquired in 20x magnification for downstream analysis with the tissue analysis software inForm® (version 2.4.1, Akoya). This procedure included first a spectral unmixing for each specific fluorophore (7, 25, 26), followed by a trainable tissue segmentation to distinguish between different TLS phenotypes. Autofluorescence was determined on an unstained representative tumor section.

TLS phenotypes were determined based on molecular and cellular marker composition and structural features along the lines of (27, 28) with some additional specifications for secondary follicular TLS. Early TLS/dense $CD20^+$ lymphocyte aggregates were trained as $CD20^+$ B cell aggregates with $CXCL13^+$ cells and the presence or absence of interspersed $CD4^+$ T cells ($CD21^-$, $CD23^-$, $BCL6^-$). Primary follicular TLS were trained as $CD20^+$ B cell aggregates interspersed with $CD4^+$ T cells and the presence of a network with $CD21^+$ immature follicular dendritic cells ($CD23^-$, $BCL6^-$). Secondary follicular TLS were trained as structures with an additional network of $CD23^+$ mature follicular dendritic cells and the presence of $CD20^+$ B cell aggregates interspersed with $CD4^+$ T cells without ($BCL6^-$) or with the accessory expression of BCL6 in lymphatic cells ($BCL6^+$). We did not use additional established markers such as DC-LAMP and PNAD, because DC-$LAMP^+$ dendritic cells and $PNAD^+$ high endothelial venules have been shown in different TLS phenotypes at a similar frequency as well as in lymphocyte-rich areas without apparent organization into TLS (28). Tissue segmentation quality was manually monitored for each image by the sample analyst (FW) who was blinded for sample identity at the time of image analysis.

Early, primary and secondary follicular TLS phenotypes were identified by tissue segmentation and analyzed for density (number per mm^2 tissue area) and relative area (mm^2 per mm^2 tissue area) in whole tissue sections. In secondary follicular TLS, we performed an additional sub-analysis for the area of $BCL6^+$ and $BCL6^-$ germinal centers, respectively. Spatial distribution of TLS was manually annotated with the digital pathology image analysis software QuPath [version 0.2.3 (29)] to intra- and peritumoral perimeters of increasing radiuses (1 – max. 6 mm) drawn around the tumor-invasive front with the help of a publicly available script (30, 31) with minor adaptations to our needs. Counts and relative area of each TLS phenotype were then normalized to the tissue area (mm^2) within the respective intra- and extratumoral perimeters. TLS overlapping two perimeters were assigned to the perimeter with the larger share. Regions of necrosis, ulceration and distinct hemorrhage were excluded from analysis as was non-infiltrated subcutaneous adipose tissue below primary melanomas due to the consistent absence of a recognizable lymphocyte infiltration.

Statistical Analysis

All statistical analyses were performed using R (version 4.0.3). As the data was generally not normally distributed, differences between two groups were assessed using the Wilcoxon rank sum test. Differences between multiple groups were assessed using the Kruskal-Wallis test. The absolute number of samples with and without TLS between two groups was assessed using Fisher's exact test. All p-values were corrected for multiple testing using the Benjamini & Hochberg method (abbreviated as "FDR" throughout the manuscript). Plots were created using ggplot2 [version 3.3.3 (32)], and GraphPad Prism (version 8.0.1). Statistical comparison of spatial distribution used data for the intratumoral compartment from 1 and >1 mm perimeters and focused on data for the extratumoral compartment from 1 and 2 mm perimeters, as around half of the samples presented without TLS within the 3 and higher mm extratumoral perimeters.

RESULTS

Experimental Strategy

There are some reports on the presence of distinct TLS-associated cell types in primary human melanoma, but no systematic analysis of TLS phenotypes. Another difficulty is a lack of consensus on

how to determine tumor-associated TLS density and distribution by a standardized evaluation methodology (33). To overcome the limitations of light microscopy, we performed 7-color multiplex immunohistochemistry on whole tissue sections from 103 human cutaneous melanoma samples with antibodies against TLS-defining molecular and cellular components: CXCL13, a key chemoattractant orchestrating the cellular composition of TLS, CD20 and CD4 for detection of B cells and T(helper) cells, CD21 and CD23 for the presence of a network of immature and mature follicular dendritic cells (FDCs), respectively, and BCL6, a key transcriptional regulator in B cells and T cells for germinal center formation. Representative stainings for detection of early, primary and secondary follicular TLS are given in **Figures 1A–C**.

We further specified the scoring of TLS density, relative area and spatial distribution by normalizing TLS counts and area to the tissue area (mm^2) within defined extra- and intratumoral perimeters around the invasive tumor front (**Figure 1D**). Routine FFPE sections allowed the application of perimeters to the extratumoral compartment ranging from 1 to 6 mm with a median 6 mm distance in primary melanomas and 5 mm distance in metastatic melanomas. In the intratumoral compartment, we detected most TLS within the 1 and 2 mm perimeters; further evaluation within perimeters of 3 and more mm proved difficult because of small tumor size or presence of regions of necrosis, ulceration and hemorrhage which were excluded from the analysis. We, therefore, subdivided the intratumoral compartment into 1 and >1 mm perimeter areas (**Supplementary Figure 1**).

This allowed us *(i)* to analyze TLS phenotypes, density and spatial distribution in primary human melanoma and the association with established prognostic clinicopathologic factors; *(ii)* to compare TLS in terms of phenotype, density and spatial distribution in different stages of disease progression; *(iii)* to describe TLS for phenotype, density and spatial distribution in metastases from different body sites; and *(iv)* to characterize the cellular composition and spatial distribution of TLS-defining cell types in human melanoma compared to secondary lymphoid organs.

Primary Human Melanomas Contain Mostly TLS of an Early Immature Phenotype

Here we demonstrate an evaluation strategy based on referring TLS counts and area to the tissue area (mm^2) to determine TLS density and relative area, respectively, within defined intra- and extratumoral perimeters around the invasive tumor front (**Figure 1D**). This strategy should allow standardized read-out with high reproducibility.

We found TLS in only 16 of 48 (33.3%) primary melanomas (**Figure 2A**). These TLS were predominantly of the early TLS phenotype (n=241 of a total 264; 91.3%; **Figure 2B**). Only four tumor samples presented with a secondary follicular TLS and one of these had $BCL6^+$ lymphatic cells. Primary follicular TLS were not identified (**Figure 2B**).

The density of early TLS ranged from 0 to 3.0 per intratumoral mm^2 and 0 to 1.1 per extratumoral mm^2; their relative area ranged from 0 to 9.3% of the intratumoral compartment and 0 to 3.3% of the extratumoral compartment. Comparison of areas of 1 and >1 mm perimeters in the intratumoral compartment was possible only in primary melanomas with a Breslow depth of ≥2 mm and the presence of TLS (n=9). In these samples, early TLS appeared at a higher density within the 1 mm perimeter of the intratumoral compartment (**Figure 2C**), often located directly at the inner invasive tumor front and/or between tumor cells without a preferential confinement to stromal septa (**Supplementary Figure 2A**). The extratumoral compartment could be analyzed in all 16 primary tumors with TLS. Extratumoral TLS were mostly present within the 1 mm perimeter with a drop in density with the 2 to 6 mm perimeters (**Figure 2C**). Densities, relative areas and spatial distribution for TLS in primary melanomas are given in **Supplementary Table 1**.

When we stratified the primary melanoma samples for the prognostically most important parameter, *i.e.* metastasis, we found no differences for the presence of TLS (P = 0.75, Fisher's exact test), or for their density, relative area and spatial distribution. The same was true for other prognostically important categorical clinicopathologic parameters such as Breslow depth, ulceration, age and sex.

Thus, only a subgroup of primary human melanoma contains TLS and if they do, they are mainly of an immature early phenotype. TLS mostly occur intratumorally within a distance of 1 mm to the invasive tumor front and their presence is not associated with prognostic clinicopathologic factors.

Melanoma Disease Progression Is Associated With an Increased Density of Extratumoral Secondary Follicular TLS

TLS phenotypes and density can vary between cancer stages and body sites. We, therefore, compared primary human melanomas with melanoma metastases, including early locoregional and late distant metastases.

We found TLS in 45 of 55 (81.2%) metastatic melanoma samples (**Figure 3A**). Early TLS were the most prevalent TLS phenotype, followed by secondary follicular TLS with a $BCL6^-$ germinal center and only small proportions of both secondary follicular TLS with a $BCL6^+$ germinal center and primary follicular TLS (**Figure 3B**). While secondary follicular TLS were rarely found in primary tumors, they were present in 54.5% of metastatic tumors. These secondary follicular TLS appeared in the tumor stroma, in stromal septa through the intratumoral compartment surrounding tumor nests, and in the peritumoral stroma at the invasive tumor front (**Supplementary Figure 2B**). TLS density in melanoma metastases ranged from 0 to 2.2, median 0.04 per intratumoral mm^2 and 0 to 2.6, median 0.30 per extratumoral mm^2; the relative area of TLS from 0 to 17.3%, median 0.06% of the intratumoral compartment and 0 to 16.8%, median 0.76% of the extratumoral compartment.

The number of tumor samples with TLS did not differ between early locoregional and late distant metastases (P = 0.45, Fisher's exact test) but was significantly increased in metastatic tumors compared with primary tumors (P < 0.001, Fisher's exact test). Both TLS density and relative area - particularly in the

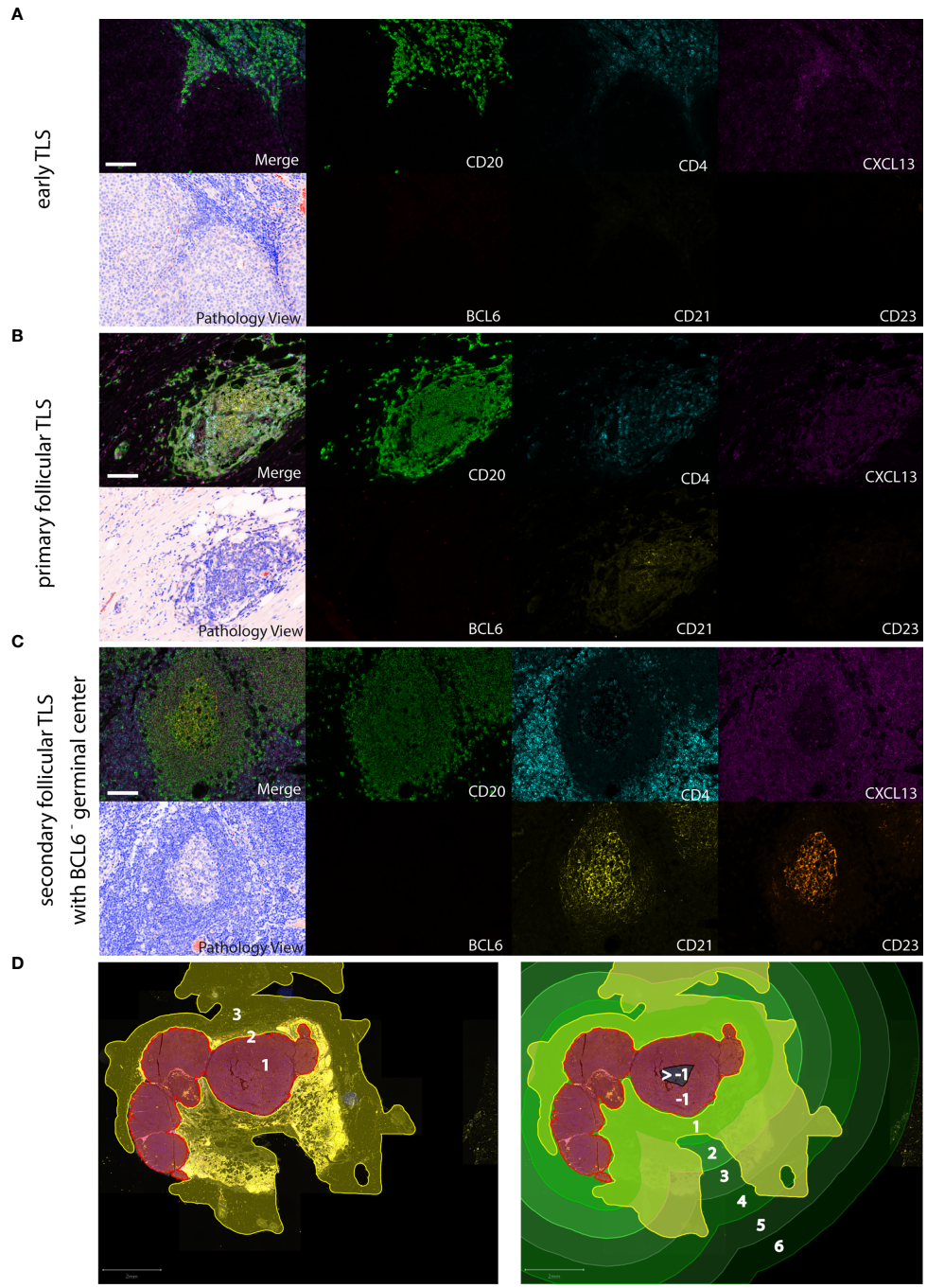

FIGURE 1 | Detection of different TLS phenotypes by 7-color multiplex immunohistochemistry in human melanoma tissues. Examples for **(A)** early TLS: dense CD20$^+$ lymphocyte aggregates with CXCL13$^+$ cells and the presence of some interspersed CD4$^+$ T cells; **(B)** primary follicular TLS: CD20$^+$ lymphocyte aggregates interspersed with CD4$^+$ T cells and the presence of a CD21$^+$ but CD23$^-$ dendritic network, surrounded by CXCL13 expressing cells; **(C)** secondary follicular TLS with a BCL6$^-$ germinal center: CD21$^+$ and CD23$^+$ dendritic networks within CD20$^+$ lymphocyte aggregates with interspersed CD4$^+$ T cells, surrounded by CXCL13 expressing cells. No accessory expression of BCL6 in lymphatic cells. Germinal centers are identifiable in routine light microscopy (see Pathology View, bottom left). An example for a BCL6$^+$ secondary follicular TLS is given in **Figure 5A**. Images for each of the individual markers and their composites (for clarity without DAPI staining) are shown, together with the corresponding Pathology View (respective bottom left). Scale bars represent 100 µm. **(D)** Spatial annotation of tumor areas. Left: Definition of the invasive tumor front (red, 2) and the respective intra- and extratumoral compartments (brown, 1 and yellow, 3, respectively) in a tissue section of a human melanoma lymph node metastasis. Extratumoral compartments include site-specific and adipose tissue (yellow). Right: Allocation of intra- (brown/black) and extratumoral perimeters (green) of increasing radiuses (1 – max. 6 mm) drawn within and around the invasive tumor front. Counts and area of TLS were referred to the tissue area (yellow) within the respective intra- and extratumoral perimeters. TLS, tertiary lymphoid structures.

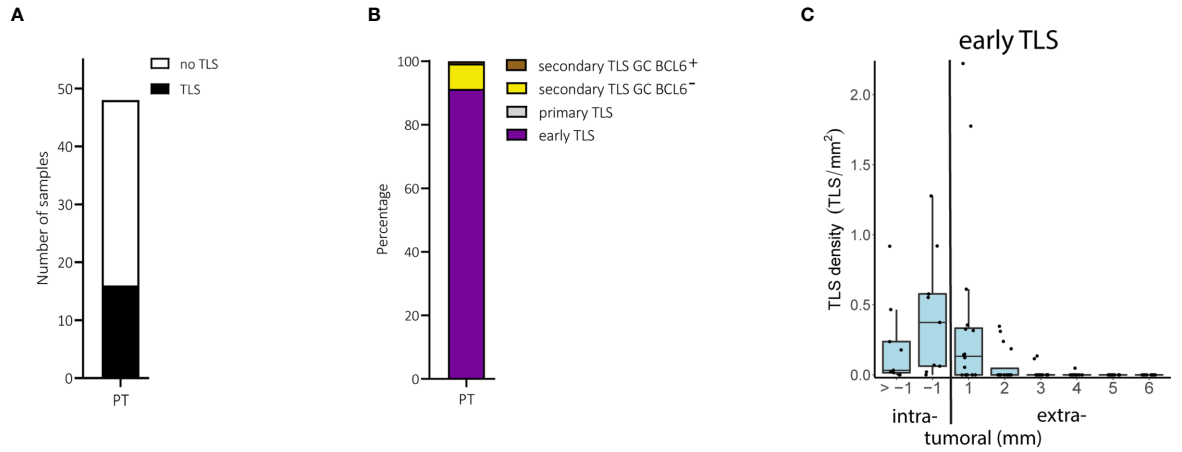

FIGURE 2 | Primary melanomas (PT): TLS phenotypes, density and spatial distribution. **(A)** Prevalence of TLS in primary tumor samples. **(B)** Relative prevalence of TLS phenotypes in primary tumors. **(C)** Density of early TLS over intra- and extratumoral compartments of primary tumors. In all boxplots, lower and upper hinges correspond to the first and third quartiles, center line to the median. Upper and lower whisker extend from the hinge to the largest value no further than 1.5 times the interquartile range. Values outside this range are shown as outliers (black circles). Individual patient values are shown as black dots. TLS, tertiary lymphoid structures; GC, germinal center.

extratumoral compartment - were also significantly increased in metastatic samples compared to primary tumors (FDR < 0.001 for both, Wilcoxon rank sum test; **Figure 3C**), mainly driven by early and secondary follicular TLS (5.9 and 34.9 fold increase in counts for early and secondary follicular TLS, respectively). Both early and secondary follicular TLS were present throughout the entire intratumoral compartment, with a higher density within the 1 mm perimeter. Extratumoral TLS were mostly present within the 1 mm perimeter, with a drop in density with the 2 to 6 mm perimeters (**Figure 3D**). Densities, relative areas and spatial distribution for TLS in melanoma metastases are given in **Supplementary Table 1**.

Thus, metastatic melanoma disease differs from local disease in the presence particularly of secondary follicular TLS phenotypes, most of which are found within the extratumoral compartment of 1 mm distance to the invasive tumor front.

Metastatic Sites Differ for Density and Spatial Distribution of Secondary Follicular TLS

When we further compared early locoregional and late distant metastatic tumors, we observed an increase in the density of particularly extratumoral secondary follicular TLS and BCL6$^-$ germinal centers in late distant metastatic tumors (P = 0.05 and 0.03, FDR = 1.0 and 0.875, respectively, Wilcoxon's rank sum test). Because early locoregional metastatic tumors were enriched for lymph node tissues, we hypothesized that a different representation of tumor sites could drive this effect.

Distant metastatic samples contained comparable numbers of lymph node and skin metastases. TLS could be detected in 13 of 13 (100%) distant metastatic lymph node samples compared with only 10 of 15 (66.7%) distant metastatic skin samples. Consistent with our hypothesis, we found an increased density of extratumoral secondary follicular TLS and extratumoral BCL6$^-$ germinal centers in metastatic lymph node samples compared with metastatic skin samples (FDR = 0.06 both, Wilcoxon's rank sum test; **Figure 4A**). We found no difference for extratumoral BCL6$^+$ germinal centers, most likely due to their small sample size. At lymph node sites, the density of secondary follicular TLS and BCL6$^-$ germinal centers was highest within the extratumoral 1 mm perimeter with a drop with the extratumoral 2 to 6 mm perimeters and the intratumoral compartment (**Figure 4B**). At skin sites, secondary follicular TLS and BCL6$^-$ germinal centers were almost exclusively present within the 1 and 2 mm extratumoral perimeters (**Figure 4B**).

A similar comparison for samples from the cohort with early locoregional metastases was not possible because of the lack of a sufficient number of skin metastases. However, the density of extratumoral secondary follicular TLS and extratumoral BCL6$^-$ germinal centers in early locoregional lymph node samples was lower than in distant late lymph node metastases (FDR = 0.002 and 0.003, respectively, Wilcoxon's rank sum test) and was not different to distant late skin metastases (FDR = 0.29 both, Wilcoxon's rank sum test). In the small number of melanoma brain metastases (n=3), secondary follicular TLS - and thus BCL6$^-$ germinal centers - were completely absent. TLS phenotypes, densities and spatial distribution for metastatic tumor samples are given in **Supplementary Table 1**.

Thus, depending on the tumor site, human melanoma metastases vary in terms of TLS density, particularly of extratumoral secondary follicular TLS with BCL6$^-$ germinal centers, and spatial distribution within intra- and extratumoral compartments.

Secondary Follicular TLS From Human Melanoma Mostly Lack Germinal Center Polarity

Secondary follicular TLS in human melanoma metastases regularly contained key cellular and molecular components in

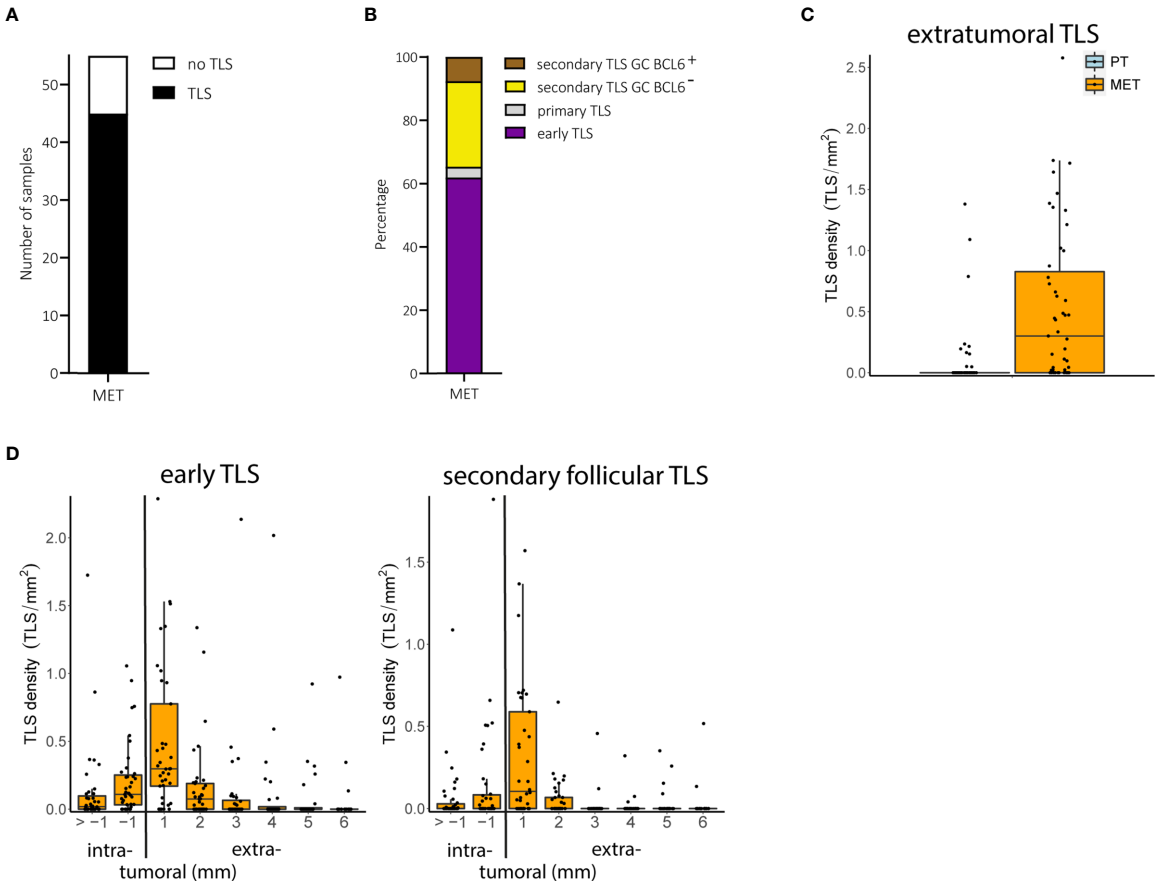

FIGURE 3 | Melanoma metastases (MET): TLS phenotypes, density and spatial distribution. **(A)** Prevalence of TLS in metastatic tumor samples. **(B)** Relative prevalence of TLS phenotypes in melanoma metastases. **(C)** Comparison of extratumoral TLS density with primary melanomas. **(D)** Densities of early TLS (left) and secondary follicular TLS (right) over intra- and extratumoral compartments of metastatic tumors. In all boxplots, lower and upper hinges correspond to the first and third quartiles, center line to the median. Upper and lower whisker extend from the hinge to the largest value no further than 1.5 times the interquartile range. Values outside this range are shown as outliers (black circles). Individual patient values are shown as black dots. TLS, tertiary lymphoid structures; GC, germinal center.

a typical spatial arrangement, but only some larger secondary follicular TLS (21.7%) contained germinal centers that included $BCL6^+CD20^+$ B cells with interspersed $BCL6^+CD4^+$ T cells (**Figures 5A, B**). Interestingly, both $BCL6^+CD20^+$ B cells and $BCL6^+CD4^+$ T cells were located within the $CD21^+$ and $CD23^+$ FDC network, which covered the entire germinal center area (**Figure 5A**). This distinct spatial arrangement differed markedly from that in canonical germinal centers of secondary lymphoid organs such as tonsillar tissue. Here, $BCL6^+$ secondary follicular structures regularly contained polarized germinal centers with the presence of dark and light zone areas. These were recognizable by light microscopy (**Figure 5C**, Pathology View) and characterized by a polarized distribution of the $CD21^+$ and $CD23^+$ FDC network together with $CD4^+$ T cells and a discernable complementary distribution of $BCL6^+$ lymphatic cells (**Figure 5C**). Tonsil germinal centers were further enriched for $BCL6^+Ki67^+$ cells with polarized distribution (**Figure 5D**, upper row). In contrast, melanoma germinal centers were smaller and had lower numbers of $BCL6^+$, $Ki67^+$ and $BCL6^+Ki67^+$ cells without polarized distribution (**Figure 5D**, lower row). Interestingly, $BCL6^-$ melanoma germinal centers showed no enrichment for $Ki67^+$ cells.

Thus, TLS in melanoma metastases reconcile the expression and spatial distribution of TLS-defining molecular and cellular markers in many aspects. However, they often lack germinal center polarity with the formation of proliferative dark zone areas enriched for $BCL6^+Ki67^+$ cells.

DISCUSSION

Here we show, *(i)* that only a subgroup of primary human melanomas contains TLS. These TLS mostly appear intratumorally within a 1 mm distance to the invasive tumor front, rarely form secondary lymphoid structures, and their presence seems not to be associated with prognostic factors; *(ii)* that melanoma metastases exhibit an increased TLS density, particularly of early and secondary follicular TLS, which are mostly found within an extratumoral 1 mm distance; *(iii)* that the density of secondary follicular TLS in metastases varies with

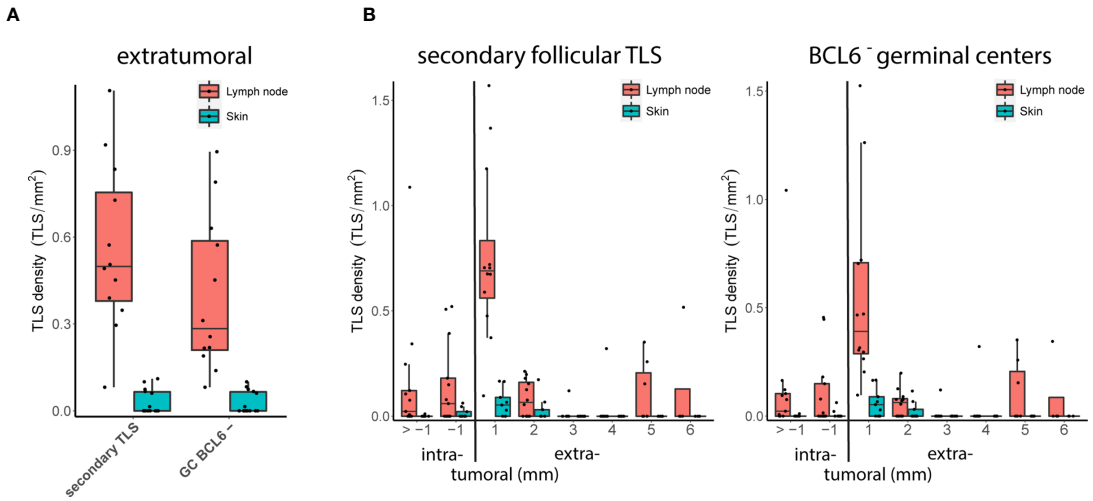

FIGURE 4 | Metastatic tumor sites: TLS density and spatial distribution. **(A)** Densities of extratumoral secondary follicular TLS (left) and BCL6$^-$ germinal centers (GC BCL6$^-$, right) in distant metastatic lymph node and skin sites. **(B)** Densities of secondary follicular TLS (left) and BCL6$^-$ germinal centers (right) over intra- and extratumoral compartments in distant metastatic lymph node and skin sites. In all boxplots, lower and upper hinges correspond to the first and third quartiles, center line to the median. Upper and lower whisker extend from the hinge to the largest value no further than 1.5 times the interquartile range. Values outside this range are shown as outliers (black circles). Individual patient values are shown as black dots.

time and disease site; and *(iv)* that secondary follicular TLS in melanoma often lack the presence of BCL6$^+$ lymphatic cells as well as germinal center polarity with the formation of dark and light zone areas.

Studies on TLS in human cancer suffer from the lack of general agreement on the definition of TLS and their quantification. This may explain why, besides reports on a positive association of the presence or density of TLS with a favorable disease outcome in several human cancers, there are also reported negative associations. This discrepancy has been linked to differences in phenotype and spatial distribution of TLS as well as disease stages (19, 33, 34). Previous studies quantified TLS density in various ways, including counting TLS within intra- and/or extratumoral tumor areas, either directly at the invasive tumor front or within different distances from it. These counts were related to the length of the invasive tumor front and to a so-called immunoreactive area around the invasive front, or were not allocated to any quantified tissue area at all [reviewed in (9, 10, 27, 28, 33, 35)]. While these differences limit the reproducibility and comparability of the data, one important advantage of our study is the use of a standardized evaluation strategy based on referring TLS counts to tissue area (mm^2) within defined intra- and extratumoral perimeters around the invasive tumor front. Another important asset is the use of multiplex immunohistochemistry for the characterization of TLS phenotypes. With the successive identification of molecular and cellular components defining and shaping TLS functionality (34) and the ability to simultaneously detect complex TLS marker combinations in histological sections (27, 28, 33), important progress has been made in identification and phenotyping of TLS in human tumor tissues. Here we applied multiplex immunohistochemistry for the simultaneous detection of six established TLS-defining molecular and cellular components (27, 28, 33, 34) and used at least two of these molecular and/or cellular markers in combination with structural features to characterize the individual TLS phenotypes. The advantage of this strategy is best exemplified by the identification of large secondary follicular TLS with germinal centers lacking the opposing polarization of CD21$^+$ and CD23$^+$ FDC networks along with CD4$^+$ cells versus BCL6$^+$ lymphatic cells with high proliferative activity as indicated by additional Ki67 staining. Given the prospectively high reproducibility of this standardized quantitative assessment approach for multiple marker expression in tumor tissues, our study may contribute to the development of a future widely accepted standard procedure for the analysis of TLS phenotypes, density and spatial distribution in human cancer.

Among various other cell types, the presence of high endothelial venules, mature dendritic cells and B cell aggregates can be indicative for the development or presence of TLS. In a small number of studies in primary cutaneous melanoma, MECA-79$^+$ high endothelial venules have been described to co-localize with mature DC-LAMP$^+$ DCs and dense lymphocyte infiltrates with CD20$^+$ B cells, and their numbers were associated with tumor regression and low Breslow depth (23). Both MECA-79$^+$ high endothelial venules and mature DC-LAMP$^+$ DCs were detected at the invasive tumor front exclusively within the extratumoral area, an observation earlier reported for mature DC-LAMP$^+$ DCs and associated dense lymphocyte infiltrates (17). In a later study by the same group, some dense lymphocyte infiltrates were characterized as follicular B cell aggregates, but their presence was not associated with improved survival (4). It is difficult to distinguish localized immune cell infiltrates from TLS and it has been subsequently shown that the presence of MECA-79$^+$ high endothelial venules and mature DC-LAMP$^+$ DCs is not sufficient to serve as

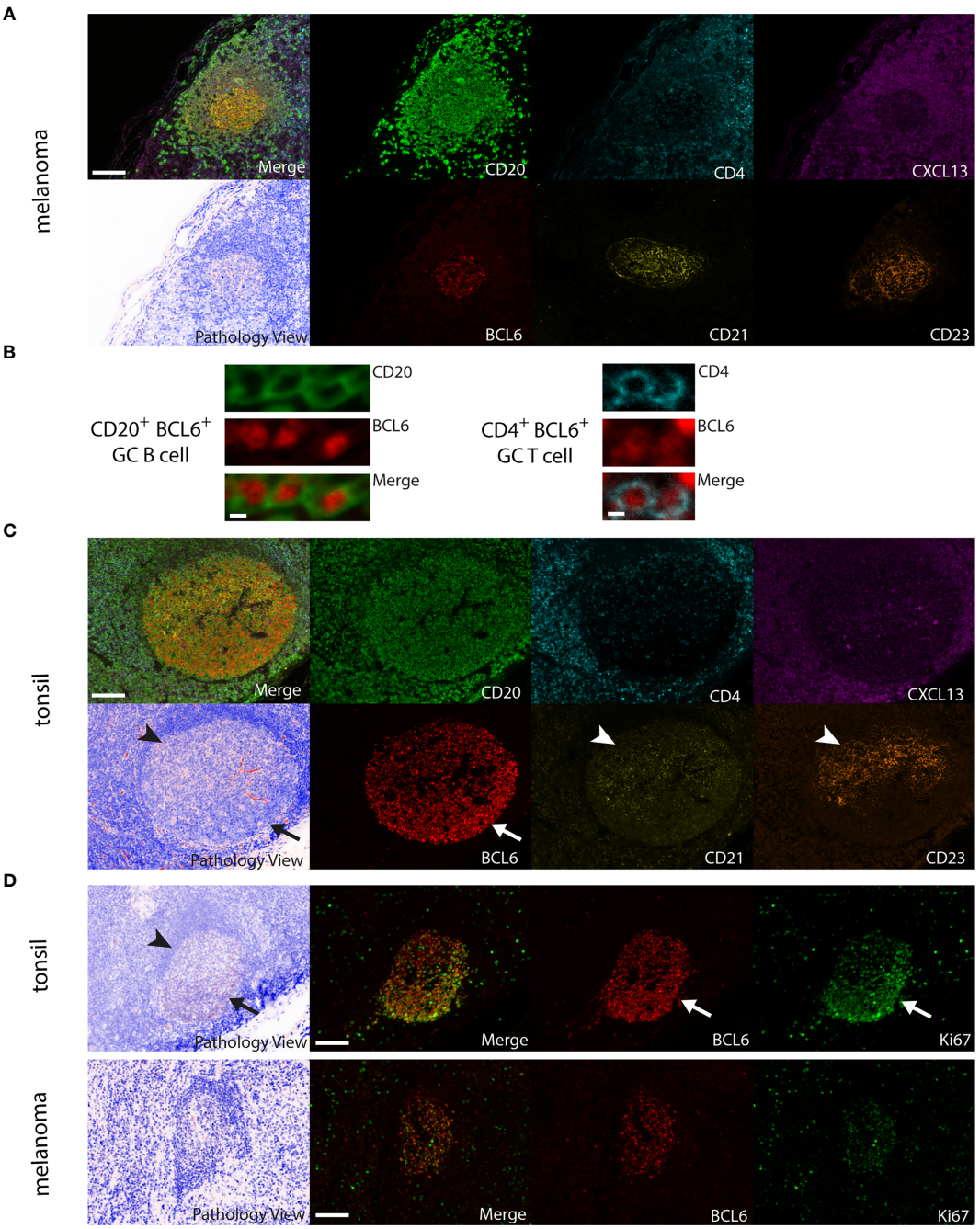

FIGURE 5 | Comparison of large BCL6$^+$ secondary follicular TLS in human melanoma to tonsil tissue. **(A)** Melanoma: CD20$^+$ lymphocyte aggregates with a germinal center surrounded by CXCL13 expressing cells. A CD21$^+$ and CD23$^+$ FDC network covers the complete germinal center area with randomly interspersed CD4$^+$ T cells and BCL6$^+$ cells. No detectable germinal center polarity, no identifiable light and dark zone areas in routine light microscopy (see Pathology View, bottom left). **(B)** Close up of BCL6$^+$CD20$^+$ B cells and BCL6$^+$CD4$^+$ T cells from a BCL6$^+$ secondary follicular TLS in human melanoma. **(C)** Tonsil: note canonical germinal center polarity with polarized spatial distribution of the CD21$^+$ and CD23$^+$ FDC network together with CD4$^+$ T cells (arrowheads) and a complementary localization of BCL6$^+$ cells (arrow). Identifiable light (arrowhead) and dark zone (arrow) areas in routine light microscopy (see Pathology View, bottom left). **(D)** Tonsil (upper row): polarized distribution of BCL6$^+$, Ki67$^+$ (arrows) and BCL6$^+$Ki67$^+$ cells in germinal centers with canonical germinal center polarity and the presence of light (arrowhead) and dark zone (arrow) areas in routine light microscopy (see Pathology View, left). Melanoma (lower row): note decreased numbers and absence of polarized distribution of BCL6$^+$, Ki67$^+$ and BCL6$^+$Ki67$^+$ cells in melanoma germinal centers. Lack of canonical germinal center polarity and absence of light and dark zone areas in routine light microscopy (see Pathology View, left). Images for each of the individual markers and their composites (for clarity without DAPI staining) are shown, together with the corresponding Pathology View (respective (bottom) left). Scale bars represent 100 μm **(A, C, D)** and 5 μm **(B)**.

surrogate parameter for the presence of TLS (12). In line with the latter observation, we found little primary or secondary follicular TLS in primary melanoma. However, in agreement with all these reports, we found dense $CD20^+$ B cell aggregates together with CXCL13-secreting cells and some interspersed $CD4^+$ T cells, which we termed early TLS.

Tumor-associated TLS are generally found in the extratumoral area (19, 36), although there are some exceptions (19, 36, 37). Interestingly, human melanoma metastases and a rare histotype of primary melanoma, namely desmoplastic melanoma, have recently been reported to contain intra- and extratumoral TLS (33, 38). We can now complement these reports with our observation on the presence of early TLS in intra- and extratumoral areas adjacent to the invasive tumor front in other histotypes. Neither density, nor area and distribution of early TLS were associated with metastasis or with other established prognostic parameters, an observation consistent with recent reports highlighting the prognostic utility particularly of mature TLS for disease and therapy outcome (9–11, 19, 27, 28).

In our study, metastases differed from local disease particularly in the presence of mature secondary follicular TLS phenotypes with germinal centers near the invasive tumor front. The presence of such secondary follicular TLS may have significant implications. In secondary lymphoid organs, such mature lymphoid structures are the site of clonal expansion, somatic hypermutation and affinity maturation of B cells and their differentiation into class-switched memory B cells and antibody secreting cells. In all likelihood, this is also true for TLS in human melanomas, as indicated by clonal amplification, somatic mutation and isotype switching of B cells in microdissected TLS from skin metastases (12) and significantly increased clonal counts for both heavy and light immunoglobulin chains and increased B cell receptor diversity in lymph node metastases with an increased density of secondary follicular TLS (10). The presence of TLS in human melanoma samples further correlates with increased frequencies of switched memory B cells, plasmablasts/plasma cells and less exhausted, activated memory-like $CD4^+$ and $CD8^+$ T cells (7, 9, 10) as well as with response to ICB therapy (9, 10).

Our data also indicate that the presence of secondary follicular TLS varies with time and site of metastasis. Originally it was reported that fully developed TLS are only present in melanoma metastases from skin, but not at several other sites (12). More recent reports, however, complemented this data for the presence of mature TLS at metastatic lymph node sites, but differed in the presence at extra-nodal sites (9, 10). In our study, the density of extratumoral secondary follicular TLS increased significantly from early regional to late distant lymph node metastasis. Distant metastases at lymph node sites also contained secondary follicular TLS at a higher density and in a different local distribution compared with skin sites. Whether these differences in TLS density and spatial distribution may reflect different immunological properties and perhaps a differential predictive value for patient survival and therapy response needs to be evaluated by site-to-site comparisons in future clinical studies. This is also true for assessing the predictive value of extratumoral TLS density, particularly within 1 mm distance to the invasive front of melanoma metastases. We further detected secondary follicular TLS in a small number of metastases from lung and kidney, but not from brain, bone and urinary bladder. These data are in line with previous reports on the absence of fully developed TLS in melanoma brain metastases (12, 39), but need to be reconciled in larger studies.

Lymph node, skin and lung metastases often exhibited TLS of different phenotypes, and a small but non-negligible number exhibited a $BCL6^+$ germinal center. In line with the previously reported expression of germinal center initiating and polarizing gene signatures in B cells of human melanoma metastases (9), these $BCL6^+$ melanoma TLS reconciled the expression of molecular and cellular markers that define mature secondary follicular structures in secondary lymphoid organs. However, melanoma TLS with $BCL6^+$ germinal centers often lacked germinal center polarization despite the expression of BCL6 in some germinal center B cells and T cells. Compared with human tonsil, germinal centers from human melanoma generally contained reduced numbers of both $BCL6^+CD20^+$ B cells and $BCL6^+CD4^+$ T cells.

Polarized cell distribution is a key feature of a functional mature germinal center and BCL6 is an important regulator of germinal center initiation and maintenance through direct and indirect regulation of genes controlling proliferation, DNA damage response, apoptosis and cell differentiation (40). The generally low expression of BCL6 in our study argues against a highly proliferative activity of germinal center B cells. This assumption is further supported by our data on the rather small size of germinal centers in melanoma with frequent lack of germinal center polarization and low expression of Ki67 compared with secondary lymphoid organs. In canonical germinal centers from secondary lymphoid organs, particularly $BCL6^+$ cells with polarized distribution are Ki67 positive. This may explain the recently published unexpectedly low number of $Ki67^+$ cells with unpolarized distribution in melanoma germinal centers (9). In contrast, repression of BCL6 expression or activity in B cells is important for differentiation and exit from the germinal center. This BCL6 repression in germinal center B cells follows B cell receptor signaling through recognition of antigens presented by mature FDCs as well as T cell help through CD40 ligation. A fine-tuned balance between the strength of B cell receptor signaling and of T cell help ultimately determines the level of BCL6 expression and thus the fate of B cells, namely induction of apoptosis or differentiation into antibody secreting cells (34). Both lead to reduced $BCL6^+$ B cell numbers as observed in our study. The expected continuous availability of tumor-associated antigens at melanoma sites together with our observation on the frequent lack of polarization of the mature FDC network rather argues more for a B cell receptor signaling-induced repression of BCL6 by comprehensive antigen presentation. Additional T cell help - as indicated by our observation on the colocalization with $CD4^+$ T cells - may then activate NFkB/IRF4-promoted memory B cell and plasmablast/plasma cell differentiation rather than apoptosis. This view is further supported by the reported high frequencies of switched

memory B cells, plasmablasts/plasma cells in human melanoma samples with mature TLS (9, 10). While these assumptions need further validation, they have some potentially important clinical implications for improving ICB therapy in melanoma, complementary to solely increasing TLS numbers. Given the already sizable numbers of early TLS and small secondary follicular TLS, our data highlight the importance of fostering TLS maturation to induce broad germinal centers with canonical germinal center polarity and the presence of light and dark zone areas for increased proliferation and differentiation of anti-tumor B cells. The rare observation of melanoma TLS with polarized germinal centers and $Ki67^{+}BCL6^{+}$ lymphatic cells gives a first hint that this ought to be possible.

CONCLUSION

This study significantly widens the knowledge of TLS phenotypes, density and spatial distribution in human melanoma. Using multiplex immunohistochemistry for TLS-defining molecular and cellular components together with a standardized evaluation strategy, our data reveal disease progression- and site-dependent changes in TLS phenotypes, density and distribution, as well as an altered germinal center formation with the frequent absence of germinal center polarity. These observations provide important premises for the further development of cancer immunotherapy and suggest that - in addition to enhancing TLS density - strategies aimed at inducing TLS maturation should be considered. The presented assessment procedure may further contribute to the development of a future widely accepted evaluation standard for TLS analysis in human cancer.

DATA AVAILABILITY STATEMENT

The original contributions presented in the study are included in the article/**Supplementary Material**. Further inquiries can be directed to the corresponding author.

ETHICS STATEMENT

The patients/participants provided their written informed consent to tumor sample collection. Tumor sample collection and the studies involving these tumor samples were reviewed and approved by the Ethikkommission Nordwest- und Zentralschweiz (votes BASEC 2016-01499 and 2019-00927). Tumor tissue analysis and read-out was additionally approved by the Ethics Committee of the Medical University of Vienna (ethics vote 1999/2019).

AUTHOR CONTRIBUTIONS

SW: conception. JG, FW, and SW: design. HL, KM, KG, FW, MS, and SW: clinical data collection and assembly, patient materials. KG and KM: Histopathology. FW, CW, MS, and SW: Multiplex immunostaining, automated imaging acquisition and data read-out. JG: Statistics. All authors contributed to the article and approved the submitted version.

FUNDING

This work received support from the Austrian Science Fund (FWF) project P31127-B28 and IPPTO project number DOC 59-B33 to SW.

ACKNOWLEDGMENTS

We thank Monika Weiss for processing human tumor samples.

SUPPLEMENTARY MATERIAL

The Supplementary Material for this article can be found online at: https://www.frontiersin.org/articles/10.3389/fimmu.2021.675146/full#supplementary-material

REFERENCES

1. Larkin J, Chiarion-Sileni V, Gonzalez R, Grob J-J, Rutkowski P, Lao CD, et al. Five-Year Survival With Combined Nivolumab and Ipilimumab in Advanced Melanoma. *N Engl J Med* (2019) 381:1535–46. doi: 10.1056/NEJMoa1910836
2. Mauri C, Menon M. Human Regulatory B Cells in Health and Disease: Therapeutic Potential. *J Clin Invest* (2017) 127:772–9. doi: 10.1172/JCI85113
3. Somasundaram R, Zhang G, Fukunaga-Kalabis M, Perego M, Krepler C, Xu X, et al. Tumor-Associated B-Cells Induce Tumor Heterogeneity and Therapy Resistance. *Nat Commun* (2017) 8:607. doi: 10.1038/s41467-017-00452-4
4. Ladányi A, Kiss J, Mohos A, Somlai B, Liszkay G, Gilde K, et al. Prognostic Impact of B-Cell Density in Cutaneous Melanoma. *Cancer Immunol Immunother* (2011) 60:1729–38. doi: 10.1007/s00262-011-1071-x
5. Garg K, Maurer M, Griss J, Brüggen MC, Wolf IH, Wagner C, et al. Tumor-Associated B Cells in Cutaneous Primary Melanoma and Improved Clinical Outcome. *Hum Pathol* (2016) 54:157–64. doi: 10.1016/j.humpath.2016.03.022
6. Erdag G, Schaefer JT, Smolkin ME, Deacon DH, Shea SM, Dengel LT, et al. Immunotype and Immunohistologic Characteristics of Tumor-Infiltrating Immune Cells are Associated With Clinical Outcome in Metastatic Melanoma. *Cancer Res* (2012) 72:1070–80. doi: 10.1158/0008-5472.CAN-11-3218
7. Griss J, Bauer W, Wagner C, Simon M, Chen M, Grabmeier-Pfistershammer K, et al. B Cells Sustain Inflammation and Predict Response to Immune Checkpoint Blockade in Human Melanoma. *Nat Commun* (2019) 10:1–14. doi: 10.1038/s41467-019-12160-2
8. Amaria RN, Reddy SM, Tawbi HA, Davies MA, Ross MI, Glitza IC, et al. Neoadjuvant Immune Checkpoint Blockade in High-Risk Resectable Melanoma. *Nat Med* (2018) 24:1649–54. doi: 10.1038/s41591-018-0197-1
9. Cabrita R, Lauss M, Sanna A, Donia M, Skaarup Larsen M, Mitra S, et al. Tertiary Lymphoid Structures Improve Immunotherapy and Survival in Melanoma. *Nature* (2020) 577:561–5. doi: 10.1038/s41586-019-1914-8
10. Helmink BA, Reddy SM, Gao J, Zhang S, Basar R, Thakur R, et al. B Cells and Tertiary Lymphoid Structures Promote Immunotherapy Response. *Nature* (2020) 577:549–55. doi: 10.1038/s41586-019-1922-8
11. Petitprez F, de Reyniès A, Keung EZ, Chen TWW, Sun CM, Calderaro J, et al. B Cells are Associated With Survival and Immunotherapy Response in Sarcoma. *Nature* (2020) 577:556–60. doi: 10.1038/s41586-019-1906-8

12. Cipponi A, Mercier M, Seremet T, Baurain JF, Theáte I, Van Den Oord J, et al. Neogenesis of Lymphoid Structures and Antibody Responses Occur in Human Melanoma Metastases. *Cancer Res* (2012) 72:3997–4007. doi: 10.1158/0008-5472.CAN-12-1377
13. Nielsen JS, Sahota RA, Milne K, Kost SE, Nesslinger NJ, Watson PH, et al. CD20+ Tumor-Infiltrating Lymphocytes Have an Atypical CD27- Memory Phenotype and Together With CD8+ T Cells Promote Favorable Prognosis in Ovarian Cancer. *Clin Cancer Res* (2012) 18:3281–92. doi: 10.1158/1078-0432.CCR-12-0234
14. Bruno TC, Ebner PJ, Moore BL, Squalls OG, Waugh KA, Eruslanov EB, et al. Antigen-Presenting Intratumoral B Cells Affect CD4+ TIL Phenotypes in non–Small Cell Lung Cancer Patients. *Cancer Immunol Res* (2017) 5:898–907. doi: 10.1158/2326-6066.CIR-17-0075
15. Colbeck EJ, Ager A, Gallimore A, Jones GW. Tertiary Lymphoid Structures in Cancer: Drivers of Antitumor Immunity, Immunosuppression, or Bystander Sentinels in Disease? *Front Immunol* (2017) 8:1830. doi: 10.3389/fimmu.2017.01830
16. Garaud S, Buisseret L, Solinas C, Gu-Trantien C, De Wind A, Van Den Eynden G, et al. Tumor-Infiltrating B Cells Signal Functional Humoral Immune Responses in Breast Cancer. *JCI Insight* (2019) 4:18. doi: 10.1172/jci.insight.129641
17. Ladányi A, Kiss J, Somlai B, Gilde K, Fejős Z, Mohos A, et al. Density of DC-LAMP(+) Mature Dendritic Cells in Combination With Activated T Lymphocytes Infiltrating Primary Cutaneous Melanoma Is a Strong Independent Prognostic Factor. *Cancer Immunol Immunother* (2007) 56:1459–69. doi: 10.1007/s00262-007-0286-3
18. Sautès-Fridman C, Lawand M, Giraldo NA, Kaplon H, Germain C, Fridman WH, et al. Tertiary Lymphoid Structures in Cancers: Prognostic Value, Regulation, and Manipulation for Therapeutic Intervention. *Front Immunol* (2016) 7:407. doi: 10.3389/fimmu.2016.00407
19. Sautès-Fridman C, Petitprez F, Calderaro J, Fridman WH. Tertiary Lymphoid Structures in the Era of Cancer Immunotherapy. *Nat Rev Cancer* (2019) 19:307–25. doi: 10.1038/s41568-019-0144-6
20. Fridman WH, Petitprez F, Meylan M, Chen TW-W, Sun C-M, Roumenina LT, et al. B Cells and Cancer: To B or Not to B? *J Exp Med* (2021) 218:1. doi: 10.1084/jem.20200851
21. Sarvaria A, Madrigal JA, Saudemont A. B Cell Regulation in Cancer and Anti-Tumor Immunity. *Cell Mol Immunol* (2017) 14:662–74. doi: 10.1038/cmi.2017.35
22. Maibach F, Sadozai H, Seyed Jafari SM, Hunger RE, Schenk M. Tumor-Infiltrating Lymphocytes and Their Prognostic Value in Cutaneous Melanoma. *Front Immunol* (2020) 11:2105. doi: 10.3389/fimmu.2020.02105
23. Martinet L, Le Guellec S, Filleron T, Lamant L, Meyer N, Rochaix P, et al. High Endothelial Venules (Hevs) in Human Melanoma Lesions: Major Gateways for Tumor-Infiltrating Lymphocytes. *Oncoimmunology* (2012) 1:829–39. doi: 10.4161/onci.20492
24. Lens MB, Newton-Bishop JA, Boon AP. Desmoplastic Malignant Melanoma: A Systematic Review. *Br J Dermatol* (2005) 152:673–8. doi: 10.1111/j.1365-2133.2005.06462.x
25. Carstens JL, De Sampaio PC, Yang D, Barua S, Wang H, Rao A, et al. Spatial Computation of Intratumoral T Cells Correlates With Survival of Patients With Pancreatic Cancer. *Nat Commun* (2017) 8:1–13. doi: 10.1038/ncomms15095
26. Gorris MAJ, Halilovic A, Rabold K, van Duffelen A, Wickramasinghe IN, Verweij D, et al. Eight-Color Multiplex Immunohistochemistry for Simultaneous Detection of Multiple Immune Checkpoint Molecules Within the Tumor Microenvironment. *J Immunol* (2018) 200:347–54. doi: 10.4049/jimmunol.1701262
27. Posch F, Silina K, Leibl S, Mündlein A, Moch H, Siebenhüner A, et al. Maturation of Tertiary Lymphoid Structures and Recurrence of Stage II and III Colorectal Cancer. *Oncoimmunology* (2018) 7:2. doi: 10.1080/2162402X.2017.1378844
28. Silina K, Soltermann A, Attar FM, Casanova R, Uckeley ZM, Thut H, et al. Germinal Centers Determine the Prognostic Relevance of Tertiary Lymphoid Structures and are Impaired by Corticosteroids in Lung Squamous Cell Carcinoma. *Cancer Res* (2018) 78:1308–20. doi: 10.1158/0008-5472.CAN-17-1987
29. Bankhead P, Loughrey MB, Fernández JA, Dombrowski Y, McArt DG, Dunne PD, et al. Qupath: Open Source Software for Digital Pathology Image Analysis. *Sci Rep* (2017) 7:1–7. doi: 10.1038/s41598-017-17204-5
30. Bankhead P. *Creating Annotations Around the Tumor* (2018). Available at: https://petebankhead.github.io/qupath/scripts/2018/08/08/three-regions.html (Accessed February 21, 2021).
31. Bankhead P. *QuPath Scripting - Combining Two Annotations* (2021). Available at: https://forum.image.sc/t/qupath-scripting-combining-two-annotations/48152/2 (Accessed February 21, 2021).
32. Wickham H. *Ggplot2: Elegant Graphics for Data Analysis*. New York: Springer-Verlag New York (2016). Available at: https://ggplot2.tidyverse.org.
33. Engelhard VH, Rodriguez AB, Mauldin IS, Woods AN, Peske JD, Slingluff CL. Immune Cell Infiltration and Tertiary Lymphoid Structures as Determinants of Antitumor Immunity. *J Immunol* (2018) 200:432–42. doi: 10.4049/jimmunol.1701269
34. Laidlaw BJ, Cyster JG. Transcriptional Regulation of Memory B Cell Differentiation. *Nat Rev Immunol* (2020) 21:209–20. doi: 10.1038/s41577-020-00446-2
35. Di Caro G, Bergomas F, Grizzi F, Doni A, Bianchi P, Malesci A, et al. Occurrence of Tertiary Lymphoid Tissue Is Associated With T-Cell Infiltration and Predicts Better Prognosis in Early-Stage Colorectal Cancers. *Clin Cancer Res* (2014) 20:2147–58. doi: 10.1158/1078-0432.CCR-13-2590
36. Hiraoka N, Ino Y, Yamazaki-Itoh R. Tertiary Lymphoid Organs in Cancer Tissues. *Front Immunol* (2016) 7:244. doi: 10.3389/fimmu.2016.00244
37. Willis SN, Mallozzi SS, Rodig SJ, Cronk KM, McArdel SL, Caron T, et al. The Microenvironment of Germ Cell Tumors Harbors a Prominent Antigen-Driven Humoral Response. *J Immunol* (2009) 182:3310–7. doi: 10.4049/jimmunol.0803424
38. Stowman AM, Hickman AW, Mauldin IS, Mahmutovic A, Gru AA, Slingluff CL. Lymphoid Aggregates in Desmoplastic Melanoma Have Features of Tertiary Lymphoid Structures. *Melanoma Res* (2018) 28:237–45. doi: 10.1097/CMR.0000000000000439
39. Lee M, Heo SH, Song IH, Rajayi H, Park HS, Park IA, et al. Presence of Tertiary Lymphoid Structures Determines the Level of Tumor-Infiltrating Lymphocytes in Primary Breast Cancer and Metastasis. *Mod Pathol* (2019) 32:70–80. doi: 10.1038/s41379-018-0113-8
40. De Silva NS, Klein U. Dynamics of B Cells in Germinal Centres. *Nat Rev Immunol* (2015) 15:137–48. doi: 10.1038/nri3804

Conflict of Interest: HL received travel grants and consultant fees from BMS and MSD. HL received research support from BMS, Anaveon, Glycoera and Palleon Pharmaceuticals.

The remaining authors declare that the research was conducted in the absence of any commercial or financial relationships that could be construed as a potential conflict of interest.

Copyright © 2021 Werner, Wagner, Simon, Glatz, Mertz, Läubli, Griss and Wagner. This is an open-access article distributed under the terms of the Creative Commons Attribution License (CC BY). The use, distribution or reproduction in other forums is permitted, provided the original author(s) and the copyright owner(s) are credited and that the original publication in this journal is cited, in accordance with accepted academic practice. No use, distribution or reproduction is permitted which does not comply with these terms.

frontiers in Immunology

REVIEW
published: 29 June 2021
doi: 10.3389/fimmu.2021.694079

The 12-CK Score: Global Measurement of Tertiary Lymphoid Structures

Roger Li[1,2], Anders Berglund[3], Logan Zemp[1], Jasreman Dhillon[4], Ryan Putney[3], Youngchul Kim[3], Rohit K. Jain[1], G. Daniel Grass[5], José Conejo-Garcia[2] and James J. Mulé[2]*

[1] Department of Genitourinary Oncology, H. Lee Moffitt Cancer Center, Tampa, FL, United States, [2] Department of Immunology, H. Lee Moffitt Cancer Center, Tampa, FL, United States, [3] Department of Biostatistics and Bioinformatics, H. Lee Moffitt Cancer Center, Tampa, FL, United States, [4] Department of Pathology, H. Lee Moffitt Cancer Center, Tampa, FL, United States, [5] Department of Radiation Oncology, H. Lee Moffitt Cancer Center, Tampa, FL, United States

There is emerging evidence that the adaptive anti-tumor activity may be orchestrated by secondary lymphoid organ-like aggregates residing in the tumor microenvironment. Known as tertiary lymphoid structures, these lymphoid aggregates serve as key outposts for lymphocyte recruitment, priming and activation. They have been linked to favorable outcomes in many tumor types, and more recently, have been shown to be effective predictors of response to immune checkpoint blockade. We have previously described a 12-chemokine (12-CK) transcriptional score which recapitulates an overwhelming enrichment for immune-related and inflammation-related genes in colorectal carcinoma. Subsequently, the 12-CK score was found to prognosticate favorable survival in multiple tumors types including melanoma, breast cancer, and bladder cancer. In the current study, we summarize the discovery and validation of the 12-CK score in various tumor types, its relationship to TLSs found within the tumor microenvironment, and explore its potential role as both a prognostic and predictive marker in the treatment of various cancers.

Keywords: tertiary lymphoid structures, 12-CK score, immune checkpoint blockade, prognostic biomarker, predictive biomarker

OPEN ACCESS

Edited by:
Catherine Sautes-Fridman, U1138 Centre de Recherche des Cordeliers (CRC) (INSERM), France

Reviewed by:
Florent Petitprez, University of Edinburgh, United Kingdom
Michael Volkmar, German Cancer Research Center (DKFZ), Germany

****Correspondence:***
Roger Li
Roger.Li@moffitt.org

Specialty section:
This article was submitted to Cancer Immunity and Immunotherapy, a section of the journal Frontiers in Immunology

Received: *12 April 2021*
Accepted: *09 June 2021*
Published: *29 June 2021*

Citation:
Li R, Berglund A, Zemp L, Dhillon J, Putney R, Kim Y, Jain RK, Grass GD, Conejo-Garcia J and Mulé JJ (2021) The 12-CK Score: Global Measurement of Tertiary Lymphoid Structures. Front. Immunol. 12:694079. doi: 10.3389/fimmu.2021.694079

INTRODUCTION

Traditionally, effective adaptive immune response against cancer requires the rendezvous between the tumor antigen/major histocompatibility complex expressed on mature dendritic cells (DC) traveling from the primary tumor site and the resident $CD4^+$ and $CD8^+$ T cells in the secondary lymphoid organs. Here, naïve $CD8^+$ T cells are primed and upregulate homing receptors that bind to cognate ligands expressed on inflamed vasculature, enabling entry into peripheral tissue (1). B cells are concurrently activated in the secondary lymphoid organs upon antigen binding and receive help from T follicular helper cells (T_{fh}) to proliferate and form a secondary follicle, which progressively becomes a germinal center that persists until antigenic clearance. Within the germinal center, B cells undergo several processes including somatic hypermutation (SHM), affinity maturation, and class switching to allow production of antibodies with increasing affinity

for the cognate antigen (2). These B cells eventually give rise to plasma cells that secrete higher-affinity and class-switched antibodies in the latter part of the primary immune response, or into memory B cells to coordinate the secondary immune response upon re-insult (2).

There is emerging evidence that adaptive anti-tumor immunity can also be orchestrated at secondary lymphoid organ-like aggregates within the tumor microenvironment (TME) called tertiary lymphoid structures (TLS) (3, 4). TLSs were first described in chronic inflammatory conditions, such as infection, autoimmune disease, and organ transplant rejection (2). They are posited to be 1) the gateway of naïve lymphocyte infiltration into the TME; 2) privileged sites for coordinated tumor antigen presentation and lymphocyte priming, differentiation, and proliferation, leading to a robust tumor-specific immune response. In line with these hypotheses, preclinical work has demonstrated the ability of adoptively transferred naïve $CD8^+$ T cells to directly enter the TME through interactions with TLS-associated high endothelial venules (HEVs) in mice devoid of secondary lymphoid organs (5). Subsequently, their differentiation into functional effectors led to improved cancer control (6). Spatially, an enriched population of naïve $CD8^+$ T cells was found to reside within the TLS, while effector memory $CD8^+$ T cells were predominantly found in the tumor stroma (6). Furthermore, activated $CD38^+$ and $CD69^+$ tumor infiltrating T lymphocytes were enriched in TLS^{Hi} tumors, implicating TLS to be the site of T cell priming and activation (7). On the other hand, there is also evidence that TLS is capable of supporting functional germinal centers to promote affinity maturation and differentiation of B cells, leading to enhanced humoral response (2). Expression of activation-induced cytidine deaminase, a marker for SHM, has been described in TLS B cells within the context of autoimmunity, infection, allograft rejection, and cancer (8). Moreover, restricted profile of variable (V)-gene repertoire usage, highly mutated V regions and oligoclonal diversification of infiltrating B cells and plasma cells found within TLS^{Hi} samples serve as circumstantial evidence for SHM taking place within the germinal centers of the TLS (8).

Consistent with their putative role in lymphocyte recruitment and activation, TLS has been found to be a favorable prognostic indicator in several tumor types (3, 7, 9–13). Although often appearing in tumors with high T cell infiltrates, the absence of TLS in tumors otherwise heavily infiltrated by T cells was associated with inferior prognosis compared to those with high TLS (7, 14). In addition, a trio of recently published studies linked the presence of TLS within the TME to increase efficacy from immune checkpoint blockade (ICB) therapy in melanoma, renal cell carcinoma and soft-tissue sarcoma (14–16). Since, the clinical benefits of TLS within the TME has also been recapitulated in the setting of immunotherapy in other tumor types (17).

TRANSCRIPTOMIC SIGNATURES

With its diverse clinical prognostic and predictive implications, several classification schemes have been proposed to semi-quantitatively assess the presence, complexity and density of the TLS within the TME (18–20). Several of these schemes have coalesced on three classes: early TLS composed of dense lymphocytic aggregates without follicular dendritic cells; primary follicle-like TLS having FDCs but no germinal center reaction; and secondary follicle-like TLS, having an active GC reaction (18, 21, 22). However, given the heterogeneity of their histology and spatial distribution, systematic evaluation of the TLS within the TME is difficult. Alternatively, we and others have leveraged bulk RNA expression data to identify signatures associated with TLS enrichment. These signatures are either related to chemokine expression and/or cell populations found within the TLS.

Based on their observation that the presence of follicular helper T (Tfh) cells within the TME were critically linked to robust tumoral immune infiltration and TLS formation, Gu-Trantien et al. (10) devised an 8-gene Tfh signature to reflect the presence of TLS. They subsequently found this signature to be prognostic in both breast cancer patients undergoing surgical resection with or without neoadjuvant chemotherapy. Amongst its components, CXCL13 expression was found to have the closest association with tumor immune infiltration and the driver of the prognostic value of the gene signature. In addition to its prognostic value in breast cancer, *CXCL13* has also been found to enable identification of TLS in colorectal cancer (23) and soft tissue sarcoma (16). In gastric cancer, Tbet+ T cells and CD20+ B-cell follicles were associated with improved relapse-free survival, serving as rationale for a coordinated Th1 and B cell stromal gene signature, which was found to predict for presence of TLS along with improved cancer specific survival (24). Finally, Cabrita et al. used differential expression analysis from melanoma samples with and without TLS to construct a gene signature consisting of B-cell specific genes such as *CD79B* and *CCR6*, TLS-hallmark genes like *CCR7*, *CXCR5* and *SELL*, as well as *CXCL13*. This TLS-signature was found to be prognostic amongst metastatic melanoma patients within TCGA and also predictive of prolonged survival following treatment with CTLA4 blockade (14). Although promising, these transcriptomic signatures have not been thoroughly examined across tumor types and may be influenced by unique expression profiles within the TME of their origin. In contrast, the most well studied transcriptomic signature recapitulating the presence of TLS is the 12-chemokine score.

12-CK Score - Origins

The 12-chemokine (12-CK) score emerged from an in-depth analysis of the immune gene expression data in colorectal carcinoma and its correlation with patterns and compositions of lymphoid infiltrates (25). Using Affymetrix microarray data derived from 326 colorectal carcinoma samples, Coppola et al. identified a metagene grouping with overwhelming enrichment for immune-related and inflammation-related genes. On histologic review, tumors highly expressive of this metagene grouping exhibited robust peri-tumoral inflammatory reactions accentuated by the presence of TLS (25). These structures contained both B and T lymphocytes, as well as $CD21^+$ dendritic cells within their germinal centers, establishing their true follicular nature. Furthermore, heat mapping analysis

revealed a strong correlation between the chemokine genes and TLS-enriched tumors. Hierarchical clustering of tumors with and without TLS was performed on a selected set of chemokine genes, which was found to also closely associate with the immune-related metagene grouping. For each gene, a single representative probe set with the highest dynamic range across all profiled samples was picked up from all probe sets that mapped to a given gene symbol. Genes were then clustered using Pearson's correlation distance metric resulting in the final 12-CK score consisting of CCL2, CCL3, CCL4, CCL5, CCL8, CCL18, CCL19, CCL21, CXCL9, CXCL10, CXCL11, and CXCL13. This signature was found to be independent of tumor stage, location, microsatellite instability status and treatment received. More importantly, the 12-CK score significantly prognosticated for improved overall survival.

That the presence of TLS was associated with a high chemokine expression signature was not surprising. While the precise sequence of TLS development has yet to be elucidated, there is now evidence demonstrating clear involvement of certain chemokine signaling pathways. Lymphotoxin (LT)-α/β are essential for the establishment and maintenance of lymphoid structures (26). Specifically, signaling through the LTβ Receptor (LTβR) is required for HEV differentiation and the formation of organized lymphoid aggregates (27). LT-α/LT-β also induce the production of CCL19, CL21, and CXCL13 through positive feedback loops, in which chemokine-producing cells expressing LTβR recruit further B cell infiltration, leading to increased production of LT-α/LT-β and in turn, further LTβR stimulation (28, 29).

LIGHT is another lymphotoxin-related cytokine expressed by T cells, immature DC, and macrophages that plays a critical role in the recruitment of $CD8^+$ T lymphocytes and their subsequent proliferation and differentiation (30). In addition, LIGHT synergizes with IFN-γ to enhance the production of CXCL9, CXCL10, and CXCL11, which serve to recruit and polarize $CXCR3^+$ mediated T_H1 response (31). LIGHT also actively recruits NK cells to the site of inflammation, which in turns produces various cytokines leading to T cell infiltration (32) and DC maturation (33). In the context of tumor immunology, LIGHT has been demonstrated to broadly convey antitumor effects in a diverse range of malignancies, including fibrosarcoma (34), melanoma (35), B cell lymphoma (36), cervical cancer (37), and breast cancer (35). Finally, LIGHT has recently been shown to trigger TLS assembly *in vivo* by inducing the production of CCL21 by tumor endothelial cells and to promote the influx of endogenous T cells. Combination therapy using LIGHT and checkpoint inhibition was able to overcome immune resistance observed in autochthonous pancreatic tumors (38).

CCL19 and CCL21 are important chemokines constitutively expressed by stromal cells that recruits $CCR7^+$ cells to the site of inflammation (39). B cell chemotaxis mediated through a CCL21 gradient is enhanced in the presence of Type-I IFN-α, which acts to decrease the ligand induced receptor internalization of CCR7 (receptor for CCL21), thereby allowing more efficient B cell trafficking within the pro-inflammatory TME (40). Ectopic expression of CCL19 or CCL21 in pancreatic islets led to organized lymphocytic infiltrates containing HEVs and stromal cells, resembling TLS (41). Furthermore, in the context of melanoma, treatment using DCs engineered to express recombinant CCL21 led to the recruitment of naïve T cells to the site of vaccination as well as increased formation of TLS (42). Through interactions between the naïve T cells and the engineered DC at the site of vaccination, the primary immune response was initiated and escalated into a more powerful systemic antitumor immunity, culminating in the regression of local and metastatic lesions (42).

Another chemokine known to play a critical role in the formation of TLS is CXCL13, through its interactions with CXCR5. Mice deficient in CXCL13 or CXCR5 lack follicular DC network and are thus devoid of any structured lymphoid organs, including lymph nodes, Peyer's patches, and spleen (28). CXCR5 is upregulated on DC and $CD4^+$ T cells in response to an infectious stimulus, promulgating the infiltration of CXCL13 expressing B cells to immune priming sites and their subsequent activation and antigen presentation (43, 44). Luther et al. showed that overexpression of CXCR5 alone was sufficient to induce the formation of TLS consisting of B and T cell zones, HEVs, and stromal cells (45).

Together, current understanding of the chemokine mediated cellular trafficking strongly support using the 12-CK score as the definitive biomarker for TLS formation. High 12-CK scores within the TME also indicates robust immunogenic activity and may serve as a marker for powerful pre-existing immunosurveillance.

Pan-Cancer 12-CK Expression Analysis

Based on our previous work in colorectal cancer, Messina et al. interrogated the 12-CK score on 14,492 distinct primary and metastatic solid tumors housed within the Moffitt Cancer Center biorepository (12). In this analysis, tumor samples harvested from the oral cavity, cervix, tongue, skin and lung were found to have the highest 12-CK scores. Expanding on our institutional cohort, we also compared the pattern of 12-CK expression across different tumor types using The Cancer Genome Atlas (TCGA) data (**Figure 1**), similar to the analysis done by Sautès-Fridman et al. (3, 4) but with normal samples added and mutational burden.

As noted by Sautès-Fridman et al. (3, 4), the 12-CK scores were highly heterogeneous across tumor types, both in level and range within a specific tumor type. The range is largest in bladder cancer (BLCA, interquartile range, IQR=11.3), cholangiocarcinoma (CHOL, IQR=10.4), sarcoma (SARC, IQR=9.1), and thyroid cancer (THCA, IQR=9.5). Heterogeneity of the 12-CK scores amongst these tumors suggest different degrees of immune activation and TLS formation. Secondly, 12-CK scores generally corresponded with the median tumor mutational burden (TMB) as previously described (46), (Spearman r=0.46, p=0.01) suggesting a link between the neoantigen burden and immune activation (47). A notable exception was the high 12-CK scores affiliated with minimally mutated testicular germ cell tumors (TGCT). Corroborating these findings, Klein et al. (48) found TLS to be prominently featured only within the microenvironment associated with testicular seminoma, but not that of tissues harvested from patients with other benign testicular pathologies. The etiology behind TLS induction in such a mutationally silent tumor remains

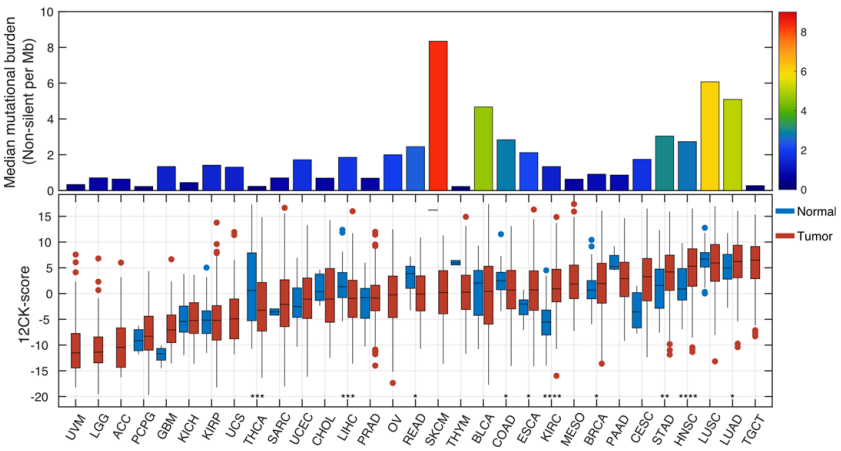

FIGURE 1 | Pan-cancer analysis of the 12-chemokine score. The 12-CK score was extracted from the RNA expression data from various tumor types within The Cancer Genome Atlas, along with expression levels in matched normal samples and their non-silent tumor mutational burden (TMB). In general, 12-CK scores corresponded with TMB. ACC, adrenocortical carcinoma; BLCA , bladder carcinoma; BRCA , breast carcinoma; CESC, cervical squamous carcinoma; CHOL , cholangiocarcinoma; COAD, colon adenocarcinoma; ESCA , oesophageal carcinoma; GBM, glioblastoma; HNSC, head and neck squamous cell carcinoma; KICH, kidney chromophobe; KIRC, kidney renal clear- cell carcinoma; KIRP, kidney renal papillary cell carcinoma; LGG, lower- grade glioma; LIHC, liver hepatocellular carcinoma; LUAD, lung adenocarcinoma; LUSC, lung squamous cell carcinoma; MESO, mesothelioma; OV, ovarian serous cystadenocarcinoma; PAAD, pancreatic adenocarcinoma; PCPG, pheochromocytoma and paraganglioma; PRAD, prostate adenocarcinoma; READ, rectum adenocarcinoma; SARC, sarcoma; SKCM, skin cutaneous melanoma; STAD, stomach adenocarcinoma; TGCT, testicular germ cell tumor; THCA , thyroid carcinoma; UCEC, uterine corpus endometrial carcinoma; UCS, uterine carcinosarcoma; UVM, uveal melanoma. *p < 0.05, **p < 0.01, ***p < 0.001, ****p < 0.0001.

to be seen. Finally, 12-CK scores were higher in tumor samples than normal controls, in esophageal cancer (ESCA), clear cell renal cell carcinoma (KIRC), breast cancer (BRCA), stomach cancer (STAD), and head and neck squamous cancer (HNSC). On the other hand, thyroid cancer (THCA), liver hepatocellular carcinoma (LIHC), and colorectal cancer (READ & COAD) demonstrated lower 12CK score than benign counterparts (**Figure 1**).

12-CK Score Identifies TLS and Is Linked to Prognosis

Since the seminal work in colorectal cancer, our group has further elucidated the implications of the 12-CK score in various other tumor types. In a cohort of 120 samples collected from metastatic lesions in patients with stage IV melanoma, Messina et al. found that patients with low 12-CK scores contained minimal to absent peritumoral lymphocytic infiltrate (12). Conversely, patients with the highest 12-CK scores all had a marked peritumoral lymphocytic host response, punctuated by an abundance of TLS. These TLS contained prominent lymphoid follicles containing $CD20^+$ B cells, with $CD3^+$ T cells clustered within the parafollicular cortex like zones. While $CD86^+$ activated T cells were diffusely present within these structures, $FoxP3^+$ T regs were excluded (**Figure 2**). Additionally, in a limited cohort of 10 patients, the presence of TLS was associated with increased survival. Of particular interest, a single patient with prolonged partial response to ipilimumab (CTLA4 blockade) exhibited TLS within their tumor sample.

In another cohort of 366 patients with breast cancer, high 12-CK scores correlated with Caucasian race (p=0.03), poorly differentiated/high grade tumors (p<0.0001), and were more likely to be ER/PR negative and HER2 positive (p=0.001) (49). In addition, higher 12-CK tumors tended to be of the basal and HER2-positive molecular subtypes as classified by PAM50. More importantly, high 12-CK scores were associated with superior RFS (HR = 0.85, p = 0.018) and OS (HR = 0.63, p < 0.01). By molecular subtypes, both basal- and HER2-subtyped patients derived survival benefit from having a high 12-CK gene expression. H&E and immunohistochemistry staining of the 12-CK high tumors yielded similar results as those seen in colorectal carcinoma and melanoma (i.e. lymphocytic aggregates with $CD20^+$ B cells concentrated as a follicle, and adjacent $CD4^+$ and $CD8^+$ T lymphocytes). Furthermore, tumors expressing high 12-CK scores also expressed genes related to immune activation, including BTLA, D274, CD69, CTLA-4, granzyme B, and IFN-γ.

12-CK in Bladder Cancer

Grounded in these works, we hypothesized that TLS played an integral role in promoting effective anti-tumor immunity in the context of bladder cancer. We collected 130 muscle invasive bladder cancer (MIBC) samples for Affymetrix microarray analysis. The 12-CK score was not found to correlate with traditional prognostic indicators such as pathologic T-staging or N-staging (**Figures 3A, B**). Moreover, no differences were observed in the 12-CK score amongst tumors that were treatment naïve *vs.* those collected following neoadjuvant chemotherapy (**Figure 3C**) (50).

To further explore the immunologic correlates of high 12CK expression, a cell type enrichment analysis from gene expression (xCell) was used to deconvolute the makeup of the TME in the mRNA microarray data. Cell type enrichment scores across 64 immune and stromal cell types were obtained. Although stromal scores were similar between the two cohorts, immune scores representing the overall immune cell content were markedly

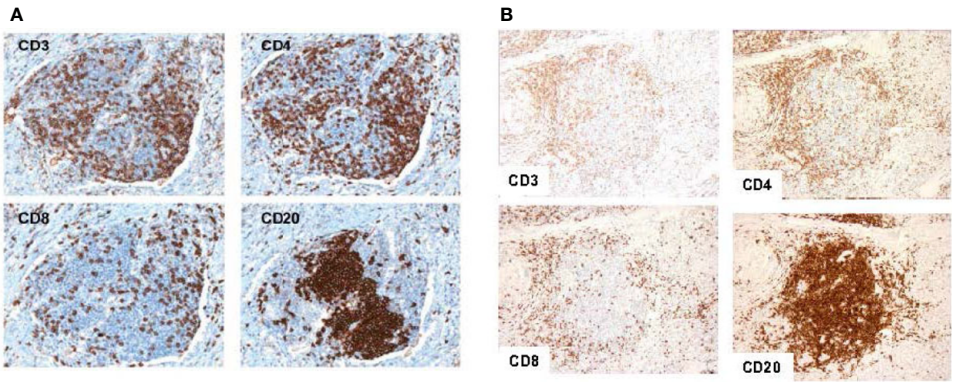

FIGURE 2 | Representative tertiary lymphoid structures found in 12-CK high samples. Typical tertiary lymphoid structure with CD20+ B cells concentrated as a follicle, and CD3+, CD4+, and CD8+ T cells appearing in the parafollicular cortex or marginal zones and with some dispersion into the follicle in a melanoma tumor sample **(A)**. Similar patterns of cellular distribution and structure are recapitulated in breast tumor samples. (Adapted from Messina et al., *Sci Rep*, 2012; Prabhakaran *et al*., *Breast Cancer Res*, 2017). Similar patterns of cellular distribution and structure are recapitulated in breast tumor samples **(B)**.

higher in the 12-CK High tumors (**Figure 3D**). The 12-CK High tumors expressed transcriptomic signatures associated with $CD4^+$ T lymphocyte, $CD8^+$ T lymphocyte, activated dendritic cells (aDC), and B lymphocytes. Furthermore, M1 macrophage, Macrophages, NK cells, $CD8^+$ Tem, $CD4^+$ Tem, and B cells were enriched in 12-CK High tumors, suggesting both a heightened innate and adaptive immune response (**Figure 3E**) (50).

These results were corroborated by findings from gene set enrichment analysis using the REACTOME gene sets, where gene sets associated with both the innate and adaptive immune response were found to be elevated in the 12CK-High tumors. In addition, other gene sets associated with immune activation including TCR signaling, CD28 co-stimulation, IFN-γ signaling, IFN-α/β signaling, cytokine signaling, chemokine receptor binding and neutrophil degranulation were correspondingly found to be elevated in the 12CK-High tumors (**Figure 3F**) (50).

To confirm these findings, immunohistochemistry (IHC) was performed using antibodies to CD4, CD8, CD20, and LAMP3, and cellular densities were quantified using the H-score. Within their TME, 12-CK High tumors consistently exhibited a more robust immuno-environment marked by a higher density of $CD4^+$ T cells ($p=0.002$), $CD8^+$ T cells ($p<0.001$), and $CD20^+$ B cells ($p=0.002$), but not $LAMP3^+$ aDC ($p=0.3$) (**Figure 4**). Next, we systematically identified the presence of TLS in the TME of 12-CK High *vs.* 12-CK Low tumors and classified them into Type I-III as previously described (19). Of the 23 12-CK High tumor samples evaluated, there were 11 with Type III TLS. In contrast, Type III TLS was only found in 1 of the 21 12-CK Low tumor samples ($p<0.002$) (50).

Kaplan-Meier survival analyses of the TCC130 cohort revealed improved progression-free survival (PFS, HR 0.29, p=0.004), disease-specific survival (DSS, HR 0.29, p=0.004), and overall survival (OS, HR 0.55, p=0.03) amongst 12CK-High patients (51). On multi-variable analysis incorporating age, pathologic T and N stage, and use of neoadjuvant chemotherapy, high 12-CK score was found to independently prognosticate improved PFS (HR 0.77, 95% CI 0.62-0.95, p=0.01), DSS (HR 0.63, 95% CI 0.49-0.81, p=0.0003), and OS (HR 0.81, 95% CI 0.65-0.998, p=0.048). To externally validate the prognostic value of the 12CK score, we interrogated data from TCGA, and found similar improvements in PFS (HR 0.55, p=0.007), DSS (HR 0.40, p=0.002), and OS (HR 0.59, p=0.01) in 12CK-High patients. Together, these findings highlight the important favorable prognostic implication of high 12CK-High scores in surgically treated MIBC patients and corroborates findings by other groups on the important prognostic implications of tumor-associated CD38+ plasma cells and TLS in bladder cancer (52).

In summary, 12-CK scores vary widely between different tumor types and within specific tumor types. In general, high scores were seen amongst cancers known to have high TMB, presumably with high neoantigenic stimuli to trigger a strong immunogenic response. On histologic review, tumors marked by high 12-CK scores consistently demonstrated a robust peritumoral inflammatory response underpinned by the presence of TLS consisting of germinal centers rich in $CD20^+$ B cells, plus an adjacent T-cell zone composed by $CD4^+$ and $CD8^+$ lymphocytes, and HEVs. Consistently across several tumor types, global high 12-CK scores were found to convey favorable oncologic outcomes.

PREDICTING RESPONSE TO IMMUNOTHERAPY

Perhaps even more relevant than its ability to prognosticate, the 12-CK score may also serve as a predictive biomarker for response to various modalities of anticancer therapies. Multiple studies have linked pathological complete response (pCR) following neoadjuvant chemotherapy in breast cancer to the presence of TLS. In a cohort of 1,058 patients, high densities of B cells in the context of TLS was found to correlate with pCR following combination neoadjuvant chemotherapy (53). Similar findings were recapitulated in another study consisting of 108 triple-negative breast cancer patients following neoadjuvant chemotherapy, in whom higher densities of HEVs, $CD20^+$ B cells and TLS were significantly associated with disease-free survival following surgery (54). In the adjuvant setting, high densities of TILs and TLS have also been demonstrated to

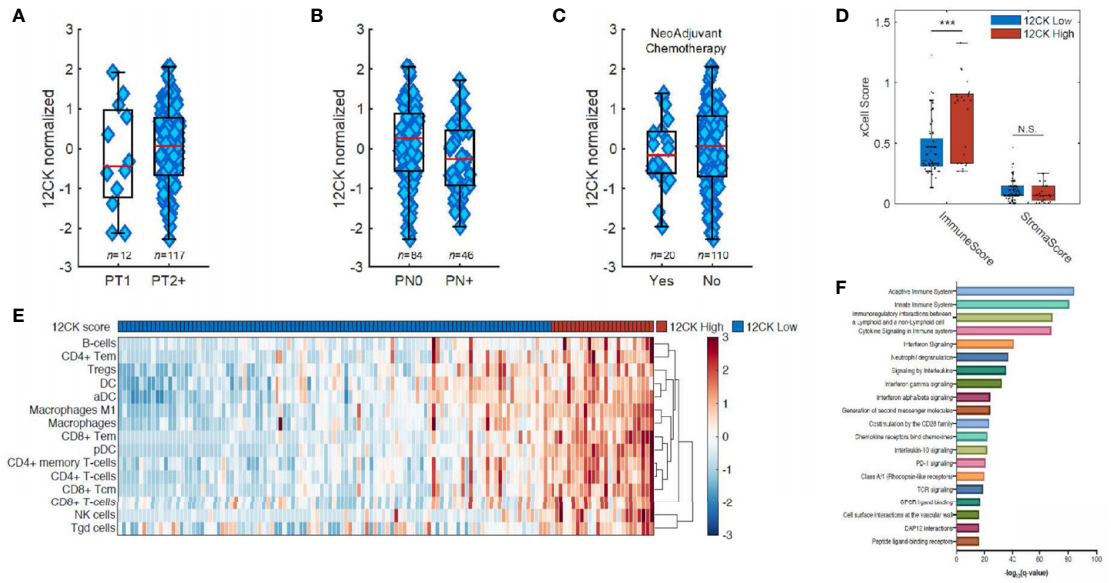

FIGURE 3 | Implications of the 12-chemokine score. The 12-CK scores were found to be independent of traditional prognostic indicators, such as pathologic **(A)** T-staging and **(B)** N-staging, as well as to **(C)** the receipt of neoadjuvant chemotherapy. **(D)** High 12-CK scores were furthermore related to elevated immune scores, but not stromal scores as delineated by the gene signature-based deconvolution method xCell. **(E)** Furthermore, 12-CK high tumors highly expressed signatures related to both innate and adaptive immune cells. **(F)** On gene set enrichment analysis, high 12-CK tumors expressed gene sets related to TCR signaling, CD28 co-stimulation, IFN-γ signaling, IFN-α/β signaling, cytokine signaling, chemokine receptor binding and neutrophil degranulation. ***p < 0.001. NS, Non-significant.

confer favorable response to chemotherapy in bladder cancer (20) and to trastuzumab in hormone receptor-negative, $HER2^+$ breast cancer (55).

Intriguingly, Messina et al. also uncovered a possible link between high 12-CK scores and response to immunotherapy. A Stage IV metastatic melanoma patient with tumor highly expressive of the 12-CK score and TLS enrichment demonstrated a more than 30 month partial response to ipilimumab (CTLA-4 antagonist) (12). Similar findings were repeated in three recent publications spanning ICB clinical trials in melanoma, renal cell carcinoma and soft tissue sarcoma (14–16), in which the presence of TLS in tumor samples were consistently associated with improved survival following therapy. The exact mechanism through which the humoral response generated from the B-cell rich TLS contributes to the overall antitumor immunity in the context of ICB treatment is unknown. Moreover, as ICB is thought to confer its antitumor effects primarily through the T cell compartment, its augmented efficacy in the B-cell enriched TME is counterintuitive.

Nevertheless, some mechanistic insights were uncovered within the three aforementioned studies (14–16). Using CyTOF, Helmink et al. (15) found memory B cells and plasma cells to be more abundant in the TME of ICB responders *vs.* non-responders. Using spatial high-plex proteomic analysis, Cabrita et al. (14) found more $CD4^+$ than $CD8^+$ T cells within or in close proximity to the TLS in metastatic melanoma samples. T cells found in the vicinity of TLS were highly expressive of the pro-survival anti-apoptotic marker BCL-2, signifying antigen-specific activation (56). Interestingly, the T cells found in tumors without TLS had increased expression of immune checkpoint receptors PD-1 and TIM3 as well as lower levels of the anti-apoptotic marker BCL-2, suggesting immune exhaustion (56). Using single cell RNA sequencing, B cell rich samples (presumably with enrichment of TLS) were confirmed to contain more $CD4^+$ and $CD8^+$ T cells with naïve and/or memory-like phenotypes. These findings were corroborated in the setting of soft tissue sarcoma in an independent study by Petitprez et al. (16) TLS containing tumors were found to have higher densities of infiltrating $CD3^+$ T cells, $CD8^+$ T cells and $CD20^+$ B cells, even while controlling for the T and B lymphocytes found within the TLSs themselves. The TLSs were also found to contain $CD4^+PD1^+CXCR5^+$ T follicular helper cells, $CD23^+CD21^+$ follicular dendritic cells, and $PNAd^+$ HEVs.

Further details on the cross-talk between the T- and B-lymphocytes in the context of ICB were uncovered by experiments using a murine triple negative breast cancer model (57). The generation of T cell memory following ICB treatment was critically dependent on B cell activity. Vice versa, tumor infiltration by B cells also hinged on concurrent T_{fh} cell activation and Regulatory T cell (Treg) inhibition. B cell activation following ICB treatment led to proliferation of classed switched plasma cells and increased production of tumor specific IgGs. Moreover, blockade of the T_{fh} cytokine IL21 completely abrogated B cell activation and therapeutic response from anti-CTLA4 therapy (57). In addition, our group has recently established the critical role of T_{fh} in initiating the formation TLS (Chaurio et al., unpublished). In sum, these studies outline a complex web of interactions between T- and B-lymphocytes following ICB treatment, with a particular focus on the importance of TLS in conferring therapeutic efficacy.

Supported by these mechanistic insights, transcriptomic signatures have been proposed by various groups as surrogate

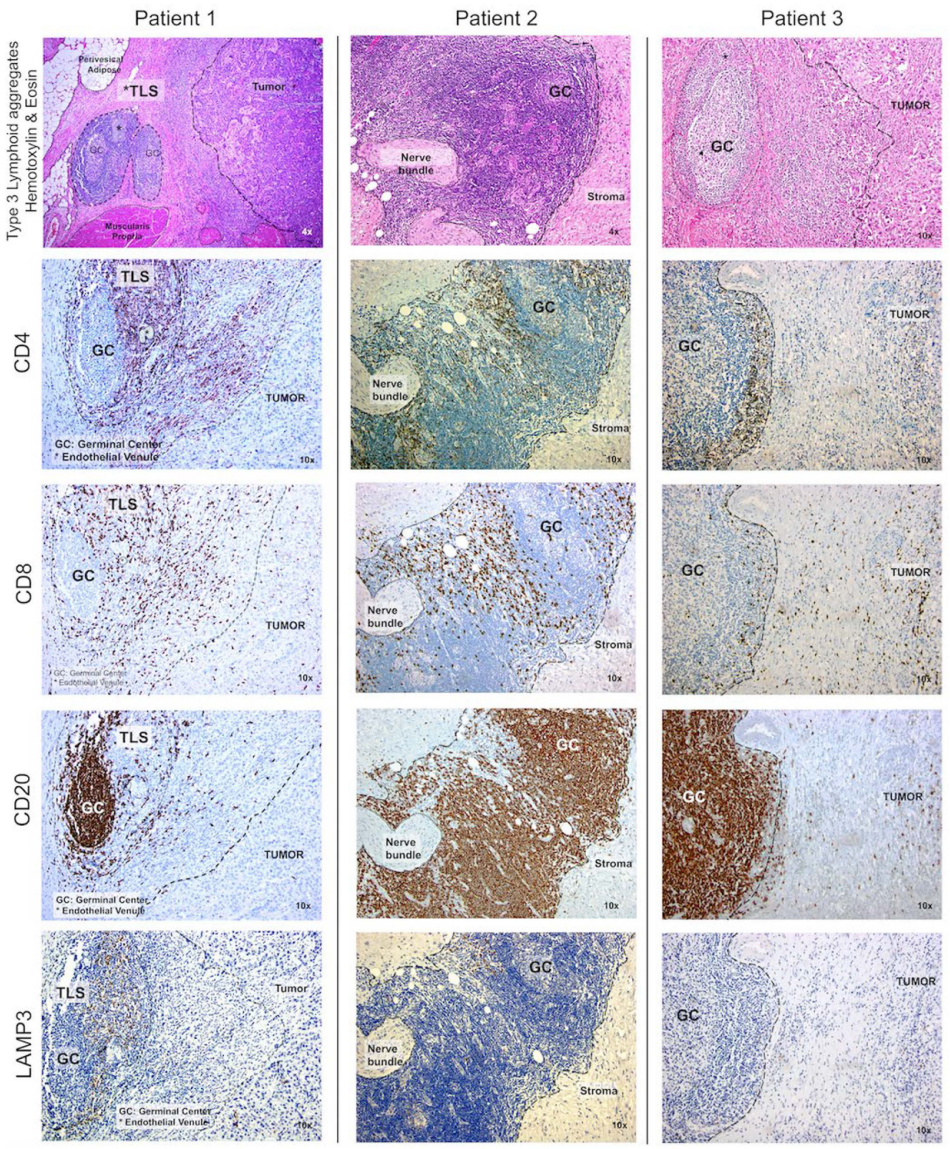

FIGURE 4 | High 12-chemokine scores correlated with higher densities of tumor infiltrating immune cells. Immunohistochemistry was performed using antibodies to CD4, CD8, CD20, and LAMP3 to mark CD4+ T cells, CD8+ T cells, B cells, and activated dendritic cells, respectively. Compared to samples with low 12-CK scores, the 12-CK high tumors were found to contain Type 3 TLS with prominent germinal centers, along with increased infiltrating CD4+ T cells, CD8+ T cells, CD20+ B cells, and comparable levels of activated dendritic cells.

markers for the presence of TLS/B cells to predict response to ICB. Cabrita et al. constructed a signature using hallmark TLS-related genes (*CCL19, CCL21,CXCL13, CCR7, CXCR5, SELL* and *LAMP3*) (14), while Helmink et al. resorted to B cell related genes (*MZB1, JCHAIN, IGLL5, FCRL5, IDO1, IFNG* and *BTLA*) (15). While both groups were able to differentiate responders from non-responders within their respective ICB trials, these signatures have not yet been tested in ICB trials involving other tumor types.

Given that the 12-CK score has been successfully deployed to both reflect the presence of TLS, and prognosticate for improved survival in multiple tumor types (12, 25, 49), we also examined its predictive role for response to ICB. We used data from a recently completed ICB trial in metastatic bladder cancer. Publicly available RNA-seq data from the IMvigor 210 study (58) was extracted. In this single-arm, phase 2 trial, patients with inoperable locally advanced or metastatic bladder cancer with disease progression following platinum-based chemotherapy were enrolled and treated with intravenous atezolizumab (1200mg, given every 3 weeks). In 310 patients receiving atezolizumab treatment, 15% objective response was observed overall, with ongoing responses observed in 84% of the responders. Stratified by treatment response, the complete responders (CR) exhibited significantly higher 12-CK scores than all other groups. Strikingly, the 12-CK High signature

conferred a median overall survival benefit of almost 1 year in the atezolizumab-treated patients (51). Similar results using the 12-CK score have also been reported in clinical trials using PD-1 inhibitor in similar patients (59).

CONCLUSION AND FUTURE DIRECTIONS

Immunotherapy has emerged as a fourth pillar in the treatment of cancer along with surgery, radiotherapy and chemotherapy. By directing the body's immune system to target cancer cells, immunotherapy has the advantages of reducing toxicity while conferring long term response. Despite the success with treatments such as ICB, its underlying mechanisms of action remain incompletely understood. To date, research in immuno-oncology has been sharply focused on the T-cell compartment. However, as efficacy rates to immunotherapy continue to stubbornly stagnate, attention has been divested to uncover the function of other immunologic cell types known to be key players in various immunogenic processes.

The discovery of TLS and their strong link to improved prognosis in multiple cancer types has shed light on the function of B cells in the context of TME. It is increasingly understood that these structures are emblems of not only a robust, but effective local anti-tumor response. As such, they may serve as reliable biomarkers for improved prognosis and/or response to immunotherapy. However, as the density, distribution and location of TLS in the TME are extremely variable, an easily attainable surrogate biomarker is needed to quantify its presence and phenotypic characteristics. Ideally, this marker should be measured objectively and reproducibly with both internal and external validity. It should also be safe to implement (60).

As demonstrated in our previous studies of the 12-CK score in the prognosis of colorectal carcinoma (25), melanoma (12), breast carcinoma (49), and urothelial carcinoma (50, 51), high scores reliably recapitulated the presence of TLS across several tumor types and prognosticated for survival following standard-of-care therapies. However, whether the score can be refined to nuances of the TLS maturation stage and/or localization within the TME remains to be seen. In addition, we are also discovering the predictive value of the 12-CK scores in the context of immunotherapy, such as ICB. Given the wide adoption of next-generation sequencing in the management of various cancers, the 12-CK score is easily attainable from tissue samples obtained for diagnostic purposes prior to the start of treatment. It may also serve to complement the existing biomarkers, such as TMB and PD-L1 status, to form a predictive nomogram used to refine selection of patients for treatment success.

On the other hand, measurement of the induction of TLS by various immunotherapeutic agents may be used to track treatment efficacy. In a clinical trial combining ipilimumab and nivolumab for preoperative treatment in locoregionally advanced urothelial cancer, responders were not necessarily found to have higher TLS in their pre-treatment samples, but rather had a higher degree of TLS induction while on-treatment (18). As repeated tissue sampling may be impractical during the treatment course, "liquid biomarkers" easily collected from the serum may be used as an alternative method to monitor response. To that end, detection of increasing levels of serum CXCL13 has been demonstrated to signify germinal center activity and broadly elevated antibody production (10, 61). Whether CXCL13 measured from the serum alone can serve to track the formation of TLS in the context of immunotherapy in cancer awaits investigation.

Finally, as more details of the B-cell mediated anti-tumor response continue to be unraveled, novel therapeutic strategies to complement ICB will undoubtedly emerge. As the key orchestrators of an effective anti-tumor immune response, TLS are front and center as the potential targets for therapeutic modification. In turn, the 12-CK score may serve as a potential biomarker to predict for response or track efficacy in many of these novel strategies, and serve as an indispensable tool for immuno-oncologists as we launch into the next phase of innovation.

AUTHOR CONTRIBUTIONS

RL: Study concept and manuscript composition. AB: Manuscript composition and critical revision. LZ: Critical revision. JD: Critical revision. RP: Critical revision. YK: Critical revision. RJ: Critical revision. GG: Critical revision. JC-G: Critical revision. JM: Study concept, critical revision, and supervision. All authors contributed to the article and approved the submitted version.

FUNDING

RL: Funding provided by the Clinical Science Division at Moffitt Cancer Center and the Campbell Family Foundation. AB and RP: This work has been supported in part by the Biostatistics and Bioinformatics Shared Resource at H. Lee Moffitt Cancer Center and Research Institute, a NCI designated Comprehensive Cancer Center (P30-CA076292). JJM: Funding provided by NCI-NIH (1R01 CA148995, 1R01 CA184845, P30 CA076292, and P50 CA168536), Cindy and Jon Gruden Fund, Chris Sullivan Fund, V Foundation, and the Dr. Miriam and Sheldon G. Adelson Medical Research.

REFERENCES

1. Engelhard VH, Rodriguez AB, Mauldin IS, Woods AN, Peske JD, Slingluff CL Jr. Immune Cell Infiltration and Tertiary Lymphoid Structures as Determinants of Antitumor Immunity. *J Immunol (Baltimore Md 1950)* (2018) 200(2):432–42. doi: 10.4049/jimmunol.1701269
2. Pitzalis C, Jones GW, Bombardieri M, Jones SA. Ectopic Lymphoid-Like Structures in Infection, Cancer and Autoimmunity. *Nat Rev Immunol* (2014) 14(7):447–62. doi: 10.1038/nri3700
3. Dieu-Nosjean MC, Antoine M, Danel C, Heudes D, Wislez M, Poulot V, et al. Long-Term Survival for Patients With Non-Small-Cell Lung Cancer With Intratumoral Lymphoid Structures. *J Clin Oncol* (2008) 26(27):4410–7. doi: 10.1200/JCO.2007.15.0284
4. Sautes-Fridman C, Petitprez F, Calderaro J, Fridman WH. Tertiary Lymphoid Structures in the Era of Cancer Immunotherapy. *Nat Rev Cancer* (2019) 19 (6):307–25. doi: 10.1038/s41568-019-0144-6
5. Thompson ED, Enriquez HL, Fu YX, Engelhard VH. Tumor Masses Support Naive T Cell Infiltration, Activation, and Differentiation Into

Effectors. *J Exp Med* (2010) 207(8):1791–804. doi: 10.1084/jem.20092454
6. Peske JD, Thompson ED, Gemta L, Baylis RA, Fu Y-X, Engelhard VH. Effector Lymphocyte-Induced Lymph Node-Like Vasculature Enables Naive T-Cell Entry Into Tumours and Enhanced Anti-Tumour Immunity. *Nat Commun* (2015) 6(1):1–15. doi: 10.1038/ncomms8114
7. Goc J, Germain C, Vo-Bourgais TK, Lupo A, Klein C, Knockaert S, et al. Dendritic Cells in Tumor-Associated Tertiary Lymphoid Structures Signal a Th1 Cytotoxic Immune Contexture and License the Positive Prognostic Value of Infiltrating CD8+ T Cells. *Cancer Res* (2014) 74(3):705–15. doi: 10.1158/0008-5472.CAN-13-1342
8. Cipponi A, Mercier M, Seremet T, Baurain JF, Theate I, van den Oord J, et al. Neogenesis of Lymphoid Structures and Antibody Responses Occur in Human Melanoma Metastases. *Cancer Res* (2012) 72(16):3997–4007. doi: 10.1158/0008-5472.CAN-12-1377
9. Coppola D, Mule JJ. Ectopic Lymph Nodes Within Human Solid Tumors. *J Clin Oncol* (2008) 26(27):4369–70. doi: 10.1200/JCO.2008.17.6149
10. Gu-Trantien C, Loi S, Garaud S, Equeter C, Libin M, de Wind A, et al. CD4(+) Follicular Helper T Cell Infiltration Predicts Breast Cancer Survival. *J Clin Invest* (2013) 123(7):2873–92. doi: 10.1172/JCI67428
11. Martinet L, Garrido I, Filleron T, Le Guellec S, Bellard E, Fournie JJ, et al. Human Solid Tumors Contain High Endothelial Venules: Association With T- and B-Lymphocyte Infiltration and Favorable Prognosis in Breast Cancer. *Cancer Res* (2011) 71(17):5678–87. doi: 10.1158/0008-5472.CAN-11-0431
12. Messina JL, Fenstermacher DA, Eschrich S, Qu X, Berglund AE, Lloyd MC, et al. 12-Chemokine Gene Signature Identifies Lymph Node-Like Structures in Melanoma: Potential for Patient Selection for Immunotherapy? *Sci Rep* (2012) 2:765. doi: 10.1038/srep00765
13. Montfort A, Pearce O, Maniati E, Vincent BG, Bixby L, Bohm S, et al. A Strong B-Cell Response Is Part of the Immune Landscape in Human High-Grade Serous Ovarian Metastases. *Clin Cancer Res* (2017) 23(1):250–62. doi: 10.1158/1078-0432.CCR-16-0081
14. Cabrita R, Lauss M, Sanna A, Donia M, Skaarup Larsen M, Mitra S, et al. Tertiary Lymphoid Structures Improve Immunotherapy and Survival in Melanoma. *Nature* (2020) 577(7791):561–5. doi: 10.1038/s41586-019-1914-8
15. Helmink BA, Reddy SM, Gao J, Zhang S, Basar R, Thakur R, et al. B Cells and Tertiary Lymphoid Structures Promote Immunotherapy Response. *Nature* (2020) 577(7791):549–55. doi: 10.1038/s41586-019-1922-8
16. Petitprez F, de Reyniès A, Keung EZ, Chen TW, Sun CM, Calderaro J, et al. B Cells Are Associated With Survival and Immunotherapy Response in Sarcoma. *Nature* (2020) 577(7791):556–60. doi: 10.1038/s41586-019-1906-8
17. Gao J, Navai N, Alhalabi O, Siefker-Radtke A, Campbell MT, Tidwell RS, et al. Neoadjuvant PD-L1 Plus CTLA-4 Blockade in Patients With Cisplatin-Ineligible Operable High-Risk Urothelial Carcinoma. *Nat Med* (2020) 26(12):1845–51. doi: 10.1038/s41591-020-1086-y
18. van Dijk N, Gil-Jimenez A, Silina K, Hendricksen K, Smit LA, de Feijter JM, et al. Preoperative Ipilimumab Plus Nivolumab in Locoregionally Advanced Urothelial Cancer: The NABUCCO Trial. *Nat Med* (2020) 26(12):1839–44. doi: 10.1038/s41591-020-1085-z
19. Kroeger DR, Milne K, Nelson BH. Tumor-Infiltrating Plasma Cells Are Associated With Tertiary Lymphoid Structures, Cytolytic T-Cell Responses, and Superior Prognosis in Ovarian Cancer. *Clin Cancer Res* (2016) 22(12):3005–15. doi: 10.1158/1078-0432.CCR-15-2762
20. Pfannstiel C, Strissel PL, Chiappinelli KB, Sikic D, Wach S, Wirtz RM, et al. The Tumor Immune Microenvironment Drives a Prognostic Relevance That Correlates With Bladder Cancer Subtypes. *Cancer Immunol Res* (2019) 7(6):923–38. doi: 10.1158/2326-6066.CIR-18-0758
21. Posch F, Silina K, Leibl S, Mündlein A, Moch H, Siebenhüner A, et al. Maturation of Tertiary Lymphoid Structures and Recurrence of Stage II and III Colorectal Cancer. *OncoImmunology* (2018) 7(2):e1378844. doi: 10.1080/2162402X.2017.1378844
22. Siliņa K, Soltermann A, Attar FM, Casanova R, Uckeley ZM, Thut H, et al. Germinal Centers Determine the Prognostic Relevance of Tertiary Lymphoid Structures and Are Impaired by Corticosteroids in Lung Squamous Cell Carcinoma. *Cancer Res* (2018) 78(5):1308–20. doi: 10.1158/0008-5472.CAN-17-1987
23. Becht E, de Reyniès A, Giraldo NA, Pilati C, Buttard B, Lacroix L, et al. Immune and Stromal Classification of Colorectal Cancer Is Associated With Molecular Subtypes and Relevant for Precision Immunotherapy. *Clin Cancer Res* (2016) 22(16):4057–66. doi: 10.1158/1078-0432.CCR-15-2879
24. Hennequin A, Derangère V, Boidot R, Apetoh L, Vincent J, Orry D, et al. Tumor Infiltration by Tbet+ Effector T Cells and CD20+ B Cells Is Associated With Survival in Gastric Cancer Patients. *Oncoimmunology* (2016) 5(2):e1054598. doi: 10.1080/2162402X.2015.1054598
25. Coppola D, Nebozhyn M, Khalil F, Dai H, Yeatman T, Loboda A, et al. Unique Ectopic Lymph Node-Like Structures Present in Human Primary Colorectal Carcinoma Are Identified by Immune Gene Array Profiling. *Am J Pathol* (2011) 179(1):37–45. doi: 10.1016/j.ajpath.2011.03.007
26. Weinstein AM, Storkus WJ. Therapeutic Lymphoid Organogenesis in the Tumor Microenvironment. *Adv Cancer Res* (2015) 128:197–233. doi: 10.1016/bs.acr.2015.04.003
27. Browning JL, Allaire N, Ngam-Ek A, Notidis E, Hunt J, Perrin S, et al. Lymphotoxin-Beta Receptor Signaling Is Required for the Homeostatic Control of HEV Differentiation and Function. *Immunity* (2005) 23(5):539–50. doi: 10.1016/j.immuni.2005.10.002
28. Ansel KM, Ngo VN, Hyman PL, Luther SA, Förster R, Sedgwick JD, et al. A Chemokine-Driven Positive Feedback Loop Organizes Lymphoid Follicles. *Nature* (2000) 406(6793):309–14. doi: 10.1038/35018581
29. Wang J, Foster A, Chin R, Yu P, Sun Y, Wang Y, et al. The Complementation of Lymphotoxin Deficiency With LIGHT, a Newly Discovered TNF Family Member, for the Restoration of Secondary Lymphoid Structure and Function. *Eur J Immunol* (2002) 32(7):1969–79. doi: 10.1002/1521-4141(200207)32:7<1969::AID-IMMU1969>3.0.CO;2-M
30. Tamada K, Ni J, Zhu G, Fiscella M, Teng B, van Deursen JM, et al. Cutting Edge: Selective Impairment of CD8+ T Cell Function in Mice Lacking the TNF Superfamily Member LIGHT. *J Immunol (Baltimore Md 1950)* (2002) 168(10):4832–5. doi: 10.4049/jimmunol.168.10.4832
31. Miyagaki T, Sugaya M, Suga H, Morimura S, Ohmatsu H, Fujita H, et al. Low Herpesvirus Entry Mediator (HVEM) Expression on Dermal Fibroblasts Contributes to a Th2-dominant Microenvironment in Advanced Cutaneous T-Cell Lymphoma. *J Invest Dermatol* (2012) 132(4):1280–9. doi: 10.1038/jid.2011.470
32. Fan Z, Yu P, Wang Y, Wang Y, Fu ML, Liu W, et al. NK-Cell Activation by LIGHT Triggers Tumor-Specific CD8+ T-Cell Immunity to Reject Established Tumors. *Blood* (2006) 107(4):1342–51. doi: 10.1182/blood-2005-08-3485
33. Holmes TD, Wilson EB, Black EV, Benest AV, Vaz C, Tan B, et al. Licensed Human Natural Killer Cells Aid Dendritic Cell Maturation *Via* TNFSF14/LIGHT. *Proc Natl Acad Sci USA* (2014) 111(52):E5688–5696. doi: 10.1073/pnas.1411072112
34. Yu P, Lee Y, Liu W, Chin RK, Wang J, Wang Y, et al. Priming of Naive T Cells Inside Tumors Leads to Eradication of Established Tumors. *Nat Immunol* (2004) 5(2):141–9. doi: 10.1038/ni1029
35. Yu P, Lee Y, Wang Y, Liu X, Auh S, Gajewski TF, et al. Targeting the Primary Tumor to Generate CTL for the Effective Eradication of Spontaneous Metastases. *J Immunol (Baltimore Md 1950)* (2007) 179(3):1960–8. doi: 10.4049/jimmunol.179.3.1960
36. Hu G, Liu Y, Li H, Zhao D, Yang L, Shen J, et al. Adenovirus-Mediated LIGHT Gene Modification in Murine B-Cell Lymphoma Elicits a Potent Antitumor Effect. *Cell Mol Immunol* (2010) 7(4):296–305. doi: 10.1038/cmi.2010.15
37. Kanodia S, Da Silva DM, Karamanukyan T, Bogaert L, Fu YX, Kast WM. Expression of LIGHT/TNFSF14 Combined With Vaccination Against Human Papillomavirus Type 16 E7 Induces Significant Tumor Regression. *Cancer Res* (2010) 70(10):3955–64. doi: 10.1158/0008-5472.CAN-09-3773
38. Johansson-Percival A, He B, Li ZJ, Kjellen A, Russell K, Li J, et al. De Novo Induction of Intratumoral Lymphoid Structures and Vessel Normalization Enhances Immunotherapy in Resistant Tumors. *Nat Immunol* (2017) 18(11):1207–17. doi: 10.1038/ni.3836
39. Legler DF, Uetz-von Allmen E, Hauser MA. CCR7: Roles in Cancer Cell Dissemination, Migration and Metastasis Formation. *Int J Biochem Cell Biol* (2014) 54:78–82. doi: 10.1016/j.biocel.2014.07.002
40. Badr G, Borhis G, Treton D, Richard Y. IFN{Alpha} Enhances Human B-Cell Chemotaxis by Modulating Ligand-Induced Chemokine Receptor Signaling and Internalization. *Int Immunol* (2005) 17(4):459–67. doi: 10.1093/intimm/dxh227
41. Luther SA, Bidgol A, Hargreaves DC, Schmidt A, Xu Y, Paniyadi J, et al. Differing Activities of Homeostatic Chemokines CCL19, CCL21, and CXCL12 in Lymphocyte and Dendritic Cell Recruitment and Lymphoid Neogenesis. *J Immunol (Baltimore Md 1950)* (2002) 169(1):424–33. doi: 10.4049/jimmunol.169.1.424

42. Mulé JJ. Dendritic Cell-Based Vaccines for Pancreatic Cancer and Melanoma. *Ann NY Acad Sci* (2009) 1174:33–40. doi: 10.1111/j.1749-6632.2009.04936.x
43. Coelho FM, Natale D, Soriano SF, Hons M, Swoger J, Mayer J, et al. Naive B-Cell Trafficking Is Shaped by Local Chemokine Availability and LFA-1–Independent Stromal Interactions. *Blood* (2013) 121(20):4101–9. doi: 10.1182/blood-2012-10-465336
44. León B, Ballesteros-Tato A, Browning JL, Dunn R, Randall TD, Lund FE. Regulation of T(H)2 Development by CXCR5+ Dendritic Cells and Lymphotoxin-Expressing B Cells. *Nat Immunol* (2012) 13(7):681–90. doi: 10.1038/ni.2309
45. Luther SA, Lopez T, Bai W, Hanahan D, Cyster JG. BLC Expression in Pancreatic Islets Causes B Cell Recruitment and Lymphotoxin-Dependent Lymphoid Neogenesis. *Immunity* (2000) 12(5):471–81. doi: 10.1016/S1074-7613(00)80199-5
46. Alexandrov LB, Nik-Zainal S, Wedge DC, Aparicio SA, Behjati S, Biankin AV, et al. Signatures of Mutational Processes in Human Cancer. *Nature* (2013) 500 (7463):415–21. doi: 10.1038/nature12477
47. Snyder A, Makarov V, Merghoub T, Yuan J, Zaretsky JM, Desrichard A, et al. Genetic Basis for Clinical Response to CTLA-4 Blockade in Melanoma. *N Engl J Med* (2014) 371(23):2189–99. doi: 10.1056/NEJMoa1406498
48. Klein B, Haggeney T, Fietz D, Indumathy S, Loveland KL, Hedger M, et al. Specific Immune Cell and Cytokine Characteristics of Human Testicular Germ Cell Neoplasia. *Hum Reproduction* (2016) 31(10):2192–202. doi: 10.1093/humrep/dew211
49. Prabhakaran S, Rizk VT, Ma Z, Cheng CH, Berglund AE, Coppola D, et al. Evaluation of Invasive Breast Cancer Samples Using a 12-Chemokine Gene Expression Score: Correlation With Clinical Outcomes. *Breast Cancer Res BCR* (2017) 19(1):71. doi: 10.1186/s13058-017-0864-z
50. Li R, Zemp L, Berglund A, Dhillon J, Putney R, Kim Y, et al. 68 the Prognostic and Predictive Implications of the 12-Chemokine Score in Muslce Invasive Bladder Cancer. *J ImmunoTherapy Cancer* (2020) 8(Suppl 3):A41. doi: 10.1136/jitc-2020-SITC2020.0068
51. Zemp L, Berglund AE, Dhillon J, Putney R, Kim Y, Jain RK, et al. The Prognostic and Predictive Implications of the 12-Chemokine Score in Muscle Invasive Bladder Cancer. *J Clin Oncol* (2021) 39(6_suppl):466–6. doi: 10.1200/JCO.2021.39.6_suppl.466
52. Zirakzadeh AA, Sherif A, Rosenblatt R, Ahlén Bergman E, Winerdal M, Yang D, et al. Tumour-Associated B Cells in Urothelial Urinary Bladder Cancer. *Scandinavian J Immunol* (2020) 91(2):e12830. doi: 10.1111/sji.12830
53. Denkert C, von Minckwitz G, Darb-Esfahani S, Lederer B, Heppner BI, Weber KE, et al. Tumour-Infiltrating Lymphocytes and Prognosis in Different Subtypes of Breast Cancer: A Pooled Analysis of 3771 Patients Treated With Neoadjuvant Therapy. *Lancet Oncol* (2018) 19(1):40–50. doi: 10.1016/S1470-2045(17)30904-X
54. Song IH, Heo S-H, Bang WS, Park HS, Park IA, Kim Y-A, et al. Predictive Value of Tertiary Lymphoid Structures Assessed by High Endothelial Venule Counts in the Neoadjuvant Setting of Triple-Negative Breast Cancer. *Cancer Res Treat* (2017) 49(2):399–407. doi: 10.4143/crt.2016.215
55. Lee HJ, Kim JY, Park IA, Song IH, Yu JH, Ahn J-H, et al. Prognostic Significance of Tumor-Infiltrating Lymphocytes and the Tertiary Lymphoid Structures in HER2-Positive Breast Cancer Treated With Adjuvant Trastuzumab. *Am J Clin pathology* (2015) 144(2):278–88. doi: 10.1309/AJCPIXUYDVZ0RZ3G
56. Rogers PR, Song J, Gramaglia I, Killeen N, Croft M. OX40 Promotes Bcl-xL and Bcl-2 Expression and Is Essential for Long-Term Survival of CD4 T Cells. *Immunity* (2001) 15(3):445–55. doi: 10.1016/S1074-7613(01)00191-1
57. Hollern DP, Xu N, Thennavan A, Glodowski C, Garcia-Recio S, Mott KR, et al. B Cells and T Follicular Helper Cells Mediate Response to Checkpoint Inhibitors in High Mutation Burden Mouse Models of Breast Cancer. *Cell* (2019) 179(5):1191–206.e1121. doi: 10.1016/j.cell.2019.10.028
58. Rosenberg JE, Hoffman-Censits J, Powles T, van der Heijden MS, Balar AV, Necchi A, et al. Atezolizumab in Patients With Locally Advanced and Metastatic Urothelial Carcinoma Who Have Progressed Following Treatment With Platinum-Based Chemotherapy: A Single-Arm, Multicentre, Phase 2 Trial. *Lancet* (2016) 387(10031):1909–20. doi: 10.1016/S0140-6736(16)00561-4
59. Sharma P, Retz M, Siefker-Radtke A, Baron A, Necchi A, Bedke J, et al. Nivolumab in Metastatic Urothelial Carcinoma After Platinum Therapy (CheckMate 275): A Multicentre, Single-Arm, Phase 2 Trial. *Lancet Oncol* (2017) 18(3):312–22. doi: 10.1016/S1470-2045(17)30065-7
60. Strimbu K, Tavel JA. What Are Biomarkers? *Curr Opin HIV AIDS* (2010) 5 (6):463–6. doi: 10.1097/COH.0b013e32833ed177
61. Havenar-Daughton C, Lindqvist M, Heit A, Wu JE, Reiss SM, Kendric K, et al. CXCL13 Is a Plasma Biomarker of Germinal Center Activity. *Proc Natl Acad Sci USA* (2016) 113(10):2702–7. doi: 10.1073/pnas.1520112113

Conflict of Interest: RL: Clinical trial protocol committee - Cold Genesys, BMS; Scientific advisor/consultant – BMS, Fergene. JM: Associate Center Director at Moffitt Cancer Center, has ownership interest in Fulgent Genetics, Inc., Aleta Biotherapeutics, Inc., CG Oncology, Inc., Myst Pharma, Inc., Verseau Therapeutics, Inc., AffyImmune, Inc., and Tailored Therapeutics, Inc., and is a paid consultant/paid advisory board member for ONCoPEP, Inc., CG Oncology, Inc., Morphogenesis, Inc., Mersana Therapeutics, Inc., GammaDelta Therapeutics, Ltd., Myst Pharma, Inc., Tailored Therapeutics, Inc., Verseau Therapeutics, Inc., Iovance Biotherapeutics, Vault Pharma, Inc., Noble Life Sciences, and Fulgent Genetics, Inc., UbiVac, LLC, Vycellix, Inc., AffyImmune, Inc., and Aleta Biotherapeutics, Inc. A patent on the 12 chemokine gene expression signature in bladder cancer was issued on March 10, 2020, titled, *"Immune Gene Signatures in Urothelial Carcinoma (UC)"* (10,583,183). Inventors are: JM, Anthony M. Magliocco, and AB. A provisional patent application was filed on August 27, 2020, titled *"Immune Gene Signature in Muscle Invasive Bladder Cancer"* (Serial No. 63/071,320). Inventors are: RL, JM, and AB.

The remaining authors declare that the research was conducted in the absence of any commercial or financial relationships that could be construed as a potential conflict of interest.

Copyright © 2021 Li, Berglund, Zemp, Dhillon, Putney, Kim, Jain, Grass, Conejo-Garcia and Mulé. This is an open-access article distributed under the terms of the Creative Commons Attribution License (CC BY). The use, distribution or reproduction in other forums is permitted, provided the original author(s) and the copyright owner(s) are credited and that the original publication in this journal is cited, in accordance with accepted academic practice. No use, distribution or reproduction is permitted which does not comply with these terms.

frontiers in Immunology

REVIEW
published: 30 June 2021
doi: 10.3389/fimmu.2021.698604

Tumor-Associated Tertiary Lymphoid Structures: From Basic and Clinical Knowledge to Therapeutic Manipulation

Charlotte Domblides[1,2,3†], *Juliette Rochefort*[1,2,3,4,5†], *Clémence Riffard*[1,2,3†], *Marylou Panouillot*[1,2,3], *Géraldine Lescaille*[1,2,3,4,5], *Jean-Luc Teillaud*[1,2,3], *Véronique Mateo*[1,2,3] *and Marie-Caroline Dieu-Nosjean*[1,2,3*]

[1] Faculté de Médecine Sorbonne Université, Sorbonne Université, UMRS 1135, Paris, France, [2] Faculté de Médecine Sorbonne Université, INSERM U1135, Paris, France, [3] Laboratory "Immune microenvironment and immunotherapy", Centre d'Immunologie et des Maladies Infectieuses Paris (CIMI-Paris), Paris, France, [4] Université de Paris, Faculté de Santé, UFR Odontologie, Paris, France, [5] Service Odontologie, Assistance Publique Hôpitaux de Paris (AP-HP), La Pitié-Salpêtrière, Paris, France

OPEN ACCESS

Edited by:
Catherine Sautes-Fridman, U1138 Centre de Recherche des Cordeliers (CRC) (INSERM), France

Reviewed by:
Jamshid Hadjati, Tehran University of Medical Sciences, Iran
Jon Zugazagoitia, Independent Researcher, Madrid, Spain

***Correspondence:**
Marie-Caroline Dieu-Nosjean
marie-caroline.dieu-nosjean@inserm.fr

[†]These authors have contributed equally to this work

Specialty section:
This article was submitted to Cancer Immunity and Immunotherapy, a section of the journal Frontiers in Immunology

Received: *21 April 2021*
Accepted: *16 June 2021*
Published: *30 June 2021*

Citation:
Domblides C, Rochefort J, Riffard C, Panouillot M, Lescaille G, Teillaud J-L, Mateo V and Dieu-Nosjean M-C (2021) Tumor-Associated Tertiary Lymphoid Structures: From Basic and Clinical Knowledge to Therapeutic Manipulation. Front. Immunol. 12:698604. doi: 10.3389/fimmu.2021.698604

The tumor microenvironment is a complex ecosystem almost unique to each patient. Most of available therapies target tumor cells according to their molecular characteristics, angiogenesis or immune cells involved in tumor immune-surveillance. Unfortunately, only a limited number of patients benefit in the long-term of these treatments that are often associated with relapses, in spite of the remarkable progress obtained with the advent of immune checkpoint inhibitors (ICP). The presence of "hot" tumors is a determining parameter for selecting therapies targeting the patient immunity, even though some of them still do not respond to treatment. In human studies, an in-depth analysis of the organization and interactions of tumor-infiltrating immune cells has revealed the presence of an ectopic lymphoid organization termed tertiary lymphoid structures (TLS) in a large number of tumors. Their marked similarity to secondary lymphoid organs has suggested that TLS are an "anti-tumor school" and an "antibody factory" to fight malignant cells. They are effectively associated with long-term survival in most solid tumors, and their presence has been recently shown to predict response to ICP inhibitors. This review discusses the relationship between TLS and the molecular characteristics of tumors and the presence of oncogenic viruses, as well as their role when targeted therapies are used. Also, we present some aspects of TLS biology in non-tumor inflammatory diseases and discuss the putative common characteristics that they share with tumor-associated TLS. A detailed overview of the different pre-clinical models available to investigate TLS function and neogenesis is also presented. Finally, new approaches aimed at a better understanding of the role and function of TLS such as the use of spheroids and organoids and of artificial intelligence algorithms, are also discussed. In conclusion, increasing our knowledge on TLS will undoubtedly improve prognostic prediction and treatment selection in cancer patients with key consequences for the next generation immunotherapy.

Keywords: artificial intelligence, biomarker, cancer, lymphoid neogenesis, organoid, tertiary lymphoid structure, therapeutic intervention, tumor model

INTRODUCTION

The study of tertiary lymphoid structure (TLS) formation, cellular content and function in tumors has progressed tremendously since the initial discovery of their presence in non-small cell lung carcinoma (NSCLC) and their association with more favorable clinical patient outcome (1). Numerous investigations on TLS have been performed with tumor biopsies, using immunohistochemical (IHC), and immunofluorescence (IF) labeling techniques and molecular analyses (transcriptomic, RNAseq, proteomic) leading to an increased knowledge of their neogenesis, composition, and immune functions (2). In particular, study of tumor biopsies has made possible to highlight the importance of tumor-infiltrating leucocytes (TIL) i.e., effector $CD8^+$ T cells and TLS-B cells with regard to the clinical outcome (3, 4) and response to anti-immune checkpoint therapies (5–7). In the present review, we will first detail how TLS are potent anti-tumor structures associated in most cases with better prognosis of cancer patients and how they can be boosters of anti-tumor responses elicited by anti-ICP (immune checkpoint) immunotherapy. We will then examine their relationship with tumor genetic instability, oncogenic drivers in cancer patients, and oncogenic viruses, with a particular focus on NSCLC and Head and Neck Squamous Cell Carcinoma (HNSCC). Second, we will discuss some aspects of TLS neogenesis and function learned from inflammatory diseases and we will present preclinical studies performed in tumor models that suggest that TLS manipulation could represent a potent new anti-cancer immunotherapy.

IMPORTANCE OF THE ORGANIZATION OF TUMOR-INFILTRATING IMMUNE CELLS IN TUMOR IMMUNOSURVEILLANCE

The efficacy of immunotherapy in cancer relies on the generation of an efficient and long-lasting adaptive immune anti-tumor response. However, objective response rates remain low, between 20% to 40%, due to tumor immune escape and to a lack of accurate predictive biomarkers (8). Furthermore, immune-related adverse events occur because of enhanced T cell activation, leading sometimes to treatment discontinuation (9). Thus, there is a crucial need to discover new immune pathways that can be manipulated to improve responses to immunotherapies and cancer patient prognosis.

A number of reports highlights growing evidence on that the development of anti-tumor immune responses at the tumor sites within organized lymphoid structures called TLS that act as local hubs where the immune response can be generated. Initially evidence in the context of autoimmune pathologies, TLS comprise the various cellular components needed to develop an adaptive anti-tumor response. They exhibit a T-cell zone containing activated T cells with Th1, cytotoxic or memory phenotypes, mature dendritic cells (DC) involved in antigen presentation, and fibroblastic reticular cells (FRC) (**Figures 1A, B**).

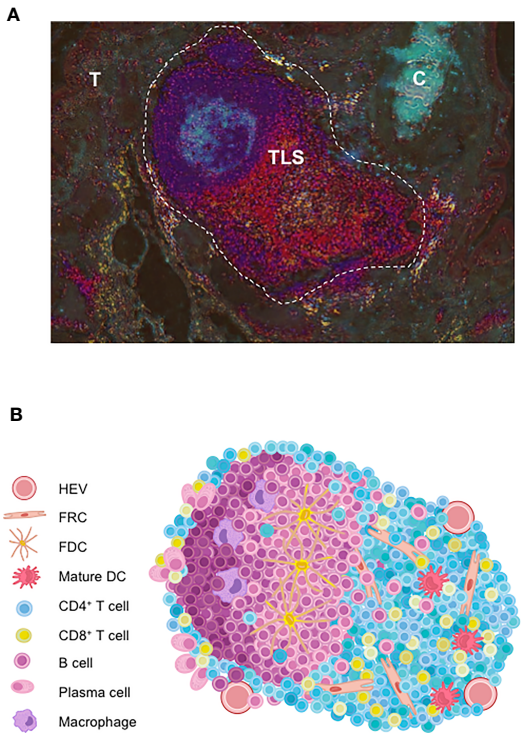

FIGURE 1 | Cellular organization of tumor-associated TLS. **(A)** Full TLS image of lung tumor sections in a NSCLC patient. Briefly, two serial tumor sections were respectively double-immunostained for CD3/DC-Lamp and CD20/CD21. Then color deconvolution and contrast inversion (using ImageJ) was applied as described (10). Shown are $CD3^+$ T cell-rich areas (red); DC-$Lamp^+$ mature DC (yellow) adjacent to the $CD20^+$ B-cell rich areas (dark blue) and $CD21^+$ FDC (light blue) of a TLS close to tumor nests (T) and bronchial cartilage (C). Magnification: x100. **(B)** TLS are well-organized functional immune ectopic aggregates in the close vicinity to HEV. TLS comprise a T-cell zone containing mature DC and FRC; and a B-cell zone with a germinal center with PC, macrophages and FDC. C, bronchial cartilage; DC, dendritic cell; FDC, follicular dendritic cell; FRC, fibroblastic reticular cell; HEV, high endothelial venule; PC, plasma cell; T, tumor nest.

A B-cell zone is also present, exhibiting a germinal center (GC) and where memory B cells and plasma cells can be detected (3, 4). On one hand, detailed cellular content and organization of ectopic lymphoid aggregates have been described, leading to the view that TLS neogenesis is a complex process that gives rise to different types of lymphoid aggregates until a fully differentiated TLS is generated. On the other hand, important features of TLS in cancer patients that have also brought new insights in their relationship with clinical status and tumor characteristics, as described below.

Prognostic Impact of Tumor-Associated TLS

TLS have been observed in numerous tumor types such as NSCLC, HNSCC, ovarian cancer, breast cancer, hepatocellular carcinoma (HCC) or gastrointestinal stromal tumor (GIST). High densities of TLS are associated with better relapse-free

survival (RFS) and overall survival (OS) in several types of solid cancer, independently of tumor TNM staging which is considered as the most important prognostic factor in cancers. The prognostic impact of TLS has been largely reviewed, and it has been shown that, alike in NSCLC, a more favorable outcome for patients is observed in a large number of other cancer types (11). Notably, the high density of TLS in OSCC patients has been associated with a better OS and RFS (12) and identified as an independent positive prognostic factor (13). However in HCC, their prognostic value remains a matter of debate with the description of a poor *versus* a favorable clinical outcome (14, 15), and HCC risk factors such as alcohol consumption, HCV and HBV infection do not account for this discrepancy as these parameters are correlated with TLS densities. Of note, regulatory T lymphocytes (Treg) have been observed in lymphoid aggregates [breast tumors (16)], and TLS [breast cancer, lung SCC, prostate cancer and lung metastasis (17–20)], and their high densities have been associated with a poor clinical outcome suggesting an immunosuppressive role of Treg in these ectopic lymphoid organizations.

Other studies also took into consideration the status of TLS maturation within the tumors, from an immature stage i.e., dense lymphoid aggregates without a network of follicular dendritic cells (FDC), to fully a mature TLS with the segregation of T and B cells segregated into two distinct areas. Thus, immature TLS are present in dysplastic nodules at a pre-neoplastic stage of HCC (21) and in colorectal carcinoma (CRC) (22), and correlate with an increased risk of cancer relapse. Thus, if it is agreed that lymphoid aggregates are immature TLS, this very early stage of TLS development appears to be unable to promote an efficient anti-tumor immune response. A higher level of TLS organization is mandatory to reach a more sophisticated structure allowing an optimal dialogue between the different actors of immune responses, namely T and B cells, macrophages, DC, and FDC (**Figure 1B**).

In addition until now, the relationship between the prognostic value of TLS and their *in situ* localization in adjacent non-tumor tissue it is still a matter of debate. TLS located in distant non-tumor tissue have been associated either with an increased rate of relapse (14), or no value in HCC (15). In contrast in breast cancer, a negative prognostic value has been reported when TLS are present in peri-tumor tissue while intra-tumor TLS are mainly associated with a favorable outcome (23). However, TLS were defined by a chemokine gene signature or by hematoxylin/eosine counterstaining in these studies, and further investigation are required to define the maturation stage of these lymphoid organizations. Thus, the localization of TLS with regard to tumor masses seems to be critical. It underlines the importance of defining the invasive margin for investigating the role of TLS in solid tumors.

Finally, TLS anti-tumor efficacy may also be dependent on tumor stage and on tumor sites where they are located. In melanoma, TLS are found in metastatic sites but not in primary sites (24), although one has to stress that it is difficult to identify primary tumors in most melanoma patients. Lung metastases from renal cell carcinoma (RCC) exhibit mostly immature TLS and correlate with short-term survival whereas in CRC lung metastases, TLS are more mature and are associated with a favorable outcome even at very advanced stage of the disease. Notably, their density was similar between the primary and their matched metastases (25). Thus, these data suggest that the tumor origin seems to be very critical in the shaping of a peculiar immune environment where TLS neogenesis can occur - or not, as compared with the metastatic sites.

Interplay Between TLS and Anti-Cancer Therapies

TLS are increasingly considered as a predictive biomarker of responses to anti-cancer therapies such as chemotherapy, immunotherapy, or targeted therapy (**Figure 2**). It is likely related to the induction of an immunogenic cell death (ICD) that leads to the release of neo-antigens that are then captured by DC, triggering an anti-tumor immune response. In triple-negative breast cancer (TNBC), the high density of high endothelial venules (HEV, as a surrogate marker of TLS) correlates with the pathologic complete response (pCR) after

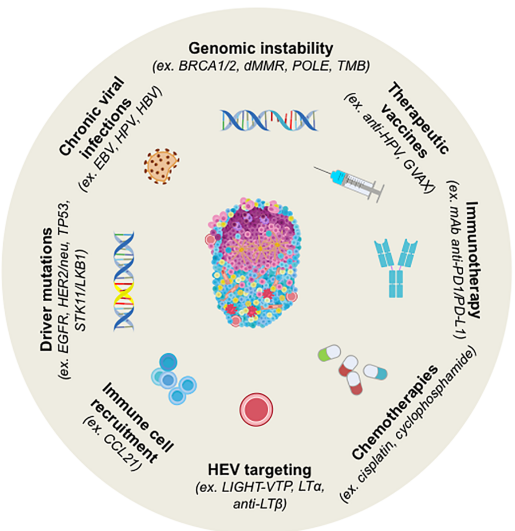

FIGURE 2 | Strategy for Induction of TLS neogenesis in human cancers and by cancer treatments. TLS are induced by chronic viral infections to which tumorigenesis has been associated with genomic instability and/or peculiar driver mutations in several tumors. Chemotherapy, immunotherapy or therapeutic vaccination can also induce TLS. In most cases, their presence is concomitant to better prognosis and higher clinical responses to treatments. Murine models have been explored for the induction of TLS by targeting HEV or the cells involved in organogenesis (i.e. CCL21). BRCA1/2, Breast cancer 1 and 2; dMMR, Deficient Mismatch Repair; EBV, Epstein-Barr Virus; EGFR, Epidermal Growth Factor Receptor; GVAX, GM-CSF-secreting allogeneic PDAC vaccine; HPV, Human Papillomavirus; LIGHT-VTP, LIGHT (stands for *homologous to lymphotoxin*)-Vascular Targeting Peptide; LKB1, Liver kinase B1; LTα, lymphotoxin alpha; LTβ, lymphotoxin beta; OSCC, Oral Squamous Cell Carcinoma; PDAC, pancreatic ductal adenocarcinoma; POLE, DNA Polymerase Epsilon, Catalytic Subunit; STK11, Serine Threonine Kinase 11; TMB, Tumor Mutational Burden.

neo-adjuvant chemotherapy (26). In addition, the presence of TLS could also predict a better outcome in patients treated with targeted therapies. Treatment of *HER2/neu*$^+$ tumors with trastuzumab, a monoclonal antibody (mAb) targeting HER2/neu, has been associated with a better disease-free survival in TLS-enriched tumors (27). In gastrointestinal stromal tumors (GIST), a high density of TLS has been associated with lower imatinib resistance, recurrence, and a more favorable survival (28). Finally, the cellular composition of TLS was found to be different in imatinib-resistant *versus* non-resistant patients, with more regulatory T cells in resistant GIST.

Anti-cancer immunotherapy has been proven one of the most important therapeutic advances in cancer treatment over the last few decade. However, all patients do not respond to these treatments, and there is a crucial need to determine accurate predictive biomarkers to better stratify patients. TLS could be one efficient biomarker. The presence and density of TLS have been correlated with responses to immune checkpoint (ICP) therapies in clear cell renal cell carcinoma (ccRCC) treated with anti-PD1 antibody, or in melanoma treated with a combination of anti-PD1 and anti-CTLA-4 antibodies (5, 6). Similarly, in soft-tissue sarcoma, the presence of TLS and B cells has been also correlated with ICP responses (7). Once again, the maturation stage of TLS and their cellular content appear to correlate their ability to represent a predictive biomarker. In the NABUCCO trial in bladder cancer, the induction of TLS with anti-PD1 and anti-CTLA-4 combination correlated with ICP responses (29). Immature TLS were observed in most non-responding patients, pinpointing again the important role of the maturation status of TLS. Also, one of the main issues of ICP treatment is the occurrence of immune-related adverse events (irAE) that sometimes leads to therapy discontinuation. While corticosteroid therapy received in response to irAE does not impair response to ICP treatment, it was reported that it dampens TLS formation and maturation in lung squamous cell carcinoma, most probably because TLS maintenance is dependent on inflammation (30).

In hepatoblastoma with *APC* mutations, an increase in TLS formation probably favored by ICD has been observed in paired biopsies from pre- and post-cisplatin-based chemotherapy (31). Similarly, NSCLC patients treated with anti-PD1 antibody in a neo-adjuvant setting showed an enrichment in TLS (32), with a positive correlation with higher response rates (33). Vaccine-based immunotherapy can also induce TLS formation (**Figure 2**). The induction of TLS upon HPV vaccination has been observed in responding patients with cervical neoplasia and correlated with CD8$^+$ T cell and Th1 infiltration (34). Moreover, it has been shown that irradiated GM-CSF-secreting allogeneic PDAC vaccine (GVAX) could switch a non-immunogenic to an immunogenic tumor in pancreatic ductal adenocarcinoma (PDAC) patients, marked by a strong T cell infiltration and TLS neogenesis (35). In line with these results, several murine models of cancer have demonstrated that induction of TLS through different strategies can overcome resistance to ICP blockade and synergize with ICP therapy (see *Learning From TLS Study in Non-Tumor Inflammatory Diseases to Better Understand TLS Role in Cancer*).

Genomic Instability, Impaired DNA Repair and TLS: A Relationship to Investigate

Due to genomic instability and impaired reparation processes, tumor cells accumulate genetic abnormalities. Few reports have focused on the molecular characteristics of tumors with regard to TLS presence and function. So far, the relationship between tumor mutational burden (TMB) and TLS in cancers has been rarely investigated (**Table 1** and **Figure 2**). Based on a 12-chemokine signature using the TCGA database, Lin et al. reported that tumors having high TMB exhibit high TLS densities in NSCLC and melanoma, two cancers types known to respond to ICP (38). This highlights the importance of assessing other molecular and cellular signatures in addition to TLS density to predict responses to cancer therapies.

Tumors are highly instable and harbor high rates of mutations leading to the expression of neo-antigens that in turn could trigger anti-tumor immune responses. This is due, at least in part, to an impairment of the DNA repair machinery through defects in homologous recombination (HR) DNA repair genes. The gene encoding *BRCA* that is involved in the detection and reparation of DNA alterations, is mutated in tumors such as breast or ovarian cancers. *BRCA*-mutated tumors exhibit a strong infiltration by CD8$^+$ T cells that harbor a high PD-1 expression in ovarian cancer and some breast cancers such as HER2/neu$^+$ tumors and TNBC (44, 47). Whereas patients with breast cancer poorly respond as well to ICP, patients with TNBC harbors response rates under ICP between 15% and 20% following ICP monotherapy and up to 58% when associated with chemotherapy (48). However, data regarding the putative link between *BRCA* mutations and TLS formation are scarce. Willard-Gallo and colleagues found no difference in the density, location or composition of TLS between *BRCA*-mutated and non-mutated TNBC in spite of a higher rate of TIL and PD-1 expression in TLS in *BRCA*-mutated tumors (36). In high-grade serous ovarian carcinoma, Nelson and colleagues did not find any correlation between a B-cell gene signature (as a likely hallmark of TLS presence (4–7), and *BRCA* mutations (37). By *in silico* analysis based on the TCGA database, Lin *et al.* elegantly showed a correlation between TLS scoring and mutation/neo-antigen loads in many solid tumors such as NSCLC, stomach adenocarcinoma, and uterine corpus endometrial carcinoma but not in others such as ovarian cancer (38). Many mutations as *BRCA* mutations positively correlate with high densities of TLS in most tumors including breast, prostate or endometrial cancers. Other mutations in genes such as *CTNNB1* and *IDH1* negatively correlate with high TLS scoring. Importantly, the correlation can be either positive or negative depending on the tumor type, as for *PIK3R1*. No common molecular feature was observed between HNSCC, lung adenocarcinoma and lung SCC that share some common risk factors. In HNSCC, TLS scoring correlates positively with *CASP8, EP300*, and *KMT2C* mutations, and negatively with *TP53* and *KMT2D* mutations. Similarly, a positive correlation was reported for *KEAP1* and *SMAD4* in lung ADC whereas a negative correlation was observed for *PIK3R1* in lung ADC and for *FBXW7* and *KMT2C* in lung SCC. Also, polymerase ϵ (POLE) mutations in endometrial carcinoma

TABLE 1 | Correlation of TLS signature with driver gene mutations in human cancers.

Mutational status	Read-out	Tumor type	Number of patients	Method of TLS detection	Correlation with mutational status	Ref.
BRCA1/2	protein	TNBC	85	IHC CD3/CD20	No correlation between TLS and BRCA-mutational status High PD-1 expression on immune cells within TLS compared with stromal immune cells Higher prevalence of PD-L1 positive tumors within the TLS positive tumors	(36)
		High-grade serous ovarian cancer	30	IHC CD3-CD8-CD20-CD21-CD208-PNAd	Correlation between TLS and TIL infiltration	(37)
	transcriptomic	Breast cancer, prostate ADC, and CESC	1119, 502, and 306	TCGA database	TLS signature correlates with BRCA1/2 for breast cancer, prostate adenocarcinoma and endometrial carcinoma	(38)
		High-grade serous ovarian cancer	30	TCGA database	Plasma cell or B cell signature correlate with TIL but not with BRCA1/2 status	(37)
MSI	protein	Colorectal cancer (stages II/III)	109	IF CD20	Higher TLS formation with MSI status Higher maturation rate of TLS with MSI status	(22)
	transcriptomic	CESC	306	TCGA database	TLS signature correlates with MSI status	(38)
		Endometrial carcinoma	119	TCGA database	TLS signature correlates with MSI status	(39)
		Colorectal cancer	975	12-chemokine transcriptomic signature	MSI status correlates with higher TLS signature	(40)
CIMP	transcriptomic	Colorectal cancer	975	12-chemokine transcriptomic signature	CIMP status associated with higher TLS signature	(40)
POLE	protein	Endometrial carcinoma	119	IF CD20, CD3, CD8, CD11c, PNAd	TLS signature correlates with POLE mutation	(39)
	transcriptomic	CESC	306	TCGA database	Trend for higher TLS signature for POLE	(38)
TMB	transcriptomic	All tumors	8672	TCGA database	TLS scoring correlates with neo-antigen burden for bladder, breast, cervical, lung adenocarcinoma, endometrial and stomach	(38)
EGFR	protein	NSCLC (ADC)	221 + 24 + 32	IHC CD3/DC-Lamp	EGFR mutations highly represented in TLS^{high} patients	(41)
EGFR	protein	NSCLC (ADC)	316	IHC CD8/DC-Lamp	Trend for higher EGFR mutations in TLS^{high} patients	(42)
Her2	protein	Breast cancer	248	IHC CD3/CD20/CD23	more TLS in $HER2^+$ compared with $Her2^-$ TLS associated with higher TIL infiltrate	(43)
		Breast cancer	95 (32/31/19/13)	IHC CD3/CD20	PD-1^{high} TIL most often found in TLS^{high} tumors (frequently TNBC and $HER2^+$ tumors)	(44)
		Breast cancer	447 $HER2^+$ (HR^+ or HR^-)	HES	TLS density correlates with HER2 expression modification	(27)
KRAS	protein	NSCLC (ADC)	221 + 24 + 32	IHC CD3/DC-Lamp	no association with KRAS mutations	(41)
BRAF	protein	NSCLC (ADC)	221 + 24 + 32	IHC CD3/DC-Lamp	no association with BRAF mutations	(41)
		Colorectal cancer (stages II/III)	109	IF CD20	Positive correlation between BRAF mutations high TLS scoring BRAF mutations correlate with presence of higher mature TLS	(22)
		Colorectal cancer (stages II/III)	351	IHC CD3/CD20	No correlation between TLS density and MSI status	(45)
		NSCLC (ADC)	316	IHC CD8/DC-Lamp	BRAF mutations correlate with low $CD8^+$ T cell and mature DC infiltrate	(42)
	transcriptomic	Colorectal cancer	975	12-chemokine transcriptomic signature	High TLS status correlates with right-sided tumor, BRAF mutations, and MSI-high status BRAF mutations correlate with high TLS signature	(40)
STK11	protein	NSCLC (ADC)	221 + 24 + 32	IHC CD3/DC-Lamp	STK11 mutations correlate with low infiltration of T cells and mature DC	(42)
		NSCLC (ADC)	316	IHC CD8/DC-Lamp	STK11 mutations correlated with low infiltration of $CD8^+$ T cells and mature DC	(42)
TP53	protein	NSCLC (ADC)	221 + 24 + 32	IHC CD3/DC-Lamp	TP53 mutations correlate with high T cell and mature DC infiltrate	(41)
		HNSCC	65	IHC CD3/CD20/CD21	TLS density associated with decreased P53 mutations	(46)
	transcriptomic	Colorectal cancer	975	12-chemokine transcriptomic signature	TP53 wt correlates with lower TLS signature in one cohort of patients	(40)
		All tumors	8672	TCGA database	Positive correlation between TLS scoring and TP53 mutations in breast cancer and low grade glioma Negative correlation between TLS scoring and TP53 mutations in HNSCC and stomach cancer No correlation between TLS scoring and lung cancers	(38)

(Continued)

TABLE 1 | Continued

Mutational status	Read-out	Tumor type	Number of patients	Method of TLS detection	Correlation with mutational status	Ref.
EBV	transcriptomic	Gastric cancer	420	TCGA database	Positive correlation between TLS signature and EBV infection	(38)
HPV	transcriptomic	HNSCC	504	TCGA database	Positive correlation between TLS signature and HPV infection	(38)
		CESC	306	TCGA database	No correlation between TLS signature and HPV infection	
HBV	transcriptomic	HCC	374	TCGA database	No correlation between TLS signature and HBV infection	(38)

Several methods have been used for the quantification of TLS, as discussed in (11).

ADC, Adenocarcinoma; CESC, Cervical Squamous cell Carcinoma and Endocervical adenocarcinoma; EBV, Epstein-Barr virus; HBV, Hepatitis B virus; HCC, HepatoCellular Carcinoma; HNSCC, Head and Neck Squamous Cell Carcinoma; HPV, Human Papilloma virus; IF, ImmunoFluorescence (staining); IHC, ImmunoHistoChemistry; MSI, Microsatellite Instability; NSCLC, Non-Small Cell Lung Carcinoma; TCGA, The Cancer Genome Atlas; TIL, Tumor-infiltrating Leukocyte; TNBC, Triple Negative Breast cancer; TMB, Tumor Mutational Burden; wt, wild type.

correlate with TLS presence (38). POLE is an enzyme involved in repair mechanisms such as base- or nucleotide-excision repair or homologous recombination, and mutations lead to hypermutations within tumors.

Moreover, the alterations of the DNA mismatch repair (MMR) system induce microsatellite instability (MSI), a condition of genome hypermutability. MSI are found in several types of cancers, such as CRC and endometrial cancers. In clinical practice, MSI tumors are associated with high response rates to PD-1 blockade (approximately 50%) whereas microsatellite stable (MSS) CRC are unresponsiveness (49). In stages II/III CRC, TLS and especially mature TLS are increased in MSI positive tumors and correlate with a better outcome compared with immature TLS (22, 50). Similar results were obtained using a 12-chemokine signature on fixed tissues or through TCGA database rather than immunohistochemistry as hallmark of TLS (38, 40), indicating that different approaches can be used for TLS quantification.

Oncogenic Drivers, TLS, and Targeted Therapies

Specific oncogenic drivers i.e., mutated molecules involved in cell proliferation, activation and survival, have been defined in many cancers. This has led to the development of targeted therapies. For instance, different response rates to ICP treatments have been observed in cancerous patients depending on the genetic profile of the tumor. In NSCLC, the presence of *EGFR* mutations is associated with a lower response rate and a worse outcome under ICP whereas a high TMB is correlated with a better response, making TMB a predictive biomarker of ICP response (51, 52). In addition, some mutations are closely associated with a particular immune profile (exclusive, "cold" or "hot" tumors) and TLS scoring (**Table 1**). In NSCLC, *EGFR*-mutated tumors respond to tyrosine kinase inhibitors such as osimertinib, but they do not respond to immunotherapy most likely due to a low immune infiltrate. Conversely, *KRAS* mutations are associated with a higher immune infiltration and *KRAS*-mutated tumors classically respond to ICP, due to high TMB induced by tobacco exposure. In lung adenocarcinoma, Biton et al. have reported that the frequency of *EGFR* mutations is higher in tumors enriched with mature DC (as a hallmark of TLS) whereas no correlation has been found with *KRAS*, *TP53 and BRAF* mutations (41).

Mutations of *BRAF* are detected in several solid cancers, such as NSCLC, melanoma, and colorectal cancers. In CRC, *BRAF* mutations are associated with a higher TLS density, and TLS are more mature compared with *BRAF* wild type (wt) tumors (22, 40). Surprisingly, little is known regarding the relationship between *BRAF* mutations and TLS presence in melanoma, although patients have benefited from anti-BRAF targeted therapies for nearly ten years. Only one study has mentioned an absence of any correlation between B-cell transcriptomic profile (as TLS signature) and *BRAF* mutations in melanoma patients treated by neo-adjuvant targeted therapy (6). Thus, the apparent opposite observations seen in CRC and melanoma means that, in

addition to *BRAF* mutations, other intrinsic parameters might be involved in the shaping of the tumor microenvironment (TME) including the development of TLS.

As discussed above, ICP response depends on various parameters among which *TP53* and *STK11* mutations. In NSCLC, *TP53* mutations are associated with better ICP responses whereas *STK11* mutations are correlated with resistance to the treatment (53). No correlation was observed between *TP53* mutations and TLS scoring in NSCLC although *TP53*-mutated tumors have a higher $CD8^+$ T cell infiltrate and PD-L1 expression (38, 41). Conversely, *STK11*-mutated tumors are characterized by a lower infiltration of $CD8^+$ T cells and TLS-mature DC infiltrate and a lower PD-L1 expression compared with *STK11*-wt tumors. Overall, the different response rates to ICP observed in NSCLC patients with either *TP53* or *STK11*-mutated tumors might be related to the composition and organization of the TME. In particular, patients with *STK11*-mutated lung tumors are not prone to respond to any ICP (at least targeting effector cells and PD-1/PD-L1 axis) as they have a marked deficit in TLS densities and PD-L1 expression.

Cancer-Induced Viruses and TLS

Some murine models have elegantly demonstrated that chronic viral infection (e.g. Influenza virus) can elicit the neogenesis of TLS. Among them, some viruses can cause cancers. Thus, an open question is to determine whether the presence of a virus might be beneficial for the host as a source of foreign antigens, or harmful because of its oncogenic properties (**Figure 2** and **Table 1**). The most studied oncovirus is the human Papilloma virus (HPV) which is involved in several types of cancers such as HNSCC, cervical carcinoma, and anal carcinoma. Transcriptomic analysis using the TCGA database has shown a positive correlation between high TLS scoring and HPV^+ HNSCC whereas no association was observed in cervical cancer (38). In gastric cancer, a high TLS signature was observed in the vast majority of EBV^+ tumors whereas it was highly heterogeneous among EBV^- tumors. Finally, hepatitis B virus (HBV) infection was not associated with TLS scoring in liver cancer. All together, these results indicate that the ability of an oncovirus to induce TLS formation is dependent on the type of cancer and its TME. Further investigation is required to decipher the mechanism by which a virus can favor – or not - the initiation of TLS neogenesis, and to evaluate whether anti-viral immune responses can take place in TLS. Such approaches could give rise to the identification of a new category of TLS-inducer candidates for therapeutic purposes.

LEARNING FROM TLS STUDY IN NON-TUMOR INFLAMMATORY DISEASES TO BETTER UNDERSTAND TLS ROLE IN CANCER

Long before they draw any interest in oncology, TLS were initially described in diseases where chronic inflammation is a shared feature. They were observed in organs that are the targets of autoimmune effector mechanisms and during solid organ transplant rejection, in some chronic infections by pathogens (bacteria and viruses), and in allergy (54–57). In autoimmune diseases and allograft rejection, their presence has been associated with an unfavorable clinical evolution (54–58), as opposed to the favorable outcome observed in cancers associated with their presence. In local infections, their role and prognostic value are more variable and depend on their location, composition and on the considered pathogen (58, 59). Remarkably, the study of TLS in these pathological conditions has provided a better understanding of the events that lead to their neogenesis in specific organs and might give some helpful clues in the field of tumor immunology (57).

In fact, as for tumor-associated TLS, tissue-related TLS also share many features with secondary lymphoid organs. Scrutiny of TLS induction in non-tumor bearing animal models has provided with crucial information for the understanding of the complex, tightly regulated, non-redundant mechanisms that lead to initiation, formation and maintenance of these lymphoid ectopic structures (55). Notably, several recent reports have shed new light in the ontogeny of TLS in mouse models of lung disorders (33, 60–66). In a model of viral infection with respiratory syncytial virus (RSV), Gassen et al. reported a RSV-dependent down-modulation of both IL-21 and IL-21R expression by lung Tfh cells, accompanied by an up-regulation of PD-L1 expression on resident B cells and DC, resulting in a defective GC formation and anti-RSV antibody response. Therapeutic blockade of PD-L1 restored IL-21R expression and increased IL-21 secretion by Tfh cells. In parallel, treatment of RSV-infected mice with IL-21 decreased the viral load and inflammation, while inducing the formation of TLS and improving the antibody response against RSV in the lung of infected animals (60). These results highlight the complex interplay between the IL-21/IL-21R and the PD-1/PD-L1 axes leading to the regulation of Tfh function and TLS formation in RSV-infected lungs. This is reminiscent of the observations made in NSCLC, where the presence of tumor-associated TLS is a favorable factor for an objective response to treatment with PD-1/PD-L1 blocking antibodies (32, 38). Thus, one can hypothesize that these anti-ICP therapies stimulate Tfh and the formation and/or maintenance of TLS in responder patients. Interestingly, an increase of IL-21 and IL21R transcripts and of IL-21 secretion is associated with the presence of TLS in Nasal Inverted Papilloma, a benign tumor, strengthening the idea that IL-21/IL21R axis plays a critical role in the response to anti-ICP therapy, possibly through the formation of TLS (67).

TLS are also involved in the control of lung bacterial infection (62, 66). In *Mycobacterium tuberculosis* (TB) infection, they have been associated with gender bias susceptibility to TB (68). More recently, the same authors demonstrated that premature death of males after TB infection is associated with smaller B-cell follicles in the lungs during the chronic phase of the infection. Moreover, the amount of IL-23, a cytokine required for IL-17 response to infection with TB was reduced in lungs of TB-susceptible males as compared with resistant females (69). This pinpoints an

underestimated gender bias in TLS formation during TB infection (65). Of note, a higher proportion of males has been observed in TLS^{low} *versus* TLS^{high} NSCLC patients (3). It will be certainly important to evaluate in retrospective studies whether such a bias exists in other infectious and malignant diseases.

Chronic Obstructive Pulmonary Disease (COPD) is often associated with airway epithelium functional defects, including a lack of secreted IgA (sIgA) and a pathological adaptive immune activation in advanced COPD patients. Richmond et al. have reported that TLS-like structures (i.e., accumulation of dense B-cell aggregates surrounded by $CD4^+$ and $CD8^+$ T cells) and myeloid DC are present in the lungs of COPD patients where no sIgA are detected, as observed in sIgA-deficient mice (64). Thus, airway bacteria induce the migration of monocyte-derived DC in the lungs through a CCR2-dependent mechanism which in turn favor T cell recruitment and TLS formation.

By the meantime, Naessens et al. have studied the lung myeloid compartment in a COPD cohort using single-cell RNA sequencing and identified type 2 conventional DC (cDC2) as being the more abundant DC in COPD lungs. These authors could show that these cells exhibit a unique migratory signature, including transcripts encoding CXCR5, CXCR4, and the oxysterol receptor EBI2, known to control the spatial organization of cells within TLS (61). Moreover, COPD cDC2 strongly express OX40L, enabling the induction of Tfh cells through the OX40–OX40L axis. Interestingly, OX40L expression by abnormal accumulation of thymic B cells has also been reported to promote Tfh cells in TLS from lupus-prone BWF1 mice (70), pinpointing the importance of this co-stimulatory molecule on B cells for ectopic GC formation in autoimmune targeted organs (71). Importantly, the level of expression of OX40L in human glioblastoma has been associated with a better prognosis, and mice bearing OX40L-expressing glioblastoma present with an improved survival rate over OX40L negative tumors (72). As lymphoid tissue inducer (LTi) cells also express OX40L, the OX40/OX40L axis is therefore likely an interesting therapeutic target for cancer therapy with regard to TLS induction. Anyhow, whether OX40/OX40L axis is implicated in tumor TLS remains to be demonstrated, and current clinical trials testing OX40 agonists for several oncology indications may provide key answers (73). However, LTi cells may not be essential for TLS formation in some situations, as illustrated in mice devoid of LTi cells (74, 75). Several immune cells have been shown to activate local resident mesenchymal stromal cells through LTα and TNF-α receptors (see *The Use of Pre-Clinical Models for studying TLS: From Imaging to Therapeutic Manipulation*), a key cross-talk enabling TLS neogenesis (76).

In an elegant model of kidney injury, Luo et al. also reported a central role of IL-17 in TLS formation. The model has the advantage to allow for a long-lasting development and maintenance of TLS, as animal are sacrificed 45 days after having ischemia reperfusion kidney injury. In this setting, the generation of TLS required fibroblastic reticular cells (FRC) that produce large amount of CXCL13 and CCL19. Interestingly, the size of kidney TLS was dependent on the concentrations of these lymphoid chemokines. Remarkably, in a cohort of patients suffering from IgA nephropathy (IgAN) condition, of whom about 30% present with renal TLS, the authors have reported a significant higher plasma level of CXCL13, CCL21, and CCL19 in patients exhibiting kidney TLS, thus representing a non-invasive renal TLS biomarker (77).

The CCL21 and CXCR3 axis have also been found central when studying a model of local TLS formation during allogeneic aortic transplant chronic rejection. By single-cell RNA sequencing, the authors identified lymphatic endothelial cells as CCL21-producing cells, recruiting into the aortic transplant $CXCR3^+$ and $CCR7^+$ cells involved in TLS formation in arteriosclerotic vessels in the recipient animals (78), confirming previous observations made in mice and humans (79). The presence of TLS induced *via* CCL21 in these pathological conditions is associated with an unfavorable prognosis, and blockade of the CCL21 and CXCR3 axis improves disease conditions (78). Surprisingly, the presence of CCL21 may be also associated with decreased autoimmune symptoms. In a diabetic NOD mouse model, Badillo et al. have interrogated the impact of CCL21 on TLS formation in diabetic animals. When comparing TLS from wild-type (WT) NOD mice and animals expressing CCL21 (ins2-CCL21-NOD) under the control of insulin, the latter mice differ from inflammatory NOD TLS found in type 1 diabetic islets isolated from WT NOD mice. As opposed to the TLS observed in the WT NOD mice, these TLS resemble lymph nodes, contain FRC-like cells expressing β-cell auto-antigens, and are able to induce systemic and antigen-specific tolerance leading to diabetes prevention (80). Remarkably, the authors noticed a redistribution of Treg to ins2-CCL21-NOD islets, presumably through the expression of CCR7 on these regulatory cells. Thus, therapeutic manipulation of CCL21 in autoimmune conditions and cancer may represent a double-edged sword approach and certainly needs further investigation.

Overall, the exploration of mice models of non-malignant inflammatory diseases has provided valuable information on TLS neogenesis. As reviewed above, a number of cellular networks and pathways have been revealed as playing an essential role in the generation of functional TLS. It will undoubtedly help to better define molecular and cellular targets aimed at manipulating the formation and the function of TLS in various diseases, including cancers.

THE USE OF PRE-CLINICAL MODELS FOR STUDYING TLS: FROM IMAGING TO THERAPEUTIC MANIPULATION

Increasing attention has been given to TLS neogenesis in the local tumor microenvironment over the last two decades, due to their negative role in inflammatory/autoimmune diseases and graft rejection on the one hand, and to their positive association with clinical responses in some infectious diseases, cancers, and in response to anti-ICP therapy.

However, the study of biopsies has important limitation for exploring the role of the different cell subsets present in TLS, their

circulation and their dynamic cognate interactions. In oncology, studies on human tumor biopsies derived from cancers such as NSCLC, have been limited in particular by a limited access to samples of sufficient sizes and, hence, the difficulty to perform *in vitro* functional studies with cells derived from these biopsies. To circumvent this bottleneck, one can take advantage of the technical advancements that have included i) the establishment of cell lines (a large majority being of human origin), ii) the use of primary cell cultures, and iii) the development of various mouse models (as illustrated in (81) for NSCLC).

This has led to the setting of preclinical tumor models to elucidate the cellular and molecular mechanisms underlying the formation and immune function of TLS. These studies go from easy-to-use syngeneic subcutaneous tumor transplants (which might fail at mimicking the relevant microenvironment conditions) to more sophisticated genetically engineered models, in which autochthonous tumors progress in the presence of a fully functional immune system, enabling the microenvironment changes and immune evolutionary adaptation that are requested for the spontaneous formation of TLS.

Deciphering Mechanisms of TLS Neogenesis to Explore Their Therapeutic Manipulation in Murine Models

Syngeneic Tumor Models

The majority of murine models used for the induction of tumor-associated TLS are based on syngeneic systems (**Figure 3A**). It is a rather simple and economic mean for studying the cellular and molecular mechanisms underlying TLS formation. However, despite the substantial advantage of an intact immune system in mice, tumor growth rate in syngeneic transplanted models is faster than in cancer patients, and might not allow to induce a

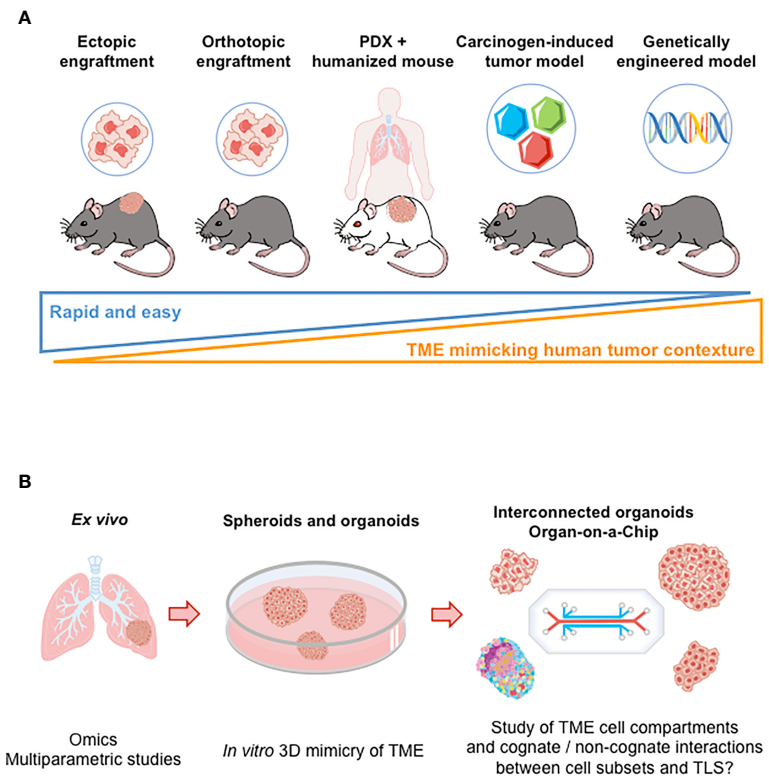

FIGURE 3 | Preclinical models for the study of TLS. **(A)** Illustration of murine models to investigate of TLS neogenesis and immune function. From the left to the right: i) Ectopic models consist in implanting syngeneic tumor cells in immunocompetent mice (subcutaneous injection). However, tumor microenvironment poorly recapitulates the immune contexture of the originating tissue; ii) Intravenous injection of tumor cells allow tumor cells to disseminate in various tissues. But TLS study is hard to perform (kinetics of tumor growth and of TLS neogenesis to be mastered); iii) Implanting tumor cells directly into the tissue from which they originate (orthotopic models) allows tumor growth in a more physiological relevant microenvironment but without rapid dissemination; iv) Patient-Derived Xenotransplantation (PDX) tumor models that use immunodeficient mice enable a better maintenance of tumor heterogeneity but do not allow to investigate anti-tumor immune responses. Mice repopulated with human immune cells ("humanized mice") can be used; v) Carcinogen-induced and genetically engineered tumor models better mimic the clinical situation. Tumors develop spontaneously and gradually in the targeted tissue, allowing for progressive immune microenvironment formation. However, an important variability in tumor development is observed (requirement for large numbers of animals to conduct experiments). **(B)** *Ex vivo* and in *vitro* models, as illustrated in lung cancer. Tumor explants enable to perform multiparametric cytometry and/or imaging, bulk or single cell RNAseq, providing data on the cellular and molecular content of TME. Spheroid and organoid cultures derived from tumor tissues allow the study of TME cellular components (or even of more complex structures such as TLS in a near future following recent progress in organoid and interconnected organoid techniques) (82). "Organ-on-a-Chips" (i.e., microfluidic tissue chips) devices make it possible to study the interaction between TME cell compartments (tumor, stromal, and immune cells). TME, tumor microenvironment.

chronic inflammation usually observed in human TME where TLS neogenesis takes place.

That being said, preclinical models aimed at enhancing a *de novo* vascularization have been nevertheless useful to decipher some of the characteristics of TLS formation. Most of these models focus on lymphotoxin signaling as lymphotoxins are known to play a crucial role in secondary lymphoid organ formation and maintenance through high HEV. These molecules belong to the TNF superfamily and are composed of two main forms, LTα and LTβ that can combine in either LTα2β1 or LTα1β2 heterodimers. The latter heterodimer is the predominant form and binds to LTβ-R receptor on epithelial cells, stromal cells present in lymphoid tissues, monocytes and DC among other cell types. There has been evidence that LTα or LTβ deficiency in mice leads to severe defects in lymphoid organs development (83, 84). Several therapeutic approaches have been considered to boost HEV formation and TLS neogenesis. An anti-disialoganglioside 2 (GD2) antibody fused to LTα has promoted anti-tumor specific T cell responses in $LT\alpha^{-/-}$ mice bearing GD2-expressing B16 melanoma (85, 86). TLS were observed at the vicinity of the tumor, and immunohistochemistry revealed an increased tumor infiltration by immune cells and the presence of B and T cell zones adjacent to the tumor site. Targeting of LTβ-R has also proven preclinical efficacy in both syngeneic and xenogeneic models of colon carcinoma. An agonist anti-LTβ-R antibody has been shown to boost HEV development and TLS induction in a syngeneic mouse colon carcinoma model (87). This was accompanied by tumor growth inhibition and a better response to chemotherapy. Anti-tumor efficacy was also reportedly greater in orthotopic models, highlighting the fact that the growth of tumors in the tissue from which tumor cells are initially derived is an important factor for immune infiltration and TLS neogenesis.

Another ligand of LTβ-R is LIGHT, a pro-inflammatory cytokine member of the tumor necrosis factor (TNF) superfamily, also termed TNFS14, and expressed on immature DC and activated T lymphocytes. Preclinical studies have demonstrated the role of LIGHT protein in activating LTβ-R signaling pathway and TLS neogenesis in solid tumors. In a mouse model of MC38 colon carcinoma, Tang et al. demonstrated that targeting the tumor with an anti-EGFR antibody fused to mutated LIGHT protein (optimized for binding to the mouse lymphotoxin-beta receptor (LTβ-R) and herpes virus entry mediator (HVEM) receptor and for preventing the spontaneous aggregation of the recombinant LIGHT molecule) enhanced T-cell anti-tumor response and contributed to overcome resistance to PD-L1 blockade by facilitating HEV induction and T-cell tumor infiltration *via* $CD68^+$ macrophages activation (88). It has been also shown that targeting tumor vessels with LIGHT fused to a vascular targeting peptide (VTP) (CRGRRST or CGKRK that have been shown to bind tumor blood vessels in murine breast, melanoma, SCC, and brain tumors), to subcutaneously implanted Lewis Lung Carcinoma (LLC) tumor cells (resistant to ICP inhibitors) induces a dose-dependent neovascularization and TLS formation, resulting in increased survival and synergistic effects with anti-tumor vaccination (89). Similar effects induced by LIGHT-VTP were observed in an immunocompetent mouse model (RIP1-Tag5 mice) where pancreatic neuroendocrine tumors arise spontaneously as well as in an orthotopic syngeneic model with the use of the CGKRK peptide as VTP fused to LIGHT after intracranial implantation of murine glioblastoma cells in C57Bl/6 mice. Intra-tumor HEV formation was enhanced, resulting in increased T cell infiltration and anti-tumor response. The effects mediated by LIGHT targeted to blood vessels were multiplied by combining CGKRK-LIGHT therapy with an anti-VEGF antibody or with ICP inhibitors (90). Interestingly, a selective binding of CGKRK-LIGHT was also observed on tumor vessels but not on normal vessels of FvB/N Rag-deficient mice implanted with human NSCG glioblastoma cells, suggesting that LIGHT-targeting strategies are translatable to human neo-angiogenic tumors.

Moreover, the role of CCL21 in the induction of TLS has been also investigated. CCL21 is a chemoattractant expressed by fibroblastic cells within lymph nodes and its role as a T lymphocyte recruiter into TLS *via* CCR7 has been extensively studied. Intra-tumor injection of the chemokine in ectopic pancreatic adenocarcinoma increased tumor immune infiltration, especially T cells, DC and NK cells, and induced a microenvironment reorganization resulting in anti-tumor immunity (91). The use of different KO mice revealed that the effect of CCL21 is mediated by these various immune cell populations and not due only to the angiostatic effect of the therapy. Also, the use of genetically engineered DC has been proven efficient in murine models. T-bet transcription factor-expressing DC induced TLS neogenesis in a model of ectopic CRC and in sarcoma (92). In these studies, TLS induction by T-bet^+ DC was found to be dependent on IL-36γ overexpressed by these cells.

Transfer of established clonal cell lines have also been reported to induce TLS *in vivo*. In an elegant study performed by Zhu et al., lymph node-derived and isolated $CD45^-$ $CD3^-$ LTβ-R^+ $VCAM\text{-}1^+$ clonal stromal cells were reinjected into mice before ectopic subcutaneous MC38 colorectal cancer engrafting. Formation of TLS, accompanied by an increased infiltration of anti-tumor specific T lymphocytes was observed in pre-injected mice (93).

In a preclinical study, combination of GVAX with TGF-β inhibitors enhanced TLS formation, $CD8^+$ T cells infiltration, and intra-tumor Treg depletion in pancreatic tumor-bearing mice, resulting in an improved anti-tumor effect of the vaccination (94). This pre-clinical study has been echoed in a clinical trial where the administration of GVAX was shown to induce TLS formation, promoting T cell infiltration and Th17 differentiation, while inhibiting Treg recruitment in PDAC patients (35). Anti-angiogenic strategies as well as ICP inhibitors combined with chemotherapy could also enhance immune infiltration through HEV and promote TLS neogenesis in breast and pancreatic cancer syngeneic models, although not in a glioblastoma model (95).

Other mouse models relying on the injection of syngeneic lung tumor cells in immunocompetent mice have been used to study lung tumor development and response to therapy but have rarely reported examination of TLS. The injection of mouse lung tumor cells such as syngeneic LLC in immunocompetent mice induced the appearance of a lymph node-like vasculature, supporting naïve T-cell entry into the tumors (96). It was found dependent on the presence of endogenous $CD8^+$ T cells but not of B cells, NKT and $CD4^+$ T cells. However, the authors also showed that cells involved in the induction of lymph node-like vasculature and cytokine production differed between tumor sites. Finally, this mouse model made it possible to show that organized lymphoid tissue develops in tumors injected intraperitoneally, although T cells were not organized in a well-defined area.

Humanized Tumor Models

TLS have been successfully induced in both ectopic and orthotopic tumors from human origin representing a variety of cancer types. They were mostly detected thanks to their specific immunohistological features that include the presence of a T cell zone and an adjacent B cell zone punctuated by clusters of follicular dendritic cells, structured by a network of HEV, and a specific chemokine expression profile such as CCL21 and CXCL13. However, the existing models have limitations as they fail at reproducing the complex human TME and tumorigenesis kinetics, both of which greatly impact TLS neogenesis and function. In addition, xenografts of human tumor cells are attractive but not workable for TLS study as they require the use of immune-deficient mice which prevents to study the immune cellular crosstalk that takes place to generate TLS. The engrafting of patient-derived tumor tissue (patient-derived xenograft, PDX) in humanized immune competent mice could enable to accurately study TLS neogenesis but remains a difficult and time-consuming task (**Figure 3A**).

Carcinogen-Induced Tumors

Carcinogen-induced tumorigenesis allows for evolutionary cellular and molecular interactions between immune cells and tumor cells before the tumor gets palpable, an advantage rarely shared by tumor cell transplantation, if any (**Figure 3A**). In carcinogen-induced advanced tumors, Treg accumulation in TLS may alter further development and effector function of the structures. Depletion of these cells in $Foxp3^{DTR}$ tumor-bearing mice boosted anti-tumor efficacy through HEV neoformation and immune cell infiltration (97, 98).

Genetically Engineered Mouse Tumor Models

Genetically engineered murine models have also been developed, marked by a slower tumor expansion and a histopathological context that better mimics human cancer progression (**Figure 3A**). However, murine tumors are also known to bear a lower mutational load than their human counterparts, and this feature could mean a lower immunogenicity, explaining the tardiness of tumor development in genetically engineered mouse models.

This has been exemplified by the elegant work of Tyler Jacks et al. that explored the role of Treg in a genetically engineered mouse model ($Kras^{G12D}$ $Trp53^{-/-}$) of autochthonous lung adenocarcinoma (97). After detecting an accumulation of activated Treg strongly expressing CTLA-4 in lungs with tumor nodules, the authors showed that these cells suppress anti-tumor responses. Depletion of Treg that were engineered to specifically express diphtheria toxin receptor fused to GFP [(DTR)-GFP fusion] provoked a massive cellular infiltration into tumors whose architecture was profoundly disrupted, as shown by CLARITY 3D confocal imaging. IHC showed that most of the infiltrating cells were $CD4^+$ and $CD8^+$ T cells located all over lung parenchyma, with a large number of macrophages infiltrating tumor masses whereas T cells were primarily found near/within blood vessels and macrophages within airway-like pockets surrounded by tumor cells when Treg were present. Treg were found mostly in perivascular and T-cell areas of TLS. Finally, HEV present in TLS exhibited T cells in their lumen, suggesting that HEV are involved in the recruitment of circulating T cells into TLS. Not only this mouse model made it possible to characterize in details the cell composition of tumor-associated TLS but also to investigate their function and regulation. First, tumor-specific activated dye-labelled T cells entered the lung tissue only when TLS were present in tumor-bearing mice. Control mice lacking TLS did not show any T cells in lung tissue. Interestingly, a majority of tumor-specific T cells were observed within TLS by contrast to control labeled T cells. These cells interacted with DC in the T-cell area. Second, when Treg were depleted, a strong increase in the area of the lung covered by TLS was observed due to local $CD4^+$ and $CD8^+$ T cell proliferation shortly after Treg depletion, an upregulation of the expression of CD80 and CD86 costimulatory molecules on DC being observed as well.

In CC10-TAg mice, intrapulmonary administration of engineered CCL21-expressing DC also induced tumor T cell infiltration and specific anti-tumor responses in spontaneous broncho-alveolar carcinoma, thus decreasing tumor burden (99). These authors could show that both ectopic syngeneic or orthotopic autochthonous tumors are infiltrated by immune cell populations following CCL21 therapy, leading to a potent anti-tumor effect. As already stated in *Learning From TLS Study in Non-Tumor Inflammatory Diseases to Better Understand TLS Role in Cancer*, CCL21 could be therefore an interesting and translatable target for TLS induction and anti-tumor immunotherapy.

Other complex genetically engineered models have been developed lately to induce tumor-associated TLS in mice. $Kras^{LSL\text{-}G12D}TP53^{flox/flox}$ mice developed lung adenocarcinoma following intra-tracheal injection of non-recombinant lentiviruses expressing tumor antigenic peptide and Cre recombinase and displayed highly organized TLS along with tumor growth (100). In this experimental model, inducible neo-antigen expression provided evidence that tumor antigens play a role in TLS formation.

Ectopic lymphoid structures histologically comparable with their human counterparts have been also induced in a genetically engineered model of $IKK\beta(EE)^{Hep}$ mice. These animals show a persistent activation of the IκB kinase (IKK) in hepatocytes and

abundance and transcriptional activity of NF-κB, similar to what is observed in chronic hepatitis (14). Following diethyl nitrosamine injection, these mice are more susceptible to hepatocellular carcinogenesis (HCC). A NF-κB dose-dependent TLS phenotype was demonstrated, as well as an association between TLS and hepatocarcinogenesis, and TLS were found to be a niche for HCC progenitor cells. The bad prognosis value of TLS in this type of cancer has led to the development of murine models where TLS formation is inhibited. In particular, depletion of thymocytes, NK cells and FDC in IKKβ(EE)^{Hep} mice was obtained with an anti-Thy1.2 antibody. Treated mice displayed a reduced TLS presence as well as fewer HCC. Similar results were obtained with Rag1$^{-/-}$ mice, lacking B and T lymphocytes. This murine model underlined an unexpected role of TLS in a subtype of HCC. It also confirmed that TLS originate from a cross-talk between innate and adaptive immune system in an inflammatory context.

Although many strategies have been successful at inducing TLS in tumor models *in vivo*, only a few murine models have shown spontaneous tumor-associated TLS formation so far. Interestingly, these tumor models have revealed various mechanisms that control TLS induction: following subcutaneous tumor implantation in Lewis lung carcinoma (96), in carcinogen-induced colorectal cancer (45), in melanoma where TLS formation was shown to be orchestrated by a network of lymphoid tissue organizer cell-like fibroblasts (101), as well as in advanced gastric cancer and in lung adenocarcinoma in genetically engineered models (97, 102). In the latter, Treg ablation led to TLS formation, suggesting that targeting Treg could be an interesting therapeutic lead for a TLS-boosting strategy.

Spheroids and Organoids, the Next Step to Study TLS

Whether mouse models mirror accurately the cellular and molecular complexity of human tumors such as NSCLC, remains an open and controversial question, even though these models have brought useful insights on TLS role and structure. One can think that the ability to recapitulate *in vitro* the complexity of TME of human tumors and its dialogue with tumor cells could allow the study of TLS formation, regulation and function in a more relevant setting. Thus, the question arises whether the current development of 3D culture models of solid tumors could make it possible to study TLS.

Tumor spheroids correspond to simple 3D structures obtained either with cells from tumor cell lines or from biopsies, digested/dissociated or not. Spheroids resemble the architecture and metabolism of the tissue of origin. They are cell aggregates that grow in 3D suspensions. Overall, their volumes are comprised between 0.5 and 1 mm^3. For tumor study, they can be obtained from cancer cell lines or from solid tumors. Spheroids have been used to screen anti-cancer drugs and oncogenic drivers, therapeutic antibodies and immune cell infiltration and trafficking. Recently, it has been shown that lung adenocarcinoma spheroids derived from cancer cell lines can be used to perform genome-wide CRISPR screens (103). Also, tissue-derived tumor spheres (TDTS) can be derived from cells obtained from partial dissociation of tumors and contain mostly tumor cells. TDTS can be used as a reliable read-out to test chemotherapeutic drugs. Spheroids can be also obtained without tissue dissociation from tumor explants without enzymatic digestion or mechanical dissociation. They are usually termed organotypic multicellular spheroids (OMS) or more simply tumor explants. Again, these multicellular spheroids have proven useful to determine the sensitivity of tumor cells to chemotherapeutic drugs or to analyze the diffusion and distribution of the anti-EGFR antibody cetuximab. They have been also used to study the content of their immune cell compartment and the impact of an anti-PD-1 antibody (nivolumab) on immune cell localization [reviewed in (104)]. However, all these types of spheroids did not make possible to obtain more complex tumor tissue organization where TLS can develop.

One step forward towards the generation of a TME favorable to TLS development might be microfluidics. These dynamic models can mimic vascularization and have been used for antibody, soluble drugs and cell diffusion within tumor spheroids. Murine and patient-derived organotypic tumor spheroids (termed MDOTS and HDOTS, respectively) loaded into 3D microfluidic devices containing immune cells have been developed in an effort to incorporate characteristics of TME and evaluate the response to ICP blockade (105). These spheroids retained autologous immune cells. The addition of anti-PD-1 antibody in the device showed that a dose-dependent killing of MDOTS in response to the treatment. This effect required the presence of CD8$^+$ T cells in the spheroids. Similarly, when HDOTS were examined, it was possible to immunophenotype a large panel of these spheroids that contain B and T cell subsets and myeloid cells. Killing and production of cytokines (IL-2, IFN-γ, TNF-α) and chemokines (CCL9, CXCL13) could be also evidenced in presence of anti-PD-1 antibody. Thus, improvement of microfluidics applied to the generation of a complex TME where immune cells are present may allow the study of TLS genesis in a near future.

Alike organotypic multicellular spheroids, organoids are obtained from tumor fragments by culture in enzyme-free culture medium that makes possible to preserve tissue integrity. By contrast to spheroids, they can then be grown *in vitro* for several weeks, although their immune components tend to decrease and disappear along the culture, preventing a detailed analysis of the microenvironment. These models mimic the cellular and architectural complexity of the TME only partially and suffer from severe limitations that hamper the generation of a more complex TME. Hypoxia and an increased production of lactic acid by tumor cells cultured in such 3D architectures play a major role in this process. However, a recent study has shown that the co-culture of tumor organoids (derived from CRC and NSCLC tumors) with autologous PBMC can generate tumor-reactive T cells (106). Using this method, the authors could show that (i) tumor-reactive CD8$^+$ T cells can be induced and expanded, (ii) expanded CD8$^+$ T cells are tumor-specific and not anti-self T-cells, (iii) tumor organoids can be killed by

autologous tumor-reactive T cells. Thus, this study shows that co-cultures of autologous primary tumor organoids and PBMC can be used to activate and expand tumor-reactive cytotoxic T cells from peripheral blood of patients. It paves the way to generate well-characterized tumor-specific T cells that could be further engineered for immunotherapy and to decipher the mechanisms leading to sensitivity or resistance to immunotherapeutic intervention. Also, one can think that co-cultures of organoids with cells that have been identified as playing a role in TLS induction could be set up. More sophisticated organoids that recapitulate the TME cellular complexity and its machinery can be envisioned. In a recent report, Kuo and colleagues have developed human and mouse cancer models to better recapitulate TME (107). These authors developed an air-liquid interface (ALI) mouse and patient-derived in bloc tumor organoid model that maintains the architecture of TME. In this setting, the patient-derived organoids (PDO) exhibit both tumor parenchyma and myofibroblast stroma, and include tumor-specific TIL, making it possible to model immune cell responses *in vitro* (107). These PDO recapitulated the parental tumor histology although continued growth did not always maintain the TME architecture, limiting the study of TME to a few weeks. Molecular analyses revealed that TIL within PDO derived from ccRCC recapitulated the TCR repertoire of the original tumor biopsies and that the immune diversity of T, B and NK cells was conserved across PDO and fresh tumors. Importantly, when human organoids derived from NSCLC, ccRCC and melanoma patients were treated with the anti-PD-1 therapeutic antibody nivolumab, a high-grade induction of *IFNG*, *PRF1*, and/or *GZMB* transcripts was observed within organoid-sorted TIL, with a pattern of TIL activation response to nivolumab similar to that observed in clinical trials. Thus, these results show that it is possible to manipulate immune cells present in organoids, suggesting that the triggering of cells present in TME and involved in TLS neogenesis is feasible.

All these studies clearly show that progress has to be made towards rendering organoid models suitable for TME studies (82) in particular if one wants to dissect complex process such as TLS neogenesis in tumors. The study by Kuo and colleagues pinpoints several important issues (107). First, a marked difference was observed between mouse and tumor patient-derived organoids. By contrast to mouse organoids, human PDO display variable growth correlating with i) high- *versus* low-grade tumor histology, ii) quality of the tumor biopsy (acquisition delay, tumor viability, pre-/post-treatment). Mouse tumors exhibit far less heterogeneity in terms of TIL activation, proliferation and cytotoxic ability than their human counterparts. Also, the contributions of the peripheral immune system and of vascularization in the shaping and control of TME are still excluded with the present PDO. It will be certainly possible in a near future to combine such PDO with other immune components from blood or/and lymph node and/or to introduce various precursor cells such as lymphoid tissue inducer (LTi) and organizer (LTo) cells within tumor organoids. Of note, Watanabe and his colleagues (108) have recently reported that immunologically active lymphoid tissues (termed by these authors aLTs) composed of human lymphoid cells and stromal cells expressing LTβR, VCAM-1, ICAM-1 and containing several lymphoid chemokines, could be stably constructed in immunodeficient mice. The spheroids were formed as the scaffolds from the stromal cells and transplanted into renal subcapsular space of immunodeficient mice together with human PBMC absorbed in collagen sponges. After a few weeks, three-dimensional organoids containing clusters of human T and B cells and scattered DC were stably formed. When PBMC prepared from healthy donors who were vaccinated against varicella zoster virus (VZV) were absorbed in the collagen sponges, a GC-like B cell proliferation, an anti-VZV specific antibody response and a human IFN-γ production were detected in these organoids.

Such steps forward will undoubtedly help to better recapitulate the cellular complexity of TME and will make it possible to study the genesis and immune function of TLS. Thus, a lot of efforts should be now devoted to the development of more complex 3D culture systems where i) additional cell partners impacting the cross-talk between cancer cells and the immune system are included, ii) hypoxia is better controlled, and iii) the quality of tumor biopsies is improved. In the long-term, interconnected organoids allowing the study of the interplay between primary tumor and metastases and immune cell trafficking should help to set-up *in vitro* model of TLS neogenesis (**Figure 3B**).

ARTIFICIAL INTELLIGENCE, A VALUABLE TOOL FOR FUNDAMENTAL AND CLINICAL RESEARCH ON TLS

Deep learning has revolutionized many machine learning tasks based on machine learning in recent years such as image and video classification, speech and natural language recognition. The complexity of graphical data has imposed significant challenges on existing machine learning algorithms. In the 1950s, a symbolic Artificial Intelligence (AI) program based on mathematical symbols was developed to represent objects and their relationship. However, a number of problems were encountered, in particular about the fluidity of the management of the symbols recognized by the machine, often too complex to be integrated in the early development of AI. New AI tools were therefore created to process signals based on a rationally-designed path through a network of simulated nodes, true counterparts of the synaptic junctions existing between human neurons. Thus, today, symbolic AI has been largely replaced by IA relying on "artificial neural networks" and "deep learning". Recently, many studies on the extension of deep learning approaches to graphical data have emerged, especially in the medical field (109).

Deep Learning and Medicine

The first deep learning studies focused on the detection or classification of radiological or clinical lesions, and reported performance superior to conventional techniques (110). To date, applying deep learning-based medical image analysis to

Computer-Assisted Diagnosis (CAD) could provide decision support to clinicians and improve the accuracy and efficiency of various processes for diagnosis and treatment (109). New tools are emerging, such as those allowing the detection of retinopathies in diabetic patients (111), enabling the analysis of images obtained by magnetic resonance imaging (MRI) of the knee (112) or in the detection of melanoma (113), as well as to the automated detection of SCC of the oral cavity (114).

Histopathology has also benefited from these technical advances. Many works have focused on the recognition of histology slides by AI mostly on the recognition of immunohistochemical stainings but also include research on the identification of cancerous invasion-related markers in many cancers (115, 116). An interesting research work currently underway is to predict the response to anti-PD-L1 antibody treatment in melanoma and lung cancer by analyzing tumor mutational burden, MSI, and PD-L1 expression using histopathological images (117).

Deep Learning and TLS

Currently, a computer tool can recognize and quantify inflammatory lymphocytic infiltrates by analyzing microscope images with reproducible measurements of the spatial composition in lymphocytes. Such a computer-based reading has been developed for analyzing renal allograft biopsies, breast cancer biopsies, and lung tissue from patients with cystic fibrosis (118). It makes it possible to quantify and spatially evaluate TLS on tissue section i.e., from dense lymphoid aggregates after hematoxylin/eosin counterstaining to multiplex staining such as CD3, CD20, DC-Lamp, CD21, and PNAd co-staining (**Figure 4**). Thanks to the identification of regions of interest, the automated detection of cells of interest within the tumor stroma (in addition to the detection of stained tumor cells and/or recognition of less dense/cohesive tissue), and the classification of immune cell clusters according to their degree of organization, the computer system generates a grading of TLS for each of these diseases (118). It has also been possible to establish multi-class segmentation of tissues in breast cancer and grading of TLS in lung cancers (119).

CONCLUSIONS AND PERSPECTIVE

The growing number of articles focusing on the study of TLS biology has led to a major advance in our knowledge of this singular immunological entity that arises in undedicated organs

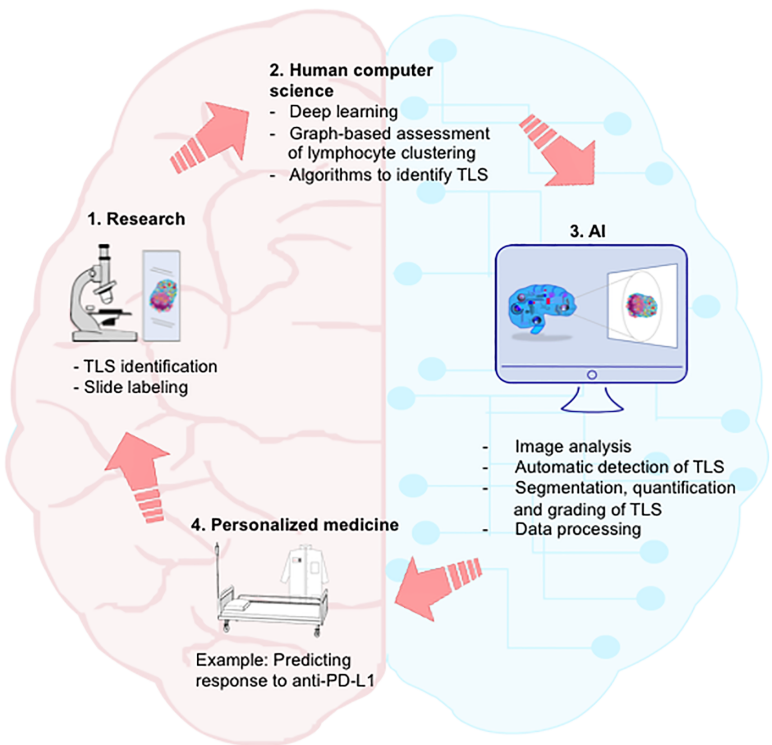

FIGURE 4 | Integration of AI in the continuum of medicine. Streamlined dialogue between human and computer may accelerate path from laboratory discovery on TLS to clinical application and personalized medicine. Step 1. Researchers and clinicians identify TLS on labeled slides. Step 2. Computer scientists develop algorithms allowing machine-learning for automatic identification of TLS. Step 3. AI performs segmentation, quantification and grading of TLS, as well as big data processing. Step 4. By integrating computerized medical data into the therapeutic decision, anticipation of clinical responses (in particular following anti-PD-L1 therapy) and development of personalized medicine would become possible. AI, artificial intelligence.

upon inflammation triggered by pathological events, including cancers.

First, apparent discrepancies in some studies highlight the importance of standardizing certain procedures and methods for the identification and quantification of TLS. Assessing several immune parameters for the determination of TLS is time-consuming and not compatible with clinical practice, highlighting the need to simplify and/or automatize their evaluation in the perspective of a TLS routine clinical protocol, in particular in human cancers. Emerging techniques of AI will certainly make it possible to standardize the recognition of TLS, leading to a reproducible reading and will therefore constitute a valuable tool for translational research and clinical practices.

It will be also necessary to find alternative identification methods that are less invasive in order to investigate TLS status, for example in cancer patients under treatment or in non-operable patients. A number of methods are currently being tested using peripheral blood or other body fluids to detect and quantify biomarkers predictive of TLS presence. In HNSCC, the analysis of saliva that is an easy-to-collect, non-invasive and easily stored fluid, could offer an alternative to facilitate the examination of tumor-associated TLS. Interestingly, this approach has already been investigated in Gougerot-Sjögren syndrome where pregnancy-associated plasma protein A (PAPPA), thrombospondin 1 and YY peptide were associated with the presence of ectopic GC that might be TLS (120).

Second, the very in-depth characterization of the cellular composition of TLS in most solid tumors has shown an heterogeneity in term of TLS organization, suggesting that the TME and tumor cells may control their neogenesis program. Deciphering the TME allowing – or not - the formation of TLS may represent a new opportunity to identify TLS inducer(s) and TLS blocker(s) that can have a direct clinical application in cancers and autoimmune diseases, respectively.

In addition, it has been shown that some cancer types are more prone to develop immature TLS (e.g. ccRCC) or mature TLS (e.g. NSCLC), whereas others exhibit mix developmental stages. Interestingly, this observation seems to correlate with response to immunotherapy. Because mature TLS are a key site where the generation of anti-tumor immunity can take place in the tumor bed, these ectopic lymphoid organizations play a dual role. On one hand, they are a powerful prognostic biomarker in almost all human cancers and on the other hand, they can predict response to ICP inhibitors (i.e., antibodies against CTLA-4, PD-1, PD-L1, or a combination). One can hypothesize that ICP blockade can reactivate protective immune responses elicited in TLS. Further investigation will be required to decipher the cellular and molecular mechanisms underlying ICP blockade efficiency as well as to extend studies to other targeted therapies. One way to understand why some patients are responders and others non-responders/progressors to ICP blockade could be through the use of spheroids and/or organoids to better recapitulate the cellular complexity of the TME and to predict the best ICP response for each cancer patient.

In conclusion, TLS are certainly an attractive target for researchers and clinicians to improve cancer patient outcome. TLS could become a new predictive biomarker of tumor development, and the capability of tumor-infiltrating immune cells to organize into TLS could be assigned as a new hallmark of cancer progression, a concept initially described by Hanahan and Weinberg (121).

AUTHOR CONTRIBUTIONS

CD, JR, CR, J-LT, VM, and M-CD-N wrote the initial draft. MP performed the multiplex staining. All authors contributed to the article and approved the submitted version.

FUNDING

This work was supported by the "Institut National de la Santé et de la Recherche Médicale (INSERM), Sorbonne Université, Fondation ARC pour la Recherche sur le Cancer (GL: PJA2017, M-CD-N: PJA20181207895 and PGA12019120000978, J-LT: PJA20191209801), the Institut National du Cancer (INCa-DGOS_10888, M-CD-N), Cancéropôle Ile de France (2021-1-EMERG-47-INSERM 6-1), AstraZeneca (Gaithersburg, USA, n° 11796A10, M-CD-N), Janssen Horizon (CT7088), and Sanofi innovation Awards Europe 2020 (201014). CR is supported by a grant from "La Ligue contre le Cancer". MP is supported by a grant from Sanofi. CD is financially supported by Bordeaux University Hospital and Bordeaux University.

ACKNOWLEDGMENTS

We are grateful to all our colleagues who have participated to the studies on and characterization of TLS over the past 15 years and to the members of the team "Immune Microenvironment and Immunotherapy" (Cimi-Paris) involved in the research programs focusing on tumor-associated TLS. We also thank all clinicians for their invaluable contribution to these studies and we thank warmly all the patients who agreed to participate to our studies.

REFERENCES

1. Dieu-Nosjean M-C, Antoine M, Danel C, Heudes D, Wislez M, Poulot V, et al. Long-Term Survival for Patients With non-Small-Cell Lung Cancer With Intratumoral Lymphoid Structures. *J Clin Oncol* (2008) 26:4410–17. doi: 10.1200/JCO.2007.15.0284
2. Gago da Graça C, van Baarsen LGM, Mebius RE. Tertiary Lymphoid Structures: Diversity in Their Development, Composition, and Role. *J Immunol* (2021) 206:273–81. doi: 10.4049/jimmunol.2000873
3. Goc J, Germain C, Vo-Bourgais TKD, Lupo A, Klein C, Knockaert S, et al. Dendritic Cells in Tumor-Associated Tertiary Lymphoid Structures Signal a Th1 Cytotoxic Immune Contexture and License the Positive Prognostic

Value of Infiltrating CD8+ T Cells. *Cancer Res* (2014) 74:705–15. doi: 10.1158/0008-5472.CAN-13-1342
4. Germain C, Gnjatic S, Tamzalit F, Knockaert S, Remark R, Goc J, et al. Presence of B Cells in Tertiary Lymphoid Structures Is Associated With a Protective Immunity in Patients With Lung Cancer. *Am J Respir Crit Care Med* (2014) 189:832–44. doi: 10.1164/rccm.201309-1611OC
5. Cabrita R, Lauss M, Sanna A, Donia M, Skaarup Larsen M, Mitra S, et al. Tertiary Lymphoid Structures Improve Immunotherapy and Survival in Melanoma. *Nature* (2020) 577:561–5. doi: 10.1038/s41586-019-1914-8
6. Helmink BA, Reddy SM, Gao J, Zhang S, Basar R, Thakur R, et al. B Cells and Tertiary Lymphoid Structures Promote Immunotherapy Response. *Nature* (2020) 577:549–55. doi: 10.1038/s41586-019-1922-8
7. Petitprez F, de Reyniès A, Keung EZ, Chen TW-W, Sun C-M, Calderaro J, et al. B Cells are Associated With Survival and Immunotherapy Response in Sarcoma. *Nature* (2020) 577:556–60. doi: 10.1038/s41586-019-1906-8
8. Mishima S, Taniguchi H, Akagi K, Baba E, Fujiwara Y, Hirasawa A, et al. Japan Society of Clinical Oncology Provisional Clinical Opinion for the Diagnosis and Use of Immunotherapy in Patients With Deficient DNA Mismatch Repair Tumors, Cooperated by Japanese Society of Medical Oncology, First Edition. *Int J Clin Oncol* (2020) 25:217–39. doi: 10.1007/s10147-019-01498-8
9. Postow MA, Sidlow R, Hellmann MD. Immune-Related Adverse Events Associated With Immune Checkpoint Blockade. *N Engl J Med* (2018) 378:158–68. doi: 10.1056/NEJMra1703481
10. Klein C, Devi-Marulkar P, Dieu-Nosjean M-C, Germain C. Development of Tools for the Selective Visualization and Quantification of TLS-Immune Cells on Tissue Sections. *Methods Mol Biol* (2018) 1845:47–69. doi: 10.1007/978-1-4939-8709-2_4
11. Dieu-Nosjean M-C. Tumor-Associated Lymphoid Structures: A Cancer Biomarker and a Target for Next-Generation Immunotherapy. In: A. Birbrair A, editor. *Tumor Microenvironment Tumor Microenvironment, Novel Concepts*, Springer Nature series. Springer (2021).
12. Li K, Guo Q, Zhang X, Dong X, Liu W, Zhang A, et al. Oral Cancer-Associated Tertiary Lymphoid Structures: Gene Expression Profile and Prognostic Value. *Clin Exp Immunol* (2020) 199:172–81. doi: 10.1111/cei.13389
13. Liu Z-H, Wang M-H, Ren H-J, Qu W, Sun L-M, Zhang Q-F, et al. Interleukin 7 Signaling Prevents Apoptosis by Regulating Bcl-2 and Bax *via* the P53 Pathway in Human Non-Small Cell Lung Cancer Cells. *Int J Clin Exp Pathol* (2014) 7:870–81.
14. Finkin S, Yuan D, Stein I, Taniguchi K, Weber A, Unger K, et al. Ectopic Lymphoid Structures Function as Microniches for Tumor Progenitor Cells in Hepatocellular Carcinoma. *Nat Immunol* (2015) 16:1235–44. doi: 10.1038/ni.3290
15. Calderaro J, Petitprez F, Becht E, Laurent A, Hirsch TZ, Rousseau B, et al. Intra-Tumoral Tertiary Lymphoid Structures are Associated With a Low Risk of Early Recurrence of Hepatocellular Carcinoma. *J Hepatol* (2019) 70:58–65. doi: 10.1016/j.jhep.2018.09.003
16. Gobert M, Treilleux I, Bendriss-Vermare N, Bachelot T, Goddard-Leon S, Arfi V, et al. Regulatory T Cells Recruited Through CCL22/CCR4 are Selectively Activated in Lymphoid Infiltrates Surrounding Primary Breast Tumors and Lead to an Adverse Clinical Outcome. *Cancer Res* (2009) 69:2000–9. doi: 10.1158/0008-5472.CAN-08-2360
17. Gu-Trantien C, Migliori E, Buisseret L, de Wind A, Brohée S, Garaud S, et al. CXCL13-Producing TFH Cells Link Immune Suppression and Adaptive Memory in Human Breast Cancer. *JCI Insight* (2017) 2(11):e91487. doi: 10.1172/jci.insight.91487
18. García-Hernández M de la L, Uribe-Uribe NO, Espinosa-González R, Kast WM, Khader SA, Rangel-Moreno J. A Unique Cellular and Molecular Microenvironment Is Present in Tertiary Lymphoid Organs of Patients With Spontaneous Prostate Cancer Regression. *Front Immunol* (2017) 8:563. doi: 10.3389/fimmu.2017.00563
19. Nishihira M, Nakazato Y, Maeda S, Inoue T, Araki O, Karube Y, et al. Impact of Tumor Infiltrating Lymphocytes and Lymphoid Follicle Formation on Patient Survival Following Surgery for Lung Squamous Cell Carcinoma. *Thorac Cancer* (2019) 10:219–25. doi: 10.1111/1759-7714.12935
20. Schweiger T, Berghoff AS, Glogner C, Glueck O, Rajky O, Traxler D, et al. Tumor-Infiltrating Lymphocyte Subsets and Tertiary Lymphoid Structures in Pulmonary Metastases From Colorectal Cancer. *Clin Exp Metastasis* (2016) 33:727–39. doi: 10.1007/s10585-016-9813-y
21. Meylan M, Petitprez F, Lacroix L, Tommaso LD, Roncalli M, Bougoüin A, et al. Early Hepatic Lesions Display Immature Tertiary Lymphoid Structures and Show Elevated Expression of Immune Inhibitory and Immunosuppressive Molecules. *Clin Cancer Res* (2020) 26:4381–9. doi: 10.1158/1078-0432.CCR-19-2929
22. Posch F, Silina K, Leibl S, Mündlein A, Moch H, Siebenhüner A, et al. Maturation of Tertiary Lymphoid Structures and Recurrence of Stage II and III Colorectal Cancer. *OncoImmunology* (2018) 7:e1378844. doi: 10.1080/2162402X.2017.1378844
23. Sofopoulos M, Fortis SP, Vaxevanis CK, Sotiriadou NN, Arnogiannaki N, Ardavanis A, et al. The Prognostic Significance of Peritumoral Tertiary Lymphoid Structures in Breast Cancer. *Cancer Immunol Immunother* (2019) 68:1733–45. doi: 10.1007/s00262-019-02407-8
24. Cipponi A, Mercier M, Seremet T, Baurain J-F, Théate I, van den Oord J, et al. Neogenesis of Lymphoid Structures and Antibody Responses Occur in Human Melanoma Metastases. *Cancer Res* (2012) 72:3997–4007. doi: 10.1158/0008-5472.CAN-12-1377
25. Remark R, Alifano M, Cremer I, Lupo A, Dieu-Nosjean M-C, Riquet M, et al. Characteristics and Clinical Impacts of the Immune Environments in Colorectal and Renal Cell Carcinoma Lung Metastases: Influence of Tumor Origin. *Clin Cancer Res* (2013) 19:4079–91. doi: 10.1158/1078-0432.CCR-12-3847
26. Song IH, Heo S-H, Bang WS, Park HS, Park IA, Kim Y-A, et al. Predictive Value of Tertiary Lymphoid Structures Assessed by High Endothelial Venule Counts in the Neoadjuvant Setting of Triple-Negative Breast Cancer. *Cancer Res Treat* (2017) 49:399–407. doi: 10.4143/crt.2016.215
27. Lee HJ, Kim JY, Park IA, Song IH, Yu JH, Ahn J-H, et al. Prognostic Significance of Tumor-Infiltrating Lymphocytes and the Tertiary Lymphoid Structures in HER2-Positive Breast Cancer Treated With Adjuvant Trastuzumab. *Am J Clin Pathol* (2015) 144:278–88. doi: 10.1309/AJCPIXUYDVZ0RZ3G
28. Lin Q, Tao P, Wang J, Ma L, Jiang Q, Li J, et al. Tumor-Associated Tertiary Lymphoid Structure Predicts Postoperative Outcomes in Patients With Primary Gastrointestinal Stromal Tumors. *OncoImmunology* (2020) 9:1747339. doi: 10.1080/2162402X.2020.1747339
29. van Dijk N, Gil-Jimenez A, Silina K, Hendricksen K, Smit LA, de Feijter JM, et al. Preoperative Ipilimumab Plus Nivolumab in Locoregionally Advanced Urothelial Cancer: The NABUCCO Trial. *Nat Med* (2020) 26:1839–44. doi: 10.1038/s41591-020-1085-z
30. Siliņa K, Soltermann A, Attar FM, Casanova R, Uckeley ZM, Thut H, et al. Germinal Centers Determine the Prognostic Relevance of Tertiary Lymphoid Structures and Are Impaired by Corticosteroids in Lung Squamous Cell Carcinoma. *Cancer Res* (2018) 78:1308–20. doi: 10.1158/0008-5472.CAN-17-1987
31. Morcrette G, Hirsch TZ, Badour E, Pilet J, Caruso S, Calderaro J, et al. APC Germline Hepatoblastomas Demonstrate Cisplatin-Induced Intratumor Tertiary Lymphoid Structures. *OncoImmunology* (2019) 8:e1583547. doi: 10.1080/2162402X.2019.1583547
32. Cottrell TR, Thompson ED, Forde PM, Stein JE, Duffield AS, Anagnostou V, et al. Pathologic Features of Response to Neoadjuvant Anti-PD-1 in Resected non-Small-Cell Lung Carcinoma: A Proposal for Quantitative Immune-Related Pathologic Response Criteria (irPRC). *Ann Oncol* (2018) 29:1853–60. doi: 10.1093/annonc/mdy218
33. Sánchez-Alonso S, Setti-Jerez G, Arroyo M, Hernández T, Martos MI, Sánchez-Torres JM, et al. A New Role for Circulating T Follicular Helper Cells in Humoral Response to Anti-PD-1 Therapy. *J Immunother Cancer* (2020) 8(2):e001187. doi: 10.1136/jitc-2020-001187
34. Maldonado L, Teague JE, Morrow MP, Jotova I, Wu TC, Wang C, et al. Intramuscular Therapeutic Vaccination Targeting HPV16 Induces T Cell Responses That Localize in Mucosal Lesions. *Sci Transl Med* (2014) 6:221ra13. doi: 10.1126/scitranslmed.3007323
35. Lutz ER, Wu AA, Bigelow E, Sharma R, Mo G, Soares K, et al. Immunotherapy Converts Nonimmunogenic Pancreatic Tumors Into Immunogenic Foci of Immune Regulation. *Cancer Immunol Res* (2014) 2:616–31. doi: 10.1158/2326-6066.CIR-14-0027

36. Solinas C, Marcoux D, Garaud S, Vitória JR, Van den Eynden G, de Wind A, et al. BRCA Gene Mutations do Not Shape the Extent and Organization of Tumor Infiltrating Lymphocytes in Triple Negative Breast Cancer. *Cancer Lett* (2019) 450:88–97. doi: 10.1016/j.canlet.2019.02.027
37. Kroeger DR, Milne K, Nelson BH. Tumor-Infiltrating Plasma Cells Are Associated With Tertiary Lymphoid Structures, Cytolytic T-Cell Responses, and Superior Prognosis in Ovarian Cancer. *Clin Cancer Res* (2016) 22:3005–15. doi: 10.1158/1078-0432.CCR-15-2762
38. Lin Z, Huang L, Li S, Gu J, Cui X, Zhou Y. Pan-Cancer Analysis of Genomic Properties and Clinical Outcome Associated With Tumor Tertiary Lymphoid Structure. *Sci Rep* (2020) 10:21530. doi: 10.1038/s41598-020-78560-3
39. Workel HH, Lubbers JM, Arnold R, Prins TM, Vlies P, Lange K D, et al. A Transcriptionally Distinct CXCL13+CD103+CD8+ T-Cell Population Is Associated With B-Cell Recruitment and Neoantigen Load in Human Cancer. *Cancer Immunol Res* (2019) 7:784–96. doi: 10.1158/2326-6066.CIR-18-0517
40. Tokunaga R, Nakagawa S, Sakamoto Y, Nakamura K, Naseem M, Izumi D, et al. 12-Chemokine Signature, a Predictor of Tumor Recurrence in Colorectal Cancer. *Int J Cancer* (2020) 147:532–41. doi: 10.1002/ijc.32982
41. Biton J, Mansuet-Lupo A, Pécuchet N, Alifano M, Ouakrim H, Arrondeau J, et al. TP53, STK11, and EGFR Mutations Predict Tumor Immune Profile and the Response to Anti–PD-1 in Lung Adenocarcinoma. *Clin Cancer Res* (2018) 24:5710–23. doi: 10.1158/1078-0432.CCR-18-0163
42. Mansuet-Lupo A, Alifano M, Pécuchet N, Biton J, Becht E, Goc J, et al. Intratumoral Immune Cell Densities Are Associated With Lung Adenocarcinoma Gene Alterations. *Am J Respir Crit Care Med* (2016) 194:1403–12. doi: 10.1164/rccm.201510-2031OC
43. Liu X, Tsang JYS, Hlaing T, Hu J, Ni Y-B, Chan SK, et al. Distinct Tertiary Lymphoid Structure Associations and Their Prognostic Relevance in HER2 Positive and Negative Breast Cancers. *Oncol* (2017) 22:1316–24. doi: 10.1634/theoncologist.2017-0029
44. Solinas C, Carbognin L, De Silva P, Criscitiello C, Lambertini M. Tumor-Infiltrating Lymphocytes in Breast Cancer According to Tumor Subtype: Current State of the Art. *Breast* (2017) 35:142–50. doi: 10.1016/j.breast.2017.07.005
45. Caro GD, Bergomas F, Grizzi F, Doni A, Bianchi P, Malesci A, et al. Occurrence of Tertiary Lymphoid Tissue Is Associated With T-Cell Infiltration and Predicts Better Prognosis in Early-Stage Colorectal Cancers. *Clin Cancer Res* (2014) 20:2147–58. doi: 10.1158/1078-0432.CCR-13-2590
46. Li Q, Liu X, Wang D, Wang Y, Lu H, Wen S, et al. Prognostic Value of Tertiary Lymphoid Structure and Tumour Infiltrating Lymphocytes in Oral Squamous Cell Carcinoma. *Int J Oral Sci* (2020) 12(1):24. doi: 10.1038/s41368-020-00092-3
47. Strickland KC, Howitt BE, Shukla SA, Rodig S, Ritterhouse LL, Liu JF, et al. Association and Prognostic Significance of BRCA1/2-Mutation Status With Neoantigen Load, Number of Tumor-Infiltrating Lymphocytes and Expression of PD-1/PD-L1 in High Grade Serous Ovarian Cancer. *Oncotarget* (2016) 7:13587–98. doi: 10.18632/oncotarget.7277
48. Kim I, Sanchez K, McArthur HL, Page D. Immunotherapy in Triple-Negative Breast Cancer: Present and Future. *Curr Breast Cancer Rep* (2019) 11:259–71. doi: 10.1007/s12609-019-00345-z
49. Le DT, Durham JN, Smith KN, Wang H, Bartlett BR, Aulakh LK, et al. Mismatch Repair Deficiency Predicts Response of Solid Tumors to PD-1 Blockade. *Science* (2017) 357:409–13. doi: 10.1126/science.aan6733
50. Alexander J, Watanabe T, Wu TT, Rashid A, Li S, Hamilton SR. Histopathological Identification of Colon Cancer With Microsatellite Instability. *Am J Pathol* (2001) 158:527–35. doi: 10.1016/S0002-9440(10)63994-6
51. Hellmann MD, Ciuleanu T-E, Pluzanski A, Lee JS, Otterson GA, Audigier-Valette C, et al. Nivolumab Plus Ipilimumab in Lung Cancer With a High Tumor Mutational Burden. *New Engl J Med* (2018) 378:2093–104. doi: 10.1056/NEJMoa1801946
52. Herbst RS, Garon EB, Kim D-W, Cho BC, Perez-Gracia JL, Han J-Y, et al. Long-Term Outcomes and Retreatment Among Patients With Previously Treated, Programmed Death-Ligand 1–Positive, Advanced Non–Small-Cell Lung Cancer in the KEYNOTE-010 Study. *J Clin Oncol* (2020) 38:1580–90. doi: 10.1200/JCO.19.02446
53. Skoulidis F, Goldberg ME, Greenawalt DM, Hellmann MD, Awad MM, Gainor JF, et al. STK11/LKB1 Mutations and PD-1 Inhibitor Resistance in KRAS-Mutant Lung Adenocarcinoma. *Cancer Discovery* (2018) 8:822–35. doi: 10.1158/2159-8290.CD-18-0099
54. Domeier PP, Schell SL, Rahman ZSM. Spontaneous Germinal Centers and Autoimmunity. *Autoimmunity* (2017) 50:4–18. doi: 10.1080/08916934.2017.1280671
55. Luo S, Zhu R, Yu T, Fan H, Hu Y, Mohanta SK, et al. Chronic Inflammation: A Common Promoter in Tertiary Lymphoid Organ Neogenesis. *Front Immunol* (2019) 10:2938. doi: 10.3389/fimmu.2019.02938
56. Chudakov DB, Ryasantsev DY, Tsaregorotseva DS, Kotsareva OD, Fattakhova GV, Svirshchevskaya EV. Tertiary Lymphoid Structure Related B-Cell IgE Isotype Switching and Secondary Lymphoid Organ Linked IgE Production in Mouse Allergy Model. *BMC Immunol* (2020) 21(1):45. doi: 10.1186/s12865-020-00376-7
57. Dorraji SE, Kanapathippillai P, Hovd A-MK, Stenersrød MR, Horvei KD, Ursvik A, et al. Kidney Tertiary Lymphoid Structures in Lupus Nephritis Develop Into Large Interconnected Networks and Resemble Lymph Nodes in Gene Signature. *Am J Pathol* (2020) 190:2203–25. doi: 10.1016/j.ajpath.2020.07.015
58. Pipi E, Nayar S, Gardner DH, Colafrancesco S, Smith C, Barone F. Tertiary Lymphoid Structures: Autoimmunity Goes Local. *Front Immunol* (2018) 9:1952. doi: 10.3389/fimmu.2018.01952
59. Silva-Sanchez A, Randall TD, Meza-Perez S. "Tertiary Lymphoid Structures Among the World of Noncanonical Ectopic Lymphoid Organizations,". In: M-C Dieu-Nosjean, editor. *Tertiary Lymphoid Structures: Methods and Protocols Methods in Molecular Biology*. New York, NY: Springer. (2018) p. 1–15. doi: 10.1007/978-1-4939-8709-2_1 (2018)
60. Gassen RB, Fazolo T, Freitas DN de, Borges TJ, Lima K, Antunes GL, et al. IL-21 Treatment Recovers Follicular Helper T Cells and Neutralizing Antibody Production in Respiratory Syncytial Virus Infection. *Immunol Cell Biol* (2021) 99(3):309–22. doi: 10.1111/imcb.12418
61. Naessens T, Morias Y, Hamrud E, Gehrmann U, Budida R, Mattsson J, et al. Human Lung Conventional Dendritic Cells Orchestrate Lymphoid Neogenesis During Chronic Obstructive Pulmonary Disease. *Am J Respir Crit Care Med* (2020) 202:535–48. doi: 10.1164/rccm.201906-1123OC
62. Regard L, Martin C, Teillaud J-L, Lafoeste H, Vicaire H, Ladjemi MZ, et al. Effective Control of S. Aureus Lung Infection Despite Tertiary Lymphoid Structures Disorganisation. *Eur Respir J* (2020) 57(4):2000768. doi: 10.1183/13993003.00768-2020
63. Weitbrecht L, Berchtold D, Zhang T, Jagdmann S, Dames C, Winek K, et al. CD4+ T Cells Promote Delayed B Cell Responses in the Ischemic Brain After Experimental Stroke. *Brain Behav Immun* (2021) 91:601–14. doi: 10.1016/j.bbi.2020.09.029
64. Richmond BW, Mansouri S, Serezani A, Novitskiy S, Blackburn JB, Du R-H, et al. Monocyte-Derived Dendritic Cells Link Localized Secretory IgA Deficiency to Adaptive Immune Activation in COPD. *Mucosal Immunol* (2021) 14(2):431–42. doi: 10.1038/s41385-020-00344-9
65. Hertz D, Dibbern J, Eggers L, von Borstel L, Schneider BE. Increased Male Susceptibility to Mycobacterium Tuberculosis Infection is Associated With Smaller B Cell Follicles in the Lungs. *Sci Rep* (2020) 10:5142. doi: 10.1038/s41598-020-61503-3
66. Teillaud J-L, Regard L, Martin C, Sibéril S, Burgel P-R. Exploring the Role of Tertiary Lymphoid Structures Using a Mouse Model of Bacteria-Infected Lungs. *Methods Mol Biol* (2018) 1845:223–39. doi: 10.1007/978-1-4939-8709-2_13
67. Bao Q, Guo X-X, Cao C, Li Q-Y, Sun L, Ye X-Y, et al. Presence of Tertiary Lymphoid Organ in Nasal Inverted Papilloma Is Correlated With Eosinophil Infiltration and Local Immunoglobulin Production. *Int Arch Allergy Immunol* (2021) 182(4):350–9. doi: 10.1159/000510966
68. Dibbern J, Eggers L, Schneider BE. Sex Differences in the C57BL/6 Model of Mycobacterium Tuberculosis Infection. *Sci Rep* (2017) 7:10957. doi: 10.1038/s41598-017-11438-z
69. Khader SA, Guglani L, Rangel-Moreno J, Gopal R, Junecko BAF, Fountain JJ, et al. IL-23 is Required for Long-Term Control of Mycobacterium Tuberculosis and B Cell Follicle Formation in the Infected Lung. *J Immunol* (2011) 187:5402–7. doi: 10.4049/jimmunol.1101377
70. Hidalgo Y, Núñez S, Fuenzalida MJ, Flores-Santibáñez F, Sáez PJ, Dorner J, et al. Thymic B Cells Promote Germinal Center-Like Structures and the Expansion of Follicular Helper T Cells in Lupus-Prone Mice. *Front Immunol* (2020) 11:696. doi: 10.3389/fimmu.2020.00696

71. Yu S, Medling B, Yagita H, Braley-Mullen H. Characteristics of Inflammatory Cells in Spontaneous Autoimmune Thyroiditis of NOD.H-2h4 Mice. *J Autoimmun* (2001) 16:37–46. doi: 10.1006/jaut.2000.0458
72. Schropp V, Rohde J, Rovituso DM, Jabari S, Bharti R, Kuerten S. Contribution of LTi and TH17 Cells to B Cell Aggregate Formation in the Central Nervous System in a Mouse Model of Multiple Sclerosis. *J Neuroinflamm* (2019) 16:111. doi: 10.1186/s12974-019-1500-x
73. Alves Costa Silva C, Facchinetti F, Routy B, Derosa L. New Pathways in Immune Stimulation: Targeting OX40. *ESMO Open* (2020) 5:e000573. doi: 10.1136/esmoopen-2019-000573
74. Aloisi F, Pujol-Borrell R. Lymphoid Neogenesis in Chronic Inflammatory Diseases. *Nat Rev Immunol* (2006) 6:205–17. doi: 10.1038/nri1786
75. Cupedo T, Mebius RE. Role of Chemokines in the Development of Secondary and Tertiary Lymphoid Tissues. *Semin Immunol* (2003) 15:243–8. doi: 10.1016/j.smim.2003.08.002
76. Jones GW, Hill DG, Jones SA. Understanding Immune Cells in Tertiary Lymphoid Organ Development: It Is All Starting to Come Together. *Front Immunol* (2016) 7:401. doi: 10.3389/fimmu.2016.00401
77. Luo R, Cheng Y, Chang D, Liu T, Liu L, Pei G, et al. Tertiary Lymphoid Organs are Associated With the Progression of Kidney Damage and Regulated by Interleukin-17A. *Theranostics* (2021) 11:117–31. doi: 10.7150/thno.48624
78. Jingjing C, Jiacheng D, Wenduo G, Zhichao N, Yuanyuan L, Yogesh K, et al. Impact of Local Alloimmunity and Recipient Cells in Transplant Arteriosclerosis. *Circ Res* (2020) 127:974–93. doi: 10.1161/CIRCRESAHA.119.316470
79. Fernandez Dawn M, Chiara G. Mapping Transplant Arteriosclerosis Cell-By-Cell. *Circ Res* (2020) 127:994–6. doi: 10.1161/CIRCRESAHA.120.317907
80. Badillo FEG, Tegou FZ, Abreu MM, Masina R, Sha D, Najjar M, et al. CCL21 Expression in β-Cells Induces Antigen-Expressing Stromal Cell Networks in the Pancreas and Prevents Autoimmune Diabetes in Mice. *Diabetes* (2019) 68:1990–2003. doi: 10.2337/db19-0239
81. Hynds RE, Frese KK, Pearce DR, Grönroos E, Dive C, Swanton C. Progress Towards non-Small-Cell Lung Cancer Models That Represent Clinical Evolutionary Trajectories. *Open Biol* (2021) 11:200247. doi: 10.1098/rsob.200247
82. Bock C, Boutros M, Camp JG, Clarke L, Clevers H, Knoblich JA, et al. The Organoid Cell Atlas. *Nat Biotechnol* (2021) 39:13–7. doi: 10.1038/s41587-020-00762-x
83. Banks TA, Rouse BT, Kerley MK, Blair PJ, Godfrey VL, Kuklin NA, et al. Lymphotoxin-Alpha-Deficient Mice. Effects on Secondary Lymphoid Organ Development and Humoral Immune Responsiveness. *J Immunol* (1995) 155:1685–93.
84. Koni PA, Sacca R, Lawton P, Browning JL, Ruddle NH, Flavell RA. Distinct Roles in Lymphoid Organogenesis for Lymphotoxins α and β Revealed in Lymphotoxin β–Deficient Mice. *Immunity* (1997) 6:491–500. doi: 10.1016/S1074-7613(00)80292-7
85. Schrama D, thor Straten P, Fischer WH, McLellan AD, Bröcker E-B, Reisfeld RA, et al. Targeting of Lymphotoxin-α to the Tumor Elicits an Efficient Immune Response Associated With Induction of Peripheral Lymphoid-Like Tissue. *Immunity* (2001) 14:111–21. doi: 10.1016/S1074-7613(01)00094-2
86. Schrama D, Voigt H, Eggert AO, Xiang R, Zhou H, Schumacher TNM, et al. Immunological Tumor Destruction in a Murine Melanoma Model by Targeted LTalpha Independent of Secondary Lymphoid Tissue. *Cancer Immunol Immunother* (2008) 57:85–95. doi: 10.1007/s00262-007-0352-x
87. Lukashev M, LePage D, Wilson C, Bailly V, Garber E, Lukashin A, et al. Targeting the Lymphotoxin-Beta Receptor With Agonist Antibodies as a Potential Cancer Therapy. *Cancer Res* (2006) 66:9617–24. doi: 10.1158/0008-5472.CAN-06-0217
88. Tang H, Wang Y, Chlewicki LK, Zhang Y, Guo J, Liang W, et al. Facilitating T Cell Infiltration in Tumor Microenvironment Overcomes Resistance to PD-L1 Blockade. *Cancer Cell* (2016) 29:285–96. doi: 10.1016/j.ccell.2016.02.004
89. Johansson-Percival A, He B, Li Z-J, Kjellén A, Russell K, Li J, et al. *De Novo* Induction of Intratumoral Lymphoid Structures and Vessel Normalization Enhances Immunotherapy in Resistant Tumors. *Nat Immunol* (2017) 18:1207–17. doi: 10.1038/ni.3836
90. He B, Jabouille A, Steri V, Johansson-Percival A, Michael IP, Kotamraju VR, et al. Vascular Targeting of LIGHT Normalizes Blood Vessels in Primary Brain Cancer and Induces Intratumoural High Endothelial Venules. *J Pathol* (2018) 245:209–21. doi: 10.1002/path.5080
91. Turnquist HR, Lin X, Ashour AE, Hollingsworth MA, Singh RK, Talmadge JE, et al. CCL21 Induces Extensive Intratumoral Immune Cell Infiltration and Specific Anti-Tumor Cellular Immunity. *Int J Oncol* (2007) 30:631–9. doi: 10.3892/ijo.30.3.631
92. Weinstein AM, Chen L, Brzana EA, Patil PR, Taylor JL, Fabian KL, et al. Tbet and IL-36γ Cooperate in Therapeutic DC-Mediated Promotion of Ectopic Lymphoid Organogenesis in the Tumor Microenvironment. *OncoImmunology* (2017) 6:e1322238. doi: 10.1080/2162402X.2017.1322238
93. Zhu G, Nemoto S, Mailloux AW, Perez-Villarroel P, Nakagawa R, Falahat R, et al. Induction of Tertiary Lymphoid Structures With Antitumor Function by a Lymph Node-Derived Stromal Cell Line. *Front Immunol* (2018) 9:1609. doi: 10.3389/fimmu.2018.01609
94. Soares KC, Rucki AA, Kim V, Foley K, Solt S, Wolfgang CL, et al. TGF-β Blockade Depletes T Regulatory Cells From Metastatic Pancreatic Tumors in a Vaccine Dependent Manner. *Oncotarget* (2015) 6:43005–15. doi: 10.18632/oncotarget.5656
95. Allen E, Jabouille A, Rivera LB, Lodewijckx I, Missiaen R, Steri V, et al. Combined Antiangiogenic and Anti–PD-L1 Therapy Stimulates Tumor Immunity Through HEV Formation. *Sci Transl Med* (2017) 9(385): eaak9679. doi: 10.1126/scitranslmed.aak9679
96. Peske JD, Thompson ED, Gemta L, Baylis RA, Fu Y-X, Engelhard VH. Effector Lymphocyte-Induced Lymph Node-Like Vasculature Enables Naive T-Cell Entry Into Tumours and Enhanced Anti-Tumour Immunity. *Nat Commun* (2015) 6:1–15. doi: 10.1038/ncomms8114
97. Joshi NS, Akama-Garren EH, Lu Y, Lee D-Y, Chang GP, Li A, et al. Regulatory T Cells in Tumor-Associated Tertiary Lymphoid Structures Suppress Anti-Tumor T Cell Responses. *Immunity* (2015) 43:579–90. doi: 10.1016/j.immuni.2015.08.006
98. Colbeck EJ, Jones E, Hindley JP, Smart K, Schulz R, Browne M, et al. Treg Depletion Licenses T Cell–Driven HEV Neogenesis and Promotes Tumor Destruction. *Cancer Immunol Res* (2017) 5:1005–15. doi: 10.1158/2326-6066.CIR-17-0131
99. Yang S-C, Batra RK, Hillinger S, Reckamp KL, Strieter RM, Dubinett SM, et al. Intrapulmonary Administration of CCL21 Gene-Modified Dendritic Cells Reduces Tumor Burden in Spontaneous Murine Bronchoalveolar Cell Carcinoma. *Cancer Res* (2006) 66:3205–13. doi: 10.1158/0008-5472.CAN-05-3619
100. Connolly KA, Nader M, Joshi N. Investigating Tumor-Associated Tertiary Lymphoid Structures in Murine Lung Adenocarcinoma. *Methods Mol Biol* (2018) 1845:259–73. doi: 10.1007/978-1-4939-8709-2_15
101. Rodriguez AB, Engelhard VH. Insights Into Tumor-Associated Tertiary Lymphoid Structures: Novel Targets for Antitumor Immunity and Cancer Immunotherapy. *Cancer Immunol Res* (2020) 8:1338–45. doi: 10.1158/2326-6066.CIR-20-0432
102. Hill DG, Yu L, Gao H, Balic JJ, West A, Oshima H, et al. Hyperactive Gp130/STAT3-Driven Gastric Tumourigenesis Promotes Submucosal Tertiary Lymphoid Structure Development. *Int J Cancer* (2018) 143:167–78. doi: 10.1002/ijc.31298
103. Han K, Pierce SE, Li A, Spees K, Anderson GR, Seoane JA, et al. CRISPR Screens in Cancer Spheroids Identify 3D Growth-Specific Vulnerabilities. *Nature* (2020) 580:136–41. doi: 10.1038/s41586-020-2099-x
104. Boucherit N, Gorvel L, Olive D. 3d Tumor Models and Their Use for the Testing of Immunotherapies. *Front Immunol* (2020) 11:603640. doi: 10.3389/fimmu.2020.603640
105. Jenkins RW, Aref AR, Lizotte PH, Ivanova E, Stinson S, Zhou CW, et al. Ex Vivo Profiling of PD-1 Blockade Using Organotypic Tumor Spheroids. *Cancer Discovery* (2018) 8:196–215. doi: 10.1158/2159-8290.CD-17-0833
106. Dijkstra KK, Cattaneo CM, Weeber F, Chalabi M, van de Haar J, Fanchi LF, et al. Generation of Tumor-Reactive T Cells by Co-Culture of Peripheral Blood Lymphocytes and Tumor Organoids. *Cell* (2018) 174:1586–98. doi: 10.1016/j.cell.2018.07.009
107. Neal JT, Li X, Zhu J, Giangarra V, Grzeskowiak CL, Ju J, et al. Organoid Modeling of the Tumor Immune Microenvironment. *Cell* (2018) 175:1972–88. doi: 10.1016/j.cell.2018.11.021
108. Watanabe T, Kobayashi Y, Kawamoto H. Formation of Human Lymphoid Organoids and Their Immunological Function. *J Immunol* (2020) 204:145.49–9.
109. Chan ,HP, Samala RK, Hadjiiski ,LM, Zhou ,C. Deep Learning in Medical Image Analysis. *Adv Exp Med Biol* (2020) 1213:3–21. doi: 10.1007/978-3-030-33128-3_1

110. Nagendran M, Chen Y, Lovejoy CA, Gordon AC, Komorowski M, Harvey H, et al. Artificial Intelligence Versus Clinicians: Systematic Review of Design, Reporting Standards, and Claims of Deep Learning Studies. *BMJ* (2020) 368: m689. doi: 10.1136/bmj.m689
111. Gulshan V, Peng L, Coram M, Stumpe MC, Wu D, Narayanaswamy A, et al. Development and Validation of a Deep Learning Algorithm for Detection of Diabetic Retinopathy in Retinal Fundus Photographs. *JAMA* (2016) 316:2402–10. doi: 10.1001/jama.2016.17216
112. Bien N, Rajpurkar P, Ball RL, Irvin J, Park A, Jones E, et al. Deep-Learning-Assisted Diagnosis for Knee Magnetic Resonance Imaging: Development and Retrospective Validation of MRNet. *PloS Med* (2018) 15:e1002699. doi: 10.1371/journal.pmed.1002699
113. Esteva A, Kuprel B, Novoa RA, Ko J, Swetter SM, Blau HM, et al. Dermatologist-Level Classification of Skin Cancer With Deep Neural Networks. *Nature* (2017) 542:115–8. doi: 10.1038/nature21056
114. Fu Q, Chen Y, Li Z, Jing Q, Hu C, Liu H, et al. A Deep Learning Algorithm for Detection of Oral Cavity Squamous Cell Carcinoma From Photographic Images: A Retrospective Study. *EClinicalMedicine* (2020) 27:100558. doi: 10.1016/j.eclinm.2020.100558
115. Sultan AS, Elgharib MA, Tavares T, Jessri M, Basile JR. The Use of Artificial Intelligence, Machine Learning and Deep Learning in Oncologic Histopathology. *J Oral Pathol Med* (2020) 49:849–56. doi: 10.1111/jop.13042
116. Zhu W, Xie L, Han J, Guo X. The Application of Deep Learning in Cancer Prognosis Prediction. *Cancers (Basel)* (2020) 12(3):603. doi: 10.3390/cancers12030603
117. Hu J, Cui C, Yang W, Huang L, Yu R, Liu S, et al. Using Deep Learning to Predict Anti-PD-1 Response in Melanoma and Lung Cancer Patients From Histopathology Images. *Transl Oncol* (2020) 14(1):100921. doi: 10.1016/j.tranon.2020.100921
118. Schaadt NS, Schönmeyer R, Forestier G, Brieu N, Braubach P, Nekolla K, et al. Graph-Based Description of Tertiary Lymphoid Organs at Single-Cell Level. *PloS Comput Biol* (2020) 16:e1007385. doi: 10.1371/journal.pcbi.1007385
119. van Rijthoven M, Balkenhol M, Siliņa K, van der Laak J, Ciompi F. HookNet: Multi-Resolution Convolutional Neural Networks for Semantic Segmentation in Histopathology Whole-Slide Images. *Med Image Anal* (2021) 68:101890. doi: 10.1016/j.media.2020.101890
120. Delaleu N, Mydel P, Brun JG, Jonsson MV, Alimonti A, Jonsson R. Sjögren's Syndrome Patients With Ectopic Germinal Centers Present With a Distinct Salivary Proteome. *Rheumatology* (2016) 55:1127–37. doi: 10.1093/rheumatology/kew013
121. Hanahan D, Weinberg RA. Hallmarks of Cancer: The Next Generation. *Cell* (2011) 144:646–74. doi: 10.1016/j.cell.2011.02.013

Conflict of Interest: The authors declare that the research was conducted in the absence of any commercial or financial relationships that could be construed as a potential conflict of interest.

Copyright © 2021 Domblides, Rochefort, Riffard, Panouillot, Lescaille, Teillaud, Mateo and Dieu-Nosjean. This is an open-access article distributed under the terms of the Creative Commons Attribution License (CC BY). The use, distribution or reproduction in other forums is permitted, provided the original author(s) and the copyright owner(s) are credited and that the original publication in this journal is cited, in accordance with accepted academic practice. No use, distribution or reproduction is permitted which does not comply with these terms.

frontiers in Immunology

MINI REVIEW
published: 15 July 2021
doi: 10.3389/fimmu.2021.696311

The Impact of Programmed Cell Death on the Formation of Tertiary Lymphoid Structures

Mélanie Dieudé[1,2,3]*, *Imane Kaci*[1,3,4] *and Marie-Josée Hébert*[1,3,5]*

[1] Research Centre, Centre Hospitalier de l'Université de Montréal (CRCHUM), Montréal, QC, Canada, [2] Department of Microbiology, Infectiology and Immunology, Faculty of Medicine, Université de Montréal, Montréal, QC, Canada, [3] Canadian Donation and Transplantation Research Program, Edmonton, AB, Canada, [4] Molecular Biology Programs, Faculty of Medicine, Université de Montréal, Montréal, QC, Canada, [5] Department of Medicine, Faculty of Medicine, Université de Montréal, Montréal, QC, Canada

Tertiary lymphoid structures are clusters of lymphoid tissue that develop post-natally at sites of chronic inflammation. They have been described in association with infection, autoimmune disorders, cancer, and allograft rejection. In their mature stage, TLS function as ectopic germinal centers, favoring the local production of autoantibodies and cytokines. TLS formation tends to parallel the severity of tissue injury and they are usually indicative of locally active immune responses. The presence of TLS in patients with solid tumors is usually associated with a better prognosis whereas their presence predicts increased maladaptive immunologic activity in patients with autoimmune disorders or allograft transplantation. Recent data highlight a correlation between active cell death and TLS formation and maturation. Our group recently identified apoptotic exosome-like vesicles, released by apoptotic cells, as novel inducers of TLS formation. Here, we review mechanisms of TLS formation and maturation with a specific focus on the emerging importance of tissue injury, programmed cell death and extracellular vesicles in TLS biogenesis.

Keywords: tertiary lymphoid structure, antibodies, inflammation, apoptosis, injury

OPEN ACCESS

Edited by:
Catherine Sautes-Fridman, U1138 Centre de Recherche des Cordeliers (CRC) (INSERM), France

Reviewed by:
Richard Chahwan, University of Zurich, Switzerland
Jon Zugazagoitia, Independent Researcher, Madrid, Spain

***Correspondence:**
Marie-Josée Hébert
marie-josee.hebert@umontreal.ca
Mélanie Dieudé
melanie.dieude@umontreal.ca

Specialty section:
This article was submitted to Cancer Immunity and Immunotherapy, a section of the journal Frontiers in Immunology

Received: *16 April 2021*
Accepted: *28 June 2021*
Published: *15 July 2021*

Citation:
Dieudé M, Kaci I and Hébert M-J (2021) The Impact of Programmed Cell Death on the Formation of Tertiary Lymphoid Structures. Front. Immunol. 12:696311. doi: 10.3389/fimmu.2021.696311

INTRODUCTION

Tertiary lymphoid structures (TLS) are ectopic aggregates of lymphocytes and stromal cells, which, at maturity, behave as functional sites of adaptive immune responses (1, 2). In contrast to secondary lymphoid organs (SLO) (such as spleen, lymph nodes and Peyer's patches), TLS are non-encapsulated and form postnatally. They exhibit plasticity and their presence is transient, correlating with active tissue injury and resolving after antigenic clearance and tissue repair (3). They are composed of T and B cells as well as stromal cells, such as follicular dendritic cells (FDCs) and αSMA+ fibroblasts. Macrophages can be found at the periphery of TLS (4) (**Figure 1**). TLS display different organization levels ranging from simple clusters of B and T lymphocytes to more mature structures where T and B cells are polarized and FDC expressing CD21 and p75 neurotrophin receptor are present, allowing the formation of germinal centers (GC) (1, 5–7). GC are characterized by expression of activation-induced cytidine deaminase (AID) that regulated immunoglobulin gene affinity maturation through somatic hypermutation and initiation of immunoglobulin class switch recombination. GC are sites of B cell proliferation and affinity

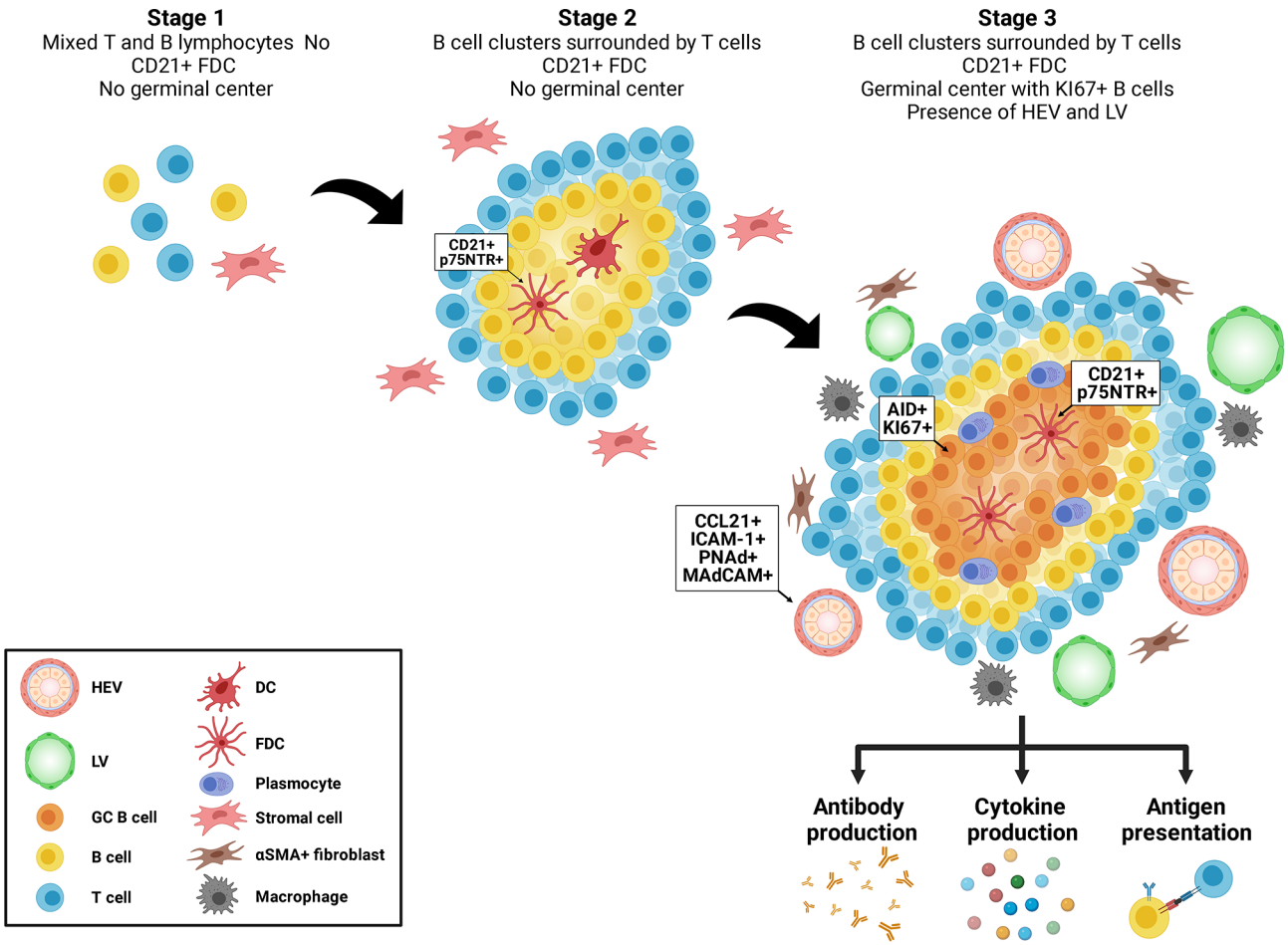

FIGURE 1 | Maturation of tertiary lymphoid structures. Tertiary lymphoid structures evolve from loose aggregates of T and B cells and stromal cells (Stage 1), to polarized clusters of T and B cells accompanied by follicular dendritic cells (FDC) (Stage 2) to mature polarized structures containing germinal centers, proliferating B cells, plasma cells, high endothelial venules (HEV) and lymphoid vessels (LV).

maturation into antibody secreting plasma cells. Lymphatic vessels and high endothelial venules (HEV), characterized by a cuboidal shape of endothelial cells and expression of CCL21, ICAM-1, PNAd and MAdCAM, are commonly found in mature stages (6) (**Figure 1**).

TLS arise in tissues whose main function is other than the generation of immune cells such as kidney, heart, pancreas, lung, colon and breast. Lymphoid neogenesis (5, 8), i.e. the process of TLS formation, can be observed in inflammatory microenvironments resulting from chronic infection, autoimmune conditions, allograft rejection and tumor growth (9, 10). Inflammatory cytokines such as TNF-α, IL-17A, IL-23 and lymphotoxins, expressed by immune cells at sites of injury induce stromal cells to produce homeostatic chemokines, such as CXCL13, CXCL12, CCL19 and CCL21. This in turn drives the recruitment of T and B cells and their organization into progressively polarized clusters (11). CXCL13 expression in TLS by CD8+ T cells and other immune cells appears pivotal to TLS maturation (12–16). Inflammation also prompts the expression of a number of chemokines and cytokines in tissue fibroblasts such as podoplanin, CCL19, IL-17, CXCL13, and adhesion molecules ICAM-1 and VCAM-1, therefore creating a microenvironment conducive to attraction and retention of lymphoid cells (17–22). Chemokines and cytokines produced by local fibroblasts and epithelial cells (19) favor the recruitment of immune cells and TLS organization. Various cytokines can also synergize and/or compensate one another, creating an environment favorable for TLS formation and maturation (2).

An important phase in TLS maturation is the formation of HEV that connect TLS with the bloodstream and enable the sustained recruitment of lymphocytes. HEVs express addressin and CCL21 allowing the entry of naïve T cells expressing the addressin ligand CD62L and CCR7, the chemokine receptor for CCL21 and CCL19. Data from tumor models also demonstrate that lymphotoxin α (LTα) and TNF receptor (TNFR) interactions, likely through infiltrating CD8+ T cells and NK cells, are also important for HEV formation (23). Others found that HEV formation can occur independently of both LTα and lymphotoxin (LT)-ß receptor (LTbR) (24). Specific requirements

for HEV formation and TLS maturation may be a consequence of the different microenvironments in which TLS are formed. The presence of FDCs within B cell follicles is another hallmark of TLS maturation. In SLO, LTbR and TNFR signaling are essential for FDC formation. In TLS, LTα1ß2 is important for FDC generation, enabling GC formation and antigen presentation (25–27). Although FDCs progenitors remain unknown, activated local stromal cells can differentiate into FDCs upon encounter with migrating immune cells in TLSs (28).

Antigenic stimulation plays an important role in the formation of TLS and, in turn, TLS are sites of antibody formation. In numerous autoimmune diseases and alloimmune conditions, pathogenic or diagnostic autoantibodies have been shown to be produced by TLS (25, 29, 30). TLS within inflamed synovium or salivary glands in patients with rheumatoid arthritis or Sjögren's syndrome, control the production of anti-citrullinated peptide antibody, anti-Ro/SSA and anti-La/SSB antibodies (3, 31, 32). In kidney and heart allografts with chronic rejection, TLS have been identified as a source of anti-HLA antibodies, the latter playing a major role in allograft rejection (33). Our group also recently identified a role for TLS in the production of autoantibodies that contribute to allograft inflammation and dysfunction (34, 35).

B cells within TLS can differentiate into antibody-producing plasma cells. They can also favor autoimmunity and alloimmunity by acting as antigen presenting cells, further perpetuating antigenic stimulation and immunogenicity (25, 29, 30). Some conflicting reports have pointed to the absence of correlation between TLS formation and autoimmunity or alloimmune disease activity. These results may stem from activation of tolerogenic pathways in certain TLS that harbor regulatory B and T cells (36, 37). While the presence of TLS is generally associated with disease severity in patients with autoimmunity and alloimmune diseases such as rheumatoid arthritis, Sjögren's syndrome, IgA nephropathy and allograft rejection (31–33, 38), TLS formation in solid tumors has been generally associated with a better prognosis. B cell aggregates in tumor TLS can participate in anti-tumor immunity by serving as antigen presenting cells and by differentiating into plasma cells producing tumor-associated antibodies. TLS B cell aggregates have generally been associated with better prognosis in lung, pancreas, colon and breast cancer (39–49).

FORMATION AND MATURATION OF TLS; FROM LYMPHOTOXINS TO IL-17

The formation and development of SLO and TLS both rely on the expression of lymphotoxins and inflammatory cytokines such as TNFα. Lymphotoxins are members of the TNF superfamily and are pivotal to the formation of SLO. Lymphoid inducer cells (LTi) arise from innate lymphoid progenitors in the fetal liver under the tight regulation of the nuclear hormone receptor retinoic acid related orphan receptor γτ (RORγτ) and the transcriptional regulator Id2 (50, 51). LTi express lymphotoxin α2ß1 on their surface and the soluble lymphotoxin α3 form. Interactions between lymphotoxins and the LTbR on stromal cells stimulate the expression of CXCL13 and CCL21, which in turn favor homing of T and B cells. Lymphotoxins-LTbR interactions are essential for the formation and maturation of SLO as HEV and FDC require persistent LTbR mediated signaling (52, 53). LTbR stimulation was originally considered also crucial for TLSs neogenesis since LTbR expression is readily upregulated in inflamed tissues and downstream signaling directly induces lymphoid neogenesis in different models (7, 17, 20, 21, 54, 55). Further studies have shown that initial recruitment of T and B cells can occur independently of LTbR signaling (18, 56) and point to IL-17 as an important regulator of TLS biogenesis.

IL-17A is the initial member of the IL-17 cytokine family that includes IL-17A, B, C, D, E and F. The IL-17 family plays important roles in host-defense against infection and behaves as a master regulator of inflammatory and autoimmune responses. It is also known to regulate the growth of several tumors, including skin, colon, pancreas, liver, lung and myeloma (57–65). A number of immune cells can produce IL-17A including LTi, Th17 T cells and γδ T cells, which has been implicated in autoimmune and inflammatory diseases such as multiple sclerosis, psoriasis, rheumatoid arthritis, crescentic glomerulonephritis, lupus nephritis and uveitis, among others (66–82).

In multiple sclerosis, IL-17-producing γδ T cells are thought to be initiators of inflammation and inductors of Th17 cells. In the experimental autoimmune encephalomyelitis (EAE) model, early accumulation of γδ T cells was observed in the central nervous system (CNS) where they release IL-17 and IL-21 to enhance the pro-inflammatory activity of αβ Th17 cells (71). Patients with multiple sclerosis also show accumulation of IL-17+ cells in chronic demyelinated areas of the CNS, and an increase in IL-17-producing γδ T cells in the cerebrospinal fluid (72, 73). Experimental models of skin inflammation identified IL-17A/F-producing γδ T cells as necessary and sufficient to trigger psoriasis-like plaque formation in IL-23- or Immiquimod-induced models (74). IL-17-secreting γδ T cells were also shown to enhance Th17 responses when skin inflammation was triggered with BCG immunization or Freund's adjuvant (75, 76). Similarly, human dermal γδ T cells are abundant in biopsies of psoriasis lesions, with an ability to produce higher levels of IL-17 compared to αβ Th17 cells upon IL-23 stimulation *in vitro* (74). In mouse models of non-autoimmune arthritis, resident and peripheral γδ T cells were reported as a major source of IL-17 (77, 78). An increase in circulating IL-17A-producing γδ T cells was also found in arthritis patients, suggesting their priming by cytokines secreted at the site of inflammation (79, 80). In Crescentic glomerulonephritis, renal IL-17A-producing γδ T cells were found to be the main contributor in the early inflammatory response by promoting kidney injury. They were predominated by IL-17A-producing Th17 at later phases (81). In the experimental autoimmune uveitis model, αβ and γδ T cells interactions was found to be important for mediation of eye inflammation. In this model, an early expansion of γδ T cells in SLO induces IL-17 production and further generation of Th17 responses by αβ cells at the inflammatory site (82).

A growing body of evidence has confirmed a role for IL-17A produced by Th17 T cells and γδ T cells in the development of TLS in the context of pulmonary infection, CNS inflammation, renal ischemia-reperfusion, obstruction and IgA nephropathy, and kidney transplantation (22, 38, 54, 83–88). In a model of LPS-

induced pulmonary infection in neonatal mice, αβ and γδ T cells were detected within Inducible Bronchus-Associated Lymphoid Tissues (iBALT). γδ T cells formed a large proportion of infiltrating cells and both contributed to IL-17 production. Adoptive transfer of these purified T cell subsets, separately or together, to LPS-treated *Tcrbd*$^{-/-}$ neonatal mice, showed preferential contribution of γδ T cells in promoting iBALT development and of αβ T cells in forming larger areas of iBALT (83). Using another model of pulmonary infection induced by *Pseudomonas aeruginosa*, γδ T cells were found to be the main source of IL-17 within iBALT, inducing CXCL-12 production by IL-17R+ stromal cells, B cell recruitment and follicles formation independent of FDC. When induced in *IL-17a/f* $^{-/-}$ or γδ T cells-deficient mice upon infection, lymphoid structures were less organized and, in the absence of γδ T cells, showed a reduction in number and size (84). In the EAE model, TLS formation in the CNS was also shown to require IL-17 production. Among various Th cell subsets adoptively transferred to mice, IL-17-secreting podoplanin-positive Th17 cells generated large organized and well structured ectopic lymphoid follicles in the CNS (22). Renal TLOs induced by ischemia-reperfusion injury in aged mice were reported to be enriched in Th17 cell differentiation, with increased expression of IL-17A and IL-23R (38). Moreover, human renal rejected graft samples show a correlation between shorter graft survival and high interstitial infiltration of Th17 cells, producing IL-17 and IL-21 and promoting lymphoid neogenesis (85).

We have recently shown that γδ T17 cells play a critical role in IL-17 overexpression and lymphoid neogenesis in a model of vascular rejection (34). The importance of IL-17 in the activation of autoimmune responses in the context of transplantation appears to stem from its capacity to initiate recruitment of immune cells to sites of injury and promote maturation of antigen-presenting cells (89–94). As Th17 cells are the classic producers of IL-17, they have been suggested to play a pivotal role in autoimmune pathways triggered following transplantation. Intriguingly, our findings demonstrate the importance of γδ T cells, rather than Th17 cells, in coordinating the IL-17 response triggered by vascular injury of vascular allografts (34). These observations are in line with previous studies showing that human IL-17-producing γδ T cells are generated in the periphery and recruited to inflamed tissues (95, 96). This process takes place more rapidly compared to the activation of conventional T lymphocytes as γδ T cells can be activated in the absence of a cognate TCR ligand (97).

Collectively, depending on the nature of the insult and the tissue implicated, peripheral or resident IL-17-producing γδ T cells may be involved at early phases to organize immunological events in response to inflammatory signals, and promote further conventional T cell responses at the site of inflammation.

TISSUE INJURY, CELL DEATH, AND EXTRACELLULAR VESICLES REGULATE TLS BIOGENESIS

The production of danger associated molecular patterns (DAMPs) at sites of injury is considered pivotal to TLS biogenesis. Various animal models and disease states in humans highlight a clear correlation between the degree of tissue injury, TLS number and maturation stages (4, 38, 98). In models of renal ischemia-reperfusion injury and ureteral obstruction in mice, the severity of renal damage is associated with TLS biogenesis. Aged mice, which show enhanced tissue injury after ischemia-reperfusion, were recently found to exhibit an increased propensity to TLS formation, translating into accentuated renal dysfunction (4, 98). Yet the precise DAMPs and mediators that are prompting TLS formation through activation of Th17 T cells and/or γδ T cells are only beginning to be characterized.

Our group and others showed that apoptosis, a type of programmed cell death classically considered non-inflammatory, can prompt the release of a number of mediators of importance in regulating immune cells towards either anti- but also pro-inflammatory and immunogenic responses (99–101). Activation of caspase-3 in dying cells leads to the release of different types of extracellular vesicles. Our group identified apoptotic exosome-like vesicles (ApoExo) as a novel type of extracellular vesicles released by endothelial cells through caspase-3 dependent pathways. ApoExo are smaller than classical apoptotic bodies, ranging from 30 to 100nm. Their protein, mRNA and microRNA contents differ from those of classical apoptotic bodies and classical exosomes (100, 102, 103). They are characterized by the presence of active 20S proteasome, perlecan LG3 C-terminal fragment and long non-coding RNAs. We showed that ApoExo are released in the bloodstream after hindlimb and renal ischemic injury resulting in higher circulating levels. In a model of vascular rejection in mice, allograft recipients injected with ApoExo showed increased TLS formation within the allograft (**Figure 2**). ApoExo injection prompted egress of γδ T cells from the spleen to the allograft leading to increased intragraft IL-17 expression, complement deposition and enhanced production of autoantibodies (34) (**Figure 2**). Mice genetically deficient in γδ T cells showed significantly less TLS formation, decreased autoantibody production and diminished allograft inflammation (**Figure 2**). Contrary to ApoExo, injection of apoptotic bodies did not foster TLS formation nor autoantibody production. The mechanism by which ApoExo activate γδ T cells and favor their homing to sites of injury remains to be fully characterized. Our results identify the proteasome activity of ApoExo as a pivotal signal regulating trafficking of γδ T cells to sites of vascular injury (34). Injection of ApoExo devoid of proteasome activity failed to induce TLS biogenesis and autoantibody formation in this system (**Figure 2**). Collectively, these recent findings identify ApoExo as novel inducers of γδ T cells activation and TLS formation and provide new clues into the mechanisms of cross talk between tissue injury and TLS biogenesis. The scope of future investigations will be to identify whether activation of γδ T cells by ApoExo is antigen specific or derives from innate signaling triggered by Toll-like receptor ligands or nonprotein mediators.

CONCLUSION

TLS are increasingly attracting interest because of their capacity to sustain local adaptive immune responses in a variety of disease

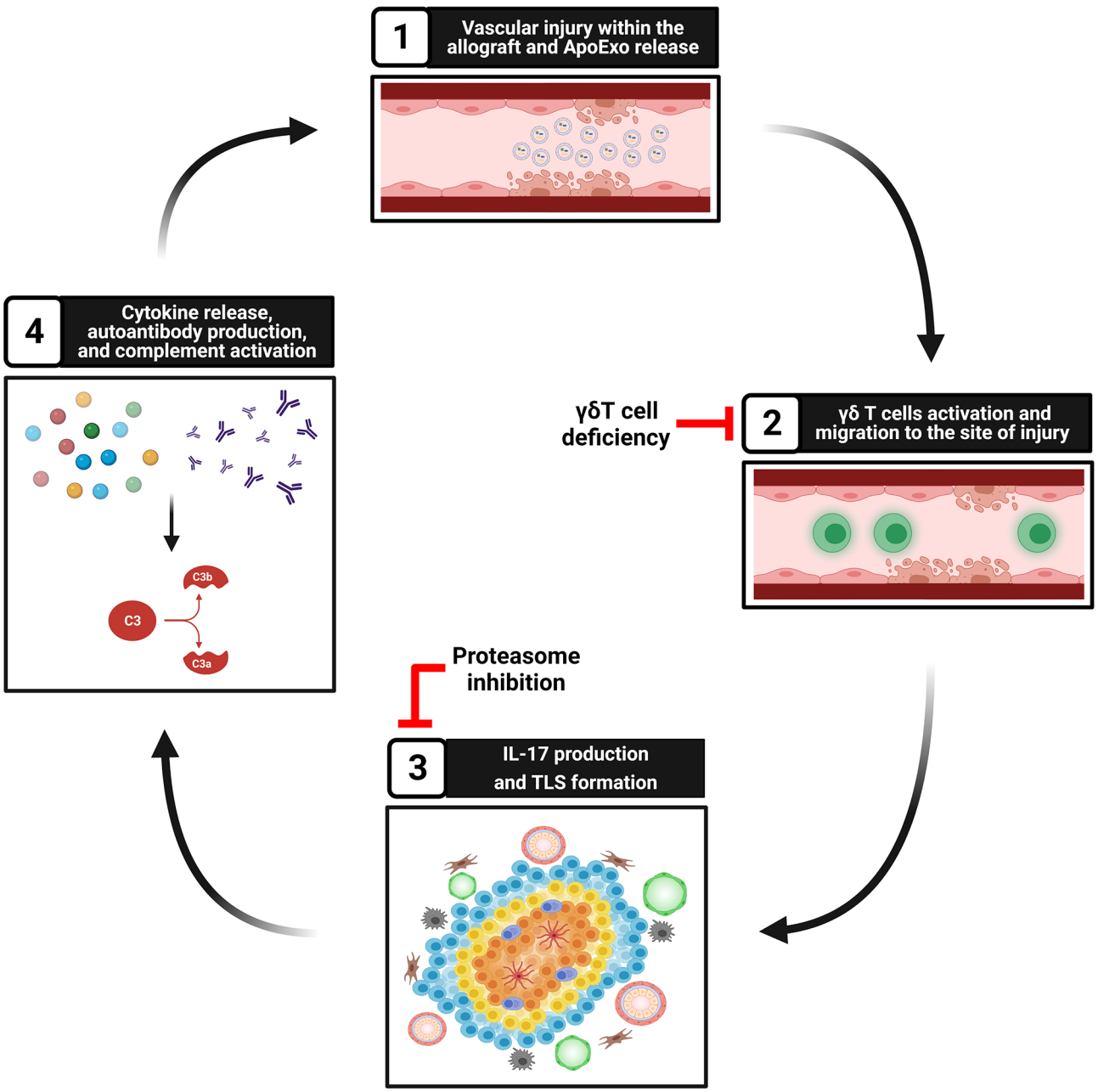

FIGURE 2 | Tissue injury, ApoExo release, and TLS formation. Step 1: Vascular injury and apoptosis of endothelial cells foster the release of apoptotic exosome-like vesicles (ApoExo) carrying active 20S proteasome. Step 2: ApoExo activate γδ T cells that migrate to the site of injury. Genetic deficiency of γδ T cells decreases TLS formation and autoantibody production. Step 3: γδ T cells produce IL-17 and favor the formation of tertiary lymphoid structures at sites of injury. Inhibition of proteasome activity within ApoExo blocks TLS biogenesis and autoantibody formation. Step 4: Tertiary lymphoid structures produce proinflammatory cytokines and autoantibodies, therefore favoring complement activation and further vascular injury.

states. Not only do TLS correlate with the severity and chronicity of tissue injury, they are increasingly recognized as pivotal players in maladaptive tissue remodeling, autoimmunity and inflammation. Although anti-tumor immune responses triggered and propagated from TLS are important pathways for controlling tumor growth, TLS are often associated with maladaptive autoimmune reactivity and tissue destruction in an array of autoimmune, alloimmune and chronic inflammatory diseases. The identification of ApoExo released by dying apoptotic cells as novel inducers of TLS biogenesis provides new insights into the mechanisms of cross talk that contribute to TLS formation at sites of injury.

AUTHOR CONTRIBUTIONS

MD, IK, and M-JH wrote the manuscript. All authors contributed to the article and approved the submitted version.

ACKNOWLEDGMENTS

The authors acknowledge support from the Canadian Donation and Transplantation Research Program (CDTRP) (MD, IK, M-JH), the Canadian Institutes of Health Research [CIHR, MOP-123436 and PJT-148884 (M-JH)], the Kidney Foundation of Canada [IP20016MDs (MD)], Shire Chair in Nephrology, Transplantation and Renal Regeneration of Université de Montréal (M-JH). M-JH is the Co-Director and MD is the Executive Director of the Canadian Donation and Transplantation Research Program (CDTRP). The authors thank the J.-L. Lévesque Foundation for renewed support. The authors thank Julie Turgeon and Francis Migneault for their help with article and figure editing. Figures were created with BioRender.com.

REFERENCES

1. Manzo A, Paoletti S, Carulli M, Blades MC, Barone F, Yanni G, et al. Systematic Microanatomical Analysis of CXCL13 and CCL21 *In situ* Production and Progressive Lymphoid Organization in Rheumatoid Synovitis. *Eur J Immunol* (2005) 35(5):1347–59. doi: 10.1002/eji.200425830
2. Gago da Graca C, van Baarsen LGM, Mebius RE. Tertiary Lymphoid Structures: Diversity in Their Development, Composition, and Role. *J Immunol* (2021) 206(2):273–81. doi: 10.4049/jimmunol.2000873
3. Corsiero E, Delvecchio FR, Bombardieri M, Pitzalis C. B Cells in the Formation of Tertiary Lymphoid Organs in Autoimmunity, Transplantation and Tumorigenesis. *Curr Opin Immunol* (2019) 57:46–52. doi: 10.1016/j.coi.2019.01.004
4. Sato Y, Boor P, Fukuma S, Klinkhammer BM, Haga H, Ogawa O, et al. Developmental Stages of Tertiary Lymphoid Tissue Reflect Local Injury and Inflammation in Mouse and Human Kidneys. *Kidney Int* (2020) 98(2):448–63. doi: 10.1016/j.kint.2020.02.023
5. Aloisi F, Pujol-Borrell R. Lymphoid Neogenesis in Chronic Inflammatory Diseases. *Nat Rev Immunol* (2006) 6(3):205–17. doi: 10.1038/nri1786
6. Ruddle NH. High Endothelial Venules and Lymphatic Vessels in Tertiary Lymphoid Organs: Characteristics, Functions, and Regulation. *Front Immunol* (2016) 7:491. doi: 10.3389/fimmu.2016.00491
7. Grabner R, Lotzer K, Dopping S, Hildner M, Radke D, Beer M, et al. Lymphotoxin Beta Receptor Signaling Promotes Tertiary Lymphoid Organogenesis in the Aorta Adventitia of Aged ApoE-/- Mice. *J Exp Med* (2009) 206(1):233–48. doi: 10.1084/jem.20080752
8. Hjelmstrom P. Lymphoid Neogenesis: *De Novo* Formation of Lymphoid Tissue in Chronic Inflammation Through Expression of Homing Chemokines. *J Leukoc Biol* (2001) 69(3):331–9. doi: 10.1189/jlb.69.3.331
9. Pitzalis C, Jones GW, Bombardieri M, Jones SA. Ectopic Lymphoid-Like Structures in Infection, Cancer and Autoimmunity. *Nat Rev Immunol* (2014) 14(7):447–62. doi: 10.1038/nri3700
10. Sautes-Fridman C, Petitprez F, Calderaro J, Fridman WH. Tertiary Lymphoid Structures in the Era of Cancer Immunotherapy. *Nat Rev Cancer* (2019) 19(6):307–25. doi: 10.1038/s41568-019-0144-6
11. McDonald KG, McDonough JS, Dieckgraefe BK, Newberry RD. Dendritic Cells Produce CXCL13 and Participate in the Development of Murine Small Intestine Lymphoid Tissues. *Am J Pathol* (2010) 176(5):2367–77. doi: 10.2353/ajpath.2010.090723
12. Koscso B, Kurapati S, Rodrigues RR, Nedjic J, Gowda K, Shin C, et al. Gut-Resident CX3CR1(hi) Macrophages Induce Tertiary Lymphoid Structures and IgA Response in Situ. *Sci Immunol* (2020) 5(46). doi: 10.1126/sciimmunol.aax0062
13. Thommen DS, Koelzer VH, Herzig P, Roller A, Trefny M, Dimeloe S, et al. A Transcriptionally and Functionally Distinct PD-1(+) CD8(+) T Cell Pool With Predictive Potential in non-Small-Cell Lung Cancer Treated With PD-1 Blockade. *Nat Med* (2018) 24(7):994–1004. doi: 10.1038/s41591-018-0057-z
14. Manzo A, Vitolo B, Humby F, Caporali R, Jarrossay D, Dell'accio F, et al. Mature Antigen-Experienced T Helper Cells Synthesize and Secrete the B Cell Chemoattractant CXCL13 in the Inflammatory Environment of the Rheumatoid Joint. *Arthritis Rheum* (2008) 58(11):3377–87. doi: 10.1002/art.23966
15. Bellamri N, Viel R, Morzadec C, Lecureur V, Joannes A, de Latour B, et al. TNF-Alpha and IL-10 Control CXCL13 Expression in Human Macrophages. *J Immunol* (2020) 204(9):2492–502. doi: 10.4049/jimmunol.1900790
16. Carlsen HS, Baekkevold ES, Morton HC, Haraldsen G, Brandtzaeg P. Monocyte-Like and Mature Macrophages Produce CXCL13 (B Cell-Attracting Chemokine 1) in Inflammatory Lesions With Lymphoid Neogenesis. *Blood* (2004) 104(10):3021–7. doi: 10.1182/blood-2004-02-0701
17. Peduto L, Dulauroy S, Lochner M, Spath GF, Morales MA, Cumano A, et al. Inflammation Recapitulates the Ontogeny of Lymphoid Stromal Cells. *J Immunol* (2009) 182(9):5789–99. doi: 10.4049/jimmunol.0803974
18. Pikor NB, Astarita JL, Summers-Deluca L, Galicia G, Qu J, Ward LA, et al. Integration of Th17- and Lymphotoxin-Derived Signals Initiates Meningeal-Resident Stromal Cell Remodeling to Propagate Neuroinflammation. *Immunity* (2015) 43(6):1160–73. doi: 10.1016/j.immuni.2015.11.010
19. Barone F, Nayar S, Campos J, Cloake T, Withers DR, Toellner KM, et al. IL-22 Regulates Lymphoid Chemokine Production and Assembly of Tertiary Lymphoid Organs. *Proc Natl Acad Sci USA* (2015) 112(35):11024–9. doi: 10.1073/pnas.1503315112
20. Link A, Hardie DL, Favre S, Britschgi MR, Adams DH, Sixt M, et al. Association of T-Zone Reticular Networks and Conduits With Ectopic Lymphoid Tissues in Mice and Humans. *Am J Pathol* (2011) 178(4):1662–75. doi: 10.1016/j.ajpath.2010.12.039
21. Olivier BJ, Cailotto C, van der Vliet J, Knippenberg M, Greuter MJ, Hilbers FW, et al. Vagal Innervation is Required for the Formation of Tertiary Lymphoid Tissue in Colitis. *Eur J Immunol* (2016) 46(10):2467–80. doi: 10.1002/eji.201646370
22. Peters A, Pitcher LA, Sullivan JM, Mitsdoerffer M, Acton SE, Franz B, et al. Th17 Cells Induce Ectopic Lymphoid Follicles in Central Nervous System Tissue Inflammation. *Immunity* (2011) 35(6):986–96. doi: 10.1016/j.immuni.2011.10.015
23. Peske JD, Thompson ED, Gemta L, Baylis RA, Fu YX, Engelhard VH. Effector Lymphocyte-Induced Lymph Node-Like Vasculature Enables Naive T-Cell Entry Into Tumours and Enhanced Anti-Tumour Immunity. *Nat Commun* (2015) 6:7114. doi: 10.1038/ncomms8114
24. Weinstein AM, Chen L, Brzana EA, Patil PR, Taylor JL, Fabian KL, et al. Tbet and IL-36gamma Cooperate in Therapeutic DC-Mediated Promotion of Ectopic Lymphoid Organogenesis in the Tumor Microenvironment. *Oncoimmunology* (2017) 6(6):e1322238. doi: 10.1080/2162402X.2017.1322238
25. Hughes CE, Benson RA, Bedaj M, Maffia P. Antigen-Presenting Cells and Antigen Presentation in Tertiary Lymphoid Organs. *Front Immunol* (2016) 7:481. doi: 10.3389/fimmu.2016.00481
26. Fu YX, Huang G, Wang Y, Chaplin DD. B Lymphocytes Induce the Formation of Follicular Dendritic Cell Clusters in a Lymphotoxin Alpha-Dependent Fashion. *J Exp Med* (1998) 187(7):1009–18. doi: 10.1084/jem.187.7.1009
27. Le Pottier L, Devauchelle V, Fautrel A, Daridon C, Saraux A, Youinou P, et al. Ectopic Germinal Centers are Rare in Sjogren's Syndrome Salivary Glands and do Not Exclude Autoreactive B Cells. *J Immunol* (2009) 182(6):3540–7. doi: 10.4049/jimmunol.0803588
28. Cupedo T, Jansen W, Kraal G, Mebius RE. Induction of Secondary and Tertiary Lymphoid Structures in the Skin. *Immunity* (2004) 21(5):655–67. doi: 10.1016/j.immuni.2004.09.006
29. Buckley CD, Barone F, Nayar S, Benezech C, Caamano J. Stromal Cells in Chronic Inflammation and Tertiary Lymphoid Organ Formation. *Annu Rev Immunol* (2015) 33:715–45. doi: 10.1146/annurev-immunol-032713-120252

30. Pipi E, Nayar S, Gardner DH, Colafrancesco S, Smith C, Barone F. Tertiary Lymphoid Structures: Autoimmunity Goes Local. *Front Immunol* (2018) 9:1952. doi: 10.3389/fimmu.2018.01952
31. Humby F, Bombardieri M, Manzo A, Kelly S, Blades MC, Kirkham B, et al. Ectopic Lymphoid Structures Support Ongoing Production of Class-Switched Autoantibodies in Rheumatoid Synovium. *PloS Med* (2009) 6(1): e1. doi: 10.1371/journal.pmed.0060001
32. Amara K, Steen J, Murray F, Morbach H, Fernandez-Rodriguez BM, Joshua V, et al. Monoclonal IgG Antibodies Generated From Joint-Derived B Cells of RA Patients Have a Strong Bias Toward Citrullinated Autoantigen Recognition. *J Exp Med* (2013) 210(3):445–55. doi: 10.1084/jem.20121486
33. Thaunat O, Field AC, Dai J, Louedec L, Patey N, Bloch MF, et al. Lymphoid Neogenesis in Chronic Rejection: Evidence for a Local Humoral Alloimmune Response. *Proc Natl Acad Sci USA* (2005) 102(41):14723–8. doi: 10.1073/pnas.0507223102
34. Dieude M, Turgeon J, Karakeussian Rimbaud A, Beillevaire D, Qi S, Patey N, et al. Extracellular Vesicles Derived From Injured Vascular Tissue Promote the Formation of Tertiary Lymphoid Structures in Vascular Allografts. *Am J Transplant* (2020) 20(3):726–38. doi: 10.1111/ajt.15707
35. Cardinal H, Dieude M, Hebert MJ. The Emerging Importance of Non-HLA Autoantibodies in Kidney Transplant Complications. *J Am Soc Nephrol* (2017) 28(2):400–6. doi: 10.1681/ASN.2016070756
36. Nova-Lamperti E, Chana P, Mobillo P, Runglall M, Kamra Y, McGregor R, et al. Increased CD40 Ligation and Reduced BCR Signalling Leads to Higher IL-10 Production in B Cells From Tolerant Kidney Transplant Patients. *Transplantation* (2017) 101(3):541–7. doi: 10.1097/TP.0000000000001341
37. Brown K, Sacks SH, Wong W. Tertiary Lymphoid Organs in Renal Allografts can be Associated With Donor-Specific Tolerance Rather Than Rejection. *Eur J Immunol* (2011) 41(1):89–96. doi: 10.1002/eji.201040759
38. Luo R, Cheng Y, Chang D, Liu T, Liu L, Pei G, et al. Tertiary Lymphoid Organs are Associated With the Progression of Kidney Damage and Regulated by Interleukin-17A. *Theranostics* (2021) 11(1):117–31. doi: 10.7150/thno.48624
39. Castino GF, Cortese N, Capretti G, Serio S, Di Caro G, Mineri R, et al. Spatial Distribution of B Cells Predicts Prognosis in Human Pancreatic Adenocarcinoma. *Oncoimmunology* (2016) 5(4):e1085147. doi: 10.1080/2162402X.2015.1085147
40. Cipponi A, Mercier M, Seremet T, Baurain JF, Theate I, van den Oord J, et al. Neogenesis of Lymphoid Structures and Antibody Responses Occur in Human Melanoma Metastases. *Cancer Res* (2012) 72(16):3997–4007. doi: 10.1158/0008-5472.CAN-12-1377
41. Di Caro G, Bergomas F, Grizzi F, Doni A, Bianchi P, Malesci A, et al. Occurrence of Tertiary Lymphoid Tissue is Associated With T-Cell Infiltration and Predicts Better Prognosis in Early-Stage Colorectal Cancers. *Clin Cancer Res* (2014) 20(8):2147–58. doi: 10.1158/1078-0432.CCR-13-2590
42. Dieu-Nosjean MC, Goc J, Giraldo NA, Sautes-Fridman C, Fridman WH. Tertiary Lymphoid Structures in Cancer and Beyond. *Trends Immunol* (2014) 35(11):571–80. doi: 10.1016/j.it.2014.09.006
43. Germain C, Gnjatic S, Tamzalit F, Knockaert S, Remark R, Goc J, et al. Presence of B Cells in Tertiary Lymphoid Structures is Associated With a Protective Immunity in Patients With Lung Cancer. *Am J Respir Crit Care Med* (2014) 189(7):832–44. doi: 10.1164/rccm.201309-1611OC
44. Ladanyi A, Kiss J, Mohos A, Somlai B, Liszkay G, Gilde K, et al. Prognostic Impact of B-Cell Density in Cutaneous Melanoma. *Cancer Immunol Immunother* (2011) 60(12):1729–38. doi: 10.1007/s00262-011-1071-x
45. Nzula S, Going JJ, Stott DI. Antigen-Driven Clonal Proliferation, Somatic Hypermutation, and Selection of B Lymphocytes Infiltrating Human Ductal Breast Carcinomas. *Cancer Res* (2003) 63(12):3275–80.
46. Posch F, Silina K, Leibl S, Mundlein A, Moch H, Siebenhuner A, et al. Maturation of Tertiary Lymphoid Structures and Recurrence of Stage II and III Colorectal Cancer. *Oncoimmunology* (2018) 7(2):e1378844. doi: 10.1080/2162402X.2017.1378844
47. Silina K, Soltermann A, Attar FM, Casanova R, Uckeley ZM, Thut H, et al. Germinal Centers Determine the Prognostic Relevance of Tertiary Lymphoid Structures and Are Impaired by Corticosteroids in Lung Squamous Cell Carcinoma. *Cancer Res* (2018) 78(5):1308–20. doi: 10.1158/0008-5472.CAN-17-1987
48. Zhu G, Falahat R, Wang K, Mailloux A, Artzi N, Mule JJ. Tumor-Associated Tertiary Lymphoid Structures: Gene-Expression Profiling and Their Bioengineering. *Front Immunol* (2017) 8:767. doi: 10.3389/fimmu.2017.00767
49. Zhu W, Germain C, Liu Z, Sebastian Y, Devi P, Knockaert S, et al. A High Density of Tertiary Lymphoid Structure B Cells in Lung Tumors is Associated With Increased CD4(+) T Cell Receptor Repertoire Clonality. *Oncoimmunology* (2015) 4(12):e1051922. doi: 10.1080/2162402X.2015.1051922
50. Grogan JL, Ouyang W. A Role for Th17 Cells in the Regulation of Tertiary Lymphoid Follicles. *Eur J Immunol* (2012) 42(9):2255–62. doi: 10.1002/eji.201242656
51. Eberl G, Marmon S, Sunshine MJ, Rennert PD, Choi Y, Littman DR. An Essential Function for the Nuclear Receptor RORgamma(t) in the Generation of Fetal Lymphoid Tissue Inducer Cells. *Nat Immunol* (2004) 5(1):64–73. doi: 10.1038/ni1022
52. Browning JL, Allaire N, Ngam-Ek A, Notidis E, Hunt J, Perrin S, et al. Lymphotoxin-Beta Receptor Signaling is Required for the Homeostatic Control of HEV Differentiation and Function. *Immunity* (2005) 23 (5):539–50. doi: 10.1016/j.immuni.2005.10.002
53. Krautler NJ, Kana V, Kranich J, Tian Y, Perera D, Lemm D, et al. Follicular Dendritic Cells Emerge From Ubiquitous Perivascular Precursors. *Cell* (2012) 150(1):194–206. doi: 10.1016/j.cell.2012.05.032
54. Moyron-Quiroz JE, Rangel-Moreno J, Kusser K, Hartson L, Sprague F, Goodrich S, et al. Role of Inducible Bronchus Associated Lymphoid Tissue (iBALT) in Respiratory Immunity. *Nat Med* (2004) 10(9):927–34. doi: 10.1038/nm1091
55. Lochner M, Ohnmacht C, Presley L, Bruhns P, Si-Tahar M, Sawa S, et al. Microbiota-Induced Tertiary Lymphoid Tissues Aggravate Inflammatory Disease in the Absence of RORgamma T and LTi Cells. *J Exp Med* (2011) 208 (1):125–34. doi: 10.1084/jem.20100052
56. Nayar S, Campos J, Smith CG, Iannizzotto V, Gardner DH, Mourcin F, et al. Immunofibroblasts are Pivotal Drivers of Tertiary Lymphoid Structure Formation and Local Pathology. *Proc Natl Acad Sci USA* (2019) 116 (27):13490–7. doi: 10.1073/pnas.1905301116
57. Wu L, Chen X, Zhao J, Martin B, Zepp JA, Ko JS, et al. A Novel IL-17 Signaling Pathway Controlling Keratinocyte Proliferation and Tumorigenesis *via* the TRAF4-ERK5 Axis. *J Exp Med* (2015) 212 (10):1571–87. doi: 10.1084/jem.20150204
58. Wang L, Yi T, Zhang W, Pardoll DM, Yu H. IL-17 Enhances Tumor Development in Carcinogen-Induced Skin Cancer. *Cancer Res* (2010) 70 (24):10112–20. doi: 10.1158/0008-5472.CAN-10-0775
59. Zepp JA, Zhao J, Liu C, Bulek K, Wu L, Chen X, et al. IL-17a-Induced PLET1 Expression Contributes to Tissue Repair and Colon Tumorigenesis. *J Immunol* (2017) 199(11):3849–57. doi: 10.4049/jimmunol.1601540
60. Zhang Y, Zoltan M, Riquelme E, Xu H, Sahin I, Castro-Pando S, et al. Immune Cell Production of Interleukin 17 Induces Stem Cell Features of Pancreatic Intraepithelial Neoplasia Cells. *Gastroenterology* (2018) 155 (1):210–23 e3. doi: 10.1053/j.gastro.2018.03.041
61. Wang K, Kim MK, Di Caro G, Wong J, Shalapour S, Wan J, et al. Interleukin-17 Receptor a Signaling in Transformed Enterocytes Promotes Early Colorectal Tumorigenesis. *Immunity* (2014) 41(6):1052–63. doi: 10.1016/j.immuni.2014.11.009
62. Sun C, Kono H, Furuya S, Hara M, Hirayama K, Akazawa Y, et al. Interleukin-17a Plays a Pivotal Role in Chemically Induced Hepatocellular Carcinoma in Mice. *Dig Dis Sci* (2016) 61(2):474–88. doi: 10.1007/s10620-015-3888-1
63. Jin C, Lagoudas GK, Zhao C, Bullman S, Bhutkar A, Hu B, et al. Commensal Microbiota Promote Lung Cancer Development *via* Gammadelta T Cells. *Cell* (2019) 176(5):998–1013 e16. doi: 10.1016/j.cell.2018.12.040
64. Calcinotto A, Brevi A, Chesi M, Ferrarese R, Garcia Perez L, Grioni M, et al. Microbiota-Driven Interleukin-17-Producing Cells and Eosinophils Synergize to Accelerate Multiple Myeloma Progression. *Nat Commun* (2018) 9(1):4832. doi: 10.1038/s41467-018-07305-8
65. Coffelt SB, Kersten K, Doornebal CW, Weiden J, Vrijland K, Hau CS, et al. IL-17-Producing Gammadelta T Cells and Neutrophils Conspire to Promote Breast Cancer Metastasis. *Nature* (2015) 522(7556):345–8. doi: 10.1038/nature14282
66. Katz Y, Nadiv O, Beer Y. Interleukin-17 Enhances Tumor Necrosis Factor Alpha-Induced Synthesis of Interleukins 1,6, and 8 in Skin and Synovial

Fibroblasts: A Possible Role as a "Fine-Tuning Cytokine" in Inflammation Processes. *Arthritis Rheum* (2001) 44(9):2176–84. doi: 10.1002/1529-0131(200109)44:9<2176::AID-ART371>3.0.CO;2-4
67. Crispin JC, Oukka M, Bayliss G, Cohen RA, Van Beek CA, Stillman IE, et al. Expanded Double Negative T Cells in Patients With Systemic Lupus Erythematosus Produce IL-17 and Infiltrate the Kidneys. *J Immunol* (2008) 181(12):8761–6. doi: 10.4049/jimmunol.181.12.8761
68. Havrdova E, Belova A, Goloborodko A, Tisserant A, Wright A, Wallstroem E, et al. Activity of Secukinumab, an Anti-IL-17A Antibody, on Brain Lesions in RRMS: Results From a Randomized, Proof-of-Concept Study. *J Neurol* (2016) 263(7):1287–95. doi: 10.1007/s00415-016-8128-x
69. Nistala K, Moncrieffe H, Newton KR, Varsani H, Hunter P, Wedderburn LR. Interleukin-17-Producing T Cells are Enriched in the Joints of Children With Arthritis, But Have a Reciprocal Relationship to Regulatory T Cell Numbers. *Arthritis Rheum* (2008) 58(3):875–87. doi: 10.1002/art.23291
70. Chabaud M, Durand JM, Buchs N, Fossiez F, Page G, Frappart L, et al. Human Interleukin-17: A T Cell-Derived Proinflammatory Cytokine Produced by the Rheumatoid Synovium. *Arthritis Rheum* (1999) 42(5):963–70. doi: 10.1002/1529-0131(199905)42:5<963::AID-ANR15>3.0.CO;2-E
71. Sutton CE, Lalor SJ, Sweeney CM, Brereton CF, EdC L, Mills KHG. Interleukin-1 and IL-23 Induce Innate IL-17 Production From γδ T Cells, Amplifying Th17 Responses and Autoimmunity. *Immunity* (2009) 31:331–41. doi: 10.1016/j.immuni.2009.08.001
72. Schirmer L, Rothhammer V, Hemmer B, Korn T. Enriched CD161^{high} CCR6^{+} γδ T Cells in the Cerebrospinal Fluid of Patients With Multiple Sclerosis. *JAMA Neurol* (2013) 70(3):345–51. doi: 10.1001/2013.jamaneurol.409
73. Tzartos JS, Friese MA, Craner MJ, Palace J, Newcombe J, Esiri MM, et al. Interleukin-17 Production in Central Nervous System-Infiltrating T Cells and Glial Cells is Associated With Active Disease in Multiple Sclerosis. *AJP* (2008) 172(1):146–55. doi: 10.2353/ajpath.2008.070690
74. Cai Y, Shen X, Ding C, Qi C, Li K, Li X, et al. Pivotal Role of Dermal IL-17-Producing γδ T Cells in Skin Inflammation. *Immunity* (2011) 35:596–610. doi: 10.1016/j.immuni.2011.08.001
75. Sumaria N, Roediger B, Ng LG, Qin J, Pinto R, Cavanagh LL, et al. Cutaneous Immunosurveillance by Self-Renewing Dermal γδ T Cells. *J Exp Med* (2011) 208(3):505–18. doi: 10.1084/jem.20101824
76. Roark CL, Huang Y, Jin N, Aydintug MK, Casper T, Sun D, et al. A Canonical Vγ4vδ4+ γδ T Cell Population With Distinct Stimulation Requirements Which Promotes the Th17 Response. *Immunol Res* (2013) 55:217–30. doi: 10.1007/s12026-012-8364-9
77. Reinhardt A, Yevsa T, Worbs T, Lienenklaus S, Sandrock I, Oberdörfer L, et al. Interleukin-23–Dependent γ/δ T Cells Produce Interleukin-17 and Accumulate in the Enthesis, Aortic Valve, and Ciliary Body in Mice. *Arthritis Rheumatol* (2016) 68(10):2476–86. doi: 10.1002/art.39732
78. Avau A, Mitera T, Put S, Put K, Brisse E, Filtjens J, et al. Systemic Juvenile Idiopathic Arthritis–Like Syndrome in Mice Following Stimulation of the Immune System With Freund's Complete Adjuvant. *Arthritis Rheumatol* (2014) 66(5):1340–51. doi: 10.1002/art.38359
79. Kenna TJ, Davidson SI, Duan R, Bradbury LA, McFarlane J, Smith M, et al. Enrichment of Circulating Interleukin-17–Secreting Interleukin-23 Receptor-Positive γ/δ T Cells in Patients With Active Ankylosing Spondylitis. *Arthritis Rheumatol* (2012) 64(5):1420–9. doi: 10.1002/art.33507
80. Kessel C, Lippitz K, Weinhage T, Hinze C, Wittkowski H, Holzinger D, et al. Proinflammatory Cytokine Environments can Drive Interleukin-17 Overexpression by γ/δ T Cells in Systemic Juvenile Idiopathic Arthritis. *Arthritis Rheumatol* (2017) 69(7):1480–94. doi: 10.1002/art.40099
81. Turner J-E, Krebs C, Tittel AP, Paust H-J, Meyer-Schwesinger C, Bennstein SB, et al. IL-17A Production by Renal γδ T Cells Promotes Kidney Injury in Crescentic GN. *J Am Soc Nephrol* (2012) 23(9):1486–95. doi: 10.1681/ASN.2012010040
82. Cui Y, Shao H, Lan C, Nian H, O'Brien RL, Born WK, et al. Major Role of Gd T Cells in the Generation of IL-17^{+} Uveitogenic T Cells. *J Immunol* (2009) 183:560–7. doi: 10.4049/jimmunol.0900241
83. Rangel-Moreno J, Carragher DM, de la Luz Garcia-Hernandez M, Hwang JY, Kusser K, Hartson L, et al. The Development of Inducible Bronchus-Associated Lymphoid Tissue Depends on IL-17. *Nat Immunol* (2011) 12(7):639–46. doi: 10.1038/ni.2053
84. Fleige H, Ravens S, Moschovakis GL, Bölter J, Willenzon S, Sutter G, et al. IL-17–Induced CXCL12 Recruits B Cells and Induces Follicle Formation in BALT in the Absence of Differentiated FDCs. *J Exp Med* (2014) 21(4):643–51. doi: 10.1084/jem.20131737
85. Deteix C, Attuil-Audenis V, Duthey A, Patey N, McGregor B, Dubois V, et al. Intragraft Th17 Infiltrate Promotes Lymphoid Neogenesis and Hastens Clinical Chronic Rejection. *J Immunol* (2010) 184(9):5344–51. doi: 10.4049/jimmunol.0902999
86. Zhang X, Lu B. IL-17 Initiates Tertiary Lymphoid Organ Formation. *Cell Mol Immunol* (2012) 9(1):9–10. doi: 10.1038/cmi.2011.48
87. Cupedo T. An Unexpected Role for IL-17 in Lymphoid Organogenesis. *Nat Immunol* (2011) 12(7):590–2. doi: 10.1038/ni.2058
88. Patakas A, Benson RA, Withers DR, Conigliaro P, McInnes IB, Brewer JM, et al. Th17 Effector Cells Support B Cell Responses Outside of Germinal Centres. *PloS One* (2012) 7(11):e49715. doi: 10.1371/journal.pone.0049715
89. Burlingham WJ, Love RB, Jankowska-Gan E, Haynes LD, Xu Q, Bobadilla JL, et al. IL-17-Dependent Cellular Immunity to Collagen Type V Predisposes to Obliterative Bronchiolitis in Human Lung Transplants. *J Clin Invest* (2007) 117(11):3498–506. doi: 10.1172/JCI28031
90. Saini D, Weber J, Ramachandran S, Phelan D, Tiriveedhi V, Liu M, et al. Alloimmunity-Induced Autoimmunity as a Potential Mechanism in the Pathogenesis of Chronic Rejection of Human Lung Allografts. *J Heart Lung Transplant* (2011) 30(6):624–31. doi: 10.1016/j.healun.2011.01.708
91. Goers TA, Ramachandran S, Aloush A, Trulock E, Patterson GA, Mohanakumar T. De Novo Production of K-Alpha1 Tubulin-Specific Antibodies: Role in Chronic Lung Allograft Rejection. *J Immunol* (2008) 180(7):4487–94. doi: 10.4049/jimmunol.180.7.4487
92. Hachem RR, Tiriveedhi V, Patterson GA, Aloush A, Trulock EP, Mohanakumar T. Antibodies to K-Alpha 1 Tubulin and Collagen V are Associated With Chronic Rejection After Lung Transplantation. *Am J Transplant* (2012) 12(8):2164–71. doi: 10.1111/j.1600-6143.2012.04079.x
93. Fukami N, Ramachandran S, Saini D, Walter M, Chapman W, Patterson GA, et al. Antibodies to MHC Class I Induce Autoimmunity: Role in the Pathogenesis of Chronic Rejection. *J Immunol* (2009) 182(1):309–18. doi: 10.4049/jimmunol.182.1.309
94. Nath DS, Ilias Basha H, Tiriveedhi V, Alur C, Phelan D, Ewald GA, et al. Characterization of Immune Responses to Cardiac Self-Antigens Myosin and Vimentin in Human Cardiac Allograft Recipients With Antibody-Mediated Rejection and Cardiac Allograft Vasculopathy. *J Heart Lung Transplant* (2010) 29(11):1277–85. doi: 10.1016/j.healun.2010.05.025
95. Papotto PH, Reinhardt A, Prinz I, Silva-Santos B. Innately Versatile: Gammadelta17 T Cells in Inflammatory and Autoimmune Diseases. *J Autoimmun* (2018) 87:26–37. doi: 10.1016/j.jaut.2017.11.006
96. Caccamo N, La Mendola C, Orlando V, Meraviglia S, Todaro M, Stassi G, et al. Differentiation, Phenotype, and Function of Interleukin-17-Producing Human Vgamma9Vdelta2 T Cells. *Blood* (2011) 118(1):129–38. doi: 10.1182/blood-2011-01-331298
97. Shiromizu CM, Jancic CC. Gammadelta T Lymphocytes: An Effector Cell in Autoimmunity and Infection. *Front Immunol* (2018) 9:2389. doi: 10.3389/fimmu.2018.02389
98. Sato Y, Mii A, Hamazaki Y, Fujita H, Nakata H, Masuda K, et al. Heterogeneous Fibroblasts Underlie Age-Dependent Tertiary Lymphoid Tissues in the Kidney. *JCI Insight* (2016) 1(11):e87680. doi: 10.1172/jci.insight.87680
99. Sirois I, Raymond MA, Brassard N, Cailhier JF, Fedjaev M, Hamelin K, et al. Caspase-3-Dependent Export of TCTP: A Novel Pathway for Antiapoptotic Intercellular Communication. *Cell Death Differ* (2011) 18(3):549–62. doi: 10.1038/cdd.2010.126
100. Dieude M, Bell C, Turgeon J, Beillevaire D, Pomerleau L, Yang B, et al. The 20S Proteasome Core, Active Within Apoptotic Exosome-Like Vesicles, Induces Autoantibody Production and Accelerates Rejection. *Sci Transl Med* (2015) 7(318):318ra200. doi: 10.1126/scitranslmed.aac9816

101. Dieude M, Cardinal H, Hebert MJ. Injury Derived Autoimmunity: Anti-Perlecan/LG3 Antibodies in Transplantation. *Hum Immunol* (2019) 80 (8):608–13. doi: 10.1016/j.humimm.2019.04.009
102. Migneault F, Dieude M, Turgeon J, Beillevaire D, Hardy MP, Brodeur A, et al. Apoptotic Exosome-Like Vesicles Regulate Endothelial Gene Expression, Inflammatory Signaling, and Function Through the NF-kappaB Signaling Pathway. *Sci Rep* (2020) 10(1):12562. doi: 10.1038/s41598-020-69548-0
103. Hardy MP, Audemard E, Migneault F, Feghaly A, Brochu S, Gendron P, et al. Apoptotic Endothelial Cells Release Small Extracellular Vesicles Loaded With Immunostimulatory Viral-Like RNAs. *Sci Rep* (2019) 9(1):7203. doi: 10.1038/s41598-019-43591-y

Conflict of Interest: The authors declare that the research was conducted in the absence of any commercial or financial relationships that could be construed as a potential conflict of interest.

Copyright © 2021 Dieudé, Kaci and Hébert. This is an open-access article distributed under the terms of the Creative Commons Attribution License (CC BY). The use, distribution or reproduction in other forums is permitted, provided the original author(s) and the copyright owner(s) are credited and that the original publication in this journal is cited, in accordance with accepted academic practice. No use, distribution or reproduction is permitted which does not comply with these terms.

frontiers in Immunology

REVIEW
published: 29 July 2021
doi: 10.3389/fimmu.2021.689270

Tertiary Lymphoid Structures in Cancer: The Double-Edged Sword Role in Antitumor Immunity and Potential Therapeutic Induction Strategies

Wendi Kang[1], *Zhichao Feng*[1,2], *Jianwei Luo*[1], *Zhenhu He*[1], *Jun Liu*[1], *Jianzhen Wu*[1] *and Pengfei Rong*[1,2*]

[1] Department of Radiology, The Third Xiangya Hospital of Central South University, Changsha, China, [2] Molecular Imaging Research Center, Central South University, Changsha, China

OPEN ACCESS

Edited by:
Catherine Sautes-Fridman, U1138 Centre de Recherche des Cordeliers (CRC) (INSERM), France

Reviewed by:
Marie-Cecile Michallet, University of Lyon, France
Yona Keisari, Tel Aviv University, Israel

***Correspondence:**
Pengfei Rong
rongpengfei66@163.com

Specialty section:
This article was submitted to Cancer Immunity and Immunotherapy, a section of the journal Frontiers in Immunology

Received: 31 March 2021
Accepted: 05 July 2021
Published: 29 July 2021

Citation:
Kang W, Feng Z, Luo J, He Z, Liu J, Wu J and Rong P (2021) Tertiary Lymphoid Structures in Cancer: The Double-Edged Sword Role in Antitumor Immunity and Potential Therapeutic Induction Strategies. Front. Immunol. 12:689270. doi: 10.3389/fimmu.2021.689270

The complex tumor microenvironment (TME) plays a vital role in cancer development and dramatically determines the efficacy of immunotherapy. Tertiary lymphoid structures (TLSs) within the TME are well recognized and consist of T cell-rich areas containing dendritic cells (DCs) and B cell-rich areas containing germinal centers (GCs). Accumulating research has indicated that there is a close association between tumor-associated TLSs and favorable clinical outcomes in most types of cancers, though a minority of studies have reported an association between TLSs and a poor prognosis. Overall, the double-edged sword role of TLSs in the TME and potential mechanisms need to be further investigated, which will provide novel therapeutic perspectives for antitumor immunoregulation. In this review, we focus on discussing the main functions of TLSs in the TME and recent advances in the therapeutic manipulation of TLSs through multiple strategies to enhance local antitumor immunity.

Keywords: tertiary lymphoid structures, tumor immunity, lymphoid neogenesis, bioengineering, immunotherapy, LIGHT

INTRODUCTION

Tumors originate and develop in a complicated and dynamic microenvironment, and there are endothelial cells, immune cells, and stromal cells existing around or within the tumor microenvironment (TME) and interacting with tumor cells (1, 2). Effective antitumor immunity is recognized to require the existence and activation of a variety of immune cells, including B cells,

$CD8^+$ T cells, and $CD4^+$ T cells, etc. This concept is confirmed by the presence of intratumoral tertiary lymphoid structures (TLSs), which are well-organized tumor-infiltrating lymphocyte (TIL) clusters and may generate an advanced immune response (3). As is known to us, immunotherapy can utilize positive feedback to activate the immune system and boost the infiltration of endogenous T cells into tumors and subsequent destruction of tumor cells (4–6). However, only 5%-30% of patients with malignancies exhibit activated intratumoral T cell immunity after anti-programmed cell death protein-1 (PD-1)/programmed death-ligand 1 (PD-L1) immunotherapy (7, 8). This failure is mainly due to the extensive immunosuppressive mechanisms in the TME that lead to the decreased number and dysfunction of infiltrating T cells (9–11).

TLSs are ectopic lymphoid organs that can develop at sites of chronic inflammation, such as those associated with infection and autoimmunity, but also form within the TME (12, 13). TLSs share similar structural and functional characteristics with secondary lymphoid organs (SLOs) (14). However, TLSs lack a capsule and can form in various nonlymphoid tissues, such as stroma and epithelium (15). The prognostic impact of TLSs has been widely explored and most reports have indicated that TLSs are associated with positive immunoreactivity and favorable clinical outcomes in most types of cancers (12, 16–20). For example, TLSs are shown to be associated with relapse-free survival in patients with oral carcinoma or early-stage hepatocellular carcinoma (21, 22). Moreover, germinal centers (GCs) in TLSs may determine the prognostic value of TLSs (23, 24). Even though, TLSs show an association with poor prognosis in a minority of studies (25–27). It is urgent to comprehensively illustrate the function of TLSs in the TME.

SLOs, such as lymph nodes (LNs), provide three-dimensional structures for immune cells to optimize cell-cell interactions and produce an effective immune response (28, 29). Effector T (Teff) cells are activated after being instructed by DCs, and migrate from external draining LNs into the tumor to exert their function (30, 31). Increasing studies have shown that the antitumor immune response originates not only in LNs but also directly in TLSs (32). In general, the cells and molecules that regulate the signaling underlying TLS formation and promote immune responses within TLS remain to be further studied. In this review, we briefly summarize the development of TLSs and focus on discussing the function of TLSs and multiple approaches that had been developed to induce TLS formation.

Abbreviations: TLSs, tertiary lymphoid structures; TILs, tumor-infiltrating lymphocytes; TME, tumor microenvironment; PD-1, programmed cell death protein-1; PD-L1, programmed death-ligand 1; SLOs, secondary lymphoid organs; GCs, germinal centers; HEVs, high endothelial venules; LN, lymph node; DCs, dendritic cells; Teff, effector T cell; FDCs, follicular DCs; PCs, plasma cells; PNAd, peripheral node addressing; TFH cells, T follicular helper cells; Treg cells, regulatory T cells; LTi, lymphoid tissue inducer; LT, lymphotoxin; LTβR, lymphotoxin-β receptor; IL, interleukin; ICB, immune checkpoint blockade; APCs, antigen-presenting cells; TGF-β, transforming growth factor-β; TNFR, tumor necrosis factor receptor; TNF-α, tumor necrosis factor-α; ACT, adoptive cell transfer; VEGF, vascular endothelial growth factor; VTP, vascular targeting peptide; TLRs, Toll-like receptors; IFN-γ, interferon-gamma; ILC3s, group 3 innate lymphoid cells; CTL, cytotoxic T lymphocyte; PLG, poly (lactide-coglycolide); TRAIL, TNF-related apoptosis-inducing ligand; MDSCs, myeloid-derived suppressor cells; GM-CSF, granulocyte-macrophage colony-stimulating factor; ICAM-1, intercellular cell adhesion molecule 1; VCAM1, vascular cell adhesion molecule 1; MADCAM1, mucosal addressable cell adhesion molecule 1.

DEVELOPMENT AND FORMATION OF TLSS

SLO development is a highly organized process that is initiated and continued during embryogenesis, which has similarities to TLS formation and provides a classical model for understanding TLS development (33). However, there are some differences between the canonical SLOs and TLSs. A chronic inflammatory state is sufficient to induce TLS formation even in the absence of lymphoid tissue inducer (LTi) cells (34), indicating that chronic inflammation may be an important factor that favors lymphoid neogenesis and promotes TLS formation (35). Some studies have revealed that DCs (36), T helper 17 (Th17) cells (37, 38), B cells (39), M1 macrophages (40), and T follicular helper (TFH) cells (41) can initiate TLS neogenesis in various pathological conditions. In addition, group 3 innate lymphoid cells (ILC3s) are associated with ectopic lymphoid aggregates (42). Tumor-infiltrating ILC3s may interact with fibroblasts and lung tumor cells to facilitate cytokine release, contributing to protective TLS formation (43). Lymphotoxin (LT) signaling plays a vital role in TLS formation (44, 45). The LTα1β2-LTβ receptor (LTβR) interaction initiates signaling that leads to the production of various chemokines and adhesion molecules, such as CCL19, CCL21, CXCL13, and CXCL12 (46). CCR7-expressing T cells are recruited by their homologous ligands CCL21 and CCL19, and this recruited population forms a T cell zone. In addition, B cells can express CXCR5 and CXCR4 on their surface to transmigrate to the follicle through the activity of the CXCL12-CXCR4 and CXCL13-CXCR5 axis (47, 48). These findings show that the CCL19/CCL21-CCR7 and CXCL13-CXCR5 axes are vital for regulating TLS development (49). Although the knowledge of TLS formation mechanisms is widely researched, the possible mechanisms and factors need to be further explored in future studies. The main molecular and cellular mechanisms of TLS formation are shown in **Figure 1**.

THE FUNCTION OF TLSS IN THE TME

Favorable Impact of TLSs on Antitumor Properties

Mature TLSs are similar to SLOs, which contain T cell-rich areas with $CD3^+$ T cells and dendritic cell (DC)-lysosomal associated membrane $protein^+$ (DC-LAMP) mature DCs and follicular $CD20^+$ B cell-rich zones (12). The B cell follicles in TLSs comprise follicular dendritic cells (FDCs), B cells, plasmablasts, and TFH cells required for GC formation and B cell differentiation (50). Macrophages, neutrophils, and regulatory T (Treg) cells have been discovered in the TLSs of lung cancer, pancreatic cancer, and ovarian cancer (51–54). TLSs are divided into classical and nonclassical structures. Classical structures are mature and contain T cells, DCs, B cells, and FDC compartments

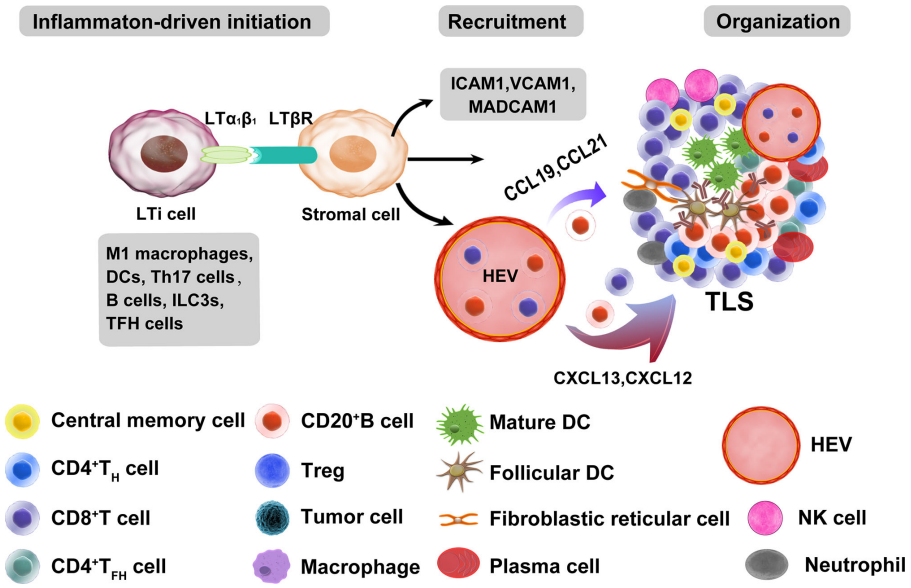

FIGURE 1 | Main molecular and cellular mechanisms of TLS formation in tumors. The development of TLSs is similar to that of SLOs. A chronic inflammatory state is sufficient to induce TLS formation in the absence of lymphoid tissue inducer (LTi) cells. Many immune cells can be used as LTi cells, such as B cells, DCs, M1 macrophages, Th17 cells, ILC3s, and TFH cells. Immune and stromal cell cross-talk mediates TLS formation mainly through the binding of lymphotoxin (LT) αβ and LTβR, which can further release many chemokines (CXCL13, CXCL12, CCL21, and CCL19) and adhesion molecules (VCAM1, ICAM1, and MADCAM1). These chemokines recruit lymphocytes from HEVs and form T and B cell zones. ILC3s, group 3 innate lymphoid cells; VCAM1, vascular cell adhesion molecule 1; ICAM1, intercellular adhesion molecule 1; MADCAM1, mucosal addressable cell adhesion molecule 1.

and comprise more active components than nonclassical structures, mainly B cells. Nonclassical TLSs usually contain B cells that are less activated than those in classical structures (14). TLSs are distributed intratumorally and peritumorally and are more abundant in the invasive margin than in the tumor core (12). Intratumoral TLSs may have greater prognostic significance, but this has not been widely established. In some studies, intratumoral TLSs are a favorable prognosticator in pancreatic cancer and hepatocellular carcinoma (20, 21). One study proposed a hypothesis to explain the better prognosis of intratumoral TLSs. Tumors with, rather than without, intratumoral TLSs are less invasive, especially regarding blood vessel invasion, and have a role related to the immune response. These tumors retain a relatively complete vascular network to transport immune cells and other molecules into the tumor and initiate a more effective antitumor immune response (17).

Increasing evidence shows that TLSs play an important role in controlling tumor invasion. Mature TLSs exhibit evidence for the formation of GCs (24) and GC B cells in TLSs are characterized by FDCs and $Ki67^+$ proliferating B cells (51). Oligoclonal B cell responses have been identified in melanoma, which suggests an active humoral antitumor response within TLSs that is driven by B cells (55). High PC counts are associated with higher numbers of TLSs and B cells in breast cancer and neck carcinomas (56, 57). PCs surrounded by TLSs are associated with the highest levels of TILs and cytotoxicity-related gene products in ovarian cancer. This study showed that $CD8^+$ TILs can predict prognosis only in combination with PCs, $CD20^+$ TILs, and $CD4^+$ TILs, suggesting that these four lymphocyte subsets work in concert to promote antitumor immunity, which indicates that TLSs may facilitate coordinated antitumor responses involving the combined actions of cytolytic T cells and PCs (58). B cells in TLSs are organized and highly differentiated and can produce tumor-specific antibodies in adenocarcinomas and ovarian cancer (59). In omental metastases from ovarian cancer, memory B lymphocytes essentially located within TLSs had higher clonality and somatic hypermutation rates, and they produced chemokines attracting DCs, T cells, and natural killer (NK) cells. The density of B cells also correlated with that of mature DCs in the stroma of tumors (53). Recent studies have shown the important role of TLSs and B cells in immunotherapy. The frequencies of memory B cells, PCs, and GC-like B cells in the tumors of responders treated with immune checkpoint blockade (ICB) therapy are significantly higher than those in nonresponders. Increased B cell proliferation indicating GC activity and formation within TLSs has been observed (60). High expression of B-lineage markers is associated with improved prognosis and TLS formation in sarcoma (61). B cells within TLSs can predict favorable prognosis in melanoma patients receiving ICB therapy. In addition, B cell-rich tumors are associated with elevated levels of initial and memory T cells. T cells in tumors without TLSs possess a dysfunctional molecular phenotype, which indicates that TLSs have a key role in the melanoma TME by conferring distinct T cell phenotypes (62). In summary, these studies demonstrate a major role of TLS-associated B cells in TLS function. B cells probably act together with key immune constituents of TLSs by altering T cell activation and function. Memory B cells may act as

antigen-presenting cells (APCs) to drive the expansion of both memory and naive T cell responses. B cells can also activate and recruit other immune effector cells by secreting an array of cytokines (60). The potential functions of TLSs in the TME are shown in **Figure 2**.

The existence of TLSs at metastatic tumor sites is the key factor in the level of TILs, which directly determines the antitumor effect (19). Moreover, the presence of TLSs led to increased infiltration and activation of T cells and other immune cells and was associated with a good prognosis in liver cancer and pancreatic carcinoma (21, 63, 64). There is evidence that TLSs can activate effector T cells in tumors (65). In MC38 tumors, T cells from TLSs exhibited a largely enhanced baseline level of IFN-γ (interferon-gamma) release. This finding revealed successful antitumor T cell priming activity within induced TLSs, and TLSs may act as immune factories where T cells activate effector cells to mediate synergistic antitumor effects (66). Studies of lung and ovarian cancers showed that TLS-associated DCs establish unique immune states characterized by a strong T helper (Th) 1 orientation and facilitate a good prognosis, indicating that antigen presentation allows local T cells to initiate responses to tumor-associated antigens in TLSs (67, 68). Whether TLS-associated DCs present tumor antigens directly to $CD8^+$ T cells or whether $CD4^+$ Th cells participate in the production of $CD8^+$ cytotoxic T cell responses in TLSs remains to be further studied. TFH cells produce CXCL13, potentially resulting in the formation of TLSs to trigger the GC B cell response (69). FDCs can also produce chemokines and cytokines involved in B cell proliferation and migration in LN, such as interleukin (IL) -6 and CXCL13 (70). B cells produce LTα1β2, which has a crucial function in the differentiation of FDCs within TLSs (71).

HEVs in TLSs are associated with T and B cell infiltration and indicate favorable outcomes in oral carcinoma and breast cancer (72, 73). The emergence of HEVs also contributes to the formation of TLSs (74). There is ample evidence that the function of HEVs in TLSs is similar to that in LNs, providing a channel for immune cells to accumulate in the tumor. HEVs in TLSs express molecules similar to those expressed in LNs, such as CCL21 and peripheral node addressing (PNAd), and cells

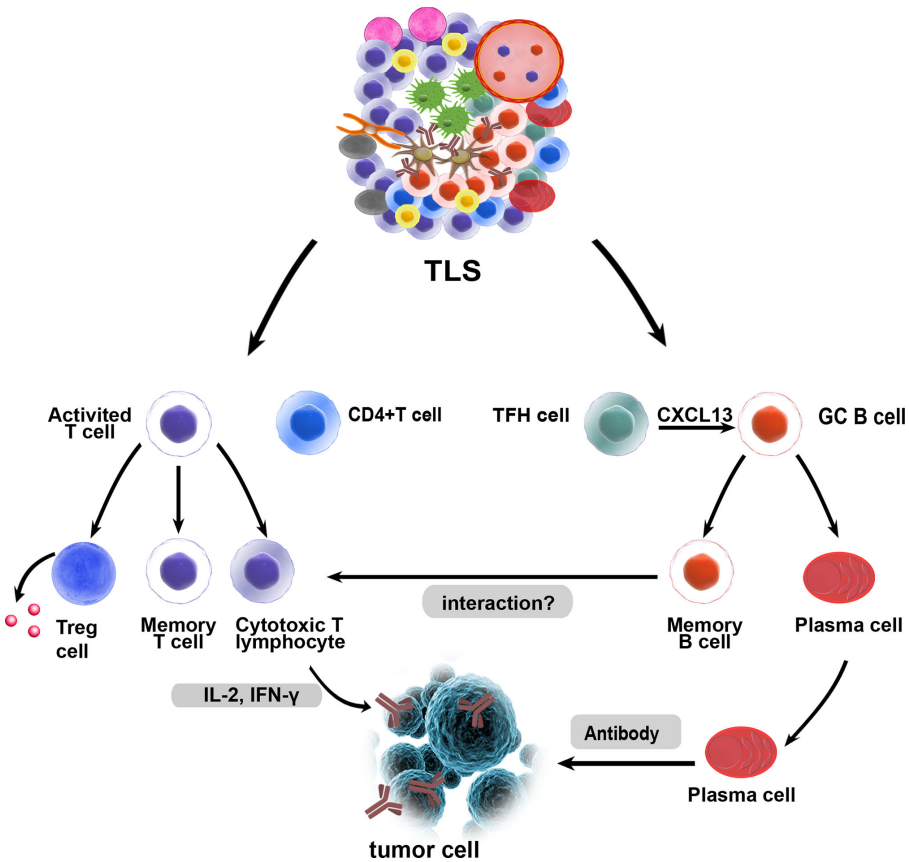

FIGURE 2 | Potential functions of tertiary lymphoid structures in the TME. As in canonical SLOs, TLSs may constitute a critical site where specific T and B cells can undergo terminal differentiation into effector cells. GC B cells can differentiate into memory B cells and plasma cells in TLSs, and fully differentiated B cells and exert their antitumor effects. T cells can differentiate and expand, and they are activated as effector cells that exert cytotoxic effects. B cells and T cells in TLSs may interact with each other and play a synergistic role, which needs to be confirmed by more studies. Treg cells within TLSs could exert a negative influence on the capacity of TLSs to generate effector and memory lymphocytes.

expressing CCR7 and L-selectin ligands for receptors on HEVs are found in TLSs (75). PNAd expression indicates that HEVs are essential for recruiting lymphocytes to lymphoid organs (76), an event that orchestrates the extravasation of Lselectin$^+$ and CCR7$^+$ immune cells into TLSs (77, 78). LTαβ plays a key role in PNAd expression in HEV (79). Single-cell analysis revealed the heterogeneity of HEVs in LN. LTβR signaling and inflammation also have crucial effects on HEV transcriptomes (80). However, the study showed that HEV neogenesis is dependent on tumor necrosis factor receptor (TNFR) rather than LTβR signaling in Treg-depleted tumors, suggesting another mechanism for HEV formation. The expression of PNAd is not dependent on the LTβR signal but is stimulated by activation of TNFR mediated by LTα3 derived from CD8$^+$ T cells (81). HEV formation is associated with increased T and B lymphocyte infiltration and activation in murine pancreatic cancer and breast cancer (82, 83). In mouse models of melanoma and lung cancer, the LN-like vasculature in tumors, characterized by the expression of PNAd and chemokine CCL21, induced by effector lymphocytes allows naive T cells to enter tumors and enhance antitumor immunity. Vasculogenesis is regulated by a mechanism involving CD8$^+$ T cells that secrete IFN-γ and LTα3 (84). In summary, T cells may contribute to the formation of the peripheral vasculature and HEV.

The Adverse Impact of TLSs on Tumors

Nevertheless, a few studies have indicated that TLSs have a negative impact on prognosis in colorectal cancer and breast cancer (25–27). The studies showed that TLSs that develop in the inflamed liver during hepatitis can function as a niche for tumor progenitor cells in hepatocellular carcinoma and are associated with an increased risk of late recurrence and decreased survival. It can be postulated that TLSs, which persist in the liver and are associated with a viral infection, play a different role than TLSs induced by tumors (25). Lymphoid aggregates are associated with more advanced diseases and indicate an adverse prognosis in colorectal cancers. These structures form in association with more advanced tumors, suggesting that they are a reaction to progressive tumor invasion, and their prognostic significance varies with disease progression and according to the inherent immunogenicity of the tumor (26). TLSs are associated with adverse prognosis in renal carcinoma with lung metastasis. TLSs are rarely found in lung metastasis of renal carcinoma, and studies speculated that the presence of T cells may not be educated in peritumoral TLSs but may reflect a chronic inflammatory response, which is known to be harmful to the host. At the same time, the high expression of vascular endothelial growth factor (VEGF) and IL-6 genes in renal carcinoma may also inhibit the differentiation of DCs, resulting in an impaired T cell response and poor prognosis (85). TLS Treg cells are detected in breast and colorectal cancers (86, 87). The decrease in the number of TLS Treg cells is associated with tumor regression in metastatic prostate cancer (88). Treg cells are present in TLSs in tumor-bearing lungs and exhibit activated phenotypes. Costimulatory ligand expression by DCs and T cell proliferation rates increased in TLSs after Treg cell depletion, enhancing the antitumor immune response. The reason may be that Treg cells in TLSs regulate DC function by reducing costimulatory levels, the immunosuppression of Treg cells to DCs is relieved after Treg cell depletion, and the TLS microenvironment may become more immunostimulatory to promote antitumor responses by T cells (54). The recruitment of Treg cells and myeloid-derived suppressor cells (MDSCs) to lymphoid aggregates in mouse B16 melanomas expressing CCL21 was found to correlate with the promotion of tumor growth (89). Therefore, TLS-associated Treg cells and MDSC presence may exert a negative influence on the capacity of TLSs to generate effector and memory lymphocytes.

DEVELOPMENT OF MULTIPLE APPROACHES TO INDUCE THE TLS FORMATION

A variety of LN modifications to improve the efficacy of tumor immunotherapy have been widely discussed and researched. Targeting LN can affect the efficacy of cancer vaccines, ICB therapy, and adoptive cell transfer (ACT) at the cellular level. Macroscopic biomaterials mimicking LN characteristics can be used as immune niches for cell reprogramming and *in vivo* transmission and can be used for preclinical testing of drugs and vaccines *in vitro* at the tissue level (90). TLSs may be the first line of T cell differentiation and expansion and are the key to inducing intratumoral immune sensitization in situ. Therefore, similar principles can be used for developing strategies to induce TLS formation, and a new antitumor immune strategy can be constructed. Although biomaterials for transporting or recruiting APCs can mimic the cellular characteristics of SLOs, other strategies aim to induce TLS formation specifically, as observed *in situ*. These strategies aim to mimic the chemokine and inflammatory signals of the main molecular and cellular mechanisms of TLS formation. In the next section, we discuss strategies that induce TLS formation through the delivery of chemokine-expressing cells or chemokines, implantation of biomaterial scaffolds containing these inflammatory factors and agents, and multiple therapeutic approaches.

Chemokines and Cytokines

A chemokine delivery strategy for TLSs provides a convenient way to generate ectopic lymphoid tissue in tumors. Recent electronic screening techniques involving the identification of TLS-related chemokine genes that induce lymphocyte chemotaxis have offered a framework for a more effective design of TLSs (91, 92). A 12-chemokine gene signature also provided a promising starting point for the potential construction of designed TLSs (93–96). In early studies, chemokines produced by lymphoid structures were expressed in various ways, which led to the formation of lymphoid tissue structures. For example, transgenic mice expressed B lymphocyte chemokines in pancreatic islets, and the expression of B lymphocyte chemokines resulted in the formation of LN-like structures that included HEVs, interstitial cells, and B and T cell zones and illustrated that the maintenance of B lymphocyte chemokine-induced lymphoid structures depends on LTβR

signaling (97). CCL21 exhibits a stronger capacity than CCL19 to induce more organized infiltrates in the islets of transgenic mice (98). Intratumoral injection of CCL21 facilitated lymphocyte infiltration into pancreatic tumors (99), and targeting lymphotoxin-α can induce lymphocyte infiltration and lymphoid-like tissue formation in B16 melanoma (100). LN-like lymphocyte infiltration was also found in transgenic mice expressing CCL21 driven by the thyroglobulin promoter in the thyroid gland and transgenic pancreas (101, 102). Type I interferon can also drive B cell recruitment by CXCR5–CXCL13 signaling and initiate ectopic GC formation within TLSs in pulmonary virus infection (103). In the salivary glands of adult mice, IL-7 regulates lymphatic vessel expansion and promotes the neogenesis of TLSs in the first phase, and LTβR signaling regulates TLS neogenesis in the second phase (104). Th17 cytokines can regulate TLS development and function. For instance, IL-22 modulates CXCL12, CXCL13, and IL-23 production, contributing to the formation of TLSs (105–107). In conclusion, these studies show that many chemokines and cytokines involved in lymphoid structure formation can be used as novel and feasible inducers in combination with other stimulants and multiple methods to induce the formation of TLSs.

LIGHT, the 14th member of the tumor necrosis factor superfamily (TNFSF14), is a protein primarily expressed on activated T cells and immature DCs (108). LIGHT can function as both a soluble and cell surface-bound type II membrane protein and interact with its two primary functional receptors: Herpes Virus Entry Mediator and LTβR (109). LIGHT can interact with Herpes Virus Entry Mediator and deliver co-stimulatory signals to T cells (44). LTβR is found on the surface of epithelial, stromal, and myeloid cells (110). LIGHT-LTβR signaling plays an important role in immune responses, functioning to repair tumor vasculature and to support effector cells cell trafficking to and infiltration into tumors (111). Recently, LTβR signal transduction induced by LIGHT has become a focus of the investigation. When combined with an anti-VEGF antibody, LIGHT can activate LTβR signaling and mediate chemokine production to recruit T cells (112). In pancreatic cancer, targeting LIGHT for homing to tumor vessels *via* a vascular targeting peptide (VTP), LIGHT-VTP showed a dual ability to induce TLS formation and regulate the angiogenic vasculature (83). LIGHT targeting to tumor vessels induces vessel normalization, and HEVs and TLS formation may occur through a self-amplifying loop in pancreatic cancer. The mechanism may involve the LIGHT-triggered expression of inflammatory cytokines in macrophages, such as IL-1β, IL-6, CXCL13, TNF, and CCL21, These chemokines further recruit T cells. Macrophages and T cells have been deemed essential for HEV and TLS formation (83, 113) (**Figure 3A**). LIGHT-VTP in combination with ICB therapy can produce intratumoral memory T cells and Teff cells and improve prognosis (114). In addition, LIGHT-VTP combined with anti-VEGF and ICB therapy can increase the frequency of HEVs and normalize tumor vessels and the accumulation of T cells in glioblastoma and lung metastases (115, 116). The LT-LIGHT axis provides key differentiation signals guiding the differentiation of the reticular network and vascular system, maintaining the mesenchymal differentiation pathway of the specialized network, and remodeling reactive LNs (117). The LTβR signaling pathway plays a critical role in HEV differentiation and function in LN (44). Because of the similarity between SLOs and TLSs, it is speculated that LTβR signaling is also involved in HEV differentiation and function in TLSs. Further studies are required to understand the precise mechanisms by which HEV formation in TLSs is induced and the effects of HEVs on different types of cancer. This knowledge may guide the therapeutic objectives of cancer interventions. Other means can also be used to deliver LIGHT to tumor sites, and the oncolytic activity of attenuated *Salmonella Typhimurium* was enhanced by the stable insertion of the gene encoding LIGHT. Attenuated *S. Typhimurium* expressing LIGHT inhibited the growth of primary tumors and the spread of lung metastasis (118). The findings suggest that avirulent bacteria can be used as targeted carriers for the local production of therapeutic proteins in tumors. In recent years, the potential use of exosomes in the treatment and control of many diseases has expanded because of their inherent characteristics in regulating complex intracellular pathways. The characteristics of exosomes can also be exploited to induce TLSs. Exosomes are extracellular vesicles derived from endosomes and have a diameter of approximately 40-160 nm. They can carry a variety of substances, such as proteins and DNA, to allow these substances to be absorbed by other cells (119, 120). Therefore, we hypothesize that exosomes can be used as carriers to load many chemokines and cytokines to induce the formation of TLSs.

Toll-like receptors (TLRs) have also been researched concerning TLS formation. Myofibroblasts were stimulated with TLR agonists and cytokines in giant cell arteritis, which upregulated B cell-activating factor and CXCL13 and resulted in the formation of TLSs (121). Inhalation of TLR9 agonists can generate profound remodeling of tumor-bearing lungs and lead to TLS formation in adjacent tumors (122). In addition, both the anti-HBV response to the TLR7 agonist GS-9620 and TLR4 agonists in mouse models of myasthenia gravis can induce TLS generation (123, 124). Transforming growth factor-β (TGF-β) plays a noncanonical role in coordinating immune responses against ovarian cancer. $CD8^+$ T cells in the presence of TGF-β upregulate the secretion of CD103 and CXCL13, and $CD8^+$ TILs play a role in mediating B cell recruitment and TLS formation (125).

Cells

An alternative approach to produce TLSs is to deliver cells that express chemokines or to engineer chemokines that are associated with lymphomagenesis. DC-based therapeutic strategies can be used therapeutically to promote the extranodal priming of antitumor immunity (126). DCs expressing T cell chemokines were injected into melanoma tumors, which yielded rapid T cell infiltration and initiation of intratumor responses (127). Additionally, intraperitoneal injection of murine DCs promoted the acute infiltration of immature T cells and NK cells into the TME, an effect related to upregulated expression of NK and T cell recruitment chemokines by murine DCs (128). DCs engineered to overexpress T-bet suppressed the growth of sarcomas *in vivo* after intratumoral injection and prolonged the overall survival of mice (126, 128). DCs promote LT signaling through LTβR for HEV

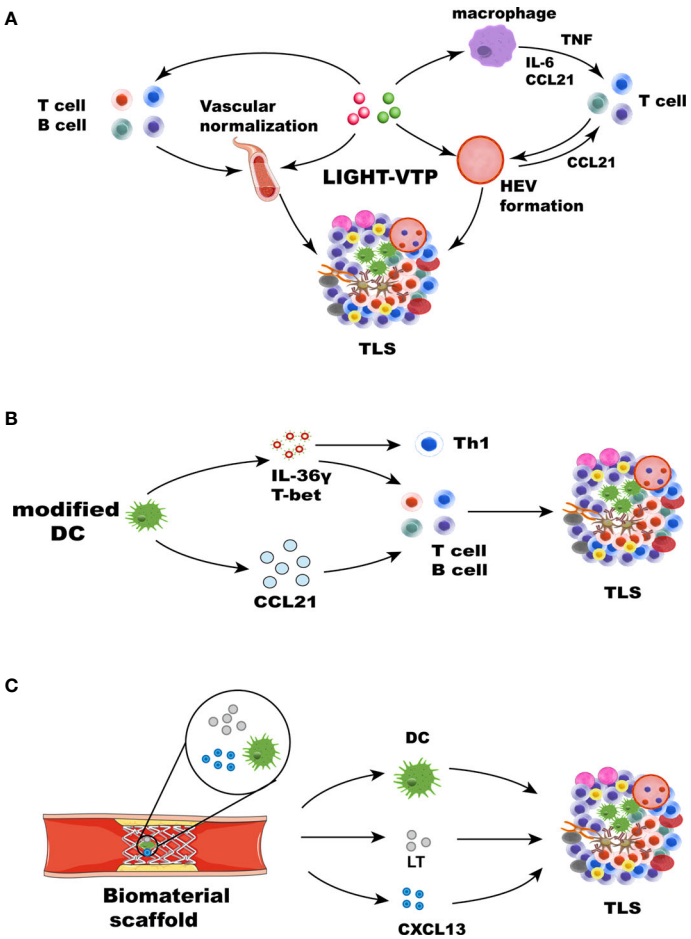

FIGURE 3 | Strategies for therapeutic induction of TLS formation. TLS inducers, such as chemokines, cytokines, DCs, and therapeutic approaches, can induce TLS formation in different ways. **(A)** Cytokines and chemokines involved in lymphogenesis, including LIGHT, CCL21, CXCL13, LT, and IFN-γ, can lead to the formation of TLSs. LIGHT-VTP targeting tumor vessels can induce vessel normalization, and HEV and TLS formation may occur through a self-amplifying loop. The mechanism may be related to the LIGHT-triggered expression of the inflammatory cytokines IL-6, TNF, and CCL21 in macrophages. These chemokines can recruit T cells. Macrophages and T cells play an important role in the formation of HEVs and TLSs (83). HEV formation and vascular normalization can also recruit more immune cells. **(B)** Some immune cells, such as modified DCs and stromal cells, leading to the formation of TLSs. DCs engineered to secrete IL-36γ also initiate therapeutic TLS formation, which can upregulate the expression of T-bet. T-bet and IL-36γ cooperate to reinforce their expression and recruit immune cells, leading to TLS formation. DCs modified with the CCL21 gene can significantly increase T cell infiltration. Activated DCs can also upregulate many factors associated with TLS formation. **(C)** Biomaterials can provide 3D scaffolds in *situ* and deliver cells and chemokines. Collagen scaffolds containing LT, CCL21, CXCL13, and activated DCs were transplanted into mice. The recruited lymphocytes can form artificial lymph node structures.

differentiation and function in LN (129). DCs, which coordinate adaptive immune responses, have historically been a promising target. DCs are a source of LT, and homeostatic chemokines (CXCL12, CXCL13, CCL19, and CCL21) are known to contribute to TLS formation in the lungs of influenza virus-infected mice. Similar to the depletion of DCs, blockade of LTβR signaling after virus clearance leads to the disintegration of TLSs and GC reactions. It is suggested that the DC-mediated LTBR pathway contributes to the formation of TLSs (36). Other methods have focused on modifying and editing DCs to express the transcription factor T-bet and secrete IL-36γ to play a vital role. IL-36 cytokines are an IL-1 subfamily consisting of three agonists that signal through the common heterodimeric receptor IL-36R (130), which is expressed on endothelial cells and many immune cells, including T cells and DCs (131). IL-36γ is involved in polarizing type-1 immune responses. It is a downstream target of the type-1 transactivator T-bet and can induce T-bet expression in target cells (132). Research has shown that IL-36γ predominantly expressed by M1 macrophages and vasculature cells, including smooth muscle cells and HEVs, mediates polarization toward a type 1 immune response. This pattern of IL-36γ expression increased $CD4^+$ central memory T cell infiltrate and the density of B cells and led to TLS formation in human colorectal cancer (133). The injection of tumors with DCs engineered to secrete a bioactive form of mIL-36γ also initiated therapeutic TLS formation and slowed tumor progression in a mouse model of colorectal carcinoma. Furthermore, DC.IL-36γ cells show strongly upregulated expression of T-bet, suggesting that T-bet and IL-36γ cooperate to reinforce each other's expression in

DCs, rendering them competent to promote TLS formation in the therapeutic TME (134) (**Figure 3B**). In lung cancer, autologous DCs transduced with an adenoviral vector modified with the CCL21 gene significantly reduced the tumor load and T cell infiltration (135), accompanied by enhanced expression of IFN-γ, IL-12, and CXCL10, as well as molecules related to reduced immunosuppression in the TME (136). Mice vaccinated with DCs charged with apoptotic/necrotic B16 cells are protected against B16 challenge, and TLSs form at the vaccination site (137). In conclusion, DCs play an important role in inducing TLS formation. These results provide a framework for the usage of DCs. Promoting the expression of multiple chemokines by targeting DCs is a valuable strategy to induce TLS formation.

LTi-like cells from newborn mouse LNs were injected intradermally into adult mice and formed TLSs in the skin, and the results indicated that hyperactivated lymphocytes can fulfill the role of LTi cells during inflammatory responses (138). Subcutaneous injection of the LN-derived stromal cell line resulted in the formation of TLSs that promote infiltration of immune cell subsets and inhibit tumor growth by improving the antitumor activity of TILs (66). Lymphoid tissue-like organoids were constructed by transplantation of stromal cells embedded in biocompatible scaffolds into the renal subcapsular space in mice. The structure is similar to that of SLOs and contains clusters of B and T cells and HEVs, DCs, and FDC networks (139). Other cells, such as immune fibroblasts, bone marrow mesenchymal stem cells (MSCs), adipocytes, and macrophages, also play their roles. Research on autoimmune conditions demonstrated that external triggers at mucosal sites can induce gradual differentiation of stromal cell populations into immune fibroblast networks, which supports the establishment of TLSs at an early stage. This process is mediated mainly by paracrine and autocrine signals regulated by IL-13. Once lymphocytes are recruited, the initial fibroblast network is expanded by local production of IL-22 and lymphotoxin. This finding demonstrates the role of immune fibroblasts in maintaining TLS and supporting their formation and identifies new therapeutic targets (140). Human MSCs stimulated with TNF-α and IL-1β significantly increased the expression of CCL19, VCAM1, ICAM1. Stimulated MSCs can induce $CD4^+$ T cell proliferation. MSCs could play a key role as LTo cells in promoting the early inflammatory and initiating the formation of kidney-specific TLSs (141). Mucosa-resident $CXCL13^+CX3CR1^{hi}$ macrophages are responsible for recruiting B cells and $CD4^+$ T cells to sites of *Salmonella* invasion and subsequently activating them, resulting in TLS formation and a local pathogen-specific IgA response (142). Recently, the combination of TNF-α and lipopolysaccharide was shown to directly induce adipocytes to produce TLS-related chemokines, thereby coordinating the formation of functional TLSs in the mesentery affected by Crohn's disease (143). In summary, these studies have further proved the various initiating factors and mechanisms of the formation of TLSs and provided more references and insights for inducing the TLS formation.

Biomaterials

Biomaterials can support the formation of TLSs by locally and controllably releasing chemokines and providing cellular support. Scaffolds are usually three-dimensional microporous structures designed to achieve cell encapsulation *in vitro* or cell penetration *in vivo* while providing mechanical support, cell adhesion capability, and a continuous supply of biological cues to promote cell migration and interaction (144). Biomaterial scaffolds can boost the efficacy of immunotherapies, such as cancer vaccines and ACT (145–147). For instance, biomaterials loaded with signaling molecules and engineered T cells have been evaluated *in vitro*. These biomaterials were surgically implanted near the tumor or under a resected tumor bed, where they maintained continuous proliferation and release of specific T cells (148).

In early cases, collagen scaffolds containing both thymus-derived stromal cells expressing LTα and activated DCs were transplanted into the renal subcapsular space of mice. The recruited lymphocytes formed artificial lymph nodes (ALN) structures, which contained FDC, T cell, and B cell regions and HEV-like structures. ALN induced a potent immune response *in vivo* and the accumulation of memory and effector T and B cells. The engineered structures elicited a humoral response after vaccination and could be transplanted into immunodeficient mice to secrete antibodies after secondary immunization (139, 149, 150) (**Figure 3C**). Based on this strategy, cell-free biomaterials have been explored. Hydrogels can provide a controlled cellular microenvironment for immune cells so that they can be recruited, expanded, and activated *in vitro* and *in vivo* (151). Hydrogels can be used to deliver antigens, chemokines, and other factors to DCs and induce T and B cell responses, and they can effectively encapsulate immunomodulators and immune cells. DCs can be activated *in vitro* in hydrogels before implantation and can be recruited and activated in gels by immobilized stimulators, as in a bioreactor (152, 153). In another study, collagen sponge scaffolds embedded with sustained-release gel beads containing LTα1β2, and many chemokines were transplanted into the subcapsular space of mice to establish ALN-like TLSs, recruiting memory T cells and B cells and induced a strong antigen-specific immune response (154). A synthetic immune priming center consisting of an *in situ* cross-linking hydrogel delivering chemokines and particles loaded with DNA and siRNA can attract numerous DCs and can both generate a strong transition to a T helper 1 response and increase the cytotoxic T lymphocyte (CTL) response. The multimode injectable system can simultaneously deliver chemokines, DNA, and siRNA antigens to DCs. This system constitutes a novel strategy to regulate immunotherapy *in situ* and could provide an effective vaccine strategy to prevent cancer (155).

Other biomaterials include polylactide-coglycolide (PLG), nano-sapper, and nanoparticles. A macroporous PLG matrix was used to deliver granulocyte-macrophage colony-stimulating factor (GM-CSF), tumor antigens, and danger signals *in vivo*. GM-CSF recruited DCs and significantly enhanced their homing to LNs, and danger signals and cancer antigens further activated the recruited DCs. These materials elicited protective antitumor immunity and showed prospects as cancer vaccines (156). A study demonstrated improved immune function by targeting DCs with adjuvant vector cells engineered from MKT cell ligands loaded with tumor antigen mRNAs. This method also enhanced the local immune response *via*

TLS formation (157). Importantly, these polymers may be designed to program the transport of various types of cells *in vivo*. Nano-sapper was co-loaded with an antifibrotic protein and a plasmid expressing LIGHT. By normalizing the tumor vasculature, reducing collagen deposition, and stimulating the expression of lymphocyte-recruiting chemokines, Nano-sapper induces TLS formation to promote CTL infiltration and remodel the TME (158). Recognition of ectopic HEVs in human pancreatic ductal adenocarcinoma by engineered MECA79-coated nanoparticles can increase the transport of Taxol to the tumor and distinctly reduce tumor growth (159). Nanomaterials are promising for inducing TLS formation. Local delivery of engineered biomaterials can play a role by establishing synthetic immune niches to enhance antitumor immunity. Immunotherapy based on biomaterials will facilitate the development of the next generation of tumor therapies.

Other Therapeutic Approaches

Multiple cancer therapeutic strategies, such as cancer vaccines, ICB therapy, antiangiogenic therapy, radiotherapy, and chemotherapy, contribute to TLS formation. After therapeutic vaccination against human papillomavirus serotype 16 with E6/E7 antigens, significant immune changes in the TME were observed in subjects with CIN2/3, and TLSs formed in the immune-infiltrated cervical tissues. At the molecular level, these histological changes in the matrix were characterized by increased gene expression and associated with immune activation (CXCR3) and effector function (T-bet and IFN-β) (160). A prominent study of patients with resected pancreatic cancer showed that 33 of the 39 patients treated with the GM-CSF vaccine exhibited TLS formation after 2 weeks. Further analysis showed that these structures could regulate adaptive immunity. Inhibition of the Treg signaling pathway and enhancement of the Th17 signaling pathway in TLS aggregates were associated with increased survival and intratumoral Teff: Treg ratios and upregulation of the mechanism of immunosuppression (161). The findings help to guide the production of the next generation of effective cancer vaccines and facilitate better responses to ICB therapy. TLSs containing lymphocytes and APCs appeared in all 11 patients who received cisplatin neoadjuvant chemotherapy in a study on hepatoblastoma, indicating that cisplatin can induce TLS infiltration and synergistically induce the death of immunogenic cells and trigger an antitumor immune response. This may involve so-called immunogenic cell death, a controlled cell death process that produces damage-associated molecular patterns that can be used as adjuvants to initiate an immune response through the recruitment and activation of DCs (162). Administration of preoperative chemoradiotherapy (neoadjuvant chemotherapy, NAC) was associated with increased TLS formation and may affect the immunological composition of the TME and confer a favorable prognosis in patients with pancreatic ductal adenocarcinoma (163). However, corticosteroid therapy during chemotherapy impaired GC formation and reduced TLS prognostic value in patients with lung cancer (164). After radiotherapy, apoptosis in tumors with TLSs increased significantly. The TLSs also showed an acute increase in apoptosis and size reduction. Although their size tended to normalize after 2 weeks, the apoptotic rate remained high, suggesting active and continuous proliferation in residual irradiated cells and providing them with a window to optimize their unique function (165). Low-dose stimulator of interferon genes (STING) agonist treatment can upregulate the expression of various cytokines and increase the infiltration of T cells and DCs to establish a proinflammatory TME, which can also lead to normalization of the tumor vasculature, ultimately inducing the formation of TLSs and controlling tumor growth. Stimulating DC maturation and local production of vascular normalization-promoting and TLS-promoting factors, such as CCL19, CCL21, LTα, LTβ, and LIGHT (166). A study showed that Treg elimination can activate $CD8^+$ T cells and promote the development of HEVs in tumors. The study proposed a model in which a positive feedback loop of T cell activation by Treg cell depletion can promote HEV development, T cell infiltration, and tumor destruction (81). A prostate cancer study showed that Treg cells and cyclooxygenase 2 are attractive therapeutic targets that can be used to strengthen TLS-driven tumor immunity. In particular, the existence of HEVs and lymphatic vessels suggests that TLSs can also be used as a platform for cell-based or cyclooxygenase 2 blockade therapy to control tumor growth (88).

$PD\text{-}L1^+$, $PD\text{-}L2^+$, $LAG3^+$, and $TIM3^+$ cells were detected in some breast cancer-related TLSs, and PD-1 was used as a marker of T cell activity in both the T and B cell areas in TLSs. The expression levels of immune checkpoint molecules were associated with the level of TILs and TLS formation (167). In a group of patients with renal carcinoma, the low expression of immune checkpoints and the localization of mature DCs in TLSs are associated with a better prognosis (168) (NCT03387761). Recently, some prominent studies have shown that B cell and TLS formation promote the immunotherapy response in patients with melanoma and sarcoma after ICB therapy (60–62). In a study of locoregionally advanced urothelial carcinoma, the formation of TLSs was observed in responding patients after treatment with combined CTLA-4 and PD-1 blockade therapy, which could be an effective preoperative treatment strategy (169). Another study compared the metabolic, transcriptional, and functional characteristics of intratumoral $CD8^+$ T cell subtypes with high, moderate, and no PD-1 expression from patients with non-small cell lung carcinoma. $PD\text{-}1^+$ high T lymphocytes produce CXCL13, which mediates the recruitment of immune cells to TLSs and has the potential to be predicted after treatment with PD-1 blockade therapy (170). Combination therapy with anti-VEGFR2 and anti-PD-L1 antibodies can induce HEV formation in pancreatic and breast cancer. LTβR signaling plays an important role in the generation and activation of tumor HEVs. HEV formation can increase the activity of CTLs, which makes tumors sensitive to ICB therapy (82). An anti-mouse LTβR agonistic antibody increased TIL infiltration in a mouse model of colon cancer. Agonistic monoclonal antibodies targeting LTβR are a novel method for treating colorectal cancer and potentially other types of cancer (171). Considering that the formation of TLSs is strongly related to the LTBR signaling pathway, targeting LTβR can also be used as an approach to induce TLS formation and enhance antitumor immunity.

TLSs formation induced by multiple therapeutic strategies may involve a complex network of mechanisms, such as various types of cells, chemokines, and molecular mechanisms. We speculate that the main reason for TLS formation may be that the immune suppression in the TME is relieved after multiple therapeutic strategies, and the function of many immune cells can be restored. These cells interact with each other to activate LTβR signaling and other pathways and induce the production of various chemokines and cytokines, which can ultimately lead to the formation of TLSs. TLSs formation further enhances antitumor immunity, which may explain why the existence of TLSs is related to a more favorable prognosis after therapy.

CONCLUSION AND FUTURE PERSPECTIVES

In summary, current research has revealed the significance of TLSs in tumor immunotherapy. TLSs may constitute a privileged niche for educating T cells and B cells, which can activate and enhance immune responses. Although the major cellular and molecular mechanisms of TLSs have been elucidated, how to utilize them as an important part of the immune-related cancer control strategy is still being developed. Targeting the molecular pathways of TLSs development to induce formation is a promising immunotherapeutic strategy, which may directly enhance the antitumor response in situ. HEV induction therapy deserves more research in the design of new immunotherapies, and a more in-depth understanding of the mechanisms in terms of the types of cytokines and chemokines leading to the formation of HEVs in different types of cancer is needed. In the future, we need to focus on the combination of methods inducing HEV and TLSs formation with new therapeutic strategies that can alleviate immunosuppression, such as chemotherapies, radiotherapies, and ICB therapies. These strategies may promote the formation of TLSs as well to synergistically enhance adaptive immunity and provide insight into ultimately effective immune-mediated tumor control.

AUTHOR CONTRIBUTIONS

Conceptualization: WK and ZH. Writing original draft: WK. Supervision: ZF and PR. All authors contributed to the article and approved the submitted version.

FUNDING

This work was supported by funding from the National Natural Science Foundation of China [grant numbers: 82071986, 81771827] and the Province Natural Science Foundation of Hunan [grant numbers: 2020JJ4855, 2020JJ4841].

REFERENCES

1. Sautès-Fridman C, Cherfils-Vicini J, Damotte D, Fisson S, Fridman WH, Cremer I, et al. Tumor Microenvironment is Multifaceted. *Cancer Metastasis Rev* (2011) 30(1):13–25. doi: 10.1007/s10555-011-9279-y
2. Maman S. Witz IP. A History of Exploring Cancer in Context. *Nat Rev Cancer* (2018) 18(6):359–76. doi: 10.1038/s41568-018-0006-7
3. Paijens ST, Vledder A, de Bruyn M, Nijman HW. Tumor-Infiltrating Lymphocytes in the Immunotherapy Era. *Cell Mol Immunol* (2020) 18 (4):842–59. doi: 10.1038/s41423-020-00565-9
4. Schumacher TN, Schreiber RD. Neoantigens in Cancer Immunotherapy. *Sci (New York NY)* (2015) 348(6230):69–74. doi: 10.1126/science.aaa4971
5. Topalian SL, Weiner GJ, Pardoll DM. Cancer Immunotherapy Comes of Age. *J Clin Oncol* (2011) 29(36):4828–36. doi: 10.1200/JCO.2011.38.0899
6. Wei SC, Levine JH, Cogdill AP, Zhao Y, Anang N-AAS, Andrews MC, et al. Distinct Cellular Mechanisms Underlie Anti-CTLA-4 and Anti-PD-1 Checkpoint Blockade. *Cell* (2017) 170(6):1120–33.e17. doi: 10.1016/j.cell.2017.07.024
7. Christofi T, Baritaki S, Falzone L, Libra M, Zaravinos A. Current Perspectives in Cancer Immunotherapy. *Cancers* (2019) 11(10):1472. doi: 10.3390/cancers11101472
8. Feng Z, Rong P, Wang W. Meta-Analysis of the Efficacy and Safety of PD-1/PD-L1 Inhibitors Administered Alone or in Combination With Anti-VEGF Agents in Advanced Hepatocellular Carcinoma. *Gut* (2020) 69(10):1904–6. doi: 10.1136/gutjnl-2019-320116
9. Devalaraja S, To TKJ, Folkert IW, Natesan R, Alam MZ, Li M, et al. Tumor-Derived Retinoic Acid Regulates Intratumoral Monocyte Differentiation to Promote Immune Suppression. *Cell* (2020) 180(6):1098–114.e16. doi: 10.1016/j.cell.2020.02.042
10. Thommen DS. Schumacher TN. T Cell Dysfunction in Cancer. *Cancer Cell* (2018) 33(4):547–62. doi: 10.1016/j.ccell.2018.03.012
11. Togashi Y, Shitara K, Nishikawa H. Regulatory T Cells in Cancer Immunosuppression - Implications for Anticancer Therapy. *Nat Rev Clin Oncol* (2019) 16(6):356–71. doi: 10.1038/s41571-019-0175-7
12. Sautès-Fridman C, Petitprez F, Calderaro J, Fridman WH. Tertiary Lymphoid Structures in the Era of Cancer Immunotherapy. *Nat Rev Cancer* (2019) 19(6):307–25. doi: 10.1038/s41568-019-0144-6
13. Di Caro G, Castino GF, Bergomas F, Cortese N, Chiriva-Internati M, Grizzi F, et al. Tertiary Lymphoid Tissue in the Tumor Microenvironment: From its Occurrence to Immunotherapeutic Implications. *Int Rev Immunol* (2015) 34(2):123–33. doi: 10.3109/08830185.2015.1018416
14. Rodriguez AB, Engelhard VH. Insights Into Tumor-Associated Tertiary Lymphoid Structures: Novel Targets for Antitumor Immunity and Cancer Immunotherapy. *Cancer Immunol Res* (2020) 8(11):1338–45. doi: 10.1158/2326-6066.CIR-20-0432
15. Pimenta EM, Barnes BJ. Role of Tertiary Lymphoid Structures (TLS) in Anti-Tumor Immunity: Potential Tumor-Induced Cytokines/Chemokines That Regulate TLS Formation in Epithelial-Derived Cancers. *Cancers* (2014) 6(2):969–97. doi: 10.3390/cancers6020969
16. Munoz-Erazo L, Rhodes JL, Marion VC, Kemp RA. Tertiary Lymphoid Structures in Cancer - Considerations for Patient Prognosis. *Cell Mol Immunol* (2020) 17(6):570–5. doi: 10.1038/s41423-020-0457-0
17. Hiraoka N, Ino Y, Yamazaki-Itoh R. Tertiary Lymphoid Organs in Cancer Tissues. *Front Immunol* (2016) 7:244. doi: 10.3389/fimmu.2016.00244
18. Li K, Guo Q, Zhang X, Dong X, Liu W, Zhang A, et al. Oral Cancer-Associated Tertiary Lymphoid Structures: Gene Expression Profile and Prognostic Value. *Clin Exp Immunol* (2020) 199(2):172–81. doi: 10.1111/cei.13389
19. Lee M, Heo S-H, Song IH, Rajayi H, Park HS, Park IA, et al. Presence of Tertiary Lymphoid Structures Determines the Level of Tumor-Infiltrating Lymphocytes in Primary Breast Cancer and Metastasis. *Mod Pathol* (2019) 32(1):70–80. doi: 10.1038/s41379-018-0113-8
20. Hiraoka N, Ino Y, Yamazaki-Itoh R, Kanai Y, Kosuge T, Shimada K. Intratumoral Tertiary Lymphoid Organ Is a Favourable Prognosticator in Patients With Pancreatic Cancer. *Br J Cancer* (2015) 112(11):1782–90. doi: 10.1038/bjc.2015.145
21. Li H, Wang J, Liu H, Lan T, Xu L, Wang G, et al. Existence of Intratumoral Tertiary Lymphoid Structures Is Associated With Immune Cells Infiltration

and Predicts Better Prognosis in Early-Stage Hepatocellular Carcinoma. *Aging (Albany NY)* (2020) 12(4):3451–72. doi: 10.18632/aging.102821
22. Li Q, Liu X, Wang D, Wang Y, Lu H, Wen S, et al. Prognostic Value of Tertiary Lymphoid Structure and Tumour Infiltrating Lymphocytes in Oral Squamous Cell Carcinoma. *Int J Oral Sci* (2020) 12(1):24. doi: 10.1038/s41368-020-00092-3
23. Posch F, Silina K, Leibl S, Mündlein A, Moch H, Siebenhüner A, et al. Maturation of Tertiary Lymphoid Structures and Recurrence of Stage II and III Colorectal Cancer. *Oncoimmunology* (2018) 7(2):e1378844. doi: 10.1080/2162402X.2017.1378844
24. Siliņa K, Soltermann A, Attar FM, Casanova R, Uckeley ZM, Thut H, et al. Germinal Centers Determine the Prognostic Relevance of Tertiary Lymphoid Structures and Are Impaired by Corticosteroids in Lung Squamous Cell Carcinoma. *Cancer Res* (2018) 78(5):1308–20. doi: 10.1158/0008-5472.CAN-17-1987
25. Finkin S, Yuan D, Stein I, Taniguchi K, Weber A, Unger K, et al. Ectopic Lymphoid Structures Function as Microniches for Tumor Progenitor Cells in Hepatocellular Carcinoma. *Nat Immunol* (2015) 16(12):1235–44. doi: 10.1038/ni.3290
26. Bento DC, Jones E, Junaid S, Tull J, Williams GT, Godkin A, et al. High Endothelial Venules are Rare in Colorectal Cancers But Accumulate in Extra-Tumoral Areas With Disease Progression. *Oncoimmunology* (2015) 4 (3):e974374. doi: 10.4161/2162402X.2014.974374
27. Figenschau SL, Fismen S, Fenton KA, Fenton C, Mortensen ES. Tertiary Lymphoid Structures Are Associated With Higher Tumor Grade in Primary Operable Breast Cancer Patients. *BMC Cancer* (2015) 15:101. doi: 10.1186/s12885-015-1116-1
28. Willard-Mack CL. Normal Structure, Function, and Histology of Lymph Nodes. *Toxicol Pathol* (2006) 34(5):409–24. doi: 10.1080/01926230600867727
29. Rosenberg SA. Cancer Immunotherapy Comes of Age. *Nat Clin Pract Oncol* (2005) 2(3):115. doi: 10.1038/ncponc0101
30. Menares E, Gálvez-Cancino F, Cáceres-Morgado P, Ghorani E, López E, Díaz X, et al. Tissue-Resident Memory CD8 T Cells Amplify Anti-Tumor Immunity by Triggering Antigen Spreading Through Dendritic Cells. *Nat Commun* (2019) 10(1):4401. doi: 10.1038/s41467-019-12319-x
31. Garris CS, Arlauckas SP, Kohler RH, Trefny MP, Garren S, Piot C, et al. Successful Anti-PD-1 Cancer Immunotherapy Requires T Cell-Dendritic Cell Crosstalk Involving the Cytokines IFN-γ and IL-12. *Immunity* (2018) 49 (6):1148–61.e7. doi: 10.1016/j.immuni.2018.09.024
32. Drayton DL, Liao S, Mounzer RH, Ruddle NH. Lymphoid Organ Development: From Ontogeny to Neogenesis. *Nat Immunol* (2006) 7 (4):344–53. doi: 10.1038/ni1330
33. Jones GW, Hill DG, Jones SA. Understanding Immune Cells in Tertiary Lymphoid Organ Development: It Is All Starting to Come Together. *Front Immunol* (2016) 7:401. doi: 10.3389/fimmu.2016.00401
34. Furtado GC, Pacer ME, Bongers G, Bénézech C, He Z, Chen L, et al. Tnfα-Dependent Development of Lymphoid Tissue in the Absence of Rorγt$^+$ Lymphoid Tissue Inducer Cells. *Mucosal Immunol* (2014) 7(3):602–14. doi: 10.1038/mi.2013.79
35. Luo S, Zhu R, Yu T, Fan H, Hu Y, Mohanta SK, et al. Chronic Inflammation: A Common Promoter in Tertiary Lymphoid Organ Neogenesis. *Front Immunol* (2019) 10:2938. doi: 10.3389/fimmu.2019.02938
36. GeurtsvanKessel CH, Willart MA, Bergen IM, van Rijt LS, Muskens F, Elewaut D, et al. Dendritic Cells Are Crucial for Maintenance of Tertiary Lymphoid Structures in the Lung of Influenza Virus-Infected Mice. *J Exp Med* (2009) 206(11):2339–49. doi: 10.1084/jem.20090410
37. Peters A, Pitcher LA, Sullivan JM, Mitsdoerffer M, Acton SE, Franz B, et al. Th17 Cells Induce Ectopic Lymphoid Follicles in Central Nervous System Tissue Inflammation. *Immunity* (2011) 35(6):986–96. doi: 10.1016/j.immuni.2011.10.015
38. Grogan JL, Ouyang W. A Role for Th17 Cells in the Regulation of Tertiary Lymphoid Follicles. *Eur J Immunol* (2012) 42(9):2255–62. doi: 10.1002/eji.201242656
39. Lochner M, Ohnmacht C, Presley L, Bruhns P, Si-Tahar M, Sawa S, et al. Microbiota-Induced Tertiary Lymphoid Tissues Aggravate Inflammatory Disease in the Absence of RORgamma T and LTi Cells. *J Exp Med* (2011) 208 (1):125–34. doi: 10.1084/jem.20100052
40. Guedj K, Khallou-Laschet J, Clement M, Morvan M, Gaston A-T, Fornasa G, et al. M1 Macrophages Act as Ltβr-Independent Lymphoid Tissue Inducer Cells During Atherosclerosis-Related Lymphoid Neogenesis. *Cardiovasc Res* (2014) 101(3):434–43. doi: 10.1093/cvr/cvt263
41. Jones GW, Jones SA. Ectopic Lymphoid Follicles: Inducible Centres for Generating Antigen-Specific Immune Responses Within Tissues. *Immunology* (2016) 147(2):141–51. doi: 10.1111/imm.12554
42. Shikhagaie MM, Björklund ÅK, Mjösberg J, Erjefält JS, Cornelissen AS, Ros XR, et al. Neuropilin-1 Is Expressed on Lymphoid Tissue Residing LTi-Like Group 3 Innate Lymphoid Cells and Associated With Ectopic Lymphoid Aggregates. *Cell Rep* (2017) 18(7):1761–73. doi: 10.1016/j.celrep.2017.01.063
43. Carrega P, Loiacono F, Di Carlo E, Scaramuccia A, Mora M, Conte R, et al. NCR (+)ILC3 Concentrate in Human Lung Cancer and Associate With Intratumoral Lymphoid Structures. *Nat Commun* (2015) 6:8280. doi: 10.1038/ncomms9280
44. Tang H, Zhu M, Qiao J, Fu Y-X. Lymphotoxin Signalling in Tertiary Lymphoid Structures and Immunotherapy. *Cell Mol Immunol* (2017) 14 (10):809–18. doi: 10.1038/cmi.2017.13
45. Wolf MJ, Seleznik GM, Zeller N, Heikenwalder M. The Unexpected Role of Lymphotoxin Beta Receptor Signaling in Carcinogenesis: From Lymphoid Tissue Formation to Liver and Prostate Cancer Development. *Oncogene* (2010) 29(36):5006–18. doi: 10.1038/onc.2010.260
46. Colbeck EJ, Ager A, Gallimore A, Jones GW. Tertiary Lymphoid Structures in Cancer: Drivers of Antitumor Immunity, Immunosuppression, or Bystander Sentinels in Disease? *Front Immunol* (2017) 8:1830. doi: 10.3389/fimmu.2017.01830
47. Nerviani A, Pitzalis C. Role of Chemokines in Ectopic Lymphoid Structures Formation in Autoimmunity and Cancer. *J Leukoc Biol* (2018) 104(2):333–41. doi: 10.1002/JLB.3MR0218-062R
48. Tokunaga R, Naseem M, Lo JH, Battaglin F, Soni S, Puccini A, et al. B Cell and B Cell-Related Pathways for Novel Cancer Treatments. *Cancer Treat Rev* (2019) 73:10–9. doi: 10.1016/j.ctrv.2018.12.001
49. Schulz O, Hammerschmidt SI, Moschovakis GL, Förster R. Chemokines and Chemokine Receptors in Lymphoid Tissue Dynamics. *Annu Rev Immunol* (2016) 34:203–42. doi: 10.1146/annurev-immunol-041015-055649
50. Teillaud J-L, Dieu-Nosjean M-C. Tertiary Lymphoid Structures: An Anti-Tumor School for Adaptive Immune Cells and an Antibody Factory to Fight Cancer? *Front Immunol* (2017) 8:830. doi: 10.3389/fimmu.2017.00830
51. Germain C, Gnjatic S, Tamzalit F, Knockaert S, Remark R, Goc J, et al. Presence of B Cells in Tertiary Lymphoid Structures is Associated With a Protective Immunity in Patients With Lung Cancer. *Am J Respir Crit Care Med* (2014) 189(7):832–44. doi: 10.1164/rccm.201309-1611OC
52. Stromnes IM, Hulbert A, Pierce RH, Greenberg PD. Hingorani SR. T-Cell Localization, Activation, and Clonal Expansion in Human Pancreatic Ductal Adenocarcinoma. *Cancer Immunol Res* (2017) 5(11):978–91. doi: 10.1158/2326-6066.CIR-16-0322
53. Montfort A, Pearce O, Maniati E, Vincent BG, Bixby L, Böhm S, et al. A Strong B-Cell Response Is Part of the Immune Landscape in Human High-Grade Serous Ovarian Metastases. *Clin Cancer Res* (2017) 23(1):250–62. doi: 10.1158/1078-0432.CCR-16-0081
54. Joshi NS, Akama-Garren EH, Lu Y, Lee D-Y, Chang GP, Li A, et al. Regulatory T Cells in Tumor-Associated Tertiary Lymphoid Structures Suppress Anti-Tumor T Cell Responses. *Immunity* (2015) 43(3):579–90. doi: 10.1016/j.immuni.2015.08.006
55. Selitsky SR, Mose LE, Smith CC, Chai S, Hoadley KA, Dittmer DP, et al. Prognostic Value of B Cells in Cutaneous Melanoma. *Genome Med* (2019) 11(1):36. doi: 10.1186/s13073-019-0647-5
56. Seow DYB, Yeong JPS, Lim JX, Chia N, Lim JCT, Ong CCH, et al. Tertiary Lymphoid Structures and Associated Plasma Cells Play an Important Role in the Biology of Triple-Negative Breast Cancers. *Breast Cancer Res Treat* (2020) 180(2):369–77. doi: 10.1007/s10549-020-05548-y
57. Lechner A, Schlößer HA, Thelen M, Wennhold K, Rothschild SI, Gilles R, et al. Tumor-Associated B Cells and Humoral Immune Response in Head and Neck Squamous Cell Carcinoma. *Oncoimmunology* (2019) 8 (3):1535293. doi: 10.1080/2162402X.2018.1535293
58. Kroeger DR, Milne K, Nelson BH. Tumor-Infiltrating Plasma Cells Are Associated With Tertiary Lymphoid Structures, Cytolytic T-Cell Responses, and Superior Prognosis in Ovarian Cancer. *Clin Cancer Res* (2016) 22 (12):3005–15. doi: 10.1158/1078-0432.CCR-15-2762
59. Schlößer HA, Thelen M, Lechner A, Wennhold K, Garcia-Marquez MA, Rothschild SI, et al. B Cells in Esophago-Gastric Adenocarcinoma Are

Highly Differentiated, Organize in Tertiary Lymphoid Structures and Produce Tumor-Specific Antibodies. *Oncoimmunology* (2019) 8(1): e1512458. doi: 10.1080/2162402X.2018.1512458
60. Helmink BA, Reddy SM, Gao J, Zhang S, Basar R, Thakur R, et al. B Cells and Tertiary Lymphoid Structures Promote Immunotherapy Response. *Nature* (2020) 577(7791):549–55. doi: 10.1038/s41586-019-1922-8
61. Petitprez F, de Reyniès A, Keung EZ, Chen TW-W, Sun C-M, Calderaro J, et al. B Cells Are Associated With Survival and Immunotherapy Response in Sarcoma. *Nature* (2020) 577(7791):556–60. doi: 10.1038/s41586-019-1906-8
62. Cabrita R, Lauss M, Sanna A, Donia M, Skaarup Larsen M, Mitra S, et al. Tertiary Lymphoid Structures Improve Immunotherapy and Survival in Melanoma. *Nature* (2020) 577(7791):561–5. doi: 10.1038/s41586-019-1914-8
63. Zhang W-H, Wang W-Q, Han X, Gao H-L, Xu S-S, Li S, et al. Infiltrating Pattern and Prognostic Value of Tertiary Lymphoid Structures in Resected Non-Functional Pancreatic Neuroendocrine Tumors. *J Immunother Cancer* (2020) 8(2):e001188. doi: 10.1136/jitc-2020-001188
64. Poschke I, Faryna M, Bergmann F, Flossdorf M, Lauenstein C, Hermes J, et al. Identification of a Tumor-Reactive T-Cell Repertoire in the Immune Infiltrate of Patients With Resectable Pancreatic Ductal Adenocarcinoma. *Oncoimmunology* (2016) 5(12):e1240859. doi: 10.1080/2162402X.2016.1240859
65. Dieu-Nosjean M-C, Giraldo NA, Kaplon H, Germain C, Fridman WH, Sautès-Fridman C. Tertiary Lymphoid Structures, Drivers of the Anti-Tumor Responses in Human Cancers. *Immunol Rev* (2016) 271(1):260–75. doi: 10.1111/imr.12405
66. Zhu G, Nemoto S, Mailloux AW, Perez-Villarroel P, Nakagawa R, Falahat R, et al. Induction of Tertiary Lymphoid Structures With Antitumor Function by a Lymph Node-Derived Stromal Cell Line. *Front Immunol* (2018) 9:1609. doi: 10.3389/fimmu.2018.01609
67. Goc J, Germain C, Vo-Bourgais TKD, Lupo A, Klein C, Knockaert S, et al. Dendritic Cells in Tumor-Associated Tertiary Lymphoid Structures Signal a Th1 Cytotoxic Immune Contexture and License the Positive Prognostic Value of Infiltrating CD8+ T Cells. *Cancer Res* (2014) 74(3):705–15. doi: 10.1158/0008-5472.CAN-13-1342
68. Truxova I, Kasikova L, Hensler M, Skapa P, Laco J, Pecen L, et al. Mature Dendritic Cells Correlate With Favorable Immune Infiltrate and Improved Prognosis in Ovarian Carcinoma Patients. *J Immunother Cancer* (2018) 6 (1):139. doi: 10.1186/s40425-018-0446-3
69. Gu-Trantien C, Migliori E, Buisseret L, de Wind A, Brohée S, Garaud S, et al. CXCL13-Producing TFH Cells Link Immune Suppression and Adaptive Memory in Human Breast Cancer. *JCI Insight* (2017) 2(11):e91487. doi: 10.1172/jci.insight.91487
70. Stranford S, Ruddle NH. Follicular Dendritic Cells, Conduits, Lymphatic Vessels, and High Endothelial Venules in Tertiary Lymphoid Organs: Parallels With Lymph Node Stroma. *Front Immunol* (2012) 3:350. doi: 10.3389/fimmu.2012.00350
71. Le Pottier L, Devauchelle V, Fautrel A, Daridon C, Saraux A, Youinou P, et al. Ectopic Germinal Centers Are Rare in Sjogren's Syndrome Salivary Glands and Do Not Exclude Autoreactive B Cells. *J Immunol* (2009) 182 (6):3540–7. doi: 10.4049/jimmunol.0803588
72. Wirsing AM, Ervik IK, Seppola M, Uhlin-Hansen L, Steigen SE, Hadler-Olsen E. Presence of High-Endothelial Venules Correlates With a Favorable Immune Microenvironment in Oral Squamous Cell Carcinoma. *Mod Pathol* (2018) 31(6):910–22. doi: 10.1038/s41379-018-0019-5
73. Martinet L, Garrido I, Filleron T, Le Guellec S, Bellard E, Fournie J-J, et al. Human Solid Tumors Contain High Endothelial Venules: Association With T- and B-Lymphocyte Infiltration and Favorable Prognosis in Breast Cancer. *Cancer Res* (2011) 71(17):5678–87. doi: 10.1158/0008-5472.CAN-11-0431
74. Daum S, Hagen H, Naismith E, Wolf D, Pircher A. The Role of Anti-Angiogenesis in the Treatment Landscape of Non-Small Cell Lung Cancer - New Combinational Approaches and Strategies of Neovessel Inhibition. *Front Cell Dev Biol* (2020) 8:610903. doi: 10.3389/fcell.2020.610903
75. Ruddle NH. High Endothelial Venules and Lymphatic Vessels in Tertiary Lymphoid Organs: Characteristics, Functions, and Regulation. *Front Immunol* (2016) 7:491. doi: 10.3389/fimmu.2016.00491
76. Ager A. High Endothelial Venules and Other Blood Vessels: Critical Regulators of Lymphoid Organ Development and Function. *Front Immunol* (2017) 8:45. doi: 10.3389/fimmu.2017.00045
77. Buckley CD, Barone F, Nayar S, Bénézech C, Caamaño J. Stromal Cells in Chronic Inflammation and Tertiary Lymphoid Organ Formation. *Annu Rev Immunol* (2015) 33:715–45. doi: 10.1146/annurev-immunol-032713-120252
78. Weinstein AM, Storkus WJ. Biosynthesis and Functional Significance of Peripheral Node Addressin in Cancer-Associated TLO. *Front Immunol* (2016) 7:301. doi: 10.3389/fimmu.2016.00301
79. Drayton DL, Ying X, Lee J, Lesslauer W, Ruddle NH. Ectopic LT Alpha Beta Directs Lymphoid Organ Neogenesis With Concomitant Expression of Peripheral Node Addressin and a HEV-Restricted Sulfotransferase. *J Exp Med* (2003) 197(9):1153–63. doi: 10.1084/jem.20021761
80. Veerman K, Tardiveau C, Martins F, Coudert J, Girard J-P. Single-Cell Analysis Reveals Heterogeneity of High Endothelial Venules and Different Regulation of Genes Controlling Lymphocyte Entry to Lymph Nodes. *Cell Rep* (2019) 26(11):3116–31.e5. doi: 10.1016/j.celrep.2019.02.042
81. Colbeck EJ, Jones E, Hindley JP, Smart K, Schulz R, Browne M, et al. Treg Depletion Licenses T Cell-Driven HEV Neogenesis and Promotes Tumor Destruction. *Cancer Immunol Res* (2017) 5(11):1005–15. doi: 10.1158/2326-6066.CIR-17-0131
82. Allen E, Jabouille A, Rivera LB, Lodewijckx I, Missiaen R, Steri V, et al. Combined Antiangiogenic and Anti-PD-L1 Therapy Stimulates Tumor Immunity Through HEV Formation. *Sci Transl Med* (2017) 9(385): eaak9679. doi: 10.1126/scitranslmed.aak9679
83. Johansson-Percival A, He B, Li Z-J, Kjellén A, Russell K, Li J, et al. De Novo Induction of Intratumoral Lymphoid Structures and Vessel Normalization Enhances Immunotherapy in Resistant Tumors. *Nat Immunol* (2017) 18 (11):1207–17. doi: 10.1038/ni.3836
84. Peske JD, Thompson ED, Gemta L, Baylis RA, Fu Y-X, Engelhard VH. Effector Lymphocyte-Induced Lymph Node-Like Vasculature Enables Naive T-Cell Entry Into Tumours and Enhanced Anti-Tumour Immunity. *Nat Commun* (2015) 6:7114. doi: 10.1038/ncomms8114
85. Remark R, Alifano M, Cremer I, Lupo A, Dieu-Nosjean M-C, Riquet M, et al. Characteristics and Clinical Impacts of the Immune Environments in Colorectal and Renal Cell Carcinoma Lung Metastases: Influence of Tumor Origin. *Clin Cancer Res* (2013) 19(15):4079–91. doi: 10.1158/1078-0432.CCR-12-3847
86. Gobert M, Treilleux I, Bendriss-Vermare N, Bachelot T, Goddard-Leon S, Arfi V, et al. Regulatory T Cells Recruited Through CCL22/CCR4 Are Selectively Activated in Lymphoid Infiltrates Surrounding Primary Breast Tumors and Lead to an Adverse Clinical Outcome. *Cancer Res* (2009) 69 (5):2000–9. doi: 10.1158/0008-5472.CAN-08-2360
87. Schweiger T, Berghoff AS, Glogner C, Glueck O, Rajky O, Traxler D, et al. Tumor-Infiltrating Lymphocyte Subsets and Tertiary Lymphoid Structures in Pulmonary Metastases From Colorectal Cancer. *Clin Exp Metastasis* (2016) 33(7):727–39. doi: 10.1007/s10585-016-9813-y
88. García-Hernández M, Uribe-Uribe NO, Espinosa-González R, Kast WM, Khader SA, Rangel-Moreno J. A Unique Cellular and Molecular Microenvironment Is Present in Tertiary Lymphoid Organs of Patients With Spontaneous Prostate Cancer Regression. *Front Immunol* (2017) 8:563. doi: 10.3389/fimmu.2017.00563
89. Shields JD, Kourtis IC, Tomei AA, Roberts JM, Swartz MA. Induction of Lymphoidlike Stroma and Immune Escape by Tumors That Express the Chemokine CCL21. *Sci (New York NY)* (2010) 328(5979):749–52. doi: 10.1126/science.1185837
90. Najibi AJ, Mooney DJ. Cell and Tissue Engineering in Lymph Nodes for Cancer Immunotherapy. *Adv Drug Deliv Rev* (2020) 161–162:42–62. doi: 10.1016/j.addr.2020.07.023
91. Yagawa Y, Robertson-Tessi M, Zhou SL, Anderson ARA, Mulé JJ, Mailloux AW. Systematic Screening of Chemokines to Identify Candidates to Model and Create Ectopic Lymph Node Structures for Cancer Immunotherapy. *Sci Rep* (2017) 7(1):15996. doi: 10.1038/s41598-017-15924-2
92. Zhu G, Falahat R, Wang K, Mailloux A, Artzi N, Mulé JJ. Tumor-Associated Tertiary Lymphoid Structures: Gene-Expression Profiling and Their Bioengineering. *Front Immunol* (2017) 8:767. doi: 10.3389/fimmu.2017.00767
93. Yagawa Y, Robertson-Tessi M, Zhou SL, Anderson ARA, Mulé JJ, Mailloux AW. Systematic Screening of Chemokines to Identify Candidates to Model and Create Ectopic Lymph Node Structures for Cancer Immunotherapy. *Sci Rep* (2017) 7(1):15996. doi: 10.1038/s41598-017-15924-2

94. Coppola D, Nebozhyn M, Khalil F, Dai H, Yeatman T, Loboda A, et al. Unique Ectopic Lymph Node-Like Structures Present in Human Primary Colorectal Carcinoma are Identified by Immune Gene Array Profiling. *Am J Pathol* (2011) 179(1):37–45. doi: 10.1016/j.ajpath.2011.03.007
95. Prabhakaran S, Rizk VT, Ma Z, Cheng C-H, Berglund AE, Coppola D, et al. Evaluation of Invasive Breast Cancer Samples Using a 12-Chemokine Gene Expression Score: Correlation With Clinical Outcomes. *Breast Cancer Res: BCR* (2017) 19(1):71. doi: 10.1186/s13058-017-0864-z
96. Tokunaga R, Nakagawa S, Sakamoto Y, Nakamura K, Naseem M, Izumi D, et al. 12-Chemokine Signature, a Predictor of Tumor Recurrence in Colorectal Cancer. *Int J Cancer* (2020) 147(2):532–41. doi: 10.1002/ijc.32982
97. Luther SA, Lopez T, Bai W, Hanahan D, Cyster JG. BLC Expression in Pancreatic Islets Causes B Cell Recruitment and Lymphotoxin-Dependent Lymphoid Neogenesis. *Immunity* (2000) 12(5):471–81. doi: 10.1016/S1074-7613(00)80199-5
98. Luther SA, Bidgol A, Hargreaves DC, Schmidt A, Xu Y, Paniyadi J, et al. Differing Activities of Homeostatic Chemokines CCL19, CCL21, and CXCL12 in Lymphocyte and Dendritic Cell Recruitment and Lymphoid Neogenesis. *J Immunol* (2002) 169(1):424–33. doi: 10.4049/jimmunol.169.1.424
99. Turnquist HR, Lin X, Ashour AE, Hollingsworth MA, Singh RK, Talmadge JE, et al. CCL21 Induces Extensive Intratumoral Immune Cell Infiltration and Specific Anti-Tumor Cellular Immunity. *Int J Oncol* (2007) 30(3):631–9. doi: 10.3892/ijo.30.3.631
100. Schrama D, thor Straten P, Fischer WH, McLellan AD, Bröcker EB, Reisfeld RA, et al. Targeting of Lymphotoxin-Alpha to the Tumor Elicits an Efficient Immune Response Associated With Induction of Peripheral Lymphoid-Like Tissue. *Immunity* (2001) 14(2):111–21. doi: 10.1016/S1074-7613(01)00094-2
101. Martin AP, Coronel EC, G-i S, Chen S-C, Vassileva G, Canasto-Chibuque C, et al. A Novel Model for Lymphocytic Infiltration of the Thyroid Gland Generated by Transgenic Expression of the CC Chemokine CCL21. *J Immunol* (2004) 173(8):4791–8. doi: 10.4049/jimmunol.173.8.4791
102. Chen S-C, Vassileva G, Kinsley D, Holzmann S, Manfra D, Wiekowski MT, et al. Ectopic Expression of the Murine Chemokines CCL21a and CCL21b Induces the Formation of Lymph Node-Like Structures in Pancreas, But Not Skin, of Transgenic Mice. *J Immunol* (2002) 168(3):1001–8. doi: 10.4049/jimmunol.168.3.1001
103. Denton AE, Innocentin S, Carr EJ, Bradford BM, Lafouresse F, Mabbott NA, et al. Type I Interferon Induces CXCL13 to Support Ectopic Germinal Center Formation. *J Exp Med* (2019) 216(3):621–37. doi: 10.1084/jem.20181216
104. Nayar S, Campos J, Chung MM, Navarro-Núñez L, Chachlani M, Steinthal N, et al. Bimodal Expansion of the Lymphatic Vessels Is Regulated by the Sequential Expression of IL-7 and Lymphotoxin $\alpha 1\beta 2$ in Newly Formed Tertiary Lymphoid Structures. *J Immunol* (2016) 197(5):1957–67. doi: 10.4049/jimmunol.1500686
105. Barone F, Nayar S, Campos J, Cloake T, Withers DR, Toellner K-M, et al. IL-22 Regulates Lymphoid Chemokine Production and Assembly of Tertiary Lymphoid Organs. *Proc Natl Acad Sci USA* (2015) 112(35):11024–9. doi: 10.1073/pnas.1503315112
106. Grogan JL, Ouyang W. A Role for Th17 Cells in the Regulation of Tertiary Lymphoid Follicles. *Eur J Immunol* (2012) 42(9):2255–62. doi: 10.1002/eji.201242656
107. Savage AK, Liang HE, Locksley RM. The Development of Steady-State Activation Hubs Between Adult LTi ILC3s and Primed Macrophages in Small Intestine. *J Immunol* (2017) 199(5):1912–22. doi: 10.4049/jimmunol.1700155
108. Wang J, Lo JC, Foster A, Yu P, Chen HM, Wang Y, et al. The Regulation of T Cell Homeostasis and Autoimmunity by T Cell-Derived LIGHT. *J Clin Invest* (2001) 108(12):1771–80. doi: 10.1172/JCI200113827
109. Rooney IA, Butrovich KD, Glass AA, Borboroglu S, Benedict CA, Whitbeck JC, et al. The Lymphotoxin-Beta Receptor is Necessary and Sufficient for LIGHT-Mediated Apoptosis of Tumor Cells. *J Biol Chem* (2000) 275(19):14307–15. doi: 10.1074/jbc.275.19.14307
110. Ware CF. Targeting Lymphocyte Activation Through the Lymphotoxin and LIGHT Pathways. *Immunol Rev* (2008) 223:186–201. doi: 10.1111/j.1600-065X.2008.00629.x
111. Skeate JG, Otsmaa ME, Prins R, Fernandez DJ, Da Silva DM, Kast WM. TNFSF14: LIGHTing the Way for Effective Cancer Immunotherapy. *Front Immunol* (2020) 11:922. doi: 10.3389/fimmu.2020.00922
112. Tang H, Wang Y, Chlewicki LK, Zhang Y, Guo J, Liang W, et al. Facilitating T Cell Infiltration in Tumor Microenvironment Overcomes Resistance to PD-L1 Blockade. *Cancer Cell* (2016) 29(3):285–96. doi: 10.1016/j.ccell.2016.02.004
113. Johansson-Percival A, He B, Ganss R. Immunomodulation of Tumor Vessels: It Takes Two to Tango. *Trends Immunol* (2018) 39(10):801–14. doi: 10.1016/j.it.2018.08.001
114. Treps L. EnLIGHTenment of Tumor Vessel Normalization and Immunotherapy in Glioblastoma. *J Pathol* (2018) 246(1):3–6. doi: 10.1002/path.5103
115. He B, Jabouille A, Steri V, Johansson-Percival A, Michael IP, Kotamraju VR, et al. Vascular Targeting of LIGHT Normalizes Blood Vessels in Primary Brain Cancer and Induces Intratumoural High Endothelial Venules. *J Pathol* (2018) 245(2):209–21. doi: 10.1002/path.5080
116. He B, Johansson-Percival A, Backhouse J, Li J, Lee GYF, Hamzah J, et al. Remodeling of Metastatic Vasculature Reduces Lung Colonization and Sensitizes Overt Metastases to Immunotherapy. *Cell Rep* (2020) 30(3):714–24.e5. doi: 10.1016/j.celrep.2019.12.013
117. Lu TT, Browning JL. Role of the Lymphotoxin/LIGHT System in the Development and Maintenance of Reticular Networks and Vasculature in Lymphoid Tissues. *Front Immunol* (2014) 5:47. doi: 10.3389/fimmu.2014.00047
118. Loeffler M, Le'Negrate G, Krajewska M, Reed JC. Attenuated Salmonella Engineered to Produce Human Cytokine LIGHT Inhibit Tumor Growth. *Proc Natl Acad Sci USA* (2007) 104(31):12879–83. doi: 10.1073/pnas.0701959104
119. O'Brien K, Breyne K, Ughetto S, Laurent LC, Breakefield XO. RNA Delivery by Extracellular Vesicles in Mammalian Cells and Its Applications. *Nat Rev Mol Cell Biol* (2020) 21(10):585–606. doi: 10.1038/s41580-020-0251-y
120. Kalluri R, LeBleu VS. The Biology Function and Biomedical Applications of Exosomes. *Sci (New York NY)* (2020) 367(6478):eaau6977. doi: 10.1126/science.aau6977
121. Ciccia F, Rizzo A, Maugeri R, Alessandro R, Croci S, Guggino G, et al. Ectopic Expression of CXCL13, BAFF, APRIL and LT-β Is Associated With Artery Tertiary Lymphoid Organs in Giant Cell Arteritis. *Ann Rheum Dis* (2017) 76(1):235–43. doi: 10.1136/annrheumdis-2016-209217
122. Gallotta M, Assi H, Degagné É, Kannan SK, Coffman RL, Guiducci C. Inhaled TLR9 Agonist Renders Lung Tumors Permissive to PD-1 Blockade by Promoting Optimal CD4 and CD8 T-Cell Interplay. *Cancer Res* (2018) 78(17):4943–56. doi: 10.1158/0008-5472.CAN-18-0729
123. Li L, Barry V, Daffis S, Niu C, Huntzicker E, French DM, et al. Anti-HBV Response to Toll-Like Receptor 7 Agonist GS-9620 Is Associated With Intrahepatic Aggregates of T Cells and B Cells. *J Hepatol* (2018) 68(5):912–21. doi: 10.1016/j.jhep.2017.12.008
124. Robinet M, Villeret B, Maillard S, Cron MA, Berrih-Aknin S, Le Panse R. Use of Toll-Like Receptor Agonists to Induce Ectopic Lymphoid Structures in Myasthenia Gravis Mouse Models. *Front Immunol* (2017) 8:1029. doi: 10.3389/fimmu.2017.01029
125. Workel HH, Lubbers JM, Arnold R, Prins TM, van der Vlies P, de Lange K, et al. A Transcriptionally Distinct CXCL13(+)CD103(+)CD8(+) T-Cell Population Is Associated With B-Cell Recruitment and Neoantigen Load in Human Cancer. *Cancer Immunol Res* (2019) 7(5):784–96. doi: 10.1158/2326-6066.Cir-18-0517
126. Chen L, Fabian KL, Taylor JL, Storkus WJ. Therapeutic Use of Dendritic Cells to Promote the Extranodal Priming of Anti-Tumor Immunity. *Front Immunol* (2013) 4:388. doi: 10.3389/fimmu.2013.00388
127. Kirk CJ, Hartigan-O'Connor D, Mulé JJ. The Dynamics of the T-Cell Antitumor Response: Chemokine-Secreting Dendritic Cells Can Prime Tumor-Reactive T Cells Extranodally. *Cancer Res* (2001) 61(24):8794–802.
128. Chen L, Taylor JL, Sabins NC, Lowe DB, Qu Y, You Z, et al. Extranodal Induction of Therapeutic Immunity in the Tumor Microenvironment After Intratumoral Delivery of Tbet Gene-Modified Dendritic Cells. *Cancer Gene Ther* (2013) 20(8):469–77. doi: 10.1038/cgt.2013.42
129. Moussion C, Girard J-P. Dendritic Cells Control Lymphocyte Entry to Lymph Nodes Through High Endothelial Venules. *Nature* (2011) 479(7374):542–6. doi: 10.1038/nature10540
130. Debets R, Timans JC, Homey B, Zurawski S, Sana TR, Lo S, et al. Two Novel IL-1 Family Members, IL-1 Delta and IL-1 Epsilon, Function as an

Antagonist and Agonist of NF-Kappa B Activation Through the Orphan IL-1 Receptor-Related Protein 2. *J Immunol* (2001) 167(3):1440–6. doi: 10.4049/jimmunol.167.3.1440
131. Bridgewood C, Stacey M, Alase A, Lagos D, Graham A, Wittmann M. IL-36γ Has Proinflammatory Effects on Human Endothelial Cells. *Exp Dermatol* (2017) 26(5):402–8. doi: 10.1111/exd.13228
132. Bachmann M, Scheiermann P, Härdle L, Pfeilschifter J, Mühl H. IL-36γ/IL-1F9, an Innate T-Bet Target in Myeloid Cells. *J Biol Chem* (2012) 287 (50):41684–96. doi: 10.1074/jbc.M112.385443
133. Weinstein AM, Giraldo NA, Petitprez F, Julie C, Lacroix L, Peschaud F, et al. Association of IL-36γ With Tertiary Lymphoid Structures and Inflammatory Immune Infiltrates in Human Colorectal Cancer. *Cancer Immunol Immunother* (2019) 68(1):109–20. doi: 10.1007/s00262-018-2259-0
134. Weinstein AM, Chen L, Brzana EA, Patil PR, Taylor JL, Fabian KL, et al. Tbet and IL-36γ Cooperate in Therapeutic DC-Mediated Promotion of Ectopic Lymphoid Organogenesis in the Tumor Microenvironment. *Oncoimmunology* (2017) 6(6):e1322238. doi: 10.1080/2162402X.2017.1322238
135. Lee JM, Lee MH, Garon E, Goldman JW, Salehi-Rad R, Baratelli FE, et al. Phase I Trial of Intratumoral Injection of CCL21 Gene-Modified Dendritic Cells in Lung Cancer Elicits Tumor-Specific Immune Responses and CD8(+) T-Cell Infiltration. *Clin Cancer Res* (2017) 23(16):4556–68. doi: 10.1158/1078-0432.Ccr-16-2821
136. Yang SC, Batra RK, Hillinger S, Reckamp KL, Strieter RM, Dubinett SM, et al. Intrapulmonary Administration of CCL21 Gene-Modified Dendritic Cells Reduces Tumor Burden in Spontaneous Murine Bronchoalveolar Cell Carcinoma. *Cancer Res* (2006) 66(6):3205–13. doi: 10.1158/0008-5472.Can-05-3619
137. Mac Keon S, Gazzaniga S, Wallerman J, Bravo AI, Mordoh J, Wainstok R. Vaccination With Dendritic Cells Charged With Apoptotic/Necrotic B16 Melanoma Induces the Formation of Subcutaneous Lymphoid Tissue. *Vaccine* (2010) 28(51):8162–8. doi: 10.1016/j.vaccine.2010.09.095
138. Cupedo T, Jansen W, Kraal G, Mebius RE. Induction of Secondary and Tertiary Lymphoid Structures in the Skin. *Immunity* (2004) 21(5):655–67. doi: 10.1016/j.immuni.2004.09.006
139. Suematsu S, Watanabe T. Generation of a Synthetic Lymphoid Tissue-Like Organoid in Mice. *Nat Biotechnol* (2004) 22(12):1539–45. doi: 10.1038/nbt1039
140. Nayar S, Campos J, Smith CG, Iannizzotto V, Gardner DH, Mourcin F, et al. Immunofibroblasts are Pivotal Drivers of Tertiary Lymphoid Structure Formation and Local Pathology. *Proc Natl Acad Sci USA* (2019) 116 (27):13490–7. doi: 10.1073/pnas.1905301116
141. Dorraji SE, Hovd A-MK, Kanapathippillai P, Bakland G, Eilertsen GØ, Figenschau SL, et al. Mesenchymal Stem Cells and T Cells in the Formation of Tertiary Lymphoid Structures in Lupus Nephritis. *Sci Rep* (2018) 8 (1):7861. doi: 10.1038/s41598-018-26265-z
142. Koscsó B, Kurapati S, Rodrigues RR, Nedjic J, Gowda K, Shin C, et al. Gut-Resident CX3CR1 Macrophages Induce Tertiary Lymphoid Structures and IgA Response *In Situ*. *Sci Immunol* (2020) 5(46):eaax0062. doi: 10.1126/sciimmunol.aax0062
143. Guedj K, Abitbol Y, Cazals-Hatem D, Morvan M, Maggiori L, Panis Y, et al. Adipocytes Orchestrate the Formation of Tertiary Lymphoid Organs in the Creeping Fat of Crohn's Disease Affected Mesentery. *J Autoimmun* (2019) 103:102281. doi: 10.1016/j.jaut.2019.05.009
144. Malafaya PB, Silva GA, Reis RL. Natural-Origin Polymers as Carriers and Scaffolds for Biomolecules and Cell Delivery in Tissue Engineering Applications. *Adv Drug Deliv Rev* (2007) 59(4-5):207–33. doi: 10.1016/j.addr.2007.03.012
145. Weber JS, Mulé JJ. Cancer Immunotherapy Meets Biomaterials. *Nat Biotechnol* (2015) 33(1):44–5. doi: 10.1038/nbt.3119
146. Weiden J, Tel J, Figdor CG. Synthetic Immune Niches for Cancer Immunotherapy. *Nat Rev Immunol* (2018) 18(3):212–9. doi: 10.1038/nri.2017.89
147. Kim J, Li WA, Choi Y, Lewin SA, Verbeke CS, Dranoff G, et al. Injectable, Spontaneously Assembling, Inorganic Scaffolds Modulate Immune Cells *In Vivo* and Increase Vaccine Efficacy. *Nat Biotechnol* (2015) 33(1):64–72. doi: 10.1038/nbt.3071
148. Stephan SB, Taber AM, Jileaeva I, Pegues EP, Sentman CL, Stephan MT. Biopolymer Implants Enhance the Efficacy of Adoptive T-Cell Therapy. *Nat Biotechnol* (2015) 33(1):97–101. doi: 10.1038/nbt.3104
149. Okamoto N, Chihara R, Shimizu C, Nishimoto S, Watanabe T. Artificial Lymph Nodes Induce Potent Secondary Immune Responses in Naive and Immunodeficient Mice. *J Clin Invest* (2007) 117(4):997–1007. doi: 10.1172/JCI30379
150. Kobayashi Y, Watanabe T. Synthesis of Artificial Lymphoid Tissue With Immunological Function. *Trends Immunol* (2010) 31(11):422–8. doi: 10.1016/j.it.2010.09.002
151. Singh A, Peppas NA. Hydrogels and Scaffolds for Immunomodulation. *Adv Mater* (2014) 26(38):6530–41. doi: 10.1002/adma.201402105
152. Gilam A, Conde J, Weissglas-Volkov D, Oliva N, Friedman E, Artzi N, et al. Local microRNA Delivery Targets Palladin and Prevents Metastatic Breast Cancer. *Nat Commun* (2016) 7:12868. doi: 10.1038/ncomms12868
153. Conde J, Oliva N, Zhang Y, Artzi N. Local Triple-Combination Therapy Results in Tumour Regression and Prevents Recurrence in a Colon Cancer Model. *Nat Mater* (2016) 15(10):1128–38. doi: 10.1038/nmat4707
154. Kobayashi Y, Watanabe T. Gel-Trapped Lymphorganogenic Chemokines Trigger Artificial Tertiary Lymphoid Organs and Mount Adaptive Immune Responses *In Vivo*. *Front Immunol* (2016) 7:316. doi: 10.3389/fimmu.2016.00316
155. Singh A, Qin H, Fernandez I, Wei J, Lin J, Kwak LW, et al. An Injectable Synthetic Immune-Priming Center Mediates Efficient T-Cell Class Switching and T-Helper 1 Response Against B Cell Lymphoma. *J Control Rel* (2011) 155(2):184–92. doi: 10.1016/j.jconrel.2011.06.008
156. Ali OA, Huebsch N, Cao L, Dranoff G, Mooney DJ. Infection-Mimicking Materials to Program Dendritic Cells in Situ. *Nat Mater* (2009) 8(2):151–8. doi: 10.1038/nmat2357
157. Shimizu K, Yamasaki S, Shinga J, Sato Y, Watanabe T, Ohara O, et al. Systemic DC Activation Modulates the Tumor Microenvironment and Shapes the Long-Lived Tumor-Specific Memory Mediated by CD8+ T Cells. *Cancer Res* (2016) 76 (13):3756–66. doi: 10.1158/0008-5472.CAN-15-3219
158. Huang Y, Chen Y, Zhou S, Chen L, Wang J, Pei Y, et al. Dual-Mechanism Based CTLs Infiltration Enhancement Initiated by Nano-Sapper Potentiates Immunotherapy Against Immune-Excluded Tumors. *Nat Commun* (2020) 11(1):622. doi: 10.1038/s41467-020-14425-7
159. Bahmani B, Uehara M, Ordikhani F, Li X, Jiang L, Banouni N, et al. Ectopic High Endothelial Venules in Pancreatic Ductal Adenocarcinoma: A Unique Site for Targeted Delivery. *EBioMedicine* (2018) 38:79–88. doi: 10.1016/j.ebiom.2018.11.030
160. Maldonado L, Teague JE, Morrow MP, Jotova I, Wu TC, Wang C, et al. Intramuscular Therapeutic Vaccination Targeting HPV16 Induces T Cell Responses That Localize in Mucosal Lesions. *Sci Transl Med* (2014) 6 (221):221ra13. doi: 10.1126/scitranslmed.3007323
161. Lutz ER, Wu AA, Bigelow E, Sharma R, Mo G, Soares K, et al. Immunotherapy Converts Nonimmunogenic Pancreatic Tumors Into Immunogenic Foci of Immune Regulation. *Cancer Immunol Res* (2014) 2 (7):616–31. doi: 10.1158/2326-6066.CIR-14-0027
162. Morcrette G, Hirsch TZ, Badour E, Pilet J, Caruso S, Calderaro J, et al. Germline Hepatoblastomas Demonstrate Cisplatin-Induced Intratumor Tertiary Lymphoid Structures. *Oncoimmunology* (2019) 8(6):e1583547. doi: 10.1080/2162402X.2019.1583547
163. Kuwabara S, Tsuchikawa T, Nakamura T, Hatanaka Y, Hatanaka KC, Sasaki K, et al. Prognostic Relevance of Tertiary Lymphoid Organs Following Neoadjuvant Chemoradiotherapy in Pancreatic Ductal Adenocarcinoma. *Cancer Sci* (2019) 110(6):1853–62. doi: 10.1111/cas.14023
164. Siliņa K, Soltermann A, Attar FM, Casanova R, Uckeley ZM, Thut H, et al. Germinal Centers Determine the Prognostic Relevance of Tertiary Lymphoid Structures and Are Impaired by Corticosteroids in Lung Squamous Cell Carcinoma. *Cancer Res* (2018) 78(5):1308–20. doi: 10.1158/0008-5472.Can-17-1987
165. Boivin G, Kalambaden P, Faget J, Rusakiewicz S, Montay-Gruel P, Meylan E, et al. Cellular Composition and Contribution of Tertiary Lymphoid Structures to Tumor Immune Infiltration and Modulation by Radiation Therapy. *Front Oncol* (2018) 8:256. doi: 10.3389/fonc.2018.00256
166. Chelvanambi M, Fecek RJ, Taylor JL, Storkus WJ. STING Agonist-Based Treatment Promotes Vascular Normalization and Tertiary Lymphoid Structure Formation in the Therapeutic Melanoma Microenvironment. *J Immunother Cancer* (2021) 9(2):e001906. doi: 10.1136/jitc-2020-001906
167. Solinas C, Garaud S, De Silva P, Boisson A, Van den Eynden G, de Wind A, et al. Immune Checkpoint Molecules on Tumor-Infiltrating Lymphocytes and Their Association With Tertiary Lymphoid Structures in Human Breast Cancer. *Front Immunol* (2017) 8:1412. doi: 10.3389/fimmu.2017.01412

168. Giraldo NA, Becht E, Pagès F, Skliris G, Verkarre V, Vano Y, et al. Orchestration and Prognostic Significance of Immune Checkpoints in the Microenvironment of Primary and Metastatic Renal Cell Cancer. *Clin Cancer Res* (2015) 21(13):3031–40. doi: 10.1158/1078-0432.CCR-14-2926
169. van Dijk N, Gil-Jimenez A, Silina K, Hendricksen K, Smit LA, de Feijter JM, et al. Preoperative Ipilimumab Plus Nivolumab in Locoregionally Advanced Urothelial Cancer: The NABUCCO Trial. *Nat Med* (2020) 26(12):1839–44. doi: 10.1038/s41591-020-1085-z
170. Thommen DS, Koelzer VH, Herzig P, Roller A, Trefny M, Dimeloe S, et al. A Transcriptionally and Functionally Distinct PD-1 CD8 T Cell Pool With Predictive Potential in Non-Small-Cell Lung Cancer Treated With PD-1 Blockade. *Nat Med* (2018) 24(7):994–1004. doi: 10.1038/s41591-018-0057-z
171. Lukashev M, LePage D, Wilson C, Bailly V, Garber E, Lukashin A, et al. Targeting the Lymphotoxin-Beta Receptor With Agonist Antibodies as a Potential Cancer Therapy. *Cancer Res* (2006) 66(19):9617–24. doi: 10.1158/0008-5472.Can-06-0217

Conflict of Interest: The authors declare that the research was conducted in the absence of any commercial or financial relationships that could be construed as a potential conflict of interest.

Publisher's Note: All claims expressed in this article are solely those of the authors and do not necessarily represent those of their affiliated organizations, or those of the publisher, the editors and the reviewers. Any product that may be evaluated in this article, or claim that may be made by its manufacturer, is not guaranteed or endorsed by the publisher.

Copyright © 2021 Kang, Feng, Luo, He, Liu, Wu and Rong. This is an open-access article distributed under the terms of the Creative Commons Attribution License (CC BY). The use, distribution or reproduction in other forums is permitted, provided the original author(s) and the copyright owner(s) are credited and that the original publication in this journal is cited, in accordance with accepted academic practice. No use, distribution or reproduction is permitted which does not comply with these terms.

frontiers in Immunology

REVIEW
published: 17 August 2021
doi: 10.3389/fimmu.2021.736670

High Endothelial Venules: A Vascular Perspective on Tertiary Lymphoid Structures in Cancer

Gerlanda Vella[1], *Sophie Guelfi*[1*] *and Gabriele Bergers*[1,2*]

[1] Laboratory of Tumor Microenvironment and Therapeutic Resistance, Department of Oncology, Vlaams Instituut voor Biotechnologie (VIB)-Center for Cancer Biology, Katholieke Universiteit (KU) Leuven, Leuven, Belgium, [2] Department of Neurological Surgery, UCSF Comprehensive Cancer Center, University of California San Francisco (UCSF), San Francisco, CA, United States

High endothelial venules (HEVs) are specialized postcapillary venules composed of cuboidal blood endothelial cells that express high levels of sulfated sialomucins to bind L-Selectin/CD62L on lymphocytes, thereby facilitating their transmigration from the blood into the lymph nodes (LN) and other secondary lymphoid organs (SLO). HEVs have also been identified in human and murine tumors in predominantly $CD3^+$T cell-enriched areas with fewer $CD20^+$B-cell aggregates that are reminiscent of tertiary lymphoid-like structures (TLS). While HEV/TLS areas in human tumors are predominantly associated with increased survival, tumoral HEVs (TU-HEV) in mice have shown to foster lymphocyte-enriched immune centers and boost an immune response combined with different immunotherapies. Here, we discuss the current insight into TU-HEV formation, function, and regulation in tumors and elaborate on the functional implication, opportunities, and challenges of TU-HEV formation for cancer immunotherapy.

Keywords: high endothelial venules, tertiary lymphoid structures, tumor endothelial cells, tumor immunity, immunotherapy, lymphotoxin beta receptor, sentinel lymph node, metastasis

OPEN ACCESS

Edited by:
Vivek Verma,
Georgetown University, United States

Reviewed by:
Ann Ager,
Cardiff University, United Kingdom
Hiroto Kawashima,
Chiba University, Japan

***Correspondence:**
Sophie Guelfi
Sophie.guelfi@kuleuven.be
Gabriele Bergers
gabriele.bergers@kuleuven.be

Specialty section:
This article was submitted to Cancer Immunity and Immunotherapy, a section of the journal Frontiers in Immunology

Received: *05 July 2021*
Accepted: *30 July 2021*
Published: *17 August 2021*

Citation:
Vella G, Guelfi S and Bergers G (2021) High Endothelial Venules: A Vascular Perspective on Tertiary Lymphoid Structures in Cancer. Front. Immunol. 12:736670. doi: 10.3389/fimmu.2021.736670

INTRODUCTION

Tumoral Angiogenesis and Immune Escape

Solid tumors are heterogeneous and complex cellular ecosystems in which cancer cells shape their microenvironment to their advantage by actively remodeling the local immune, vascular and stromal compartments (1). Thus, tumors have also been considered as "wounds that never heal" because they increasingly promote immunosuppression and neovascularization to sustain the rapid growth of cancer cells (2, 3). Due to the anomalous proangiogenic signals, these tumors exhibit a continuously growing tumor vasculature with a chaotic composition of venules, postcapillary venules, arterioles, and capillaries. Consequently, angiogenic tumor vessels typically exhibit abnormal structural and functional characteristics of poor vessel maturation, leakiness, and staggered blood flow due to the elevated interstitial pressure (4–6) (**Figure 1**). With these vascular aberrations, hypoxic, acidic, and necrotic regions appear in tumors that induce an additional wave of proangiogenic signals, exacerbating disease because they support metastasis by enabling tumor cell intravasation into the bloodstream and obstructing adequate delivery of anti-cancer drugs (4, 7). Importantly, as part of the wound repair program, angiogenic factors including vascular endothelial growth factor (VEGF) and angiopoietins also convey immunosuppressive

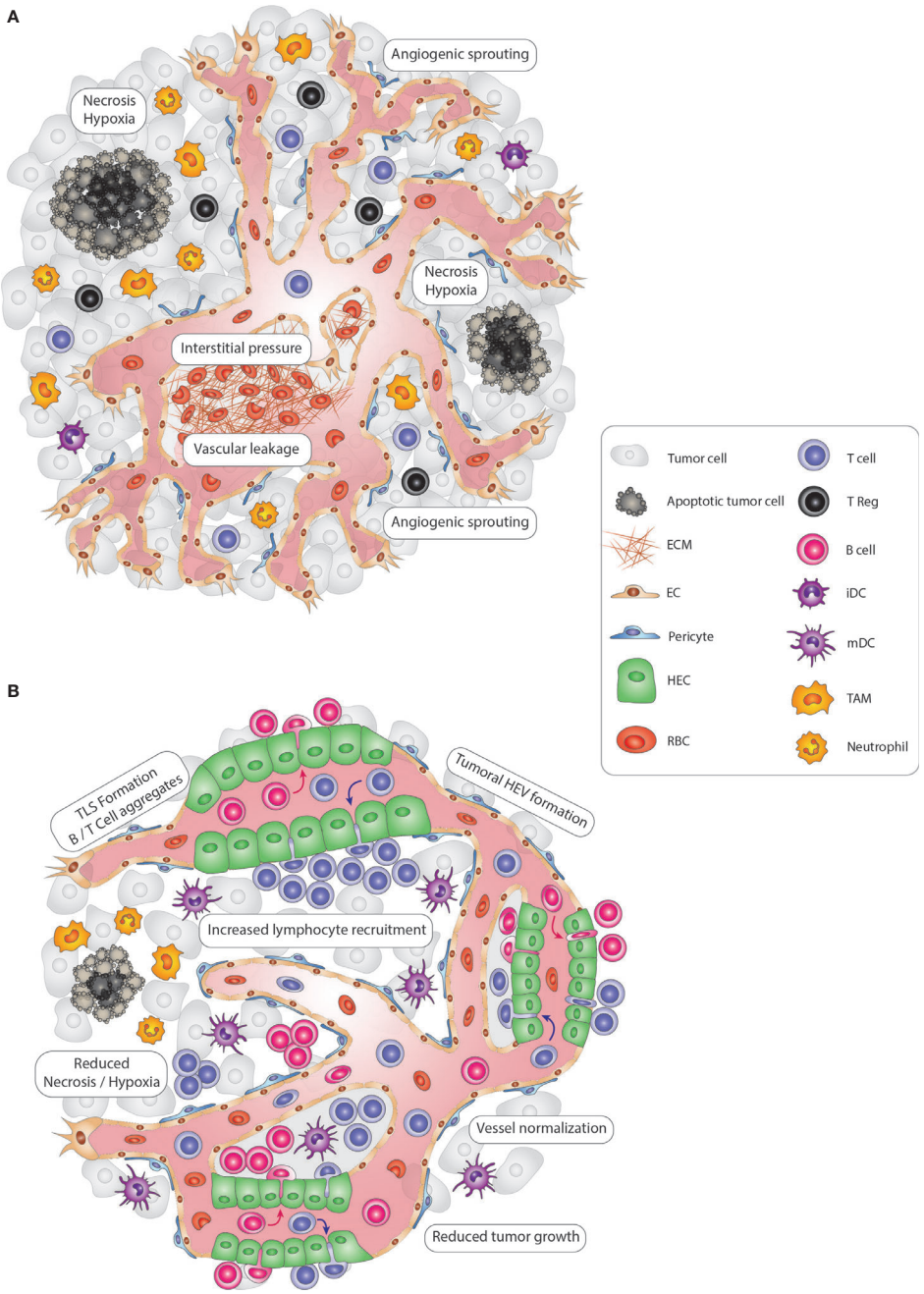

FIGURE 1 | Modulating vascular-immune interactions in solid tumors *via* TLS and HEV formation. **(A)** In solid tumors, vascular-immune interactions promote immunosuppression and neovascularization to allow the growth of cancer cells. Continuous angiogenic sprouting of ECs leads to an abnormal, less mature tumor vasculature with poor pericyte coverage leading to leakiness, dysfunctional blood flow and increased interstitial pressure which in turn promotes hypoxia and necrosis. Importantly, tumor blood vessels convey immunosuppressive signals that inhibit $CD4^+$ and $CD8^+$ lymphocyte infiltration, DC maturation and activate immunosuppressive regulatory T-cells (Tregs). Finally, innate immune cells, including TAMs and neutrophils, also suppress immunosurveillance and promote vascular remodeling. **(B)** Tumoral TLS and HEV induction promote anti-tumor immunity. In an immune-stimulatory setting, the tumor vasculature becomes transiently normalized with increased pericyte coverage, thus re-establishing blood flow and perfusion and reducing hypoxic and necrotic areas of the tumor. Due to the enhanced functionality, vessels are angiostatic and more prone to recruit immune cells which can lead to the formation of HEVs. Subsequently, HEV-containing TLSs form, with immune cell centers composed of CD4+ and CD8+ T, B lymphocytes, and mature DCs that promote an anti-tumor immune response. Tregs, TAMs, and neutrophils are less abundant, thus no longer exerting an immunosuppressive function. Altogether, re-awakening and boosting the immune system *via* TLS and HEV formation leads to reduced tumor cell growth and is ultimately beneficial for cancer progression. ECM, extra-cellular matrix; EC, endothelial cell; TLS, tertiary-lymphoid structure; HEV, high endothelial venule; HEC, high endothelial cell; iDC, immature dendritic cell; mDC, mature dendritic cell NK, Natural Killer cell; TAM, tumor-associated macrophage; RBC, red blood cell.

signals. They reduce the expression of ICAM1 and VCAM1 lymphocyte adhesion molecules in endothelial cells that limit vascular adhesion of lymphocytes and subsequent infiltration into the tumor (8, 9). Further, VEGF can directly inhibit dendritic cell (DC) maturation and activate antigen-specific regulatory T-cells (8, 9). Tumor-recruited innate immune cells, including macrophages, myeloid-derived suppressor cells (MDSC), and neutrophils, are an additional source of angiogenic and immunosuppressive factors to suppress immunosurveillance and promote vascular and matrix remodeling **(Figure 1)** (3, 10). Thus, tumors employ multiple mechanisms of the tissue repair program to keep their environment in a favorable, immunosuppressive and angiogenic state.

TLSs in Tumors

The *in situ* detection of tumor-infiltrating lymphocytes has been commonly used in the clinic because the degree of CD8 T cell infiltration often correlates with patient survival (11). Such histopathological studies revealed substantial lymphocyte aggregates in some tumors of patients who had a predominantly favorable outcome compared to those who did not. These structures display variably organized T- and B cell aggregates, sometimes even a T cell-rich zone with mature DCs juxtaposing a B cell follicle with germinal center characteristics. They are commonly located at the tumor interphase or in adjacent areas to the tumor and entail blood and lymphatic vessels and other stromal cells that are commonly observed in secondary lymphoid organs (SLOs). Indeed, due to their resemblance with SLOs, these ectopic lymphoid-like structures have been coined tertiary lymphoid structures (TLS) and have been observed in the pathological contexts of chronic inflammatory and autoimmune diseases (12, 13); including rheumatoid arthritis (14, 15), autoimmune thyroiditis (16), inflammatory bowel disease (17, 18), and *H. pylori gastritis* infections (19, 20). The reader can refer to (21–23) for their detailed description. Under these conditions, TLSs are abnormal structures of an active immune response against self-antigen, promote autoimmune reactions, and subsequently aggravate the disease. Since TLSs in solid tumors are mostly associated with improved tumor response, it is conceivable that they are also sites of activated lymphocytes generating an immune response (22). This raises the question as to how lymphocytes can preferentially infiltrate these locations despite the presence of an overall immunosuppressive vascular environment.

TLSs, Like SLOs, Contain High Endothelial Venules

While histopathological studies have extensively characterized immune infiltrates and defined tumoral TLSs in human cancer for the last 30 years (22), less is known regarding the vascular components of tumoral TLSs. TLS vessels present a resemblance to those in lymph nodes and other SLOs. Lymphatic vessels (LV) have been identified around multiple TLSs and are recognized by the typical lymphatic markers such as LYVE-1, PROX-1, and podoplanin (24). LVs remove interstitial fluid (containing plasma proteins, lipids etc.) that extravasate from blood capillary filtrates back into the blood circulation. They serve as the main route for dendritic cells, antigens, and inflammatory mediators into the lymph node (LN) and are essential players in peripheral tolerance, immunosurveillance, and resolution of inflammation (25). Only about a decade ago, Martinet and colleagues made the first observations of unusual blood vessels in human solid cancer samples which resembled high endothelial venules (HEV) in SLOs (26). HEVs are morphologically and functionally specialized blood vessels that deliver naïve lymphocytes from the bloodstream into the LN, in which lymphocytes become primed and educated by antigen-presenting cells (APC) (e.g., DCs) (**Figure 1**). Lymphocytes exit then through efferent LVs, which lead into the blood vascular system *via* the thoracic duct to circulate the cells through the body (27–31).

These observations beg the question as to whether HEVs and LVs in TLSs play comparable roles and are regulated similarly to those in LNs. In this review, we will focus on recent advances in HEV formation, function, and regulation in the tumoral context. From observations in human cancer, we will highlight studies of intratumoral HEVs in several mouse cancer models and describe the morphological and functional HEV alterations in premetastatic and metastatic LNs. Finally, we will discuss the functional implication, opportunities, and challenges of tumoral HEV formation for cancer immunotherapy.

PHYSIOLOGICAL HEVS IN SLOS

Characteristics of HEVs

HEVs develop from postcapillary venules in LN, Peyer's patches (PPs), and other SLOs but are absent in the spleen. In SLOs, adaptive immune responses are initiated through the active recruitment of naïve lymphocytes, which is facilitated by HEVs. In contrast to the common flat appearance of endothelial cells (EC), ECs lining HEVs have a cuboidal appearance with a prominent glycocalyx for which they have been coined "high" endothelial cells (HEC) (27, 32). HEVs form a thick basal lamina and are encompassed by a perivascular sheath of fibroblastic reticular cells (FRC) (33–36). Due to their specialized function as lymphocyte portals, HEVs express high levels of the ligand of L-Selectin/CD62L, the classic homing receptor for T and B-lymphocytes. L-Selectin ligands are sialomucins that entail sulfated mucin-like glycoproteins, including podocalyxin, endomucin, CD34, nepmucin, and GlyCAM-1 (rodent-specific) (30, 37). Importantly, sialomucins bind more effectively L-selectin after HEV-specific post-translational modifications by sulfotransferases and glycosyltransferases, including Carbohydrate Sulfotransferase 4 (CHST4) (38, 39) and Alpha-(1,3)-Fucosyltransferase VII (FucT-VII) (40, 41), which are highly expressed in HECs but not in other endothelial cells. Thus, antibodies have been developed that recognize HEVs by binding to these modified sialomucins. The most prominent antibody MECA79 ("Mouse Endothelial Cell Antigen-79") detects sulfated peripheral node addressin

(PNAd) that is decorated with the carbohydrate element 6-sulfo sialyl Lewis^X, (sialic acidα2-3Galβ1-4(Fucα1-3(sulfo-6) GlcNAcβ1-R) (37, 42, 43). Aside from these HEV-specific characteristics, HEVs express different vascular addressins in an SLO-dependent manner. While PNAd$^+$ HEVs are mainly found in peripheral LNs (pLN), HEVs in PPs express mucosal addressin cell adhesion molecule-1 (MAdCAM-1) but not PNAd (44). Notwithstanding, neonatal pLN-HEVs first express MAdCAM-1 for 3-4 weeks after birth before they switch to the PNAd$^+$ phenotype concomitant with HEV maturation, suggesting that MAdCAM-1 is an immature HEV marker in pLNs (45). Finally, mesenteric, sacral, and cervical LN-HEVs display expression of both PNAd and MAdCAM-1 vascular addressins (46, 47). It is noteworthy that most of our knowledge of HEV biology is derived from studies on pLNs.

HEVs Facilitate the Transmigration of Lymphocytes

The detailed migration process of lymphocytes across endothelial cells, including HEVs has been thoroughly studied by intravital microscopy (48, 49). This multistep event of lymphocyte tethering, rolling, sticking, and transmigration is tightly regulated by a coordinated interplay of adhesion molecules, integrins, and chemokines (37, 45, 48, 50). Migration of naïve and central memory T cells, as well as naïve B cells, starts with the binding of L-selectin to the 6-sulfo sialyl Lewis^X on the HEV walls. This tethering interaction reduces lymphocyte rolling and enables binding to the chemokines CCL19, CCL21, CXCL12, and CXCL13, which are presented on the luminal surface of HEVs, *via* CCR7, CXCR4, and CXCR5 receptors (51–53).

The chemoattractant-chemoattractant receptor axes that predominately govern the trafficking of lymphocytes into and out of LNs are CCL19/CCR7 and sphingosine 1-phosphate (S1P)/sphingosine 1 receptor 1 (S1PR1), respectively (30, 54). Blood-borne lymphocytes downregulate S1PR1 and use CCR7 signaling to adhere to HEVs for transmigration. During their LN residency, recirculating lymphocytes reacquire S1PR1 and attenuate their sensitivity to chemokines. Eventually, lymphocytes exit the LN by entering the cortical or medullary lymphatics, a process that depends upon S1PR1 signaling. Upon entering into the lymph, lymphocytes lose their polarity, downregulate their sensitivity to S1P due to the high concentration of S1P, and upregulate their sensitivity to chemokines (55). However, many of the details of lymphocyte transmigration across endothelial barriers remain poorly understood.

The integrin lymphocyte function-associated antigen 1(LFA-1/αLβ2) on lymphocytes interacts with the ICAM1 and ICAM2 adhesion molecules on the HEV surface, which leads to a firm arrest and subsequent paracellular or transcellular lymphocyte transmigration into the LN parenchyma (56, 57). Another notable characteristic of HEVs is their ability to form HEV pockets in which lymphocytes can be temporarily retained before their egress (56, 58). Although their function remains obscure, it is tempting to speculate that they exhibit specific lymphocyte communication centers and/or form when an overflow of lymphocytes arrives.

While HEVs typically recruit naïve and central memory lymphocytes in homeostatic LNs (30), HEVs of inflamed LNs become phenotypically remodeled, expand, and are capable of recruiting novel immune subsets into the LN. Specifically, they upregulate P-selectin, E-selectin, and CXCL9 and appear less mature because they induce gene expression of MAdCAM-1 while reducing *Fut7* and *Glycam1* transcription (59–61). Inflamed LN-HEVs can therefore recruit activated/effector T cells, plasmacytoid DCs, monocytes and neutrophils, whereas their capability to enroll naïve lymphocytes is not compromised (59, 60, 62–64)

HEV Regulation and Signaling in Lymph Nodes

The development of LNs is a well-organized event that involves the crosstalk between the hematopoietic lymphoid tissue inducer (LTi) cells and the mesenchymal lymphoid-tissue organizer (LTo) cells (65). It is thought that HEVs develop concomitantly with the accumulation of LTi cells to form the lymphoid anlagen; however, the developmental ontogeny of HEVs in lymphoid organs as well as the stepwise transcriptional program of HEV specification has not been clearly identified so far (66). The most important signaling pathway that has been directly linked to developmental LN-HEV formation and maintenance is the lymphotoxin- (LT)/ lymphotoxin β receptor (LTβR)–signaling pathway (67–69). LTβR is a member of the TNF receptor superfamily which binds the LTα1β2 heterotrimers or LIGHT ("homologous to **l**ymphotoxin, exhibits **i**nducible expression and competes with HSV **g**lycoprotein D for binding to **h**erpesvirus entry mediator, a receptor expressed on **T** lymphocytes") also known as TNSF14 (tumor necrosis factor superfamily member 14). Although the LTβR can activate both the canonical and non-canonical NFκB pathways, the non-canonical axis appears to be preferentially activated, specifically through the NIK kinase and the RelB/p52 transcriptional complex (70). Deletion of LTβR in ECs impaired the formation of HEVs in LN and subsequently LN homeostasis (69).

More recently, the S1P/S1PR1 axis has also been proposed to regulate HEV integrity in an autocrine manner and to facilitate HEV-DC interactions in LNs (71), thus suggesting the involvement of alternative signaling pathways regulating LN-HEV maintenance.

HIGH ENDOTHELIAL VENULES IN HUMAN CANCER

Martinet and colleagues made the first and formal observations of ectopic HEVs in human cancer samples (26). They observed MECA79$^+$ vessels by immunohistochemistry in a subset of human primary and naïve melanoma and breast, ovarian, colon, and lung tumor sections. They further confirmed with additional human HEV-specific marker HECA-452 (72) and

human HEV-specific antibodies G72 and G152 (73) that these vessels phenotypically resembled LN-HEVs and thus, termed them tumor HEVs (TU-HEV). Importantly, TU-HEVs were specifically located within lymphocyte-rich areas and frequently contained luminally-attached or extravasating $CD3^+$ cells. Indeed, the density of TU-HEVs in breast cancer was a predictor of CD3 T cell and B cell infiltration, suggesting that TU-HEVs, like their homologs in LNs, are major gateways for lymphocyte infiltration (26). Importantly, the density of TU-HEVs positively correlated with disease-free, metastasis-free, and overall survival rates in a retrospective cohort of primary breast cancer patients, thus suggesting their implication in the formation of immune-active TLS-like structure (74).

To date, these seminal results have been confirmed by other groups in breast cancer (75) and extended to a broader panel of other human cancers (76–79). Thus, $MECA79^+$ vessel-containing lymphocyte aggregates were described in renal (80), gastric (81), pancreatic (82–84), and head and neck carcinomas (85–88), among many other cancer types (89).

Although these studies defined a common TU-HEV phenotype by MECA79-positivity across the different human tumor types, they also described a more heterogeneous phenotype in comparison to that of LN-HEVs. For instance, in lung cancer, $MECA79^+$ blood vessels were also shown to express high levels of MAdCAM-1 (78). Additionally, in human melanoma (90) and oral squamous cell carcinoma (85, 88), the typical thick $MECA79^+$ vasculature with cuboidal ECs coexists with thin-walled $MECA79^+$ vessels displaying a flattened EC morphology and dilated lumens. It is conceivable that these observations could reflect different degrees and stages of TU-HEV maturation, thus implying functional differences among intratumoral $MECA79^+$ vessels. Indeed, plump TU-HEVs, that are surrounded by substantial lymphocyte aggregates are thought to be more mature than some isolated and flat TU-HEVs located at the periphery.

Since these observations are, however, only correlative, there is still a debate to which extent TU-HEVs are necessary to actively influence cancer progression in TLSs or TLS-like structures. Certainly, there are discrepancies between studies that are not only inherent to the considered tumor type but also dependent on intratumoral heterogeneity of TU-HEVs and TLSs, respectively. For instance, TU-HEVs can be present in T cell- and DC-rich areas (74, 91) while also present in B cell-rich areas (92, 93). Moreover, TU-HEVs appear to be more frequent than TLSs in breast cancer (26, 94) and melanoma (79, 91). Thus, it appears that the presence of TU-HEVs does not always correlate with *bona fide* intratumoral TLSs that inherit a "strict" definition but instead with a broader spectrum of TLS-like structures (23).

As the correlation of spontaneous TU-HEV and TLS formation with a positive outcome is preferentially observed in specific cancer types, one can envision that these naïve cancers have obtained a permissive environment for ectopic HEV formation. In line with this idea, "hot" tumors may be more prone to TU-HEV formation while "cold" tumors remain anergic (95).

This further raises the question as to whether cancer therapies and specifically those generating an immune-stimulating reaction, can instigate HEV and TLS formation. So far, only a few reports in breast (75, 96) and colorectal (97) tumors have correlated the presence of tumoral TLSs/HEVs with a favorable response to combined radio- and chemotherapy (22). Given the plethora of ongoing clinical trials evaluating the effects of immune checkpoint inhibitors (ICI), it is of great interest to evaluate thoroughly TU-HEV/TLS formation and its correlation with patient response. In support, higher TLS density in tumors correlated with an improved response to ICIs and increased survival in melanoma and soft-tissue sarcoma patients (92, 93, 98),

In summary, there is accumulating evidence from these clinical data that the formation of HEV-containing TLSs can be a marker of good prognosis but whether TU-HEV formation is a prerequisite for instigating TLS formation and antitumor response in human cancer remains obscure.

LESSONS LEARNED FROM HEVS IN MURINE TUMORS

Spontaneous TU-HEV Formation

Why do some tumors spontaneously form HEVs while others do not? One clue comes from the observation that spontaneous HEV formation in tumors of mice was only observed when tumor cells expressed strong antigens, i.e., the commonly used OVA-antigen peptide in tumor cell lines or the viral oncoprotein simian virus SV40 large T-antigen to drive endogenous tumor formation in pancreatic islets (99, 100). The presence of such antigens suggests that strongly antigenic tumors may have a more robust lymphocyte activity and, thus, be better poised to instigate TU-HEV formation.

So far, observations of spontaneous TU-HEVs in mice are rare and only reported in B16-OVA melanomas, LLC-OVA lung carcinomas and Rip1Tag5 (RT5) pancreatic neuroendocrine premalignant lesions (99–101). In line with the requirement of a tumor antigen to elicit a robust immune response, expression of SV40 Tag in the beta cells of pancreatic islets in RT5 mice does not commence before 10–12 weeks of age, leading to the recognition of Tag as a nonself protein (102). In contrast, pancreatic beta cells express Tag in Rip1Tag2 (RT2) mice already during embryonic development, probably due to differences in the site of integration of the transgene, and thus become tolerant to Tag (103). As a consequence, Tag expression in RT5 mice causes a severe immune response with intense infiltration of CD4 and CD8 T cells, B cells, and macrophages in hyperplastic RT5 islets, while islets of RT2 mice display a paucity of lymphocytes and do not become inflamed. This leads to the formation of immature $MAdCAM\text{-}1^+$ HEVs in inflamed RT5 hyperplastic islets but not in non-inflamed RT2 hyperplastic islets suggesting that immune cell infiltrates are required to initiate HEV formation although they appear not to be fully developed (100). Similarly, the spontaneously formed TU-HEVs in B16-OVA melanoma and LLC-OVA exhibited much weaker

PNAd positivity compared to LN-HEVs likely reflective of an immature HEV phenotype similar to that observed in RT5 hyperplastic islets (99, 100). What these data also imply is the necessity of reactive immune cells to enable HEV formation in tumors.

Immune Cells Regulate HEV Neogenesis in Tumors

The first evidence that hematopoietic cells can regulate LN-HEVs in adulthood comes from the study of Moussion and Girard (68). Depleting $CD11c^+$ DCs in adult CD11c-DTR mice by administering diphtheria toxin (DTX) degenerated HEVs and reverted them to a $MAdCAM\text{-}1^+$ immature stage reminiscent of neonatal HEVs. Congruently, $CD11c^+$ DCs are crucial for the switch from MAdCAM-1 to MECA79/PNAd expression during neonatal development of peripheral LNs (104). Consequently, due to the reduced HEV ability to recruit lymphocytes into the LN, LN size and cellularity was reduced (68).

Observations of $DC\text{-}LAMP^+$ mature DCs in close proximity of TU-HEVs in human breast cancer and melanoma tissue led to the initial proposition that DCs may also regulate HEVs in cancer (74, 105, 106) **(Figure 2)**. Nevertheless, most of the studies in mouse tumor models point to a more predominant role of lymphocytes. Spontaneous HEVs did not occur in B16-OVA tumors grown in Rag2-/- mice, lacking B and T lymphocytes but appeared when Rag2-/- mice were reconstituted with CD8 T cells before tumor implantation (99). Similarly, CD3 and CD8 T cell depletion led to a reduction of TU-HEV frequency and lymphocyte infiltrates in the pancreatic RIP1-Tag5 and a methylcholanthrene-induced fibrosarcoma tumor models (107, 108). The role of CD8 T cells as critical inducers of TU-HEV formation is further underscored by the observation that depletion of immunosuppressive CD4 T regulatory (Treg) cells renders tumors permissive to TU-HEV and TU-TLS neogenesis (108–110) **(Figure 2)**. Noteworthy, $FoxP3^+$Treg cell depletion with DTX using the FoxP3-DTR system, also disrupted the physiological LN-HEV network (108). DCs were, however, not required to form HEVs in Treg-depleted fibrosarcomas because HEVs were unaffected upon DC depletion (108). Although CD11c is a marker traditionally associated with pan-DCs, the expression of CD11c often overlaps in macrophages and DCs in non-lymphoid tissues (111). Therefore, the depletion of $CD11c^+$ cells in the before-mentioned study may not be restricted to the intratumoral DCs. So far, it remains unknown whether Tregs may directly suppress HEV neogenesis by interacting with tumor endothelial cells or indirectly by inhibiting CD4 and CD8 lymphocytes and creating an immunosuppressive environment.

Although lymphocytes appear to be the main regulators of TU-HEV neogenesis, innate immune cells have also been proposed as potential candidates (107, 112). Particularly, $CD68^+$ macrophages have also been shown to facilitate TU-HEV formation in the Rip1Tag5 tumor model by producing the TNF receptor ligands TNFα and LTα (107). Moreover, in a Kras (G12D)-driven mouse model of lung cancer, the depletion of $GR1^+$ neutrophils increased the intensity of MECA79 staining in $CD31^+$ ECs, indicating that $Gr1^+$ neutrophils are negative regulators of TU-HEVs (112) **(Figure 2).**

What are then the signaling pathways in ECs that instigate HEV formation in tumors? So far, it appears that the signaling cues and mechanisms involved in LN-HEV formation are also involved in tumoral HEV neogenesis. Several studies point to the lymphotoxin (LIGHT, LTα1β2)/LTβR pathway as the prevailing signaling cue in inducing TU-HEVs. Treatment with the LTβR agonist or the LTβR ligand LIGHT, which had been targeted to the tumor vasculature by fusing it to a vascular zip code peptide, induced $MECA79^+$ HEVs in various mouse tumor models, including those of breast cancer, neuroendocrine pancreatic tumors, and glioblastomas (107, 113–115).

Important to note is that anti-angiogenic immunotherapy in the form of anti-VEGF plus anti-PDL1 induced the noncanonical LTβR pathway in ECs of breast and pancreatic endocrine tumors, which enabled HEV formation, enhanced lymphocyte infiltration, and prolonged survival of tumor-bearing mice (113). The addition of agonistic LTβR antibodies to anti-VEGF plus anti-PDL1 therapy, thus fully activating the LTβR signaling cues, further increased HEV numbers and maturation in breast and pancreatic cancer and sensitized glioblastoma to the therapy. Combination treatment with LTβR antagonists, however, reversed these effects (113, 114) **(Figure 2)**.

Further, TNFR1 stimulation *via* TNFα or LTα3 seems to be accountable for spontaneous TU-HEV formation independent of LTβR. While LTβR-Ig blockade did not alter spontaneous HEVs in B16-OVA melanomas, HEVs were absent in these tumors when grown in $TNFR1/2^{-/-}$ mice or $Rag2^{-/-}$ mice replenished with $LT\alpha^{-/-}$ CD8 T cells (99). In a carcinogen-induced fibrosarcoma model, Treg depletion increased numbers, proliferation, and activation of TNFα-producing intratumoral $CD8^+$ T cells, which then induced the formation of intratumoral HEVs in a TNFR-dependent manner. Blockade of TNFR with TNFRII.Ig, anti-TNF antibodies, or *via* anti-LTα treatment reduced TU-HEV areas specifically in Treg-depleted fibrosarcomas, while LTbR-Ig had no effect (108). Targeting an LTα fusion protein to the tumor site has been shown to be another strategy to successfully induce $MECA79^+$ HEVs and lymphoid aggregates in the tumor microenvironment. In this study, electron microscopy observations confirmed the HEV morphology of around 30% of the blood vessels. Moreover, the therapy was efficient in eradicating subcutaneous B78-D14 melanomas and their established pulmonary metastases (116). These observations are in line with a study conducted in chronic inflammation where the transgenic expression of LTα under the control of a rat insulin promoter generated structures resembling lymph nodes concerning the cellular composition and HEV detection (117).

Another potential signaling molecule involved in HEV formation is IFNγ produced by NK cells and T cells because it stimulates the expression of the CXCR3 ligands CXCL9 and CXCL10, and the CCR7 ligand CCL21 as well as ICAM-1 in ECs, which all together induce T cell recruitment and infiltration (118). Although IFNγ is not sufficient to directly induce HEV

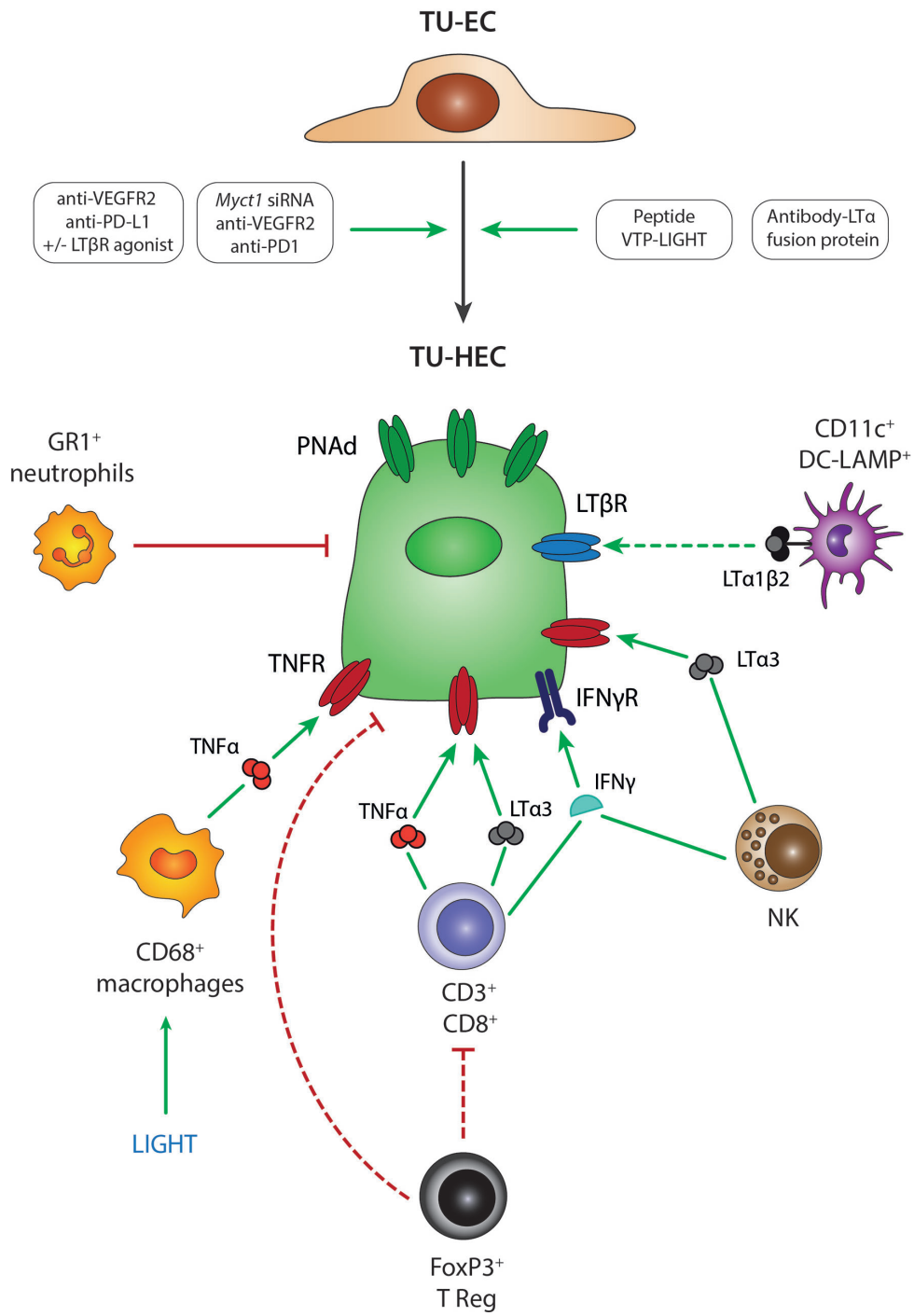

FIGURE 2 | Mechanisms of TU-HEV formation and maintenance. Several treatment regimens in mouse model studies have demonstrated the transition from TU-ECs to TU-HECs expressing PNAd; including 1- the combination of anti-VEGFR2 anti-angiogenic therapy with anti-PD-L1 immunotherapy, 2- the single activation of the LTβR axis with LTβR agonists, 3- the triple combination of anti-VEGFR2 anti-angiogenic therapy with anti-PD-L1 immunotherapy and LTβR agonists, 4- the triple combination of anti-VEGFR2 anti-angiogenic therapy with anti-PD1 immunotherapy and *Myct1* siRNA-mediated silencing, 5- engineered EC-specific VTP peptides expressing LIGHT and 6- fusion protein antibodies delivering LTα to the tumors (antibody-LTα fusion protein). TU-HECs are regulated by specific immune cell types and signaling cues within the tumor microenvironment; including 1- $CD3^+/CD8^+$ T cells *via* TNFα, LTα3 and IFNγ, 2- $FoxP3^+$ Tregs that either directly regulate PNAd expression or indirectly by exerting an immune-suppressive effect on $CD3^+CD8^+$ T cells, 3- NK cells *via* LTα3 and IFNγ, 4- $CD11c^+$ $DC\text{-}LAMP^+$ DCs *via* membrane-bound LTα1β2, 4- LIGHT-induced $CD68^+$ macrophages *via* TNFα and 5- $GR1^+$ neutrophils. TU-EC, tumoral endothelial cell; TU-HEC, tumoral high endothelial cell; PNAd, peripheral node addressin; DC, dendritic cell; NK, Natural Killer cell.

neogenesis (99), it may have supporting functions in instigating TU-HEVs by increasing lymphocyte influx. This may have important implications because the signaling pathways described above, induce vessel normalization. During this process, excessive immature tumor vessels become pruned, lymphocyte adhesion molecules increase, and pericytes align more closely to and stabilize the vasculature which leads to enhanced blood flow and T-cell infiltration. Vessel-targeted LIGHT normalized blood vessels in murine primary tumors and metastases (107, 114, 115, 119) and antiangiogenic therapy, alone and in combination with checkpoint blockade induced vessel normalization and boosted by further activation of the LTβR signaling using a LTβR agonistic antibody (113). In addition, a recent study has shown that genetic deletion of Myct1, a direct target gene of ETV2, was sufficient to normalize tumor vessels and induce TU-HEV formation in subcutaneous sarcoma, concomitant with antitumoral immunity. Myct1 deletion combined with immunotherapy was successful in increasing long-term survival in anti-PD1 refractory breast cancer model (120).

Thus, although it remains obscure whether vessel normalization is a prerequisite for HEV formation, it is tempting to speculate that vessel normalization in tumors is a trigger to enhance lymphocyte infiltration which in certain areas reaches a signaling threshold that could lead to HEV neogenesis.

What these studies also reveal is that the complex process of TU-HEV development likely involves multiple pathways and signals, and requires further investigation. It is plausible that a process similar to the proposed two-step differentiation model of HEV formation in chronic inflammation, may take place. In accordance with this model, TNFR1 is required in the initial stages of chronic inflammation and induces flat MECA79$^+$ blood vessels, whereas the LTβR pathway is involved for the additional maturation and acquisition of a fully mature HEV phenotype (121, 122).

Do Tumoral HEVs Generate Specific Immune-Reactive Centers?

Naïve T cells are thought to become primed and activated by tumor antigen-presenting DCs, expand and differentiate in the tumor-draining lymph node, also referred to as sentinel LN, from which they home to the tumor site (123).

Interestingly, analysis of T cell clonality and homing indicate that TU-HEVs can facilitate infiltration of naïve T cells *via* the selectin L/CD62L axis into the tumor (99, 116). T cell activation, therefore, not only occurs in the sentinel LN, but may also take place at the tumor site (22, 116, 124). The recruitment of naïve T cells into the tumor, bypassing the activation in the sentinel LN, may help to speed up and favor the generation of an *in situ* antitumoral response but also requires antigen presentation by DCs and other APCs for T cell activation (125). Congruently, TLSs have been shown to facilitate interactions between T cells and tumor-antigen-presenting CD11c$^+$ DCs in a genetically engineered mouse model of lung adenocarcinoma. Staining of γ-tubulin (a marker of the microtubule-organizing center [MTOC]) depicted immunological synapses between DCs and CD8 T cells, in the tumors, which in turn upregulated the early activation marker (CD69) and became proliferative (109). The concept that naïve T cells may be educated within the tumor has also been observed in human tumors. Mature LAMP$^+$ DCs closely associated with CD3 T-cells have been identified in juxtaposition to TU-HEVs in human breast cancer (74). Importantly, dense aggregates of MHC-II$^+$ APCs and CD8 T cells have been identified in human renal cell carcinomas (RCC). These niches contain TCF1$^+$PD1$^+$stem-like CD8 T-cells that undergo slow self-renewal and give rise to terminally differentiated CD8 T cells. They provide the proliferative burst and thereby foster the antitumoral immune response seen after anti-PD1-immunotherapy (126, 127). Interestingly, these T cell-enriched nests appear to be active immune centers that closely resembled the extrafollicular regions of the lymph node and were quite distinct from the typical B cell-enriched-identified TLSs found in RCCs which did not exhibit closely interacting DCs and T cells (126). Whether TU-HEVs are also an integral part of these APC niches remains to be investigated.

Besides therapeutically exploiting TU-HEVs as lymphocyte gateways, they also offer a "route" to deliver chemotherapeutic agents. One of the key features of the pancreatic ductal adenocarcinoma (PDAC) is the dense and poor vascularized microenvironment which limits the penetrance of drugs to the site of the tumor. TU-HEVs have been identified in the stroma of human PDAC implanted in a humanized mouse model (84). Targeting TU-HEVs with MECA79-Taxol-nanoparticles has been shown to improve efficacy in delivering Paclitaxel to the tumor, resulting in tumor growth inhibition (84). Similarly, in preclinical models of breast as well as pancreatic tumors, an antibody (MHA112)-based strategy has been used to directly deliver the chemotherapeutic agent to tumors *via* targeting of TU-HEVs (128). Given these results, combining HEV-inducing strategies with HEV-specific deliverables of chemotherapeutical agents may represent a synergistic approach for future cancer therapy.

HEV ALTERATIONS IN SENTINEL LNS

LNs are critical for immune surveillance, providing a highly organized hub to obtain optimal conditions for naïve lymphocytes to interact with APCs. In response to certain stimuli such as infection and inflammation, the draining LNs undergo considerable expansion, known as lymphadenopathy, to accommodate the increased need of lymphocyte priming. This process is characterized by increased blood flow and lymphocyte trafficking while the lymphocyte exit *via* lymphatics is temporarily blocked (129–131). These changes increase the probability of antigen presentation and ensure the initiation of the appropriate antigen-specific immunity. LN expansion is orchestrated by transient LN-vasculature remodeling. Upon inflammation, HEVs quickly expand by undergoing clonal proliferation of a putative progenitor cell and succumb upon cessation of inflammation to return to their homeostatic stage (132). LN-HEV plasticity and remodeling upon inflammation

are controlled by extensive reprogramming and have been comprehensively investigated at the transcriptional level (59).

Sentinel LNs are considered the major site at which the anti-tumoral immunity is initiated, but they also represent a privileged site for cancer cell dissemination (133) **(Figure 3)**.

Similar to inflamed LNs, sentinel LNs also undergo vascular remodeling (88, 134–137). Sentinel LN-HEVs often show dramatic morphological changes, shifting from thick-walled blood vessels with a small lumen to a thin-walled vasculature with an enlarged lumen and abundant red blood cells (RBC). Moreover, HEVs of sentinel LNs can display loss in PNAd/MECA79 expression in association with dysregulation of CCL21 in perivascular FRCs (134–136). Given the importance of PNAd and CCL21 in the recruitment remodeling of naïve T cells and initiation of the adaptive response, the dysregulation of these components in sentinel LNs may indicate impaired LN functionality.

Noteworthy, experiments in nude mice have shown that these dramatic changes occur only in tumor-reactive LNs and not in endotoxin-induced lymphadenopathy, indicating that the mechanism of vascular reorganization in sentinel LN may differ from that of inflammatory-reactive LNs. Importantly, these studies have also shown that T cells are not the major players in the vascular remodeling of sentinel LN (135).

HEV abnormality has been observed in sentinel LNs of breast cancer, melanoma, and squamous cell cancer patients (88, 134–137). As these modifications occur before detection of metastatic cancer cells in the sentinel LN (135, 136), it is conceivable that tumor-emanating factors induce LN-HEV alterations to establish a pre-metastatic niche permissive for tumor cells. One could also speculate that the presence of enlarged HEV lumen engorged with RBC, could enhance oxygen and nutrient delivery for arriving cancer cells.

The majority of cancers invade the sentinel LN *via* lymphatic vessels before spreading to distant organs (138). Until recently, it was expected that metastatic cancer cells would also leave the LN through the efferent lymphatic vessels, the LNs of higher echelons, and the thoracic duct (139) **(Figure 3)**. However, two recent seminal studies in mice have revealed that cancer cell dissemination can occur through the LN-HEVs by intravital microscopy. In the first study, murine 4T1 breast cancer cells intra-lymphatically infused into the subcapsular sinus of pLNs, migrated towards the LN center, then localized around HEVs, transmigrated through HEVs, and subsequently disseminated into the lungs. Importantly, lymphatic ligation did not compromise the capability of cancer cells to colonize the distal organs (140). Similar results were obtained in the second study, in which, using time-lapse multiphoton intravital microscopy, the photo-converted metastatic cancer cells were first seen in the subcapsular sinus and later invaded the cortex of the LN where they transmigrated into HEV^+ vessels. Metastatic cancer cells were then eventually detected in the systemic blood circulation and in the lungs (141).

Overall, these experimental studies revealed that LN-HEVs serve as a gateway not only for lymphocyte trafficking into the LN but can also enable tumor cell intravasation into the bloodstream. Concomitantly, HEV alterations into flattened, dilated blood vessels occur that have lost their morphological and likely functional properties and may likely be induced by the tumor. To this end, the implication of tumor-emanating factors in HEV remodeling in the premetastatic niche in LNs is unknown (**Figure 3**). In addition, whether tumor cell dissemination in human LNs also occurs through HEVs, remains to be clarified, but substantial LN-HEV remodeling preceding LN metastasis has also been shown in human breast cancer patients (136). The premetastatic LN alterations also provide an opportunity for identifying biomarkers of vascular changes in sentinel LNs that could be used to predict disease progression in human cancer (136).

CONCLUDING REMARKS AND FUTURE DIRECTIONS

Since sufficient infiltration of intratumoral T cell effector cells in malignant lesions is a major hurdle in anti-cancer immunotherapy (11, 142), therapeutic induction of HEVs represents a compelling approach to boost effective transmigration of lymphocytes into the tumor. This may increase the benefits of immune checkpoint blockade and improve cell-based immunotherapies using chimeric antigen receptor (CAR) T cells in solid tumors. An additional and specific advantage of therapeutic HEV induction may be the creation of immune-reactive niches that spurt T cell activation and differentiation and replace exhausted and dysfunctional effector T cells.

Although these are tantalizing concepts, they also raise several questions about the tumor-specific ontogeny, regulation, and function of HEVs. Studies in mouse tumor models have provided the first insight into the cellular and molecular regulators of HEV formation and maintenance, partly resembling those of LN-HEVs and partly depicting disparities. The varying degrees of HEV morphology in tumors may also affect HEV functionality, as shown in sentinel LNs, raising concerns about the implication of HEVs in recruiting tolerance-promoting lymphocytes in tumors. Indeed, TLSs are correlated with a worse prognosis in some tumor types, including hepatocellular carcinomas, RCC lung metastases, and head and neck cancer, although the reasons are unknown (22, 143, 144).

An accumulation of Tregs has been observed in TLSs of a lung cancer mouse model (109). However, Treg depletion enhanced HEVs and improved an immune response in these tumors (109), as also observed in fibrosarcoma (108). Recent single-cell transcriptomic analyses of homeostatic and inflamed LNs (59, 145) have provided a specific transcriptional signature of LN-HEVs that has shed some light on LN-HEV-specific signals (146). Comparing transcriptomics between LN-HEVs and TU-HEVs will be important to inform about general and tumor-specific HEV characteristics and functions. To this end, HEV development in LNs and in tumors remains obscure. When LNs become inflamed and enlarged, HEVs quickly expand in part by progenitor cell propagation but by what means HEVs arise from

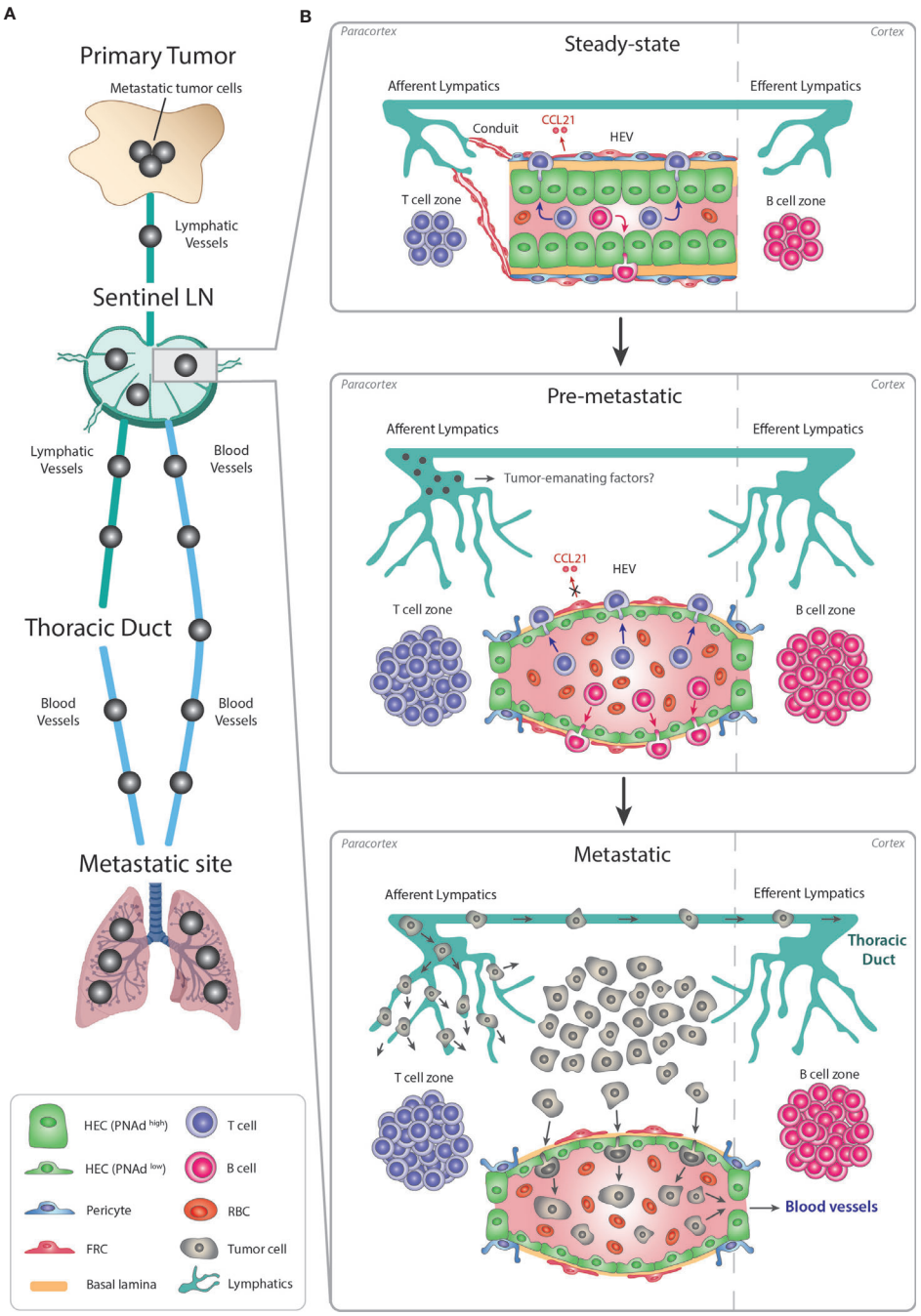

FIGURE 3 | Remodeling of LN-HEVs during cancer metastasis. **(A)** Metastasis is a stepwise process leading to the dissemination of cancer cells from the primary tumor towards preferential metastatic sites. Most commonly, metastatic cancer cells use the lymphatic system to exit the primary tumor, reach a proximal sentinel LN, circulate into adjacent LNs and eventually drain from the thoracic duct into the systemic venous system, thus spreading towards metastatic sites (e.g., lungs). Metastatic tumor cells in the LN parenchyma can also directly intravasate into the bloodstream *via* LN-HEVs and disseminate towards metastatic sites. **(B)** This alternative route involves an important remodeling of the sentinel LN already at the pre-metastatic stage, in preparation for the arrival of cancer cells. Overall, the sentinel LN expands, as evidenced by 1- expanded T and B cell compartments in the paracortex and cortex, respectively, and by 2- an extensive lymphangiogenesis. Importantly, HEVs are remodeled as 1- HECs switch to a PNAd^{low} flat phenotype with thin-walled basal lamina and enlarged lumens filled with numerous RBCs, and 2- CCL21 expression is dysregulated in FRCs, suggesting impaired lymphocyte-recruiting functions of sentinel LN-HEVs. Whether tumor cells from the primary site secrete specific factors preparing this pre-metastatic niche prior to their circulation into the sentinel LN remains to be elucidated. Altogether, the expanded sentinel LN and remodeled HEVs allow the direct spreading of cancer cells from afferent lymphatics into the venous bloodstream during the metastatic stage. LN, lymph node; HEV, high endothelial venule; HEC, high endothelial cell; RBC, red blood cell; FRC, fibroblastic reticular cell.

tumor endothelial cells and expand is unknown. Such knowledge, however, will be crucial to therapeutically switch on and off HEV formation in a controlled manner in malignant lesions to avoid potential autoimmune reactions.

Finally, *in situ* HEV model systems can help to dissect the cellular and molecular circuits controlling TU-HEV neogenesis. To date, nonetheless, HEVs cannot be cultured and maintained *ex vivo*, thus rendering mechanistic analyses difficult. Indeed, several attempts to culture purified HEV-ECs have failed due to a rapid loss of their unique features once plated as monolayers suggesting the necessity of additional cell types, factors and specific growth conditions (147–150). One attractive model system may be *bona fide* vascular organoids that have been successfully generated from human ES cells and fully recapitulate the heterogeneity and functionality of vessels *in vitro* and *in vivo* upon transplantation (151–153). Other systems involve microfluidics (154) or EC reprogramming (155) which could serve as more relevant platforms to induce and maintain HEV *ex vivo*.

High endothelial venules display a unique specialization of blood endothelial cells and due to their explicit interaction with lymphocytes, only arise in specific lymphoid organs during development. The fact that they can also ectopically develop in non-lymphoid organs during chronic (tumor) inflammation in the adult is again linked to their intimate relationship with lymphocytes, which may go far beyond mere lymphocyte transportation. Looking into the future, further investigations of TU-HEV blood vessels are timely to better comprehend their nature and functionality because enabling their therapeutic induction in tumors offers promising avenues, not only for immunotherapies, but also for other types of cancer treatment.

AUTHOR CONTRIBUTIONS

All authors contributed to the article and approved the submitted version.

FUNDING

This work was supported by grants from the Flemish government FWO (G0A0818N to GV and GB, G072021N to SG and GB) and the National Institute of Health NIH/NCI (R01CA201537 to GB).

REFERENCES

1. Hanahan D, Weinberg RA. Hallmarks of Cancer: The Next Generation. *Cell* (2011) 144(5):646–74. doi: 10.1016/j.cell.2011.02.013
2. Dvorak HF. Tumors: Wounds That do Not Heal. Similarities Between Tumor Stroma Generation and Wound Healing. *N Engl J Med* (1986) 315 (26):1650–9. doi: 10.1056/NEJM198612253152606
3. Hua Y, Bergers G. Tumors *vs.* Chronic Wounds: An Immune Cell's Perspective. *Front Immunol* (2019) 10:2178. doi: 10.3389/fimmu.2019.02178
4. Baluk P, Hashizume H, McDonald DM. Cellular Abnormalities of Blood Vessels as Targets in Cancer. *Curr Opin Genet Dev* (2005) 15(1):102–11. doi: 10.1016/j.gde.2004.12.005
5. Jain RK. Normalizing Tumor Vasculature With Anti-Angiogenic Therapy: A New Paradigm for Combination Therapy. *Nat Med* (2001) 7(9):987–9. doi: 10.1038/nm0901-987
6. Jain RK. Normalization of Tumor Vasculature: An Emerging Concept in Antiangiogenic Therapy. *Science* (2005) 307(5706):58–62. doi: 10.1126/science.1104819
7. Carmeliet P. Angiogenesis in Life, Disease and Medicine. *Nature* (2005) 438 (7070):932–6. doi: 10.1038/nature04478
8. Motz GT, Santoro SP, Wang LP, Garrabrant T, Lastra RR, Hagemann IS, et al. Tumor Endothelium FasL Establishes a Selective Immune Barrier Promoting Tolerance in Tumors. *Nat Med* (2014) 20(6):607–15. doi: 10.1038/nm.3541
9. Rodig N, Ryan T, Allen JA, Pan H, Grabie N, Chernova T, et al. Endothelial Expression of PD-L1 and PD-L2 Down-Regulates CD8+ T Cell Activation and Cytolysis. *Eur J Immunol* (2003) 33(11):3117–26. doi: 10.1002/eji.200324270
10. Rivera LB, Bergers G. Intertwined Regulation of Angiogenesis and Immunity by Myeloid Cells. *Trends Immunol* (2015) 36(4):240–9. doi: 10.1016/j.it.2015.02.005
11. Galon J, Costes A, Sanchez-Cabo F, Kirilovsky A, Mlecnik B, Lagorce-Pagès C, et al. Type, Density, and Location of Immune Cells Within Human Colorectal Tumors Predict Clinical Outcome. *Science* (2006) 313 (5795):1960–4. doi: 10.1126/science.1129139
12. Aloisi F, Pujol-Borrell R. Lymphoid Neogenesis in Chronic Inflammatory Diseases. *Nat Rev Immunol* (2006) 6(3):205–17. doi: 10.1038/nri1786
13. Pitzalis C, Jones GW, Bombardieri M, Jones SA, et al. Ectopic Lymphoid-Like Structures in Infection, Cancer and Autoimmunity. *Nat Rev Immunol* (2014) 14(7):447–62. doi: 10.1038/nri3700
14. Takemura S, Braun A, Crowson C, Kurtin PJ, Cofield RH, O'Fallon WM, et al. Lymphoid Neogenesis in Rheumatoid Synovitis. *J Immunol* (2001) 167 (2):1072–80. doi: 10.4049/jimmunol.167.2.1072
15. Humby F, Bombardieri M, Manzo A, Kelly S, Blades MC, Kirkham B, et al. Ectopic Lymphoid Structures Support Ongoing Production of Class-Switched Autoantibodies in Rheumatoid Synovium. *PloS Med* (2009) 6(1): e1. doi: 10.1371/journal.pmed.0060001
16. Armengol MP, Juan M, Lucas-Martín A, Fernández-Figueras MT, Jaraquemada D, Gallart T, et al. Thyroid Autoimmune Disease: Demonstration of Thyroid Antigen-Specific B Cells and Recombination-Activating Gene Expression in Chemokine-Containing Active Intrathyroidal Germinal Centers. *Am J Pathol* (2001) 159(3):861–73. doi: 10.1016/S0002-9440(10)61762-2
17. Surawicz CM, Belic L. Rectal Biopsy Helps to Distinguish Acute Self-Limited Colitis From Idiopathic Inflammatory Bowel Disease. *Gastroenterology* (1984) 86(1):104–13. doi: 10.1016/0016-5085(84)90595-X
18. Carlsen HS, Baekkevold ES, Johansen FE, Haraldsen G, Brandtzaeg P, et al. B Cell Attracting Chemokine 1 (CXCL13) and its Receptor CXCR5 Are Expressed in Normal and Aberrant Gut Associated Lymphoid Tissue. *Gut* (2002) 51(3):364–71. doi: 10.1136/gut.51.3.364
19. Mazzucchelli L, Blaser A, Kappeler A, Schärli P, Laissue JA, Baggiolini M, et al. BCA-1 Is Highly Expressed in Helicobacter Pylori-Induced Mucosa-Associated Lymphoid Tissue and Gastric Lymphoma. *J Clin Invest* (1999) 104(10):R49–54. doi: 10.1172/JCI7830
20. Winter S, Loddenkemper C, Aebischer A, Rabel K, Hoffmann K, Meyer TF, et al. The Chemokine Receptor CXCR5 Is Pivotal for Ectopic Mucosa-Associated Lymphoid Tissue Neogenesis in Chronic Helicobacter Pylori-Induced Inflammation. *J Mol Med (Berl)* (2010) 88(11):1169–80. doi: 10.1007/s00109-010-0658-6
21. Stranford S, Ruddle NH. Follicular Dendritic Cells, Conduits, Lymphatic Vessels, and High Endothelial Venules in Tertiary Lymphoid Organs: Parallels With Lymph Node Stroma. *Front Immunol* (2012) 3:350. doi: 10.3389/fimmu.2012.00350
22. Sautes-Fridman C, Petitprez F, Calderaro J, Fridman WH, et al. Tertiary Lymphoid Structures in the Era of Cancer Immunotherapy. *Nat Rev Cancer* (2019) 19(6):307–25. doi: 10.1038/s41568-019-0144-6
23. Neyt K, Perros F, GeurtsvanKessel CH, Hammad H, Lambrecht BN, et al. Tertiary Lymphoid Organs in Infection and Autoimmunity. *Trends Immunol* (2012) 33(6):297–305. doi: 10.1016/j.it.2012.04.006

24. Ruddle NH. Lymphatic Vessels and Tertiary Lymphoid Organs. *J Clin Invest* (2014) 124(3):953–9. doi: 10.1172/JCI71611
25. Alitalo K. The Lymphatic Vasculature in Disease. *Nat Med* (2011) 17 (11):1371–80. doi: 10.1038/nm.2545
26. Martinet L, Garrido I, Filleron T, Le Guellec S, Bellard E, Fournie JJ, et al. Human Solid Tumors Contain High Endothelial Venules: Association With T- and B-Lymphocyte Infiltration and Favorable Prognosis in Breast Cancer. *Cancer Res* (2011) 71(17):5678–87. doi: 10.1158/0008-5472.CAN-11-0431
27. Girard JP, Springer TA. High Endothelial Venules (HEVs): Specialized Endothelium for Lymphocyte Migration. *Immunol Today* (1995) 16 (9):449–57. doi: 10.1016/0167-5699(95)80023-9
28. Butcher EC, Picker LJ. Lymphocyte Homing and Homeostasis. *Science* (1996) 272(5258):60–6. doi: 10.1126/science.272.5258.60
29. Miyasaka M, Tanaka T. Lymphocyte Trafficking Across High Endothelial Venules: Dogmas and Enigmas. *Nat Rev Immunol* (2004) 4(5):360–70. doi: 10.1038/nri1354
30. Girard JP, Moussion C, Förster R. HEVs, Lymphatics and Homeostatic Immune Cell Trafficking in Lymph Nodes. *Nat Rev Immunol* (2012) 12 (11):762–73. doi: 10.1038/nri3298
31. von Andrian UH, Mempel TR. Homing and Cellular Traffic in Lymph Nodes. *Nat Rev Immunol* (2003) 3(11):867–78. doi: 10.1038/nri1222
32. Thomé R. Endothelien Als Phagocyten (Aus Den Lymphdrüsen Von Macacus Cynomolgus). *Arch Mikrosk Anat* (1898) 52(4):820–42. doi: 10.1007/BF02977038
33. Roozendaal R, Mebius RE, Kraal G. The Conduit System of the Lymph Node. *Int Immunol* (2008) 20(12):1483–7. doi: 10.1093/intimm/dxn110
34. Anderson AO, Anderson ND. Studies on the Structure and Permeability of the Microvasculature in Normal Rat Lymph Nodes. *Am J Pathol* (1975) 80 (3):387–418.
35. Gretz JE, Kaldjian EP, Anderson AO, Shaw S, et al. Sophisticated Strategies for Information Encounter in the Lymph Node: The Reticular Network as a Conduit of Soluble Information and a Highway for Cell Traffic. *J Immunol* (1996) 157(2):495–9.
36. Gretz JE, Norbury CC, Anderson AO, Proudfoot AE, Shaw S, et al. Lymph-Borne Chemokines and Other Low Molecular Weight Molecules Reach High Endothelial Venules *via* Specialized Conduits While a Functional Barrier Limits Access to the Lymphocyte Microenvironments in Lymph Node Cortex. *J Exp Med* (2000) 192(10):1425–40. doi: 10.1084/jem.192.10.1425
37. Rosen SD. Ligands for L-Selectin: Homing, Inflammation, and Beyond. *Annu Rev Immunol* (2004) 22:129–56. doi: 10.1146/annurev.immunol.21.090501.080131
38. Kawashima H, Petryniak B, Hiraoka N, Mitoma J, Huckaby V, Nakayama J, et al. N-Acetylglucosamine-6-O-Sulfotransferases 1 and 2 Cooperatively Control Lymphocyte Homing Through L-Selectin Ligand Biosynthesis in High Endothelial Venules. *Nat Immunol* (2005) 6(11):1096–104. doi: 10.1038/ni1259
39. Uchimura K, Gauguet JM, Singer MS, Tsay D, Kannagi R, Muramatsu T, et al. A Major Class of L-Selectin Ligands Is Eliminated in Mice Deficient in Two Sulfotransferases Expressed in High Endothelial Venules. *Nat Immunol* (2005) 6(11):1105–13. doi: 10.1038/ni1258
40. Homeister JW, Thall AD, Petryniak B, Malý P, Rogers CE, Smith PL, et al. The Alpha(1,3)Fucosyltransferases FucT-IV and FucT-VII Exert Collaborative Control Over Selectin-Dependent Leukocyte Recruitment and Lymphocyte Homing. *Immunity* (2001) 15(1):115–26. doi: 10.1016/S1074-7613(01)00166-2
41. Malý P, Thall A, Petryniak B, Rogers CE, Smith PL, et al. The Alpha(1,3) Fucosyltransferase Fuc-TVII Controls Leukocyte Trafficking Through an Essential Role in L-, E-, and P-Selectin Ligand Biosynthesis. *Cell* (1996) 86 (4):643–53. doi: 10.1016/S0092-8674(00)80137-3
42. Streeter PR, Rouse BT, Butcher EC. Immunohistologic and Functional Characterization of a Vascular Addressin Involved in Lymphocyte Homing Into Peripheral Lymph Nodes. *J Cell Biol* (1988) 107(5):1853–62. doi: 10.1083/jcb.107.5.1853
43. Yeh JC, Hiraoka N, Petryniak B, Nakayama J, Ellies LG, Rabuka D, et al. Novel Sulfated Lymphocyte Homing Receptors and Their Control by a Core1 Extension Beta 1,3-N-Acetylglucosaminyltransferase. *Cell* (2001) 105 (7):957–69. doi: 10.1016/S0092-8674(01)00394-4
44. Berg EL, McEvoy LM, Berlin C, Bargatze RF, Butcher EC, et al. L-Selectin-Mediated Lymphocyte Rolling on MAdCAM-1. *Nature* (1993) 366 (6456):695–8. doi: 10.1038/366695a0
45. Mebius RE, Streeter PR, Michie S, Butcher EC, Weissman IL, et al. A Developmental Switch in Lymphocyte Homing Receptor and Endothelial Vascular Addressin Expression Regulates Lymphocyte Homing and Permits CD4+ CD3- Cells to Colonize Lymph Nodes. *Proc Natl Acad Sci USA* (1996) 93(20):11019–24. doi: 10.1073/pnas.93.20.11019
46. Ager A. High Endothelial Venules and Other Blood Vessels: Critical Regulators of Lymphoid Organ Development and Function. *Front Immunol* (2017) 8:45. doi: 10.3389/fimmu.2017.00045
47. Csencsits KL, Jutila MA, Pascual DW. Mucosal Addressin Expression and Binding-Interactions With Naive Lymphocytes Vary Among the Cranial, Oral, and Nasal-Associated Lymphoid Tissues. *Eur J Immunol* (2002) 32 (11):3029–39. doi: 10.1002/1521-4141(200211)32:11<3029::AID-IMMU3029>3.0.CO;2-9
48. von Andrian UH. Intravital Microscopy of the Peripheral Lymph Node Microcirculation in Mice. *Microcirculation* (1996) 3(3):287–300. doi: 10.3109/10739689609148303
49. Warnock RA, Askari S, Butcher EC, von Andrian UH, et al. Molecular Mechanisms of Lymphocyte Homing to Peripheral Lymph Nodes. *J Exp Med* (1998) 187(2):205–16. doi: 10.1084/jem.187.2.205
50. Kikuta A, Rosen SD. Localization of Ligands for L-Selectin in Mouse Peripheral Lymph Node High Endothelial Cells by Colloidal Gold Conjugates. *Blood* (1994) 84(11):3766–75. doi: 10.1182/blood.V84.11.3766.bloodjournal84113766
51. Bao X, Moseman EA, Saito H, Petryniak B, Thiriot A, Hatakeyama S, et al. Endothelial Heparan Sulfate Controls Chemokine Presentation in Recruitment of Lymphocytes and Dendritic Cells to Lymph Nodes. *Immunity* (2010) 33(5):817–29. doi: 10.1016/j.immuni.2010.10.018
52. Tsuboi K, Hirakawa J, Seki E, Imai Y, Yamaguchi Y, Fukuda M, et al. Role of High Endothelial Venule-Expressed Heparan Sulfate in Chemokine Presentation and Lymphocyte Homing. *J Immunol* (2013) 191(1):448–55. doi: 10.4049/jimmunol.1203061
53. Okada T, Ngo VN, Ekland EH, Förster R, Lipp M, Littman DR, et al. Chemokine Requirements for B Cell Entry to Lymph Nodes and Peyer's Patches. *J Exp Med* (2002) 196(1):65–75. doi: 10.1084/jem.20020201
54. Cyster JG, Schwab SR. Sphingosine-1-Phosphate and Lymphocyte Egress From Lymphoid Organs. *Annu Rev Immunol* (2012) 30:69–94. doi: 10.1146/annurev-immunol-020711-075011
55. Arnon TI, Xu Y, Lo C, Pham T, An J, Coughlin S, et al. GRK2-Dependent S1PR1 Desensitization Is Required for Lymphocytes to Overcome Their Attraction to Blood. *Science* (2011) 333(6051):1898–903. doi: 10.1126/science.1208248
56. Yan SLS, Hwang IY, Kamenyeva O, Kehrl JH, et al. *In Vivo* F-Actin Filament Organization During Lymphocyte Transendothelial and Interstitial Migration Revealed by Intravital Microscopy. *iScience* (2019) 16:283–97. doi: 10.1016/j.isci.2019.05.040
57. Schoefl GI. The Migration of Lymphocytes Across the Vascular Endothelium in Lymphoid Tissue. A Reexamination. *J Exp Med* (1972) 136(3):568–88. doi: 10.1084/jem.136.3.568
58. Mionnet C, Sanos SL, Mondor I, Jorquera A, Laugier JP, Germain RN, et al. High Endothelial Venules as Traffic Control Points Maintaining Lymphocyte Population Homeostasis in Lymph Nodes. *Blood* (2011) 118 (23):6115–22. doi: 10.1182/blood-2011-07-367409
59. Veerman K, Tardiveau C, Martins F, Coudert J, Girard JP, et al. Single-Cell Analysis Reveals Heterogeneity of High Endothelial Venules and Different Regulation of Genes Controlling Lymphocyte Entry to Lymph Nodes. *Cell Rep* (2019) 26(11):3116–31.e5. doi: 10.1016/j.celrep.2019.02.042
60. Janatpour MJ, Hudak S, Sathe M, Sedgwick JD, McEvoy LM, et al. Tumor Necrosis Factor-Dependent Segmental Control of MIG Expression by High Endothelial Venules in Inflamed Lymph Nodes Regulates Monocyte Recruitment. *J Exp Med* (2001) 194(9):1375–84. doi: 10.1084/jem.194.9.1375
61. Martín-Fontecha A, Baumjohann D, Guarda G, Reboldi A, Hons M, Lanzavecchia A, et al. CD40L+ CD4+ Memory T Cells Migrate in a CD62P-Dependent Fashion Into Reactive Lymph Nodes and License Dendritic Cells for T Cell Priming. *J Exp Med* (2008) 205(11):2561–74. doi: 10.1084/jem.20081212

62. Guarda G, Hons M, Soriano SF, Huang AY, Polley R, Martín-Fontecha A, et al. L-Selectin-Negative CCR7- Effector and Memory CD8+ T Cells Enter Reactive Lymph Nodes and Kill Dendritic Cells. *Nat Immunol* (2007) 8 (7):743–52. doi: 10.1038/ni1469
63. Yoneyama H, Matsuno K, Zhang Y, Nishiwaki T, Kitabatake M, Ueha S, et al. Evidence for Recruitment of Plasmacytoid Dendritic Cell Precursors to Inflamed Lymph Nodes Through High Endothelial Venules. *Int Immunol* (2004) 16(7):915–28. doi: 10.1093/intimm/dxh093
64. Bogoslowski A, Butcher EC, Kubes P. Neutrophils Recruited Through High Endothelial Venules of the Lymph Nodes *via* PNAd Intercept Disseminating Staphylococcus Aureus. *Proc Natl Acad Sci USA* (2018) 115(10):2449–54. doi: 10.1073/pnas.1715756115
65. van de Pavert SA, Mebius RE. New Insights Into the Development of Lymphoid Tissues. *Nat Rev Immunol* (2010) 10(9):664–74. doi: 10.1038/nri2832
66. Hayasaka H, Taniguchi K, Fukai S, Miyasaka M, et al. Neogenesis and Development of the High Endothelial Venules That Mediate Lymphocyte Trafficking. *Cancer Sci* (2010) 101(11):2302–8. doi: 10.1111/j.1349-7006.2010.01687.x
67. Browning JL, Allaire N, Ngam-Ek A, Notidis E, Hunt J, Perrin S, et al. Lymphotoxin-β Receptor Signaling Is Required for the Homeostatic Control of HEV Differentiation and Function. *Immunity* (2005) 23(5):539–50. doi: 10.1016/j.immuni.2005.10.002
68. Moussion C, Girard J-P. Dendritic Cells Control Lymphocyte Entry to Lymph Nodes Through High Endothelial Venules. *Nature* (2011) 479 (7374):542–6. doi: 10.1038/nature10540
69. Onder L, Danuser R, Scandella E, Firner S, Chai Q, Hehlgans T, et al. Endothelial Cell–Specific Lymphotoxin-β Receptor Signaling Is Critical for Lymph Node and High Endothelial Venule Formation. *J Exp Med* (2013) 210(3):465–73. doi: 10.1084/jem.20121462
70. Jeucken KCM, Koning JJ, Mebius RE, Tas SW, et al. The Role of Endothelial Cells and TNF-Receptor Superfamily Members in Lymphoid Organogenesis and Function During Health and Inflammation. *Front Immunol* (2019) 10:2700. doi: 10.3389/fimmu.2019.02700
71. Simmons S, Sasaki N, Umemoto E, Uchida Y, Fukuhara S, Kitazawa Y, et al. High-Endothelial Cell-Derived S1P Regulates Dendritic Cell Localization and Vascular Integrity in the Lymph Node. *eLife* (2019) 8:e41239. doi: 10.7554/eLife.41239
72. Duijvestijn AM, Horst E, Pals ST, Rouse BN, Steere AC, Picker LJ, et al. High Endothelial Differentiation in Human Lymphoid and Inflammatory Tissues Defined by Monoclonal Antibody HECA-452. *Am J Pathol* (1988) 130 (1):147–55.
73. Mitsuoka C, Mitsuoka M, Mitsuoka K, Mitsuoka M, Mitsuoka H, Nakamura S, et al. Identification of a Major Carbohydrate Capping Group of the L-Selectin Ligand on High Endothelial Venules in Human Lymph Nodes as 6-Sulfo Sialyl Lewis X. *J Biol Chem* (1998) 273(18):11225–33. doi: 10.1074/jbc.273.18.11225
74. Martinet L, Filleron T, Guellec S, Rochaix P, Garrido I, Girard JPO, et al. High Endothelial Venule Blood Vessels for Tumor-Infiltrating Lymphocytes Are Associated With Lymphotoxin β-Producing Dendritic Cells in Human Breast Cancer. *J Immunol* (2013) 191(4):2001–8. doi: 10.4049/jimmunol.1300872
75. Song IH, Heo SH, Bang WS, Park HS, Park IA, Kim YA, et al. Predictive Value of Tertiary Lymphoid Structures Assessed by High Endothelial Venule Counts in the Neoadjuvant Setting of Triple-Negative Breast Cancer. *Cancer Res Treat* (2017) 49(2):399–407. doi: 10.4143/crt.2016.215
76. Kroeger DR, Milne K, Nelson BH. Tumor-Infiltrating Plasma Cells Are Associated With Tertiary Lymphoid Structures, Cytolytic T-Cell Responses, and Superior Prognosis in Ovarian Cancer. *Clin Cancer Res* (2016) 22 (12):3005–15. doi: 10.1158/1078-0432.CCR-15-2762
77. Pfuderer PL, Ballhausen A, Seidler F, Stark HJ, Grabe N, Frayling IM, et al. High Endothelial Venules Are Associated With Microsatellite Instability, Hereditary Background and Immune Evasion in Colorectal Cancer. *Br J Cancer* (2019) 121(5):395–404. doi: 10.1038/s41416-019-0514-6
78. de Chaisemartin L, Goc J, Damotte D, Validire P, Magdeleinat P, Alifano M, et al. Characterization of Chemokines and Adhesion Molecules Associated With T Cell Presence in Tertiary Lymphoid Structures in Human Lung Cancer. *Cancer Res* (2011) 71(20):6391–9. doi: 10.1158/0008-5472.CAN-11-0952
79. Cipponi A, Mercier M, Seremet T, Baurain JF, Théate I, van den Oord J, et al. Neogenesis of Lymphoid Structures and Antibody Responses Occur in Human Melanoma Metastases. *Cancer Res* (2012) 72(16):3997–4007. doi: 10.1158/0008-5472.CAN-12-1377
80. Giraldo NA, Becht E, Pagès F, Skliris G, Verkarre V, Vano Y, et al. Orchestration and Prognostic Significance of Immune Checkpoints in the Microenvironment of Primary and Metastatic Renal Cell Cancer. *Clin Cancer Res* (2015) 21(13):3031–40. doi: 10.1158/1078-0432.CCR-14-2926
81. Hong SA, Hwang HW, Kim MK, Lee TJ, Yim K, Won HS, et al. High Endothelial Venule With Concomitant High CD8+ Tumor-Infiltrating Lymphocytes Is Associated With a Favorable Prognosis in Resected Gastric Cancer. *J Clin Med* (2020) 9(8):2628. doi: 10.3390/jcm9082628
82. Hiraoka N, Ino Y, Yamazaki-Itoh R, Kanai Y, Kosuge T, Shimada K, et al. Intratumoral Tertiary Lymphoid Organ Is a Favourable Prognosticator in Patients With Pancreatic Cancer. *Br J Cancer* (2015) 112(11):1782–90. doi: 10.1038/bjc.2015.145
83. Castino GF, Cortese N, Capretti G, Serio S, Di Caro G, Mineri R, et al. Spatial Distribution of B Cells Predicts Prognosis in Human Pancreatic Adenocarcinoma. *Oncoimmunology* (2016) 5(4):e1085147. doi: 10.1080/2162402X.2015.1085147
84. Bahmani B, Uehara M, Ordikhani F, Li X, Jiang L, Banouni N, et al. Ectopic High Endothelial Venules in Pancreatic Ductal Adenocarcinoma: A Unique Site for Targeted Delivery. *EBioMedicine* (2018) 38:79–88. doi: 10.1016/j.ebiom.2018.11.030
85. Wirsing AM, Rikardsen OG, Steigen SE, Uhlin-Hansen L, Hadler-Olsen E, et al. Presence of Tumour High-Endothelial Venules Is an Independent Positive Prognostic Factor and Stratifies Patients With Advanced-Stage Oral Squamous Cell Carcinoma. *Tumour Biol* (2016) 37(2):2449–59. doi: 10.1007/s13277-015-4036-4
86. Wirsing AM, Ervik IK, Seppola M, Uhlin-Hansen L, Steigen Se, Hadler-Olsen E, et al. Presence of High-Endothelial Venules Correlates With a Favorable Immune Microenvironment in Oral Squamous Cell Carcinoma. *Mod Pathol* (2018) 31(6):910–22. doi: 10.1038/s41379-018-0019-5
87. Li Q, Liu X, Wang D, Wang Y, Lu H, Wen S, et al. Prognostic Value of Tertiary Lymphoid Structure and Tumour Infiltrating Lymphocytes in Oral Squamous Cell Carcinoma. *Int J Oral Sci* (2020) 12(1):24. doi: 10.1038/s41368-020-00092-3
88. Shen H, Wang X, Shao Z, Liu K, Xia XY, Zhang HZ, et al. Alterations of High Endothelial Venules in Primary and Metastatic Tumors Are Correlated With Lymph Node Metastasis of Oral and Pharyngeal Carcinoma. *Cancer Biol Ther* (2014) 15(3):342–9. doi: 10.4161/cbt.27328
89. Blanchard L, Girard JP. High Endothelial Venules (HEVs) in Immunity, Inflammation and Cancer. *Angiogenesis* (2021). doi: 10.1007/s10456-021-09792-8
90. Avram G, Sánchez-Sendra B, sMartín JM, TerrÁdez L, Ramos D, Monteagudo C, et al. The Density and Type of MECA-79-Positive High Endothelial Venules Correlate With Lymphocytic Infiltration and Tumour Regression in Primary Cutaneous Melanoma. *Histopathology* (2013) 63 (6):852–61. doi: 10.1111/his.12235
91. Martinet L, Le Guellec S, Filleron T, Lamant L, Meyer N, Rochaix P, et al. High Endothelial Venules (HEVs) in Human Melanoma Lesions: Major Gateways for Tumor-Infiltrating Lymphocytes. *Oncoimmunology* (2012) 1 (6):829–39. doi: 10.4161/onci.20492
92. Helmink BA, Reddy SM, Gao J, Zhang S, Basar R, Thakur R, et al. B Cells and Tertiary Lymphoid Structures Promote Immunotherapy Response. *Nature* (2020) 577(7791):549–55.
93. Petitprez F, de Reyniès A, Keung EZ, Chen TW, Sun CM, Calderaro J, et al. B Cells Are Associated With Survival and Immunotherapy Response in Sarcoma. *Nature* (2020) 577(7791):556–60. doi: 10.1038/s41586-019-1906-8
94. Liu X, Tsang JYS, Hlaing T, Hu J, Ni YB, Chan SK, et al. Distinct Tertiary Lymphoid Structure Associations and Their Prognostic Relevance in HER2 Positive and Negative Breast Cancers. *Oncologist* (2017) 22(11):1316–24. doi: 10.1634/theoncologist.2017-0029
95. Duan Q, Zhang H, Zheng J, Zhang L, et al. Turning Cold Into Hot: Firing Up the Tumor Microenvironment. *Trends Cancer* (2020) 6(7):605–18. doi: 10.1016/j.trecan.2020.02.022

96. Gu-Trantien C, Loi S, Garaud S, Equeter C, Libin M, de Wind A, et al. CD4+ Follicular Helper T Cell Infiltration Predicts Breast Cancer Survival. *J Clin Invest* (2013) 123(7):2873–92. doi: 10.1172/JCI67428
97. Prabhakaran S, Rizk VT, Ma Z, Cheng CH, Berglund AE, Coppola D, et al. Evaluation of Invasive Breast Cancer Samples Using a 12-Chemokine Gene Expression Score: Correlation With Clinical Outcomes. *Breast Cancer Res* (2017) 19(1):71. doi: 10.1186/s13058-017-0864-z
98. Cabrita R, Lauss M, Sanna A, Donia M, Skaarup Larsen M, Mitra S, et al. Tertiary Lymphoid Structures Improve Immunotherapy and Survival in Melanoma. *Nature* (2020) 577(7791):561–5. doi: 10.1038/s41586-019-1914-8
99. Peske JD, Thompson ED, Gemta L, Baylis RA, Fu Y-X, Engelhard VH, et al. Effector Lymphocyte-Induced Lymph Node-Like Vasculature Enables Naive T-Cell Entry Into Tumours and Enhanced Anti-Tumour Immunity. *Nat Commun* (2015) 6(1):7114. doi: 10.1038/ncomms8114
100. Onrust SV, Hartl PM, Rosen SD, Hanahan D, et al. Modulation of L-Selectin Ligand Expression During an Immune Response Accompanying Tumorigenesis in Transgenic Mice. *J Clin Invest* (1996) 97(1):54–64. doi: 10.1172/JCI118406
101. Hanahan D. Heritable Formation of Pancreatic Beta-Cell Tumours in Transgenic Mice Expressing Recombinant Insulin/Simian Virus 40 Oncogenes. *Nature* (1985) 315(6015):115–22. doi: 10.1038/315115a0
102. Grant SG, Jessee J, Bloom FR, Hanahan D, et al. Differential Plasmid Rescue From Transgenic Mouse DNAs Into Escherichia Coli Methylation-Restriction Mutants. *Proc Natl Acad Sci USA* (1990) 87(12):4645–9. doi: 10.1073/pnas.87.12.4645
103. Alpert S, Hanahan D, Teitelman G. Hybrid Insulin Genes Reveal a Developmental Lineage for Pancreatic Endocrine Cells and Imply a Relationship With Neurons. *Cell* (1988) 53(2):295–308. doi: 10.1016/0092-8674(88)90391-1
104. Zhang Z, Li J, Zheng W, Zhao G, Zhang H, Wang X, et al. Peripheral Lymphoid Volume Expansion and Maintenance Are Controlled by Gut Microbiota *Via* RALDH+ Dendritic Cells. *Immunity* (2016) 44(2):330–42. doi: 10.1016/j.immuni.2016.01.004
105. Martinet L, Garrido I, Girard JP. Tumor High Endothelial Venules (HEVs) Predict Lymphocyte Infiltration and Favorable Prognosis in Breast Cancer. *Oncoimmunology* (2012) 1(5):789–90. doi: 10.4161/onci.19787
106. Martinet L, Girard JP. Regulation of Tumor-Associated High-Endothelial Venules by Dendritic Cells: A New Opportunity to Promote Lymphocyte Infiltration Into Breast Cancer? *Oncoimmunology* (2013) 2(11):e26470. doi: 10.4161/onci.26470
107. Johansson-Percival A, He B, Li ZJ, Kjellén A, Russell K, Li J, et al. De Novo Induction of Intratumoral Lymphoid Structures and Vessel Normalization Enhances Immunotherapy in Resistant Tumors. *Nat Immunol* (2017) 18 (11):1207–17. doi: 10.1038/ni.3836
108. Colbeck EJ, Jones E, Hindley JP, Smart K, Schulz R, Browne M, et al. Treg Depletion Licenses T Cell–Driven HEV Neogenesis and Promotes Tumor Destruction. *Cancer Immunol Res* (2017) 5(11):1005–15. doi: 10.1158/2326-6066.CIR-17-0131
109. Joshi NS, Akama-Garren EH, Lu Y, Lee DY, Chang GP, Li A, et al. Regulatory T Cells in Tumor-Associated Tertiary Lymphoid Structures Suppress Anti-Tumor T Cell Responses. *Immunity* (2015) 43(3):579–90. doi: 10.1016/j.immuni.2015.08.006
110. Hindley JP, Jones E, Smart K, Bridgeman H, Lauder SN, Ondondo B, et al. T-Cell Trafficking Facilitated by High Endothelial Venules Is Required for Tumor Control After Regulatory T-Cell Depletion. *Cancer Res* (2012) 72 (21):5473–82. doi: 10.1158/0008-5472.CAN-12-1912
111. Gautier EL, Shay T, Miller J, Greter M, Jakubzick C, Ivanov S, et al. Gene-Expression Profiles and Transcriptional Regulatory Pathways That Underlie the Identity and Diversity of Mouse Tissue Macrophages. *Nat Immunol* (2012) 13(11):1118–28. doi: 10.1038/ni.2419
112. Faget J, Groeneveld S, Boivin G, Sankar M, Zangger N, Garcia M, et al. Neutrophils and Snail Orchestrate the Establishment of a Pro-Tumor Microenvironment in Lung Cancer. *Cell Rep* (2017) 21(11):3190–204. doi: 10.1016/j.celrep.2017.11.052
113. Allen E, Jabouille A, Rivera LB, Lodewijckx I, Missiaen R, Steri V, et al. Combined Antiangiogenic and Anti-PD-L1 Therapy Stimulates Tumor Immunity Through HEV Formation. *Sci Transl Med* (2017) 9(385): eaak9679. doi: 10.1126/scitranslmed.aak9679
114. He B, Jabouille A, Steri V, Johansson-Percival A, Michael IP, Kotamraju R, et al. Vascular Targeting of LIGHT Normalizes Blood Vessels in Primary Brain Cancer and Induces Intratumoural High Endothelial Venules. *J Pathol* (2018) 245(2):209–21. doi: 10.1002/path.5080
115. He B, Johansson-Percival A, Backhouse J, Li J, Lee GYF, Hamzah J, et al. Remodeling of Metastatic Vasculature Reduces Lung Colonization and Sensitizes Overt Metastases to Immunotherapy. *Cell Rep* (2020) 30(3):714–24.e5. doi: 10.1016/j.celrep.2019.12.013
116. Schrama D, thor Straten P, Fischer WH, McLellan AD, Bröcker EB, Reisfeld RA, et al. Targeting of Lymphotoxin-Alpha to the Tumor Elicits an Efficient Immune Response Associated With Induction of Peripheral Lymphoid-Like Tissue. *Immunity* (2001) 14(2):111–21. doi: 10.1016/S1074-7613(01)00094-2
117. Kratz A, Campos-Neto A, Hanson MS, Ruddle NH, et al. Chronic Inflammation Caused by Lymphotoxin Is Lymphoid Neogenesis. *J Exp Med* (1996) 183(4):1461–72. doi: 10.1084/jem.183.4.1461
118. Tian L, Goldstein A, Goldstein H, Ching H, Sun Kim I, Welte T, et al. Mutual Regulation of Tumour Vessel Normalization and Immunostimulatory Reprogramming. *Nature* (2017) 544(7649):250–4. doi: 10.1038/nature21724
119. Johansson-Percival A, Li ZJ, Lakhiani DD, He B, Wang X, Hamzah J, et al. Intratumoral LIGHT Restores Pericyte Contractile Properties and Vessel Integrity. *Cell Rep* (2015) 13(12):2687–98. doi: 10.1016/j.celrep.2015.12.004
120. Kabir AU, Subramanian M, Lee DH, Wang X, Krchma K, Wu J, et al. Dual Role of Endothelial Myct1 in Tumor Angiogenesis and Tumor Immunity. *Sci Transl Med* (2021) 13(583):eabb6731. doi: 10.1126/scitranslmed.abb6731
121. Cuff CA, Schwartz J, Bergman CM, Russell KS, Bender JR, Ruddle NH, et al. Lymphotoxin Alpha3 Induces Chemokines and Adhesion Molecules: Insight Into the Role of LT Alpha in Inflammation and Lymphoid Organ Development. *J Immunol* (1998) 161(12):6853–60.
122. Noort AR, van Zoest KP, van Baarsen LG, Maracle CX, Helder B, Papazian N, et al. Tertiary Lymphoid Structures in Rheumatoid Arthritis: NF-κB-Inducing Kinase-Positive Endothelial Cells as Central Players. *Am J Pathol* (2015) 185(7):1935–43. doi: 10.1016/j.ajpath.2015.03.012
123. Chen DS, Mellman I. Elements of Cancer Immunity and the Cancer-Immune Set Point. *Nature* (2017) 541(7637):321–30. doi: 10.1038/nature21349
124. Thompson ED, Enriquez HL, Fu YX, Engelhard VH, et al. Tumor Masses Support Naive T Cell Infiltration, Activation, and Differentiation Into Effectors. *J Exp Med* (2010) 207(8):1791–804. doi: 10.1084/jem.20092454
125. Zhang N, Bevan MJ. CD8(+) T Cells: Foot Soldiers of the Immune System. *Immunity* (2011) 35(2):161–8. doi: 10.1016/j.immuni.2011.07.010
126. Jansen CS, Prokhnevska N, Master VA, Sanda MG, Carlisle JW, Bilen MA, et al. An Intra-Tumoral Niche Maintains and Differentiates Stem-Like CD8 T Cells. *Nature* (2019) 576(7787):465–70. doi: 10.1038/s41586-019-1836-5
127. Miller BC, Sen DR, Al Abosy R, Bi K, Virkud YV, LaFleur MW, et al. Subsets of Exhausted CD8(+) T Cells Differentially Mediate Tumor Control and Respond to Checkpoint Blockade. *Nat Immunol* (2019) 20(3):326–36. doi: 10.1038/s41590-019-0312-6
128. Jiang L, Jung S, Zhao J, Kasinath V, Ichimura T, Joseph J, et al. Simultaneous Targeting of Primary Tumor, Draining Lymph Node, and Distant Metastases Through High Endothelial Venule-Targeted Delivery. *Nano Today* (2021) 36:101045. doi: 10.1016/j.nantod.2020.101045
129. Mackay CR, Marston W, Dudler L. Altered Patterns of T Cell Migration Through Lymph Nodes and Skin Following Antigen Challenge. *Eur J Immunol* (1992) 22(9):2205–10. doi: 10.1002/eji.1830220904
130. Cahill RN, Frost H, Trnka Z. The Effects of Antigen on the Migration of Recirculating Lymphocytes Through Single Lymph Nodes. *J Exp Med* (1976) 143(4):870–88. doi: 10.1084/jem.143.4.870
131. Hay JB, Hobbs BB. The Flow of Blood to Lymph Nodes and its Relation to Lymphocyte Traffic and the Immune Response. *J Exp Med* (1977) 145(1):31–44. doi: 10.1084/jem.145.1.31
132. Mondor I, Jorquera A, Sene C, Adriouch S, Adams RH, Zhou B, et al. Clonal Proliferation and Stochastic Pruning Orchestrate Lymph Node Vasculature Remodeling. *Immunity* (2016) 45(4):877–88. doi: 10.1016/j.immuni.2016.09.017
133. Milutinovic S, Abe J, Godkin A, Stein JV, Gallimore A, et al. The Dual Role of High Endothelial Venules in Cancer Progression *Versus* Immunity. *Trends Cancer* (2021) 7(3):214–25. doi: 10.1016/j.trecan.2020.10.001

134. Lee SY, Qian CN, Ooi AS, Chen P, Tan VK, Chia CS, et al. 2011 Young Surgeon's Award Winner: High Endothelial Venules: A Novel Prognostic Marker in Cancer Metastasis and the Missing Link? *Ann Acad Med Singap* (2012) 41(1):21–8.
135. Qian CN, Berghuis B, Tsarfaty G, Bruch M, Kort EJ, Ditlev J, et al. Preparing the "Soil": The Primary Tumor Induces Vasculature Reorganization in the Sentinel Lymph Node Before the Arrival of Metastatic Cancer Cells. *Cancer Res* (2006) 66(21):10365–76. doi: 10.1158/0008-5472.CAN-06-2977
136. Bekkhus T, Martikainen T, Olofsson A, Franzén Boger M, Vasiliu Bacovia D, Wärnberg F, et al. Remodeling of the Lymph Node High Endothelial Venules Reflects Tumor Invasiveness in Breast Cancer and Is Associated With Dysregulation of Perivascular Stromal Cells. *Cancers (Basel)* (2021) 13(2). doi: 10.3390/cancers13020211
137. Chung MK, Do IG, Jung E, Son YI, Jeong HS, Baek CH, et al. Lymphatic Vessels and High Endothelial Venules Are Increased in the Sentinel Lymph Nodes of Patients With Oral Squamous Cell Carcinoma Before the Arrival of Tumor Cells. *Ann Surg Oncol* (2012) 19(5):1595–601. doi: 10.1245/s10434-011-2154-9
138. Karaman S, Detmar M. Mechanisms of Lymphatic Metastasis. *J Clin Invest* (2014) 124(3):922–8. doi: 10.1172/JCI71606
139. Burn JI, Watne AL, Moore GE. The Role of the Thoracic Duct Lymph in Cancer Dissemination. *Br J Cancer* (1962) 16(4):608–15. doi: 10.1038/bjc.1962.71
140. Brown M, Assen FP, Leithner A, Abe J, Schachner H, Asfour G, et al. Lymph Node Blood Vessels Provide Exit Routes for Metastatic Tumor Cell Dissemination in Mice. *Science* (2018) 359(6382):1408–11. doi: 10.1126/science.aal3662
141. Pereira ER, Kedrin D, Seano G, Gautier O, Meijer EFJ, Jones D, et al. Lymph Node Metastases can Invade Local Blood Vessels, Exit the Node, and Colonize Distant Organs in Mice. *Science* (2018) 359(6382):1403–7. doi: 10.1126/science.aal3622
142. Peranzoni E, Lemoine J, Vimeux L, Feuillet V, Barrin S, Kantari-Mimoun C, et al. Macrophages Impede CD8 T Cells From Reaching Tumor Cells and Limit the Efficacy of Anti–PD-1 Treatment. *Proc Natl Acad Sci* (2018) 115 (17):E4041–50. doi: 10.1073/pnas.1720948115
143. Finkin S, Yuan D, Stein I, Taniguchi K, Weber A, Unger K, et al. Ectopic Lymphoid Structures Function as Microniches for Tumor Progenitor Cells in Hepatocellular Carcinoma. *Nat Immunol* (2015) 16(12):1235–44. doi: 10.1038/ni.3290
144. Remark R, Alifano M, Cremer I, Lupo A, Dieu-Nosjean MC, Riquet M, et al. Characteristics and Clinical Impacts of the Immune Environments in Colorectal and Renal Cell Carcinoma Lung Metastases: Influence of Tumor Origin. *Clin Cancer Res* (2013) 19(15):4079–91. doi: 10.1158/1078-0432.CCR-12-3847
145. Lee M, Kiefel H, LaJevic MD, Macauley MS, Kawashima H, O'Hara E, et al. Transcriptional Programs of Lymphoid Tissue Capillary and High Endothelium Reveal Control Mechanisms for Lymphocyte Homing. *Nat Immunol* (2014) 15(10):982–95. doi: 10.1038/ni.2983
146. Brulois K, Rajaraman A, Szade A, Nordling S, Bogoslowski A, Dermadi D, et al. A Molecular Map of Murine Lymph Node Blood Vascular Endothelium at Single Cell Resolution. *Nat Commun* (2020) 11(1):3798. doi: 10.1038/s41467-020-17291-5
147. Baekkevold ES, Jahnsen FL, Johansen FE, Bakke O, Gaudernack G, Brandtzaeg P, et al. Culture Characterization of Differentiated High Endothelial Venule Cells From Human Tonsils. *Lab Invest* (1999) 79(3):327–36.
148. Girard JP, Baekkevold ES, Yamanaka T, Haraldsen G, Brandtzaeg P, Amalric F, et al. Heterogeneity of Endothelial Cells: The Specialized Phenotype of Human High Endothelial Venules Characterized By Suppression Subtractive Hybridization. *Am J Pathol* (1999) 155: (6):13. doi: 10.1016/S0002-9440(10)65523-X
149. Lacorre D-A. Plasticity of Endothelial Cells: Rapid Dedifferentiation of Freshly Isolated High Endothelial Venule Endothelial Cells Outside the Lymphoid Tissue Microenvironment. *Blood* (2004) 103(11):4164–72. doi: 10.1182/blood-2003-10-3537
150. Nowak-Sliwinska P, Alitalo K, Allen E, Anisimov A, Aplin AC, Auerbach R, et al. Consensus Guidelines for the Use and Interpretation of Angiogenesis Assays. *Angiogenesis* (2018) 21(3):425–532. doi: 10.1007/s10456-018-9613-x
151. Dutta D, Heo I, Clevers H. Disease Modeling in Stem Cell-Derived 3D Organoid Systems. *Trends Mol Med* (2017) 23(5):393–410. doi: 10.1016/j.molmed.2017.02.007
152. Wimmer RA, Leopoldi A, Aichinger M, Wick N, Hantusch B, Novatchkova M, et al. Human Blood Vessel Organoids as a Model of Diabetic Vasculopathy. *Nature* (2019) 565(7740):505–10. doi: 10.1038/s41586-018-0858-8
153. Wimmer RA, Leopoldi A, Aichinger M, Kerjaschki D, Penninger JM, et al. Generation of Blood Vessel Organoids From Human Pluripotent Stem Cells. *Nat Protoc* (2019) 14(11):3082–100. doi: 10.1038/s41596-019-0213-z
154. Andrique L, Recher G, Alessandri K, Pujol N, Feyeux M, Bon P, et al. A Model of Guided Cell Self-Organization for Rapid and Spontaneous Formation of Functional Vessels. *Sci Adv* (2019) 5(6):eaau6562. doi: 10.1126/sciadv.aau6562
155. Palikuqi B, Nguyen DT, Li G, Schreiner R, Pellegata AF, Liu Y, et al. Adaptable Haemodynamic Endothelial Cells for Organogenesis and Tumorigenesis. *Nature* (2020) 585(7825):426–32.

Conflict of Interest: The authors declare that the research was conducted in the absence of any commercial or financial relationships that could be construed as a potential conflict of interest.

Publisher's Note: All claims expressed in this article are solely those of the authors and do not necessarily represent those of their affiliated organizations, or those of the publisher, the editors and the reviewers. Any product that may be evaluated in this article, or claim that may be made by its manufacturer, is not guaranteed or endorsed by the publisher.

Copyright © 2021 Vella, Guelfi and Bergers. This is an open-access article distributed under the terms of the Creative Commons Attribution License (CC BY). The use, distribution or reproduction in other forums is permitted, provided the original author(s) and the copyright owner(s) are credited and that the original publication in this journal is cited, in accordance with accepted academic practice. No use, distribution or reproduction is permitted which does not comply with these terms.

frontiers in Immunology

MINI REVIEW
published: 01 September 2021
doi: 10.3389/fimmu.2021.724739

Tertiary Lymphoid Structures in the Central Nervous System: Implications for Glioblastoma

Tiarne van de Walle[†], *Alessandra Vaccaro*[†], *Mohanraj Ramachandran*[†], *Ilkka Pietilä*, *Magnus Essand*[*] *and Anna Dimberg*[*]

Department of Immunology, Genetics and Pathology, Science for Life Laboratory, The Rudbeck Laboratory, Uppsala University, Uppsala, Sweden

Glioblastoma is the most common and aggressive brain tumor, which is uniformly lethal due to its extreme invasiveness and the absence of curative therapies. Immune checkpoint inhibitors have not yet proven efficacious for glioblastoma patients, due in part to the low prevalence of tumor-reactive T cells within the tumor microenvironment. The priming of tumor antigen-directed T cells in the cervical lymph nodes is complicated by the shortage of dendritic cells and lack of appropriate lymphatic vessels within the brain parenchyma. However, recent data suggest that naive T cells may also be primed within brain tumor-associated tertiary lymphoid structures. Here, we review the current understanding of the formation of these structures within the central nervous system, and hypothesize that promotion of tertiary lymphoid structures could enhance priming of tumor antigen-targeted T cells and sensitize glioblastomas to cancer immunotherapy.

Keywords: tertiary lymphoid structure, immunotherapy, glioma, central nervous system, brain, glioblastoma

OPEN ACCESS

Edited by:
Eyad Elkord,
University of Salford, United Kingdom

Reviewed by:
Walter J. Storkus,
University of Pittsburgh, United States
Victor Engelhard,
University of Virginia, United States

***Correspondence:**
Anna Dimberg
Anna.Dimberg@igp.uu.se
Magnus Essand
Magnus.Essand@igp.uu.se

[†]*These authors have contributed equally to this work*

Specialty section:
This article was submitted to Cancer Immunity and Immunotherapy, a section of the journal Frontiers in Immunology

Received: *14 June 2021*
Accepted: *16 August 2021*
Published: *01 September 2021*

Citation:
van de Walle T, Vaccaro A, Ramachandran M, Pietilä I, Essand M and Dimberg A (2021) Tertiary Lymphoid Structures in the Central Nervous System: Implications for Glioblastoma. Front. Immunol. 12:724739. doi: 10.3389/fimmu.2021.724739

INTRODUCTION

Glioblastoma (GBM) is a grade IV astrocytoma with dismal prognosis. The overall survival is only 12-15 months despite conventional therapy, which includes maximal surgical resection, adjuvant temozolomide chemotherapy and radiotherapy (1). Immunotherapy using immune checkpoint inhibitors (ICI) has revolutionized cancer treatment but GBM patients have not yet benefited from this breakthrough (2). Adjuvant α-PD-1 therapy has not proven effective and neoadjuvant α-PD-1 therapy results in only a modest improvement in immune activation (3, 4). ICI therapy 'releases the brakes' on T cell activity, and therefore strictly relies on a preexisting T cell response towards the tumor. The lack of response in GBM is likely due to the scarcity of tumor antigen-directed T cells within the tumor microenvironment (TME).

Priming of naïve tumor antigen-directed T cells in lymphoid organs occurs when their cognate antigens are presented on the surface of professional antigen-presenting cells (APCs). While lymphatic vessels have been found within the meninges (5), there are no lymphatic vessels present within the brain parenchyma. Instead, fluid transport is mediated by the glymphatic system, a waste clearance system consisting of perivascular tunnels formed by astroglial cells, which does not allow for the migration of APCs (6). As such, the mechanisms that enable the priming of glioma antigen-directed T cells have not yet been elucidated, but likely rely on the transportation of antigens *via* the glymphatic system to the meningeal lymphatics. The antigens can then be taken up by meningeal

APCs, which migrate through the dural lymphatics to cervical lymph nodes for priming of naïve T cells (5, 7, 8). Brain tumor immunity and the response to ICI can be improved through ectopic expression of vascular endothelial growth factor (VEGF)-C, which enhances lymphangiogenesis in the dura mater and thereby antigen transport to cervical lymph nodes in mouse models of glioma (9, 10). T cells primed against tumor-associated antigens then travel through the blood circulation and extravasate into the TME *via* activated tumor vasculature (11). This process, referred to as the cancer-immunity cycle, is less efficient in the central nervous system (CNS) than in the periphery.

The presence of tertiary lymphoid structures (TLS) in association with brain tumors (12, 13) suggests that these structures may serve as alternative sites for antigen presentation and T cell priming. Since the formation of TLS is a dynamic process that can be manipulated, this offers exciting new possibilities for enhancing the priming of brain tumor-reactive T cells. In this review, we briefly summarize the current understanding of the immunosuppressive GBM microenvironment, the formation and function of TLS in the CNS, and the putative implications for GBM immunity and immunotherapy.

THE IMMUNE MICROENVIRONMENT OF GBM

The brain as an immune-privileged organ is a notion of the past: it is rather an actively regulated site of immune surveillance maintained by the meningeal lymphatic system (5, 14). Communication with the immune system differs significantly between the various CNS compartments, which are separated by specific brain barriers [reviewed in (15)]. Immune cells can readily enter the CNS through the subarachnoid space *via* the leptomeningeal vessels as well as the highly vascularized choroid plexus (16, 17). However, the immune trafficking in and out of the brain parenchyma is strictly controlled by the blood-brain barrier (BBB). The BBB consists of specialized brain microvascular endothelial cells and pericytes as well as the astrocyte endfeet and basal lamina, which comprise the glia limitans (15). This tight regulation is necessary to protect the brain from damaging inflammation, but it is also a significant hurdle for efficient immune responses against brain cancer.

Tumors can be classified as immune 'desert', 'excluded' or 'inflamed' based on the extent of infiltrating cytotoxic $CD8^+$ T lymphocytes (CTLs) (18). Inflamed tumors are more likely to respond to ICI therapy, and accordingly a higher abundance of tumor-infiltrating $CD8^+$ T cells is associated with improved prognosis and is a predictor of clinical outcome in GBM (19). However, the majority of GBM tumors are 'immune-desert' and essentially lack CTLs due to a number of tumor-related factors. Indeed, these tumors are poorly immunogenic as a result of low mutational burden and a scarcity of professional APCs in the GBM TME, which leads to decreased tumor antigen presentation (20). Furthermore, downregulation of MHC-I expression on the tumor cells limits their recognition by cytotoxic T cells (20). Newly diagnosed GBM patients may exhibit lymphopenia (21) due to the sequestration of T cells in the bone marrow (22). This results from GBM-induced downregulation of the G protein-coupled receptor S1P1, which controls egression of T cells from the secondary lymphoid organs (22). Low T cell levels are further exacerbated by conventional GBM treatments (21, 23).

The vasculature plays a critical role in immune cell extravasation into tissues. Infiltration of T cells across the BBB depends on the multistep process of lymphocyte diapedesis, mediating capture, rolling, adhesion and transendothelial migration, and subsequent re-activation of T cells by APCs in the perivascular space in order to cross the glia limitans [reviewed in (24)]. In GBM, the inflammatory milieu compromises the integrity of the BBB (25) but the vasculature is highly abnormal, which is in part due to pro-angiogenic factors such as VEGF in the TME (26, 27). This likely contributes to the poor T cell infiltration observed in GBM, as increased VEGF signaling in endothelial cells can reduce leukocyte recruitment by inhibiting the expression of adhesion molecules and chemokines required for T cell recruitment (28–30). Notably, vessel phenotype is heterogeneous in GBM and varies both between patients and within a single tumor (31). Single cell mRNA sequencing of endothelial cells isolated from human GBM demonstrated that while activated endothelial cells are detected in some patients, the majority of endothelial cells within the tumor are angiogenic and express low levels of adhesion molecules and chemokines (31).

In addition to their low abundance, T cells in GBM patients typically have a lower activation and proliferation status (32), are profoundly exhausted (33) and frequently express natural killer (NK) cell-related inhibitory receptors that further suppress their anti-tumor activity (23). Myeloid cells also contribute to T cell dysfunctionality in GBM. The immune-microenvironment of GBM is composed predominantly of highly plastic glioma-associated macrophages, which increase in number with tumor grade and are associated with poor prognosis (34, 35). Glioma-associated macrophages promote T cell anergy in GBM due to deficits in expression of costimulatory molecules and cytokines (36). Furthermore, professional APCs such as dendritic cells (DCs) are few in number in the CNS (37, 38), and their function can be impaired by tumor-derived factors in the GBM microenvironment. Fibrinogen-like protein 2 and other glioma-derived factors can impair differentiation of DCs in both the GBM microenvironment and tumor-draining lymph nodes by multiple mechanisms, including the overexpression of Nrf2 (39, 40). Furthermore, prostaglandin E2 produced by glioma cells can enhance interleukin (IL)-10 production in DCs, leading to increased immunosuppression (41). Each of these mechanisms ultimately leads to reduced effector T cell activation.

Overall, by establishing such a complex immunosuppressive ecosystem, GBMs can effectively evade immune recognition.

TERTIARY LYMPHOID STRUCTURES IN ASSOCIATION WITH BRAIN TUMORS

TLS are ectopic aggregates of lymphoid and stromal cells that are transiently formed in non-lymphoid environments in association

with chronic inflammatory conditions, including autoimmunity and cancer (42). The definition of a TLS is not conclusive and varies across studies, but they are generally accepted to be non-encapsulated aggregates of B cells and T cells. The maturity of TLS is believed to range from loose lymphoid clusters to highly organized structures resembling secondary lymphoid organs (SLOs), containing defined B cell follicles with active germinal centers as well as T cell zones (43). Other components of TLS can include DCs, follicular DCs (fDCs) and high endothelial venules (HEVs) which specialize in the recruitment of naïve lymphocytes (43). The mechanisms of TLS formation may vary in different biological systems. Similar to SLOs, the formation of TLS can be initiated by immune cells which take on the role of lymphoid tissue inducer cells (LTis), such as B cells and Th17 cells (44, 45). These cells secrete factors such as lymphotoxin-αβ and stimulate lymphotoxin-β-receptor (LTβR)-expressing cells that function as lymphoid tissue organizer cells (LTos). As a result, cytokines and chemokines are secreted that attract immune cells and induce angiogenesis (46). Once organized and mature, TLS encompass all cell types that are necessary for the priming of lymphocytes.

TLS are present in many types of solid tumors and are generally associated with positive prognosis and improved response to immunotherapy (42, 47, 48). Furthermore, they have recently been observed in treatment-naïve human gliomas (12). TLS were also found in untreated glioma-bearing mice, and their formation was augmented by agonistic CD40 antibody therapy (αCD40) (12). Similarly, the delivery of an adenovirus expressing the CD40 ligand to murine brainstem tumors resulted in B cell aggregation in the surrounding meninges which was reminiscent of TLS (13). In orthotopic CT-2A and GL261 models, TLS were found close to the meninges or ventricles of the tumor-bearing hemisphere, but not always in direct contact with the tumor mass (12) (**Figure 1A**). Glioma-associated murine TLS contained B cells, T cells, DCs and fDCs, similar to those found in peripheral tumors, but were uniquely encapsulated by extracellular matrix molecules such as collagen and fibronectin, and exhibited an elongated morphology, likely due to the anatomical location (12) (**Figure 1**). TLS were also present in a subset of human WHO grade II-IV gliomas, not only in meningeal regions but also in the white matter proximal to the tumor as well as within the tumor tissue itself (12) (**Figure 2**). The TLS in human gliomas formed around peripheral node addressin (PNAd)-expressing vessels resembling HEVs (**Figure 2**). Interestingly, the presence of TLS in human gliomas correlated with higher infiltration of T cells (12), which may suggest local TLS-associated priming and expansion of tumor-infiltrating lymphocytes.

TLS IN CNS AUTOIMMUNITY – SIMILARITIES AND DIFFERENCES

TLS observed in autoimmune diseases of the CNS show some similarities and differences to those discovered in glioma, which may provide insight into their development and function in the brain cancer setting.

Multiple sclerosis (MS) is a neuroinflammatory autoimmune disease in which TLS have been described and are thought to exacerbate the characteristic autoreactive immune responses against CNS self-antigens. TLS containing B cell follicles, T cell zones and a network of fDCs have been observed in about 40% of secondary-progressive MS patients (49, 50). Interestingly, patient samples from earlier MS stages exhibited no TLS-like structures,

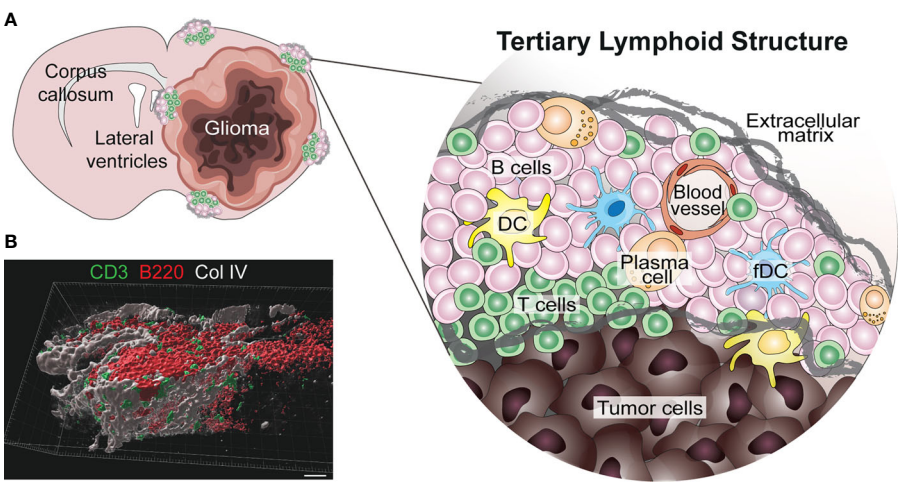

FIGURE 1 | Known location and composition of TLS in murine glioma. **(A)** The image shows a schematic representation of the location and composition of TLS in murine glioma models (12). TLS form in the meningeal and ventricular regions of the tumor-bearing hemisphere, either in direct contact with the tumor or in its proximity. These structures form around blood vessels and are composed of B cells, T cells, dendritic cells (DCs), follicular DCs (fDCs) and a few plasma cells. Interestingly, murine glioma-associated TLS are surrounded by a network of extracellular matrix. **(B)** A 3D rendering of a cortical TLS (identified by $B220^+$ B cells in red and $CD3^+$ T cells in green) formed in a treatment-naïve GL261 glioma-bearing mouse, indicating how the structure is surrounded by a network of collagen IV (Col IV) in grey (scale bar 30 μm).

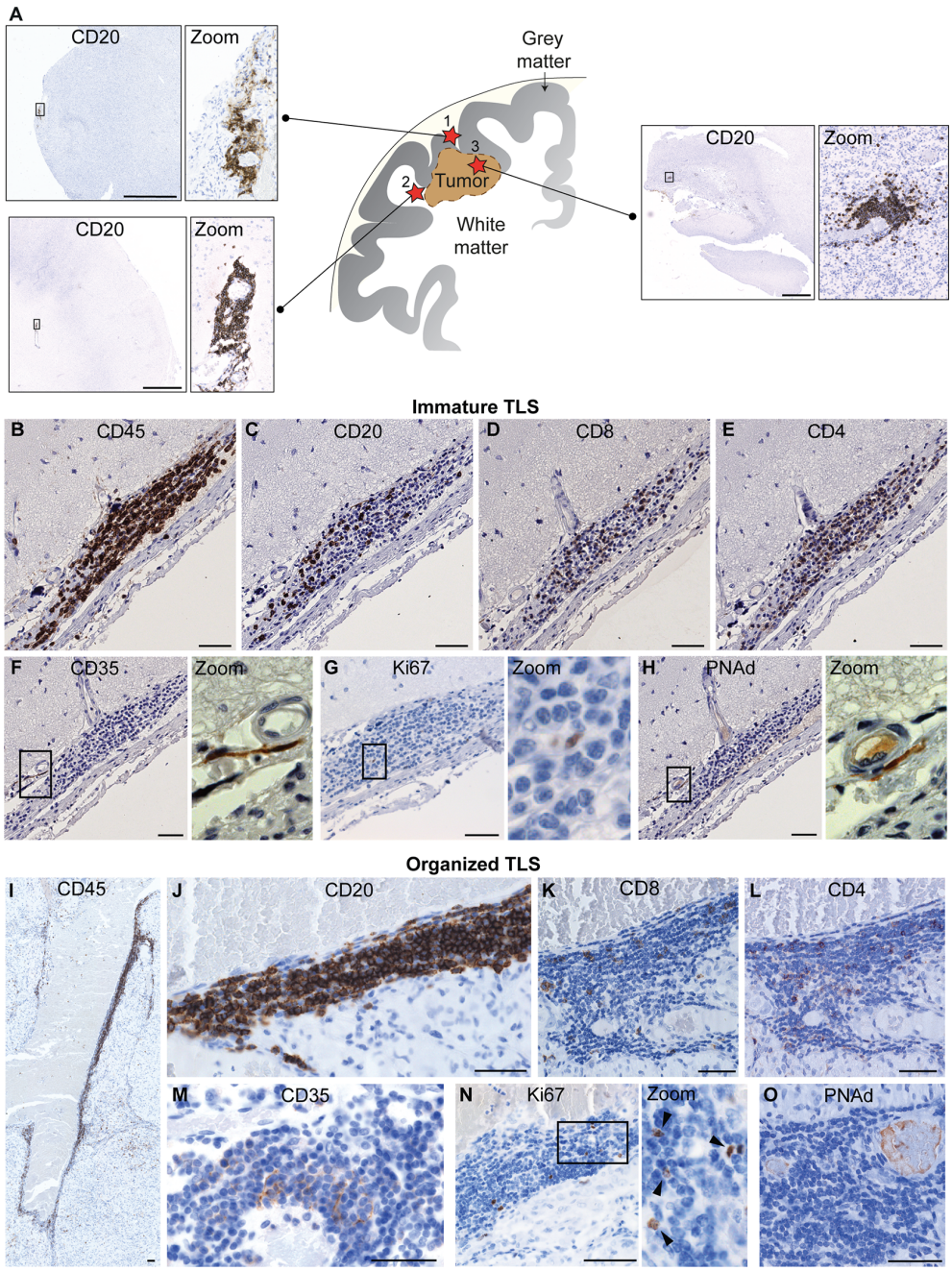

FIGURE 2 | Known location and composition of TLS in human glioma. **(A)** The image shows a schematic representation of the known location of TLS in human glioma. To date, TLS have been identified in three main locations in glioma patients: (1) in direct proximity of the meningeal tissue, (2) in the white matter close to the tumor and (3) within the tumor tissue. A representative image of a TLS (identified by $CD20^+$ B cell staining) is shown for each of the three locations. Scale bars: 2 mm. **(B–O)** illustrate the main cellular components of immature and organized TLS, respectively. While immature TLS contain dispersed B cells, organized TLS are characterized by a tight B cell core. Both immature and organized TLS contain $CD8^+$ and $CD4^+$ T cells and $CD35^+$ follicular dendritic cells (fDCs), include proliferating cells, and form around $PNAd^+$ high endothelial venules. Scale bars: 50μm. All images shown in this figure are reproduced from the original publication - *van Hooren, Vaccaro et al., Nature Communications, 2021* (12) under the terms of the Creative Commons Attributions License (CC BY).

emphasizing that chronic inflammatory signals are required for their development. Meningeal immune infiltrates containing both B cells and T cells were identified, but had no defined zones, follicles or fDC networks (45, 51). The presence of this infiltration correlated with increased levels of neurite loss and demyelination (45, 51), just as the presence of TLS in secondary-progressive MS patients was associated with underlying cortical damage and accelerated clinical disease (49, 50). This supports

the popular hypothesis that TLS act as local sites for reinforcement of autoreactive immune responses in MS patients.

TLS were also observed in experimental autoimmune encephalomyelitis (EAE), the murine model of MS, where their formation was induced by Th17 cells (52). As with TLS in murine glioma, those in EAE were encapsulated by collagen fibers that extended into the structure, resembling the collagen-lined passages within lymph nodes (52). TLS in MS patients were observed exclusively in the meninges and were not found in the healthy or diseased parenchyma (49, 50), suggesting that proximity to the meningeal layer may be required for these structures to form. The MS TLS were closely associated with inflamed blood vessels which were not positive for the HEV marker PNAd (49, 53), while HEVs are largely unreported in EAE. An exception to this is a study on a B cell-dependent model of EAE in which both $PNAd^+$ and $MAdCAM\text{-}1^+$ HEVs were reported in TLS, however the majority of these structures formed in the cerebellum and the few within the cerebrum were confined to the ventricles (54). Therefore, it is of note that $PNAd^+$ HEVs were present in cerebral human glioma TLS, which formed not only in the meninges but also in the white matter and tumor tissue (12) (**Figure 2**). This contrasts with the hypothesis that TLS can only form in the meninges and suggests that there may be multiple mechanisms for the formation and maintenance of TLS in the brain.

Ocular lymphoid clusters have been characterized in spontaneous murine and equine models of autoimmune uveitis, an autoimmune disease involving the attack of the healthy neuroretina (55–57). In the murine setting, distinct zones of B cells and T cells as well as the presence of fDC networks defined these clusters as TLS (55, 56). The structures were B cell-dominated (55, 56), but did not consistently associate with more severe disease as they do in MS (49, 50, 55). In earlier disease stages, the presence of organized TLS correlated with retained visual acuity (55). Interestingly, the TLS became more diffuse and disorganized as the disease progressed, and mice with these structures had poorer visual function than those without (55). This indicates that TLS may not uniformly function to progress autoimmune diseases, but that functional, well-organized TLS may hold autoimmune attacks at bay. In comparison, lymphocytic aggregates in the equine setting were T cell-rich and contained very few B cells, but were still defined by the authors as TLS (57). The relation between presence of these structures and disease severity was not determined, and the functions of different types of ectopic lymphoid clusters including TLS and other lymphoid aggregates should be further elucidated.

THE POTENTIAL ROLE OF STROMAL NICHES IN CNS TLS FORMATION

To date, it remains unclear which cells initiate and maintain TLS development in the inflamed CNS, and why they form in close proximity to meningeal tissues. The answers to these questions may be intertwined and connected to the unique organization of stromal cells in the CNS.

CNS stromal cells include fibroblasts, lymphatic endothelial cells (LECs), blood endothelial cells, pericytes and choroid epithelial cells, which are uniquely compartmentalized within specific stromal niches (58). Fibroblasts and LECs are selectively present within the meninges, indicating that they could be involved in the induction or maintenance of meningeal TLS. Both cell types have been implicated in TLS establishment during chronic inflammation in other organs (59–61). A recent study showed that dural LECs are involved in the regulation of brain tumor immunity (10), however their potential role in the formation of CNS TLS has not yet been investigated. The presence of TLS in a murine model of MS was associated with an increased proportion of meningeal $PDPN^+PDGFR\alpha^+PDGFR\beta^+$ fibroblastic reticular cells, which expressed LTβR and CXCL13 (62), localized within meningeal TLS and were closely connected to a network of fibronectin and reticular fibers, similar to in lymph nodes. Likewise, it was demonstrated that these mice formed spinal cord TLS which were encapsulated by collagen (52). This data suggests that meningeal fibroblasts may produce lymphoid chemokines and extracellular matrix networks that support meningeal TLS formation during chronic inflammation.

CNS immune responses are generally initiated in the meninges, which are rich in immune cells, have access to the lymphatic system through the dura mater, and contain postcapillary venules that support immune cell trafficking (63). Vessels of the choroid plexus, which comprise the blood-CSF barrier, can also be readily activated upon systemic inflammation and participate in recruiting immune cells into the CNS (64). This may explain why CNS TLS are mostly found in the meninges or choroid plexus but not within the parenchyma, where immune cell recruitment is more strictly regulated by the BBB (12, 49, 50, 62). An exception to this is TLS in human glioma, which can also form in the cortical space close to the tumor around HEVs (12). Thus, it is possible that the formation of HEVs can allow TLS to form in locations other than the meninges. HEV formation has been associated with an active ongoing immune response, and can be enhanced by Treg depletion in peripheral tumors (65, 66). In murine glioma, HEV formation was induced by treatment with a vascular targeting peptide delivering LIGHT/TNFSF14 or when using a lymphotoxin β receptor agonist, and was further enhanced by anti-VEGF and ICI therapy (67, 68). HEV formation was associated with an accumulation of T cells, however it was not investigated whether these lymphoid aggregates included other TLS-related cell types, or if they were reminiscent of the antigen-presenting niches recently described to maintain stem-like T cells in tumors (69). The relative importance of HEV formation and different lymphoid niches for immune response in glioma is an important area of further investigation. Another possibility is that the cortical TLS have a direct connection to meningeal tissue through Virchow-Robin spaces, which are perivascular spaces lined by pia mater and fibroblastic cells that originate in the leptomeninges and penetrate the cortex surrounding venules or arterioles (70–72).

Altogether, current experimental evidence indicates that multiple CNS stromal cell types could be involved in the formation of meningeal and cortical TLS. Elucidating their specific functions may offer new targets for regulation of TLS induction in CNS pathologies.

FUTURE DIRECTIONS – CAN TLS INDUCTION IN THE CNS IMPROVE ANTI-TUMOR IMMUNITY?

The correlation of intratumoral TLS formation with positive prognosis and patient survival in many forms of cancer (42) has led to attempts to induce TLS as a form of immunotherapy (73, 74). TLS are associated with enhanced T cell presence in human tumors, and similar observations in GBM patients indicate that TLS induction may be beneficial in this setting. Notably, enhanced TLS formation was observed in glioma-bearing mice treated with αCD40, confirming that induction of TLS is feasible in brain cancer (12). However, αCD40 also induced T cell hypofunction. This was associated with a systemic upregulation of regulatory B cells, which was not related to TLS induction. Therefore, the potential benefit of TLS induction in GBM should be investigated using other inducers. Moreover, it is possible that not only the presence but also the composition of TLS is important for guiding the immune response. Indeed, the existence of regulatory T cells within TLS has been associated with suppression of anti-tumor immunity (75). A deeper knowledge of how TLS composition affects anti-GBM immune responses is necessary to enable the development of therapies that can efficiently induce TLS and consequently boost T cell priming and activation.

Strong immune activation within the CNS is associated with certain risks, including oedema and autoimmunity. CNS oedema is limited by the cranium and can have devastating effects: the swelling can lead to raised intracranial pressure, impaired function and even death. CNS tumors such as GBM display increased vascular permeability, giving rise to peritumoral oedema (76) which would likely be enhanced by strengthening immune activation. Additionally, immunotherapy aiming for TLS induction in the meningeal space may lead to local activation of autoreactive lymphocytes and thus the attack of normal CNS tissue. Such adverse events could resemble MS, where formation of TLS has been associated with subpial cortical damage and disease progression (77). Similarly, TLS formation is often observed in affected organs in other autoimmune diseases and has been associated with both autoantibody production and disease progression (78), but this has not been studied in glioma. Corticosteroids can be used to reduce symptoms of oedema, inflammation and autoimmune attack in the CNS, but can also dampen the effects of immunotherapy and TLS formation. For GBM patients who received ICI therapy, the use of dexamethasone was associated with shorter survival (79). Furthermore, corticosteroid treatment during chemotherapy negatively affected the development of TLS and abrogated their prognostic value in lung cancer patients (43). Therefore, treatment with corticosteroids should be used with caution in association with immunotherapy as this may counteract TLS formation and result in reduced anti-tumor immune responses.

In conclusion, GBM-associated TLS correlate with an influx of T cells in the tumors, indicating that adaptive immune responses can form locally in the CNS in this setting. However, many questions remain to be answered. Is TLS formation in GBM associated with a survival benefit? Which are the molecular cues for TLS formation in GBM? How does this connect with immune activation and T cell infiltration in the tumors? The answers to these questions can enable the development of new strategies to enhance immune responses in brain cancer.

AUTHOR CONTRIBUTIONS

All authors listed have made a substantial, direct, and intellectual contribution to the work and approved it for publication.

FUNDING

This work was supported by grants from the Swedish Cancer Society [20 1008 PjF], [20 1010 UsF], [190184Pj]; the Swedish Childhood Cancer Fund [PR2018-0148], [PR2020-0167]; the Swedish Research Council [2020-02563], [2019-01326]; Knut and Alice Wallenberg foundation [KAW 2019.0088]. MR was supported by a postdoctoral grant from the Swedish Childhood Cancer Fund [TJ 2019-0014]. AD was supported by a Senior Investigator Award from the Swedish Cancer Society [CAN 2015/1216].

ACKNOWLEDGMENTS

We apologize to the authors of original work that was not cited in this mini-review due to space constraint.

REFERENCES

1. Stupp R, Mason WP, van den Bent MJ, Weller M, Fisher B, Taphoorn MJ, et al. Radiotherapy Plus Concomitant and Adjuvant Temozolomide for Glioblastoma. *N Engl J Med* (2005) 352(10):987–96. doi: 10.1056/NEJMoa043330
2. Khasraw M, Reardon DA, Weller M, Sampson JH. PD-1 Inhibitors: Do They Have a Future in the Treatment of Glioblastoma? *Clin Cancer Res* (2020) 26 (20):5287–96. doi: 10.1158/1078-0432.CCR-20-1135
3. Cloughesy TF, Mochizuki AY, Orpilla JR, Hugo W, Lee AH, Davidson TB, et al. Neoadjuvant Anti-PD-1 Immunotherapy Promotes a Survival Benefit With Intratumoral and Systemic Immune Responses in Recurrent Glioblastoma. *Nat Med* (2019) 25(3):477–86. doi: 10.1038/s41591-018-0337-7
4. Schalper KA, Rodriguez-Ruiz ME, Diez-Valle R, Lopez-Janeiro A, Porciuncula A, Idoate MA, et al. Neoadjuvant Nivolumab Modifies the Tumor Immune Microenvironment in Resectable Glioblastoma. *Nat Med* (2019) 25(3):470–6. doi: 10.1038/s41591-018-0339-5
5. Louveau A, Smirnov I, Keyes TJ, Eccles JD, Rouhani SJ, Peske JD, et al. Structural and Functional Features of Central Nervous System Lymphatic Vessels. *Nature* (2015) 523(7560):337–41. doi: 10.1038/nature14432

6. Mestre H, Mori Y, Nedergaard M. The Brain's Glymphatic System: Current Controversies. *Trends Neurosci* (2020) 43(7):458–66. doi: 10.1016/j.tins.2020.04.003
7. Jessen NA, Munk AS, Lundgaard I, Nedergaard M. The Glymphatic System: A Beginner's Guide. *Neurochem Res* (2015) 40(12):2583–99. doi: 10.1007/s11064-015-1581-6
8. Rustenhoven J, Drieu A, Mamuladze T, de Lima KA, Dykstra T, Wall M, et al. Functional Characterization of the Dural Sinuses as a Neuroimmune Interface. *Cell* (2021) 184(4):1000–16.e27. doi: 10.1016/j.cell.2020.12.040
9. Song E, Mao T, Dong H, Boisserand LSB, Antila S, Bosenberg M, et al. VEGF-C-Driven Lymphatic Drainage Enables Immunosurveillance of Brain Tumours. *Nature* (2020) 577(7792):689–94. doi: 10.1038/s41586-019-1912-x
10. Hu X, Deng Q, Ma L, Li Q, Chen Y, Liao Y, et al. Meningeal Lymphatic Vessels Regulate Brain Tumor Drainage and Immunity. *Cell Res* (2020) 30(3):229–43. doi: 10.1038/s41422-020-0287-8
11. Chen DS, Mellman I. Oncology Meets Immunology: The Cancer-Immunity Cycle. *Immunity* (2013) 39(1):1–10. doi: 10.1016/j.immuni.2013.07.012
12. van Hooren L, Vaccaro A, Ramachandran M, Vazaios K, Libard S, van de Walle T, et al. Agonistic CD40 Therapy Induces Tertiary Lymphoid Structures But Impairs Responses to Checkpoint Blockade in Glioma. *Nat Commun* (2021) 12(1):4127. doi: 10.1038/s41467-021-24347-7
13. Wongthida P, Schuelke MR, Driscoll CB, Kottke T, Thompson JM, Tonne J, et al. Ad-CD40L Mobilizes CD4 T Cells for the Treatment of Brainstem Tumors. *Neuro Oncol* (2020) 22(12):1757–70. doi: 10.1093/neuonc/noaa126
14. Aspelund A, Antila S, Proulx ST, Karlsen TV, Karaman S, Detmar M, et al. A Dural Lymphatic Vascular System That Drains Brain Interstitial Fluid and Macromolecules. *J Exp Med* (2015) 212(7):991–9. doi: 10.1084/jem.20142290
15. Engelhardt B, Vajkoczy P, Weller RO. The Movers and Shapers in Immune Privilege of the CNS. *Nat Immunol* (2017) 18(2):123–31. doi: 10.1038/ni.3666
16. Korin B, Ben-Shaanan TL, Schiller M, Dubovik T, Azulay-Debby H, Boshnak NT, et al. High-Dimensional, Single-Cell Characterization of the Brain's Immune Compartment. *Nat Neurosci* (2017) 20(9):1300–9. doi: 10.1038/nn.4610
17. Wilson EH, Weninger W, Hunter CA. Trafficking of Immune Cells in the Central Nervous System. *J Clin Invest* (2010) 120(5):1368–79. doi: 10.1172/JCI41911
18. Chen DS, Mellman I. Elements of Cancer Immunity and the Cancer-Immune Set Point. *Nature* (2017) 541(7637):321–30. doi: 10.1038/nature21349
19. Han S, Zhang C, Li Q, Dong J, Liu Y, Huang Y, et al. Tumour-Infiltrating CD4(+) and CD8(+) Lymphocytes as Predictors of Clinical Outcome in Glioma. *Br J Cancer* (2014) 110(10):2560–8. doi: 10.1038/bjc.2014.162
20. Facoetti A, Nano R, Zelini P, Morbini P, Benericetti E, Ceroni M, et al. Human Leukocyte Antigen and Antigen Processing Machinery Component Defects in Astrocytic Tumors. *Clin Cancer Res* (2005) 11(23):8304–11. doi: 10.1158/1078-0432.CCR-04-2588
21. Kim WJ, Dho YS, Ock CY, Kim JW, Choi SH, Lee ST, et al. Clinical Observation of Lymphopenia in Patients With Newly Diagnosed Glioblastoma. *J Neurooncol* (2019) 143(2):321–8. doi: 10.1007/s11060-019-03167-2
22. Chongsathidkiet P, Jackson C, Koyama S, Loebel F, Cui X, Farber SH, et al. Sequestration of T Cells in Bone Marrow in the Setting of Glioblastoma and Other Intracranial Tumors. *Nat Med* (2018) 24(9):1459–68. doi: 10.1038/s41591-018-0135-2
23. Mathewson ND, Ashenberg O, Tirosh I, Gritsch S, Perez EM, Marx S, et al. Inhibitory CD161 Receptor Identified in Glioma-Infiltrating T Cells by Single-Cell Analysis. *Cell* (2021) 184(5):1281–98.e26. doi: 10.1016/j.cell.2021.01.022
24. Marchetti L, Engelhardt B. Immune Cell Trafficking Across the Blood-Brain Barrier in the Absence and Presence of Neuroinflammation. *Vasc Biol* (2020) 2(1):H1–H18. doi: 10.1530/VB-19-0033
25. Arvanitis CD, Ferraro GB, Jain RK. The Blood-Brain Barrier and Blood-Tumour Barrier in Brain Tumours and Metastases. *Nat Rev Cancer* (2020) 20(1):26–41. doi: 10.1038/s41568-019-0205-x
26. Ahir BK, Engelhard HH, Lakka SS. Tumor Development and Angiogenesis in Adult Brain Tumor: Glioblastoma. *Mol Neurobiol* (2020) 57(5):2461–78. doi: 10.1007/s12035-020-01892-8
27. Dieterich LC, Mellberg S, Langenkamp E, Zhang L, Zieba A, Salomaki H, et al. Transcriptional Profiling of Human Glioblastoma Vessels Indicates a Key Role of VEGF-A and TGFbeta2 in Vascular Abnormalization. *J Pathol* (2012) 228(3):378–90. doi: 10.1002/path.4072
28. Lanitis E, Irving M, Coukos G. Targeting the Tumor Vasculature to Enhance T Cell Activity. *Curr Opin Immunol* (2015) 33:55–63. doi: 10.1016/j.coi.2015.01.011
29. Huang H, Langenkamp E, Georganaki M, Loskog A, Fuchs PF, Dieterich LC, et al. VEGF Suppresses T-Lymphocyte Infiltration in the Tumor Microenvironment Through Inhibition of NF-kappaB-Induced Endothelial Activation. *FASEB J* (2015) 29(1):227–38. doi: 10.1096/fj.14-250985
30. Griffioen AW, Damen CA, Blijham GH, Groenewegen G. Tumor Angiogenesis Is Accompanied by a Decreased Inflammatory Response of Tumor-Associated Endothelium. *Blood* (1996) 88(2):667–73. doi: 10.1182/blood.V88.2.667.bloodjournal882667
31. Xie Y, He L, Lugano R, Zhang Y, Cao H, He Q, et al. Key Molecular Alterations in Endothelial Cells in Human Glioblastoma Uncovered Through Single-Cell RNA Sequencing. *JCI Insight* (2021) 6(15):150861. doi: 10.1172/jci.insight.150861
32. Friebel E, Kapolou K, Unger S, Nunez NG, Utz S, Rushing EJ, et al. Single-Cell Mapping of Human Brain Cancer Reveals Tumor-Specific Instruction of Tissue-Invading Leukocytes. *Cell* (2020) 181(7):1626–42.e20. doi: 10.1016/j.cell.2020.04.055
33. Woroniecka K, Chongsathidkiet P, Rhodin K, Kemeny H, Dechant C, Farber SH, et al. T-Cell Exhaustion Signatures Vary With Tumor Type and Are Severe in Glioblastoma. *Clin Cancer Res* (2018) 24(17):4175–86. doi: 10.1158/1078-0432.CCR-17-1846
34. Komohara Y, Ohnishi K, Kuratsu J, Takeya M. Possible Involvement of the M2 Anti-Inflammatory Macrophage Phenotype in Growth of Human Gliomas. *J Pathol* (2008) 216(1):15–24. doi: 10.1002/path.2370
35. Wei J, Chen P, Gupta P, Ott M, Zamler D, Kassab C, et al. Immune Biology of Glioma-Associated Macrophages and Microglia: Functional and Therapeutic Implications. *Neuro Oncol* (2020) 22(2):180–94. doi: 10.1093/neuonc/noz212
36. Matyszak MK, Denis-Donini S, Citterio S, Longhi R, Granucci F, Ricciardi-Castagnoli P. Microglia Induce Myelin Basic Protein-Specific T Cell Anergy or T Cell Activation, According to Their State of Activation. *Eur J Immunol* (1999) 29(10):3063–76. doi: 10.1002/(SICI)1521-4141(199910)29:10<3063::AID-IMMU3063>3.0.CO;2-G
37. Ochocka N, Segit P, Walentynowicz KA, Wojnicki K, Cyranowski S, Swatler J, et al. Single-Cell RNA Sequencing Reveals Functional Heterogeneity of Glioma-Associated Brain Macrophages. *Nat Commun* (2021) 12(1):1151. doi: 10.1038/s41467-021-21407-w
38. Srivastava S, Jackson C, Kim T, Choi J, Lim M. A Characterization of Dendritic Cells and Their Role in Immunotherapy in Glioblastoma: From Preclinical Studies to Clinical Trials. *Cancers (Basel)* (2019) 11(4):537. doi: 10.3390/cancers11040537
39. Yan J, Zhao Q, Gabrusiewicz K, Kong LY, Xia X, Wang J, et al. FGL2 Promotes Tumor Progression in the CNS by Suppressing CD103(+) Dendritic Cell Differentiation. *Nat Commun* (2019) 10(1):448. doi: 10.1038/s41467-018-08271-x
40. Wang J, Liu P, Xin S, Wang Z, Li J. Nrf2 Suppresses the Function of Dendritic Cells to Facilitate the Immune Escape of Glioma Cells. *Exp Cell Res* (2017) 360(2):66–73. doi: 10.1016/j.yexcr.2017.07.031
41. Akasaki Y, Liu G, Chung NH, Ehtesham M, Black KL, Yu JS. Induction of a CD4+ T Regulatory Type 1 Response by Cyclooxygenase-2-Overexpressing Glioma. *J Immunol* (2004) 173(7):4352–9. doi: 10.4049/jimmunol.173.7.4352
42. Sautes-Fridman C, Petitprez F, Calderaro J, Fridman WH. Tertiary Lymphoid Structures in the Era of Cancer Immunotherapy. *Nat Rev Cancer* (2019) 19(6):307–25. doi: 10.1038/s41568-019-0144-6
43. Silina K, Soltermann A, Attar FM, Casanova R, Uckeley ZM, Thut H, et al. Germinal Centers Determine the Prognostic Relevance of Tertiary Lymphoid Structures and Are Impaired by Corticosteroids in Lung Squamous Cell Carcinoma. *Cancer Res* (2018) 78(5):1308–20. doi: 10.1158/0008-5472.CAN-17-1987
44. Lochner M, Ohnmacht C, Presley L, Bruhns P, Si-Tahar M, Sawa S, et al. Microbiota-Induced Tertiary Lymphoid Tissues Aggravate Inflammatory Disease in the Absence of RORgamma T and LTi Cells. *J Exp Med* (2011) 208(1):125–34. doi: 10.1084/jem.20100052
45. Lucchinetti CF, Popescu BF, Bunyan RF, Moll NM, Roemer SF, Lassmann H, et al. Inflammatory Cortical Demyelination in Early Multiple Sclerosis. *N Engl J Med* (2011) 365(23):2188–97. doi: 10.1056/NEJMoa1100648
46. Neyt K, Perros F, GeurtsvanKessel CH, Hammad H, Lambrecht BN. Tertiary Lymphoid Organs in Infection and Autoimmunity. *Trends Immunol* (2012) 33(6):297–305. doi: 10.1016/j.it.2012.04.006

47. Helmink BA, Reddy SM, Gao J, Zhang S, Basar R, Thakur R, et al. B Cells and Tertiary Lymphoid Structures Promote Immunotherapy Response. *Nature* (2020) 577(7791):549–55. doi: 10.1038/s41586-019-1922-8
48. Cabrita R, Lauss M, Sanna A, Donia M, Skaarup Larsen M, Mitra S, et al. Tertiary Lymphoid Structures Improve Immunotherapy and Survival in Melanoma. *Nature* (2020) 577(7791):561–5. doi: 10.1038/s41586-019-1914-8
49. Serafini B, Rosicarelli B, Magliozzi R, Stigliano E, Aloisi F. Detection of Ectopic B-Cell Follicles With Germinal Centers in the Meninges of Patients With Secondary Progressive Multiple Sclerosis. *Brain Pathol* (2004) 14 (2):164–74. doi: 10.1111/j.1750-3639.2004.tb00049.x
50. Magliozzi R, Howell O, Vora A, Serafini B, Nicholas R, Puopolo M, et al. Meningeal B-Cell Follicles in Secondary Progressive Multiple Sclerosis Associate With Early Onset of Disease and Severe Cortical Pathology. *Brain* (2007) 130(Pt 4):1089–104. doi: 10.1093/brain/awm038
51. Choi SR, Howell OW, Carassiti D, Magliozzi R, Gveric D, Muraro PA, et al. Meningeal Inflammation Plays a Role in the Pathology of Primary Progressive Multiple Sclerosis. *Brain* (2012) 135(Pt 10):2925–37. doi: 10.1093/brain/aws189
52. Peters A, Pitcher LA, Sullivan JM, Mitsdoerffer M, Acton SE, Franz B, et al. Th17 Cells Induce Ectopic Lymphoid Follicles in Central Nervous System Tissue Inflammation. *Immunity* (2011) 35(6):986–96. doi: 10.1016/j.immuni.2011.10.015
53. Dang AK, Tesfagiorgis Y, Jain RW, Craig HC, Kerfoot SM. Meningeal Infiltration of the Spinal Cord by Non-Classically Activated B Cells Is Associated With Chronic Disease Course in a Spontaneous B Cell-Dependent Model of CNS Autoimmune Disease. *Front Immunol* (2015) 6:470. doi: 10.3389/fimmu.2015.00470
54. Kuerten S, Schickel A, Kerkloh C, Recks MS, Addicks K, Ruddle NH, et al. Tertiary Lymphoid Organ Development Coincides With Determinant Spreading of the Myelin-Specific T Cell Response. *Acta Neuropathol* (2012) 124(6):861–73. doi: 10.1007/s00401-012-1023-3
55. Kielczewski JL, Horai R, Jittayasothorn Y, Chan CC, Caspi RR. Tertiary Lymphoid Tissue Forms in Retinas of Mice With Spontaneous Autoimmune Uveitis and Has Consequences on Visual Function. *J Immunol* (2016) 196 (3):1013–25. doi: 10.4049/jimmunol.1501570
56. Heng JS, Hackett SF, Stein-O'Brien GL, Winer BL, Williams J, Goff LA, et al. Comprehensive Analysis of a Mouse Model of Spontaneous Uveoretinitis Using Single-Cell RNA Sequencing. *Proc Natl Acad Sci U S A* (2019) 116 (52):26734–44. doi: 10.1073/pnas.1915571116
57. Kleinwort KJ, Amann B, Hauck SM, Feederle R, Sekundo W, Deeg CA. Immunological Characterization of Intraocular Lymphoid Follicles in a Spontaneous Recurrent Uveitis Model. *Invest Ophthalmol Vis Sci* (2016) 57 (10):4504–11. doi: 10.1167/iovs.16-19787
58. Pikor NB, Cupovic J, Onder L, Gommerman JL, Ludewig B. Stromal Cell Niches in the Inflamed Central Nervous System. *J Immunol* (2017) 198(5): 1775–81. doi: 10.4049/jimmunol.1601566
59. Barone F, Gardner DH, Nayar S, Steinthal N, Buckley CD, Luther SA. Stromal Fibroblasts in Tertiary Lymphoid Structures: A Novel Target in Chronic Inflammation. *Front Immunol* (2016) 7:477. doi: 10.3389/fimmu.2016.00477
60. Buckley CD, Barone F, Nayar S, Benezech C, Caamano J. Stromal Cells in Chronic Inflammation and Tertiary Lymphoid Organ Formation. *Annu Rev Immunol* (2015) 33:715–45. doi: 10.1146/annurev-immunol-032713-120252
61. Ruddle NH. Lymphatic Vessels and Tertiary Lymphoid Organs. *J Clin Invest* (2014) 124(3):953–9. doi: 10.1172/JCI71611
62. Pikor NB, Astarita JL, Summers-Deluca L, Galicia G, Qu J, Ward LA, et al. Integration of Th17- and Lymphotoxin-Derived Signals Initiates Meningeal-Resident Stromal Cell Remodeling to Propagate Neuroinflammation. *Immunity* (2015) 43(6):1160–73. doi: 10.1016/j.immuni.2015.11.010
63. Rua R, McGavern DB. Advances in Meningeal Immunity. *Trends Mol Med* (2018) 24(6):542–59. doi: 10.1016/j.molmed.2018.04.003
64. Solar P, Zamani A, Kubickova L, Dubovy P, Joukal M. Choroid Plexus and the Blood-Cerebrospinal Fluid Barrier in Disease. *Fluids Barriers CNS* (2020) 17 (1):35. doi: 10.1186/s12987-020-00196-2
65. Hindley JP, Jones E, Smart K, Bridgeman H, Lauder SN, Ondondo B, et al. T-Cell Trafficking Facilitated by High Endothelial Venules Is Required for Tumor Control After Regulatory T-Cell Depletion. *Cancer Res* (2012) 72 (21):5473–82. doi: 10.1158/0008-5472.CAN-12-1912
66. Milutinovic S, Abe J, Godkin A, Stein JV, Gallimore A. The Dual Role of High Endothelial Venules in Cancer Progression Versus Immunity. *Trends Cancer* (2021) 7(3):214–25. doi: 10.1016/j.trecan.2020.10.001
67. Allen E, Jabouille A, Rivera LB, Lodewijckx I, Missiaen R, Steri V, et al. Combined Antiangiogenic and Anti-PD-L1 Therapy Stimulates Tumor Immunity Through HEV Formation. *Sci Transl Med* (2017) 9(385): eaak9679. doi: 10.1126/scitranslmed.aak9679
68. He B, Jabouille A, Steri V, Johansson-Percival A, Michael IP, Kotamraju VR, et al. Vascular Targeting of LIGHT Normalizes Blood Vessels in Primary Brain Cancer and Induces Intratumoural High Endothelial Venules. *J Pathol* (2018) 245(2):209–21. doi: 10.1002/path.5080
69. Jansen CS, Prokhnevska N, Master VA, Sanda MG, Carlisle JW, Bilen MA, et al. An Intra-Tumoral Niche Maintains and Differentiates Stem-Like CD8 T Cells. *Nature* (2019) 576(7787):465–70. doi: 10.1038/s41586-019-1836-5
70. Brinker T, Stopa E, Morrison J, Klinge P. A New Look at Cerebrospinal Fluid Circulation. *Fluids Barriers CNS* (2014) 11:10. doi: 10.1186/2045-8118-11-10
71. Vanlandewijck M, He L, Mae MA, Andrae J, Ando K, Del Gaudio F, et al. A Molecular Atlas of Cell Types and Zonation in the Brain Vasculature. *Nature* (2018) 554(7693):475–80. doi: 10.1038/nature25739
72. Hannocks MJ, Pizzo ME, Huppert J, Deshpande T, Abbott NJ, Thorne RG, et al. Molecular Characterization of Perivascular Drainage Pathways in the Murine Brain. *J Cereb Blood Flow Metab* (2018) 38(4):669–86. doi: 10.1177/0271678X17749689
73. Aoyama S, Nakagawa R, Mule JJ, Mailloux AW. Inducible Tertiary Lymphoid Structures: Promise and Challenges for Translating a New Class of Immunotherapy. *Front Immunol* (2021) 12:675538. doi: 10.3389/fimmu.2021.675538
74. Filderman JN, Appleman M, Chelvanambi M, Taylor JL, Storkus WJ. STINGing the Tumor Microenvironment to Promote Therapeutic Tertiary Lymphoid Structure Development. *Front Immunol* (2021) 12:690105. doi: 10.3389/fimmu.2021.690105
75. Joshi NS, Akama-Garren EH, Lu Y, Lee DY, Chang GP, Li A, et al. Regulatory T Cells in Tumor-Associated Tertiary Lymphoid Structures Suppress Anti-Tumor T Cell Responses. *Immunity* (2015) 43(3):579–90. doi: 10.1016/j.immuni.2015.08.006
76. Qin X, Liu R, Akter F, Qin L, Xie Q, Li Y, et al. Peri-Tumoral Brain Edema Associated With Glioblastoma Correlates With Tumor Recurrence. *J Cancer* (2021) 12(7):2073–82. doi: 10.7150/jca.53198
77. Pikor NB, Prat A, Bar-Or A, Gommerman JL. Meningeal Tertiary Lymphoid Tissues and Multiple Sclerosis: A Gathering Place for Diverse Types of Immune Cells During CNS Autoimmunity. *Front Immunol* (2015) 6:657. doi: 10.3389/fimmu.2015.00657
78. Pipi E, Nayar S, Gardner DH, Colafrancesco S, Smith C, Barone F. Tertiary Lymphoid Structures: Autoimmunity Goes Local. *Front Immunol* (2018) 9:1952. doi: 10.3389/fimmu.2018.01952
79. Iorgulescu JB, Gokhale PC, Speranza MC, Eschle BK, Poitras MJ, Wilkens MK, et al. Concurrent Dexamethasone Limits the Clinical Benefit of Immune Checkpoint Blockade in Glioblastoma. *Clin Cancer Res* (2021) 27(1):276–87. doi: 10.1158/1078-0432.CCR-20-2291

Conflict of Interest: The authors declare that the research was conducted in the absence of any commercial or financial relationships that could be construed as a potential conflict of interest.

Publisher's Note: All claims expressed in this article are solely those of the authors and do not necessarily represent those of their affiliated organizations, or those of the publisher, the editors and the reviewers. Any product that may be evaluated in this article, or claim that may be made by its manufacturer, is not guaranteed or endorsed by the publisher.

Copyright © 2021 van de Walle, Vaccaro, Ramachandran, Pietilä, Essand and Dimberg. This is an open-access article distributed under the terms of the Creative Commons Attribution License (CC BY). The use, distribution or reproduction in other forums is permitted, provided the original author(s) and the copyright owner(s) are credited and that the original publication in this journal is cited, in accordance with accepted academic practice. No use, distribution or reproduction is permitted which does not comply with these terms.

frontiers in Immunology

MINI REVIEW
published: 03 September 2021
doi: 10.3389/fimmu.2021.716860

Current Clinical and Pre-Clinical Imaging Approaches to Study the Cancer-Associated Immune System

Christopher G. Mueller[1]*, *Christian Gaiddon*[2] *and Aïna Venkatasamy*[2,3]

[1] CNRS UPR 3572, University of Strasbourg, Immunologie-Immunopathologie-Chimie Thérapeutique, Strasbourg, France, [2] Inserm UMR_S 1113, University of Strasbourg, Interface de Recherche Fondamentale et Appliquée en Cancérologie (IRFAC), Strasbourg, France, [3] IHU-Strasbourg (Institut Hospitalo-Universitaire), Strasbourg, France

In the light of the success and the expected growth of its arsenal, immuno-therapy may become the standard neoadjuvant procedure for many cancers in the near future. However, aspects such as the identity, organization and the activation status of the peri- and intra-tumoral immune cells would represent important elements to weigh in the decision for the appropriate treatment. While important progress in non-invasive imaging of immune cells has been made over the last decades, it falls yet short of entering the clinics, let alone becoming a standard procedure. Here, we provide an overview of the different intra-vital imaging approaches in the clinics and in pre-clinical settings and discuss their benefits and drawbacks for assessing the activity of the immune system, globally and on a cellular level. Stimulated by further research, the future is likely to see many technological advances both on signal detection and emission as well as image specificity and resolution to tackle current hurdles. We anticipate that the ability to precisely determine an immune stage of cancer will capture the attention of the oncologist and will create a change in paradigm for cancer therapy.

Keywords: imaging, immune cells, cancer, lymph node, tertiary lymphoid structure

OPEN ACCESS

Edited by:
Anna Dimberg,
Uppsala University, Sweden

Reviewed by:
Joanna Bandola-Simon,
National Institutes of Health (NIH), United States
Thuy Tran,
Karolinska Institutet (KI), Sweden

***Correspondence:**
Christopher G. Mueller
c.mueller@unistra.fr

Specialty section:
This article was submitted to Cancer Immunity and Immunotherapy, a section of the journal Frontiers in Immunology

Received: *29 May 2021*
Accepted: *16 August 2021*
Published: *03 September 2021*

Citation:
Mueller CG, Gaiddon C and Venkatasamy A (2021) Current Clinical and Pre-Clinical Imaging Approaches to Study the Cancer-Associated Immune System. Front. Immunol. 12:716860. doi: 10.3389/fimmu.2021.716860

INTRODUCTION

The success of immune checkpoint blockade has initiated a shift in the way we view the relationship between the immune system and cancer. The immune system is no longer seen as the underdog in an unequal duel with cancer but increasingly as a powerful system, potentially capable of fighting and even eradicating tumor cells. While formerly relatively little attention has been paid to the immune system in cancer therapy, it has now been recognized to provide precious information regarding tumor staging and to present a serious therapeutic option, in particular when amplified after releasing it from immune-checkpoint blockades. This raises the question of preserving rather than resecting the local immune tissues, especially the sentinel lymph node, where many critical immune-stimulatory and modulatory processes take place. Along the same lines, preserving and amplifying existing intra-tumoral immune cells, structured or not as tertiary lymphoid tissue may benefit patients in the long run. However, this depends on an accurate means to non-invasively estimate the activity of the immune system in order to make the right choice between resection, chemotherapy and/or immune stimulatory treatment. Over the last decade, efforts to image precisely and specifically tissue and tissue-resident single cell-types have

greatly accelerated so that the capacity to accurately visualize immune cells *in vivo* becomes reality (1). These technologies have seen applications to observe lymph nodes, especially its architecture and the presence of micro-metastasis, with further clinical applications including pre-operative guidance for selected lymph node resection. Intra-vital imaging techniques are being refined for direct antitumor therapy and will provide the basis for further development towards pre-operative immune cell imaging (2). Here, we review the current approaches for *in vivo* imaging in clinical and pre-clinical settings and how these technologies and methods could pave the way to intra-vital imaging of immune cells to guide oncologists in the choice of the best treatment option.

LYMPH NODE IMAGING IN THE CLINICS

The spatial resolution of standard imaging modalities does not enable the direct visualization of immune cells. However, a variety of conventional imaging techniques (e.g., lymphography, ultrasound, computed tomography, magnetic resonance imaging and positron emission tomography) may be used to detect and visualize normal and pathological human lymph nodes (**Table 1**). For instance, lymphography has been widely used to image the lymph nodes and the lymphatic system (3). This technique bears the unique ability to demonstrate changes in the internal architecture of lymph nodes (with normal nodes appearing homogeneous with a fine granularity owing to the opacification of the sinus and the non-opacification of the lymphoid follicles) especially useful in pathological nodes such as in hemopathies (e.g. lymphomas) and/or genitourinary cancers. Similarly, ultrasound (US) has been extensively used to detect superficial lymph nodes and guide needle biopsies. It provides a real-time, radiation-free, access to the lymph node substructure, visualizing micro-metastasis (0.2 - 2 mm) as well as inflammatory changes within the node, resulting from either tissue inflammation or metastatic invasion (4–6). On US, inflamed lymph nodes usually present with increased size (small axis >10 mm), a thicker cortex and increased vascular flow (using Doppler mode). Such findings are not specific and it may sometimes be difficult to differentiate inflamed nodes from metastatic ones. The use of microbubble-based contrast agent, Doppler imaging (with blood flow velocity measures of microvascular network) and elastrography (using tissue stiffness) improved the US-detection of lymph node metastasis and the distinction between malignant (harder) and benign (softer) nodes (4–6). However, US is observer-dependent, limited by the depth of tissue penetration and subject to air/bone artifacts. Presently, routine lymph node imaging relies on multimodal imaging by CT (computed tomography), PET (positron emission tomography) and/or MRI (magnetic resonance imaging), which are free from limitations imposed by the type of surrounding tissue and the depth of exploration. Validated morpho-functional criteria applied to the node (i.e., small axis > 10mm, presence of necrosis, round shape) are used to detect metastasis on imaging (8, 13). Unfortunately, all techniques reveal several limitations (**Table 1**). For instance, due to their current spatial resolution and acquisition time, CT, PET and MRI are currently insufficient to detect micro-metastasis (< 2 mm), which can be an issue for the accurate preoperative staging of cancers. Additionally, they fail to provides architectural information on the lymph nodes, and CT mostly reveals changes in nodal size. Yet, enlargement of the organ may be secondary to a metastatic invasion, inflammation and/or follicular hyperplasia (9). Therefore, evaluation of lymph node size or shape is no longer sufficient and more functional approaches are required. For instance, metastatic lymph nodes present with restricted diffusion on MRI and lower rADC (apparent diffusion coefficient ratio) than inflammatory ones (21). Additionally, [18F] Fluorodeoxyglucose ([18F] FDG) uptake on PET appears more sensitive and more specific than restricted diffusion on MRI to detect metastatic nodes (14). Similarly, dual-energy CT techniques have been used to differentiate between normal, inflammatory and metastatic lymph nodes in cervical squamous cell carcinoma (10). Unfortunately, despite constant progress, the current imaging approaches remain limited to lymph nodes and have not yet reached the cellular level.

TABLE 1 | Critical assessment of the imaging modalities for intravital immune assessment.

Modalities (References)	Clinical uses	Lymphatic tissue	Single cells	Limitations	Advantages	Spatial resolution
Lymphography (3)	+	+	–	Resolution, contrast agents	LN architecture, lower cost	10-20 mm
Ultrasound (4–7)	+	+ (superficial)	+ (contrast agents)	Depth, contrast agents	Lower cost	0.2-2 mm
CT (8–12)	+	+	+ (contrast agents)	Radiation	Depth	~ 1 mm (clinical) Lower (preclinical)
PET/SPECT (13–20)	+	+	+ (radioisotopes contrast agents)	Radiation, higher costs	Depth, activity quantification	~ 4-5 mm (clinical)
MRI (8, 9, 14, 21–30)	+	+	+ (contrast agents)	Higher costs	Depth Radiation-free	~ 1-2 mm (clinical) Lower (preclinical)
PA (7, 31–35)	+	+	+ (contrast/fluorescent agents)	Clinical applications	Depth, combination with NIR/ ultrasound imaging	< 5 µm
OCT (36–40)	+	-/+	–	Depth	Needle OCT	< 2 mm, depth
Fluorescence (41–48)	–	-/+	+ (fluorescent probes)	Depth, clinical use	NIR, multimodalities, theranostics	NA

NA, Not available.

FROM LYMPHATIC TISSUE TO IMMUNE CELLS

Pre-clinical *in vivo* micro-imaging techniques offer superior technical possibilities compared to current human imaging modalities because of *i)* the immobility of the studied specimen (e.g., *ex vivo* lymph node, anesthetized animal), *ii)* higher spatial resolutions (e.g., special coils, higher frequency probes or higher magnetic fields) and the possible use of novel contrast-agents, not approved for clinical use. Pre-clinical multimodal imaging, especially in mice, progressed from a macroscopic lymph node-centered approach to a cellular and functionally-driven aspect of imaging. For instance, the introduction of gold-nanoparticles (AuNPs) as CT contrast agent allows the detection of T cells (11) or monocytes (12). Concerning MRI, an *ex vivo* study on a limited number of samples of normal and metastatic lymph nodes produced a series of images of the node substructure and metastatic changes that presented a good correlation with the corresponding histological slides, using very high sub-millimetric spatial resolution and longer scanning time (22). Additionally, cell-specific imaging approaches make use of contrast or tracer agents to label and track cells after their intravenous injection (23, 24). Similarly, Magnetic particle imaging (MPI) of superparamagnetic iron oxide SPIO nanoparticles are promising, with new cell-specific applications awaiting further development (25–27). Recently, large progress has been made in immuno-imaging with the development of new probes targeting endogenous immune cells for PET or SPECT (single-photon emission computed tomography) and a large toolbox of lymphocyte and myeloid cell-targeting antibodies is becoming available (15). Molecular imaging has a pivotal role to visualize immune cells, such as the different immune cells and structures in the tumor microenvironment. Several advances within PET imaging of immune checkpoint blockade (e.g., PD-L1, PD-1) and CD8 have been evaluated on animal models and are now finding their way to the clinics. For instance, site-specific immune-PET tracers (64Cu-NOTA-αPD-L1 or 68Ga-NOTA-Nb109) has been developed to image PD-L1 and PD1 (68Ga-DOTA-HACA-PD1) (16–18). Additionally, specific immune-PET tracers for endogenous CD8 imaging have also been developed (19) and one of them (89Zr-IAB22M2C) is currently undergoing a human phase I clinical trial (20). Similarly, the tumor-associated-macrophages localized in a tumor microenvironment that can represent up to 50% of a tumor mass can now be visualized using macrophage-directed radiotracers in PET (e.g., using 64 Cu-labeled polyglucose nanoparticles) and MRI (28, 29). The non-invasive detection of tumor-associated-macrophages appears promising to monitor cancer immunotherapies, especially when combined with iron oxide nanoparticles, emerging as a novel prognostic assay for more refined patient stratification and personalized therapeutic choices (30).

Alternative imaging systems have been developed. Here, the challenges are specificity, sensitivity and penetrance that preclude so-far the dominance of one particular imaging approach (**Table 1**). Optoacoustic or photoacoustic tomography (PA) is based on the generation of an acoustic wave resulting from the absorption of optical energy and combines optical contrast and high ultrasonic resolution in a single modality (31). It has a spatial resolution of less than 5 μm and higher imaging depth than US. PA combined with ultrasound proved useful to image sentinel lymph node metastasis *in vivo* in a rabbit compared to histology (7). Using multi-wavelength measurements and the hemoglobin as endogenous contrast agent, venous and arterial blood flow can be imaged. Multispectral optoacoustic tomography (MSOT) offers the possibility of simultaneously imaging cell-specific signals with high tissue penetration. Near infrared (NIR) fluorescent dyes, such as indocyanine green, widely used in angiography, can detect immune cells such as macrophages in mice (41). AuNPs have seen increased use as contrast agents for PA with the advantage of different absorption spectra and multiplex targeting moieties (32). Coupled to tumor cell-specific antibodies, they allow simultaneous detection of different tumor cells (33) and antigen delivery to dendritic cells (34). NIR excitation combined with photoacoustics efficiently tracks T cells in mouse tumor models (35). Optical coherence tomography (OCT) uses interference of light rather than the sound exploited in US to generate two-dimensional cross-sectional images. Although its resolution is higher than US, it suffers from a low (~1-2 mm) penetration depth. Small lymph nodes such as those of rodents can be entirely analyzed, whereas the analysis of the larger human lymph nodes is restricted to its periphery (36–38). A means to overcome this constraint is to minimize the imaging probe to the size of a needle allowing tissue-imaging biopsies. Thus, internal human nodal B cell follicles and germinal centers can be observed (39) making it in theory possible to detect intra-tumoral tertiary lymphoid structures. Because of lack of molecular sensitivity, there have been efforts to combine OCT with fluorescence detection systems (40).

Analogous to radioisotopes or contrast NPs, various optical tags such as fluorescent dyes can be used to observe cells *in vivo*. Fluorescence imaging is well established for superficial investigations, but at the generally-employed wavelengths (from 450 nm [ultraviolet] to 650 nm [visible]) the strong interaction between the photon and the tissue that it traverses causes image inaccuracy. Photon scattering is therefore dependent on wavelength, tissue optical properties and depth of imaging (42). Confocal and multiphoton microscopy have greatly improved image resolution, with depth reaching several hundreds of μm. Further improvements were made with selective plane illumination microscopy (light sheet) and optical clearing of tissue allowing a depth of up to 2 mm. These improvements are welcomed in research laboratories but are unlikely to see clinical pre-operative applications. More promising are fluorophores with excitation and emission spectra in the NIR wavelength range (700–900 nm) or the second NIR range (up to 1700 nm) owing to their improved depth penetration (43). The cancer-cell targeting antibody recognizing EGFR (Cetuximab) coupled to IRDye800CW allows the visualization of tumor margins and the identification of lymph nodes with micro-metastasis (44, 45). Other therapeutic antibodies are undergoing repurposing with fluorescent dyes (46). In pre-clinical models, myeloid cells were detected using dual NIR imaging with NPs coupled to anti-Gr-1 and to anti-CD11b antibodies (47). Likewise, the use of anti-CD5 and anti-CD20 antibodies, coupled to

NIR emitting NPs allowed the detection of CD5+ CD20+ mantle cell lymphoma (48).

A FINE LINE BETWEEN IMAGING AND THERAPEUTICS: THERANOSTICS/ THERAGNOSTICS

Before fluorescence is applied to the detection of specific immune cells *in vivo*, hurdles such as the toxicity of fluorophores and the feasibility of imaging instrumentation must be taken. In this context, photoactivated therapy for directed cancer treatment should be considered. Several NPs used for imaging present themselves intrinsic cytotoxicity by liberating - upon illumination - reactive oxygen species (PDT, Photo-Dynamic Therapy), bioactive chemicals (Photo-Activated Chemotherapy, PACT), or even heat (Photo-Thermal Therapy, PTT) (49–51). Hence, these bifunctional NPs are valuable tools to simultaneously treat and assess treatment efficacy by visualizing the tumor or the immune cells. This combined approach defines the concept of theranostics. The NPs used for theranostics are of multiple sorts that can be categorized into at least two types based on the principal constituent: either purely organic or containing one or multiple metals (such as silica, zinc, gold, or ruthenium) (52, 53). The metal present in the NPs can either function as structural support for light-emitting compounds or for bioactive molecules. It can also be exploited for its intrinsic physicochemical properties. For instance, in PDT, light-sensitive transition metals, such as ruthenium, can change their peripheral electronic content to generate reactive oxygen species after reacting with O_2. The reactive oxygen species degrade several intracellular biological macromolecules, including DNA (54). Besides directly inducing cancer cell death by apoptosis, PDT can produce danger signals that recruit and activate cytotoxic immune cells (55). Indeed, PLGA-PEG NPs stimulate the accumulation of myeloid cells within the tumor microenvironment (56). This opens interesting opportunities to assess immune cell localization within the tumors while releasing compounds capable of recruiting and activating immune cells with antitumor activity. For PACT, bioactive ligands are liberated from the bond with the metal core to stimulate immune cells or directly kill cancer cells. Similar to the NPs that are used in diagnostics, the NPs with therapeutic properties can be functionalized for targeting specifically the tumors or infiltrating cells by using antibodies or other bioactive molecules (57). So far, only a limited number of tumors are targeted by these light-induced therapies, such as head and neck cancer, melanoma and bladder cancers. A better translation of theranostics from the pre-clinical stage to the clinic is likely to depend on the ability of NPs to be activated within the tissues. In line with the trend seen in imaging, the development of NPs for theranostics is moving toward the conception of NIR-sensitive compounds. Other innovative strategies include self-illuminating NPs that would avoid the requirement of external illumination while auto-generating light for PDT and imaging (58). Another complexing factor is the choice of the necessity of oxygen within the tumor for PDT and the choice of the target when considering the development of targeted NPs using monoclonal antibodies.

OUTLOOK AND CHALLENGES

The imaging of immune entities, such as different immune cells and structures in the tumor microenvironment represents an area of molecular imaging that has a pivotal role for the development of personalized and modern medicine. With the rise of immunotherapy for cancer treatment, one of the main issues on imaging is the enlargement of tumors related to the infiltration of the tumor microenvironment by immune cells that may be misinterpreted for tumor progression due to cancer growth (especially as both cases would show increased [^{18}F]-FDG uptake on PET). Therefore, the non-invasive molecular imaging approaches of different immune cell subtypes would represent a change of paradigm, especially in the era of immunotherapy and personalized medicine (59). While cutting-edge non-invasive imaging modalities, coupled to contrast agents with optimized cell specificity had been restricted to pre-clinical tests for years, they are now mature and are likely to reach the routine clinic in the near future. These include specific PET radiotracers for the immune checkpoint blockade or CD8/TAM that can be of crucial help for assessing the immune status of tumors and help select the patients who have the highest probability to respond to immunotherapy. Challenges will be to control cell toxicity in a way to avoid adverse effects, while preserving the option of targeted cell death for direct tumor destruction and to create inflammation. Another issue will be to refine the measures in a way to allow the distinction between pro- versus anti-inflammatory immune cell infiltration. The direct way to tackle this difficulty would be to distinguish between cell types such as M1 versus M2 macrophages or the release of inflammatory mediators such as IFN-γ, TNF-α or IL-1 versus anti-inflammatory IL-10 or TGF-β. An alternative, probably technically less challenging, could be to consider not only the number but also the localization of the immune cells. Their tumor-peripheral residence is likely characteristic of an inactive immune system and an ability of the tumor to resist immune attack, while an infiltrated tumor translates to an active immune cell response. To take this further, the presence of tertiary lymphoid structures comprising a large variety of hematopoietic cells including B cells in an organized fashion would suggest a chronic inflammatory and a potent anti-tumoral activity. In this general context of questioning anti- versus pro-inflammatory immune cell activity, it is important to also consider the draining lymph node. A pro-inflammatory immune cell activity in the tumor will necessarily translate into active draining lymph nodes characterized by increased size, rich immune cell traffic and extensive vascularization. All things considered, by bringing the immune cell into the foreground of the oncologist's attention new diagnostic and therapeutic possibilities will certainly emerge. Molecular imaging and nanomedicine will probably help to improve the cancer patient management, for improved patient

stratification for a more personalized care, providing a novel axis of success that has the potential to revolutionize cancer immunotherapy.

AUTHOR CONTRIBUTIONS

All authors contributed to the article and approved the submitted version.

FUNDING

CM acknowledges the support by grants 10-IDEX-0002, 20-SFRI-0012, 11-EQPX-022, ANR-20-CE93-0006 and ANR-19-CE14-0021-02. AV is supported by French state funds managed within the "Plan Investissements d'Avenir" and by the ANR (ANR-10-IAHU-02). CG is CNRS scientist supported by grants Ligue Contre le Cancer, Strasbourg university IDEX-excellence, ITMO Cancer (TPDTRu), ITMO Cancer (HNCARTMOL), ANR-10-IDEX-0002, ANR-20-SFRI-0012, PHC-Proteus (44234XC), Alsace Contre le Cancer, ECOS-Nord (M15PS01).

ACKNOWLEDGMENTS

We thank Alain Jung, ICANS, Strasbourg for critical reading of the manuscript.

REFERENCES

1. McCarthy CE, White JM, Viola NT, Gibson HM. *In Vivo* Imaging Technologies to Monitor the Immune System. *Front Immunol* (2020) 11:1067. doi: 10.3389/fimmu.2020.01067
2. Abadjian MZ, Edwards WB, Anderson CJ. Imaging the Tumor Microenvironment. *Adv Exp Med Biol* (2017) 1036:229–57. doi: 10.1007/978-3-319-67577-0_15
3. Guermazi A, Brice P, Hennequin C, Sarfati E. Lymphography: An Old Technique Retains Its Usefulness. *Radiographics: Rev Publ Radiol Soc North America Inc* (2003) 23(6):1541–58. doi: 10.1148/rg.236035704
4. Saegusa-Beecroft E, Machi J, Mamou J, Hata M, Coron A, Yanagihara ET, et al. Three-Dimensional Quantitative Ultrasound for Detecting Lymph Node Metastases. *J Surg Res* (2013) 183(1):258–69. doi: 10.1016/j.jss.2012.12.017
5. Belanger AR, Hollyfield J, Yacovone G, Ceppe AS, Akulian JA, Burks AC, et al. Incidence and Clinical Relevance of Non-Small Cell Lung Cancer Lymph Node Micro-Metastasis Detected by Staging Endobronchial Ultrasound-Guided Transbronchial Needle Aspiration. *J Thorac Dis* (2019) 11(8):3650–8. doi: 10.21037/jtd.2019.05.36
6. Tucker NS, Cyr AE, Ademuyiwa FO, Tabchy A, George K, Sharma PK, et al. Axillary Ultrasound Accurately Excludes Clinically Significant Lymph Node Disease in Patients With Early Stage Breast Cancer. *Ann Surg* (2016) 264 (6):1098–102. doi: 10.1097/sla.0000000000001549
7. Kang J, Chang JH, Kim SM, Lee HJ, Kim H, Wilson BC, et al. Real-Time Sentinel Lymph Node Biopsy Guidance Using Combined Ultrasound, Photoacoustic, Fluorescence Imaging: *In Vivo* Proof-of-Principle and Validation With Nodal Obstruction. *Sci Rep* (2017) 7:45008. doi: 10.1038/srep45008
8. Chong V. Cervical Lymphadenopathy: What Radiologists Need to Know. *Cancer Imaging: Off Publ Int Cancer Imaging Soc* (2004) 4(2):116–20. doi: 10.1102/1470-7330.2004.0020
9. Studer UE, Scherz S, Scheidegger J, Kraft R, Sonntag R, Ackermann D, et al. Enlargement of Regional Lymph Nodes in Renal Cell Carcinoma Is Often Not Due to Metastases. *J Urol* (1990) 144(2 Pt 1):243–5. doi: 10.1016/s0022-5347(17)39422-3
10. Tawfik AM, Razek AA, Kerl JM, Nour-Eldin NE, Bauer R, Vogl TJ. Comparison of Dual-Energy CT-Derived Iodine Content and Iodine Overlay of Normal, Inflammatory and Metastatic Squamous Cell Carcinoma Cervical Lymph Nodes. *Eur Radiol* (2014) 24(3):574–80. doi: 10.1007/s00330-013-3035-3
11. Meir R, Shamalov K, Betzer O, Motiei M, Horovitz-Fried M, Yehuda R, et al. Nanomedicine for Cancer Immunotherapy: Tracking Cancer-Specific T-Cells *In Vivo* With Gold Nanoparticles and CT Imaging. *ACS Nano* (2015) 9 (6):6363–72. doi: 10.1021/acsnano.5b01939
12. Chhour P, Naha PC, O'Neill SM, Litt HI, Reilly MP, Ferrari VA, et al. Labeling Monocytes With Gold Nanoparticles to Track Their Recruitment in Atherosclerosis With Computed Tomography. *Biomaterials* (2016) 87:93–103. doi: 10.1016/j.biomaterials.2016.02.009
13. Torabi M, Aquino SL, Harisinghani MG. Current Concepts in Lymph Node Imaging. *J Nucl Med: Off Publication Soc Nucl Med* (2004) 45(9):1509–18.
14. Stecco A, Buemi F, Cassarà A, Matheoud R, Sacchetti GM, Arnulfo A, et al. Comparison of Retrospective PET and MRI-DWI (PET/MRI-DWI) Image Fusion With PET/CT and MRI-DWI in Detection of Cervical and Endometrial Cancer Lymph Node Metastases. *La Radiol Med* (2016) 121 (7):537–45. doi: 10.1007/s11547-016-0626-5
15. Mayer AT, Gambhir SS. The Immunoimaging Toolbox. *J Nucl Med: Off Publication Soc Nucl Med* (2018) 59(8):1174–82. doi: 10.2967/jnumed.116.185967
16. Wissler HL, Ehlerding EB, Lyu Z, Zhao Y, Zhang S, Eshraghi A, et al. Site-Specific Immuno-PET Tracer to Image PD-L1. *Mol Pharm* (2019) 16 (5):2028–36. doi: 10.1021/acs.molpharmaceut.9b00010
17. Mayer AT, Natarajan A, Gordon SR, Maute RL, McCracken MN, Ring AM, et al. Practical Immuno-PET Radiotracer Design Considerations for Human Immune Checkpoint Imaging. *J Nucl Med: Off Publication Soc Nucl Med* (2017) 58(4):538–46. doi: 10.2967/jnumed.116.177659
18. Lv G, Sun X, Qiu L, Sun Y, Li K, Liu Q, et al. PET Imaging of Tumor PD-L1 Expression With a Highly Specific Nonblocking Single-Domain Antibody. *J Nucl Med: Off Publication Soc Nucl Med* (2020) 61(1):117–22. doi: 10.2967/jnumed.119.226712
19. Tavaré R, Escuin-Ordinas H, Mok S, McCracken MN, Zettlitz KA, Salazar FB, et al. An Effective Immuno-PET Imaging Method to Monitor CD8-Dependent Responses to Immunotherapy. *Cancer Res* (2016) 76(1):73–82. doi: 10.1158/0008-5472.Can-15-1707
20. Farwell MD, Gamache RF, Pandit-Taskar N, Postow M, Gordon MS, Wilson IA, et al. eds. CD8 PET Imaging of Tumor Infiltrating T Cells in Advanced Solid Tumors. In: *Society for Immunotherapy of Cancer*.
21. Wang J, Liao Q, Zhang Y, Yu C, Bai R, Sun H. Differential Diagnosis of Axillary Inflammatory and Metastatic Lymph Nodes in Rabbit Models by Using Diffusion-Weighted Imaging: Compared With Conventional Magnetic Resonance Imaging. *Korean J Radiol* (2012) 13(4):458–66. doi: 10.3348/kjr.2012.13.4.458
22. Dashevsky BZ, D'Alfonso T, Sutton EJ, Giambrone A, Aronowitz E, Morris EA, et al. The Potential of High Resolution Magnetic Resonance Microscopy in the Pathologic Analysis of Resected Breast and Lymph Tissue. *Sci Rep* (2015) 5:17435. doi: 10.1038/srep17435
23. Ahrens ET, Bulte JW. Tracking Immune Cells *In Vivo* Using Magnetic Resonance Imaging. *Nat Rev Immunol* (2013) 13(10):755–63. doi: 10.1038/nri3531
24. Zanganeh S, Spitler R, Hutter G, Ho JQ, Pauliah M, Mahmoudi M. Tumor-Associated Macrophages, Nanomedicine and Imaging: The Axis of Success in the Future of Cancer Immunotherapy. *Immunotherapy* (2017) 9(10):819–35. doi: 10.2217/imt-2017-0041
25. Talebloo N, Gudi M, Robertson N, Wang P. Magnetic Particle Imaging: Current Applications in Biomedical Research. *J Magn Reson Imaging: JMRI* (2020) 51(6):1659–68. doi: 10.1002/jmri.26875
26. Sehl OC, Gevaert JJ, Melo KP, Knier NN, Foster PJ. A Perspective on Cell Tracking With Magnetic Particle Imaging. *Tomogr (Ann Arbor Mich)* (2020) 6 (4):315–24. doi: 10.18383/j.tom.2020.00043

27. Furtado AD, Ceschin R, Blüml S, Mason G, Jakacki RI, Okada H, et al. Neuroimaging of Peptide-Based Vaccine Therapy in Pediatric Brain Tumors: Initial Experience. *Neuroimaging Clin N Am* (2017) 27(1):155–66. doi: 10.1016/j.nic.2016.09.002
28. Kim HY, Li R, Ng TSC, Courties G, Rodell CB, Prytyskach M, et al. Quantitative Imaging of Tumor-Associated Macrophages and Their Response to Therapy Using (64)Cu-Labeled Macrin. *ACS Nano* (2018) 12 (12):12015–29. doi: 10.1021/acsnano.8b04338
29. Yang R, Sarkar S, Yong VW, Dunn JF. In Vivo MR Imaging of Tumor-Associated Macrophages: The Next Frontier in Cancer Imaging. *Magn Reson Insights* (2018) 11:1–8. doi: 10.1177/1178623x18771974
30. Mukherjee S, Sonanini D, Maurer A, Daldrup-Link HE. The Yin and Yang of Imaging Tumor Associated Macrophages With PET and MRI. *Theranostics* (2019) 9(25):7730–48. doi: 10.7150/thno.37306
31. Wang LV. Prospects of Photoacoustic Tomography. *Med Phys* (2008) 35 (12):5758–67. doi: 10.1118/1.3013698
32. Li W, Chen X. Gold Nanoparticles for Photoacoustic Imaging. *Nanomed (London England)* (2015) 10(2):299–320. doi: 10.2217/nnm.14.169
33. Li PC, Wang CR, Shieh DB, Wei CW, Liao CK, Poe C, et al. *In Vivo* Photoacoustic Molecular Imaging With Simultaneous Multiple Selective Targeting Using Antibody-Conjugated Gold Nanorods. *Opt Express* (2008) 16(23):18605–15. doi: 10.1364/oe.16.018605
34. Liang R, Xie J, Li J, Wang K, Liu L, Gao Y, et al. Liposomes-Coated Gold Nanocages With Antigens and Adjuvants Targeted Delivery to Dendritic Cells for Enhancing Antitumor Immune Response. *Biomaterials* (2017) 149:41–50. doi: 10.1016/j.biomaterials.2017.09.029
35. Zheng S, Li H, Lai K, Chen M, Fu G, Liu WH, et al. Noninvasive Photoacoustic and Fluorescent Tracking of Optical Dye Labeled T Cellular Activities of Diseased Sites at New Depth. *J Biophotonics* (2018) 11(9):e201800073. doi: 10.1002/jbio.201800073
36. Nguyen FT, Zysk AM, Chaney EJ, Adie SG, Kotynek JG, Oliphant UJ, et al. Optical Coherence Tomography: The Intraoperative Assessment of Lymph Nodes in Breast Cancer. *IEEE Eng Med Biol Mag: Q Mag Eng Med Biol Soc* (2010) 29(2):63–70. doi: 10.1109/memb.2009.935722
37. Jung Y, Zhi Z, Wang RK. Three-Dimensional Optical Imaging of Microvascular Networks Within Intact Lymph Node *In Vivo*. *J Biomed Opt* (2010) 15(5):050501. doi: 10.1117/1.3496301
38. Galanzha EI, Zharov VP. Circulating Tumor Cell Detection and Capture by Photoacoustic Flow Cytometry *In Vivo* and *Ex Vivo*. *Cancers* (2013) 5 (4):1691–738. doi: 10.3390/cancers5041691
39. Shostak E, Hariri LP, Cheng GZ, Adams DC, Suter MJ. Needle-Based Optical Coherence Tomography to Guide Transbronchial Lymph Node Biopsy. *J Bronchol Intervent Pulmonol* (2018) 25(3):189–97. doi: 10.1097/lbr.0000000000000491
40. Gora MJ, Suter MJ, Tearney GJ, Li X. Endoscopic Optical Coherence Tomography: Technologies and Clinical Applications [Invited]. *Biomed Opt Express* (2017) 8(5):2405–44. doi: 10.1364/boe.8.002405
41. Tzoumas S, Zaremba A, Klemm U, Nunes A, Schaefer K, Ntziachristos V. Immune Cell Imaging Using Multi-Spectral Optoacoustic Tomography. *Opt Lett* (2014) 39(12):3523–6. doi: 10.1364/ol.39.003523
42. Ntziachristos V. Going Deeper Than Microscopy: The Optical Imaging Frontier in Biology. *Nat Methods* (2010) 7(8):603–14. doi: 10.1038/nmeth.1483
43. Zhang RR, Schroeder AB, Grudzinski JJ, Rosenthal EL, Warram JM, Pinchuk AN, et al. Beyond the Margins: Real-Time Detection of Cancer Using Targeted Fluorophores. *Nat Rev Clin Oncol* (2017) 14(6):347–64. doi: 10.1038/nrclinonc.2016.212
44. Rosenthal EL, Warram JM, de Boer E, Chung TK, Korb ML, Brandwein-Gensler M, et al. Safety and Tumor Specificity of Cetuximab-IRDye800 for Surgical Navigation in Head and Neck Cancer. *Clin Cancer Res: Off J Am Assoc Cancer Res* (2015) 21(16):3658–66. doi: 10.1158/1078-0432.Ccr-14-3284
45. Rosenthal EL, Moore LS, Tipirneni K, de Boer E, Stevens TM, Hartman YE, et al. Sensitivity and Specificity of Cetuximab-IRDye800CW to Identify Regional Metastatic Disease in Head and Neck Cancer. *Clin Cancer Res: Off J Am Assoc Cancer Res* (2017) 23(16):4744–52. doi: 10.1158/1078-0432.Ccr-16-2968
46. Hernot S, van Manen L, Debie P, Mieog JSD, Vahrmeijer AL. Latest Developments in Molecular Tracers for Fluorescence Image-Guided Cancer Surgery. *Lancet Oncol* (2019) 20(7):e354–67. doi: 10.1016/s1470-2045(19)30317-1
47. Yu GT, Luo MY, Li H, Chen S, Huang B, Sun ZJ, et al. Molecular Targeting Nanoprobes With Non-Overlap Emission in the Second Near-Infrared Window for in Vivo Two-Color Colocalization of Immune Cells. *ACS Nano* (2019) 13(11):12830–9. doi: 10.1021/acsnano.9b05038
48. Yang G, Cao Y, Yan B, Lv Q, Yu J, Zhao F, et al. Application of a Double-Colour Upconversion Nanofluorescent Probe for Targeted Imaging of Mantle Cell Lymphoma. *Oncotarget* (2018) 9(24):16758–74. doi: 10.18632/oncotarget.23860
49. Kim H, Chung K, Lee S, Kim DH, Lee H. Near-Infrared Light-Responsive Nanomaterials for Cancer Theranostics. *WIREs Nanomed Nanobiotechnol* (2016) 8(1):23–45. doi: 10.1002/wnan.1347
50. Imberti C, Zhang P, Huang H, Sadler PJ. New Designs for Phototherapeutic Transition Metal Complexes. *Angew Chem Int Ed* (2020) 59(1):61–73. doi: 10.1002/anie.201905171
51. Yang Y, Mu J, Xing B. Photoactivated Drug Delivery and Bioimaging. *WIREs Nanomed Nanobiotechnol* (2017) 9(2):e1408. doi: 10.1002/wnan.1408
52. Aranda-Lara L, Morales-Avila E, Luna-Gutiérrez MA, Olivé-Alvarez E, Isaac-Olivé K. Radiolabeled Liposomes and Lipoproteins as Lipidic Nanoparticles for Imaging and Therapy. *Chem Phys Lipids* (2020) 230:104934. doi: 10.1016/j.chemphyslip.2020.104934
53. Osterrieth JWM, Fairen-Jimenez D. Metal–Organic Framework Composites for Theragnostics and Drug Delivery Applications. *Biotechnol J* (2021) 16 (2):2000005. doi: 10.1002/biot.202000005
54. Kessel D. Photodynamic Therapy: Apoptosis, Paraptosis and Beyond. *Apoptosis: Int J Programmed Cell Death* (2020) 25(9-10):611–5. doi: 10.1007/s10495-020-01634-0
55. Alzeibak R, Mishchenko TA, Shilyagina NY, Balalaeva IV, Vedunova MV, Krysko DV. Targeting Immunogenic Cancer Cell Death by Photodynamic Therapy: Past, Present and Future. *J ImmunoTher Cancer* (2021) 9(1):e001926. doi: 10.1136/jitc-2020-001926
56. Huis in 't Veld RV, Ritsma L, Kleinovink JW, Que I, Ossendorp F, Cruz LJ. Photodynamic Cancer Therapy Enhances Accumulation of Nanoparticles in Tumor-Associated Myeloid Cells. *J Controlled Release* (2020) 320:19–31. doi: 10.1016/j.jconrel.2019.12.052
57. Vijayan V, Uthaman S, Park I-K. Cell Membrane-Camouflaged Nanoparticles: A Promising Biomimetic Strategy for Cancer Theragnostics. *Polymers* (2018) 10(983):1–25. doi: 10.3390/polym10090983
58. Xu X, An H, Zhang D, Tao H, Dou Y, Li X, et al. A Self-Illuminating Nanoparticle for Inflammation Imaging and Cancer Therapy. *Sci Adv* (2019) 5(1):eaat2953. doi: 10.1126/sciadv.aat2953
59. Galli F, Aguilera JV, Palermo B, Markovic SN, Nisticò P, Signore A. Relevance of Immune Cell and Tumor Microenvironment Imaging in the New Era of Immunotherapy. *J Exp Clin Cancer Res: CR* (2020) 39(1):89. doi: 10.1186/s13046-020-01586-y

Conflict of Interest: The authors declare that the research was conducted in the absence of any commercial or financial relationships that could be construed as a potential conflict of interest.

Publisher's Note: All claims expressed in this article are solely those of the authors and do not necessarily represent those of their affiliated organizations, or those of the publisher, the editors and the reviewers. Any product that may be evaluated in this article, or claim that may be made by its manufacturer, is not guaranteed or endorsed by the publisher.

Copyright © 2021 Mueller, Gaiddon and Venkatasamy. This is an open-access article distributed under the terms of the Creative Commons Attribution License (CC BY). The use, distribution or reproduction in other forums is permitted, provided the original author(s) and the copyright owner(s) are credited and that the original publication in this journal is cited, in accordance with accepted academic practice. No use, distribution or reproduction is permitted which does not comply with these terms.

frontiers in Immunology

ORIGINAL RESEARCH
published: 20 December 2021
doi: 10.3389/fimmu.2021.793964

The Tumor Immune Landscape and Architecture of Tertiary Lymphoid Structures in Urothelial Cancer

Nick van Dijk[1†], Alberto Gil-Jimenez[2,3†], Karina Silina[4], Maurits L. van Montfoort[5], Sarah Einerhand[1], Lars Jonkman[6], Charlotte S. Voskuilen[1], Dennis Peters[7], Joyce Sanders[5], Yoni Lubeck[5], Annegien Broeks[7], Erik Hooijberg[5], Daniel J. Vis[2,3], Maries van den Broek[4], Lodewyk F. A. Wessels[2,3,8], Bas W. G. van Rhijn[9,10] and Michiel S. van der Heijden[1,2]*

[1] Department of Medical Oncology, The Netherlands Cancer Institute, Amsterdam, Netherlands, [2] Department of Molecular Carcinogenesis, The Netherlands Cancer Institute, Amsterdam, Netherlands, [3] Oncode Institute, Utrecht, Netherlands, [4] Institute of Experimental Immunology, University of Zurich, Zurich, Switzerland, [5] Department of Pathology, The Netherlands Cancer Institute, Amsterdam, Netherlands, [6] Department of Medical Oncology, Maastricht University Medical Center, Maastricht, Netherlands, [7] Core Facility Molecular Pathology & Biobanking, The Netherlands Cancer Institute, Amsterdam, Netherlands, [8] Department of Electrical Engineering, Mathematics and Computer Science, Delft University of Technology, Delft, Netherlands, [9] Department of Urology, The Netherlands Cancer Institute, Amsterdam, Netherlands, [10] Department of Urology, Caritas St. Josef Medical Center, University of Regensburg, Regensburg, Germany

OPEN ACCESS

Edited by:
Anna Dimberg,
Uppsala University, Sweden

Reviewed by:
Alain Le Moine,
Université libre de Bruxelles, Belgium
Frank James Ward,
University of Aberdeen, United Kingdom

***Correspondence:**
Michiel S. van der Heijden
ms.vd.heijden@nki.nl

†These authors have contributed equally to this work and share first authorship

Specialty section:
This article was submitted to Cancer Immunity and Immunotherapy, a section of the journal Frontiers in Immunology

Received: *12 October 2021*
Accepted: *30 November 2021*
Published: *20 December 2021*

Citation:
Dijk Nv, Gil-Jimenez A, Silina K, Montfoort MLv, Einerhand S, Jonkman L, Voskuilen CS, Peters D, Sanders J, Lubeck Y, Broeks A, Hooijberg E, Vis DJ, Broek Mvd, Wessels LFA, Rhijn BWGv and Heijden MSvd (2021) The Tumor Immune Landscape and Architecture of Tertiary Lymphoid Structures in Urothelial Cancer. Front. Immunol. 12:793964. doi: 10.3389/fimmu.2021.793964

Candidate immune biomarkers have been proposed for predicting response to immunotherapy in urothelial cancer (UC). Yet, these biomarkers are imperfect and lack predictive power. A comprehensive overview of the tumor immune contexture, including Tertiary Lymphoid structures (TLS), is needed to better understand the immunotherapy response in UC. We analyzed tumor sections by quantitative multiplex immunofluorescence to characterize immune cell subsets in various tumor compartments in tumors without pretreatment and tumors exposed to preoperative anti-PD1/CTLA-4 checkpoint inhibitors (NABUCCO trial). Pronounced immune cell presence was found in UC invasive margins compared to tumor and stroma regions. $CD8^+PD1^+$ T-cells were present in UC, particularly following immunotherapy. The cellular composition of TLS was assessed by multiplex immunofluorescence (CD3, CD8, FoxP3, CD68, CD20, PanCK, DAPI) to explore specific TLS clusters based on varying immune subset densities. Using a k-means clustering algorithm, we found five distinct cellular composition clusters. Tumors unresponsive to anti-PD-1/CTLA-4 immunotherapy showed enrichment of a $FoxP3^+$ T-cell-low TLS cluster after treatment. Additionally, cluster 5 (macrophage low) TLS were significantly higher after pre-operative immunotherapy, compared to untreated tumors. We also compared the immune cell composition and maturation stages between superficial (submucosal) and deeper TLS, revealing that superficial TLS had more pronounced T-helper cells and enrichment of early TLS than TLS located in deeper tissue. Furthermore, superficial TLS displayed a lower fraction of secondary follicle like TLS than deeper TLS. Taken together, our results provide a detailed quantitative overview of the tumor immune landscape in UC, which can provide a basis for further studies.

Keywords: immunotherapy, tertiary lymphoid structures (TLS), multiplex immunofluorescence, urothelial cancer, tumor microenvironment, bladder cancer

1 INTRODUCTION

Muscle-invasive urothelial cancer (UC) is an aggressive disease with limited treatment options that originates in the bladder and parts of the urinary tract. Although UC can be cured by resection of the bladder (cystectomy), recurrence rates are high and 5-year survival is only 60-70% for pT2N0 tumors, and even worse for high-risk patients having pT3-4aN0 (40-50%) or pTxN+ (10-35%) at cystectomy. Immune checkpoint inhibitors (ICIs) have changed the treatment paradigm in metastatic urothelial cancer. Currently, ICIs have been approved for the first-line and second-line treatment (1–5), and are being tested in the adjuvant and preoperative setting. In the PURE-01 trial (6) and ABACUS trial (7), preoperative pembrolizumab (anti-PD-1) and atezolumab (anti-PD-L1) were clinically tested in patients diagnosed with cT2-4N0 UC, respectively. These trials revealed promising pathological complete response (pCR) rates upon treatment with neo-adjuvant pembrolizumab and atezolizumab. However, pCR to ICI monotherapy was primarily found in patients having less extensive disease (cT2N0), whereas patients with more extensive disease (cT3-4N0) or loco-regional lymph node involvement (T2-4N+) showed only limited pCR to anti-PD1 or anti-PD-L1. Recent clinical studies testing combination strategies targeting PD-1/PD-L1 plus CTLA-4 in the metastatic setting found higher response rates than in trials testing anti-PD1 or anti-PD-L1 alone (8, 9). In the NABUCCO trial (10), preoperative ipilimumab plus nivolumab was tested in high-risk patients having locoregionally-advanced UC (cT3-4N0/cT2-4N1-3) without distant metastases. Histopathological examination showed that 58% of patients in NABUCCO had no remaining invasive disease (pT0 or CIS/pTa) after ipilimumab plus nivolumab (10). A study testing preoperative tremelimumab plus durvalumab in cT2-4N0 UC observed a pCR in 37.5% (pT0 or CIS) of patients having surgery, whereas the pCR rate was 31.7% in all patients analyzed (8).

Associations between ICI response and candidate biomarkers, such as PD-L1 immunohistochemistry and tumor mutational burden (TMB), have been observed in metastatic UC. These biomarkers are currently imperfect and lack sufficient predictive power for clinical utility (11, 12). In addition, comparison of biomarker findings across trials is complicated by variability in biomarker assays (i.e. PD-L1 assessment) and heterogeneity in tumor tissue used to assess biomarkers. In the preoperative setting, the pCR rate to pembrolizumab in the PURE-01 study was high in TMB-high and PD-L1-high (PD-L1 >10%; tumor plus immune cells combined) tumors (6), whereas no significant associations were found for TMB-high and PD-L1-high (PD-L1 >5% of immune cells) subgroups in anti-PD-L1 treated patients in ABACUS (7). Both studies found that baseline pre-existing $CD8^+$ T-cell immunity based on high CD8 presence and interferfon-γ signaling was associated with pCR to ICI monotherapy. Qualification of immune phenotypes by CD8 immunohistochemistry showed that "immune desert" tumors in ABACUS were unresponsive to ICI (7). In sharp contrast, the clinical response to combination ICI in NABUCCO was independent of baseline $CD8^+$ T-cell density by multiplex immunofluorescence and inflammatory signatures such as interferon-gamma, tumor inflammation and T-cell effector signatures (10). Similarly, baseline pre-existing $CD8^+$ T-cell immunity did not differ between responders and non-responders to neo-adjuvant tremelimumab plus durvalumab (13), suggesting that the addition of anti-CTLA4 can induce responses in immunologically "cold" tumors.

Tertiary lymphoid structures (TLS) are ectopic lymph node formations that share functional features such as antigen presentation and B-cell activation with secondary lymphoid organs. TLS emerge upon chronic inflammatory stimuli in non-lymphoid tissues and can also be found in the tumor micro-environment. In an analysis of the presence of TLS, responders to tremelimumab plus durvalumab showed higher baseline TLS and B-cell abundance than non-pCR tumors. Intriguingly, baseline TLS and B-cell abundance did not differ between responders and non-responders in NABUCCO. However, both studies found that responders to combination ICI showed a higher TLS abundance in post-treatment tissue than non-responders (10, 13). Thus, conflicting results on baseline candidate biomarkers for immunotherapy response were found between comparable studies. The complex interplay between immune cells in the UC tumor-immune microenvironment and TLS is still poorly understood, hampering the discovery and development of novel cancer immunotherapy as well as predictive biomarkers for immunotherapy response, underscoring the urgent need to better characterize the tumor immune landscape in UC.

In this study, we employ quantitative multiplex immuno-fluorescence to assess the UC tumor-immune contexture in untreated and immunotherapy-treated tumors. We first provide a general overview of the UC tumor-immune microenvironment, followed by a more detailed assessment of the TLS immune composition in untreated and immunotherapy-treated tumors.

2 RESULTS

2.1 Untreated Urothelial Cancer Demonstrates Heterogeneous Immune Cell Infiltration

To examine the UC immune context, we analyzed immune cell infiltration by multiplex immunofluorescence (IF) on whole-slide cystectomy tissue sections from untreated (n=32, **Table 1**) and ipilimumab (anti- CTLA-4) plus nivolumab (anti-PD1) treated (n=24, **Table 2**) UC patient cohorts (**Figure 1A**). In the current study, cystectomy specimens obtained from NABUCCO are analyzed, while we previously (10) reported $CD8^+$ and $CD20^+$ immune cell presence in pretreatment biopsies. Additionally, we segmented tumor areas into various regions of interest. Our antibody panel allowed the quantitation of immune cells actively involved in anti-tumor immunity and response, such as B-cells ($CD20^+$), macrophages ($CD68^+$) and distinct $CD3^+$ T-cell populations. $CD3^+$ T-cell populations were further specified by expression of CD8 or FoxP3, resulting in CD8 T-cells ($CD3^+CD8^+$), FoxP3 T-cells ($CD3^+FoxP3^+$) and CD4 T-cells ($CD3^+CD8^-FoxP3^-$), a non-$CD8^+$/$FoxP3^+$ T-cell population which is likely to involve primarily CD4 T-cells. $CD3^+FoxP3^-CD8^-$ was thus used as an approximation of $CD4^+$ T-cells to make the manuscript easier to

TABLE 1 | Untreated cohort characteristics.

Baseline characteristics	Total (n = 31)
Male sex, n (%)	24 (77%)
Median age – years [range]	64.79 [45.7, 78.7]
Pathological T stage, (%)	
pT1-4/pTis/pTaN0M0	20 (65%)
pT3-4N1-2M0	11 (35%)
Histology, (%)	
Urothelial Carcinoma	29 (94%)
Urothelial Carcinoma and Small cell carcinoma	1 (3%)
Urothelial Carcinoma and Squamous differentiation	1 (3%)
Adjuvant treatment, (%)	
No adjuvant treatment	25 (81%)
Adjuvant chemotherapy	2 (6%)
Adjuvant radiotherapy	3 (10%)
Adjuvant chemotherapy and adjuvant radiotherapy	1 (3%)

read. CD4 IF was not used in our multiplex panel given the expression of CD4 on other immune cells (including macrophages and dendritic cells) when using CD4 antibodies in our pilot studies. Immune cells were separately quantified for tumor and stroma areas within the central tumor and square grids were computed for spatial sampling to assesses heterogeneity of immune subsets within tumors (**Figure 1B** and **Supplementary Methods 1**). We additionally quantified immune cell abundance in the tumor margin and TLS. The tumor margin was annotated from the outermost edge of the invasive tumor, with an extend of 250μm (**Supplementary Methods 1**). To promote readability, immune cell labels and not markers are reported throughout the results.

We first examined immune cell infiltration by multiplex IF for tumor and stroma areas to provide a comprehensive overview of the UC immune contexture and assess intratumor heterogeneity. We observed that the median density of immune subsets varied greatly across the untreated tumor cohort, particularly for B-cells, FoxP3 T-cells and CD8 T-cells (**Figure 1C**). Variable intratumoral heterogeneity existed for specific immune cells upon a comparison of separate tiles in the computed square grid (**Figure 1C).** Next, we examined the relative abundance of T-cell subsets in the total T-cell population. We found that the fraction of CD4 T-cells was highly heterogeneous across tumors in the untreated cohort (**Supplementary Figure 1A**). Further explorative analysis revealed that tumors having a low CD8 T-cell ratio demonstrated a higher proportion of FoxP3 T-cells in tumor (**Figure 1D** and **Supplementary Figure 1B**). We then compared the immune cell density between central tumor regions and the tumor margin. A significantly higher presence of immune cells was found in tumor margins when compared to the tumor region ($p<0.02$ **Figure 1E**). In non-recurring tumors, the tumor margins displayed a significantly higher CD8 T-cell presence than in recurring tumors ($p=0.0097$, **Figure 1F**), while immune cell presence in tumor and stroma did not inform clinical outcome in untreated tumors. In conclusion, the UC immune landscape is heterogeneous between tumors, and pronounced immune infiltration is found in the UC tumor margin (7, 14).

TABLE 2 | Ipilimumab plus nivolumab treated cohort (NABUCCO Cohort 1) characteristics.

Study population characteristics	Total (n = 24)
Male sex, n (%)	18 (75%)
Median age – years [range]	65 [50, 81]
Baseline clinical T stage, (%)	
cT3-4N0M0	14 (58%)
cT3-4N1	5 (21%)
cT2-3N2M0	5 (21%)
Post-treatment clinical stage, (%)	
ypT0/pTa/pTisN0M0/Mx	14 (58%)
ypT2-3N0M0	2 (8.5%)
ypT0-4N1M0	6 (25%)
ypT3N2-3M0	2 (8.5%)
Immunotherapy cycles, (%)	
2	6 (25%)
6	18 (75%)

2.2 Urothelial Cancer Immune Phenotypes Show Distinct Patterns of Cytotoxic T-Cell Exclusion in the Stroma and Tumor Margin

CD8 T-cell tumor infiltration patterns can be segregated into three immune phenotypes ("immune-inflamed", "immune-excluded" and "immune-desert") of pre-existing tumor-immunity (15). Previous studies found that these distinct immune phenotypes harbor prognostic relevance (16) and predictive value (17, 18) for an immunotherapy response, including in UC (7, 14). Currently, limited knowledge exists on the presence of distinct immune subsets beyond cytotoxic T-cells across CD8-based immune phenotypes in UC, while their presence may impact CD8 effector function and the extend of CD8 tumor-immunity. Using multiplex IF, immune phenotypes (**Figure 2A**) were classified based on CD8 T-cell density (**Supplementary Methods 1.2**) in the tumor and stroma compartment and the tumor margin in the untreated UC cohort. We first explored the distribution of tumor immune phenotypes in the untreated cohort and assessed possible correlations with prognosis for "inflamed", "excluded" and "desert" tumors separately. In line with results in the ABACUS study (7), "immune-inflamed" (42%) tumors were most abundant in our cohort, whereas 32% and 26% of tumors exhibited the "excluded" and "desert" phenotype, respectively. The separate tumor immune phenotypes did not inform recurrence outcome in the untreated cohort (**Figure 2B**), although tumors qualified as "immune-desert" showed a high recurrence rate (87.5%, $p=0.1$). Next, we explored the immune composition in tumor subgroups qualified as "immune-inflamed", "immune-excluded" and "immune-desert" based on CD8-based immune phenotypes. Intratumoral immune cell densities were generally higher in "inflamed" tumors compared to "excluded" and "desert" tumors, as shown for the significantly higher macrophages compared to "desert" tumors ($p=0.006$. **Figure 2C**). In the stroma compartment, immune cell densities were lowest in "desert" tumors, as shown for the significantly lower CD4 T-cells when compared to "excluded" ($p=0.027$) and "inflamed" tumors ($p=0.013$) (**Figure 2D**). Interestingly, FoxP3

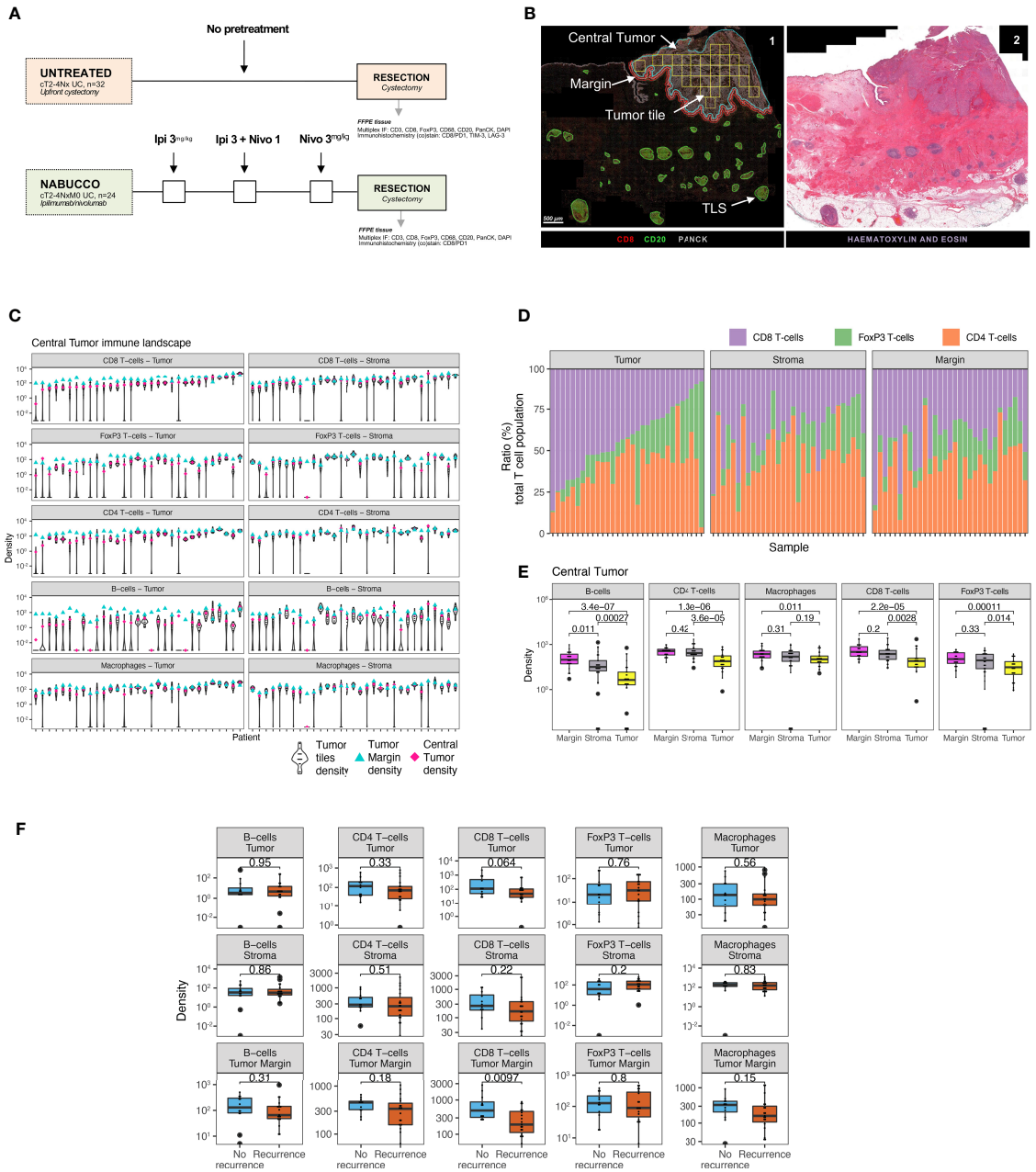

FIGURE 1 | Untreated urothelial cancer demonstrates heterogeneous immune cell infiltration. **(A)** Cohort interventions and timepoints of tissue collection for biomarker analysis. **(B)** *1)* Example of annotated regions of interest in untreated urothelial cancer analyzed by multiplex immunofluorescence and HALO image analysis, involving annotations of central tumor (blue), central tumor tiles (yellow, n = 30 tiles per slide), tumor margin (red, 250 micrometers diameter and tertiary lymphoid structures (green). Central tumor area can be distinguished in tumor and stroma area by employing and training a tissue classifier. *2)* Corresponding H&E slides were consulted to support annotation of regions of interest. **(C)** Intratumoral and stroma immune subset densities per mm^2 within tumor tiles (violin plots, n = 30 tiles per sample), whole tumor (pink) and tumor margin (cyan) for the untreated UC cohort (n = 31). The median immune subset densities and distribution across tumor tiles were analyzed by quantitative multiplex immunofluorescence. Samples were sorted by intratumoral CD8 T-cell central tumor density. **(D)** Relative abundance of T-cell subsets in the total T-cell population in central tumor tissue classes and tumor margin by multiplex IF (n = 31). Samples were sorted by CD8 T-cell ratio. **(E)** Immune subset densities per mm^2 for tumor tissue regions in the untreated UC cohort (n = 31). **(F)** Intratumoral, stroma and tumor margin immune subset densities per mm^2 for the combined untreated UC cohort (n = 31) between recurrence (n = 19) and non-recurrence (n = 12) groups. The boxplots from the panels display the median and 25th and 75th percentiles, and the whiskers expand from the hinge to the largest value not exceeding the hinge 1.5×Interquantile range. Unless otherwise stated, a two-sided Mann-Whitney test was used for the comparison between distributions. The p-value is presented in-between boxplots. No adjustments were implemented for multiple comparisons. IF, Immuno-fluorescence; FFPE, Formalin-fixed paraffin-embedded tissue; Ipi, Ipilimumab; Nivo, Nivolumab; TLS, Tertiary lymphoid structure.

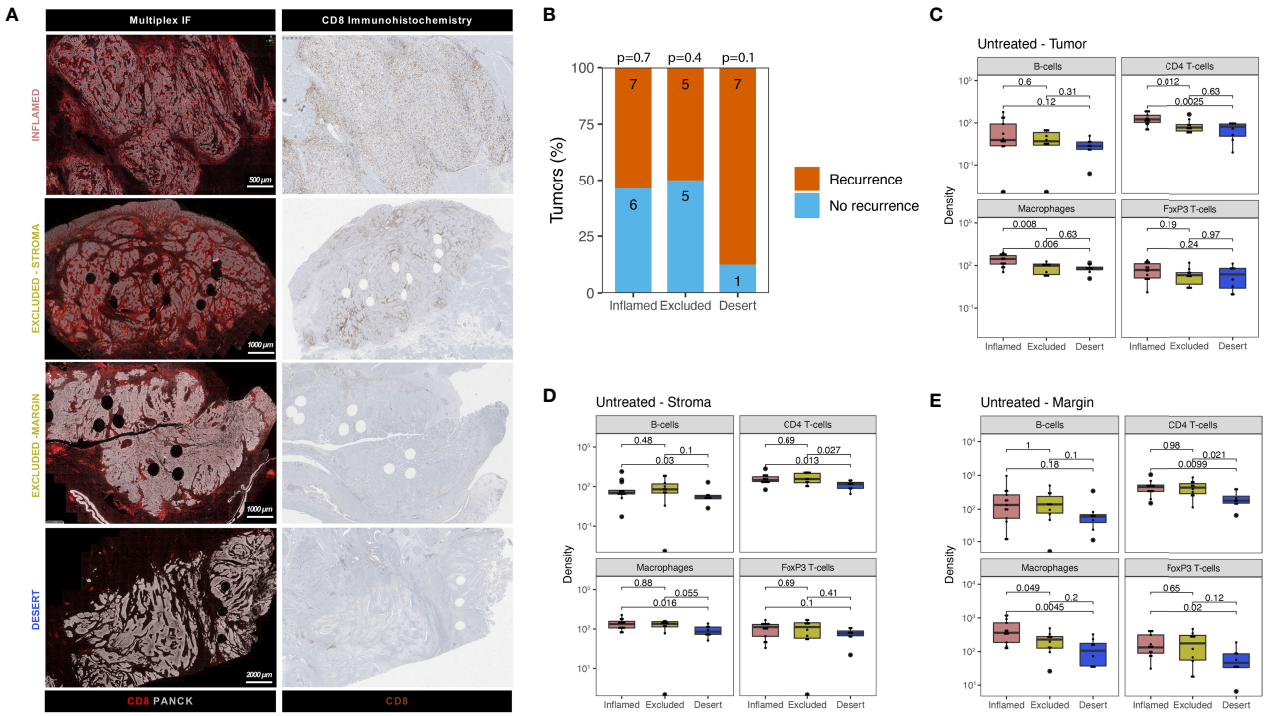

FIGURE 2 | Urothelial cancer immune phenotypes display a varying abundance of immune cells and distinct patterns of cytotoxic T-cell exclusion in stroma and tumor margins. **(A)** Examples of tumor immune phenotypes by multiplex immunofluorescence and CD8 immunohistochemistry in untreated urothelial cancer **(B)**. Proportion of patients having recurrence (n = 19) and no recurrence (n = 12) stratified by immune phenotype for the untreated UC cohort. The group size is indicated on each bar. A Fisher's exact test was implemented on a 2x2 contingency table between recurrence and immune phenotype (i.e. Desert *vs* No Desert) for each phenotype. The p-value for each phenotype is indicated at the top of each bar. All statistical tests were two-sided. C-E. Comparison of immune subset densities per mm^2 in central tumor parenchyma **(C)**, central tumor stroma **(D)** and tumor margin **(E)** between inflamed (n = 13), excluded (n = 10) and desert (n = 8) tumors by quantitative multiplex IF. The boxplots from the panels display the median and 25th and 75th percentiles, and the whiskers expand from the hinge to the largest value not exceeding the hinge 1.5×Interquantile range. Unless otherwise stated, a two-sided Mann-Whitney test was used for the comparison between distributions. The p-value is presented in-between boxplots. No adjustments were implemented for multiple comparisons. IF, immunofluorescence.

T-cells were an exception, as these cells were similar across immune phenotypes in absolute density and higher as a percentage of total T-cells in "desert" tumors, compared to "inflamed" tumors (p=0.037, **Supplemental Figure 2A**). Macrophage abundance in tumor margins of "inflamed" tumors was significantly higher than in "excluded" (p=0.049) and "desert" (p=0.005) tumors, (**Figure 2E**).

2.3 Markers of T-Cell Exhaustion in Untreated and Immunotherapy Treated UC

Exhausted CD8 T-cells are characterized by impaired effector function and sustained expression of immune inhibitory checkpoints such as TIM3, LAG3 and PD1 (19). Immunotherapies targeting these checkpoints demonstrate promising therapeutic potential in several studies (20–26), presumably by reinvigorating exhausted T-cells. Given the implication of T-cell exhaustion as a target of immunotherapy, we employed immunohistochemistry in our untreated cohort to examine the expression of TIM3 and LAG3, as well as co-expression of CD8 and PD1. In untreated tumors, we observed considerable TIM-3 expression (example image in **Figure 3A**) on tumor-infiltrating lymphocytes (15% median positivity, range 5%-30%, **Supplementary Figure 3A**) in most central tumors, as well as in lymph nodal T-cell zones in rare cases having perivesical lymph nodes adjacent to the central tumor (**Supplementary Figure 3B**). In contrast to TIM-3, expression of LAG-3 was virtually non-existent in untreated tumors (**Supplementary Figure 3C**), as illustrated in **Supplementary Figure 3D**. Following CD8/PD1 co-staining, an algorithm was trained (**Supplementary methods 1.3**), based on a similar approach as in colorectal cancer (20), to assess $CD8^+PD1^+$ T-cells in tumor and stroma. $CD8^+PD1^+$ T-cells were clearly present in untreated UC, as shown in **Figure 3B**. Upon quantitation, we found that $CD8^+PD1^+$ T-cell abundance in tumor and stroma did not inform recurrence (**Figure 3C**). We then examined $CD8^+PD1^+$ T-cells in NABUCCO tumors having complete response (CR, qualified as pCR or CIS/pTa) and non-CR following ipilimumab plus nivolumab. $CD8^+PD1^+$ T-cells were enriched irrespective of response compared to untreated cystectomies, whereas $CD8^+PD1^+$ T-cells were highest in tumors achieving CR to immunotherapy

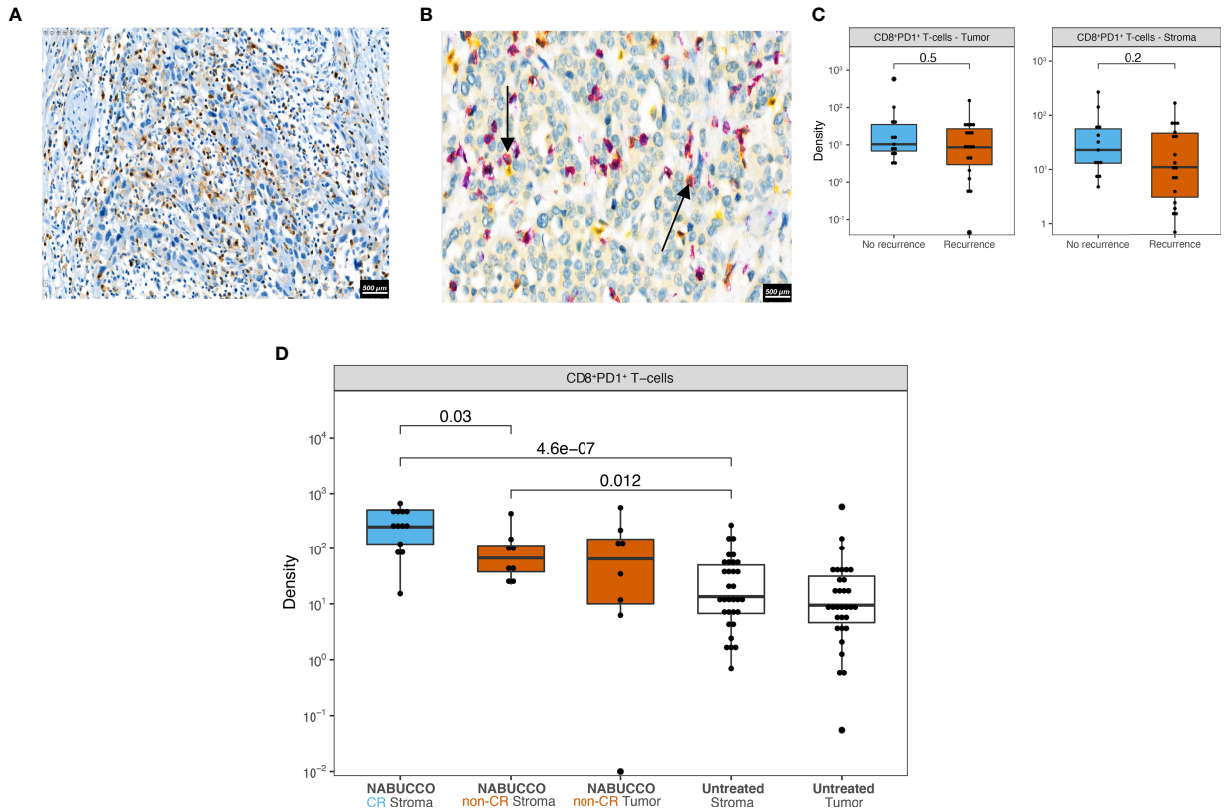

FIGURE 3 | Markers of T-cell exhaustion in untreated and immunotherapy treated UC. **(A)** Representative tumor analyzed by TIM-3 immunohistochemistry. **(B)** Representative tumor analyzed by CD8 (purple) PD1 (yellow) co-stainings in untreated UC, showing $CD8^+PD1^+$ (red) T-cells marked by black arrows. **(C)** $CD8^+PD\text{-}1^+$ cell densities in central tumor regions stratified by recurrence outcome in untreated UC ($n_{Recurrence}$ = 19, $n_{No\ recurrence}$ = 13). **(D)** $CD8^+PD\text{-}1^+$ cell densities in central tumor regions in untreated ($n_{Untreated\ Stroma}$ = 32, $n_{Untreated\ Tumor}$ = 32) and immunotherapy treated cystectomies ($n_{NABUCCO\ CR\ Stroma}$ = 13, $n_{NABUCCO\ non\text{-}CR\ Stroma}$ = 8, $n_{NABUCCO\ non\text{-}CR\ Tumor}$ = 8). Non-significant comparisons, as well as comparisons between tumor and stroma regions, were excluded from the plot. The boxplots from the panels display the median and 25th and 75th percentiles, and the whiskers expand from the hinge to the largest value not exceeding the hinge 1.5×Interquantile range. Unless otherwise stated, a two-sided Mann-Whitney test was used for the comparison between distributions. The p-value is presented in-between boxplots. No adjustments were implemented for multiple comparisons. CR, complete response; non-CR, no complete response.

(**Figure 3D**). Altogether, TIM-3 was highly expressed on lymphocytes and abundant $CD8^+PD1^+$ T-cells were found in cystectomies, particularly following immunotherapy, in both responders and non-responders.

2.4 Urothelial Cancer TLS Display Distinct Cellular Composition Clusters and Checkpoint Inhibitor-Induced Changes

In many cancers, the immune landscape exhibits highly organized B-cell-rich clusters related to TLS formation. The presence of TLS has been associated with favorable clinical outcomes in untreated and treated malignancies (13, 27–29), whereas other studies found no correlation or immunosuppressive TLS function (30–33). We hypothesized that heterogeneity in TLS immune composition might impact anti-tumor-immunity and patient outcome in the untreated and treated setting. We employed multiplex IF to assess the cellular composition of TLS and associations with clinical outcome in our untreated cohort. TLS were automatically annotated by a trained algorithm and manually revised when needed. In total, 754 TLS aggregates were identified in untreated tumors mainly found around the muscularis propria regions, fatty tissue and fibroinflammatory regression beds (**Figure 4A**). TLS often co-localized with nerve bundles as confirmed on the corresponding H&E slide (**Supplementary Figure 4A**). Following TLS assessment by multiplex IF, the majority of untreated tumors showed notable TLS presence, but no differences in TLS abundance were observed between recurrence groups (**Supplementary Figure 4B**). Upon quantitative analysis, TLS revealed a heterogeneous cellular immune composition, accompanied by strong variations in TLS size between TLS in untreated tumors (**Figure 4B**). No differences were found for immune subset density in aggregated TLS between recurrence groups (**Figure 4C**). As limited knowledge exists on TLS immune architecture and how immune composition impacts the clinical outcome, we grouped TLS based on immune cell density and

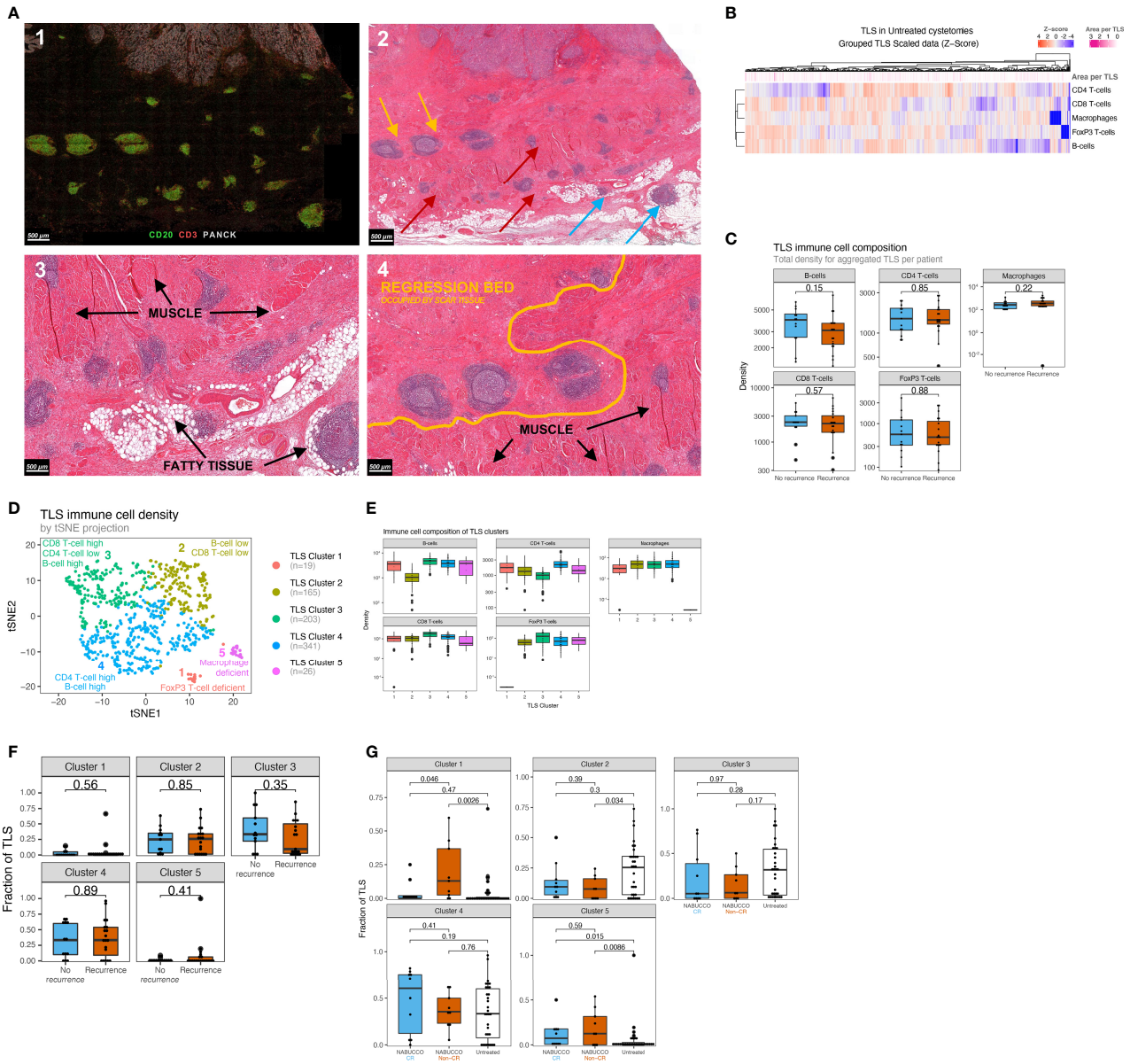

FIGURE 4 | Urothelial cancer displays distinct TLS clusters and differences in treatment effect on TLS composition between responders and non-responders. **(A)** 1) Multiplex immunofluorescence example showing substantial peritumoral TLS formation. 2) Corresponding hematoxylin and eosin stain, showing TLS formation in muscle (red arrow), fatty tissue (blue arrow) and fibroinflammatory regression bed (yellow). 3). Close-up image of A2, showing TLS formation around muscle, fatty tissue and in regression bed. 4) Regression bed TLS and depositions of scar tissue in areas previously harboring muscle suggest that pre-existing invasive tumor has been cleared and replaced by scar tissue, suggesting pre-existing antitumor immunity. **(B)** Heatmap showing the variability of immune cell density in untreated UC TLS. Each column represents an individual TLS (n=754) from n=32 patients. Z-score high expression levels (red) and low expression levels (blue) and varying TLS size (pink) are indicated for each TLS. **(C)** TLS immune subset densities per mm^2, stratified by recurrence outcome groups ($n_{Recurrence}$=19, $n_{No\ Recurrence}$=13). **(D)** Clustering map upon computing a trained k-means model using 754 untreated TLS from 32 unique patients of the untreated cohort (Median 16.5 TLS per patient, Mean 24 TLS per patient, Materials and Methods 3). Each TLS type is assigned a color label and an interpretation. **(E)** Abundance of Immune subsets per mm^2 for each TLS cluster. TLS clusters are depicted in distinct colors. ($n_{Cluster1\ =}$ 19, $n_{Cluster\ 2\ =}$ 165, $n_{Cluster\ 3\ =}$ 203, $n_{Cluster\ 4\ =}$ 341, $n_{Cluster\ 5\ =}$ 26) **(F)**. Comparisons of TLS relative area per cluster based on multiplex immunofluorescence between non-recurring tumors (n = 13) and tumors having recurrence (n = 19). **(G)** Comparisons of post-treatment TLS cluster fractions between untreated tumors (n = 32) and complete-responders (n = 10) and non-responders (n = 9) in NABUCCO. The boxplots from the panels display the median and 25th and 75th percentiles, and the whiskers expand from the hinge to the largest value not exceeding the hinge 1.5×Interquantile range. Unless otherwise stated, a two-sided Mann-Whitney test was used for the comparison between distributions. The p-value is presented in-between boxplots. No adjustments were implemented for multiple comparisons. CR, complete response; non-CR, no complete response; TLS, Tertiary lymphoid structures.

their relative abundance in untreated tumors using a k-means clustering algorithm. We identified five distinct TLS clusters in untreated tumors (**Figure 4D**), characterized by varying abundance of immune cells (**Figure 4E**), whereas TLS cluster presence was balanced between immune phenotype subgroups (**Supplementary Figure 4C**). No differences were observed for TLS cluster abundance between outcome groups (**Figure 4F**) in untreated UC. Next, the relative abundance of TLS clusters was compared between untreated tumors and anti-PD-1/CTLA-4 treated tumors to examine how immunotherapy impacts these TLS clusters. In NABUCCO non-responders, cluster 1 (FoxP3 T-cell low) TLS were significantly enriched when compared to untreated tumors or NABUCCO responders (**Figure 4G**). Furthermore, cluster 5 (macrophage low) TLS were significantly higher in NABUCCO (non-CR or CR) tumors compared to untreated tumors (**Figure 4G**). These findings suggest that UC displays distinct TLS clusters that change in cellular composition upon immunotherapeutic treatment.

2.5 Discrepant TLS Patterns and Variable Expression of CD4 T-Cells Between Superficial and Deeper TLS in Urothelial Cancer

Although pretreatment B-cell and TLS enrichment has been associated with favorable clinical outcomes and immunotherapy response, other studies reported no positive associations (10, 13), suggesting that B-cells and TLS can have opposite roles. In NABUCCO, we previously found that immature TLS, B-cells, and genes associated with B-cell proliferation and plasma cells were enriched in pretreatment biopsies in non-CR tumors, compared to CR tumors (10). Conversely, a study testing preoperative tremelimumab plus durvalumab in UC reported higher pretreatment TLS and B-cells in responders (13). As other stimuli have been shown to induce TLS (31, 34, 35), we hypothesized that a subset of TLS may be unrelated to anti-tumor immunity, particularly in pretreatment tissue obtained by transurethral resection (TUR, debulking of a tumor from the luminal layer of the bladder). TUR biopsies primarily collect superficial tissue that is highly exposed to urinary toxins, microbial pathogens (especially in the presence of a bladder tumor) and inflammatory mediators (**Supplementary Figure 5A, B**). These TLS could cloud the tumor-associated TLS analysis, particularly in superficial parts of the tumor. To examine this, we explored whether TLS composition in superficial regions differed from TLS in deeper tissue regions. In line with quantitated results in our previous report (10), a high TLS presence was observed in NABUCCO pretreatment TUR, especially in non-CR tumors, while TLS abundance was limited in their corresponding post-treatment tissues (**Figure 5A**). TLS abundance in pretreatment TUR was particularly high in the urothelial submucosa (**Figure 5B**). TLS present in the urothelial submucosa (Superficial TLS) were characterized by pronounced CD4 T-cell presence, whereas deeper TLS showed only limited CD4 T-cell contribution to the immune cell composition (**Figure 5B**). The predominant abundance of superficial TLS was also found in a subset of post-treatment specimens from NABUCCO (**Supplementary Figure 5C**) and untreated tumors (**Supplementary Figure 5D**), further supporting the existence of a distinct TLS population in superficial tissue. Next, we stratified superficial and deep TLS in untreated UC to compare TLS composition and the relative abundance of TLS clusters. In untreated tumors, superficial TLS showed a significantly higher CD4 T-cell presence (p=0.012, **Figure 5C**), which is in line with our visual observations. Next, we quantified TLS maturation stages for superficial and deep TLS using a 7-plex multiplex immunofluorescence panel on a separate, larger cohort (n=40, involving 20 patients from the original untreated cohort, **Supplementary Table 1**). Upon assigning TLS maturation, we found that superficial TLS displayed a higher fraction of early TLS and lower germinal center positive TLS when compared to deeper TLS (p=0.001 and p=0.01, respectively **Figure 5D**).

Altogether, our findings suggest that superficial TLS may be compositionally different from deeper TLS. These observations could impact the approach to immune biomarkers in UC and provides the rationale to dissect TLS populations further and study their precise role in anti-tumor immunity in the UC tumor-immune microenvironment.

3 DISCUSSION

The introduction of ICI changed the treatment landscape of UC. Despite recent successes, a substantial proportion of patients do not respond to immunotherapy (36, 37). As the biology driving anti-tumor immunity is still poorly understood, the characterization of the tumor immune contexture is critical to broaden our understanding of the immune landscape to ultimately improve immunotherapeutic treatment of UC patients (11).

The aim of our study was to characterize the immune landscape in tumor, stroma and TLS using computational analysis of multiplex IF. We started with a general overview of the UC immune landscape and observed substantial variation in immune subset presence across untreated tumors. Immune cells were more abundantly present in the tumor margin, compared to tumor and stroma. In previous UC immune biomarker studies, the tumor margin immune infiltrate was not specifically reported (6) or incorporated into the immune phenotype classification system (7, 14). In other cancer types such as colorectal cancer, breast cancer and melanoma, tumor margins have been extensively used for immune phenotype assessment (38). In UC, T-cell exclusion by TGF-beta signaling has been proposed as a mechanism of resistance by excluding T-cells, emphasizing the importance of incorporating the tumor margin compartment in biomarker assessment in UC.

Tumor-specific T-cells can be re-activated through blocking immune inhibitory checkpoints (20–26). We observed high TIM-3 expression and abundant $CD8^+PD1^+$ T-cell presence in UC. $CD8^+PD1^+$ T-cells were enriched upon immunotherapy, and surprisingly, also in immunotherapy non-responders. These data suggest that, despite the immune system being able to mount an anti-cancer response upon checkpoint blockade, resistance mechanisms beyond the CTLA-4 and PD-1 checkpoints may limit cytotoxic T-cell effector function and tumor elimination in these cases. A further dissection of the

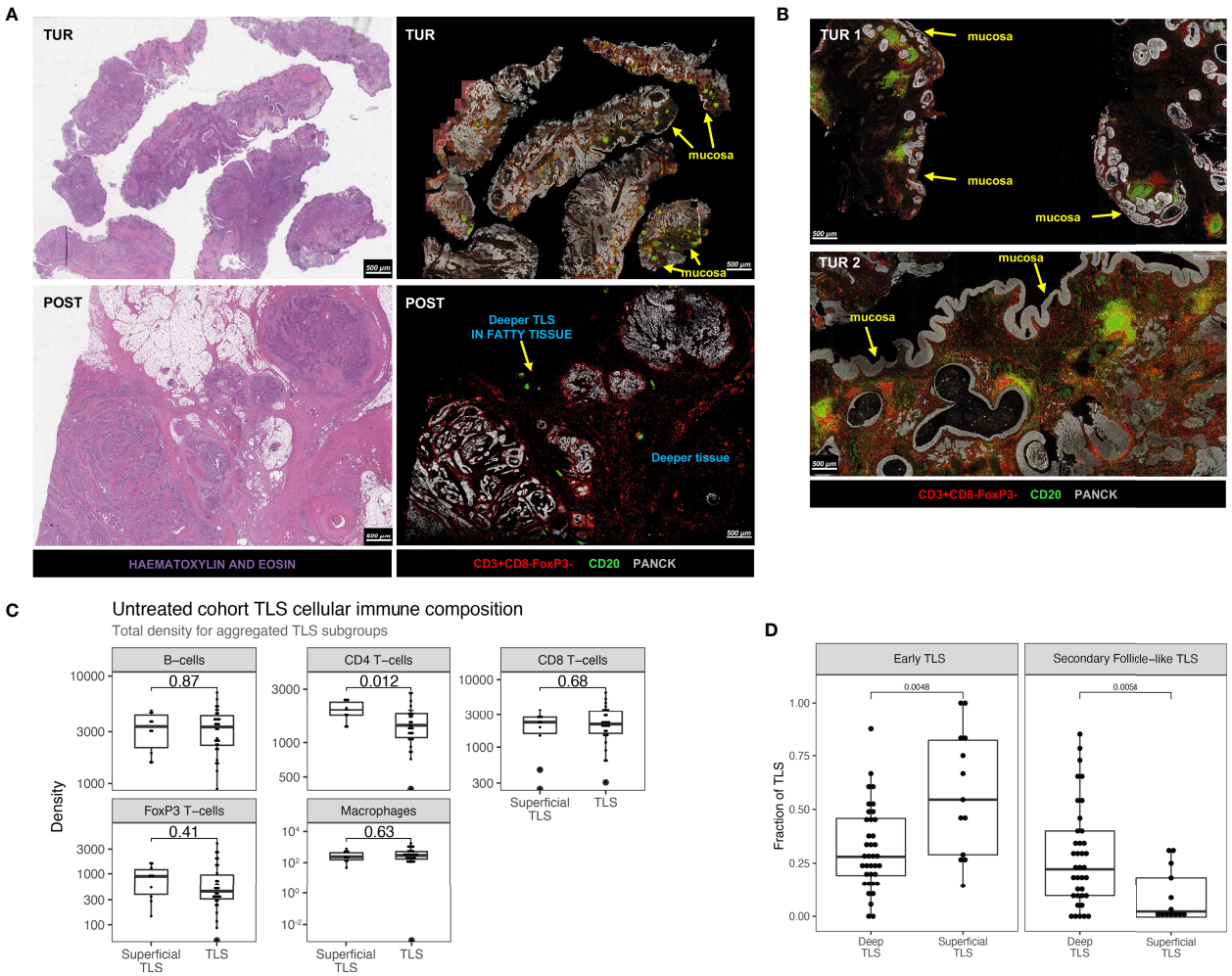

FIGURE 5 | Discrepant TLS patterns and variable expression of T-helper cells between superficial and deeper TLS in urothelial cancer. **(A)** Example of TLS abundance in baseline TUR and post-treatment cystectomy by multiplex immunofluorescence and hematoxylin and eosin stain in a non-responding patient in NABUCCO. Baseline TUR tissue shows a higher TLS presence than in the post-treatment specimen, particularly in submucosal regions. **(B)** Two different TUR examples showing TLS that display pronounced CD4 T-cell presence. **(C)** Comparison of TLS aggregated immune cell density (counts per mm^2) between superficial (n = 10 patients) and deeper TLS (n = 30 patients). **(D)** TLS maturation states quantified by CD21-expressing Follicular Dendritic Cell networks and CD23+ Germinal center zones by multiples IF (Materials and Methods). Quantifications were done on 40 untreated UC cystectomies (18 patients from the original untreated cohort (**Figure 1A**) and 22 additional untreated UC cystectomies, **Supplementary Table 1**). Fraction of TLS maturation states are depicted for Deep TLS (n = 37) and Superficial TLS (n = 13), for Early TLS (germinal center negative) and Secondary Follicle-like TLS (germinal Center positive). 27 patients had only Deep TLS present, 3 patients had only Superficial TLS present, and 10 patients had both Superficial and Deep TLS present. The boxplots from the panels display the median and 25th and 75th percentiles, and the whiskers expand from the hinge to the largest value not exceeding the hinge 1.5×Interquantile range. Unless otherwise stated, a two-sided Mann-Whitney test was used for the comparison between distributions. The p-value is presented in-between boxplots. No adjustments were implemented for multiple comparisons. TLS, Tertiary lymphoid structures; TUR, Transurethral Resection; UC, Urothelial Carcinoma.

tumor-immune landscape in non-responders is crucial to identify the resistance mechanism limiting the efficacy of checkpoint blockade.

In this study, we found that UC exhibits distinct TLS clusters with varying cellular composition. We observed that upon CTLA-4/PD-1 blockade, the fraction of TLS clusters 1 (FoxP3 T-cell low) was enriched in non-responding tumors when compared to untreated tumors and responding tumors. Tregs are generally believed to have immune-suppressive functions, though limited data exist on the function of these cells within TLS. In a lung cancer mouse model, Treg presence in TLS was associated with a suppressed T-cell function (39). Studies in colorectal cancer (40) and melanoma (41) found no correlation between Treg presence in TLS and patient survival. A possible reason for the enrichment of Treg-low TLS may be a direct therapeutic effect of anti-CTLA4, depleting Tregs in TLS. Despite Treg depletion, these tumors did not respond, suggesting that other causes for resistance might be present in these tumors (11, 42).

Generally, TLS in the tumor-microenvironment is considered tumor-associated. Our findings suggest that superficial TLS may define a distinct TLS category in UC that may not be tumor-responsive. Superficial bladder tissue may exhibit immune features (e.g., TLS) unrelated to anti-tumor immunity, given the high exposure to urinary toxins or microbial pathogens, especially in the presence of a bladder tumor disrupting the mucosal barrier. We found that these superficial TLS had a higher density of CD4 T-cells. The proportion of secondary follicle-like TLS, which are required for the prognostic benefit of TLS in other cancer types (27, 43), was significantly lower in superficial TLS compared to deep TLS. Given the similar characteristics, we hypothesize that superficial TLS may be related to Hunner-type interstitial cystitis, an idiopathic inflammatory disease characterized by submucosal lymphocytic pan-cystitis, lymphoid aggregates (Hunner lesions) with varying maturation stages (44) and expression of follicular T-helper cell markers (45). In addition, a recent study showed that Hunner-type interstitial cystitis was associated with enrichment of B-cell receptor signaling genes and B-cell clonal expansion (46). In line with these findings, we previously found that immature TLS, B-cells and genes associated with B-cell proliferation and plasma cells were enriched in baseline TUR tissue in non-CR tumors (10). These discrepant findings in NABUCCO may be explained by the presence of tumor-unrelated TLS such as Hunner-type aggregates in the TUR samples. One can even speculate that high numbers of superficial TLS indicate prominent chronic inflammation with adverse effects on anti-tumor immunity, explaining the association with non-response. This hypothesis needs further testing. In biomarker assessments, the presence of submucosal TLS may possibly enrich B-cell and TLS levels independent of anti-tumor immunity, particularly in TUR (which removes superficial layers) and smaller biopsies. In non-UC patients, the prevalence of interstitial cystitis is 0.5% in the western world (47). No data exists on interstitial cystitis in muscle-invasive bladder cancer, because of the prognostic impact of bladder cancer and overlapping locoregional symptoms.

The strengths of the current study are the comprehensive computational analysis and the automated nature of our assessments, enabling 1) in-depth analysis of the tumor bed, and 2) systematic assessment of tertiary lymphoid structure's immune architecture in untreated and ICI treated tumors. Combined, our study provides a unique overview of the UC immune landscape. Limitations include the limited sample size, which precluded robust assessment of associations with outcome, and the number of immune markers profiled, which limited insight into the functional relevance of immune cells. Further limitations include the retrospective nature of our study and the risk of overinterpretation due to multiple testing.

In conclusion, our study provides a comprehensive overview of the tumor immune landscape and architecture of TLS in UC. We established distinct TLS clusters based on their cellular compositions. Compared to untreated tumors, TLS clusters showed a distinct immune cell composition in anti-CTLA-4/PD-1 ICI treated tumors. In addition, we identified a superficial TLS population, characterized by more pronounced CD4 T-cell expression than deeper TLS. The relevance of the superficial TLS population for antitumor immunity is currently unknown and warrants further investigation.

4 MATERIALS AND METHODS

4.1 Study Cohort Characteristics

Tumors were obtained from untreated patients and a prospective clinical trial testing the efficacy of preoperative ipilimumab (anti-CTLA-4) plus nivolumab (anti-PD-1) (NABUCCO: NCT03387761). In NABUCCO, a total of 24 patients with stage III resectable urothelial cancer (cT3-4aN0M0 and cT1-4aN1-3M0) were treated with preoperative ipilimumab 3 mg/kg (day 1), ipilimumab 3 + nivolumab 1 mg/kg (day 22), and nivolumab 3 mg/kg (day 43) followed by surgical resection. In the untreated cohort (n=31), patients had upfront cystectomy without prior systemic therapy following diagnosis of muscle-invasive carcinoma in pretreatment transurethral resection (TUR) specimen. Cystectomy specimens were preferred over TUR, given that TUR specimens provide a limited overview of the overarching tumor contexture, as shown in **Supplementary Figure 5**. The NABUCCO trial was approved by the institutional review board of the Netherlands Cancer Institute and was executed in accordance with the protocol and Good Clinical Practice Guidelines defined by the International Conference on Harmonization and the principles of the Declaration of Helsinki. Use of the cohort of untreated cystectomies was approved by the NKI-AVL institutional research board, following national regulations. Archival FFPE tumor tissue cystectomy specimens were used for immunohistochemistry and multiplex immunofluorescent analysis. Non-recurring patients and patients having recurrence were compared for explorative biomarker analysis. In NABUCCO, tumors with complete response (CR, defined as pCR, pTis or pTaN0) were compared to non-CR tumors for biomarker exploration. We included non-invasive disease in the CR definition, which is generally believed to be cured by surgery.

4.2 Multiplex Immunofluorescence Analysis and Immunohistochemistry

4.2.1 Multiplex Immunofluorescence of CD8/CD4 T-Cells, B-Cells, Macrophages, and B-Cells

Analysis of immune cell subsets was performed by multiplex Immunofluorescence (IF) technology using an automated multiplex staining on a Discovery Ultra Stainer. Prior to multiplex staining, 3µm slides were cut on DAKO Flex IHC slides. Slides were then dried overnight and stored in +4°C. Before a run was started tissue slides were baked for 30 minutes at 70°C in an oven. Opan 7-color manual IHC kit (50 slides kit, Perkin Elmer, cat NEL81101KT) was used for staining. The protocol was initiated by heating the FFPE cuts for 28 minutes at 75°C, followed by dewaxing with Discovery Wash using the standard setting of 3 cycles of 8 minutes at 69°C. Cell Conditioning 1 (CC1, Ventana Medical Systems) was performed with Discovery CC1 buffer for 32 minutes at 95°C, after which Discovery Inhibitor was applied for 8 minutes to block endogenous peroxidase activity. Specific markers were detected consecutively on

the same slide with the following antibodies, which included anti-CD3 (SP7, Cat RM-9107-S, ThermoScientific, 1/400 dilution 1 hour at RT), anti-CD8 (Clone C8/144B, Cat M7103, DAKO, 1/100 dilution 1 hour at RT), anti-CD68 (Clone KP1, M0814, Dako, 1/500 dilution, 1 hour at RT), anti-FoxP3 (clone 236A/47, Cat ab20034, Abcam, 1/50 dilution, 2 hours at RT), anti-CD20 (Clone L26, cat M0755, Dako, 1/500 dilution, 1 hour at RT) anti-PanCK (Clone AE1AE3, Cat MS-343P, Thermo Scientific, 1/100 dilution, 2 hours at RT).

Each staining cycle consisted of four steps: Primary Antibody incubation, Opal polymer HRP Ms+Rb secondary antibody incubated for 32 minutes at RT, OPAL dye incubation (OPAL520, OPAL540, OPAL570, OPAL620, OPAL650, OPAL690, 1/50 or 1/75 dilution as appropriate for 32 minutes at RT) and an antibody denaturation step using CC2 buffer for 20minutes at 95°C. Cycles were repeated for each new antibody to be stained. At the end of the protocol slides were incubated with DAPI (1/25 dilution in Reaction Buffer) for 12 minutes. After the run was finished slides were washed with demi water and mounted with Fluoromount-G (SouthernBiotech, cat 0100-01) mounting medium. After staining, imaging of the slides was done using the Vectra 3.0 automated imaging system (PerkinElmer). First, whole slide scans were made at 10x magnification. After selection of the region of interest, multispectral images were taken at 20x magnification. Library slides were created by staining a representative sample with each of the specific dyes. Using the InForm software version 2.4 and the library slides the multispectral images were unmixed into 8 channels: DAPI, OPAL520, OPAL540, OPAL570, OPAL620, OPAL650, OPAL690 and Auto Fluorescence and exported to a multilayered TIFF file. The multilayered TIFF's were fused with HALO software (Indica Labs, v2.3). Analysis was done using HALO (Indica Labs, v2.3) image analysis. Pragmatic definitions and delineation of tumor regions in a spatial context are described in **Supplementary Methods 1.1**. Tumor and stroma regions were classified by HALO automated tissue segmentation. Quantitative assessment of central tumors was assessed in 31/32 patients, as one slide involved insufficient tumor material for appropriate assessment but did involve notable TLS (**Supplementary Methods 1.4**).

4.2.2 Multiplex Immunofluorescence of Tertiary Lymphoid Structures Maturation States

TLS maturation was analyzed in tissue sections by 7-plex multiplex IF as previously described (Silina et al., 2018, Springer Protocols) (48). Briefly, tissue sections were deparaffinized, rehydrated and retrieved all in one step using the Trilogy buffer (CellMarque) for 10 min at 110°C in a pressure cooker. The following antibodies and dilutions were used for a 7-plex IF; CD21 (1:5000, clone 2G9 Leica), DC-LAMP (1:1000, clone 1010E1.01, Dendritics), CD23 (1:1000, clone SP3, Abcam), PNAd (1:5000, clone MECA-79, Biolegend), CD20 (1:5000, clone L26, Dako), CD3 (1:1000, clone SP7, ThermoScientific) and 200x magnified images were acquired by Vectra 3.0 multispectral microscope (PerkinElmer/Akoya). Area segregation was done by Inform tissue segmentation algorithm of the Inform software (Akoya).

TLS maturation stages were defined by the presence or absence of $CD21^+$ Follicular Dendritic cells (FDC) networks and $CD23^+$ Germinal Center (GC) cells in dense $CD20^+$ B-cell regions. Proportions of early TLS (no FDCs, no GC), primary follicle-like (PFL) TLS (has FDCs but no GC) and secondary follicle-like (SFL) TLS were determined as fractions out of all analyzed TLS for each patient.

4.2.3 Staining of TIM3, LAG3, and Co-Staining of CD8 and PD1

Stainings and co-stainings were performed by immunohistochemistry. Prior to the staining, 3μm sections were cut and dried overnight and subsequently transferred to Ventana Discovery Ultra autostainer. Briefly, paraffin sections were cut at 3 μm, heated at 75°C for 28 minutes, and deparaffinized in the instrument with EZ prep solution (Ventana Medical Systems). Heat-induced antigen retrieval was carried out using Cell Conditioning 1 (CC1, Ventana Medical Systems) for 64 minutes at 95°C. For the detection of TIM3, the clone D5D5R (Cell Signaling) was used (1/200 dilution, 1 hour, 370°C), and for the detection of LAG3, the clone 11E3 (1/50 dilution, 1 hour at 370°C, AbCam). The bound antibodies were detected using either Anti-Rabbit HQ (Ventana Medical Systems), 12 minutes at 37°C (TIM-3) or anti-mouse HQ (Ventana Medical Systems) for 12 minutes at 37°C (LAG-3) followed by Anti-HQ HRP (Ventana Medical Systems) for 12 minutes at 37°C and ChromoMap DAB Detection (Ventana Medical Systems). Slides were counterstained with Hematoxylin and Bluing Reagent (Ventana Medical Systems). For untreated tumors, the percentage of TIM-3 and LAG-3 expression on lymphocytes tumors was scored upon visual inspection of digital slides in Slidescore by a pathologist.

For the co-staining of PD-1 (yellow) and CD8 (purple), the protocol was adjusted. Detection of PD-1 was done using the antibody clone NAT105 (Ready-to-Use, 32 minutes at 37°C, Roche Diagnostics) in the first sequence. Visualization of the PD-1-bound antibody was done using anti-mouse NP (Ventana Medical Systems) for 12 minutes at 37°C, and subsequent anti-NP AP (Ventana Medical Systems) for 12 minutes at 37°C followed by the Discovery Yellow Detection Kit (Ventana Medical Systems). In the double-stain second sequence, CD8 was detected using the antibody clone C8/144B (Agilent, 1:200, 32 minutes at 37°C). CD8 was detected using anti-mouse HQ (Ventana Medical Systems) for 12 minutes at 37°C and subsequent anti-HQ horseradish peroxidase (Ventana Medical Systems) for 12 minutes at 37°C, followed by the Discovery Purple Detection Kit (Ventana Medical Systems). Slides were counterstained with Hematoxylin and Bluing Reagent (Ventana Medical Systems). All immunohistochemistry slides were uploaded to SlideScore for visual exploration.

4.3 TLS Clustering Approach

We employed an unsupervised learning strategy to identify TLS clusters with distinct immune cell composition. A k-Means algorithm was trained with the cellular densities (cells/mm2) of B-cells, CD4 T-cells, CD8 T-cells, FoxP3 T-cells, and macrophages in TLS using input from all TLS identified in the untreated cohort (n=754, **Figure 1A**, **Table 1**). Cellular densities per TLS (with a pseudo-count of 0.01 cells/mm2 to account for null densities) were transformed to a logarithmic scale and scaled by the standard deviation after subtracting the mean. The k-means clustering algorithm was trained by testing 1 to 10

centroids with a maximum of 300 iterations. An optimal number of k=5 clusters was selected based on a reduction or decrease of the total within-cluster sum of squares observed from k=5 to k=6 (**Supplementary Figure 6**), by visual exploration of the separation on a tSNE plot (**Figure 4D**), and by taking into account that only 5 features (distinct immune cell densities) were used to train the k-means algorithm.

To assign clusters to TLS identified in the treated NABUCCO cohort, cellular densities (with a pseudo-count of 0.01 cells/mm2 to account for null densities) were transformed to a logarithmic scale, followed by subtraction of means computed on the untreated, and scaling by the standard deviations computed on the untreated cohort. Then, we computed the distances between each TLS and each of the 5 centroids trained with the k-means clustering on the untreated cohort and predicted each TLS subtype by selecting the nearest centroid.

DATA AVAILABILITY STATEMENT

Multiplex Immunofluorescence raw data will be made available upon reasonable request for academic use by the corresponding author within the restrictions of the informed consent. A data access agreement will need to be signed with the Netherlands Cancer Institute, and reviewed by the institutional review board of the Netherlands Cancer Institute after approval.

ETHICS STATEMENT

The studies involving human participants were reviewed and approved by Institutional review board of The Netherlands Cancer Institute - Antoni van Leeuwenhoek. The patients/participants provided their written informed consent to participate in this study.

AUTHOR CONTRIBUTIONS

ND, MH, SE, LJ, BR, and CV: Interpreted and addressed clinical data. ND, SE, BR, and CV: Collected clinical data. AG-J, DV, LW, and KS: Performed and interpreted bioinformatics and statistical analysis. ND, AG-J, KS, MB, and MH: Analysed translational data. DP: Carried out immunohistochemical and multiplex immunofluorescence staining. ND, YL: Performed HALO AI Image analysis. KS and MB: Contributed to work related to Tertiary Lymphoid Structures. EH, AB, and MM: Supervised immunohistochemical/multiplex immunofluorescence quantifications, and assessed tissue availability. MM and JS: Carried out histopathological assessment and assessed tissue availability. KS and MB: Performed immunohistochemical/multiplex immunofluorescence work on the TLS panel. KS, MB, LW, LJ, and BR: Scientific input and critical review. MH, ND, and AG-J: Wrote the manuscript together with all co-authors, who approved the data accuracy, edited and approved the manuscript. All authors contributed to the article and approved the submitted version.

FUNDING

MB was financially supported by the Swiss National Science Foundation (CRSII5_177208 and 310030_175565), the University of Zurich Research Priority Program 'Translational Cancer Research', the Cancer Research Center Zurich and Worldwide Cancer Research (18–0629). The NABUCCO study was financially supported by Brystol-Myers Squibb (BMS). The funder was not involved in the study design, collection, analysis, interpretation of data, the writing of this article or the decision to submit it for publication.

ACKNOWLEDGMENTS

We would like to acknowledge the Core Facility Molecular Pathology and Biobanking (I. Hofland, S. Vonk, I. Seignette, W. Kieviet and J. Sanders) for support, and the Research High-Performance Computing facility, all at the Netherlands Cancer Institute.

SUPPLEMENTARY MATERIAL

The Supplementary Material for this article can be found online at: https://www.frontiersin.org/articles/10.3389/fimmu.2021.793964/full#supplementary-material

REFERENCES

1. Rosenberg JE, Hoffman-Censits J, Powles T, van der Heijden MS, Balar AV, Necchi A, et al. Atezolizumab in Patients With Locally Advanced and Metastatic Urothelial Carcinoma Who Have Progressed Following Treatment With Platinum-Based Chemotherapy: A Single-Arm, Multicentre, Phase 2 Trial. *Lancet* (2016) 387(10031):1909–20. doi: 10.1016/S0140-6736(16)00561-4
2. Bellmunt J, de Wit R, Vaughn DJ, Fradet Y, Lee JL, Fong L, et al. Pembrolizumab as Second-Line Therapy for Advanced Urothelial Carcinoma. *N Engl J Med* (2017) 376(11):1015–26. doi: 10.1056/NEJMoa1613683
3. Powles T, Durán I, van der Heijden MS, Loriot Y, Vogelzang NJ, De Giorgi U, et al. Atezolizumab Versus Chemotherapy in Patients With Platinum-Treated Locally Advanced or Metastatic Urothelial Carcinoma (IMvigor211): A Multicentre, Open-Label, Phase 3 Randomised Controlled Trial. *Lancet* (2018) 391(10122):748–57. doi: 10.1016/S0140-6736(17)33297-X
4. Sharma P, Retz M, Siefker-Radtke A, Baron A, Necchi A, Bedke J, et al. Nivolumab in Metastatic Urothelial Carcinoma After Platinum Therapy (CheckMate 275): A Multicentre, Single-Arm, Phase 2 Trial. *Lancet Oncol* (2017) 18(3):312–22. doi: 10.1016/S1470-2045(17)30065-7
5. Massard C, Gordon MS, Sharma S, Rafii S, Wainberg ZA, Luke J, et al. Safety and Efficacy of Durvalumab (MEDI4736), an Anti–Programmed Cell Death Ligand-1 Immune Checkpoint Inhibitor, in Patients With Advanced Urothelial Bladder Cancer. *J Clin Oncol* (2016) 34(26):3119–25. doi: 10.1200/JCO.2016.67.9761
6. Necchi A, Anichini A, Raggi D, Briganti A, Massa S, Lucianò R, et al. Pembrolizumab as Neoadjuvant Therapy Before Radical Cystectomy in Patients With Muscle-Invasive Urothelial Bladder Carcinoma (PURE-01): An Open-Label, Single-Arm, Phase II Study. *J Clin Oncol* (2018) 36:(34):3353–60. doi: 10.1200/JCO.18.01148

7. Powles T, Kockx M, Rodriguez-Vida A, Duran I, Crabb SJ, van der Heijden MS, et al. Clinical Efficacy and Biomarker Analysis of Neoadjuvant Atezolizumab in Operable Urothelial Carcinoma in the ABACUS Trial. *Nat Med* (2019) 25(11):1706–14. doi: 10.1038/s41591-019-0628-7
8. Sharma P, Siefker-Radtke A, de Braud F, Basso U, Calvo E, Bono P, et al. Nivolumab Alone and With Ipilimumab in Previously Treated Metastatic Urothelial Carcinoma: CheckMate 032 Nivolumab 1 Mg/Kg Plus Ipilimumab 3 Mg/Kg Expansion Cohort Results. *J Clin Oncol* (2019) 37(19):1608–16. doi: 10.1200/JCO.19.00538
9. Powles T, van der Heijden MS, Castellano D, Galsky MD, Loriot Y, Petrylak DP, et al. Durvalumab Alone and Durvalumab Plus Tremelimumab Versus Chemotherapy in Previously Untreated Patients With Unresectable, Locally Advanced or Metastatic Urothelial Carcinoma (DANUBE): A Randomised, Open-Label, Multicentre, Phase 3 Trial. *Lancet Oncol* (2020) 21(12):1574–88. doi: 10.1016/S1470-2045(20)30541-6
10. van Dijk N, Gil-Jimenez A, Silina K, Hendricksen K, Smit LA, de Feijter JM, et al. Preoperative Ipilimumab Plus Nivolumab in Locoregionally Advanced Urothelial Cancer: The NABUCCO Trial. *Nat Med* (2020) 26:1839–44. doi: 10.1038/s41591-020-1085-z
11. van Dijk N, Funt SA, Blank CU, Powles T, Rosenberg JE, van der Heijden MS. The Cancer Immunogram as a Framework for Personalized Immunotherapy in Urothelial Cancer. *Eur Urol* (2019) 75(3):435–44. doi: 10.1016/j.eururo.2018.09.022
12. McGrail DJ, Pilié PG, Rashid NU, Voorwerk L, Slagter M, Kok M, et al. High Tumor Mutation Burden Fails to Predict Immune Checkpoint Blockade Response Across All Cancer Types. *Ann Oncol* (2021) 32(5):661–72. doi: 10.1016/j.annonc.2021.02.006
13. Gao J, Navai N, Alhalabi O, Siefker-Radtke A, Campbell MT, Tidwell RS, et al. Neoadjuvant PD-L1 Plus CTLA-4 Blockade in Patients With Cisplatin-Ineligible Operable High-Risk Urothelial Carcinoma. *Nat Med* (2020) 26:1845–51. doi: 10.1038/s41591-020-1086-y
14. Mariathasan S, Turley SJ, Nickles D, Castiglioni A, Yuen K, Wang Y, et al. TGFbeta Attenuates Tumour Response to PD-L1 Blockade by Contributing to Exclusion of T Cells. *Nature* (2018) 554(7693):544–8. doi: 10.1038/nature25501
15. Chen DS, Mellman I. Oncology Meets Immunology: The Cancer-Immunity Cycle. *Immunity* (2013) 39(1):1–10. doi: 10.1016/j.immuni.2013.07.012
16. Echarti A, Hecht M, Büttner-Herold M, Haderlein M, Hartmann A, Fietkau R, et al. CD8+ and Regulatory T Cells Differentiate Tumor Immune Phenotypes and Predict Survival in Locally Advanced Head and Neck Cancer. *Cancers* (2019) 11(9):1398. doi: 10.3390/cancers11091398
17. Rizvi H, Sanchez-Vega F, La K, Chatila W, Jonsson P, Halpenny D, et al. Molecular Determinants of Response to Anti–Programmed Cell Death (PD)-1 and Anti–Programmed Death-Ligand 1 (PD-L1) Blockade in Patients With Non–Small-Cell Lung Cancer Profiled With Targeted Next-Generation Sequencing. *J Clin Oncol* (2018) 36(7):633–41. doi: 10.1200/JCO.2017.75.3384
18. Chen DS, Mellman I. Elements of Cancer Immunity and the Cancer-Immune Set Point. *Nature* (2017) 541(7637):321–30. doi: 10.1038/nature21349
19. Wherry EJ. T Cell Exhaustion. *Nat Immunol* (2011) 12(6):492–9. doi: 10.1038/ni.2035
20. Chalabi M, Fanchi LF, Dijkstra KK, Van den Berg JG, Aalbers AG, Sikorska K, et al. Neoadjuvant Immunotherapy Leads to Pathological Responses in MMR-Proficient and MMR-Deficient Early-Stage Colon Cancers. *Nat Med* (2020) 26:566–76. doi: 10.1038/s41591-020-0805-8
21. Ngiow SF, von Scheidt B, Akiba H, Yagita H, Teng MW, Smyth MJ. Anti-TIM3 Antibody Promotes T Cell IFN-Gamma-Mediated Antitumor Immunity and Suppresses Established Tumors. *Cancer Res* (2011) 71(10):3540–51. doi: 10.1158/0008-5472.CAN-11-0096
22. Kumagai S, Togashi Y, Kamada T, Sugiyama E, Nishinakamura H, Takeuchi Y, et al. The PD-1 Expression Balance Between Effector and Regulatory T Cells Predicts the Clinical Efficacy of PD-1 Blockade Therapies. *Nat Immunol* (2020) 21:1346–58. doi: 10.1038/s41590-020-0769-3
23. Das M, Zhu C, Kuchroo VK. Tim-3 and its Role in Regulating Anti-Tumor Immunity. *Immunol Rev* (2017) 276(1):97–111. doi: 10.1111/imr.12520
24. Thommen DS, Koelzer VH, Herzig P, Roller A, Trefny M, Dimeloe S, et al. A Transcriptionally and Functionally Distinct PD-1+ CD8+ T Cell Pool With Predictive Potential in non-Small-Cell Lung Cancer Treated With PD-1 Blockade. *Nat Med* (2018) 24(7):994–1004. doi: 10.1038/s41591-018-0057-z
25. Rotte A, Jin JY, Lemaire V. Mechanistic Overview of Immune Checkpoints to Support the Rational Design of Their Combinations in Cancer Immunotherapy. *Ann Oncol* (2018) 29(1):71–83. doi: 10.1093/annonc/mdx686
26. Lipson EJ, Tawbi HA-H, Schadendorf D, Ascierto PA, Matamala L, Gutiérrez EC, et al. Relatlimab (RELA) Plus Nivolumab (NIVO) Versus NIVO in First-Line Advanced Melanoma: Primary Phase III Results From RELATIVITY-047 (CA224-047). *JCO* (2021) 39(15_suppl):9503–3. doi: 10.1200/JCO.2021.39.15_suppl.9503
27. Siliņa K, Soltermann A, Attar FM, Casanova R, Uckeley ZM, Thut H, et al. Germinal Centers Determine the Prognostic Relevance of Tertiary Lymphoid Structures and Are Impaired by Corticosteroids in Lung Squamous Cell Carcinoma. *Cancer Res* (2018) 78(5):1308–20. doi: 10.1158/0008-5472.CAN-17-1987
28. Helmink BA, Reddy SM, Gao J, Zhang S, Basar R, Thakur R, et al. B Cells and Tertiary Lymphoid Structures Promote Immunotherapy Response. *Nature* (2020) 577(7791):549–55. doi: 10.1038/s41586-019-1922-8
29. Cabrita R, Lauss M, Sanna A, Donia M, Skaarup Larsen M, Mitra S, et al. Tertiary Lymphoid Structures Improve Immunotherapy and Survival in Melanoma. *Nature* (2020) 577(7791):561–5. doi: 10.1038/s41586-019-1914-8
30. Goeppert B, Frauenschuh L, Zucknick M, Stenzinger A, Andrulis M, Klauschen F, et al. Prognostic Impact of Tumour-Infiltrating Immune Cells on Biliary Tract Cancer. *Br J Cancer* (2013) 109(10):2665–74. doi: 10.1038/bjc.2013.610
31. Hill DG, Yu L, Gao H, Balic JJ, West A, Oshima H, et al. Hyperactive Gp130/STAT3-Driven Gastric Tumourigenesis Promotes Submucosal Tertiary Lymphoid Structure Development: Gp130/STAT3 Regulates TLSs in Gastric Cancer. *Int J Cancer* (2018) 143(1):167–78. doi: 10.1002/ijc.31298
32. Figenschau SL, Fismen S, Fenton KA, Fenton C, Mortensen ES. Tertiary Lymphoid Structures Are Associated With Higher Tumor Grade in Primary Operable Breast Cancer Patients. *BMC Cancer* (2015) 15(1):101. doi: 10.1186/s12885-015-1116-1
33. Lee HJ, Kim JY, Park IA, Song IH, Yu JH, Ahn J-H, et al. Prognostic Significance of Tumor-Infiltrating Lymphocytes and the Tertiary Lymphoid Structures in HER2-Positive Breast Cancer Treated With Adjuvant Trastuzumab. *Am J Clin Pathol* (2015) 144(2):278–88. doi: 10.1309/AJCPIXUYDVZ0RZ3G
34. Pipi E, Nayar S, Gardner DH, Colafrancesco S, Smith C, Barone F. Tertiary Lymphoid Structures: Autoimmunity Goes Local. *Front Immunol* (2018) 9:1952. doi: 10.3389/fimmu.2018.01952
35. Rubio CA, Ásmundsson J, Silva P, Illies C, Hartman J, Kis L. Lymphoid Aggregates in Crohn's Colitis and Mucosal Immunity. *Virchows Arch* (2013) 463(5):637–42. doi: 10.1007/s00428-013-1474-5
36. Szabados B, van Dijk N, Tang YZ, van der Heijden MS, Wimalasingham A, Gomez de Liano A, et al. Response Rate to Chemotherapy After Immune Checkpoint Inhibition in Metastatic Urothelial Cancer. *Eur Urol* (2018) 73(2):149–52. doi: 10.1016/j.eururo.2017.08.022
37. Gómez de Liaño Lista A, van Dijk N, de Velasco Oria de Rueda G, Necchi A, Lavaud P, Morales-Barrera R, et al. Clinical Outcome After Progressing to Frontline and Second-Line Anti–PD-1/PD-L1 in Advanced Urothelial Cancer. *Eur Urol* (2020) 77(2):269–76. doi: 10.1016/j.eururo.2019.10.004
38. Kather JN, Suarez-Carmona M, Charoentong P, Weis C-A, Hirsch D, Bankhead P, et al. Topography of Cancer-Associated Immune Cells in Human Solid Tumors. *eLife* (2018) 7:e36967. doi: 10.7554/eLife.36967
39. Joshi NS, Akama-Garren EH, Lu Y, Lee D-Y, Chang GP, Li A, et al. Regulatory T Cells in Tumor-Associated Tertiary Lymphoid Structures Suppress Anti-Tumor T Cell Responses. *Immunity* (2015) 43(3):579–90. doi: 10.1016/j.immuni.2015.08.006
40. Yamaguchi K, Ito M, Ohmura H, Hanamura F, Nakano M, Tsuchihashi K, et al. Helper T Cell-Dominant Tertiary Lymphoid Structures Are Associated With Disease Relapse of Advanced Colorectal Cancer. *OncoImmunology* (2020) 9(1):1724763. doi: 10.1080/2162402X.2020.1724763
41. Lynch KT, Young SJ, Meneveau MO, Wages NA, Engelhard VH, Slingluff CL Jr, et al. Heterogeneity in Tertiary Lymphoid Structure B-Cells Correlates With Patient Survival in Metastatic Melanoma. *J Immunother Cancer* (2021) 9(6):e002273. doi: 10.1136/jitc-2020-002273
42. Blank CU, Haanen JB, Ribas A, Schumacher TN. The "Cancer Immunogram." *Science* (2016) 352(6286):658–60. doi: 10.1126/science.aaf2834
43. Posch F, Silina K, Leibl S, Mündlein A, Moch H, Siebenhüner A, et al. Maturation of Tertiary Lymphoid Structures and Recurrence of Stage II and

III Colorectal Cancer. *Oncoimmunology* (2017) 7(2):e1378844–e1378844. doi: 10.1080/2162402X.2017.1378844
44. Akiyama Y, Luo Y, Hanno PM, Maeda D, Homma Y. Interstitial Cystitis/Bladder Pain Syndrome: The Evolving Landscape, Animal Models and Future Perspectives. *Int J Urol* (2020) 27(6):491–503. doi: 10.1111/iju.14229
45. Lu K, Wei S, Wang Z, Wu K, Jiang J, Yan Z, et al. Identification of Novel Biomarkers in Hunner's Interstitial Cystitis Using the CIBERSORT, an Algorithm Based on Machine Learning. *BMC Urol* (2021) 21(1):109. doi: 10.1186/s12894-021-00875-8
46. Akiyama Y, Maeda D, Katoh H, Morikawa T, Niimi A, Nomiya A, et al. Molecular Taxonomy of Interstitial Cystitis/Bladder Pain Syndrome Based on Whole Transcriptome Profiling by Next-Generation RNA Sequencing of Bladder Mucosal Biopsies. *J Urol* (2019) 202(2):290–300. doi: 10.1097/JU.0000000000000234
47. Hanno PM, Erickson D, Moldwin R, Faraday MM. Diagnosis and Treatment of Interstitial Cystitis/Bladder Pain Syndrome: AUA Guideline Amendment. *J Urol* (2015) 193(5):1545–53. doi: 10.1016/j.juro.2015.01.086
48. Siliņa K, Burkhardt C, Casanova R, Solterman A, van den Broek M. A Quantitative Pathology Approach to Analyze the Development of Human Cancer-Associated Tertiary Lymphoid Structures. In: M-C Dieu-Nosjean, editor. *Tertiary Lymphoid Structures*. New York, NY: Springer New York (2018). p. 71–86. Available at: http://link.springer.com/10.1007/978-1-4939-8709-2_5. (Methods in Molecular Biology; vol. 1845).

Conflict of Interest: MH received research funding from Bristol Myers Squibb, AstraZeneca, 4SC and Roche, and consultancy fees from Bristol Myers Squibb, Roche, Merck Sharp & Dohme, Merck, AstraZeneca, Pfizer, Janssen and Seattle Genetics which were all paid to the Netherlands Cancer Institute. LW received research funding from Genmab.

The remaining authors declare that the research was conducted in the absence of any commercial or financial relationships that could be construed as a potential conflict of interest.

Publisher's Note: All claims expressed in this article are solely those of the authors and do not necessarily represent those of their affiliated organizations, or those of the publisher, the editors and the reviewers. Any product that may be evaluated in this article, or claim that may be made by its manufacturer, is not guaranteed or endorsed by the publisher.

Copyright © 2021 Dijk, Gil-Jimenez, Silina, Montfoort, Einerhand, Jonkman, Voskuilen, Peters, Sanders, Lubeck, Broeks, Hooijberg, Vis, Broek, Wessels, Rhijn and Heijden. This is an open-access article distributed under the terms of the Creative Commons Attribution License (CC BY). The use, distribution or reproduction in other forums is permitted, provided the original author(s) and the copyright owner(s) are credited and that the original publication in this journal is cited, in accordance with accepted academic practice. No use, distribution or reproduction is permitted which does not comply with these terms.

frontiers in Immunology

ORIGINAL RESEARCH
published: 25 January 2022
doi: 10.3389/fimmu.2021.793992

Molecular, Immunological, and Clinical Features Associated With Lymphoid Neogenesis in Muscle Invasive Bladder Cancer

Fabio Pagliarulo[1], Phil F. Cheng[2], Laurin Brugger[1], Nick van Dijk[3], Michiel van den Heijden[3], Mitchell P. Levesque[2], Karina Silina[1†] and Maries van den Broek[1†]*

[1] Institute of Experimental Immunology, University of Zurich, Zurich, Switzerland, [2] Department of Dermatology, University Hospital Zurich, University of Zurich, Zurich, Switzerland, [3] Department of Medical Oncology, The Netherlands Cancer Institute, Amsterdam, Netherlands

OPEN ACCESS

Edited by:
Catherine Sautes-Fridman, INSERM U1138 Centre de Recherche des Cordeliers (CRC), France

Reviewed by:
Walter J. Storkus, University of Pittsburgh, United States
Lloyd Bod, Brigham and Women's Hospital and Harvard Medical School, United States

***Correspondence:**
Karina Silina
karina@biomed.lu.lv

†These authors have contributed equally to this work

Specialty section:
This article was submitted to Cancer Immunity and Immunotherapy, a section of the journal Frontiers in Immunology

Received: 12 October 2021
Accepted: 29 December 2021
Published: 25 January 2022

Citation:
Pagliarulo F, Cheng PF, Brugger L, van Dijk N, van den Heijden M, Levesque MP, Silina K and van den Broek M (2022) Molecular, Immunological, and Clinical Features Associated With Lymphoid Neogenesis in Muscle Invasive Bladder Cancer. Front. Immunol. 12:793992. doi: 10.3389/fimmu.2021.793992

Lymphoid neogenesis gives rise to tertiary lymphoid structures (TLS) in the periphery of multiple cancer types including muscle invasive bladder cancer (MIBC) where it has positive prognostic and predictive associations. Here, we explored molecular, clinical, and histological data of The Cancer Genome Atlas, as well as the IMvigor210 dataset to study factors associated with TLS development and function in the tumor microenvironment (TME) of MIBC. We also analyzed tumor immune composition including TLS in an independent, retrospective MIBC cohort. We found that the combination of TLS density and tumor mutational burden provides a novel independent prognostic biomarker in MIBC. Gene expression profiles obtained from intratumoral regions that rarely contain TLS in MIBC showed poor correlation with the prognostic TLS density measured in tumor periphery. Tumors with high TLS density showed increased gene signatures as well as infiltration of activated lymphocytes. Intratumoral B-cell and $CD8^+$ T-cell co-infiltration was frequent in TLS-high samples, and such regions harbored the highest proportion of PD-1^+TCF1$^+$ progenitor-like T cells, naïve T cells, and activated B cells when compared to regions predominantly infiltrated by either B cells or $CD8^+$ T cells alone. We found four TLS maturation subtypes; however, differences in TLS composition appeared to be dictated by the TME and not by the TLS maturation status. Finally, we identified one downregulated and three upregulated non-immune cell-related genes in TME with high TLS density, which may represent candidates for tumor-intrinsic regulation of lymphoid neogenesis. Our study provides novel insights into TLS-associated gene expression and immune contexture of MIBC and indicates towards the relevance of B-cell and $CD8^+$ T-cell interactions in anti-tumor immunity within and outside TLS.

Keywords: tertiary lymphoid structures, lymphoid neogenesis, tumor mutational burden, cancer immunology, immune checkpoint inhibition, survival, prognosis, tumor microenvironment

INTRODUCTION

In chronically inflamed tissues including cancer, infiltrating lymphocytes can form ectopic lymphoid organs termed tertiary lymphoid structures (TLS) *via* lymphoid neogenesis (1, 2). TLS structurally resemble follicles of secondary lymphoid organs (SLO) like lymph nodes and can exert similar functions such as priming of antigen-specific T cells and mounting ectopic germinal center (GC) reactions (3, 4). TLS density in the tumor microenvironment (TME) correlates with increased infiltration of adaptive immune cells and improved patient survival in a growing list of solid tumors (5, 6) including muscle invasive bladder cancer (MIBC) (7). Along the same lines, TLS density as well as mRNA expression of CXCL13, a crucial regulator of lymphoid neogenesis, has a favorable prognostic association in the context of immune checkpoint inhibition (ICI) therapy of MIBC (8–10). Similar observations were reported in sarcoma, melanoma, and renal cell carcinoma patients (11–13). This has fueled the hypothesis that TLS are drivers of anti-tumor immunity and that, consequently, TLS induction could be considered as a therapeutic strategy (5, 6).

Lymphoid neogenesis and lymphoid organogenesis share central regulatory molecules such as CXCL13, surface lymphotoxin ($LT\alpha_1\beta_2$), CCL21, and CCL19 (14). During embryogenesis, lymphoid tissue inducer (LTi) cells of hematopoietic origin and lymphoid tissue organizer (LTo) cells of mesenchymal origin interact *via* the abovementioned chemokines and receptor/ligand pairs to establish the developing SLO (15). Such cells are absent in adult organs but various hematopoietic cells like B cells, T cells, and dendritic cells (DC) exhibit functions of LTi cells (16), and stromal cells perform as LTo cells during lymphoid neogenesis (17). Lymphoid organogenesis takes place under sterile conditions, while lymphoid neogenesis requires antigenic stimulation (14). Particularly, T cells and B cells upregulate surface lymphotoxin expression upon activation (18). In peripheral organs, perivascular LTBR-expressing mesenchymal cells respond to surface lymphotoxin-expressing B cells and differentiate into follicular dendritic cells (FDCs), which govern B-cell zone organization and GC activation in TLS as well as in SLO (19–24). In the TME, targeted delivery of LIGHT, an alternative ligand of LTBR produced by activated T cells (25), drives vascular normalization and TLS formation (26, 27). Additionally, the extent of lymphoid neogenesis in a given organ depends also on composition of mesenchymal cells including fibroblasts (14), which affects the overall TLS development in different tumor-bearing organs (28).

Variation in TLS density is observed also between patients of the same tumor type and has significant prognostic associations (5, 6). IL-1R (29, 30) and IFNAR (31) signaling have been implicated as upstream events of lymphoid neogenesis in different inflammatory contexts. Here, we hypothesized that also non-immune, tumor cell-derived factors influence TLS development. To address this, we analyzed MIBC patient data of The Cancer Genome Atlas (TCGA) and the IMvigor210 dataset (32) as well as clinical samples from a retrospective MIBC cohort. Our data demonstrate a significant interaction between TLS density and tumor mutational burden (TMB) as well as increased T-cell activation. A particular feature of TLS-high tumors was the frequent co-infiltration of B cells and $CD8^+$ T cells as well as the highest proportion of PD-1^+TCF1^+ progenitor-like T cells (33) in intratumoral regions. We found four TLS subtypes based on the presence of FDC and $CD8^+$ T cell frequency. As in tumor regions, the highest proportion of PD-1^+TCF1^+ progenitor-like $CD8^+$ T cells was found in the TLS subtype with the highest B cell and $CD8^+$ T cell frequency. However, the main differences in TLS composition were found between TLS from TLS-high and TLS-low tumors rather than between their maturation stages. Finally, we identified one downregulated and three upregulated non-immune-related genes in tumors with high TLS density that are candidates for further studies of tumor-intrinsic regulation of lymphoid neogenesis.

MATERIALS AND METHODS

Patient Cohorts

There are 412 MIBC patient cases available from TCGA. We excluded patients who had no diagnostic images available (n = 31) as well as patients for whom there was no peritumoral region visible in the diagnostic image (n = 77) (no tumor invasive margin and adjacent organ parenchyma). In total, 304 patients were included in the histological and molecular analyses. From these, 2 patients had no available survival information, 2—no available transcriptomic data and 1—no genomic data, and were thus excluded from the respective analyses. Cohort characteristics are shown in **Supplementary Table 1**.

There are 348 patients available in the IMVigor210 dataset obtained from a multicenter, single-arm, phase 2 trial that investigated efficacy and safety of atezolizumab in metastatic urothelial cancer (32). Clinical response, survival, and gene expression data of these patients were obtained from http://research-pub.gene.com/IMvigor210CoreBiologies/ (34). Cohort details and response criteria were described previously (32). For 50 patients, clinical response was not evaluated, while 25 patients had a complete response, 167—progressive disease, 43—partial response, and 63—stable disease.

A retrospective patient cohort of untreated MIBC patients (n = 40) was obtained from the Netherlands Cancer Institute (NKI) (**Supplementary Table 2**). TLS density was assessed in this cohort by mIF. We then selected 12 patients with highest and 11 with lowest TLS density for characterization of TLS-associated tumor immune infiltrates by mIF. Use of retrospective anonymized patient material for research was approved by NKI-AVL institutional research board, following national regulations.

The use of patient material in different analyses of this study is depicted in the study design schematic (**Supplementary Figure 1**).

TLS Quantification in Histological Images From TCGA

All diagnostic [formalin-fixed paraffin-embedded (FFPE)] and matched cryopreserved sample histology images (H&E staining)

of the TCGA MIBC cohort were downloaded through the GDC portal. Dense lymphocytic clusters were marked as TLS annotations using the QuPath software. Presence of GC was also marked in TLS with the characteristic central morphology (**Supplementary Figure 2**). The generated annotations were exported to ImageJ software for automated measurement of TLS and GC number and size as well as total tissue area in each image. In diagnostic images, TLS and GC density was calculated as the number of TLS or GC annotations per measured tissue area. Average TLS or GC size was calculated as the mean area of the TLS or GC annotations for each patient. In cryopreserved sample images, TLS were assessed as present or absent.

Survival Analysis

Comparison of overall survival across different clinical, histological, and molecular parameters was performed by Kaplan–Meier curve and log-rank test. Patient groups were defined by median cutoffs for all continuous variables. Death was considered as event and patients alive at the last follow-up were censored. Hazard ratio for the different parameters was calculated by univariate Cox regression analysis. Prognostic independence of parameters with significant survival associations in univariate Cox regression was tested by multivariate Cox regression analysis.

Analysis of Molecular Data

All analysis were performed using R version 4.1.0.

MIBC RNA count, somatic mutation, copy number, and methylation data were downloaded with TCGAbiolinks (35). RNA count data were normalized with edgeR (36) and log2+1 transformed. Genes with less than 1 read per million in less than 10 samples were removed.

Gene expression was compared between TLS density groups. A change in average expression level of 50% (corresponding to fold change of 1.5 and log2 fold change of 0.585) was considered relevant. Two group comparisons were done by two-tailed *t*-test followed by Benjamini and Hochberg adjustment for multiple testing. Genes with adjusted *p*-value <0.05 (corresponding to log10 *p*-value of <−1.3) were considered as differentially expressed. Multiple group comparisons were done by one-way ANOVA.

Pathway analysis of identified differentially expressed genes (DEGs) was done using enrichplot and DOSE (37) for the gene ontology Biological Processes.

Gene signature encompassing the 122 significant TLS-associated DEGs was generated using GSVA (38).

Tumor mutation burden (TMB) was calculated by taking the sum of non-synonymous mutations and insertions and deletions (indels) per patient. Immune cluster and neoantigen data were acquired from Thorsson et al. (39) Abundance of cell population gene signatures was estimated by MCP counter (40).

ImVigor210 data were obtained from http://research-pub.gene.com/IMvigor210CoreBiologies/ (34). RNA count data were normalized with edgeR and log2 +1 transformed, and genes with less than 1 read per million in less than 10 samples were removed. Gene expression was compared between complete responders ($n = 25$) and progressive disease patients ($n = 167$) as described above for TLS density groups.

TLS–TMB Score

We integrated TLS density and TMB into a joint TLS-TMB score as follows: patients were split into four groups based on the median TLS density (1.08 TLS/cm^2) and the median mutation count (166 mutations). The categorical score was obtained with 85 patients having both parameters above their medians (HiHi), 86 with both parameters below the medians (LoLo), and 65 patients in each of the mixed groups (HiLo and LoHi, respectively).

The same principle was applied to integrate TLS density and predicted neoantigen load.

Gene expression was compared between TLS-TMB groups (HiHi versus all other) as described above for TLS density groups.

Immunofluorescence

TLS were analyzed in a retrospective patient cohort by mIF as described before (41). Briefly, 4-µm-thick FFPE tissue sections were treated in Trilogy™ buffer (CellMarque) for 10 min in a pressure cooker at 110°C, blocked in 4% bovine serum albumin/PBS/0.1% Triton X solution, and subjected to sequential detection of CD23 (SP23, Abcam, 1:1,000), CD21 (2G9, Leica, 1:5,000), PNAD (MECA-79, BioLegend, 1:5,000), DC-LAMP (1010E1.01, Dendritics, 1:1,000), CD3 (SP7, ThermoFisher, 1:1,000), and CD20 (L26, Dako, 1:5,000), here referred to as the TLS panel, using tyramide-conjugated fluorophores of the 7-plex Opal system (Akoya). Multispectral images of 200× high-power fields were acquired for all TLS in each patient using the Vectra 3.0 microscope (PerkinElmer/Akoya) with one TLS per image.

For tumor immune infiltrate analysis, tissue processing prior to mIF was done as described above for TLS analysis. The following markers were sequentially detected using a 9-plex Opal system (Akoya): PD-1 (D4W2J, Cell Signaling Technology, 1:8,000), TCF1 (C63D10, Cell Signaling Technology, 1:5,000), CD3 (SP7, ThermoFisher, 1:2,000), CD8 (4B11, Bio-Rad, 1:5,000), CD20 (L26, Dako, 1:5,000), CD21 (2G9, Leica, 1:5,000), Pan-cytokeratin (h-240, Santa Cruz, 1:2,000), and SH2D2A (OTI3C7, ThermoFisher, 1:1,000), here referred to as the TIL panel. A representative set of intratumoral and peritumoral regions as well as all TLS regions in each patient were imaged in high power (200×) using a Vectra Polaris multispectral slide scanner (Akoya). Intratumoral regions were defined as regions not in direct contact with the normal organ parenchyma within the 200× high-power field (**Supplementary Figure 1C**). No intratumoral regions were defined for four patients with highly fragmented tumors that were dispersed throughout the organ parenchyma.

Quantitative Image Analysis

The workflow of multispectral image analysis of the TLS panel included the following steps: (1) spectral unmixing; (2) tissue segmentation of the following TLS regions: B-cell zone, T-cell zone, follicular dendritic cell (FDC) zone, GC zone, and the

remaining non-TLS tissue; (3) measurement of whole TLS area as the sum of the different TLS regions per image; and (4) measurement of total tissue area from the whole slide image. Steps 1–3 were done using the Inform software (version 2.5.1), and step 4 was done using the ImageJ software. TLS maturation stage was determined by the presence or absence of FDC and GC zones in images containing B-cell zones. We did not implement PNAd staining to define TLS area as HEVs are also detected in TLS-non-related regions of the tissue (42). TLS density was calculated as the number of TLS per measured tissue area.

The workflow of multispectral image analysis of the TIL panel (**Supplementary Figure 3**) included the following steps: (1) spectral unmixing; (2) tissue segmentation of tumor, stromal, and TLS regions (B-cell zone, T-cell zone, and FDC zone); (3) measurement of whole TLS area as the sum of the different TLS regions per image; (4) individual cell segmentation; (5) extraction of per-cell fluorescent data, all using the Inform software (version 2.5.1); (6) image data file conversion into flow cytometry data file format using Biobase and flowCore (43); and (7) identification and quantification of different cell phenotypes using flow cytometry data analysis software FlowJo (version 10.8.0) (**Supplementary Figure 3**). The maturation of each TLS was assessed by the presence or absence of the FDC zone by tissue segmentation or by the presence of $CD21^+$ cells in single-cell analysis. Tumor, stromal, and TLS tissue segments containing less than 100 cells were excluded from single-cell analysis. Cell frequencies were assessed as the proportion of all cells in each tissue category per image and averaged per patient in peritumoral and intratumoral regions as well as in early and mature TLS.

The immune composition of each tumor and stromal tissue segment was defined based on their frequency of B cells, $CD8^+$ T cells, and $CD8^-$ T cells, and for TLS composition, $CD21^+$ cells were also included. Tissue segments with similar immune composition were identified using hierarchical clustering (R package pheatmap). Frequencies of the identified immune clusters were calculated for each patient as a proportion of the respective tissue segments (tumor, stroma, or TLS).

Cell and cluster frequencies were compared between two groups by two-tailed *t*-test and by one-way ANOVA for multiple group comparisons. No correction for multiple testing was done.

RESULTS

TLS Density Is a Significant Positive Prognosticator in Diagnostic Images of MIBC

We quantified TLS in images from diagnostic (FFPE) samples (**Figure 1A**) and matched cryopreserved samples (**Figure 1B**) of the TCGA MIBC cohort ($n = 304$). Cryosample images displayed tissues that were used for the acquisition of TCGA molecular data, and mainly represented intratumoral regions without invasive margin. TLS detected in the cryosamples are here referred to as c-TLS. The diagnostic images always contained intra- and peritumoral regions. We refer to TLS detected in the diagnostic images as d-TLS density (number per tissue area). We found concordance in the histological assessment of TLS between the two sampling methods for approximately 50% of patients: 17 patients with high d-TLS density contained TLS in the matched cryosample (c-TLS-positive) (**Figures 1A, B** and **Supplementary Figure 2A**), and 140 patients with low d-TLS density had no c-TLS. However, a considerable discrepancy was found in 135 cases with high d-TLS density that had no detectable c-TLS (**Figures 1C, D** and **Supplementary Figure 2B**), and in 12 cases with low d-TLS density that had TLS in their cryosample (**Supplementary Figure 2C**). Overall, we detected dense lymphocytic aggregates in approximately 10% of cryosamples ($n = 29$) and in approximately 75% of diagnostic images ($n = 224$) (**Figure 1E**, **Supplementary Figure 2**). Thus, the sensitivity of TLS detection was significantly higher in the diagnostic samples (Fisher's exact test $p = 0.000$), which may be explained by the fact that intratumoral TLS were considerably less frequent than peritumoral TLS within the same diagnostic image (**Supplementary Figures 2A–E**). Consequently, we used d-TLS density for survival analysis. Patient groups split by median d-TLS density showed a significant difference in overall survival (**Figure 1F**), while groups defined as d-TLS-positive or -negative showed only a trend (**Supplementary Figure 4**), establishing the cohort median as a biologically relevant threshold. We observed that the average size of TLS and GC, as well as the density of GC was positively associated with TLS density (**Figures 1G, H** and **Supplementary Figures 6A–D**), suggesting that tumor microenvironments where TLS are initiated also allow subsequent maturation and generation of GC.

Intratumoral Gene Expression Poorly Correlates With d-TLS Density

We next investigated whether gene expression profiles obtained from intratumoral regions (cryosamples) could be used as proxies for d-TLS density substituting the necessity of histological evaluation. We thus compared d-TLS-high and -low patient groups and found 123 DEGs (**Figure 2A** and **Supplementary Figure 5A**). Many of these DEGs were canonical TLS-associated genes, like *CR2* (encoding CD21), multiple B cell lineage markers such as *MS4A1* (encoding CD20), *CD19*, and *CD79A*, as well as TLS-relevant chemokines including *CXCL13*, *LTB*, *CCL21*, and *CCL19*. However, we found only weak direct correlations between d-TLS density and the intratumoral mRNA abundance of the DEGs (**Figure 2B** and **Supplementary Table 4**). Similar results were obtained when all TLS-associated DEGs were analyzed as a joint signature (**Supplementary Table 4**), or when immune cell abundance estimated with MCP counter was analyzed (**Supplementary Figures 5B, C**). In fact, most of the identified DEGs showed a much more pronounced expression difference between tumors that did or did not contain c-TLS (**Figure 2C** and **Supplementary Table 5**). Furthermore, we found no association between d-TLS density and the previously published TCGA immune subtypes (immune gene signatures) with prognostic relevance in a pan-cancer setting (39) (**Supplementary Figures 5D, E**). When the MIBC cohort was analyzed

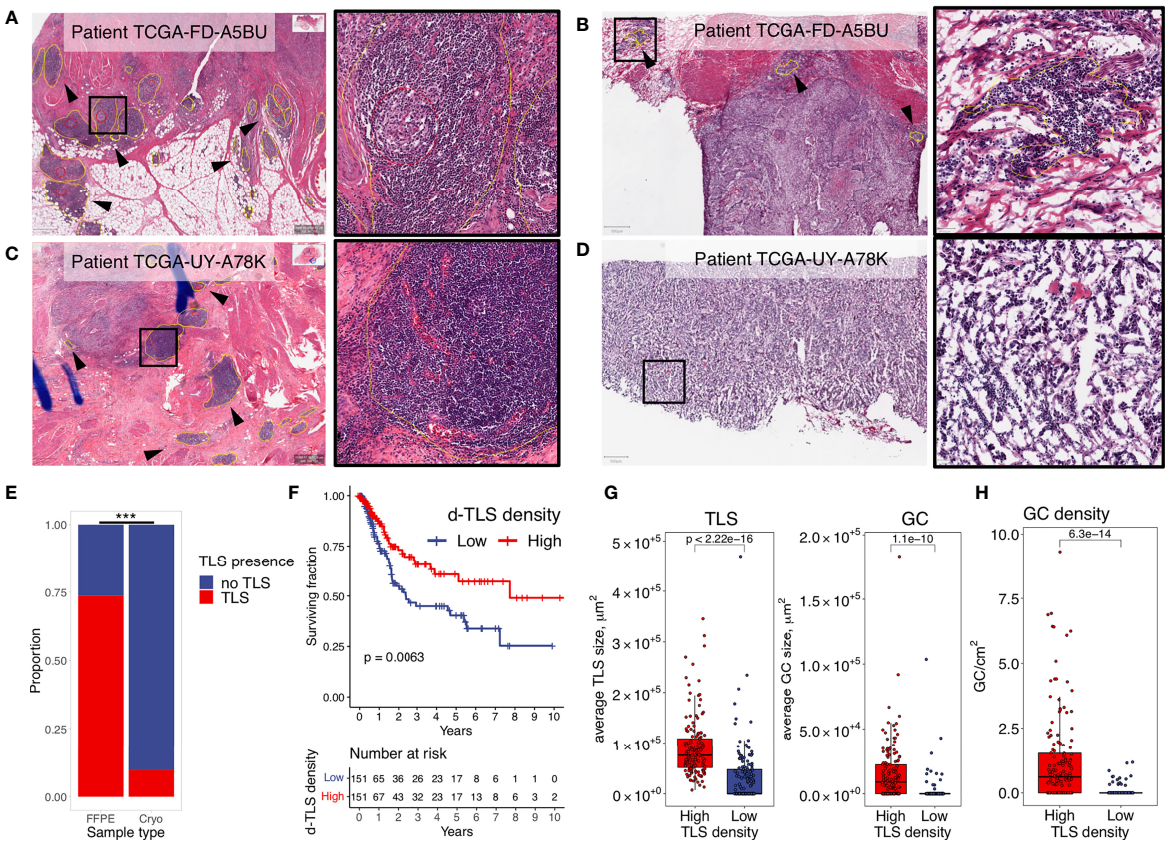

FIGURE 1 | TLS density is a significant positive prognosticator in diagnostic images of MIBC. Dense lymphocytic aggregates were assessed in histology images from diagnostic (FFPE) and matched cryopreserved (Cryo) samples of the TCGA MIBC cohort. TLS (yellow circles) and GC (red circles) were annotated using the Qupath software. Their counts and sizes were measures by ImageJ software. **(A, B)** Representative examples of concordant histology assessment between the two sampling methods: high d-TLS density **(A)** and TLS positivity in the matched cryosample **(B)**. **(C, D)** Representative examples of discordant histology assessment between the two sampling methods: high d-TLS density **(C)** but no TLS in the matched cryosample **(D)**. **(E)** Proportion of TLS-containing images from the diagnostic and cryopreserved samples were compared by Fisher's exact test (***$p < 0.000$). **(F)** Median d-TLS density (TLS count per tissue area) was used to define TLS-high and TLS-low patient groups for comparison of overall survival by Kaplan–Meier curve and log-rank test. **(G)** Average size of d-TLS and GC was calculated in each patient and compared between d-TLS density groups by two-tailed *t*-test. **(H)** GC density (count per tissue area) was compared between d-TLS density groups by two-tailed t test.

separately, the pan-cancer immune subtypes did not show any correlation with survival (**Supplementary Figure 5F**). These results indicate that mRNA profiles obtained from intratumoral regions, which rarely contain TLS (**Supplementary Figure 2D**), cannot be reliably used as proxy for the detection of tumor-associated TLS, which largely develop in the periphery of MIBC (**Supplementary Figure 2D**) and other solid tumors (8, 42, 44).

Genes Associated With d-TLS Density in the TME Are Dominantly Immune Cell-Related

To search for tumor-intrinsic gene expression alterations with potential impact on lymphoid neogenesis, we first excluded the DEGs that would be derived directly from TLS such as all DEGs overlapping between d-TLS and c-TLS group comparison (**Supplementary Table 5**). As a result, a set of 44 DEGs unique to the d-TLS group comparison remained (**Supplementary Table 6**). Next, we interrogated the published literature and online expression databases to identify potential tumor cell-, immune cell-, and stromal cell-derived genes. Out of the 44 d-TLS-associated genes, 38 were protein coding. Four of those, namely, *NDGR4, ZFP57, THEM5*, and *HRCT1*, did not show an immune cell-associated expression pattern (**Supplementary Table 6**). *NDGR4* was in fact the only gene associated with reduced TLS development in the DEG analysis, while *ZFP57, THEM5*, and *HRCT1* showed increased expression in TLS-high tumors (**Figure 3A**). We found that multiple immune population gene signatures were positively associated with the expression of ZFP57 and HRCT1, and a negative association was found for NDGR4 (**Supplementary Figure 5G**); however, no correlation with patient survival was found for these genes (**Supplementary Table 6**). Furthermore, three genes—*Cxorf65, SSTR3*, and *ART3*—had a testis-associated expression pattern (**Supplementary Table 6**) and might represent novel Cancer/Testis antigens. The majority of the remaining DEGs were, however, associated with activated immune response, in particular, with T-cell activation as

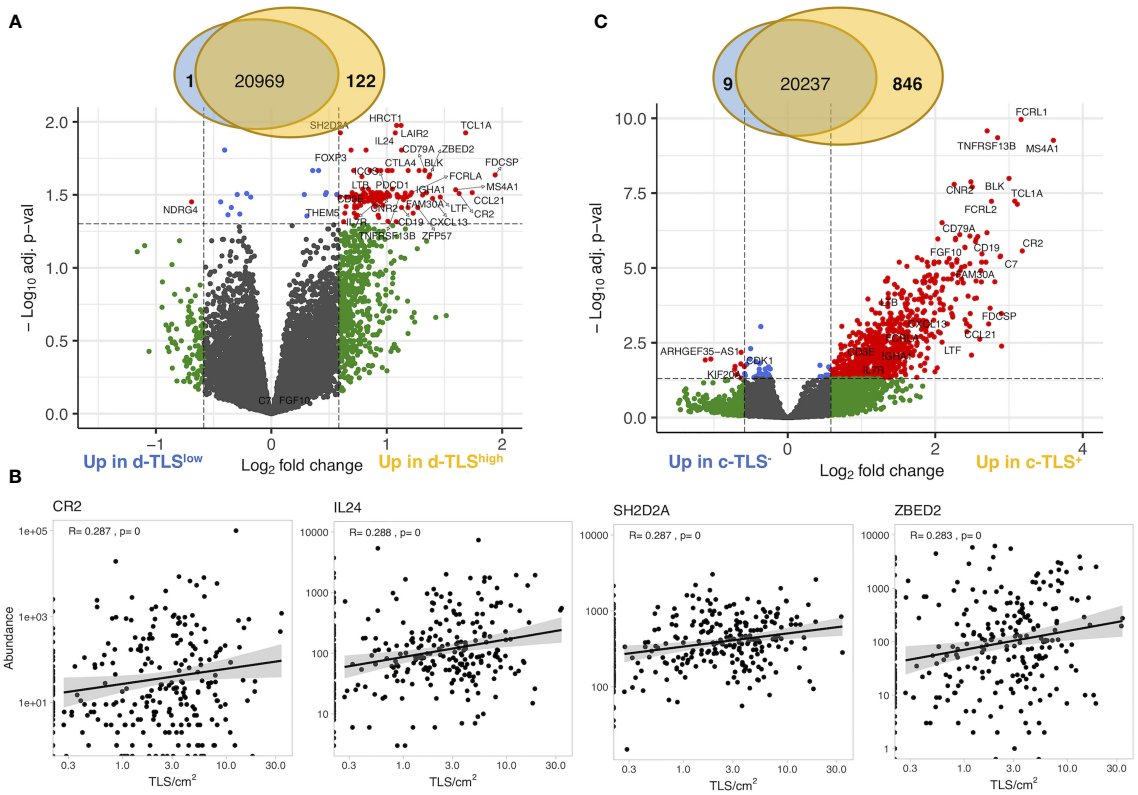

FIGURE 2 | Gene expression in intratumoral regions poorly correlates with d-TLS density. **(A)** Gene expression measured by bulk tumor RNA sequencing of intratumoral regions (cryosamples) was compared in d-TLS density groups by two-tailed *t*-test with Benjamini–Hochberg adjustment for multiple testing. Differentially expressed genes were defined as genes with expression change of 50% (log2 fold change of 0.585) and adjusted *p*-value <0.05 (log10 adj. *p*-value <-1.3) and are displayed as red dots in the Volcano plot. **(B)** Spearman correlation analysis was done to establish the direct relationship between intratumoral DEG abundance and d-TLS density. Representative plots of the most significant correlations are shown. **(C)** Gene expression was compared in patient groups defined by the presence or absence of TLS in their cryosamples (c-TLS) by two-tailed *t*-test and Benjamini–Hochberg adjustment for multiple testing. Significant DEGs were defined and visualized as in **(A)**.

demonstrated by pathway enrichment analysis (**Figure 3A**). Expression of most of these genes showed significant correlation with improved patient survival in the TCGA MIBC cohort as well as with response to immune checkpoint inhibition and survival analyzed in the IMVigor210 data set (**Figures 3B, C** and **Supplementary Table 6**). Taken together, TLS in the TME are associated with expression changes of predominantly immune response-related genes; nevertheless, also non-immune genes were found to be altered in TLS density groups and represent candidates for studying tumor-intrinsic regulation of lymphoid neogenesis.

Joint TLS–TMB Score Is a Novel Independent Prognosticator in MIBC

We next explored genetic and epigenetic features in MIBC such as copy number variation, methylation profile, TMB, and mutation frequency of individual genes in the context of TLS development. Among these, we found significant differences in TLS density groups only for TMB; the number of nonsynonymous mutations was significantly increased in patients with high d-TLS density (**Figure 4A**). However, there was no direct correlation between TMB and d-TLS density, size, or GC formation (**Figure 4B** and **Supplementary Figures 6A–D**). Since TMB by itself also conferred favorable prognosis in MICB (**Figure 4C**), we tested whether there is a potential biomarker synergy between TLS and TMB. Indeed, patients with high d-TLS density and high TMB (both parameters above the cohort medians) had a superior overall survival than all other patients (**Figure 4D**). The favorable prognostic interaction was particularly evident in advanced stage patients (**Figures 4E, F**). Neither TLS density nor TMB was associated with tumor stage (**Supplementary Figures 6E, F**). The integrated TLS-TMB score was an independent prognostic marker of survival when tested in a multivariate Cox regression model together with tumor stage and vascular invasion parameters (**Table 1**), while TLS density and TMB as separate parameters showed independence from each other (**Supplementary Table 3**, Model 1) but not from tumor stage or vascular invasion (**Supplementary Table 3**, Model 2). Like TMB, predicted neoantigen count was also increased in patients with high d-TLS density (**Supplementary Figure 3G**). Subsequently, we obtained similar survival associations when TLS density was integrated with predicted neoantigen count (**Supplementary**

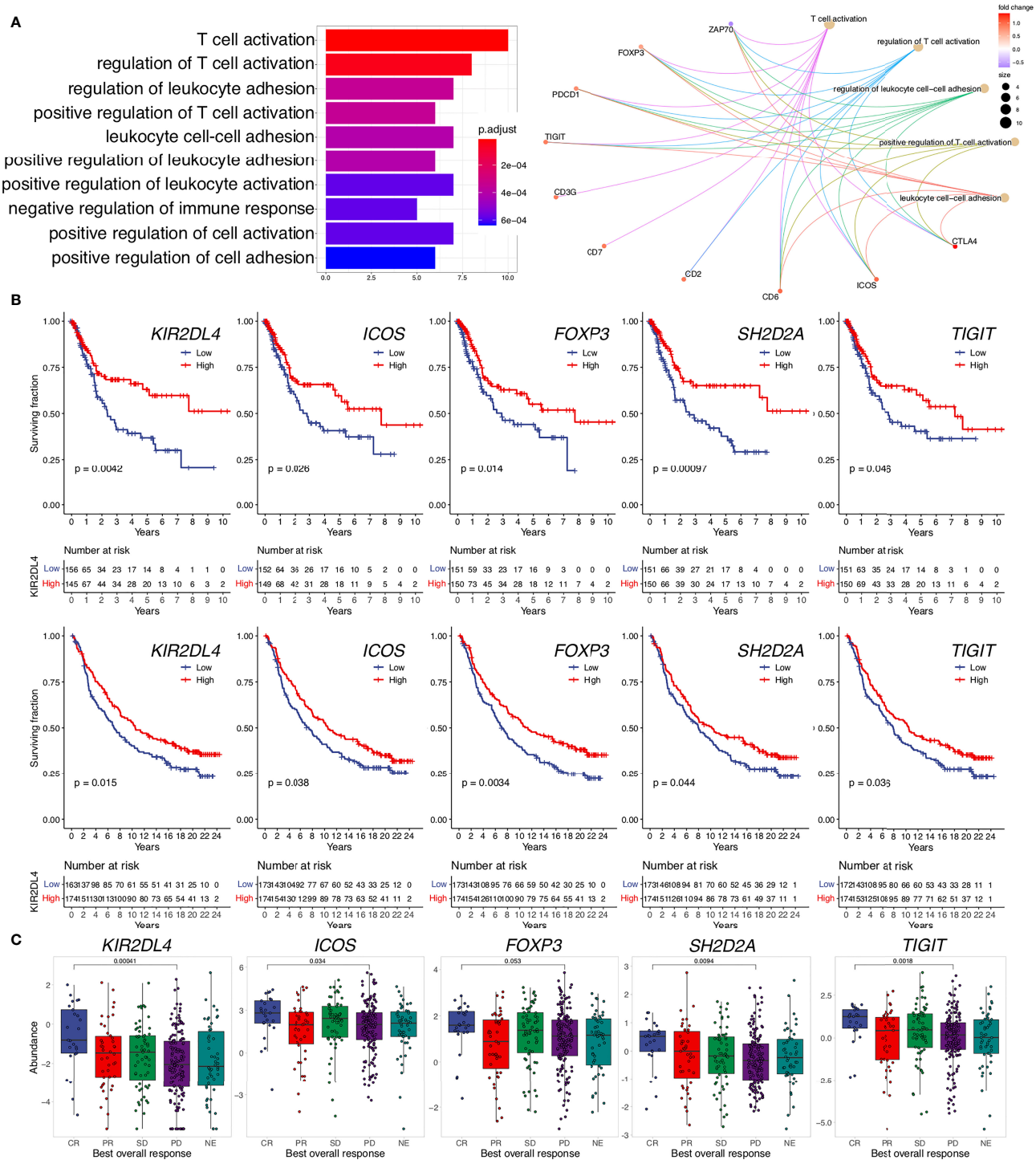

FIGURE 3 | Genes upregulated in TLS-high tumors are related to immune response activation, improved survival, and response to ICI. **(A)** Pathway enrichment analysis of TLS-associated DEGs unique to the d-TLS group comparison (n = 44) was performed using gene ontology "Biological Processes". The number of corresponding DEGs is visualized for the top ten enriched processes (left). The contribution of specific genes to the top five enriched pathways is visualized (right). **(B)** Overall survival was compared for gene expression groups defined by cohort medians in the TCGA MIBC cohort (top row) and IMvigor210 cohort (bottom row) using Kaplan–Meier curve and log-rank test for each unique DEG. **(C)** Expression comparison of the identified unique DEGs between complete response (CR) and progressive disease (PD) after ICI in the IMVigor210 dataset was performed by two-tailed t-test. Genes that showed significant favorable prognostic associations in both cohorts are shown.

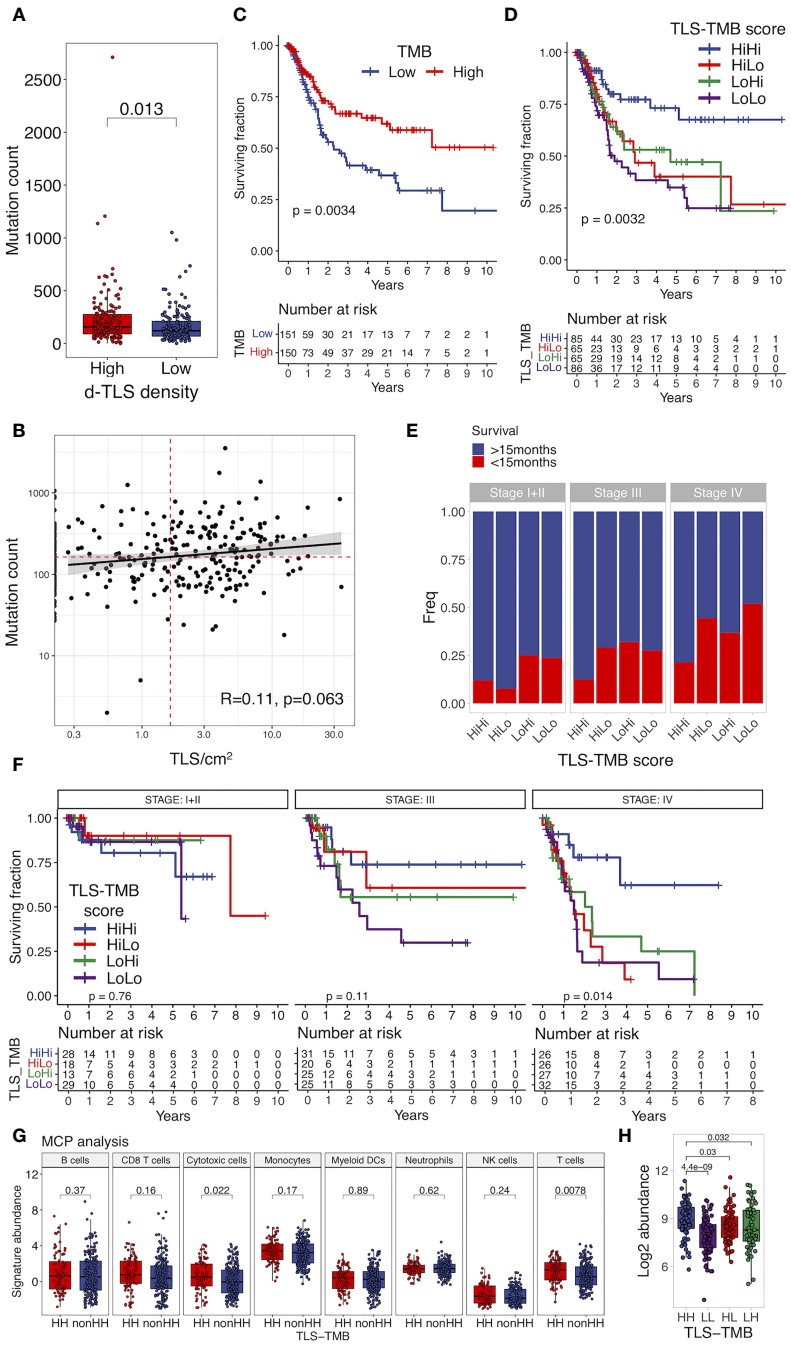

FIGURE 4 | Joint TLS-TMB score is a novel independent prognostic biomarker in MIBC. **(A)** Tumor mutational burden (TMB) was measured as the count of nonsynonymous mutations and was compared in patients with high and low d-TLS densities by two-tailed *t*-test. **(B)** Direct correlation between TMB and d-TLS density was analyzed by Spearman correlation. Red dotted lines represent cohort medians of the TMB and TLS density, respectively. **(C)** Patients with high and low TMB were defined by the cohort median TMB. Overall survival was compared in TMB-high and TMB-low patients by Kaplan–Meier curve and log-rank test. **(D)** MIBC patients were split into four groups based on their high or low d-TLS density in combination with high or low TMB creating a joint TLS-TMB score. Overall survival was compared in the four patient groups by Kaplan–Meier curve and log-rank test. **(E)** Patients were stratified into short-term and long-term survivors by using 15-month survival as cutoff. The proportion of patients with short- and long-term survival in the different TLS-TMB groups was compared in the context of tumor stage. **(F)** Overall survival of different TLS-TMB groups was analyzed in each MIBC stage separately by Kaplan–Meier curve and log-rank test. **(G)** Log2 abundance of cell population gene signatures was determined using the R package MCP counter and compared between TLS-TMB high–high (HH) and other (nonHH) patients by two-tailed *t*-test. **(H)** Gene expression measured by bulk tumor RNA sequencing was compared between TLS-TMB high–high and all other patients by two-tailed *t*-test with Benjamini–Hochberg adjustment for multiple testing. The expression of the only identified protein-coding DEG, SH2D2A, was compared for the TLS-TMB high–high group against all other groups' two-tailed *t*-test with no adjustment for multiple testing.

TABLE 1 | Multivariate Cox regression analysis.

Parameter	HR	95% CI		P value
		lower	upper	
Stage III vs Stage I+II	1.47	0.77	2.81	0.24
Stage IV vs stage I+II+III	3.22	1.65	6.28	0.001
Vascular invasion (Yes vs No)	1.77	1.12	2.80	0.014
TLS-TMB score (nonHiHi vs HiHi)	2.14	1.27	3.60	0.004

Figure 3H). The MCP counter analysis revealed that patients with TLS-TMB high–high status had significantly higher expression of cytotoxic cell- or T cell-related gene signatures in comparison to all other patients (**Figure 4G**). We observed similar trends when comparing stage IV patients with high–high versus high–low status (**Supplementary Figure 6I**). Differential gene expression analysis returned a single protein coding gene that was associated with the high–high status—SH2D2A, a T cell-specific adaptor protein with poorly understood functions (45) (**Figure 4H**). Thus, TLS in the context of potentially increased tumor antigenicity (46) provide a prognostic advantage especially for late-stage MIBC patients.

TLS-Rich TME Is Associated With Increased Infiltration of Activated Lymphocytes

We then analyzed tumor immune infiltration in the context of TLS density in a retrospective MIBC cohort. We performed tissue segmentation of 9-plex mIF images to address immune infiltration separately in tumor nests and tumor stroma obtained from peri- and intratumoral regions as well as in TLS (**Supplementary Figure 1C**). To characterize T cells, we selected SH2D2A, which, although with a low fold change, was among the top significant d-TLS-associated DEGs (**Figure 2B**, **Supplementary Figure 5A**, **Supplementary Table 6**), and was uniquely associated with the TLS-TMB high–high status (**Figure 4H**). Additionally, we used PD-1 to detect activated B cells (47–50) and T cells [PD-1^+ $TCF1^-$ (51)], and TCF1 to detect naïve [PD-1^- $TCF1^+$ (51)] or progenitor-like [PD-1^+ $TCF1^+$ (51)] T cells with known association to improved survival and response to immunotherapy (33) (**Figure 5A** and **Supplementary Figure 3**). In line with a previous report (52), we found that $CD8^+$ T cells were the most prominent TIL population in MIBC followed by B cells and $CD8^-$ T cells (**Figures 5B-D**). Intratumoral heterogeneity of immune cell infiltration was observed in all patients (**Supplementary Figure 7A**). In line with the variability and average abundance of immune population gene signatures observed by the MCP counter analysis (**Supplementary Figure 5B**), we saw increased average B-cell infiltration and trends towards increased total T-cell frequencies in TLS-high tumors; however, the effect was confined mainly to the peritumoral regions (**Figures 5B-D**). The average frequencies of SH2D2A-expressing cells, PD-$1^-$$TCF1^-$ $CD8^+$ T cells, or all subpopulations of $CD8^-$ T cells were not altered in d-TLS density groups (**Supplementary Figures 7B–D**). In contrast, $CD8^+$ T-cell and B-cell subpopulations expressing PD-1 were significantly increased in the peritumoral areas of TLS-high patients (**Figures 5E, F, H**). CD21-expresing B cells were found rarely outside mature TLS and showed a trend towards increased infiltration in TLS-high tumors (**Figure 5G**). Furthermore, naïve $CD8^+$ T cells (**Figure 5I**) as well as PD-1^- B cells (**Supplementary Figure 7C**) were increased in the periphery of TLS-high tumors, while progenitor-like PD-$1^+$$TCF1^+$ $CD8^+$ T cells infiltrated intratumoral regions significantly less in TLS-low patients (**Figure 5J**). Together, TLS are associated with increased infiltration of $CD8^+$ T cells and B cells in the TME, recapitulating the result of TCGA gene expression analysis.

TLS-High Tumors Show Frequent B- and T-Cell Co-Infiltration Harboring Naïve and Progenitor-Like T Cells and Activated B Cells

To study possible co-infiltration patterns of TILs across different tumor regions, we performed hierarchical clustering of all acquired tumor and stromal tissue segments by their frequencies of B cells, $CD8^-$ T cells, and $CD8^+$ T cells. We found similar infiltration patterns in tumor nests and stroma, which were classified into five main groups: (1) predominant $CD8^+$ T-cell infiltration with high frequency, (2) predominant $CD8^+$ T-cell infiltration with low frequency, (3) co-infiltration of $CD8^+$ T cells and B cells, (4) predominant infiltration of B cells, and (5) no infiltration (**Figure 6A**). As expected, we found a higher prevalence of non-infiltrated tumor regions in the TLS-low patients, while B-cell dominant and B-cell and $CD8^+$ T-cell co-infiltrated regions were more frequent in TLS-high tumors (**Figure 6B**). In fact, B- and T-cell co-infiltration was found in around 20% of tumor regions from 2/3 of the TLS-high patients, which contrasts with less than 10% of tumor regions in 1/4 of TLS-low patients (**Supplementary Figure 8A**). While B- and T-cell co-infiltrated tumor areas had similar total T-cell frequency when compared to T-cell-dominant areas, the proportion of $TCF1^+$ T cells (both, $CD8^-$ and $CD8^+$) was significantly higher (**Figure 6C**). Similarly, PD-1-expressing B cells were enriched in co-infiltrated regions in comparison to B-cell-dominant regions with matching total B-cell infiltration (**Figure 6D**). The same results were obtained for stromal regions (**Supplementary Figure 8B**) that also displayed a significant increase in PD-$1^+$$TCF1^+$ T-cell proportion (**Figure 6E**). Although the proportion dynamic of the above cell subpopulations in the different immune clusters was similar in both TLS density groups (**Supplementary Figure 8C**), TLS-low tumors exhibited significant reduction in the proportion of these phenotypes compared to TLS-high tumors (**Figure 6F**).

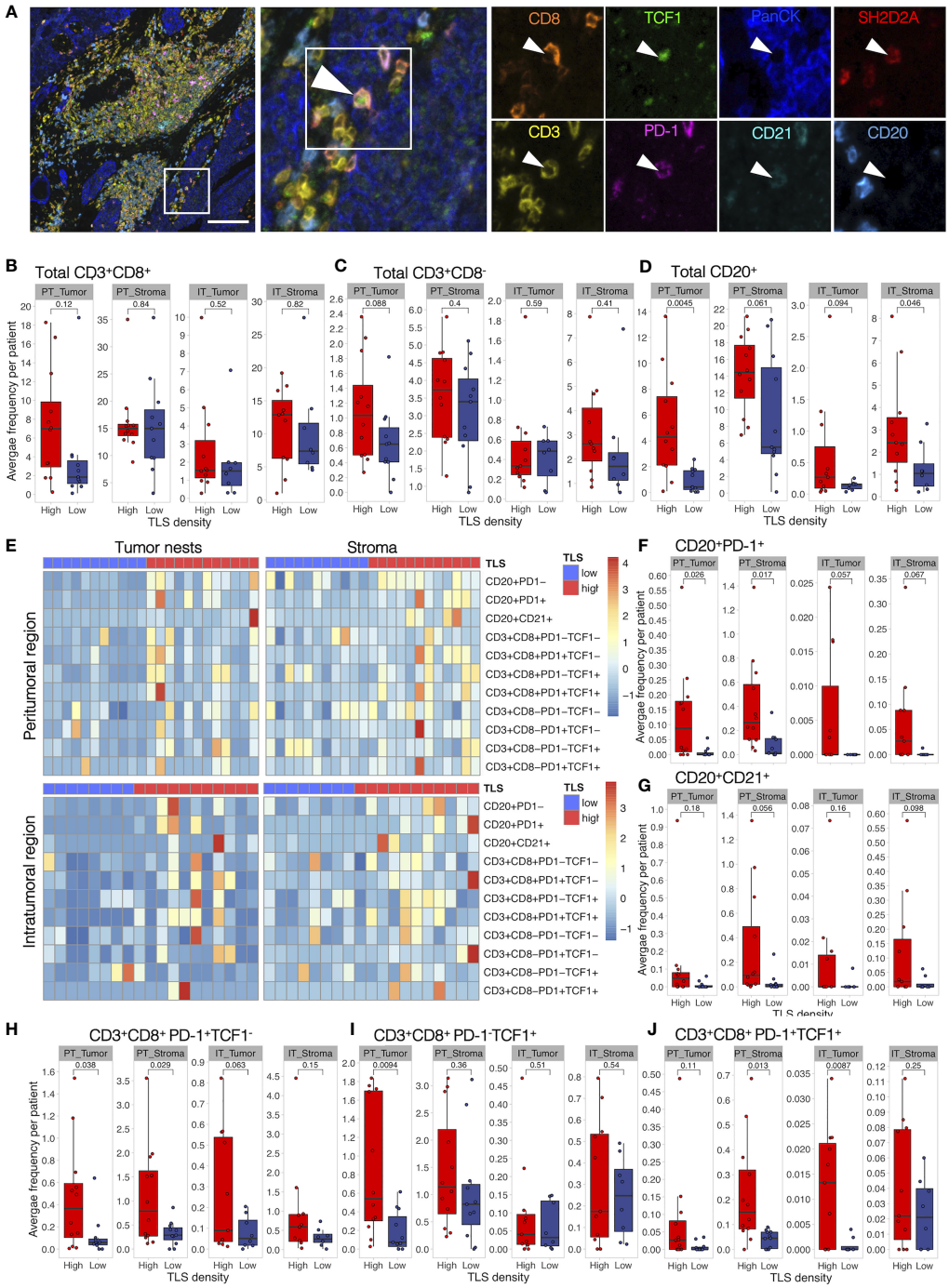

FIGURE 5 | Activated B cells and progenitor-like T cells are increased in TLS-high tumors. Characterization of immune cell phenotypes in TME was performed by mIF staining of CD20 (B cells), CD21 (FDCs), CD3 (total T cells), CD8 (cytotoxic T cells), PD-1 (activation marker), TCF1 (marker of naïve cells), SH2D2A (T cell-specific adaptor protein), and PanCK (tumor cells). Images were acquired by multispectral microscopy from a representative set of peritumoral (PT) and intratumoral (IT) regions. Per-cell fluorescent data were obtained by cell segmentation in tumor nests and stromal regions. **(A)** A representative image of a TLS-high tumor and corresponding mIF staining identifying PD-1^{+}TCF1^{+} (progenitor-like) CD8^{+} T cell infiltrating a tumor nest. Scale bar = 100 µm. **(B–D)** Total CD8^{+} **(B)** and CD8^{-} T-cell **(C)** and B-cell **(D)** frequencies were measured as the proportion of all cells within the respective tissue categories (tumor or stroma) and averaged per patient in peritumoral (PT) and intratumoral (IT) regions. Infiltration in the two d-TLS density groups was compared by two-tailed *t*-test. No correction for multiple testing was done. **(E)** Heatmaps displaying z-scaled average frequencies of each measured subpopulation in each tissue category (tumor or stroma) in peritumoral and intratumoral regions for all analyzed patients. **(F–J)** Frequencies of PD-1^{+} **(E)** and CD21^{+} **(G)** B cells, PD-1^{+}TCF1^{-} **(H)**, PD-1^{-}TCF1^{+} **(I)**, as well as PD-1^{+}TCF1^{+} **(J)** CD8^{+} T cells were quantified and compared as described in **(B)**.

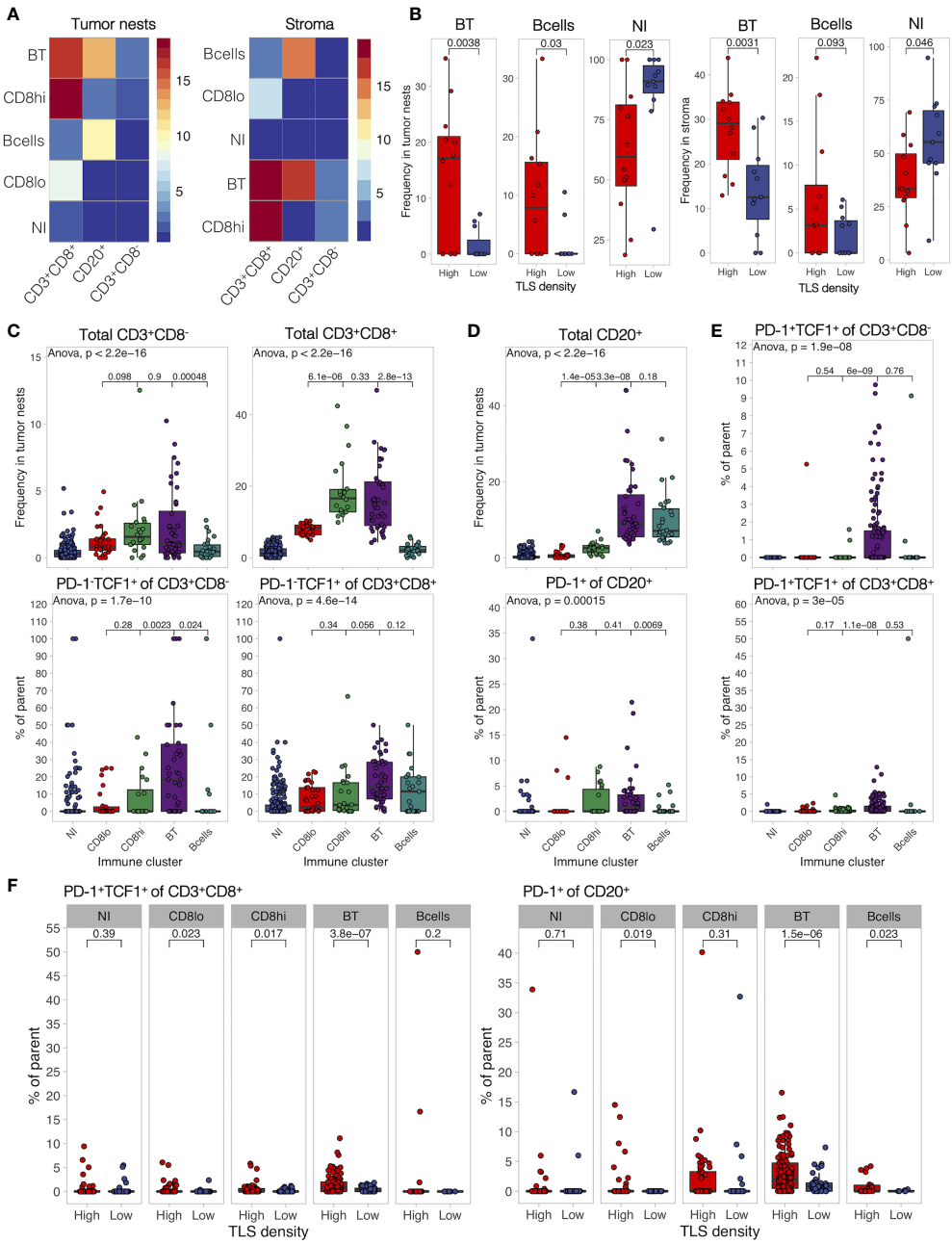

FIGURE 6 | B- and T-cell co-infiltration is common in TLS-high tumors and shows differential immune composition. **(A)** Tumor and stromal regions were classified based on their composition of B cells, $CD8^-$, and $CD8^+$ T cells by hierarchical clustering. Five immune clusters were identified in both regions: (1) B- and T-cell co-infiltrated (BT, both populations with frequency >5%), (2) B cell-dominant (B cells, B cells >5%, and $CD8^+$ T cells <5%), (3) $CD8^+$ T cell-dominant high frequency (CD8hi, >10% of cells are $CD8^+$ T cells, B cells <5%), (4) $CD8^+$ T cell-dominant low frequency (CD8lo, >5% < 10% of cells are $CD8^+$ T cells, B cells <5%), and (5) non-infiltrated (NI) (B cells and $CD8^+$ T cells both <5%). Heatmaps display the average frequency of the measured cell populations in the identified immune clusters. **(B)** Frequency of each identified immune cluster was determined as the proportion out of all analyzed tumor and stromal segments in each patient. Immune cluster frequencies were compared between TLS-high and TLS-low patients. **(C)** Frequency of infiltrating total $CD8^-$ and $CD8^+$ T cells (top panels) as well as their proportion of PD-1^-TCF1^+ naïve cells (bottom panels) was measured in each individual tissue segment (image) and compared in different tumor immune clusters. **(D)** Frequency of infiltrating total $CD20^+$ B cells (top panels) as well as their proportion of PD-1^+ activated cells (bottom panels) was measured in each individual tissue segment (image) and compared in different stromal immune clusters. **(E)** Proportion of PD-1^+TCF1^+ progenitor-like cells from total $CD8^-$ (top) and $CD8^+$ (bottom) T cells was measured in each tissue category per image and compared in different stromal immune clusters. **(F)** Proportion of PD-1^+TCF1^+ progenitor-like $CD8^+$ T cells and PD-1^+ B cells was measured in each individual tissue segment (image) and compared between different TLS density groups for each stromal immune cluster separately. In all panels, two groups (as indicated by group connectors below *p*-values) were compared by two-tailed *t*-test without correction for multiple testing. More than two groups were compared by one-way ANOVA.

Taken together, TLS presence in TME is associated with increased co-infiltration of B cells and $CD8^+$ T cells within tumor nests and tumor stroma. Co-infiltrated regions show increased frequencies of naïve ($PD\text{-}1^-TCF1^+$) T cells and activated B cells ($PD\text{-}1^+$) as well as an almost exclusive presence of progenitor-like ($PD\text{-}1^+TCF1^+$) T cells when compared to areas predominantly infiltrated by B cells or $CD8^+$ T cells alone. These data indicate towards a potential role of B-cell and $CD8^+$ T-cell interactions in generating or sustaining $PD\text{-}1^+TCF1^+$ T cells.

Lymphocyte Activation in TLS Is Defined by TME and Not TLS Maturation Stage

Finally, we characterized the development, maturation, and composition of TLS in MIBC patients. We defined TLS stages by the presence of $CD21^+$ FDC networks and $CD23^+$ GC cells (**Figure 7A**) using image tissue segmentation. Similarly to our previous findings in untreated lung and colorectal cancer (42, 44) as well as the d-TLS assessment in TCGA MIBC cohort (**Figures 2G, H**), TLS were more mature in MIBC patients with high TLS density (**Figure 7B**), suggesting that TLS initiation and maturation in the TME are naturally linked.

Analysis of the cellular composition of TLS by 9-plex mIF revealed that immature TLS had an increased proportion of T cells and reduced proportion of B cells when compared to mature TLS (**Figure 7C**), a feature present in both TLS-high and TLS-low tumors (**Supplementary Figure 9A**). No major differences were seen for the proportions of total B cells and $CD8^+$ T cells when each TLS maturation stage was compared in TLS-high and TLS-low tumors separately (**Supplementary Figure 6B**). However, the proportions of $PD\text{-}1^+TCF1^+$ T cells and $PD\text{-}1^+$ B cells in TLS were significantly increased in TLS-high tumors independently of TLS maturation stage (**Figure 7D** and **Supplementary Figure 9C**).

We next analyzed TLS composition following a similar approach as above for tumor and stromal regions. Due to the high cell density within TLS, B cells in contact with FDCs were detected as $CD21^+$ and were used here to define the maturation status of TLS subtypes identified by hierarchical clustering analysis (**Figure 7E**). Two mature and two immature TLS clusters were found based on their proportion of $CD8^+$ T cells—high and low, respectively, using 10% frequency as the cutoff. As expected, enrichment of mature and immature clusters was observed in TLS-high and TLS-low tumors, respectively (**Supplementary Figures 9D, E**). Interestingly, $PD\text{-}1^+TCF1^+$ $CD8^+$ T cells, as well as $PD\text{-}1^+$ B cells and T cells, were highest in the mature-CD8high TLS subtype (**Figure 7F**). However, this effect was only partially preserved when TLS density groups were analyzed separately (**Supplementary Figure 9F**); in TLS-low tumors, these phenotypes were significantly reduced in almost all TLS subtypes (**Figure 7G** and **Supplementary Figure 9G**). To summarize, TLS have reduced T-cell and B-cell activation and progenitor-like T-cell frequency within the TLS-low TME compared to their counterparts in TLS-high TME and independently of maturation stage. Mirroring the findings from the co-infiltrated tumor regions, TLS with high $CD8^+$ T-cell and B-cell frequency (such as the mature-CD8high subtype) had the highest proportion of progenitor-like $CD8^+$ T cells and $PD\text{-}1^+$ B cells, which implies the possible role of local interactions between B cells and $CD8^+$ T cells in immune response regulation by supporting $PD\text{-}1^+TCF1^+$ $CD8^+$ T cells.

DISCUSSION

We have performed comprehensive molecular and histological characterization of MIBC samples in the context of TLS density. We found that TLS formed in the periphery of MIBC in most cases and, in line with previous reports (7, 53), their density correlated with improved survival. We (42) and others [reviewed in (54)] showed that the expression of lymphoid neogenesis-associated chemokines like *CXCL13* and *LTB* as well as lineage markers of TLS components such as B cells is increased in samples containing lymphocytic clusters. Therefore, we reasoned that gene expression signatures could serve as a proxy for TLS quantification in cases where histological material is unavailable. We found that d-TLS density determined by histology of diagnostic sections did not correlate with TLS-related gene expression profiles in intratumoral regions obtained from matched cryosamples. The most likely explanation for this finding is that TCGA transcripts are determined in intratumoral regions that largely lack invasive margins, whereas d-TLS are mostly present around the tumor. The fact that we found a better correlation between TLS-related gene expression and c-TLS positivity supports this explanation. Spatial heterogeneity within tumor samples may further complicate such correlations. Taken together, our data suggest that intratumoral mRNA expression profiles cannot be used as surrogates for adequate TLS assessment in solid tumors with predominantly peritumoral TLS development like lung squamous cell carcinoma (42), CRC (44), and MIBC (8). Consequently, using tumor center-oriented sampling (including TCGA gene expression data or tissue microarray studies) for TLS assessment may not be reliable.

Analysis of genomic alterations revealed that TLS-high tumors were characterized by increased TMB in line with our previous work on colorectal cancer (44). This may be explained by the fact that tumor cells with high TMB potentially contain more neo-antigens and thus better elicit T-cell and B-cell responses (55). In support of this, a study in ovarian and uterine tumors showed that increased TMB was associated with increased infiltration of $CD8^+$ T cells expressing *CXCL13* and TLS development (56). Along the same line, higher neoantigen load in pancreatic cancer was observed in patients with increased number of GC-positive TLS and long-term survival (57). Additionally, we found upregulated expression of three testis-associated genes in TLS-high tumors suggesting that these may be candidate Cancer/Testis antigens (58) and further supports the idea of tumor antigenicity as a relevant factor in TLS development. Indeed, a recent report studying an i.p. B16F10 melanoma model showed significantly more spontaneous TLS in ovalbumin-overexpressing than parental tumors, and demonstrated a crucial role of antigen-specific $CD8^+$ T cells and activated B cells in the development and maturation of TLS (28).

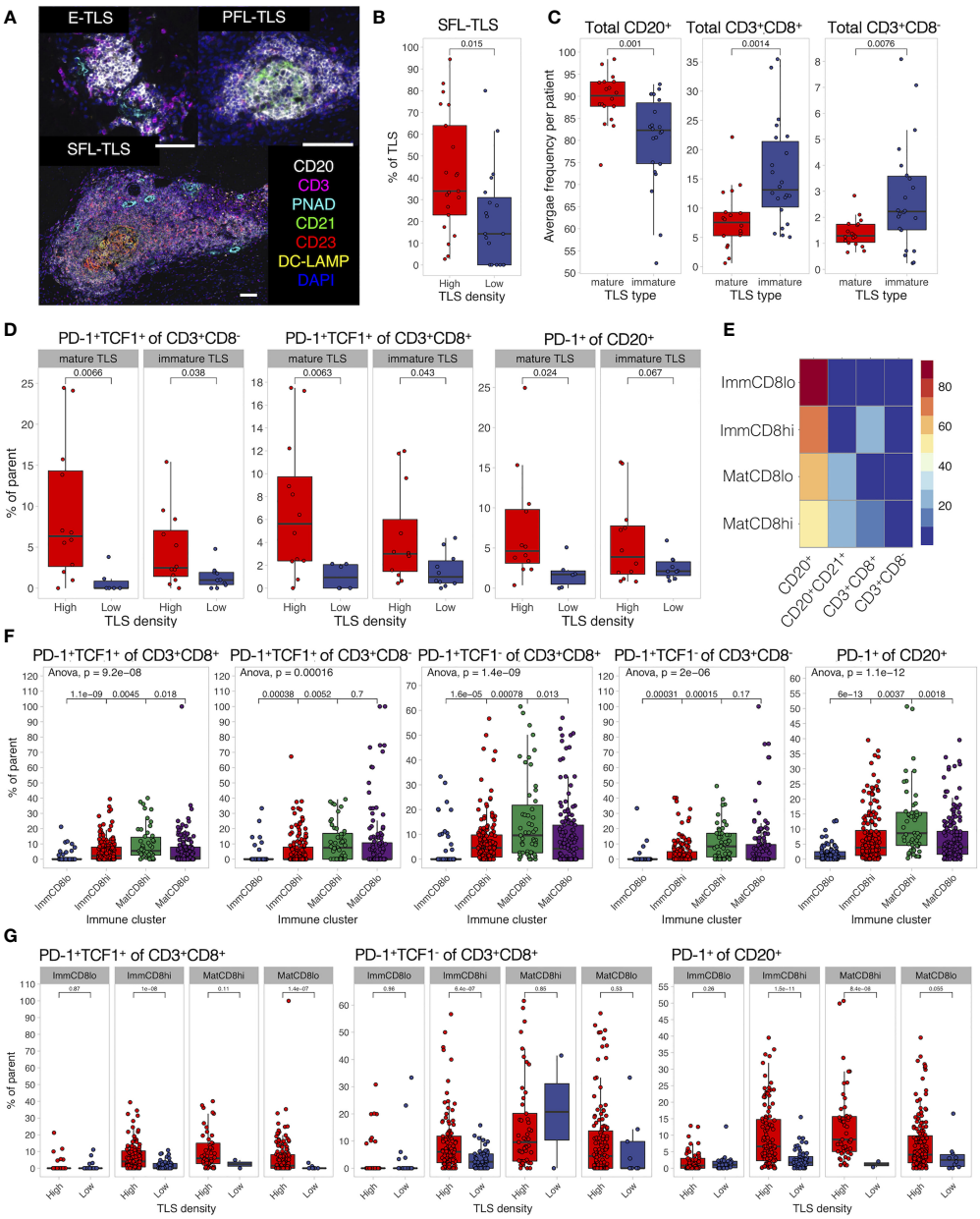

FIGURE 7 | TLS composition depends on TME and differs between maturation clusters. **(A)** TLS quantification and assessment of maturation was performed by mIF staining of CD20 (B cells), CD21 (FDCs), CD3 (total T cells), CD23 (GC cells), PNAd (high endothelial venules), and DC-LAMP (antigen-presenting DCs). Images were acquired by multispectral microscopy from all TLS. Tissue segmentation was used to detect FDC and GC presence in TLS for the assignment of TLS maturation stages as follows: no FDC and GCs—early TLS (E-TLS), FDC networks present but no GC cells—primary follicle-like TLS (PFL-TLS), GC cells present in FDC network—secondary follicle-like TLS (SFL-LS). Representative images of each maturation stage are shown. Scale bar = 100 µm. **(B)** The proportion of each TLS maturation stage was assessed as percentage of total TLS in each patient. The proportion of GC-containing TLS (SFL-TLS) was compared between TLS-high and TLS-low patients. **(C)** Characterization of immune cell infiltration in TLS was performed by mIF staining as described in **Figure 5**. Presence of CD21+ cells was used to define a TLS as mature or immature. Frequencies of B cells and T cells were averaged per patient and compared between TLS maturation stages. **(D)** Proportions of PD-1$^+$TCF1$^+$ progenitor-like cells from total CD8$^-$ (left) and CD8$^+$ (center) T cells, as well as PD-1$^+$ cells from total B cells (right) were averaged per patient per TLS maturation stage and compared in TLS-high and TLS-low groups. **(E)** Hierarchical clustering was used to identify TLS with similar composition based on B-cell, CD21$^+$ B-cell, and T-cell frequencies. Four clusters (TLS subtypes) were identified as follows: immature TLS with high or low CD8$^+$ T-cell infiltration (ImmCD8hi and ImmCD8lo, respectively), and mature TLS with high or low CD8$^+$ T-cell infiltration (MatCD8hi and MatCD8lo, respectively). Heatmap displays the average frequency of the measured cell populations in the identified TLS subtypes. **(F)** Proportions of PD-1-expressing lymphocytes and PD-1$^+$TCF1$^+$ progenitor-like T cells were compared in different TLS clusters. **(G)** Proportion of PD-1$^+$TCF1$^+$ progenitor-like CD8$^+$ T cells, PD-1$^+$ B cells, and CD8$^+$ T cells was measured in each individual TLS and compared between different TLS density groups for each TLS subtype separately. In all panels, two groups (as indicated by group connectors below *p*-values) were compared by two-tailed *t*-test without correction for multiple testing. More than two groups were compared by one-way ANOVA.

In our current study, TLS density and TMB did not directly correlate, and were independently associated with patient survival. Combining TLS density with TMB into a joint TLS-TMB score generated a novel prognostic biomarker that, in contrast to either TLS density of TMB alone, was independent from tumor stage and vascular invasion. These results together with previous reports (56, 57) suggest that the improved prognosis of the TLS-TMB high–high patients signifies ongoing anti-tumor immunity. Indeed, increased gene expression related to cytotoxic cells and T cells was found in patients with the TLS-TMB high–high status in comparison to other groups. It will be interesting to investigate the relevance of the joint TLS-TMB score in predicting the clinical response to immunotherapy, especially in the context of PD-1/PD-L1 blockade monotherapies where pre-existing immunity is a relevant biomarker of response (59).

Type I interferons may drive TLS development. In a model of influenza infection, type I interferons induced CXCL13 production in lung fibroblasts, which resulted in the development of TLS (60). We found a potential link between TLS and type I interferons as well: Two genes with known direct involvement in type I IFN signaling—*ZBP1* and *ZBED2*—were upregulated in TLS-high tumors. ZBP1 is a Z-nucleic acid sensing protein that triggers type I IFN production and programmed cell death (61). ZBED2 is a transcriptional repressor of IFN-stimulated genes (62) and has been implicated as a transcription factor typical for antigen-responsive $CD8^+$ T cells (63).

Besides type I interferons, we found IL24 as a novel immune-related factor associated with TLS in MIBC. Myofibroblasts and keratinocytes have been reported to produce IL24 in response to inflammatory stimulation, as well as lymphocytes in response to antigen receptor stimulation [reviewed in (64)]. The relevant source of IL24 in the context of TLS development, however, remains to be detemined.

Also, activated T cells correlated with the presence of TLS: Genes related to T-cell activation (*ICOS, FOXP3, SH2D2A*, and others) were among the genes with the highest direct correlation to TLS density. Human *FOXP3* is transiently induced in response to TCR engagement of effector T cells (65); thus, the increased *FOXP3* expression here may signify increased infiltration of activated effector T cells rather than T regulatory cells. In addition, the frequency of activated B cells, T cells, and progenitor-like $CD8^+$ T cells was increased in the TME of TLS-high tumors. Furthermore, we observed significantly higher TLS densities as a result of successful ICI in MIBC patients in comparison to non-responders (8).

Previously, we proposed that immature and mature TLS are sequential developmental states in the TME leading to functional TLS (42). Thus, one would anticipate to find increased proportions of activated lymphocytes in TLS with increasing maturation. In contrast to this assumption, however, we found that the proportions of activated B and T cells as well as progenitor-like $CD8^+$ T cells were similar when comparing TLS maturation stages defined by the presence of FDCs. The main differences were found instead between TLS from TLS-high and TLS-low TME. Therefore, our results rather suggest that the composition of TLS is orchestrated by the TME. In light of this, we suggest that TLS are a consequence of activated adaptive immunity rather than a prerequisite for the latter. This has important implications for the considerations of potential TLS-targeted therapeutic protocols, suggesting that TLS induction without overcoming the immunosuppressive mechanisms in a TME will not be effective. Furthermore, these results emphasize the importance of in-depth analysis of B- and T-cell zones in the TLS for TLS subtype classification, as suggested by other studies [van Dijk et al., *Frontiers in Immunology*, 2021 (back-to-back submission), and (66)].

We noticed that TLS-high tumors were frequently co-infiltrated by B cells and $CD8^+$ T cells. Such tumor regions were enriched with activated B cells, naïve T cells, and progenitor-like T cells, thus mirroring the immune composition of the mature-CD8hi TLS subtype. These data point towards the importance of local B-cell and $CD8^+$ T-cell interactions in supporting the progenitor-like T-cell phenotype.

Finally, we identified only a handful of TLS-associated genes that had no known association to immune cells. A single gene was upregulated in TLS-low TME, *NDGR4* (N-Myc downstream-regulated gene 4), which affects cell migration and proliferation. Downregulation of this gene was implicated in promoting breast cancer metastasis (67), although conflicting oncogenic and tumor-suppressive properties have been reported in multiple other tumor types. *HRCT1, THEM5*, and *ZFP57* were upregulated in TLS-high MIBC samples. The functions of HRCT1 are unknown, while THEM5 is required for normal mitochondrial function (68) and ZFP57 is involved in maintaining maternal and paternal gene imprinting (69). These are potential candidate genes for further research on tumor-intrinsic regulation of lymphoid neogenesis.

CONCLUSIONS

We have identified the joint TLS-TMB score as a novel independent biomarker for MIBC patient prognosis. We show that gene expression profiles cannot be extrapolated to TLS density, unless TLS-containing biological samples were used for RNA extraction. This limits TLS analysis to cohorts of solid tumors with available histological images or samples that include peritumoral regions.

We demonstrate that TLS-high tumors are characterized by increased expression of genes related to T-cell activation and contained regions of co-infiltrating B cells and $CD8^+$ T cells. Such regions as well as TLS in such tumors hosted increased proportions of progenitor-like $CD8^+$ T cells. The composition of TLS seemed to mirror the composition of the TME, and therefore, TLS development may be downstream of an ongoing adaptive immune response.

DATA AVAILABILITY STATEMENT

The raw data supporting the conclusions of this article will be made available by the authors, without undue reservation.

ETHICS STATEMENT

The studies involving human participants were reviewed and approved by NKI-AVL. The patients/participants provided their written informed consent to participate in this study.

AUTHOR CONTRIBUTIONS

KS and MB designed the study. KS wrote the manuscript. FP performed histological assessment of TCGA images. KS and LB performed mIF experiments. PC and ML performed bioinformatics analysis of TCGA molecular data. KS performed the analysis of mIF data and TCGA clinical data. ND and MH provided clinical material and data of the NKI cohort. All authors contributed to the article and approved the submitted version.

ACKNOWLEDGMENTS

This work was funded by grants from the WWCR (grant number 18-0629) and SNSF Sinergia (grant number CRSII5_177208) and Zurich Cancer League (grant without number). We are very thankful to Dr. Ruben Casanova for providing the R-based solution for single cell imaging data conversion into fcs file format and his advice on bioinformatics analyses.

SUPPLEMENTARY MATERIAL

The Supplementary Material for this article can be found online at: https://www.frontiersin.org/articles/10.3389/fimmu.2021.793992/full#supplementary-material

REFERENCES

1. Luo S, Zhu R, Yu T, Fan H, Hu Y, Mohanta SK, et al. Chronic Inflammation: A Common Promoter in Tertiary Lymphoid Organ Neogenesis. *Front Immunol* (2019) 10:2938. doi: 10.3389/fimmu.2019.02938
2. van de Pavert SA, Mebius RE. New Insights Into the Development of Lymphoid Tissues. *Nat Rev Immunol* (2010) 10:664–74. doi: 10.1038/nri2832
3. Carragher DM, Rangel-Moreno J, Randall TD. Ectopic Lymphoid Tissues and Local Immunity. *Semin Immunol* (2008) 20:26–42. doi: 10.1016/j.smim.2007.12.004
4. Jones GW, Jones SA. Ectopic Lymphoid Follicles: Inducible Centres for Generating Antigen-Specific Immune Responses Within Tissues. *Immunology* (2016) 147:141–51. doi: 10.1111/imm.12554
5. Sautès-Fridman C, Petitprez F, Calderaro J, Fridman WH. Tertiary Lymphoid Structures in the Era of Cancer Immunotherapy. *Nat Rev Cancer* (2019) 19:307–25. doi: 10.1038/s41568-019-0144-6
6. Silina K, Rulle U, Kalnina Z, Line A. Manipulation of Tumour-Infiltrating B Cells and Tertiary Lymphoid Structures: A Novel Anti-Cancer Treatment Avenue? *Cancer Immunol Immunother* (2014) 63:643–62. doi: 10.1007/s00262-014-1544-9
7. Pfannstiel C, Strissel PL, Chiappinelli KB, Sikic D, Wach S, Wirtz RM, et al. The Tumor Immune Microenvironment Drives a Prognostic Relevance That Correlates With Bladder Cancer Subtypes. *Cancer Immunol Res* (2019) 7:923–38. doi: 10.1158/2326-6066.CIR-18-0758
8. van Dijk N, Gil-Jimenez A, Silina K, Hendricksen K, Smit LA, de Feijter JM, et al. Preoperative Ipilimumab Plus Nivolumab in Locoregionally Advanced Urothelial Cancer: The NABUCCO Trial. *Nat Med* (2020) 26:1839–44. doi: 10.1038/s41591-020-1085-z
9. Gao J, Navai N, Alhalabi O, Siefker-Radtke A, Campbell MT, Tidwell RS, et al. Neoadjuvant PD-L1 Plus CTLA-4 Blockade in Patients With Cisplatin-Ineligible Operable High-Risk Urothelial Carcinoma. *Nat Med* (2020) 26:1845–51. doi: 10.1038/s41591-020-1086-y
10. Groeneveld CS, Fontugne J, Cabel L, Bernard-Pierrot I, Radvanyi F, Allory Y, et al. Tertiary Lymphoid Structures Marker CXCL13 is Associated With Better Survival for Patients With Advanced-Stage Bladder Cancer Treated With Immunotherapy. *Eur J Cancer* (2021) 148:181–9. doi: 10.1016/j.ejca.2021.01.036
11. Petitprez F, de Reyniès A, Keung EZ, Chen TWW, Sun CM, Calderaro J, et al. B Cells are Associated With Survival and Immunotherapy Response in Sarcoma. *Nature* (2020) 577:556–60. doi: 10.1038/s41586-019-1906-8
12. Helmink BA, Reddy SM, Gao J, Zhang S, Basar R, Thakur R, et al. B Cells and Tertiary Lymphoid Structures Promote Immunotherapy Response. *Nature* (2020) 577:549–55. doi: 10.1038/s41586-019-1922-8
13. Cabrita R, Lauss M, Sanna A, Donia M, Skaarup Larsen M, Mitra S, et al. Tertiary Lymphoid Structures Improve Immunotherapy and Survival in Melanoma. *Nature* (2020) 577:561–5. doi: 10.1038/s41586-019-1914-8
14. Aloisi F, Pujol-Borrell R. Lymphoid Neogenesis in Chronic Inflammatory Diseases. *Nat Rev Immunol* (2006) 6:205–17. doi: 10.1038/nri1786
15. Drayton DL, Liao S, Mounzer RH, Ruddle NH. Lymphoid Organ Development: From Ontogeny to Neogenesis. *Nat Immunol* (2006) 7:344–53. doi: 10.1038/ni1330
16. Jones GW, Hill DG, Jones SA. Understanding Immune Cells in Tertiary Lymphoid Organ Development: It Is All Starting to Come Together. *Front Immunol* (2016) 7:401. doi: 10.3389/fimmu.2016.00401
17. Buckley CD, Barone F, Nayar S, Bénézech C, Caamaño J. Stromal Cells in Chronic Inflammation and Tertiary Lymphoid Organ Formation. *Annu Rev Immunol* (2015) 33:715–45. doi: 10.1146/annurev-immunol-032713-120252
18. De Togni P, Goellner J, Ruddle NH, Streeter PR, Fick A, Mariathasan S, et al. Abnormal Development of Peripheral Lymphoid Organs in Mice Deficient in Lymphotoxin. *Science* (1994) 264:703–7. doi: 10.1126/science.8171322
19. Krautler NJ, Kana V, Kranich J, Tian Y, Perera D, Lemm D, et al. Follicular Dendritic Cells Emerge From Ubiquitous Perivascular Precursors. *Cell* (2012) 150:194–206. doi: 10.1016/j.cell.2012.05.032
20. Tumanov A, Kuprash D, Lagarkova M, Grivennikov S, Abe K, Shakhov A, et al. Distinct Role of Surface Lymphotoxin Expressed by B Cells in the Organization of Secondary Lymphoid Tissues. *Immunity* (2002) 17:239–50. doi: 10.1016/S1074-7613(02)00397-7
21. Schaeuble K, Britschgi MR, Scarpellino L, Favre S, Xu Y, Koroleva E, et al. Perivascular Fibroblasts of the Developing Spleen Act as LTalpha1beta2-Dependent Precursors of Both T and B Zone Organizer Cells. *Cell Rep* (2017) 21:2500–14. doi: 10.1016/j.celrep.2017.10.119
22. Endres R, Alimzhanov MB, Plitz T, Futterer A, Kosco-Vilbois MH, Nedospasov SA, et al. Mature Follicular Dendritic Cell Networks Depend on Expression of Lymphotoxin Beta Receptor by Radioresistant Stromal Cells and of Lymphotoxin Beta and Tumor Necrosis Factor by B Cells. *J Exp Med* (1999) 189:159–68. doi: 10.1084/jem.189.1.159
23. Fu YX, Huang G, Wang Y, Chaplin DD. B Lymphocytes Induce the Formation of Follicular Dendritic Cell Clusters in a Lymphotoxin Alpha-Dependent Fashion. *J Exp Med* (1998) 187:1009–18. doi: 10.1084/jem.187.7.1009
24. Chaplin D, Huang G, Wang Y, Fu Y-X. B Lymphocytes Deliver Lymphotoxin-Dependent Signals for the Development of Follicular Dendritic Cell Clusters. *FASEB J* (1998) 12:A1072.
25. Mauri DN, Ebner R, Montgomery RI, Kochel KD, Cheung TC, Yu G-L, et al. LIGHT, a New Member of the TNF Superfamily, and Lymphotoxin α Are Ligands for Herpesvirus Entry Mediator. *Immunity* (1998) 8:21–30. doi: 10.1016/S1074-7613(00)80455-0
26. Johansson-Percival A, He B, Li ZJ, Kjellen A, Russell K, Li J, et al. *De Novo* Induction of Intratumoral Lymphoid Structures and Vessel Normalization Enhances Immunotherapy in Resistant Tumors. *Nat Immunol* (2017) 18:1207–17. doi: 10.1038/ni.3836
27. Huang Y, Chen Y, Zhou S, Chen L, Wang J, Pei Y, et al. Dual-Mechanism Based CTLs Infiltration Enhancement Initiated by Nano-Sapper Potentiates Immunotherapy Against Immune-Excluded Tumors. *Nat Commun* (2020) 111(11):1–15. doi: 10.1038/s41467-020-14425-7

28. Rodriguez AB, Peske JD, Woods AN, Leick KM, Mauldin IS, Young SJ, et al. Immune Mechanisms Orchestrate Tertiary Lymphoid Structures in Tumors *Via* Cancer-Associated Fibroblasts. *Cell Rep* (2021) 36:109422. doi: 10.1016/j.celrep.2021.109422
29. Kuroda E, Ozasa K, Temizoz B, Ohata K, Koo CX, Kanuma T, et al. Inhaled Fine Particles Induce Alveolar Macrophage Death and Interleukin-1alpha Release to Promote Inducible Bronchus-Associated Lymphoid Tissue Formation. *Immunity* (2016) 45:1299–310. doi: 10.1016/j.immuni.2016.11.010
30. Morissette MC, Jobse BN, Thayaparan D, Nikota JK, Shen P, Labiris NR, et al. Persistence of Pulmonary Tertiary Lymphoid Tissues and Anti-Nuclear Antibodies Following Cessation of Cigarette Smoke Exposure. *Respir Res* (2014) 15:49. doi: 10.1186/1465-9921-15-49
31. Filderman JN, Appleman M, Chelvanambi M, Taylor JL, Storkus WJ. STINGing the Tumor Microenvironment to Promote Therapeutic Tertiary Lymphoid Structure Development. *Front Immunol* (2021) 0:1826. doi: 10.3389/fimmu.2021.690105
32. Balar AV, Galsky MD, Rosenberg JE, Powles T, Petrylak DP, Bellmunt J, et al. Atezolizumab as First-Line Treatment in Cisplatin-Ineligible Patients With Locally Advanced and Metastatic Urothelial Carcinoma: A Single-Arm, Multicentre, Phase 2 Trial. *Lancet* (2017) 389:67–76. doi: 10.1016/S0140-6736(16)32455-2
33. Siddiqui I, Schaeuble K, Chennupati V, Fuertes Marraco SA, Calderon-Copete S, Pais Ferreira D, et al. Intratumoral Tcf1+PD-1+CD8+ T Cells With Stem-Like Properties Promote Tumor Control in Response to Vaccination and Checkpoint Blockade Immunotherapy. *Immunity* (2019) 50:195–211.e10. doi: 10.1016/j.immuni.2018.12.021
34. Mariathasan S, Turley SJ, Nickles D, Castiglioni A, Yuen K, Wang Y, et al. Tgfβ Attenuates Tumour Response to PD-L1 Blockade by Contributing to Exclusion of T Cells. *Nature* (2018) 554:544–8. doi: 10.1038/nature25501
35. Colaprico A, Silva T, Olsen C, Garofano L, Cava C, Garolini D, et al. TCGAbiolinks: An R/Bioconductor Package for Integrative Analysis of TCGA Data. *Nucleic Acids Res* (2016) 44:e71–1. doi: 10.1093/NAR/GKV1507
36. Robinson MD, McCarthy DJ, Smyth GK. Edger: A Bioconductor Package for Differential Expression Analysis of Digital Gene Expression Data. *Bioinformatics* (2010) 26:139–40. doi: 10.1093/bioinformatics/btp616
37. Yu G, Wang L-G, Yan G-R, He Q-Y. DOSE: An R/Bioconductor Package for Disease Ontology Semantic and Enrichment Analysis. *Bioinformatics* (2015) 31:608–9. doi: 10.1093/bioinformatics/btu684
38. Hänzelmann S, Castelo R, Guinney J. GSVA: Gene Set Variation Analysis for Microarray and RNA-Seq Data. *BMC Bioinform* (2013) 141(14):1–15. doi: 10.1186/1471-2105-14-7
39. Thorsson V, Gibbs DL, Brown SD, Wolf D, Bortone DS, Ou Yang TH, et al. The Immune Landscape of Cancer. *Immunity* (2018) 48:812–30.e14. doi: 10.1016/j.immuni.2018.03.023
40. Becht E, Giraldo NA, Lacroix L, Buttard B, Elarouci N, Petitprez F, et al. Estimating the Population Abundance of Tissue-Infiltrating Immune and Stromal Cell Populations Using Gene Expression. *Genome Biol* (2016) 171 (17):1–20. doi: 10.1186/S13059-016-1070-5
41. Silina K, Burkhardt C, Casanova R, Solterman A, van den Broek M. Quantitative Pathology Approach to Analyze the Development of Human Cancer-Associated Tertiary Lymphoid Structures. *Methods Mol Biol* (2018) 1845:71–86. doi: 10.1007/978-1-4939-8709-2_5
42. Silina K, Solterman A, Movahedian Attar F, Casanova R, Uckeley ZM, Thut H, et al. Germinal Centers Determine the Prognostic Relevance of Tertiary Lymphoid Structures and are Impaired by Corticosteroids in Lung Squamous Cell Carcinoma. *Cancer Res* (2018) 78:1308–20. doi: 10.1158/0008-5472.CAN-17-1987
43. Hahne F, LeMeur N, Brinkman RR, Ellis B, Haaland P, Sarkar D, et al. Flowcore: A Bioconductor Package for High Throughput Flow Cytometry. *BMC Bioinform* (2009) 101(10):1–8. doi: 10.1186/1471-2105-10-106
44. Posch F, Silina K, Leibl S, Mundlein A, Moch H, Siebenhuner A, et al. Maturation of Tertiary Lymphoid Structures and Recurrence of Stage II and III Colorectal Cancer. *Oncoimmunology* (2018) 7:e1378844. doi: 10.1080/2162402X.2017.1378844
45. Borowicz P, Chan H, Hauge A, Spurkland A. Adaptor Proteins: Flexible and Dynamic Modulators of Immune Cell Signalling. *Scand J Immunol* (2020) 92: e12951. doi: 10.1111/sji.12951
46. Schumacher TN, Schreiber RD. Neoantigens in Cancer Immunotherapy. *Science* (2015) 348:69–74. doi: 10.1126/science.aaa4971
47. Agata Y, Kawasaki A, Nishimura H, Ishida Y, Tsubata T, Yagita H, et al. Expression of the PD-1 Antigen on the Surface of Stimulated Mouse T and B Lymphocytes. *Int Immunol* (1996) 8:765–72. doi: 10.1093/intimm/8.5.765
48. Thibult ML, Mamessier E, Gertner-dardenne J, Pastor S, Just-landi S, Xerri L, et al. PD-1 Is a Novel Regulator of Human B-Cell Activation. *Int Immunol* (2013) 25:129–37. doi: 10.1093/intimm/dxs098
49. Zhong X, Bai C, Gao W, Strom TB, Rothstein TL. Suppression of Expression and Function of Negative Immune Regulator PD-1 by Certain Pattern Recognition and Cytokine Receptor Signals Associated With Immune System Danger. *Int Immunol* (2004) 16:1181–8. doi: 10.1093/intimm/dxh121
50. Floudas A, Neto N, Marzaioli V, Murray K, Moran B, Monaghan MG, et al. Pathogenic, Glycolytic PD-1+ B Cells Accumulate in the Hypoxic RA Joint. *JCI Insight* (2020) 5:e139032. doi: 10.1172/jci.insight.139032
51. Zhao X, Shan Q, Xue H-H. TCF1 in T Cell Immunity: A Broadened Frontier. *Nat Rev Immunol* (2021) 2021:1–11. doi: 10.1038/s41577-021-00563-6
52. Wahlin S, Nodin B, Leandersson K, Boman K, Jirström K. Clinical Impact of T Cells, B Cells and the PD-1/PD-L1 Pathway in Muscle Invasive Bladder Cancer: A Comparative Study of Transurethral Resection and Cystectomy Specimens. *Oncoimmunology* (2019) 8:e1644108. doi: 10.1080/2162402X.2019.16441088
53. Sarma KP. The Role of Lymphoid Reaction in Bladder Cancer. *J Urol* (1970) 104:843–9. doi: 10.1016/S0022-5347(17)61849-4
54. Sautes-Fridman C, Lawand M, Giraldo NA, Kaplon H, Germain C, Fridman WH, et al. Tertiary Lymphoid Structures in Cancers: Prognostic Value, Regulation, and Manipulation for Therapeutic Intervention. *Front Immunol* (2016) 7:407. doi: 10.3389/fimmu.2016.00407
55. Rizvi NA, Hellmann MD, Snyder A, Kvistborg P, Makarov V, Havel JJ, et al. Mutational Landscape Determines Sensitivity to PD-1 Blockade in Non-Small Cell Lung Cancer. *Science* (2015) 348:124–8. doi: 10.1126/science.aaa1348
56. Workel HH, Lubbers JM, Arnold R, Prins TM, van der Vlies P, de Lange K, et al. A Transcriptionally Distinct CXCL13(+)CD103(+)CD8(+) T-Cell Population Is Associated With B-Cell Recruitment and Neoantigen Load in Human Cancer. *Cancer Immunol Res* (2019) 7:784–96. doi: 10.1158/2326-6066.CIR-18-0517
57. Gunderson AJ, Rajamanickam V, Bui C, Bernard B, Pucilowska J, Ballesteros-Merino C, et al. Germinal Center Reactions in Tertiary Lymphoid Structures Associate With Neoantigen Burden, Humoral Immunity and Long-Term Survivorship in Pancreatic Cancer. *Oncoimmunology* (2021) 10:1900635. doi: 10.1080/2162402X.2021.1900635
58. Whitehurst AW. Cause and Consequence of Cancer/Testis Antigen Activation in Cancer. *Annu Rev Pharmacol Toxicol* (2014) 54:251–72. doi: 10.1146/annurev-pharmtox-011112-14032654
59. Pilard C, Ancion M, Delvenne P, Jerusalem G, Hubert P, Herfs M. Cancer Immunotherapy: It's Time to Better Predict Patients' Response. *Br J Cancer* (2021) 1257(125):927–38. doi: 10.1038/s41416-021-01413-x
60. Denton AE, Innocentin S, Carr EJ, Bradford BM, Lafouresse F, Mabbott NA, et al. Type I Interferon Induces CXCL13 to Support Ectopic Germinal Center Formation. *J Exp Med* (2019) 216:621–37. doi: 10.1084/jem.20181216
61. Kuriakose T, Kanneganti T-D. ZBP1: Innate Sensor Regulating Cell Death and Inflammation. *Trends Immunol* (2018) 39:123. doi: 10.1016/j.it.2017.11.002
62. Somerville TDD, Xu Y, Wu XS, Maia-Silva D, Hur SK, de Almeida LMN, et al. ZBED2 is an Antagonist of Interferon Regulatory Factor 1 and Modifies Cell Identity in Pancreatic Cancer. *Proc Natl Acad Sci* (2020) 117:11471–82. doi: 10.1073/pnas.1921484117
63. Fuchs YF, Sharma V, Eugster A, Kraus G, Morgenstern R, Dahl A, et al. Gene Expression-Based Identification of Antigen-Responsive CD8+ T Cells on a Single-Cell Level. *Front Immunol* (2019) 0:2568. doi: 10.3389/fimmu.2019.02568
64. Mitamura Y, Nunomura S, Furue M, Izuhara K. IL-24: A New Player in the Pathogenesis of Pro-Inflammatory and Allergic Skin Diseases. *Allergol Int* (2020) 69:405–11. doi: 10.1016/j.alit.2019.12.003
65. Wang J, Ioan-Facsinay A, van der Voort EIH, Huizinga TWJ, Toes REM. Transient Expression of FOXP3 in Human Activated Nonregulatory CD4+ T Cells. *Eur J Immunol* (2007) 37:129–38. doi: 10.1002/eji.200636435
66. Yamaguchi K, Ito M, Ohmura H, Hanamura F, Nakano M, Tsuchihashi K, et al. Helper T Cell-Dominant Tertiary Lymphoid Structures are Associated With Disease Relapse of Advanced Colorectal Cancer. *Oncoimmunology* (2020) 9:1724763. doi: 10.1080/2162402X.2020.1724763
67. Jandrey EHF, Moura RP, Andrade LNS, Machado CL, Campesato LF, Leite KRM, et al. NDRG4 Promoter Hypermethylation is a Mechanistic Biomarker

Associated With Metastatic Progression in Breast Cancer Patients. *NPJ Breast Cancer* (2019) 5:1–12. doi: 10.1038/s41523-019-0106-x
68. Zhuravleva E, Gut H, Hynx D, Marcellin D, Bleck CKE, Genoud C, et al. Acyl Coenzyme A Thioesterase Them5/Acot15 is Involved in Cardiolipin Remodeling and Fatty Liver Development. *Mol Cell Biol* (2012) 32:2685–97. doi: 10.1128/MCB.00312-12
69. Takahashi N, Coluccio A, Thorball CW, Planet E, Shi H, Offner S, et al. ZNF445 Is a Primary Regulator of Genomic Imprinting. *Genes Dev* (2019) 33:49–54. doi: 10.1101/gad.320069.118

Conflict of Interest: The authors declare that the research was conducted in the absence of any commercial or financial relationships that could be construed as a potential conflict of interest.

Publisher's Note: All claims expressed in this article are solely those of the authors and do not necessarily represent those of their affiliated organizations, or those of the publisher, the editors and the reviewers. Any product that may be evaluated in this article, or claim that may be made by its manufacturer, is not guaranteed or endorsed by the publisher.

Copyright © 2022 Pagliarulo, Cheng, Brugger, van Dijk, van den Heijden, Levesque, Silina and van den Broek. This is an open-access article distributed under the terms of the Creative Commons Attribution License (CC BY). The use, distribution or reproduction in other forums is permitted, provided the original author(s) and the copyright owner(s) are credited and that the original publication in this journal is cited, in accordance with accepted academic practice. No use, distribution or reproduction is permitted which does not comply with these terms.

Advantages of publishing in Frontiers

OPEN ACCESS
Articles are free to read for greatest visibility and readership

FAST PUBLICATION
Around 90 days from submission to decision

HIGH QUALITY PEER-REVIEW
Rigorous, collaborative, and constructive peer-review

TRANSPARENT PEER-REVIEW
Editors and reviewers acknowledged by name on published articles

Frontiers
Avenue du Tribunal-Fédéral 34
1005 Lausanne | Switzerland

Visit us: www.frontiersin.org
Contact us: frontiersin.org/about/contact

REPRODUCIBILITY OF RESEARCH
Support open data and methods to enhance research reproducibility

DIGITAL PUBLISHING
Articles designed for optimal readership across devices

FOLLOW US
@frontiersin

IMPACT METRICS
Advanced article metrics track visibility across digital media

EXTENSIVE PROMOTION
Marketing and promotion of impactful research

LOOP RESEARCH NETWORK
Our network increases your article's readership